DOCTOR OF PHILOSOPHY

The anti-tumour activity and mode of action of artesunate and dihydroartemisinin (alone and in combination with aspirin) against human leukaemia HL-60 and colorectal HT-29-AK cancer cells

Maryniak, Lidia Barbara

Award date:
2016

Awarding institution:
Coventry University

The anti-tumour activity and mode of action of artesunate and dihydroartemisinin (alone and in combination with aspirin) against human leukaemia HL-60 and colorectal HT-29-AK cancer cells

Thesis submitted by:

Lidia Barbara Maryniak

Supervisory team: Dr Christopher J. Mee, Dr Omar Janneh, Dr Afthab Hussain, Dr Martin Cox

January 2016

In partial fulfilment for the requirements for the degree of Doctor of Philosophy

Faculty of Health and Life Sciences

Acknowledgements

I would like to thank my supervisors Dr Christopher Mee, Dr Omar Janneh, Dr Afthab Hussain and Dr Martin Cox for their guidance and support throughout my PhD project. I am especially grateful to Dr Omar Janneh for introducing me to the Cancer Research and all help given over the years despite moving to a new job. I deeply appreciate support and kindness of Dr Martin Cox and Dr Afthab Hussain during all difficult times and Dr Christopher Mee for patience during my writing up stage.

Special acknowledgment for a PhD student Aaron Nagra and past Laboratory Manager Neil Thompson for providing constant assistance in changing nitrogen cylinders for my hypoxic studies as without their help no data would be gathered. I also appreciate the assistance and technical support provided by laboratory technicians, Susan Thompset, Angela Lester and Victoria Greenwood.

I would like to express my humongous thanks to my labmates (Maryam Babba, Oana Chiuzbaian, Samantha Cooper, Hardip Sandhu, Eliot Barson, James Dayus and Mayel Gharanei) who made more enjoyable atmosphere in the lab throughout this research.

I am truly thankful to my beloved parents and siblings (Rafał, Paweł, Ewa and Katarzyna) for their unlimited love, support and endless encouragement during my PhD. I extend gratitude to my second ‘better’ half, my husband Jerzy Maryniak for believing in me, patience and tones of happiness and love given me in the last 10 years. Many thanks go to my close friends for their continous friendship and empathy.

Finally, I would like to thank Coventry University for the Research Scholarship to support this work.

Dedications

To my parents, Bronisława and Andrzej Pisuła

Abstract

Despite the considerable progress in cancer research which has been translated into better cancer care and decreased overall mortality rates in the last decade for numerous cancers, colorectal carcinoma (CRC) and leukaemia remain still one of the commonest malignancies worldwide. The compounds with improved anti-cancer activity that circumvent limitations of conventional chemotherapeutic agents are urgently searched. Artesunate (ART) and dihydroartemisinin (DHA) are the most active compounds of all semisynthetic derivatives of artemisinin (a natural extract of the Chinase plant, *Artemisia annua L.*) that have been proven to exert potent anti-cancer activity *in vitro*, *in vivo* and under human clinical trials.

ART and DHA contain a labile ring system, an endoperoxide bridge, which reductive cleavage by iron is a necessary prerequisite in their cytotoxicity. With ample evidence showing that the cytotoxicity of ART and DHA against cancer cells is linked with targeting a number of cellular proteins promoting tumorigenesis, the aim of this study was to provide additional molecular basis of ART and DHA activities in CRC HT-29-AK and leukaemia HL-60 cells *in vitro*.

Since the interior of most solid tumours are hypoxic (~1% O_2), which has implications for cancer metastasis and resistance to anti-cancer agents clinically, the anti-cancer effects of ART and DHA were performed under laboratory standard normoxic condition (20% O_2) and low oxygen tension (1% O_2), which mimics the tumour microenvironment. With reported ability of aspirin (acetylsalicylic acid; ASA) to enhance the cytotoxicity of other anti-cancer agents, we postulated that ASA would equally enhance the cytotoxic effects of ART and DHA. The mechanistic basis of this interaction was evaluated in cultured HT-29-AK and HL-60 cells in normoxia (20% O_2) and hypoxia (1% O_2).

This study shows that ART and DHA treatment of HT-29-AK and HL-60 cells in normoxia effectively inhibited the growth of both cell lines and this inhibition was affected by oxygen availability. Upon combination, ART and DHA with ASA could reverse decreased susceptibility of HT-29-AK cells under hypoxic conditions to ART and DHA alone.

In conclusion, these data illustrate the importance of modeling the tumour microenvironment when developing novel therapeutic drug applications. We also show that ART and DHA co-treated with ASA might be effective combination regimen to enhance efficacy of chemotherapy in cancer cells. Given the broad spectrum of mediators involved in ART and DHA anti-cancer effects (alone and in combination with ASA), further studies are required to validate our observations and translate them into significance for cancer therapy.

Table of contents

Acknowledgements I
Dedications I
Abstract II
Table of contents III
List of figures IX
List of tables XV
Abbreviations XVI

CHAPTER 1 1

INTRODUCTION 1
1.1. Artemisinin and its derivatives 1
1.2. The mechanism of action of artemisinin and its derivatives against malaria parasites 2
1.2.1. Activation of endoperoxide bridge 3
1.2.2. Alkylation of *Plasmodium*-specific proteins and lipids 4
1.3. Pharmacological activity of 1,2,4-trioxanes against malaria parasites *in vitro* 4
1.4. Anti-cancer effects of 1,2,4-trioxanes are linked with anti-malarial mechanisms . 6
1.4.1. Regulatory mechanisms of iron homeostasis in cells 6
1.4.2. Selective targeting of cancer cells by 1,2,4-trixanes 7
1.4.3. TfR1s as an indicator of malignant phenotype 8
1.4.4. Anti-cancer effects of 1,2,4-trioxanes are associated with a decrease in TfR1 levels 10
1.4.5. Enhanced delivery of 1,2,4-trioxanes into cancer cells through TfR1 13
1.5. Colorectal carcinoma and inflammation 15
1.5.1. Molecular mechanisms governing the development of inflammation-associated CRC 18
1.5.2. Importance of cytokine IL-6 in CRC 20
1.5.3. Inflammation promotes carcinogenesis through high TfR1 in cells 21
1.6. Leukaemia and inflammation 22
1.6.1. Molecular mechanisms promoting the development of inflammation-associated leukaemia 23
1.7. Inflammation as an anti-cancer therapeutic opportunity: use of NSAIDs 25

1.8. Molecular mechanisms of ASA anti-cancer effects 28
1.8.1. COX-1 and COX-2 enzymes 28
1.8.2. Molecular targets of ASA in cancer cells 30
1.8.3. ASA in combination with other therapeutic compounds shows increased activity against cancer cells 33
1.9. Anti-inflammatory effects of 1,2,4-trioxanes 34
1.9.1. Activities of 1,2,4-trioxanes in non-cancerous models 34
1.9.2. Activities of 1,2,4-trioxanes in cancer models 35
1.10. Inflammatory cytokines promote epithelial-mesenchymal transition 37
1.10.1. Loss of function of cell adhesion molecules supports invasive characteristics of cancer cells 37
1.10.2. Restored adhesion of cancer cells through 1,2,4-trioxanes activities 40
1.11. Inhibition of cell migration, invasion and metastasis by 1,2,4-trioxanes. 41
1.12. Angiogenesis as a anti-cancer target of 1,2,4-trioxanes 44
1.12.1. Inhibition of the VEGF gene family by 1,2,4-trioxanes 44
1.12.2. Regulation of HIF-1α transcription activator protein by 1,2,4-trioxanes 46
1.13. 1,2,4-trioxanes as a hypoxia selective agents 50
1.14. Induction of the apoptosis of cancer cells by 1,2,4-trioxanes 54
1.15. Combination therapy for cancer with 1,2,4-trioxanes and future prospectives. 60
1.16. Aim of the study 63

CHAPTER 2 66

MATERIALS & METHODS 66
2.1. REAGENTS AND CHEMICALS 66
2.2. PROPAGATION OF CANCER CELLS 67
2.2.1. Cell lines and culture 67
2.2.2. Cell harvesting 68
2.2.3. Cell counting 68
2.2.4. Cryopreservation of cells 69
2.2.5. Recovery of cryopreserved cells 69
2.3. Drug solutions 70
2.4. MTT ASSAY 70
2.4.1. Measurement of cytotoxicity of ART, DHA and ASA 70

2.4.2. Data analysis 72
2.4.3. Cytotoxicity of ART and DHA against confluent HT-29-AK cells 72
2.4.4. Effect of iron on the activity of ART and DHA 72
2.4.5. Cell rate of growth measurements 73
2.4.6. Irreversibility of cancer cell growth upon ART and DHA treatments 73
2.4.7. Combination studies 74
2.5. ENZYME-LINKED IMMUNOSORBENT ASSAYS (ELISAs) 75
2.5.1. The Quantikine® Human sTfR1 immunoassay 75
2.5.2. The Quantikine® Human IL-6 immunoassay 76
2.5.3. The Quantikine® Human VEGF-α_{165} immunoassay 76
2.5.4. The Quantikine® Human Survivin immunoassay 77
2.5.5. Data analysis 77
2.6. REAL-TIME QUANTITATIVE POLYMERASE CHAIN REACTION (RT-qPCR) 77
2.6.1. RNA extraction 78
2.6.2. RNA concentration and quality 79
2.6.3. NanoDrop™ ND-1000 Sectrophotometer 79
2.6.4. Agilent 2100 Bioanalyser 79
2.6.5. cDNA synthesis 81
2.6.6. qRT-PCR 81
2.6.7. Quality determination of qRT-PCR products 83
2.6.8. mRNA concentration calculations 83
2.7. IMMUNOCYTOCHEMISTRY STAINING 84
2.7.1. Paraformaldehyde fixation method and primary antibody staining 84
2.7.2. Methanol fixation method and primary antibody staining 84
2.7.3. Secondary antibody staining and confocal microscopic analysis 85
2.7.4. Data analysis 85
2.8. *IN VITRO* CELL SCRATCH WOUND ASSAY 85
2.8.1. Scratch wound assay of confluent HT-29-AK cells 85
2.8.2. Data analysis 87
2.9. FLOW CYTOMETRIC ANALYSIS OF PROTEIN LEVELS 87
2.9.1. Intracellular protein staining 87
2.9.1.1. Intracellular expression levels of COX-2, CLDN-1, catalytically active caspase-3, phospho-Akt, MMP-2 and MMP-9 87
2.9.1.2. Intracellular levels of HIF-1α 88

2.9.2. Cell surface protein staining 88
2.9.2.1. Cell surface levels of E-cadherin and CA-9 88
2.9.3. Data analysis 89
2.10. WESTERN BLOTTING 89
2.10.1. Extraction of protein from cultured cells 89
2.10.1.1. Extraction of protein using syringe with a 27-gauge hypodermic needle 89
2.10.1.2. Extraction of protein using sonicator 90
2.10.2. Sodium dodecyl sulphate-polyacrylamide gel electrophoresis (SDS-PAGE) 91
2.10.3. Transfer to PVDF membrane 91
2.10.4. Immunolabelling and detection 92
2.10.5. Membrane stripping and re-probing 93
2.10.6. Densitometry 93
2.11. APO-BrdU™ TUNEL ASSAY 94
2.12. AGAROSE GEL ELECTROPHORESIS OF DNA 95
2.13. STATISTICAL ANALYSIS 96

CHAPTER 3 97

RESULTS 97

3.1. ART and DHA display growth inhibitory activities against HL-60, HT-29-AK and Caco-2 cells *in vitro* under standard normoxic conditions. 97

3.2. Cytotoxicity of ART and DHA against HT-29-AK is dependent on the proliferation state of the cells. 105

3.3. Cytotoxicity of ART and DHA against HL-60 and HT-29-AK cells is iron-dependent 107

3.4. ART and DHA altered the secretion of sTfR1 in HL-60 and HT-29-AK cells in normoxia 108

3.5. DHA altered the secretion of IL-6 in HL-60 and HT-29 cells in normoxia 112

3.6. ART and DHA down-regulated intracellular protein levels of COX-2 in HT-29-AK cells in normoxia 114

3.7. Effect of ART and DHA on mRNA and protein expression levels of E-cadherin and its localisation. 116

3.8. Effect of ART and DHA on protein, mRNA and cellular localisation of CLDN-1131

3.9. ART and DHA reduced the wound healing capacity of HT-29-AK cells under normoxic conditions 139

3.10. Effect of ART and DHA on irreversibility of cell growth in normoxia 149

3.11. Effect of ART and DHA on the expression of MMP-2 and MMP-9 proteins ... 153

3.12. ART and DHA alter secretions and mRNA levels of pro-angiogenic VEGF-α in HT-29-AK and HL-60 cells 162

3.13. Effect of ART and DHA on HIF-1α protein and mRNA expression levels 167

3.14. Effect of ART and DHA on CA-9 localisation in HT-29-AK cells 180

3.15. ART and DHA treatment altered the cellular and mRNA survivin levels in HL-60 and HT-29-AK cells 185

3.16. Effect of ART and DHA on phospho-Akt expression levels 195

3.17. ART and DHA increased caspase-3-dependent apoptosis of HT-29-AK and HL-60 cells 200

3.18. DHA induces DNA strand breaks in treated HL-60 and HT-29-AK cells as measured by 5-bromo-2'-deoxyuridine (BrdU) assay under normoxic conditions ... 204

3.19. ART and DHA induced DNA fragmentation in HT-29-AK and HL-60 cells in normoxia 206

CHAPTER 4 213

RESULTS 213

4.1. ART and DHA inhibit the growth of HL-60 and HT-29-AK cells in low oxygen tension 213

4.2. Cytotoxicity of ART and DHA in hypoxia against HL-60 and HT-29-AK cells was affected by the presence of DFO and haemin. 218

4.3. Hypoxia modulates the effects of ART and DHA on the cellular secretion of sTfR1 in HL-60 and HT-29-AK cells 220

4.4. The proliferation rate of HL-60 and HT-29-AK cells is affected by oxygen availabilty 224

4.5. DHA treatment altered the secretion of cytokine IL-6 in HL-60 and HT-29-AK cells in hypoxia 226

4.6. ART and DHA reduced the levels of $VEGF\alpha_{165}$ in HL-60 and HT-29-AK cells in hypoxia 227

4.7. ART and DHA treatment altered cellular survivin levels in HL-60 and HT-29-AK cells in hypoxia 230

4.8. ART and DHA induced the release of phospho-Akt in HT-29-AK cells in hypoxia 232

4.9. ART and DHA induced the release of cleaved caspase-3 in HL-60 and HT-29-AK cells under hypoxic conditions 233

4.10. DHA induced DNA damage as measured by BrdU staining in HL-60 and HT-29-AK cells under hypoxia 235

4.11. DHA induced DNA fragmentation in HL-60 cells in hypoxia 236

CHAPTER 5.....238

RESULTS 238

5.1. Cytotoxicity of ASA against HT-29-AK and HL-60 cells is dependent on oxygen availability 238

5.2. ASA modulates the cytotoxicity of ART and DHA against cancer cells..... 240

5.3. Effect of ART and DHA (alone and in combination with ASA) on COX-2 protein 243

5.4. Effect of ART and DHA (alone and in combination with ASA) on survivin cellular and mRNA levels 244

5.5. Effect of ART and DHA (alone and in combination with ASA) on HIF-1α mRNA levels 245

5.6. Effect of ART and DHA (alone and in combination with ASA) on VEGF-α mRNA levels 247

5.7. ASA combination with ART and DHA increased cellular phospho-Akt levels .. 248

5.8. ASA enhanced ART- and DHA- caspase-3-dependent apoptosis 250

CHAPTER 6.....253

DISCUSSION 253

Part 1: THE MOLECULAR BASIS OF THE ANTI-CANCER EFFECTS OF ART AND DHA AGAINST HT-29-AK AND HL-60 CELLS IN NORMOXIA AND HYPOXIA 253

6.1. Cytotoxicity of ART and DHA under normoxic and hypoxic conditions..... 253

6.2. Cytotoxicity of ART and DHA in cancer cells is iron-dependent 257

6.3. Effect of ART and DHA on IL-6 and COX-2 levels..... 261

6.4. Effect of ART and DHA on expression and localisation of E-cadherin and CLDN-1 in cancer cells 262

6.5. Inhibition of cell migration and invasion by ART and DHA..... 267

6.6. ART and DHA to modulate VEGF-α and HIF-1α levels 269

6.7. ART and DHA modulate the expression of proteins which are responsible for caspase-dependent cell death 272
6.8. Conclusions and future studies 276

CHAPTER 7 277

DISCUSSION 2 277
Part 2: THE MOLECULAR BASIS OF THE ANTI-CANCER EFFECTS OF ART AND DHA COMBINED WITH ASA AGAINST HT-29-AK AND HL-60 CELLS IN NORMOXIA AND HYPOXIA 277
7.1. Anti-cancer effects of ART and DHA (alone and in combination with ASA) against HL-60 and HT-29-AK cells under normoxic and hypoxic conditions 277
7.2. Conclusions and future directions 288
References 291

List of figures

CHAPTER 1 1

Figure 1: The proposed mechanism of the iron-mediated activation of ART and DHA within cancer cells. 12
Figure 2: COX- dependent and independent mechanisms of action of ASA in cancer cells. 32
Figure 3: Schematic representation of the mechanisms by which 1, 2,4-trioxanes inhibit spread of cancer cells to distant parts in the body. 49
Figure 4: Tumour hypoxic mass features and their effect on inhibited responsiveness to standard radio- and chemo-therapy treatments. 53
Figure 5: Non-tumorigenic cells with damaged DNA can be self repair or be utilized by self-destruct mechanism, an apoptosis. 56
Figure 6: Simplified proposed mechanisms of DHA and ART-mediated cell death in cancer cells 58
Figure 7: Chemical structures of the test compounds used in this study. 65

CHAPTER 2 66

Figure 8: Simplified principle of MTT tetrazolium conversion into formazan crystals. 71

Figure 9: Electrophoretic separation of HT-29-AK cells total RNA upon drug treatment with the Agilent 2100 Bioanalyser using RNA 6000 Pico Chip. 80
Figure 10: Representative Images of protein transfer and separation using a stain-free Gel Doc™ EZ imaging system (Bio-Rad, UK). 92
Figure 11: The principle of APO-BrdU™ TUNEL Assay. 95
CHAPTER 3 97
Figure 12: Concentration- and time-response effects of ART and DHA on the growth of HL-60 leukaemia cancer cells cultured in normoxia for 24-72h. 100
Figure 13: Concentration- and time-response effects of ART and DHA on the growth of HT-29-AK CRC cells cultured in normoxia for 24-72h. 102
Figure 14: Concentration- and time-response effects of ART and DHA on the growth of Caco-2 CRC cells cultured in normoxia for 24-72h. 104
Figure 15: The secretion levels of sTfR1 in cancer cells upon ART and DHA treatments in normoxia. 110
Figure 16: The secretion levels of pro-inflammatory cytokine IL-6 in cancer cells upon DHA treatment at 24h and 72h in normoxia. 114
Figure 17: ART and DHA decreases the intracellular protein levels of COX-2 in HT-29-AK cells at 72h in normoxia. 116
Figure 18: The effect of ART on E-cadherin mRNA expression in HT-29-AK cells at 24h and 72h in normoxia. 118
Figure 19: Normalisation of immunocytochemistry staining method for E-cadherin localisation in HT-29-AK cells. 119
Figure 20: The effect of ART on E-cadherin cellular protein localisation in HT-29-AK cells at 24h in normoxia. 123
Figure 21: The effect of ART on E-cadherin cellular protein localisation in HT-29-AK cells at 72h in normoxia 125
Figure 22: The effect of DHA on E-cadherin cellular protein localisation in HT-29-AK cells at 24h in normoxia. 128
Figure 23: The effect of DHA on E-cadherin cellular protein localisation in HT-29-AK cells at 72h in normoxia. 129

Figure 24: The effect of ART and DHA on surface E-cadherin protein expression levels in HL-60 cells at 72h in normoxia. 131
Figure 25: The effect of ART on CLDN-1 mRNA expression in HT-29-AK cells at 24h and 72h in normoxia. 133
Figure 26: The effect of ART on intracellular CLDN-1 protein levels in HT-29-AK cells at 72h in normoxia. 134
Figure 27: The effect of ART on CLDN-1 cellular protein localisatin in HT-29-AK cells at 72h in normoxia. 135
Figure 28: DHA decreases up-regulated levels of intracellular CLDN-1 in HT-29-AK cells at 72h in normoxia. 136
Figure 29: ART and DHA increase production of CLDN-1 intracellular protein in HL-60 cells at 72h in normoxia. 138
Figure 30: Wound healing capacity of HT-29-AK monolayers after treatment with ART in normoxia. 143
Figure 31: ART increases the diamater of the wound and the number of dead cells in HT-29-AK monolayers in normoxia. 144
Figure 32: Wound healing capacity of HT-29-AK monolayers after treatment with DHA in normoxia. 147
Figure 33: DHA increases the diamater of the wound and the number of dead cells in HT-29-AK monolayers in normoxia. 148
Figure 34: ART and DHA inhibit the re-growth of HT-29-AK cells cultured in normoxia 150
Figure 35: ART and DHA inhibit the re-growth of HL-60 cells cultured in normoxia.152
Figure 36: The effect of ART on intracellular MMP-2 and MMP-9 protein levels in HT-29-AK cells at 72h in normoxia. 155
Figure 37: The effect of DHA on the protein expression of MMP-2 and MMP-9 in HT-29-AK cells at 72h in normoxia. 157
Figure 38: The effect of ART on the intracellular MMP-2 and MMP-9 protein expression in HL-60 cells at 72h in normoxia. 159
Figure 39: The effect of DHA on the intracellular MMP-2 and MMP-9 protein expression in HL-60 cells at 72h in normoxia. 161

Figure 40: The effect of ART on VEGF-α mRNA expression levels and cellular VEGF-α165 secretion in HT-29-AK cells in normoxia. 164
Figure 41: The effect of DHA on VEGF-α165 cellular secretion in HT-29-AK cells at 24h and 72h in normoxia. 165
Figure 42: The effect of ART and DHA on VEGF-α165 cellular secretion in HL-60 cells in normoxia. 167
Figure 43: The effect of ART on HIF-1α mRNA expression and intracellular protein HIF-1α levels in HT-29-AK cells in normoxia. 170
Figure 44: The effect of DHA on the mRNA expression and intracellular protein levels of HIF-1α in HT-29-AK cells in normoxia. 173
Figure 45: The effect of ART on the mRNA expression and intracellular protein levels of HIF-1α in HL-60 cells in normoxia. 176
Figure 46: The effect of DHA on the mRNA expression and intracellular protein levels of HIF-1α in HL-60 cells in normoxia. 179
Figure 47: The effect of ART and DHA treatment on CA-9 intracellular protein localisation in HT-29-AK cells at 24h and 72h in normoxia. 185
Figure 48: The effect of ART on the mRNA expression levels of survivin in HT-29-AK and HL-60 cells at 24h and 72h in normoxia. 187
Figure 49: The effect of ART on cellular protein levels of survivin in HT-29-AK and HL-60 cells at 24h and 72h in normoxia. 188
Figure 50: The effect of DHA on the mRNA expression and cellular protein levels of survivin in HT-29-AK cells at 24h and 72h in normoxia. 191
Figure 51: The effect of DHA on the mRNA expression and cellular protein levels of survivin in HL-60 cells at 24h and 72h in normoxia. 194
Figure 52: ART increases the protein levels of phospho-Akt in HT-29-AK cells at 72h in normoxia. 196
Figure 53: The effect of DHA on phospho-Akt intracellular protein levels in HT-29-AK cells at 24h and 72h in normoxia. 198
Figure 54: The effect of ART and DHA on phospho-Akt intracellular protein levels in HL-60 cells at 72h in normoxia. 200

Figure 55: The effect of ART and DHA on the activity of cellular cleaved caspase-3 in HT-29-AK cells at 72h in normoxia. 202
Figure 56: The effect of ART and DHA on the activity of cellular cleaved caspase-3 in HL-60 cells at 72h in normoxia. 203
Figure 57: The effect of DHA on the presence of BrdU-labelled nicks in DNA in HT-29-AK cells at 24h and 72h in normoxia. 205
Figure 58: The effect of DHA on the presence of BrdU-labelled nicks in DNA in HL-60 cells at 24h and 72h in normoxia. 206
Figure 59: HT-29-AK cells DNA fragmentation analysis upon ART and DHA treatment for 72h in normoxia. 208
Figure 60: HL-60 cells DNA fragmentation analysis upon ART treatment for 24-72h in normoxia. 210
Figure 61: HL-60 cells DNA fragmentation analysis upon DHA treatment at 24h and 72h in normoxia. 212
CHAPTER 4 213
Figure 62: The secretion levels of sTfR1 in HL-60 cells upon ART and DHA treatments in hypoxia. 222
Figure 63: The secretion levels of sTfR1 in HT-29-AK cells upon ART and DHA treatments in hypoxia. 224
Figure 64: The growth kinetics of A) HL-60 and B) HT-29-AK cells cultured in normoxia and hypoxia. 225
Figure 65: The secretion levels of pro-inflammatory cytokine IL-6 in HL-60 and HT-29-AK cells upon DHA treatment for 72h in hypoxia. 227
Figure 66: The effect of ART and DHA on VEGF-α165 cellular secretion in HL-60 cells at 72h in hypoxia. 228
Figure 67: The effect of ART and DHA on VEGF-α165 cellular secretion in HT-29-AK cells under hypoxia. 229
Figure 68: The effect of ART and DHA on cellular survivin levels in HL-60 cells at 72h in hypoxia. 231
Figure 69: The effect of ART and DHA on cellular survivin levels in HT-29-AK cells in hypoxia. 232

Figure 70: ART and DHA increase the protein levels of phospho-Akt in HT-29-AK cells at 72h in hypoxia. 233
Figure 71: The effect of ART and DHA on the activity of cellular cleaved caspase-3 in HL-60 cells at 72h in hypoxia. 234
Figure 72: The effect of ART and DHA on the activity of cellular cleaved caspase-3 in HT-29-AK cells in hypoxia. 235
Figure 73: The effect of DHA on the presence of BrdU-stained cells as a marker of DNA damage in HL-60 and HT-29-AK cells in hypoxia. 236
Figure 74: A representative DNA fragmentation analysis of DHA-treated HL-60 cells for 72h in hypoxia using agarose gel electrophoresis. 237
CHAPTER 5 238
Figure 75: The effect of ART, DHA and ASA (alone and in combination) on cellular COX-2 protein levels in HT-29-AK cells. 244
Figure 76: The effect of ART, DHA and ASA (alone and in combination) on survivin mRNA levels in HT-29-AK cells. 245
Figure 77: The effect of ART, DHA and ASA (alone and in combination) on HIF-1α mRNA levels in HT-29-AK cells. 246
Figure 78: The effect of ART, DHA and ASA (alone and in combination) on VEGF-α mRNA levels in HT-29-AK cells. 248
Figure 79: The effect of ART, DHA and ASA (alone and in combination) on cellular phospho-Akt levels in HT-29-AK cells in normoxia. 249
Figure 80: The effect of ART, DHA and ASA (alone and in combination) on cellular cleaved caspase-3 levels in HL-60 cells. 251
Figure 81: The effect of ART, DHA and ASA (alone and in combination) on cellular cleaved caspase-3 levels in HT-29-AK cells. 252
CHAPTER 7 277
Figure 82: The proposed shema of the mechanisms of action of ART and DHA combined with ASA in induced apostosis in human colorectal HT-29-AK cancer cells under normoxic conditions. 290

List of tables

CHAPTER 1 1

Table 1: Association between chronic inflammation and cancer development (taken from Boland *et al.* 2005; Tanaka 2012)..... 17

CHAPTER 2 66

Table 2: Primer sequences for qPCR and expected PCR products (bp). 82

CHAPTER 3 97

Table 3: The effect of ART and DHA against HL-60, HT-29-AK and Caco-2 cells for 24h, 48h or 72h cultured in normoxia. 99

Table 4: The effect of ART and DHA against HT-29-AK cells, at time 0h and confluent cells, cultured in normoxia for 24h. 106

Table 5: The effect of ART and DHA alone and in the presence of deferiprone, DFO (60µM) and haemin (1µM or 3µM) against HL-60 and HT-29-AK cells for 24h cultured in normoxia. 108

CHAPTER 4 213

Table 6: The cytotoxic effect of ART and DHA alone at 24h, 48h or 72h incubation in hypoxia. 215

Table 7: The cytotoxic effect of ART and DHA alone and in the presence of deferiprone (60µM) and haemin (1µM and 3µM) against HL-60 and HT-29-AK cells at 24h incubation in hypoxia. 219

CHAPTER 5 238

Table 8: The effect of ASA on the growth of HL-60 and HT-29-AK cells cultured for 24h, 48h or 72h under normoxic or hypoxic conditions. 240

Table 9: The effect of ART and DHA alone and in the presence of fixed concentrations of ASA against HT-29-AK and HL-60 cells in normoxic conditions. 241

Table 10: The effect of ART and DHA alone and in the presence of fixed concentrations of ASA against HT-29-AK and HL-60 cells in hypoxic conditions.. 242

Abbreviations

%	Percentage
µM	Micromolar
ACT	Artemisinin-based combination therapy
ALL	Acute lymphoblastic leukaemia
AML	Acute myeloid leukaemia
AP-1, and -2	Activator protein-1, and -2
APC	Adenomatous polyposis coli
ART	Artesunate
ASA	Aspirin, acetylsalicylic acid
ATRA	All-trans retinoic acid
B-CLL	B-cell chronic lymphocytic leukaemia
BM	Bone marrow
CA-9	Carbonic anhydrase IX
CAM	Chicken charioallantoic membrane
CCR	Carbon centred free radical
CLDN-1	Claudin-1
CML	Chronic myelocytic leukaemia
COX-1 and -2	Cyclooxygenase-1 and -2
COPD	Chronic obstructive pulmonary disease
CRC	Colorectal carcinoma
DFO	Deferiprone
DHA	Dihydroartemisinin, β-dihydroartemisinin, artenimol
DMSO	Dimethyl sulfoxide
DR-5	Death receptor -5
EGF	Epidermal growth factor
EMT	Epithelial-mesenchymal transition
ERK	Extracellular signal-regulated kinase
EM	Extracellular matrix
FACS	Fluorescence activated cell sorting
FAP	Familial adenomatous polyposis
Fe	Iron

5-FU	5-fluorouracil
Haeme	Fe^{2+} protoporphyrin-IX
Haemin	Ferric haeme, Fe^{3+} protoporphyrin-IX
•HO	Hydroxyl radical
H_2O_2	Hydrogen peroxide
HIF-1α	Hypoxia inducible factor-1α
HPV	Human Papillomavirus
IBD	Inflammatory bowel disease
IC_{50}	the 50% growth-inhibition concentration
ICAM-1	Intracellular adhesion molecule-1
IEC	Intestinal epithelial cell
IL	Interleukin
JAK	Janus kinase
K-ras	Kirsten-ras
LLC	Lewis lung carcinoma
Mad1	MAX dimerization protein 1
MAPK	Mitogen-activated protein kinase
Mdm2	Murine double minute
mM	Millimolar
MMP (-1,-2,-7,-9)	Matrix metalloproteinase (-1,-2,-7,-9)
MS	Myelodysplastic syndrome
MT1-MMP	Membrane-type 1 matrix metalloproteinase
MTT	3-(4,5-dimethyl-thizol-2-yl)-2,5-diphenyltetrazolium bromide
nM	Nanomolar
NF-κβ	Nuclear factor kappa beta
NK	Natural killer cell
Nlrp-3	NOD-like receptor protein 3
NSAID	Non-steroidal anti-inflammatory drug
O_2	Oxygen
$O_2^{\bullet-}$	Superoxide
OR	Odd ratio
PARP	Poly-ADP ribose polymerase
PI3-kinase/Akt	Phosphoinosine 3-kinase/serine-threonine protein kinase

P. falciparum	*Plasmodium falciparum*
PG	Prostaglandin
PML- RAR-α	Promyelocytic leukaemia-retinoic acid receptor -α Fusion Transcript
PVDF	Polyvinylidene fluoride membrane
RB	Retinoblastoma cancer cells
RNI	Reactive nitrogen intermediate
ROS	Reactive oxygen species
RR	Rate ratio
SERCA	the sarco/endoplasmatic reticulum Ca^{2+} ATPase
STAT	Signal transducers and activators of transcription
TCTP	Translationally controlled tumour protein
TfR1, CD71	Transferrin receptor 1
TIMP-2	Tissue inhibitor of metalloproteinase -2
TLR-1,-2,-4 and -8	Toll-like receptor-1, -2,-4 and -8
TNF-α	Tumour necrosis factor- α
TX	Thromboxane
UC	Ulcerative colitis
uPA	Urokinase-type plasminogen activator
1,2,4-trioxanes	Artemisinin and its derivatives
VEGF	Vascular endothelial growth factor
WHO	World Health Organization
Wnt	Wingless-type MMTV integration site family

CHAPTER 1

INTRODUCTION

1.1. Artemisinin and its derivatives

The genus *Artemisia L.*, (Asteraceae) compromises about 180 species of herbs, including some important medical plants, such as *Artemisia annua L.* being native to East and Southeastern Europe, the Caucasus, and Western and Middle Asia (GRIN Taxonomy Databases, 2015). Artemisinin (qinghaosu, sweet wormwood or armoise annuelle), is a pharmaco-dynamically active 15-carbon sesquiterpene trioxane 6-lactone endoperoxide isolated in 1971 from the Chinese herb *Artemisia annua L.* (Efferth *et al.* 2004; Krungkrai *et al.* 2010; Sertel *et al.* 2010). Though it has been used for over 2000 years particularly in China as a folk remedy against fever and haemorrhoids, it is mostly readily known as a treatment against the malaria parasite (Meshnick *et al.* 1996; Laman *et al.* 2014).

To overcome the solubility limitations of artemisinin (in water and oil), limited routes of administration (oral and rectal), its poor bioavailability (30% rectal relative to oral) and a short elimination half-life *in vivo* (~2.59+/-0.55h) having all impact on decreased effectiveness as an anti-malarial, semi-synthetic derivatives of artemisinin were developed (Duc *et al.* 1994; de Vries and Dien 1996; Ashton *et al.* 1998). A more water-soluble active metabolite of artemisinin, dihydroartemisinin (β-dihydroartemisinin, artenimol, DHA) is the chemical intermediate in production of water-soluble artesunate (ART) (de Vries and Dien 1996). Other semi-synthetic artemisinin derivatives include artemether and arteether (artemotil), which are both fat-soluble and around twice as active as artemisinin (de Vries and Dien 1996).

Today, artemisinin-compounds are not used in monotherapy against malaria as it is associated with comparatively high recrudescence rates of infections after 5-day treatments of ~10% (de Vries and Dien 1996). In fact, with the World Health Organization (WHO) policy guidelines artemisinin and its derivatives should be only used in combination with other not failing anti-malarial compounds in a malaria treatment regimen, artemisinin-based combination therapy (ACT) (Cui and Su 2009). ACT with conventional anti-malarial agents, such as amodiaquine, mefloquine, piperaquine, lumefantrine are at present widely used drugs to treat severe and multidrug-resistant strains of *Plasmodium falciparum* (*P. falciparum)* clinically because of their lack of severe side effects and rapid parasite clearance within approximately 48h (de Vries and Dien 1996; Tran *et al.* 2004; Nosten and White 2007). However, parasite resistance to ACT has emerged recently in seven provinces along Thai-Cambodia border (Southeast Asia) (Noedl *et al.* 2010; Satimai *et al.* 2012; Ashley *et al.* 2014). The threat of malaria resistance to ACT globally prompts an urgent need to design and develop novel treatments regimens that will overcome the increasing burden caused by *P. falciparum.*

1.2. The mechanism of action of artemisinin and its derivatives against malaria parasites

The active moiety of artemisinin and its derivatives is the endoperoxide in a labile 1,2,4-trioxane heterocyclic ring system (Meshick *et al.* 1996; Kaiser *et al.* 2007; Antoine *et al.* 2014). In *Plasmodium* parasite, artemisinin and its derivatives (for simplification hereafter the 1,2,4-trioxanes) are bio-activated by high intraparasetic-haem-iron content leading to cleavage of the endoperoxide bridge (C-O-O-C) in the two seqentional steps: activation followed by alkylation, resulting in

the formation of toxic molecules which kill parasite (Meshick *et al.* 1996; O'Neill *et al.* 2010; Antoine *et al.* 2014; Gopalakrishnan and Kumar 2015).

1.2.1. Activation of endoperoxide bridge

In the activation step, the 1,2,4-trioxane bond requires reductive cleavage by haem-derived iron (Fe) through two mechanisms including reductive scission and open peroxide model, resulting in formation of carbon centred free radicals (CCR) and/or reactive oxygen species (ROS) (Efferth *et al.* 2004; Mercer *et al.* 2007; Cui and Su 2009; O'Neill *et al.* 2010; Antoine *et al.* 2014; Gopalakrishnan and Kumar 2015). In the reductive scission model, Drew *et al.* (2007), Cui and Su (2009), and O'Neill *et al.* (2010) propose that formation of a bond between low-valent transition irons (ferrous haem or non-haem, exogenous Fe^{2+}) and either oxygen-(O)1 or O2 within peroxide skeleton of 1,2,4-trioxanes results in its reductive scission and the formation of an unstable O-centred radical. The un-symmetrical structure of the peroxide group triggers further rapid intra-molecular re-arrangements to produce O-centred radical and the formation of more stable primary or secondary C-centred radicals (Cui and Su 2009; O'Neill *et al.* 2010). In alternative open peroxide model, the peroxide bond cleavage involves protonation or complexation with ferrous Fe^{2+} (Cui and Su 2009; O'Neill *et al.* 2010). In the Fenton reaction, created hydroperoxides (H_2O_2) during cleavage of the 1,2,4-trioxane bond are catalysed by Fe^{2+} to form ROS, such as hydroxyl radicals (•HO), peroxyl radicals and (protonated) superoxide anions within *Plasmodium*-infected erythrocytes (O'Neill *et al.* 2010; Antoine *et al.* 2014).

1.2.2. Alkylation of *Plasmodium*-specific proteins and lipids

The haem(II)-iron mediated reductive decomposition of 1,2,4-trioxane results in the release of highly reactive alkylating CCR and ROS, which target pivotal *Plasmodium*-specific macromolecules including proteins and lipids, leading to DNA damage and eradication of the parasite (Cui and Su 2009; Krungkrai *et al.* 2010;O'Neill *et al.* 2010; Gopalakrishnan and Kumar 2015). Iron-activated 1,2,4-trioxanes may target membrane containing organelles, such as the mitochondria, endoplastic reticulum, nuclear envelope and the food vacuole membranes (Cui and Su 2009). Other primary targets of 1,2,4-trioxanes in *Plasmodium* include haem alkylation, inhibition of endocytosis, inhibition of inosine monophosphate dehydrogenase and succinic acid dehydrogenase resulting in loss of mitochondrial potential, inhibition of cytochrome oxidase activity and inhibiting alkylation of membrane associated *Plasmodium*-specific proteins (Krungkrai *et al.* 2010; Antoine *et al.* 2014). These include translationally controlled tumour protein (TCTP; 25kDa), histidine-rich protein (42 kDa), and pfATP6, the sarco/endoplasmatic reticulum Ca^{2+} ATPase (SERCA) (Eckstein-Ludwig *et al.* 2003; Kaiser *et al.* 2007; Nagamune *et al.* 2007; Cui and Su 2009; Krungkrai *et al.* 2010; O'Neill *et al.* 2010*)*.

1.3. Pharmacological activity of 1,2,4-trioxanes against malaria parasites *in vitro*

1,2,4-trioxanes-family of anti-malarial agents are active against sensitive and multidrug resistant isolates of *Plasmodium* species at low (nM) concentrations *in vitro* (Krishna *et al.* 2004; Jones *et al.* 2009; Nsobya *et al.* 2010). In a chloroquine sensitive 3D7 strain of *P. falciparum*, DHA and artemether treatment for 24h displayed high activity, resulting in IC_{50} values (the 50% growth-inhibition concentrations) of 2.30 ± 1.50nM and 3.53 ± 1.91nM, respectively (Jones *et al.*

2009). After 72h incubation, in *P. falciparum* strains resistant to chloroquine (IC_{50} value of 101.1nM) and monodesethylamodiaquine (IC_{50} value of 66.4nM) being above standard cutoffs for resistance for both compounds (100nM and 60nM, respectively), DHA was shown to effectively kill parasites with mean IC_{50} value at subnanomolar concentration (0.55nM) with narrow concentration range across all 212 samples of IC_{50} values <5nM (Nsobya *et al.* 2010). More recently, *P.falciparum* (3D7 strain) parasites treated *in vitro* with a panel of 1,2,4-trioxanes showed growth inhibition IC_{50} values of 7.50 ± 0.2nM, 3.48 ± 0.60nM, 1.60 ± 0.40nM and 4.46 ± 0.75nM for artemisinin, DHA, ART and artemether, respectively (Antoine *et al.* 2014). The growth of parasites was not inhibited (IC_{50} value of >10 000nM) when using deooxyartemisinin, a compound without endoperoxide bridge (Antoine *et al.* 2014). Additionally, deooxyartemisinin showed no effect on parasite membrane potential, thus confirming the importance of the endoperoxide bond in the activation of 1,2,4-trioxanes (Antoine *et al.* 2014). During the single-cell assays (<6mins), depolarisation of the parasite membrane potential was abolished when artemisinin (100nM) was co-treated with iron chelators, desferrioxamide (100µM) and deferiprone (DFO, 100µM), which are selective for non-haem Fe^{3+} (Antoine *et al.* 2014). Because artemisinin alone has been reported previously to induce membrane depolarisation of the malaria parasite, the findings of Antoine *et al.* (2014) indicate the role of Fe^{3+} in the cleavage of 1,2,4-trioxanes' endoperoxide bond.

1.4. Anti-cancer effects of 1,2,4-trioxanes are linked with anti-malarial mechanisms

1.4.1. Regulatory mechanisms of iron homeostasis in cells

Interestingly, the same way that iron plays a central role in the mechanisms of action of 1,2,4-trioxanes against malaria parasites, the mode of action of these agents against cancer cells has been reported to be iron-dependent (Efferth 2005; O'Neill *et al.* 2010). Malignant cells are characterised by rapid proliferation where high intracellular iron content is needed as a cofactor of haem synthesis and DNA metabolism to help promote continued cell proliferation (O'Donnell *et al.* 2006; Mercer *et al.* 2007; Oh *et al.* 2009; O'Neill *et al.* 2010). Synthesized in hepatocytes, human serum transferrin (an 80kDa bilobal glycoprotein) is secreted into the bloodstream where is responsible for binding iron from diet (Eckenroth *et al.* 2011). Iron-loaded transferrin is subsequently internalised into cells through type II transmembrane proteins, transferrin receptors (TfR1, CD71), which are expressed on the cell surface (Dautry-Varsat *et al.* 1983; Eckenroth *et al.* 2011). The low pH (~5.6 or below) of the endocytic vesicle facilitates the release of iron within the cell from the transferrin-receptor complex (Dautry-Varsat *et al.* 1983; Eckenroth *et al.* 2011). The apotransferrin (iron-free transferrin)-receptor complex is recycled to the cell surface and apotransferrin upon increased pH dissociates from the cell and is ready to bind iron again (Dautry-Varsat *et al.* 1983; Eckenroth *et al.* 2011). Iron homeostasis is tightly controlled by transferrin, TfRs and regulatory iron proteins, including hypoxia inducible factor (HIF)-1α (Lok and Ponka 1999; Takami and Sakaida 2011). Imbalanced iron homeostasis may contribute to excess reactive iron, which produces toxic free radicals causing cellular damage via Fenton reaction (Fe^{2+}/hydrogen peroxide H_2O_2) or Haber-Weiss reaction, where a large amount of

highly reactive hydroxyl radicals (•OH) can be generated from an interaction between H_2O_2 and superoxide ($O_2^{\bullet-}$) (Kehrer 2000; Takami and Sakaida 2011).

1.4.2. Selective targeting of cancer cells by 1,2,4-trixanes

The expression of TfR1 in cancer cells is higher compared to normal cells, which is required for increased iron up-take to maintain robust cell proliferation (O'Donnell *et al.* 2006). It has been reported that cancer cells may possess up to five times more TfR1 than normal cells, and its expression varies between different cell lines (Efferth 2005; Cheung *et al.* 2010). For example, the expression of TfR1 at the plasma membrane in retinoblastoma cancer (RB) cells reached ~70% and it was more than 2 times higher than in normal retina cells (Zhao *et al.* 2013). Therefore, the high requirement on iron by tumour cells makes them more susceptible to selective targeting by 1,2,4-trioxanes. It was confirmed by Zhao *et al.* 2013 where ART-mediated toxic effects to cells (reffered as cytotoxicity) at 24h and 48h treatment was selective towards highly proliferating RB cells, whereas minimal cell death with the same ART concentrations (12.5-200µg/ml) was observed against normal retina cell lines. Similarly, a potent and selective cytotoxicity of DHA following 48h incubation was observed towards a panel of ovarian cancer cells with the highest inhibition observed against ovarian OVCA-439 cells (IC_{50} value of 3.83 ± 0.14µM; 14.33-folds), as compared with normal HOSE642 ovarian epithelial cells (IC_{50} value of 54.9 ± 1.67µM) (Jiao *et al.* 2007). The use of compounds without the endoperoxide bridge, such as deoxy-10-(p-fluorophenoxy)DHA demonstrated low levels of cytotoxicity against human promyelogenous leukaemic HL-60 cells (50-fold less active) and human T lymphocyte Jurkat cells (130-fold less active), as compared to its parent drug, DHA (Mercer *et al.* 2007). These observations further confirm the

importance of iron in the activation of 1,2,4-trioxanes' endoperoxide bridge and their anti-cancer effects.

1.4.3. TfR1s as an indicator of malignant phenotype

The density of TfR1s was reported to be a useful prognostic marker and an indicator of malignant phenotype in several tumours, including pancreatic and colorectal cancers (Ryschich *et al.* 2004; Prutki *et al.* 2006). In contrast to normal pancreatic tissue, the immunohistochemical analysis of specimens derived from patients with primary pancreatic cancer showed a positive expression of TfR1 (more than 80% of cells stained) in 82 % of tumour cell samples, 11% of samples had heterogenous expression (25-80% of cells positively stained) and 7% of samples were negative (staining of <5% of cells) (Ryschich *et al.* 2004). In pancreatic specimens with distant metastasis, 75% of samples showed positive expression of TfR1, 8% of samples had heterogenous TfR1 expression, whereas negative staining was observed in 17% of analysed samples (Ryschich *et al.* 2004). Additionally, the flow cytometric analysis showed that the expression of TfR1 in highly proliferating pancreatic cell lines *in vitro* was very low, and was ranging from 2% in Capan1 to 19% in KCIMOH1 pancreatic cancer cells (Ryschich *et al.* 2004). The differences arising between the observations *in vivo* and in cultured pancreatic cancer cells could be linked with the tumour local microenvironment. A high-iron supply *in vitro* does not necessitate the up-regulation of TfR1 cell surface levels (Ryschich *et al.* 2004). However, samples derived from patients during surgery could be characterised by tumour heterogeneity (Ryschich *et al.* 2004; Fisher *et al.* 2013). The heterogeneity of a tumour mass refers to the existence of subpopulations of cells within a tumour characterised by the presence of distinct genotypes and phenotypes (Fisher *et al.* 2013). This results in adaptation of

different subpopulations of cells to a fluctuating tumour microenvironment and competing for iron under limited supply (Ryschich *et al.* 2004; Fisher *et al.* 2013).

In the immunohistochemical analysis, the expression of TfR1 was positively correlated with the grandular formation (tumour grading) of colorectal carcinoma (CRC) samples derived from sixty-three patients (Prutki *et al.* 2006). Well-differentiated CRC cells (>95% of the tumour is gland forming) and CRC samples of Duke A and B grade had significantly higher levels of TfR1 expression than those with poorly-differentiated characteristics (<50% gland formation) and samples of Dukes C and D grade (Prutki *et al.* 2006; Fleming *et al.* 2012). In CRC patients with lymph node infiltration and distant metastasis, TfR1 staining was categorised as absent-weak (Prutki *et al.* 2006). A high expression of TfR1 on well-differentiated cells which were associated with decreased bowel penetration could be linked with adaptation to the local tumour microenvironment with limited supply of iron (Prutki *et al.* 2006). The presence of increased bowel well penetration, which is often characterised with higher number of blood vessels and distant metastasis in poorly-differentiated malignant samples, support the spread of cancer cells to a different microenvironment (Prutki *et al.* 2006). It is suggested by Prutki *et al.* (2006) that cancer cells within a new tumour microenvironment have increased supply of oxygen and are exposed to oxygen stress partly linked with an overload of reactive iron acting as a pro-oxidant, which result in decreased TfR1 levels on CRC samples. From the reports of Ryschich *et al.* (2004) and Prutki *et al.* (2006) it can be summarised that the density of TfR1s can be a useful prognostic marker and an indicator of malignant phenotype. The reports further provide evidence for targeting TfR1 in cancer therapy.

1.4.4. Anti-cancer effects of 1,2,4-trioxanes are associated with a decrease in TfR1 levels

There are increasing reports describing that the cytotoxicity of ART and DHA against cancer cells is mediated by inhibition of the normal function and expression of TfR1. DHA inhibited the growth of leukaemic HL-60 cells in a dose-dependent (0.25-8μmol/l) and time-dependent (12-72h) manner, which was associated with decreasing TfR1 content on cell surface, reduced mRNA and protein expression of intracellular TfR1 (Zhou *et al.* 2008). In human hepatoma HepG2 cell line, DHA (5-25μM) decreased cell-surface TfR1 levels in concentration and time-dependent manners with concomitant decreasing levels of internal plasma glycoprotein transferrin levels observed with DHA at 10 and 25μM after 24h incubation (Ba *et al.* 2012). DHA (5-25μM) for 24h caused TfR1 internalisation in HepG2 cells with similar observations when cells were treated with DHA 25μM for different times, resulting in disruption of iron uptake and in a cell death due to overall inhibition of iron endocytosis needed by cancer cells to proliferate (Ba *et al.* 2012). The pretreatment of breast cancer MCF7 cells for 30mins with 20mM NAC, an antioxidant which was used to mimic the inhibition of DHA-mediated ROS production at 20μM after 24h incubation in the cells, showed that DHA disturbed intracellular iron homeostasis possibly through an alternative mechanism independent of oxidation damage (Ba *et al.* 2012). In similar investigations, Zhao *et al.* (2013) showed increased ART internalisation in RB cells upon treating the cells with increasing ART concentrations (15-40μg/ml) for 24h, which was partly linked with the decreased expression of the membrane TfR1. The findings indicate that ART is transported into the cell through an endocytic pathway together with its receptor CD71. The hypothesis arising from these reports could be that 1,2,4-trioxanes after activation by iron released from TfR1-transferrin complex within the cell inhibit recycling of apotransferrin-receptor

complex to the cell surface. Thus, only TfR1 which were not earlier activated by 1,2,4-trioxanes facilitate agents transport onto cells, and these TfR1 once within the cells are not used again. The proposed effects of 1,2,4-trioxanes on TfR1-transferrin complex upon activation by iron is presented in figure 1.

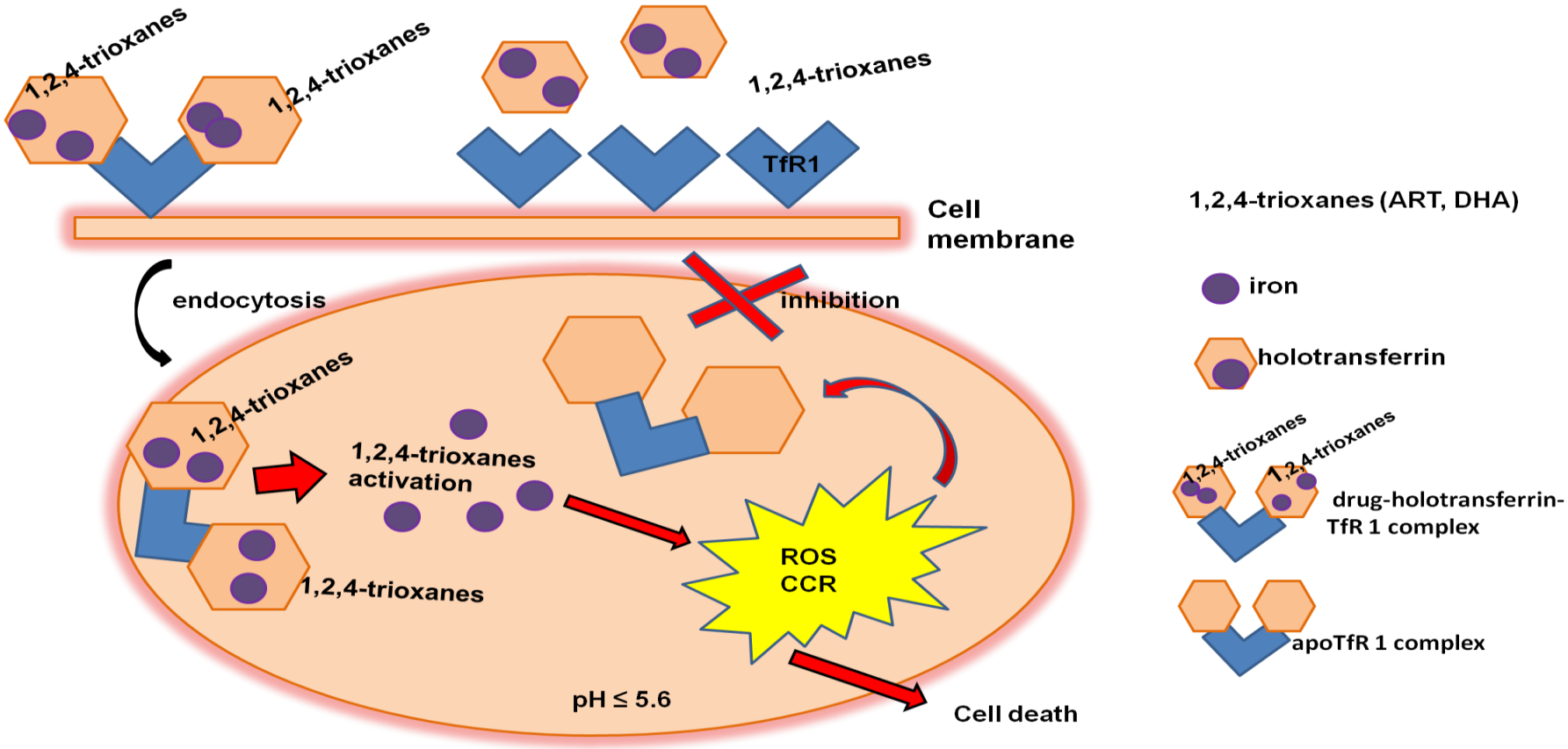

Figure 1: The proposed mechanism of the iron-mediated activation of ART and DHA within cancer cells. Iron loaded transferrin (holotransferrin) with 1,2,4-trioxanes (ART, DHA) binds cell surface TfR1. Holotransferrin-TfR1-drug complex is internalised into the cell through endocytosis. Within an endosome, a low 5.6pH facilitate the release of iron and drug from the complex. Iron catalyses the cleavage of 1,2,4-trioxanes' endoperoxide bridge resulting in the generation of free radicals which contribute to the inhibition of recycling of apotransferrin (iron-free transferrin)-receptor complex to the cell surface.

1.4.5. Enhanced delivery of 1,2,4-trioxanes into cancer cells through TfR1

The iron-binding ability of TfR1 has been used to enhance the delivery of 1,2,4-trioxanes into malignant cells since they require iron for their activation (figure 1). Artemisinin covalently attached to iron-carrying transferrin was transported onto human leukaemia Molt-4 cancer cells through endocytosis where released iron from transferrin package activated artemisinin and resulted in a more potent and selective killing of cancer cells, as compared to artemisinin alone (Lai *et al.* 2005). The pre-treatment of Molt-4 cells with 12µM holotransferrin (i.e., iron loaded transferrin) for 1h resulted in enhanced cytotoxicity of DHA (200µM) by ~10-fold, as compared to DHA alone after 8h incubation (Singh and Lai 2004). Enhanced killing of cancer cells was reported also with synthesized covalent conjugates of artemisinin and a transferrin-receptor targeting peptide (Oh *et al.* 2009). Iron (II) glycine sulphate (Ferrosanol®, 10µg/ml) increased the cytotoxicity of ART, artemisinin and ART-maltosyl-β-cyclodextrin (a compound with the endoperoxide bridge) in the dose range 0.001 to 30µg/ml against human CCRF-CEM leukaemia and human astrocytoma U373 cells following 7 days treatment (Efferth *et al.* 2004). Similar studies in a panel of 36 cell lines showed that Ferrosanol® (10µg/ml) increased the cytotoxicity of ART in most of cell lines, including colon HT-29 cells (23.91% enhancement; ART IC_{50} value of 1.38µM vs. ART+Ferrosanol IC_{50} value of 1.06µM), whereas some cell lines, including breast cancer MCF7 cells showed decreased efficacy to ART when co-treated with Ferrosanol® (10µg/ml) (17.66-fold inhibition; ART IC_{50} value of 1.68µM vs. ART+Ferrosanol IC_{50} value of 29.67µM) (Kelter *et al.* 2007). The cytotoxicity of 1,2,4-trioxanes have been shown to be further increased by the addition of free ferrous haeme (Fe^{2+} protoporphyrin-IX) (Efferth *et al.* 2004; Zhang and Gerhard 2008; Zhang and Gerhard 2009). However, there are conflicting reports on the

activation of artemisinin by haemin (ferric haeme; Fe^{3+} protoporphyrin-IX) (Haynes and Vonwiller 1995; Zhang and Gerhard 2008; Zhang and Gerhard 2009). For example, Zhang and Gerhard (2008) using spectrophotometry to measure the absorption spectra have shown that haemin (20µM) has not enhanced the activity of artemisinin, whereas haeme (20µM) more effectively potentiated the inhibitory effect of artemisinin. In contrast, the concentration of haemin at 2µM which had no significant inhibitory effect on neurite outgrowth alone, has shown to enhance effectively the inhibition of neurite outgrowth in the neuroblastoma cell line NB2a when co-administrated with DHA and artemether, as compared to single drugs treatments (at 100, 200 and 300nM) (Smith *et al.* 1997). There was no effect on neurite outgrowth when haemin (2µM) was co-administrated with desoxyarteether (at 100, 200 and 300nM), a compound without the endoperoxide bridge (Smith *et al.* 1997). The observations of Smith *et al.* (1997) indicate that haemin is involved in 1,2,4-trioxanes activation and their enhanced neurotoxicity. However, the differences arising between the effects of Ferrosanol® in combination with ART against various cancer cell lines and conflicting effects of haemin in drugs-mediated activity in different experimental settings show the need of testing these mediators further *in vitro* and *in vivo* before use in clinical therapy.

Further evidence that iron is central to the cytotoxicity of 1,2,4-trioxanes stemmed from the observation that chelation of cellular iron using deferoxamine (20µM and 100µM) antagonised the cytotoxic activity of DHA (0.50µM and 0.80µM, respectively) in HL-60 cells after 24h incubation through inhibition of caspase-3 dependent apoptosis (Lu *et al.* 2008; Zhao *et al.* 2015).

1.5. Colorectal carcinoma and inflammation

Drug regimens with mode of action targeting multiple aspects of cancer development are needed for CRC. This is important because despite of considerable decrease in overall mortality rates in the last decade due to improvements in CRC therapy regimens, CRC still remains the third commonest malignancy worldwide. It is responsible for 9.67% of all new cancer cases and caused 694 000 deaths in 2012, with nearly 317 525 new cases estimated to be diagnosed by 2020 (Ferlay *et al.* 2016).

The same as other cancers, CRC is a multistage genetic and epigenetic disease arising from a single replication-competent cell (stem cell or proliferative progenitor cell) (Greenhough *et al.* 2009). CRC is characterised by dysregulation of the normal mechanisms controlling cell survival, proliferation, migration, invasion and the cell-cell interactions (Greenhough *et al.* 2009). These distinct characteristics developed by cancer cells have been linked to the inflammatory response, with the first inflammation-cancer connection reported in 1863 by German pathologist Rudolf Virchow and was observed as the presence of leukocytes within tumours (Heidland *et al.* 2006). The inflammatory response is sub-divived into acute inflammation that leads to therapeutic recovery or chronic inflammation, which is a predisposing factor for the development of pro-cancerous dysplastic lesions and promoting cancer progression (Nesaretnam and Meganathan 2011; Cooks *et al.* 2013). The presence of inflammatory cells witin injured intenstinal cells initiate cancer development through promoting complex interactions between cytokines, chemokines, growth factors, reactive nitrogen intermediates (RNI) and ROS (Grivennikov *et al.* 2010; Qiao and Li 2014). RNI and ROS are capable of inducing oxidative stress, which

causes DNA mutations and genomic instability (Nishikawa *et al.* 2005; Grivennikov *et al.* 2010).

In CRC mucosa samples derived from patients with ulcerative colitis (UC) there was a higher incidence of the mutation of mitochondrial DNA elicited by chronic inflammation and oxidative stress than that from control samples (Nishikawa *et al.* 2005). The results indicate the strong relationship between chronic inflammation and precancerous status in UC patients (Nishikawa *et al.* 2005). In addition, as presented in table 1, chronic inflammation associated with infection is extensively reported as a predisposing factor to many cancers, including CRC in patients suffering inflammatory bowel diseases (IBDs), such as UC, Crohn's disease and chronic subclinical bowel inflammation in obese people (Dambacher *et al.* 2007; John *et al.* 2007; Waldner *et al.* 2010).

1.5.1. Molecular mechanisms governing the development of inflammation-associated CRC

Chronic inflammation in the intestine can be promoted by intrinsic factors (host mutations), which include accumulation of mutations in specific genes, including tumour suppressor p53, Kirsten-ras (K-ras), adenomatous polyposis coli (APC) and NOD-like receptor protein Nlp3 (Xie and Itzkowitz 2007; Zaki *et al.* 2010; Cooks *et al.* 2013). There are many environmental factors which promote chronic inflammation within the gut, such as viral or bacterial infections, obesity and dietary products (Gunter and Leitzmann 2006; Bonnett *et al.* 2013; Li. *et al.* 2015). The inflammatory process is driven by growth factors, cytokines and chemokines, which are secreted by immune cells recruited to the local microenvironment, or can be secreted by the tumour cells themselves (Grivennikov *et al.* 2010; Qiao and Li 2014). The proinflammatory cytokine IL-31, which is primary expressed in activated lymphocytes, increased the expression of cytokine IL-8 in CRC derived intestinal epithelial cell (IEC) lines (Dambacher *et al.* 2007). The IL-31 cytokine in IEC lines activated a network of signaling mediatos, including extracellular signal-regulated kinase (ERK)-1/2, serine-threonine protein kinase (Akt), the signal transducers and activators of transcription (STAT) 1/3), which resulted in enhanced migration of the cells (Dambacher *et al.* 2007). Later work by Cooks *et al.* (2013) showed that mutant p53 prolonged the activation of a key regulator of inflammation and a modulator of inflammation-associated cancer, nuclear factor (NF)-κβ which was induced by pro-inflammatory cytokine tumour necrosis factor (TNF)-α in cultured cells and intestinal organoid cultures. A germline p53 mutation in mice was responsible for the development of severe chronic inflammation and persistent tissue damage (Cooks *et al.* 2013).

It is documented that augumented activation of NF-κβ, STAT-1/3 and mitogen-activated protein kinase (MAPK) transcriptional modulators create a network interaction that enhance the synthesis and secretion of pro-inflammatory cytokines, which all together promote CRC through the growth of adenomatous polyps (non-malignant disease) in sporadic carcinoma, or by dysplasia sequence in colitis and IBD (Dambacher *et al.* 2007; Xie and Itzkowitz 2007; Harpaz and Polydorides 2010; Zaki *et al.* 2010; Cooks *et al.* 2013; Rokavec *et al.* 2014). Cytokines, such as IL-6, IL-8, IL-18, IL-31 and TNF-α have been extensively reported to increase ulceration, and hyperplasia in inflammed colon (Dambacher *et al.* 2007; Harpaz and Polydorides 2010; Wang *et al.* 2013). Over-expressed cytokine levels are reported in CRC tissue samples and further contribute to cancer progression throuth a negative loop system enhancing and activating other factors (Dambacher *et al.* 2007; Szkaradkiewicz *et al.* 2009; Harpaz and Polydorides 2010; Wang *et al.* 2013). These include up-regulation of pro-angiogenic vascular endothelial growth factor (VEGF) and pro-invasive and pro-matastatic matrix metalloproteinases (MMP), dysregulation of cell-cell adhesion molecules, including E-cadherin, activation of pro-survival PI3K/AKT (phosphoinosine 3-kinase/serine-threonine protein kinase) pathway, thus contributing to CRC tumour progression, invasion, angiogenesis and metastasis (Waldner *et al.* 2010; Zaki *et al.* 2010; Cooks *et al.* 2013; Wang *et al.* 2013; Rokavec *et al.* 2014). Mechanisms promoting carcinogenesis in CRC are reported to be complex with not completely defined first trigger leading to disease. Recent study of Li. *et al.* 2015 confirms complexity of CRC development by introducing Human Papillomavirus (HPV) as important high-risk infection in CRC patients (reported in 46 out of 95 CRC patients; 48.4%). HPV infection in CRC tissues strongly correlated with poorer clinical stages (III and IV) of cancer and higher Stat3 activities ($P<0.01$)

and IL-17 levels (P<0.01), as compared to adjacent healthy tissues, which together may promote accumulation of other tumour-promoting downstream cytokines and activate other signaling mediators within gut microenvironment (Li *et al.* 2015).

1.5.2. Importance of cytokine IL-6 in CRC

Especially, a multifunctional pro-tumourigenic IL-6 cytokine is extensively reported to have a broad range of biological functions, including in CRC tumour cell proliferation, survival, invasiveness and metastasis of cancer through various mediators, such as the oncogenic STAT-3 transcription factor activation (Grivennkov *et al.* 2009; Nagasaki *et al.* 2014; Rokavec *et al.* 2014). In a study of Sasaki *et al.* (2012) of 118 male individuals with colorectal adenoma, serum IL-6 concentrations in samples of venous blood were significantly (1.24 vs. 1.04 pg/mL, p=0.01) higher as compared to samples from 218 age-matched control patients. Uchiyama *et al.* (2012) documented higher levels of IL-6 in sporadic CRC patients and an increased expression of IL-6 in CRC tissues, as compared with the levels in a control group and in patients with adenoma. Uchiyama *et al.* (2012) suggest that IL-6 promotes JAK/STAT signaling through the phosphorylation of membrane-associated gp130 subunit in sporadic CRC, but not in adenoma or normal colorectal tissues. In addition, higher levels of IL-6 in patients might be mediated through increased expressions of chemokine CXCL7 and its receptor CXCR2 (Uchiyama *et al.* 2012). Lu *et al.* (2015) reported that elevated concentrations of IL-6 (p=0.002) and IL-8 (p=0.038) in CRC patients when compared to healthy volunteers correlated with a higher risk of recurrence. Gene expression of members of Toll-like receptors (TLRs) family including TLR-1, TLR2, TLR4 and TLR8 (mediators of innate and adaptive immune responses) were reported to induce the release of IL-6 and IL-8 mRNA levels and detection of these levels can be used as a marker in CRC (Lu *et al.* 2015). Groblewska *et al.* (2008)

reported a high-level of IL-6 serum concentrations in CRC patients, as compared to samples from adenoma and healthy patients, which contributed to suggestion of the usefulness of IL-6 in the diagnosis of CRC.

1.5.3. Inflammation promotes carcinogenesis through high TfR1 in cells

The mucosal TfR1 expression was increased in samples from patients with IBD and in the colonic epithelium of rats induced with experimental colitis, as compared to normal colonic mucosa (Harel *et al.* 2011). The study of Harel *et al.* (2011) showed also that TfR1 expression in the normal colonic mucosa had basolateral localisation, wherase the samples derived from IBD patients had apical TfR1 expression. These observations indicate that chronic inflammation might not only increase the expression of TfR1 but also changes its localisation. The pretreatment of human colorectal Caco-2 cells with a pro-inflammatory cytokine TNF-α increased the iron uptake by the cells, suggesting the role of TNF-α in increasing the expression of TfR1 on cell surface (Harel *et al.* 2011). Similar observations were reported earlier by Han *et al.* (2010) where incubation of Caco-2 cells with a mixture of cytokines (TNF-α, IL-1β and IL-6) increased transferrin-iron absorption by 70%. The observations indicate that pro-inflammatory cytokines are capable of modulating iron metabolism in gut epithelial cells and might contribute to CRC progression, through increasing iron up-take by cells and possibly increasing TfR1 expression. There are several reports describing that the cytotoxicity of ART and DHA against cancer cells is mediated by inhibition of the normal function and expression of TfR1 (Zhou *et al.* 2008; Ba *et al.* 2012). Therefore, the involvement of TfR1 in the activity of ART and DHA is not limited only to drug transport. ART and DHA by selective decresing TfR1 levels might inhibit the intiation and progression of CRC.

1.6. Leukaemia and inflammation

Leukaemia, the most common white blood cell malignancy is the 11th leading cause of cancer-related deaths globally, accounting for 2.5% of all new cancer cases and 265 461 deaths in 2012 (Ferlay *et al.* 2016). More commonly leukaemia is reported as secondary cancer after treatment for metastatic colorectal or breast cancer (Shapiro *et al.* 2007; Valentini *et al.* 2011). The highest proportion of adult leukaemia dignosed clinically constitute acute leukaemia, which is sub-classified into two main types: acute lymphoblastic leukaemia (ALL) and acute myeloid leukaemia (AML) (Meenaghan *et al.* 2012). Acute leukaemia is a clonal malignancy of haematopoietic stem cells maturation failure, leading to accumulation of immature cells in the bone marrow, referred as blasts, which prevent the normal production of healthy red cells, white cells and platelets (Meenaghan *et al.* 2012). Acute promyelocytic leukaemia (APL), constitutes around 10-15% of all AML and is characterised by the translocation between chromosomes 15 and 17 and promyelocytic leukaemia (PML)-retinoic acid receptor (RAR)-α fusion transcript (de Botton *et al.* 2006; Mohamed *et al.* 2013). Other features include increase in abnormal promyelocytes, large blasts, pancytopenia and coagulopathy which can lead to serious bleeding manifestations, including fatal intracranial haemorrhage (Mohamed *et al.* 2013). At early APL diagnosis and treatment with standard regimen of all-trans retinoic acid (ATRA) combined with anthracycline or other chemotherapeutic agens, including idarubicin there is a high cure rate of ~90% (Tsimberidou *et al.* 2004; Mohamed *et al.* 2013). However, higher mortality is observed in refractory (chemo-resistant) and in relapsed APL patients who constitute up to ~23% of cases (de Botton *et al.* 2006; Gallagher *et al.* 2012; Zhu *et al.* 2014). High-relapse incidence of bone marrow (BM) and extramedullary disease involving the central nervous system, leukaemia cutis and

retinoic acid syndrome indicates of urgent need for more effective and safer chemotherapeutic agents for APL treatment, which provide improvements of long-term outcomes (Chang *et al.* 1999; de Botton *et al.* 2006).

1.6.1. Molecular mechanisms promoting the development of inflammation-associated leukaemia

A functional link between inflammation and cancer development in solid tumours, especially CRC is broadly investigated and reported (Zaki *et al.* 2010; Cooks *et al.* 2013; Rokavec *et al.* 2014). However, the role of different molecular pathways and mediators governing the development of leukaemia in relation with inflammation has scarcely been documented. In human chronic myelocytic leukaemia (CML) K562 cells, the numbers of TfR1 increased when the cells were incubated with TNF-α for 24h (Nezu *et al.* 1994). A high expression of TfR1 was concomitant with increased cell proliferation (higher G2/M phase ratio), thus suggesting a key role of inflammation in leukaemogenesis (Nezu *et al.* 1994). Once initiated, leukaemia progression implicates new factors, including the activation of NF-κβ, which is a critical survival factor of B-cell chronic lymphocytic leukaemia (B-CLL) cells (Ringshausen *et al.* 2004). Additional factors, such as the activation of MAPK p38, STAT-3/5 and ERK 1/2 pathways and their down-stream proteins, including high levels of angiogenic factors VEGF-α and MMP-9 (92-kDa gelatinase) have been reported to promote leukaemia progression (Kolonics *et al.* 2001; Ringshausen *et al.* 2004; Ueda *et al.* 2005). Frequent methylation of SHP1, a negative regulator of Jak/STAT signaling pathway was also shown to be important in AML pathogenesis (Chim *et al.* 2004). In adult T-cell leukaemia, cytokine IL-21 activated phosphorylation of STAT -3 and -5, thus contributing to leukaemia progression (Ueda *et al.* 2005). Uncontrolled and rapid growth of leukaemia cells results in

hypoxic microenvironment within blast cells. A key regulator of hypoxia, hypoxia inducible factor-(HIF)-α was shown to enhance aggressiveness of leukaemia by over-expressing TfR1 on cell surface through binding to iron-responsive elements in the 3'-untranslated region of TfR1 (Lok and Ponka 1999). Interestingly, investigations of Luger and colleagues in 1989 on cultured human peripheral blood mononuclear cells (PBMCs) showed for the first time potential positive role of IL-6 in destroying of malignant cells, through IL-6-mediated enhancement of the cytolytic activity of CD3-natural killer (CD3-NK) cells via IL-2 production. Enhanced NK cell activity was further reported by Ress *et al.* (1990) in a patient during the course of 13-year disease-free survival after therapy for acute non-lymphoblastic leukaemia and with concurrent tuberculosis. Ress *et al.* (1990) suggested that chronic inflammation caused by tuberculosis may have augumented the cytotoxicity of NK cells, thus changed clinical and haematological course of malignancy and resulted in a prolonged survival. From combined results of Luger *et al.* (1989) and Ress *et al.* (1990) it can be hypothesized that IL-6 over-production triggered by stimuli, such as some chronic infections (e.g. tuberculosis) or acute inflammation from cytotoxic agents (e.g. anti-cancer drugs) may lead to spontaneous cytolytic activity of NK cells against tumour cells, resulting in a better therapeutic outcome. With conflicting differences in IL-6 functions observed in CRC and leukaemia, it is crucial to undertake subsequent research studies investigating the anti-cancer effects of cytotoxic agents, including 1,2,4-trioxanes on IL-6 expression and their possible implications for cancer treatment.

1.7. Inflammation as an anti-cancer therapeutic opportunity: use of NSAIDs

With increasing evidence of inflammation being associated with carcinogenesis, the most known anti-inflammatory drugs, NSAIDs (non-steroidal anti-inflammatory drugs) are more commonly investigated for their anti-cancer effects. The first suggestions that NSAIDs might have beneficial therapeutic implications in cancer were developed in the 1970s when Jaffe (1974) and Bennett *et al.* (1977) showed that human colon cancer cells in tissue culture had often more prostaglandins (PGs) E_2 than in the surrounding non-tumourigenic mucosa. Recent studies have shown that an NSAID and a selective cyclooxygenase (COX)-2 inhibitor, celecoxib (400mg twice daily for 7 days) in patients with hereditary colon cancer syndrome, familial adenomatous polyposis (FAP), effectively reduced tumour progression (Dovizio *et al.* 2012). The administration of celecoxib in FAP patients resulted in PGE_2 suppression via COX-2 inhibition, thus further confirming inflammation-colon cancer association (Dovizio *et al.* 2012). One of the most used NSAIDs, aspirin (acetylsalicylic acid; ASA) being used traditionally as an analgesic, antipyretic and anti-inflammatory agent has been showed to significantly suppress CRC mucosal PGE_2 at daily doses of 40.5, 81, 162, 324 or 648mg for 14 days (Ruffin *et al.* 1997). The measured lowest effective doses of ASA causing colorectal mucosal PGE_2 suppression were 81mg and 40.5mg, respectively and daily dose of 81mg ASA was recommended to be used as a chemo-preventative (reducing the development of cancer) (Ruffin *et al.* 1997). In clinical studies, long-term use of ASA and other NSAIDs showed that the reduced risk of tumour formation is not limited only to CRC (Martinez *et al.* 1995; Din *et al.* 2010). Similar chemo-preventative effects of ASA and other NSAIDs were observed in variety of other cancers including breast (Johnson *et al.* 2002), oesophageal (Farrow *et al.* 1998), lung (Moysich *et al.*

2002) and ovarian (Moysich *et al.* 2001). A population-based case-control study on the chemo-preventative effects of ASA indicated that doses as low as 75mg/day (>4 tablets/week) effectively decreased the risk of CRC after only 1 year, and that these benefits increased with the duration of ASA use (Din *et al.* 2010). In addition, ASA (80mg/day and 30mg/day in 95% and 5% of patients, respectively) in initiated or continued use after colon cancer diagnosis in patients (chosen between 1998 and 2007) was associated with decreased mortality (survival gain with adjusted rate ratio (RR) 0.65; P=0.001), but ASA regimen was not associated with increased survival in rectal patients (adjusted RR 1.10; P=0.6) (Bastiaannet *et al.* 2012). Encouragingly, a few studies indicate a chemo-preventative activity of ASA in haematologic cancer, an adult leukaemia. In epidemiological study of Kasum *et al.* (2003) in over 28,000 postmenopausal woman (55-69 years of age) during the 8-year follow-up period, it was reported that multivariate-adjusted RR of leukaemia was decreased to 0.45 (95% confidence interval; 0.27-0.75) for woman using ASA two or more times per week (doses not stated) when compared to nonusers. Similar inverse associations were observed for AML (RR of 0.30, 95% confidence interval = 0.11-0.84; P=0.02) and CLL (RR of 0.38, 95% confidence interval = 0.18-0.81; P=0.009) when sub-categorised from main leukaemia (Kasum *et al.* 2003). In contrast, woman being reported to use non-aspirin NSAIDs (ibuprofen, naproxen, sulindac and piroxicam) for at least two times a week were 1.31 times (95% confidence interval: 0.77-2.22) as likely to develop leukaemia as those being non-users, but these differences were not significant (Kasum *et al.* 2003). These arising differences between ASA and other NSAIDs in their effectiveness in cancer prevention were reported further in other studies. Weiss *et al.* (2006) showed that ASA led to a modest decrease in adult acute leukaemia risk (adjusted odd ration 0.84; 95%CI, 0.59-1.21; 169 cases, 676

controls), whereas users of acetaminophen, also known as paracetamol were 1.53 times (95%CI, 1.03-2.26) as likely to develop leukaemia as nonusers. Acetaminophen has an ability to decrease transiently DNA repair, and because lymphocytes may be more likely to undergo DNA damage, patients taking acetaminophen may have increased risk of acute leukaemia (Weiss *et al.* 2006). A population-base case-control study (420 AML, 186 CML and 701 controls aged 20-79) performed by Ross *et al.* (2011) showed that ASA (325mg) was associated with a decreased risk of myeloid leukaemia in woman (odd ratio-(OR)=0.59, 95%=0.37-0.93; 14% patients) but not man (OR=0.85, 95Cl=0.58-1.24; 21% patients). These differences were more prominent with increased ASA tablets per week (<7 for women OR=0.56, 95%=0.26-1.20; 4% patients, man OR=0.73, 95%=0.37-1.46; 4% patients; and ≥7 for women OR=0.60, 95%=0.35-1.02; 10% patients, man OR=0.89, 95%=0.58-1.36; 16% patients) and duration of ASA use (<10 years and >10 years). Similarly to Weiss *et al.* 2006 results, Ross *et al.* (2011) demonstrated that acetaminophen was related with increased risk of myeloid leukaemia but this relation was observed only for women (OR=1.60, 95%=1.04-2.47; 23% patients) and was significantly higher with number of tablets (≥7 equal to OR=2.37, 95%=1.34-4.18; P=0.003 vs. <7 tablets/week). These studies show benefits of ASA chemo-preventive therapy over other NSAIDs agents in CRC and leukaemia cancers. At the same time, however, the same studies show the importance to study further molecular mechanisms of NSAIDs actions due to extensive reports of severe adverse effects in patients undertaking ASA therapy. For example, low-dose prophylactic ASA regimens for cardiovascular disease of 75mg-300mg daily for at least a month were reported to be associated with a dose-dependent increased risk (compared with controls: 75mg with OR: 2.3; 150mg, with OR; 3.2; and 300mg with

OR: 3.9) of severe side-effects, such as gastrointestinal bleeding from peptic ulcer (Weil *et al.* 1995). More currently, García Rodríguez *et al.* (2011) showed that ASA low-dose (75 to 325mg/day) in patients within 40 to 84 years of age resulted in an almost 2-fold increase in the risk of upper gastrointenstinal bleeding when compared with nonuse. This bleeding risk was observed to be similar across duration of time studied (>1year and for ≤1 year) and higher with concurrent use of clopidogrel and some other medications being known to increase gastrointestinal bleeding (García Rodríguez *et al.* 2011). Therefore, despite widely reported benefits of low-dose ASA use in cancer prevention, the toxicity observed within gastrointestinal tract limit ASA high-dose regimen for cancer treatment. These reports also provide a rationale to combine ASA with current chemo-therapeutic agents to improve their therapeutic effectiveness and decrease side effects for the treatment of human cancers.

1.8. Molecular mechanisms of ASA anti-cancer effects

1.8.1. COX-1 and COX-2 enzymes

The mechanism of action responsible for the effects of ASA on cancer cells is associated with its ability to non-specifically suppress the COX enzymes (COX-1 and -2, known as prostaglandin endoperoxide synthase (Dovizio *et al.* 2012; Rahman *et al.* 2012). These COX enzymes are membrane-bound haemo- and glycol-proteins with a molecular weight of 72kDa which catalyze the conversion of arachidonic acid (a 20-carbon, 4-double bond fatty acid) to prostanoids (Vane and Botting 2003). COX-1 is expressed constitutively in many normal tissues and mediates the release of thromboxanes (TXs) and PGs, which are mainly involved in platelet aggregation (TXA_2) (Patrono 2015), gastric cytoprotection (PGE_2) (Takeuchi *et al*. 2001) and ASA induced gastrointestinal bleedings (TXA_2) (Patrono 2015). Additionally, increasing

experimental studies indicate a key role of COX-1 in carcinogenesis (Rossiello *et al.* 2007; Dovizio *et al.* 2012; Yang *et al.* 2014). In contrast, COX-2 is found in greatest amounts in the human kidney and spinal cord and induces the release of PGs (e.g. PGE_2 and PGI_2) and TXA_2 involved in inflammatory, cell proliferation and angiogenesis processes correlated with the development of cancer (Pai *et al.* 2003; Holla *et al.* 2005; Holla *et al.* 2006; Kim *et al.* 2011; Dovizio *et al.* 2012; Yang *et al.* 2014). COX-2-dependent inhibition of its primary metabolite, PGE_2 has been reported to reduce tumour progression in patients with FAP and inhibit the invasiveness of colon cancer cells (Pai *et al.* 2003; Dovizio *et al.* 2012). COX-2 is over-expressed in various cancer cell lines, mainly CRC, breast, endometrial, ovarian, bladder, pancreatic and Kaposi's sarcoma (Johnson *et al.* 2002; Din *et al.* 2004; Banović *et al.* 2005; Rossiello *et al.* 2007; Dhawan *et al.* 2010; Rahman *et al.* 2012). Most prominently, higher basal levels of COX-2 gene expression were observed in CRC, including cells being chemo-resistant to 5-fluorouracil (5-FU) and irinotecan, as compared with their respective sensitive cells, which clinically was linked with a 68% enhanced risk of mortality (Rahman *et al.* 2012; Roelofs *et al.* 2014). The pre-treatment of sensitive and chemo-resistant MIP101 and RKO colorectal cell lines *in vitro* with 1.8mM ASA or 30μM celecoxib (selective COX-2 inhibitor) for 48h followed by addition of 5-FU (5 μM) for additional 24h resulted in greater inhibition of cell growth, as compared to 5-FU alone (Rahman *et al*. 2012). Those reports show that the more potent inhibitory effects of 5-FU when co-treated with ASA against cancer cells might indicate the possibility to use of ASA in cancer therapy in combination with other currently used chemo-therapeutic agents to enhance their anti-cancer effects. The observations can be further supported by the fact that the use of ASA (25mg/kg) in children suffering from autoimmune diseases

resulted in average serum concentrations of 5.2mM, ranging from 0.38 to 10.26mM ASA (Juárez Olguin *et al.* 2004). At this therapeutic dose, ASA reached safely systemic levels in patients with a concentration as high as 10.26mM (Juárez Olguin *et al.* 2004).

1.8.2. Molecular targets of ASA in cancer cells

Growing reports from *in vitro* and *in vivo* studies indicate that ASA mediated anti-cancer effects are not limited only to COX-2 inhibition and involve other targets (see figure 2). ASA has been reported to inhibit cell growth and induce apoptosis in several cancer cell lines, namely CRC, leukaemic, prostate and oral squamous carcinoma cells (Bellosillo *et al.* 1998; Din *et al*. 2004; Yoo and Lee 2007; Iglesias-Serret *et al.* 2010; Xiang *et al.* 2010; Park *et al.* 2010; Im and Jang 2012; Pathi *et al.* 2012). ASA at different concentrations (2.5-10mM) inhibited the growth of four cell lines of CRC (SW480, RKO, HT-29 and HCT116 cell lines) over a period of 3 days with IC_{50} values ranging from 2.5 to 5mM, which are within the range of clinically safe ASA serum levels (Juárez Olguin *et al.* 2004; Pathi *et al.* 2012). These inhibitory effects of ASA were accompanied by the inhibition of pro-survival survivin, anti-apoptotic Bcl-2 and induction of pro-apoptotic Poly(ADP-ribose) polymerase (PARP) proteins cleavage in all four cell lines (Pathi *et al.* 2012). The authors further reported that following 48h incubation, ASA (0-10mM) induced the production of multiple caspases (-3.-7,-8, and -9) in colorectal RKO and SW480 cells (Pathi *et al.* 2012). Similarly, after 24h incubation with ASA (0-10mM), the IC_{50} values for a panel of human CRC cells (HRT-18, SW480, HT-29, DLD-1, LoVo and HCT116) were ranging from 1.48 to 3.12mM ASA (mean 2.38mM ASA) (Din *et al.* 2004). These inhibitory effects of ASA against a panel of CRC cell lines were accompanied by the

induction of apoptosis, which was dependent on IκBα degradation and NF-κB nuclear translocation (Din *et al.* 2004).

In addition, the cytotoxic effects of ASA were reported to differ between CRC and other cancer types (breast, endometrial and ovarian) and were most likely to be linked with molecular mechanisms other than apoptosis dependent (Din *et al.* 2004). More recent study has shown that ASA (0.25-1mmol/L) following 48h incubation inhibited the growth of human ovarian cancer OVCAR-3 cells, which was COX-1-dependent and correlated with blocking Epidermal Growth Factor (EGF)-activated the phosphorylation levels of Akt and Erk (Cho *et al.* 2013). Other mechanisms contributing to ASA (0-10mM) cytotoxicty against colorectal cells were attributed to the inhibition of Sp transcriptional factors (Sp 1, Sp 3 and Sp 4) and their downstream molecules, including pro-angiogenic VEGF-α and its receptor, pro-inflammatory NFκB-p50, NFκB-p65 and pro-invasive β-catenin, which is down-stream product of Wnt (wingless-type MMTV integration site family) signaling pathway (Pathi *et al.* 2012). Such multifaceted activities of ASA towards cancer cells which are attributed to targeting many distinct molecular molecules, makes ASA an attractive therapeutic agent for numerous cancers, including CRC and leukaemia. These reports provide a rationale to combine ASA with current chemotherapeutic agents to improve their therapeutic effectiveness and decrease side effects.

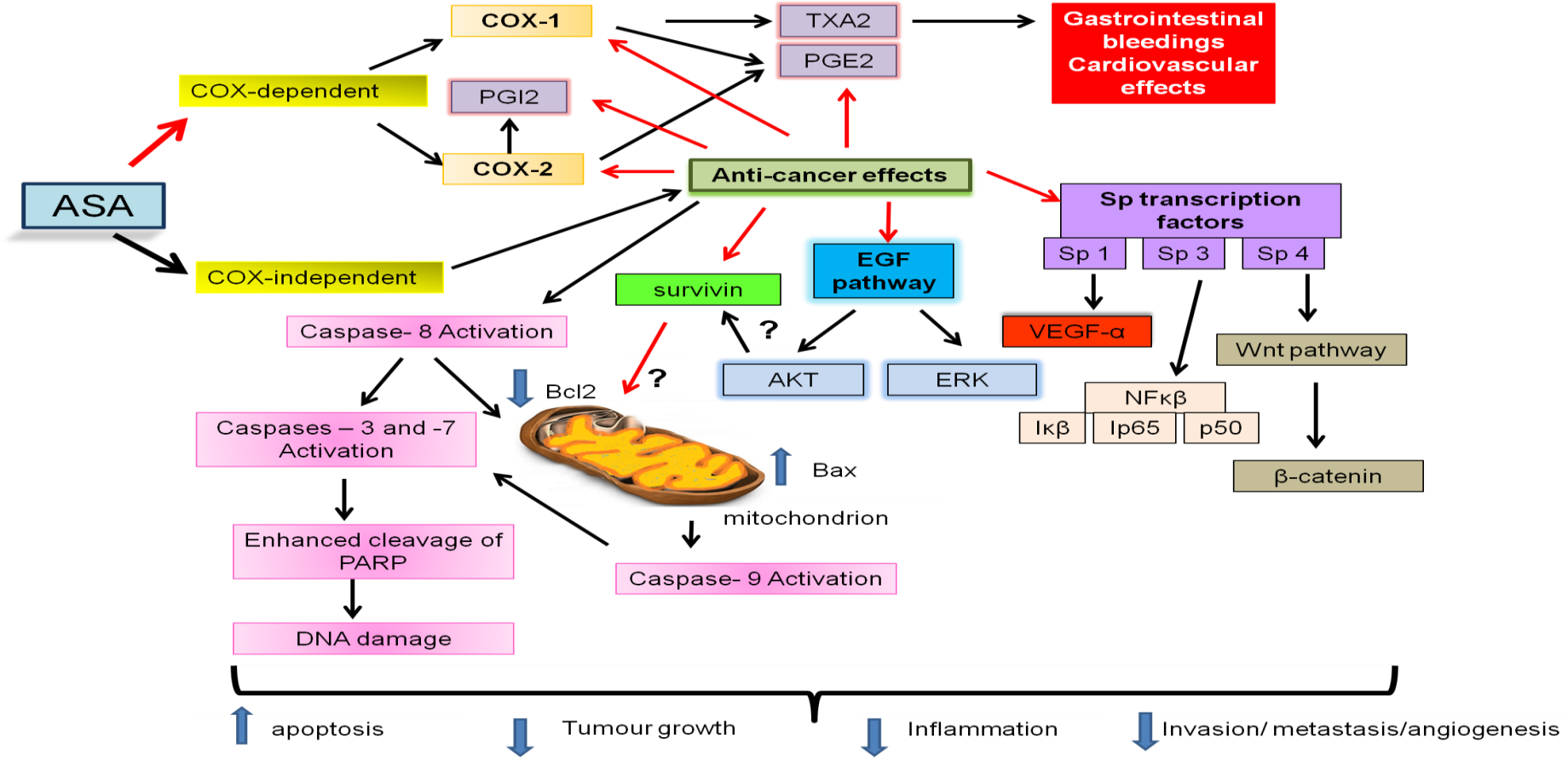

Figure 2: COX- dependent and independent mechanisms of action of ASA in cancer cells. ASA is able to induce caspase-dependent tumour cell death (apoptosis) by inhibiting the expression of key transcription factors, including Sp transcription factor, Wnt pathway, EGF pathway and NFκB pathway and its main down-stream mediators such as Akt, Erk, VEGF-α, survivin and increasing Bcl2/Bax ration in a way dependent and independent of inhibition of COX enzymes. Caspases (-3, -7, -8, -9) induced apoptosis lead to inhibition of proliferation and growth of cancer cells, suppressed inflammation, invasion, angiogenesis and inhibit the spread to distinct organs by decreasing cell metastasis. Red arrows indicate inhibition while black induction. The suggested mechanism of survivin impact on the inhibition of apoptosis is marked with '?' symbol.

1.8.3. ASA in combination with other therapeutic compounds shows increased activity against cancer cells

Due to the anti-inflammatory properties of ASA and its ability to inhibit cancer cell growth and induce apoptosis, ASA has become an attractive agent to invastigate in combination with currently used chemo-therapeutic agents. ASA increased the cytotoxic effects of many anti-cancer agents, such as reversine, doxorubicin, cisplatin and valproic acid in several cancer cell lines, including gastric SGC7901 cells, hepatoma (HepG2 and SMMC-7721) cells, cervical (HeLa, U14, Siha, Caski and C33A) cells and T cell lymphoma (Kumar and Singh 2012; Li *et al.* 2013, Qin *et al.* 2013; Dong *et al.* 2014). [a]Yan and co-workers (2010) reported that ASA when co-administered in combination with troglitazone (oral anti-type II diabetes drug with anti-cancer properties) resulted in a marked synergistic effect in growth inhibition and apoptosis (programmed cell death) induction of lung cancer CL1-0 and A549 cells. In human hepatoma HepG2 cells, ASA (5µmol/ml) when co-administrated with doxorubicin (0.25nmol/ml) for 48h significantly enhanced cell death (by 13%; $P<0.05$), as compared to doxorubicin alone (Hossain *et al.* 2012). This was concomitant with augumented release of pro-apoptotic caspases (-3,-8 and -9), increased Bax/Bcl-2 ratio and more prominent DNA damage (Hossain *et al.* 2012). After 72h incubation, combination of ASA (1mM), curcumin (10µM) and sulforaphane (5µM) showed a synergistic effect on the reduction of pancreatic Panc-1 cancer cells cell viability, which was associated with the activation of caspase-3-dependent apoptosis (Thakkar *et al.* 2013).

1.9. Anti-inflammatory effects of 1,2,4-trioxanes

1.9.1. Activities of 1,2,4-trioxanes in non-cancerous models

ART and DHA have demonstrated to display potent anti-inflammatory effects in many immune-related diseases, including human rheumatoid arthritis, bacterial sepsis, allergic asthma and cancer (Cheng *et al.* 2011; He *et al.* 2011; Jiang *et al.* 2011; Zuo *et al.* 2014). For more detailed anti-inflammatory and immune-regulatory activities of 1,2,4-trioxanes refer to recent article reviews (Ho *et al.* 2014; Shi *et al.* 2015). Unlike ASA and other NSAIDs, treatment with 1,2,4-trioxanes against malaria, cancer and other diseases is associated with high efficacious and safety, and no serious adverse effects resulting in growing interest in 1,2,4-trioxanes as therapeutic regimen against diseases associated with chronic inflammation (Weil *et al.* 1995; Tran *et al.* 2004; García Rodríguez *et al.* 2011; Ross *et al.* 2011; Hakacova *et al.* 2013; Krishna *et al.* 2015). For example, in a 14-month-old child with severe herpesvirus 6B myocarditis where previous treatment was unsuccessful (with inotropics, diuretics, immunoglobulin and ganciclovir), ART treatment (5mg/kg/day intravenously for 10 days and subsequent oral therapy with ART 2x5mg/kg for 10 days) resulted in a full recovery evidenced by lack of CD3+ T lymphocytes and no serious adverse effects (Hakacova *et al.* 2013). However, the exact molecular mechanisms underlying ant-inflammatory activities of 1,2,4-trioxanes are not completely defined. Ng *et al.* (2014) showed the utility of ART against chronic obstructive pulmonary disease (COPD) in cigarette smokers. The molecular mechanisms of action of ART in COPD were linked mainly with the inhibition of pro-inflammatory PI3K/Akt and p44/42 MAPK signaling pathways, and inhibition of pro-inflammatory cytokines, including IL-1β and TNF-1α (Ng *et al.* 2014). A high anti-inflammatory properties of 1,2,4-trioxanes in non-cancer settings, such as COPD

may show their preventative benefits against the development of lung cancer. This hypothesis is based on the COPD-lung cancer association reported extensively and the cytotoxic effects of 1,2,4-trioxanes shown against both diseases. Other examples may include utility of 1,2,4-trioxanes against chronic oesteomyelitis, pelvic inflammatory disease, chronic pancreatitis, ulcerative colitis as their potent anti-cancer activities were demonstrated against osteosarcoma, ovarian, pancreatic and colorectal tumours, respectively (Jiao *et al.* 2007; Li *et al.* 2008; Wang *et al.* 2011; Xu *et al.* 2011; Kong *et al.* 2012).

1.9.2. Activities of 1,2,4-trioxanes in cancer models

Similarly with non-cancer studies (Wu *et al.* 2010), in experimental cancer settings, ART and DHA were capable to exert potent anti-inflammatory activities mainly through suppression of the signaling pathways NF-κB, ERK and STAT, the expression of COX-2 and pro-inflammatory cytokines, including IL-8 and IL-1β (Wang *et al.* 2008; Wang *et al.* 2011; Li *et al.* 2014). In CML xenograft mouse model (ART 50-200mg/kg thrice/week for 4 weeks) and in human myeloid leukaemia KBM-5 cells *in vitro*, ART (50-100μM) following 4h incubation suppressed phosphorylation of STAT-5 pathway, protein levels of ERK, JAK-2 and p-38, which were activated by MAPK pathway being strongly linked with inflammation and cancer progression (Kim *et al.* 2015). It can be hypothesized that the ability of ART to inhibit STAT-5 and ERK pathways in leukaemia could find therapeutic benefits to treat myelodysplastic syndrome (MS). MS is a condition characterised by abnormal activation of innate immunity mediators, where both pathways were documented to be key modulators in phenotypic transformation to acute leukaemia (Kolonics *et al.* 2001, Wei *et al.* 2013). First initial *in vitro* reports of ART effects against MS were published recently (Wang *et al.* 2014). Zuo *et al.* 2014 showed that the suppression of COX-2 (mRNA and

protein levels) and its product PGE_2 in ART- treated (20, 100, 200mg/kg) bladder T24 and RT4 cancer cells for 24h correlated with miR-16 expression (reported tumour suppressor). Together with observation that exogenous PGE_2 inhibited ART-mediated caspase-3-dependent apoptosis in these cells (Zuo *et al.* 2014). The growth inhibition of human gastric HGC-27 cancer cells by ART (20, 40, 80mg/l) for 48h was associated with COX-2 inhibition and induction of caspase-3 and -9-dependent apoptosis (Zhang *et al.* 2015). ART-induced apoptosis in HGC-27 cells was further associated with increased levels of pro-apoptotic Bax, decreased levels of anti-apoptotic Bcl-2, and the loss of mitochondrial membrane potential via rhodamine 123 fluorescence inhibition (Zhang *et al.* 2015). The anti-inflammatory effects of DHA against pancreatic BxPC-3 cancer cells *in vitro* and in nude BALB/c mice were through NF-κB-mediated inhibition of COX-2, cytokine IL-8, as well as pro-angiogenic VEGF-α and MMP-9 gene levels (Wang *et al.* 2011). In addition, artemisinin (and MAPKp38 inhibitor SB-203580) in Lewis lung carcinoma (LLC) mediated down-regulation of IL-1β-induced p38 MAPK activation and decreased high levels of pro-angiogenic VEGF-C, thus reducing tumour lymphangiogenesis (Wang *et al.* 2008). With increasing reports of the anti-inflammatory effects of ART and DHA due to COX-2 down-regulation in solid tumours, there is limited experimental data showing their anti-inflammatory effects in human leukaemia cancer cells, thus future studies are needed.

Bachmeier *et al.* (2011) documented the development of resistance and induced invasion and metastasis in ART-treated highly metastatic human breast MDA-MB-231 cancer cells. These effects of ART in MDA-MB-231 cancer cells were attributed with the activation of the transcription factor activator protein (AP)-2, which is involved in cell proliferation (Bachmeier *et al.* 2011). Moreover, augumented

activation of NF-κB resulted in increased levels of bcl-2 and reduced levels of bax (Bachmeier *et al.* 2011). Induced resistance in MDA-MB-231 cancer cells upon activation of AP-2 and NF-κB resulted in increased transcription, expression and activity of matrix-degrading enzyme MMP-1 (collagenase-1), which promote invasion and migration of cancer cells (Bachmeier *et al.* 2011). Therefore, the threat of resistance development in cancer cells to 1,2,4-trioxanes monotherapy emphasize the need to investigate better therapeutic regimens against cancer. Given that available evidence suggest that COX inhibitors enhance the cytotoxic effects of anti-cancer agents, it can be postulated that ASA would equally enhance the cytotoxic effects of ART and DHA. The mechanistic basis of the interaction of ASA with these cytotoxic agents warrants to be evaluated.

1.10. Inflammatory cytokines promote epithelial-mesenchymal transition

1.10.1. Loss of function of cell adhesion molecules supports invasive characteristics of cancer cells

Increasing invasive and the migratory potential of cells in cancer progression is facilitated by epithelial-mesenchymal transition (EMT) (Jang *et al.* 2009; Gu *et al.* 2015). EMT process converts immotile, epithelial cells into mesenchymal derivatives, which are characterised by a spindle-like or fibroblastoid morphology and the loss of cell-cell interactions and polarity (Imbert *et al.* 2012; Yao *et al.* 2014; Gu *et al.* 2015). The mesenchymal properties of epithelial cells initiate malignant transformation by allowing the mesenchymal cells to migrate, invade and promoting the acquisition of metastatic potential (Imbert *et al.* 2012; Yao *et al.* 2014; Gu *et al.* 2015). EMT initiation and progression requires the vast majority of distinct signaling molecules, including pro-inflammatory mediator COX-2, and cytokines IL-6, IL-17 and TNF-1α (Jang *et al.* 2009; Yadav *et al.* 2011; Rokavec *et al.* 2014; Saito *et al.* 2014; Gu *et al.*

2015). Multiple transcriptional repressors have been reported to induce EMT, including vimentin, ZEB1, the zinc finger protein Snail 1, Slug and the basic helix-loop-helix factor Twist1 (Chen *et al.* 2010; Yadav *et al.* 2011; Xiong *et al.* 2012; Deep *et al.* 2014). A variety of signal transduction pathways, such as the NF-κB, Wnt/β-catenin, and JAK-STAT-3 signaling pathways have been implicated in EMT process (Chen *et al.* 2010; Yadav *et al.* 2011; Xiong *et al.* 2012 Rokavec *et al.* 2014; Gu *et al.* 2015). Even more remarkable, it has been documented that micro-environmental stressors, including tumour hypoxia represent a key contributor to EMT initiation and progression (Chen *et al.* 2010). The culture of human breast cancer cells under hypoxic conditions (1% O_2) resulted in enhanced activation of Notch signaling pathway and increased migratory and invasive abilities of cells, as compared to standard normoxic conditions (21% O_2) (Chen *et al.* 2010). A considerable number of experimental reports have demonstrated that many of these signaling factors down-regulate the expression of EMT pre-requisite, E-cadherin (Jang *et al.* 2009; Chen *et al.* 2010; Yadav *et al.* 2011; Xiong *et al.* 2012; Deep *et al.* 2014; Saito *et al.* 2014). E-cadherin (CDH1 gene), is a 120kDa cell-cell adhesion type I cadherin belonging to the family of transmembrane glycoproteins (Pećina-Šlaus 2003). E-cadherin is located at the baso-lateral membrane of epithelial cells and regulates their Ca^{2+}-dependent intracellular adhesion, being critical for the maintaining of tissue structure and morphogenesis (Pećina-Šlaus 2003; Fujii *et al.* 2014). E-cadherin is frequently reported to be absent or down-regulated in diverse metastatic and invasive human tumours of epithelial origin, including CRC, breast, pancreatic, hepatocellular carcinoma, ovarian and endometrial cancers (Deep *et al.* 2014; He *et al.* 2013; Zhou *et al.* 2013; Kashiwagi *et al*. 2010; Jang *et al.* 2009; Sawada *et al.* 2008; Mell *et al.* 2003). Clinically, down-regulated expression of

E-cadherin was reported to be associated with worse survival rate in patients with CRC (Elzagheid *et al.* 2012; He *et al.* 2013).

Conversely, the up-regulation of E-cadherin was partialy involved in the inhibition of doxorubicin chemo-resistance in cultured breast cancer cells through microRNA-200c (regulator of cancer chemoresistance) induced inhibition of Akt signaling pathway (Chen *et al.* 2013). In HepG2 liver carcinoma, E-cadherin inhibited nuclear accumulation of Nrft2 (promoter of cancer chemoresistance), indicating that chemoresistance in cancer cells upon the loss of E-cadherin might be linked with Nrft2 (Kim *et al.* 2012). These reports further suggest that anti-cancer agents which increase expression of E-cadherin may decrease the risk of chemo-resistance and offer effective therapeutic strategy for epithelial cancers. Besides E-cadherin, a tight junction integral membrane protein CLDN-1 (member of claudin family) also plays a fundamental role in maintaining cell-cell contacts (Bezdekova *et al.* 2012). CLDNs contribute to the formation of ion selective pores or barriers that regulate the flow of ions and small molecules, together with a role in maintaining epithelial cell polarity (Bezdekova *et al.* 2012). Conflicting reports have been published with respect of CLDN-1 expression in human cancers and its clinical outcome. Shibutani *et al.* (2013) reported that low expression of CLDN-1 in stage II and III colorectal cancer was correlated with poor survival. In contrast, other studies demonstrated that up-regulation of CLDN-1 expression in colon cancer was linked with the tumour growth and disease progression (Dhawan *et al.* 2005). Increased CLDN-1 expression has been reported in several other malignancies, including breast, ductal adenocarcinoma and squamous lung and esophagus cell carcinomas (Dhawan *et al.* 2005; Gyõrffy *et al.* 2005; Borka *et al.* 2007; Paschoud *et al.* 2007; Blanchard *et al.* 2013). Loss of CLDN-1 function through its up-regulation was observed to be

associated with the alteration of expression of EMT molecules (e.g. SNAIL-2), increasing cellular transformation and metastatic potential of cancer cells (Dhawan *et al.* 2005; Blanchard *et al.* 2013; Huang *et al*. 2015). There is some evidence that CLDN-1 up-regulates the repressor Zeb-1, thereby suppressing E-cadherin levels in colon carcinoma, which was demonstrated to be associated with poor survival (Singh *et al.* 2011). This data suggest that CLDN-1 has a key role in modulating other proteins/signaling pathways during tumorigenesis. The role of E-cadherin and CLDN-1 is extensively studied in epithelial cancers whereas their role in haematological malignancies is limited and emphasize the need of urgent further work. Experimental studies with 1,2,4-trioxanes may also provide additional molecular mechanisms of action to understand better their role in carcinogenesis.

1.10.2. Restored adhesion of cancer cells through 1,2,4-trioxanes activities

Recently, some research studies reported that anti-cancer activities of 1,2,4-trioxanes correlate with their effects on EMT mediators. The inhibitory effect of ART (40µg/ml) in human endometrial carcinoma HEC-1B cells as investigated by RT-PCR demonstrated lower expression of COX-2 mRNA, increased expressions of E-cadherin and caspase-3 mRNA when compared to respective controls (Lijuan *et al.* 2010). Experimental studies of Weifeng *et al.* (2011) showed that artemisinin (50µM) increased adhesion of human hepatocarcinoma HepG2 cells by β-catenin down-regulation and concomitant increase in Cdc42-mediated activation of E-cadherin. In human cultured CRC cell lines (CLY, HT-29 and Lovo), ART treatment (0-100µM for 24-72h) led to the inhibition of cell growth in concentration and time-dependent manners and simultaneously ART modulated the expressions of E-cadherin and β-catenin, which was linked with differentiation state of these cells (Li *et al.* 2008). It was confirmed using a Western blotting analysis where ART treatment

at 0-200μM for 72h in well-differentiated HT-29 cells showed a decreasing E-cadherin protein expression with concomitant no significant changes in β-catenin protein levels (Li *et al.* 2008). In contrast, poorly-differentiated CLY and moderately-differentiated Lovo cells showed higher E-cadherin expression and reduction in β-catenin protein levels (at 200μM ART) (Li *et al.* 2008). Immunofluorescence detection of E-cadherin and β-catenin upon ART treatment (50μM) for 72h showed membranous localisation of E-cadherin and β-catenin proteins, loss of E-cadherin and nuclear β-catenin accumulation in CLY cells and Lovo cells with cytoplasmic staining of both proteins (Li *et al.* 2008). The corresponding differences in E-cadherin and β-catenin expression and localisation levels in ART-treated CLY and Lovo cells were indicated to correspond with the suppression of hyperactive Wnt signaling pathway, thus showing the importance of ART in the reversion of EMT in cancer cells. Much of these research studies with 1,2,4-trioxanes on EMT mediators have been performed in regards of E-cadherin alone. However due to reported inverse relationship between E-cadherin and CLDN-1, it is challenging to further investigate how ART and DHA affect the expression and cellular localisation of these proteins evaluated simultaneously.

1.11. Inhibition of cell migration, invasion and metastasis by 1,2,4-trioxanes.

Activated by cytokines and signaling modulators, MMP-2 (72-kDa gelatinase) and MMP-9 proteins are members of Zn^{2+} metalloendopeptidases matrix family, which have been shown to enhance migration, invasion, metastasis and promote angiogenesis in many human solid cancers, including gastric, lung, ovarian and neuroblastoma (Jodale *et al.* 2005; Hung *et al.* 2010; Kumar *et al.* 2010; Yan *et al.* 2010; [b]Kim *et al.* 2012; Ji *et al.* 2014). In addition, the mRNA expression of MMP-2

and MMP-9 proteins as analysed by RT-PCR was demonstrated in CML, indicating the role of MMPs in haematological malignancies (de Bont *et al.* 2001). MMP-2 and MMP-9 are responsible for disorganising highly regulated cell-cell interactions, degradation of extracellular matrix (EM) and disabling normal functions of other molecules, including cleavage of growth factor β-induced protein and E-cadherin loss, thus contributing to cell invasion and decreased cell-EM interactions ([b]Kim *et al.* 2012). The potential of the primary malignant cells to metastasize and establish secondary tumours in other organs, such as leukaemia as a result of CRC has been related with high mortality (Steeg *et al.* 2006; Shapiro *et al.* 2007). Therefore, inhibition of any of these MMPs may increase the efficacy of current cancer therapies, reduce mortality and improve of life of patients.

Studies reveal that 1,2,4-trioxanes (artemisinin, ART and DHA) inhibit cell migration, invasion and metastasis *in vitro* and in *vivo* by altering the expression of MMP gene family and other factors (Buommino *et al.* 2009; Rasheed *et al.* 2010; Wang *et al.* 2011; Weifeng *et al.* 2011). The inhibitory effects of artemisinin against melanoma A375M cell line was shown by reducing the production of MMP-2 and decreasing αvβ3 integrin expression (Buommino *et al.* 2009). In PMA (30nm) pretreated human fibrosarcoma HT-1080 cells, DHA at increasing concentrations ranging between 0-50μM for 24h reduced the levels of MMP-2 and MMP-9 through decreased AP-1 and NF-κβ expression, and induced low levels of membrane-type 1 MMP (MT1-MMP) (at 50μM DHA) (Hwang *et al.* 2010). A low concentration of ART (at 2.5μM and 5μM) for 24h in human non-small cell lung cancer effectively decreased transcriptional expressions of MMP-2 and MMP-7 (small uterine metalloproteinase), together with down-regulation of mRNA and protein expression of urokinase-type plasminogen activator (uPA), which is involved in promoting degradation of extracellular matrix

(Rasheed *et al.* 2010). In human HCC hepatoma cells, ART (0-75µM) for 48h treatment showed a concentration-dependent decrease in MMP-2 levels and increase of tissue inhibitor of metalloproteinase (TIMP)-2 (suppressor of metastasis) as evaluated with Western blotting analysis (Weifeng *et al.* 2011). Similar results in both proteins were observed by gelatinase zymography analysis with hepatoma HepG2 cells upon treting the cells with ART (0-50µM) for 24h (Weifeng *et al.* 2011). Additionally, ART, DHA and artemisinin have demonstrated to inhibit cell migration and invasion in other experimental settings including 2D wound healing assays, 3D transwell chamber invasion assays and *in vivo* metastasis assays in several cancer types, including lung and hepatoma cancers (Hwang *et al.* 2010; Rasheed *et al.* 2010; Weifeng *et al.* 2011; [a]Chen *et al.* 2013). For example, inhibited migration and invasion of hepatoma cells (HepG2 and SMMC-7721) in 2D wound-healing assay upon artemisinin treatment (0-75µM) for 24-48-72h was observed in concentration- and time- dependent manners and was characterised by blocking the ability of cells to close the wound gap (Weifeng *et al.* 2011). Chen *et al.* (2013) have demonstrated that ART treatment (10-40mg/kg) in lung adenocarcinoma A549 cell xenograft tumour decreased dose-dependently the protein expressions of MMP-9 and ICAM-1 (intracellular adhesion molecule-1), suppressed tumour growth with concomitant inhibition of cell invasion *in vitro* (at ART 1.25µg/L) as evaluated with 3D transwell chamber invasion assay. In human cervical cancer (Hela and Caski) cells, DHA at 20µmol/L for 48h treatment up-regulated mRNA and protein levels of metastatic inhibitor, RKIP *in vitro,* which was accompanied by significant ($P<0.001$) reduction in tumour volume in Balb/c nude mice xenografts by ~5.25-folds in Hela and ~5.95-folds in Caski cells when compared to controls (Hu *et al.* 2014). These reports indicate that 1,2,4-trioxanes are potent anti-cancer agents, with the ability to inhibit

cell metastasis by blocking migratory and invasive abilities of cells through changes on several signaling mediators, especially MMPs. However, in literature there are no reports on ART and DHA effects to block the ability of the cells to re-growth post drug treatment, which may have significant meaning for patient survival outcome and the development of secondary cancers. Therefore, new studies designed to evaluate this concept are needed. In addition, the effects of ART and DHA on MMPs in human colorectal and leukaemia cancer cells are not completely defined and require further investigations.

1.12. Angiogenesis as a anti-cancer target of 1,2,4-trioxanes

The rapid and uncontrolled growth of malignant tissues causes inefficient tissue oxygenation (hypoxia) leading to angiogenesis (Duffy *et al.* 2003). Angiogenesis is an active process of the outgrowth of new structurally and functionally abnormal blood micro-vessels from pre-existing vessels being characterised by dilated, chaotic and hyperpermeable vasculature (Aguayo *et al.* 2000; Goel *et al.* 2011). In more invasive rectal cancers (T- and N-stages), high micro-vessel density correlates with poor prognosis in patients (Rasheed *et al.* 2009). Significantly increased number of blood vessels was widely reported in the leukaemogenic processes of several leukaemias, including AML (median: 16.1, range 1.2-32.8; $P<0.02$) and CML (median: 21.4, range 4.7-41.7; $P<0.03$), as compared to control BM (median: 11.2; range 1.2-24), which could be linked with a high risk of poor prognosis for these patients (Aguayo *et al.* 2000).

1.12.1. Inhibition of the VEGF gene family by 1,2,4-trioxanes

The human VEGFs are encoded by three separate genes which include VEGF-α, VEGF-β and VEGF-C (Anfosso *et al.* 2006). The secretion of the main cancer pro-

angiogenic factor VEGF-α is enhanced during angiogenesis and occurs via multiple processes, including hypoxia-mediated activation of HIF-1α (Faderl *et al.* 2005; Yoshioka *et al.* 2012; Li *et al.* 2014). Human VEGF-α is a homodimeric glycoprotein which form five main isoforms: $VEGF_{121}$, $VEGF_{145}$, $VEGF_{165}$, $VEGF_{189}$ and $VEGF_{206}$ (Panoilia *et al*. 2015). The $VEGF_{165}$ isoform is most abundant and enhances angiogenesis and vascular permeability by binding to vascular endothelial cells through interaction with tyrosine kinase receptor-2 (VEGFR-2 or KDR/Flk-1) and 1 (VEGFR-1 or Flt-1) (Cohen *et al.* 1996; Schneider *et al.* 2011; Yoshioka *et al.* 2012; Panoilia *et al*. 2015). The expression of VEGF-α in cancer cells is up-regulated by oxygen radicals within hypoxic tumours, directly by hypoxia-mediated HIF-1α over-expression, and indirectly by inflammatory cytokines such as TNF-α, IL-1β, IL-6 and IL-8 via activation of PI3K/Akt signaling pathway (Cohen *et al.* 1996; Neufeld *et al.* 1999; Faderl *et al.* 2005; Huang *et al.* 2008; Li *et al.* 2012). The expression of VEGF-α has been reported to be quite low under normoxic conditions (~20% O_2) but high in hypoxia (~1% O_2) (Yoshioka *et al.* 2012). Elevated levels of VEGF-α are reported to play a critical role in the tumour progression, disease stage and poor survival prognosis not only in solid tumours, including colorectal, osteosarcoma and cervical cancers but also in haematological malignances, including leukaemia (Aguayo *et al.* 2000; Koomagi *et al.* 2001; Faderl *et al.* 2005; Des Guetz *et al.* 2006; Lyu *et al.* 2007; Zhou *et al.* 2011; Katanyoo *et al.* 2013).

1,2,4-trioxanes (ART, DHA, artemisinin) were reported to elicit potent anti-antigenesis properties through in several experimental settings *in vitro,* and *in vivo* (Aung *et al.* 2011; Wang *et al.* 2008; Wang *et al.* 2011). The anti-angiogenic effects of ART (at 7.20μM) in Dell'Eva *et al.* (2004) research study were linked with strongly reduced vascularization of Matrigel plugs pretreated earlier with angiogenic stimuli

mix (VEGF-α of 100ng/ml; TNF-α of 2ng/ml and heparin (24-26U/ml) and injected subcutaneously into syngenic mice, or when ART (100mg/kg/day) was administrated with water of the animals for 4 days. In addition, orally administrated artemisinin (50mg/kg/day) in mouse Lewis lung carcinoma study reduced VEGF-C mediated lymphangiogenesis (Wang *et al.* 2008). Conditioned media analysed by ELISA from chronic myelogenous leukaemia K562 cells upon treatment with ART (2μmol/) for 48h, showed that the VEGF-α secretion and mRNA levels were significantly ($P<0.01$) inhibited (by 25.7% and 27.1%, respectively) (Zhou *et al*. 2007). The VEGF-α secretion and mRNA levels were decreased accordingly with increasing ART concentrations (5 and 10μmol/L), as compared to control cells (Zhou *et al*. 2007). Interestingly, in the same study of Zhou *et al.* 2007, the inhibitory effect of ART (1.2μmol/100μl per egg for 48h) on angiogenesis in chicken charioallantoic membrane (CAM) *in vivo* model was associated with the presence of an inflammation of cells infiltration (Zhou *et al*. 2007). It can be hypothesized that ART (1.2μmol/100μl per egg for 48h) in CAM induced transient inflammatory response, which led to IL-6-mediated activation of NK cells, thus potent anti-angiogenic effects of ART, as compared to untreated CAM.

1.12.2. Regulation of HIF-1α transcription activator protein by 1,2,4-trioxanes

Besides the VEGF gene family, new mutations taking place as tumour grows facilitate the over-expression of other pro-angiogenic proteins including HIF-1. HIF-1 is a heterodimer which belongs to the basic helix-loop-helix family of transcription activator proteins (Duffy *et al.* 2003). HIF-1 is responsible for transcription of several genes associated with key cellular functions including cell adhesion, cell-extracellular matrix interactions, inflammation, iron homeostasis, angiogenesis and inhibition of apoptosis (Duffy *et al.* 2003; Harada *et al.* 2005; Jeong *et al.* 2005). HIF-1 consists of

two subunits: the β/ aryl hydrocarbon receptor nuclear translocator subunit which is constitutively present, and α subunit which in the presence of iron and oxygen is rapidly degraded ($t_{1/2}$ of 5 mins) by ubiquitin-mediated proteolysis in normoxia but becomes stable in hypoxia (Harada *et al.* 2005; Duffy *et al.* 2003; Romney *et al.* 2011).

Recent studies have shown that HIF-1α increases the transcription of TfR by binding to its hypoxia-responsive elements which promote tumour growth and tumour aggressiveness by enhancing cell proliferation and activation of other factors, including IL-6, MMP-2 and -9 (Tacchini *et al.* 1999; Jeong *et al.* 2005; Choi *et al.* 2011). Using a microarray-based approach, Anfosso *et al.* (2006) showed that the cytotoxic effects of 1,2,4-trioxanes (e.g. ART, arteether, artemisetene) in 60 human cancer cell lines, including leukaemic HL-60 and colorectal HT-29 cells correlated with the expression of 30 genes being regulated actively by angiogenesis. For example, high mRNA expression of MMP-9 correlated significantly ($P<0.01$) with low IC_{50} values (inverse correlation) for ART, arteether and artemisetene (Anfosso *et al.* 2006). In direct correlation, high mRNA expression of MMP-11 correlated significantly ($P<0.05$) with high IC_{50} values for ART, arteether and artemisinin (Anfosso *et al.* 2006). In addition, the high expression of VEGF-C and HIF-1α correlated with ART and arteether at a significance level of $P<0.01$ (Anfosso *et al.* 2006). Interestingly, high IC_{50} values for ART, arteether correlated with high IL-6 signal transducer expression ($P<0.05$) indicating potential role of IL-6 in 1,2,4-trioxanes' activities (Anfosso *et al.* 2006).

There are also some inconsistent reports regarding the effect of DHA on HIF-1α production. The generation of ROS in rat C6 glioma cells when treated with DHA (5-25μM) resulted in inhibited HIF-1α expression and cell-growth inhibition (Huang *et*

al. 2007). In contrast, as measured in Western blotting analysis, the protein expression of HIF-1α in human hepatoma cell line HepG2 increased in a DHA concentration-dependent manner (1-25μM) for 24h and with DHA at 25μM in increasing incubation times from 0h to 24h, which was shown to be independent of ROS production but induced by cellular iron depletion (Ba *et al.* 2012). As the effects of 1,2,4-trioxanes on HIF-1α expression are not completely defined, we aimed to examine in this study the effect of ART and DHA against cultured HT-29-AK and HL-60 cells. Based on the above reports, the simplified postulated mechanisms of 1,2,4-trioxanes inhibition of cancer spread within the body is depicted in figure 3.

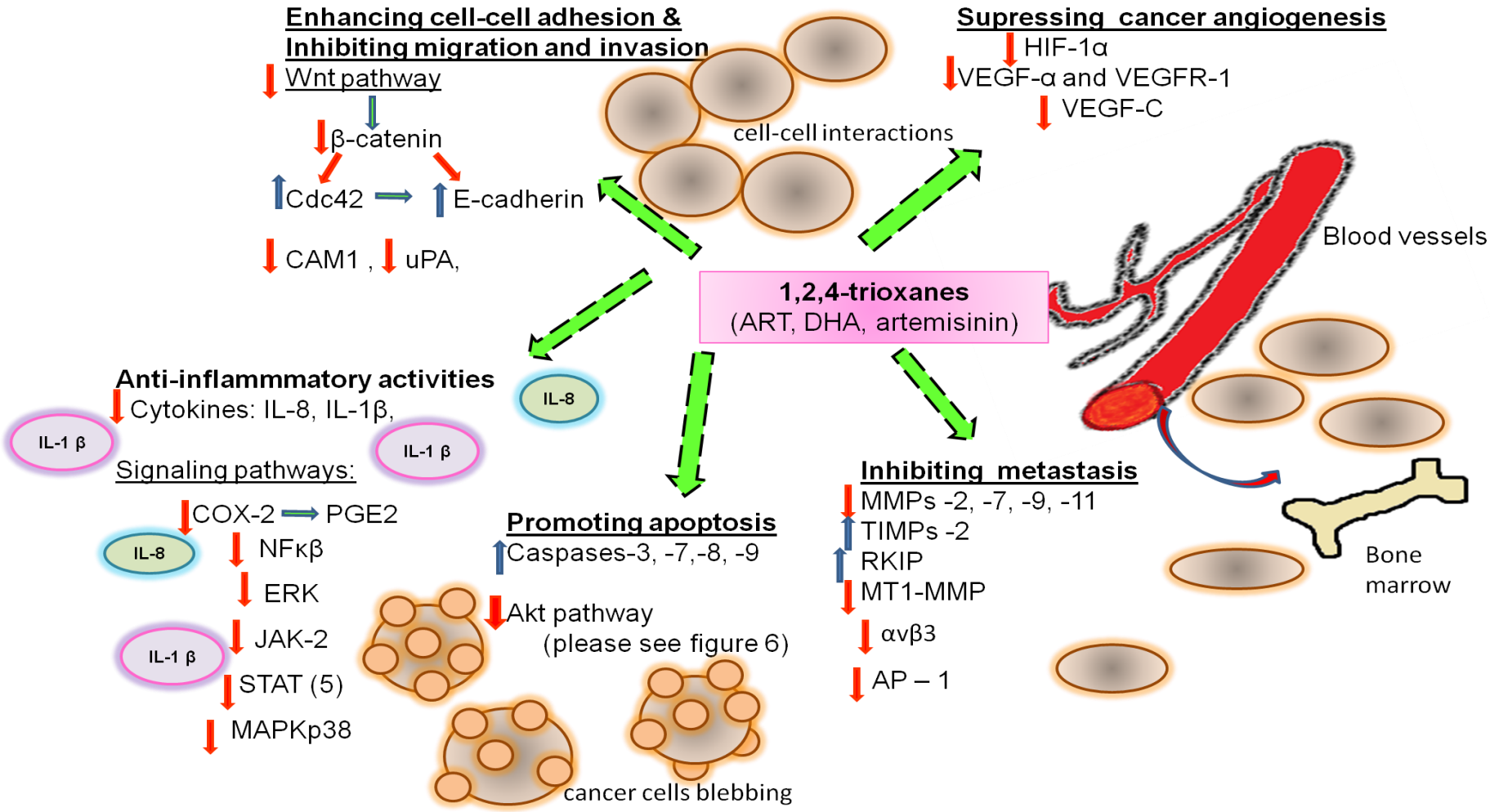

Figure 3: Schematic representation of the mechanisms by which 1, 2,4-trioxanes inhibit spread of cancer cells to distant parts in the body.

1.13. 1,2,4-trioxanes as a hypoxia selective agents

Hypoxia is a condition of decreased availability of oxygen in the interior of most, if not all solid tumours (Suzuki *et al.* 1998; Ke and Costa 2006; Brahimi-Horn *et al.* 2007). It occurs due to robust tumour growth with resulting long distances (~100-150µm) to local blood vessels (diffusion-limited hypoxia) (Brahimi-Horn *et al.* 2007; Vordermark 2010). Hypoxia is associated with poor vasculature of tumour vessels leading to inadequate oxygen and nutrient supply in certain tumour areas (perfusion-limited hypoxia) (Brahimi-Horn *et al.* 2007; Vordermark 2010). Thus, the resultant cellular hypoxia and metabolic stress leads to the recruitment of additional abnormal blood vessels through the process of angiogenesis (Faderl *et al.* 2005; Rustum *et al.* 2010). The disproportional and incomplete vasculature in hypoxic tumours often is linked with the development of resistance to non-surgical cancer therapies, mainly radiation and chemo-therapy (Bhattacharya *et al.* 2004; Goel *et al.* 2011; Milosevic *et al.* 2012). Radiation is insufficient in enhancing the cytotoxicity of agents because of low oxygen levels in highly hypoxic areas (Milosevic *et al.* 2012). The transport of anti-cancer agents at therapeutically meaningful concentrations via blood flow to hypoxic cells is inadequate by limited convection and diffusion (Bhattacharya *et al.* 2004; Rustum *et al.* 2010; Goel *et al.* 2011). The effectiveness of some chemotherapeutic drugs which target highly proliferating cancer cells is also decreased at high cell density hypoxic, well-differentiated regions of tumour due to slower cell proliferation rate (Bhattacharya *et al.* 2004; Rustum *et al.* 2010). Remaining alive hypoxic cells enhance tumour aggressiveness through inhibition of cancer cell death and increasing the expression of pro-angiogenic and metastatic factors, especially activated HIF-1α mediated over-expression of Mad1 (MAX dimerization protein 1), which has been shown experimentally to be associated with

treatment failure, therapeutic resistance and cancer recurrence (Milosevic *et al.* 2012; [b]Cho *et al.* 2013; Chen *et al.* 2014; Dekervel *et al.* 2014).

Other regulatory activities of HIF-1α in hypoxic niches include activation of carbonic anhydrase IX (CA-9), a glycotransmembrane protein of zinc metalloenzymes responsible for acid-base balance and intracellular interactions (Saarnio *et al.* 1998; Rasheed *et al.* 2009). A high protein expression and staining of CA-9 were shown to be usefull in diagnosis and survival prognosis in many carcinomas, including CRC, bladder, breast and non-small cell lung cancer (Saarnio *et al.* 1998; Rasheed *et al.* 2009; Ilie *et al.* 2010; Lock *et al.* 2012; Li *et al.* 2014; Cheng *et al.* 2015; de Martino *et al.* 2015). Over-expression of CA-9 was reported to enhance EMT transformation and metastaic potential in cancer cells through reducining cell adhesion capacity linked with modulation of E-cadherin localisation (from membrane to cytoplasm) via β-catenin (Švastová *et al.* 2003). Therefore, there is currently much ongoing research focused on targeting tumour hypoxic microenvironment and its regulators, which could represent promising therapeutic approach (Chen *et al.* 2009; [b]Cho *et al.* 2013; Chen *et al.* 2014).

Recently, there are some reports showing that 1,2,4-trioxanes target cancer cells with similar potency profiles in normoxic and hypoxic experiments and are able to modulate the expression of important signaling mediators, such as VEGF-α and HIF-α under both conditions. For example, DHA (0-80μM) for 48h in human CRC cell lines (HCT15, HCT116, and Coco 205) effectively inhibited the growth of cells under normoxic (21% O_2) and strongly hypoxic (0.2% O_2) conditions (Ontikatze *et al.* 2014). Hypoxia was induced in CRC cells for 2h prior DHA treatment and was associated with DHA-induced cell apoptosis and necrosis (Ontikatze *et al.* 2014). In BxPc3-RFP pancreatic cancer cell line, cytotoxic effects

of DHA in normoxia increased with higher DHA concentrations (0-80µM) over a period of time (24-48-72h) *in vitro,* whereas DHA (25mg/kg for 4 weeks) reduced the tumour growth in nude mice models (Aung *et al.* 2011). Subsequent mechanistic basis of DHA (0-80µM) anti-cancer effects in cultured pancreatic BxPc3-RFP cells following 18h incubation showed increasing down-regulation of VEGF-α protein expression with increasing DHA concentrations under standard normoxic conditions (20% O_2), whereas unchanged expression levels of VEGF-α under hypoxic conditions (1% O_2) (Aung *et al.* 2011). More prominent results were obtained for HIF-1α were its levels were not detected in all DHA-untreated and treated samples under normoxic conditions but decreased in hypoxia, as compared to control (Aung *et al.* 2011). These evidence indicate potential applications of 1,2,4-trioxanes for cancer therapies especially for highly aggressive and resistant tumours to current chemotherapies, thus becoming first anti-malarial agents selectively targeting hypoxia (figure 4).

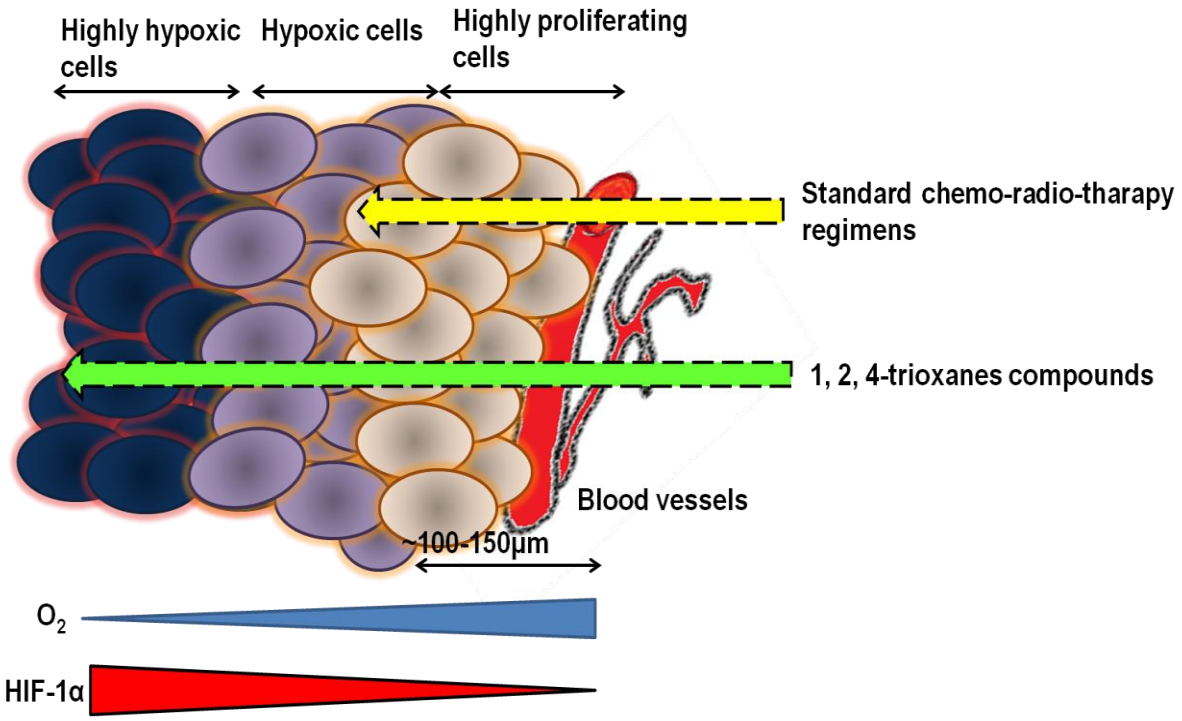

Figure 4: Tumour hypoxic mass features and their effect on inhibited responsiveness to standard radio- and chemo-therapy treatments. Poor vasculature of tumour blood vessels leads to inadequate oxygen and nutrient supply resulting in highly hypoxic areas dominated by HIF-α factor linked with treatment failure, therapeutic resistance and cancer recurrence. Low levels of oxygen within hypoxia interior restricts radiation and transport of chemo-therapeutic agents due to their limited convection, diffusion and being inactive towards slowly proliferating highly hypoxic cells. Increasing reports indicate high potency of 1,2,4-trioxanes (ART and DHA) towards highly hypoxic cells, thus showing potential benefits in cancer treatment.

However, above studies concentrated only on the evaluation of DHA effects under both conditions without testing other 1,2,4-trioxanes, such as ART. In addition, the effects of ART and DHA under both conditions were not explored against cancers of different phenotypic state, including adherent human colorectal HT-29-AK cells and suspension human leukaemic HL-60 cells, investigated alone and in combination with other chemotherapeutic

agents, such as ASA, which could additionally enhance the effects of the agents. Other study design are also needed, including longer pre-incubation of cells under hypoxic conditions, thus allowing the low oxygen microenvironment in cell culture to induce changes in expression of signaling factors such as VEGF-α and HIF-1α which normally are taking place in tumour hypoxia.

1.14. Induction of the apoptosis of cancer cells by 1,2,4-trioxanes

In principle, the major aim of current chemotherapy approaches is to selectively induce the apoptosis of cancer cells. Apoptosis, or programmed cell death is a highly regulated mechanism used to regulate tissue homeostasis, including in gut mucosal and leukaemic mast cells microenvironment through removal of superfluous, damaged or potentially deleterious cells (Zhang *et al.* 2004; Greenhough *et al.* 2009; Hassan *et al.* 2014). Apoptosis signaling that leads to caspase activation is mediated through two major pathways, the death receptor pathway (extrinsic) and the mitochondrial pathway (intrinsic) (Hector and Prehn 2009; Sanmartin *et al.* 2012). Caspases are cysteine-dependent, aspartate-specific proteases, which belong to the familily of more than 14 enzymes where only seven actively participate in the apoptosis program (Herr and Debatin 2001). Of these, caspases -2, -8, -9 and -10 constitute initiator caspases, which activation leads to proteolytic activation of the downstream effector or executioner caspases-3,-6, and -7 (Herr and Debatin 2001). Especially, caspase-3 (known as CPP32, Yama and apopain) is reported to be required for the execution of apoptosis by cleaving a number of key cellular proteins, including other caspases -6 and -7 (Yang *et al.* 2001; Devarajan *et al.* 2002). Caspase-3 activity induces the classical morphological and biochemical of apoptosis, such as internucleosomal DNA fragmentation, membrane damage, chromatin condensation and

hypodiploid DNA content (Coalho *et al.* 2000; Bestwick *et al.* 2006; Sanmartin *et al.* 2012). Escape from cell death being associated with dysfunction, down-regulation or loss of caspase-3 has been shown in several cancer types, including acute myeloid leukaemia, colorectal, breast and non-small cell lung carcinoma and has been linked with therapy failure and the development of resistance to standard chemotherapies (Joseph *et al.* 2001; Yang *et al.* 2001; Devarajan *et al.* 2002; Zhang *et al.* 2004; Hector *et al.* 2012). For example, a breast cancer MCF-7 cell line, deficient of caspase-3 and resistant to many chemothatapeutic agents was shown to be sensitive towards doxorubicin and etoposide when caspase-3 was reconstituted, which led to enhanced cancer cells death (Yang *et al.* 2001). The proposed mechanism of the defective apoptosis in cancer progression and potential responses to cancer therapy is presented in figure 5. Therefore, there is great therapeutic potential to investigate the mechanistic role of current chemotherapeutic agents on caspase-3-dependent apoptosis.

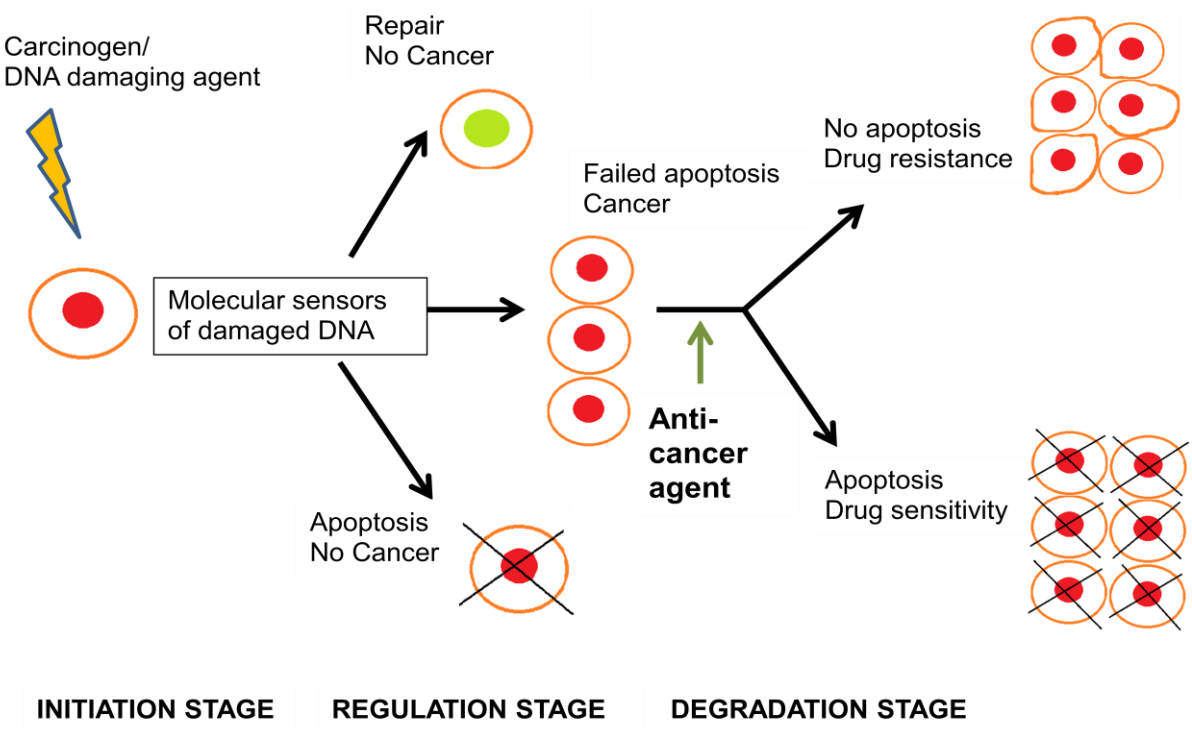

Figure 5: Non-tumorigenic cells with damaged DNA can be self repair or be utilized by self-destruct mechanism, an apoptosis. Escape from the apoptosis by cells with dysfunctional apoptotic genes may lead to therapy failure and the development of resistance to standard chemotherapies (re-drawn from Kelly *et al.* 1999).

As presented in figure 6, the primary mechanism by which 1,2,4-trioxanes exert their anti-tumour activities is through the induction of caspase-dependent apoptotic cell death via the extrinsic (He *et al.* 2010; Kong *et al.* 2012) or the intrinsic effector mechanisms (Mercer *et al.* 2007; Lu *et al.* 2008; Hamacher-Brady *et al*. 2010; Xu *et al.* 2011; Kim *et al.* 2015; Zhang *et al.* 2015; Zhao *et al.* 2015). In pancreatic BxPC-3 and PANC-1 cancer cells, DHA (0-100µM/L) following 48h incubation increased the ROS- and Apo2L/TRAIL *(*Apo2 ligand or tumour necrosis factor-related apoptosis-inducing ligand*)* mediated protein expression of Death Receptor (DR)-5 (initiator of the extrinsic pathway), which led to cleavage of initiator caspase-8 and its downstream effector caspases -9 and -3 (Kong *et al.* 2012). A reductive

cleavage of DHA by CCR in leukaemic HL-60 cells induced a time- (for up to 24h) and concentration-dependent (0.1-10μM) mitochondrial membrane depolarisation, which is characteristic for the intrinsic pathway, and the cell cycle arrest at the G_o/G_1 phase with degraded DNA as investigated by flow cytometric analyses (Mercer *et al.* 2007). By employing Western blotting analysis, it was shown that DHA in HL-60 cells was responsible for activation of caspases- 3 and -7, which was time- (for up to 24h) and concentration-dependent (0.1-10μM) (Mercer *et al.* 2007). Partialy ROS-dependent induced apoptosis by DHA (2.5 to 40μM/L) for up to 24h in Jurkat T-lymphoma cells resulted in the release of cytochrome c from damaged mitochondria, activation of caspases (-3 and -8), cleavage and up-regulation of the DNA repair enzyme PARP and induction of pivotal characteristics of apoptotic cell death, including chromatin condensation, hypodiploid nuclei or nuclear fragmentation (Handrick *et al.* 2010). The genotoxicity (DNA damage) directly induced by DHA and ART was also evidence with DNA gel electrophoresis in some cell lines, including leukaemia and ovarian cancers (Jiao *et al.* 2007; Li *et al.* 2009; Yang *et al*. 2009).

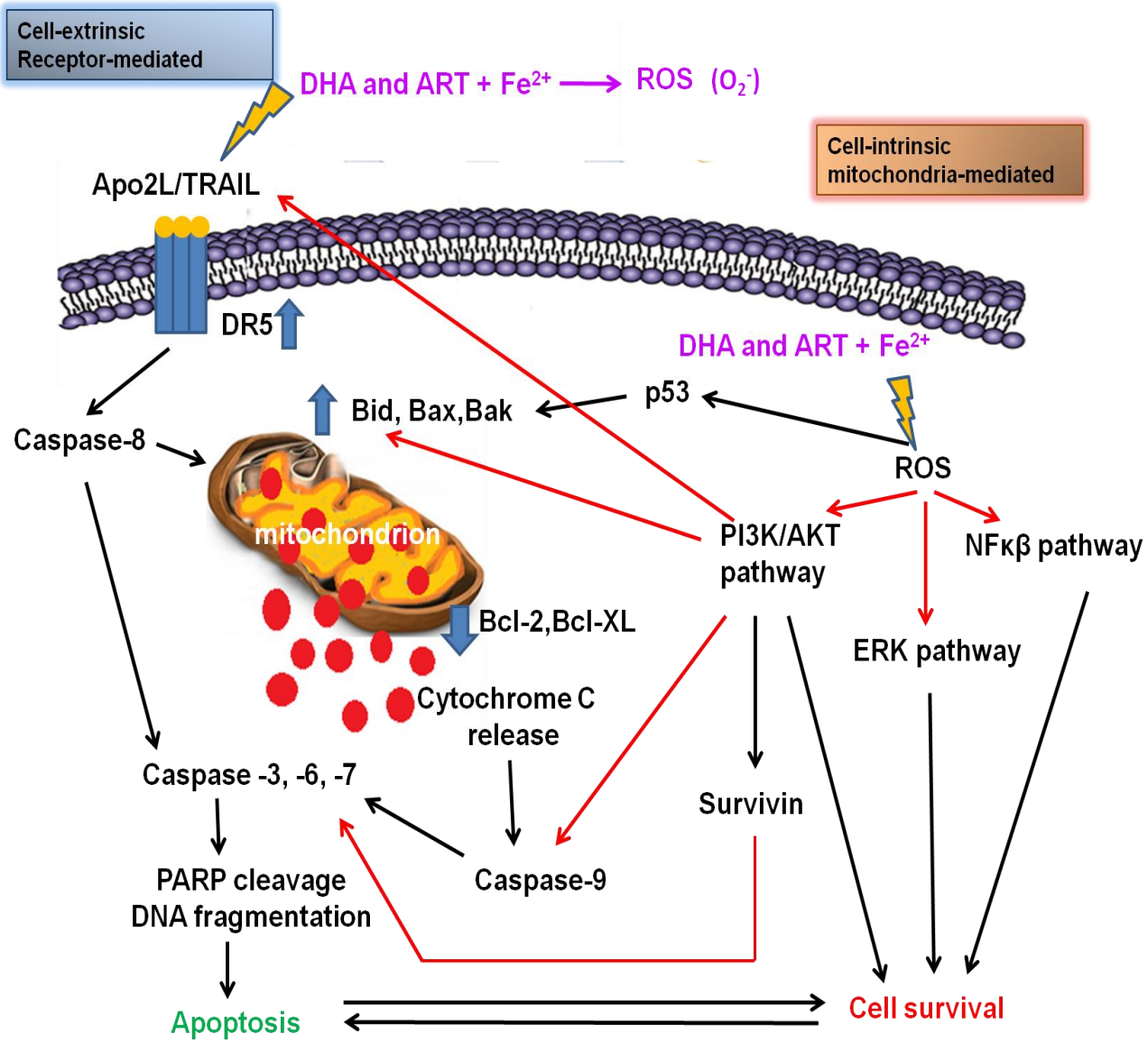

Figure 6: Simplified proposed mechanisms of DHA and ART-mediated cell death in cancer cells. The apoptosis signaling pathway induced by ART and DHA includes the cell extrinsic mechanisms triggered by Apo2L/TRAIL/DR5 activation and cell-intrinsic mechanisms linked with induced cell mitochondria damage and results in DNA fragmentation. Crosstalk between both pathways involves activation of Bid, Bax, Bak proteins and the inhibition of the cell proliferation survival pathways (PI3K/AKT, ERK and NFκβ pathways).

Survivin is an oncofetal protein (16.5-kDa) implicated in inhibition of apoptosis (binds directly to caspase-3 and caspase-7) and has a role in enhancement of motility and metastatic abilities of CRC (Shin *et al.* 2001; Ye *et al.* 2014). Together with stimulating angiogenesis, survivin has prognostic implications in cancer patients and promotes resistance to chemo-therapy, thus making survivin an attractive target in cancer therapy (Ko *et al.* 2010; Ye *et al.* 2014). The inhibitory effects of DHA against colorectal SW480 cells were linked with survivin inhibition whereas in other experimental study with DHA (25-100μM/L) in BxPC-3 and PANC-1 pancreatic cells for 72h incubation, it was observed that survivin levels were unchanged (Shao *et al.* 2008; Kong *et al.* 2012). In leukaemic KBM-5 cells *in vitro* and in CML xenograft model, ART (at 50-100μM for 4h and 50-200mg/kg thrice/week for 4 weeks, respectively) down-regulated survivin mRNA and protein levels as evaluated by Western blotting (Kim *et al.* 2015). In osteosarcoma HOS cells, ART (10-80μmol/L) following 48h treatment decreased in a concentration-dependent manner protein survivin as measured by Western blotting (Xu *et al.* 2011). Therefore, the investigation and understanding of the differences arising in the effects of 1,2,4-trioxanes on survivin expression in various cancers could provide additional knowledge on their mode of action.

In addition, in cultured human prostate malignant cells have shown that DHA (30μM for PC-3 and DU145, 50μM LNCaP cells) for 24h inhibited the PI3-kinase/Akt and ERKsurvival/proliferation pathways with concomitant cleavage of caspases (-3, -8, -9) at 50μM for 24h due to TRAIL/DR5 activation (He *et al.* 2010). Similar inhibitory effects of ART and DHA against phosho-Akt were observed in some other *in vitro* and *in vivo* studies (Ma *et al.* 2011; Thanaketpaisarn *et al.* 2011; Lee *et al.* 2013; Odaka *et al.* 2014). Akt is reported to promote resistance to 5-FU and inhibition of apoptosis through numerous mechanisms, such as direct inhibition of caspase-3 and the inactivation of some other

pro-apoptotic proteins (e.g. Bad, caspase-9) and up-regulation of anti-apoptotic proteins (e.g. survivin, Bcl-2, Mcl-1), thus preventing caspases cascade activation (Bortul *et al.* 2003; Zhang *et al.* 2004; Zhang *et al.* 2014; Ye *et al.* 2014). Elevated Akt protein levels have been reported in haematological malignancies, including HL-60 cells which correlated with decreased sensitivity induced by TRIAL (Bortul *et al.* 2003). In colorectal HCT116 cells, TNF-α activated Akt pathway contributed to inflammation-induced EMT, enhanced invasion and metastasis of cells (Wang *et al.* 2013). Due to broad-spectrum functions of Akt in cancer development it is important to further explore its function in ART- and DHA-mediated anti-cancer effects to better understand their molecular basis of action. Other key mechanisms of ART- and DHA- induced apoptosis in cancer cells are associated with the regulation of BcL-2 family proteins, including inhibition of anti-apoptotic Bcl-2 and up-regulation of pro-apoptotic Bax, Bim and Bak proteins, activation of p53 and inhibition of NFκβ signaling pathways (Hou *et al.* 2008; Li *et al.* 2009; Handrick *et al.* 2010; Xu *et al.* 2011; Kong *et al.* 2012; Du *et al.* 2013; Zhao *et al.* 2015).

1.15. Combination therapy for cancer with 1,2,4-trioxanes and future prospectives

Major shortcomings of many current chemotherapeutic agents, such as cisplatin, doxorubicin, 5-FU, irinotecan, oxaliplatin, oral fluoropyrimidines and raltitrexed (given either alone or in combination) include lack of specificity resulting in unfavourable side effects (such as hypotrophy, leukopenia or stomatitis) and the development of drug resistance (Shahrokni *et al.* 2009; Rasheed *et al.* 2010; Feng *et al.* 2014). Complete remission of cancer without toxic effects to healthy cells in the rest of the body is the main aim in the clinical anticancer treatment. 1,2,4-trioxanes are broad-spectrum natural *Artemisia annua L.*-derived compounds that have been proven to elicit potent cytotoxic activities towards

rapidly dividing cancer cells *in vitro* and *in vivo*. Additionally, ART and DHA have been shown to be effective towards cancer cell lines being resistant to current chemo-therapeutic agents. ART (1µg/ml) following 24h incubation has been shown to be effective against doxorubicin (0.5µg/ml)-resistant T leukaemia cells through induction of apoptosis and DNA fragmentation (Efferth *et al.* 2007). Other study showed that DHA inhibited the growth of imatinib-resistant CML (Lee *et al.* 2013). Encourangingly, increasing reports are describing that 1,2,4-trioxanes (ART, artemether) are effective to combat cancer clinically where are well tolerated without causing serious side effects (Singh and Verma 2002; Singh and Panwar 2006; Jansen *et al.* 2011; Krishna *et al.* 2015). This include a pilot study of ART-treated patients with advanced cervical cancer led to disease remission of about 6 months (after 28-day treatment), prolonged survival for about 12 months, improved clinical symptoms (reduced vaginal discharge and pain) and was well tolerated (Jansen *et al.* 2011). Recently, in double-blinded pilot study, Krishna *et al.* (2015) reported higher recurrence-free survival probability at 3 years of follow-up after ART treatment at daily dose of 200mg orally for 2 weeks in CRC. Treatment was well tolerated with some adverse effects, including leucopenia but no reports of nausea (Krishna *et al.* 2015). Despite these promising reports there is a global threat that relatively short half-life of 1,2,4-trioxanes linked with repeated administrations and high drug doses could eventually lead to the development of drug resistance in cancer cells due to their metabolic adaptation. Therefore, there is pressing need for undertaking additional molecular investigations enhancing current understanding of 1,2,4-trioxanes anti-cancer actions. Additional molecular mechanisms governing the anti-cancer effects of 1,2,4-trioxanes could provide a solid background for novel drug combinations for the cancer treatment. The combination therapies are attractive because they could overcome drug resistance and possibly yield even better therapeutic

effects than monotherapy. There are several reports of the ability of ART and DHA to enhance therapeutic effectiveness *in vitro* and animal settings of other anti-cancer agents, including cisplatin (Efferth *et al.* 2007; Wang *et al.* 2010; Thanaketpaisarn *et al.* 2011; Krusche *et al.* 2013; Liu and Cui 2013; Zhang *et al.* 2013; Feng *et al.* 2014). Most recently, in human myeloid leukaemic KBM-5 cells, combination of ART (10µM) with either, doxorubicin (30µM), paclitaxel (1.50nM) or docetaxel (1.50nM) for 24h significantly ($P<0.001$) potentiated the cytotoxicity of all drugs through enhanced down-regulation of survivin and augumented cleavage of PARP (Kim *et al.* 2015). Clinically, ART in combination with decarbazine was successfully used in the treatment of stage IV uveal melanoma (median survival of 2-5 months) where subject was alive after 47 months of diagnosis with progressive decline of splenic and lung metastases (Berger *et al.* 2005). A randomized open-controlled trial in patients with advanced lung cancer showed that ART (120 mg/day intravenously for 8 days) combined with vinorelbine (25 mg reconstituted in 2ml H_2O m(2) and used once-a-day intravenously, at the 1st and 8th day) and cisplatin (25 mg/m(2), once-a day intravenously, at the 2nd to 4th day) used for at least two three-week cycles significantly improved disease control, prolonged time to progression with no additional toxic effects as those observed in control vinorelbine/cisplatin group (myelosuppression and digestion reaction) (Zhang *et al.* 2008). Reports from pre-clinical and clinical studies make the point evident that cancer monotherapy is not enough and combination therapies would add necessary new regimens to current cancer treatment tools.

1.16. Aim of the study

The main aim of the current study was to evaluate anti-cancer effects of ART and DHA (figure 7) against human promyelocytic leukaemia HL-60, human colorectal carcinoma HT-29-AK and Caco-2 human epithelial colorectal adenocarcinoma cell lines. Of particular interest was to elucidate the mechanism of action of ART and DHA in both cell lines. For that purposes following objectives were established:

1. Using the MTT assay, to evaluate the cytotoxicity of ART and DHA against both cell lines at increasing incubation time points (24-48-72h) under standard normoxic condition (20% O_2) and to compare the results with the drugs cytotoxicity determined under low oxygen tension (1% O_2).

2. To determine the role of iron in drugs-mediated cytotoxicity against cancer cells through incubation of ART and DHA for 24h with iron carrying molecule, haemin (1µM and 3µM) and iron chelator deferiprone (DFO) (60µM) at concentrations of these modulators having no toxic impact on cells.

3. To evaluate the effects of ART and DHA on sTfR1 needed for drug and iron endocytosis.

4. Using basis wound scratch and growth irreversibility assays to study anti-invasive and anti-metastatic effects of ART and DHA against cancer cells.

5. To provide characteristics of the proliferation kinetics of both cell lines under different tumour microenvironments (20% vs. 1% O_2).

6. Using ELISA, qPCR, immunocytochemical staining, gel electrophoresis, flow cytometric and Western blotting analyses to indicate the role of pivotal signaling

molecules involved in inflammatory responses (COX-2, IL-6), proliferation and survival mechanisms (survivin, Akt), cell-cell interactions, pro-invasive and metastatic abilities (E-cadherin, CLDN-1, MMP-2 and MMP-9), functions in angiogenesis (VEGF-α, HIF-1α and CA-9) and apoptotic cell death mechanisms (caspase-3, BrDu assay, DNA fragmentation assay).

7. Employing experimental techniques listed above, to elucidate the anti-cancer activities and underlying mechanisms of action of ART and DHA alone and in combination with ASA as a chemo-sensitising agent, in cultured HL-60 and HT-29-AK cells under different oxygen tensions (20% vs. 1% O_2). Because the primary mechanisms of action of ART and DHA and ASA are linked with the inhibition of COX-2 and induction of caspase-dependent apoptosis it was hypothesized that ASA would enhance the cytotoxic effects of ART and DHA.

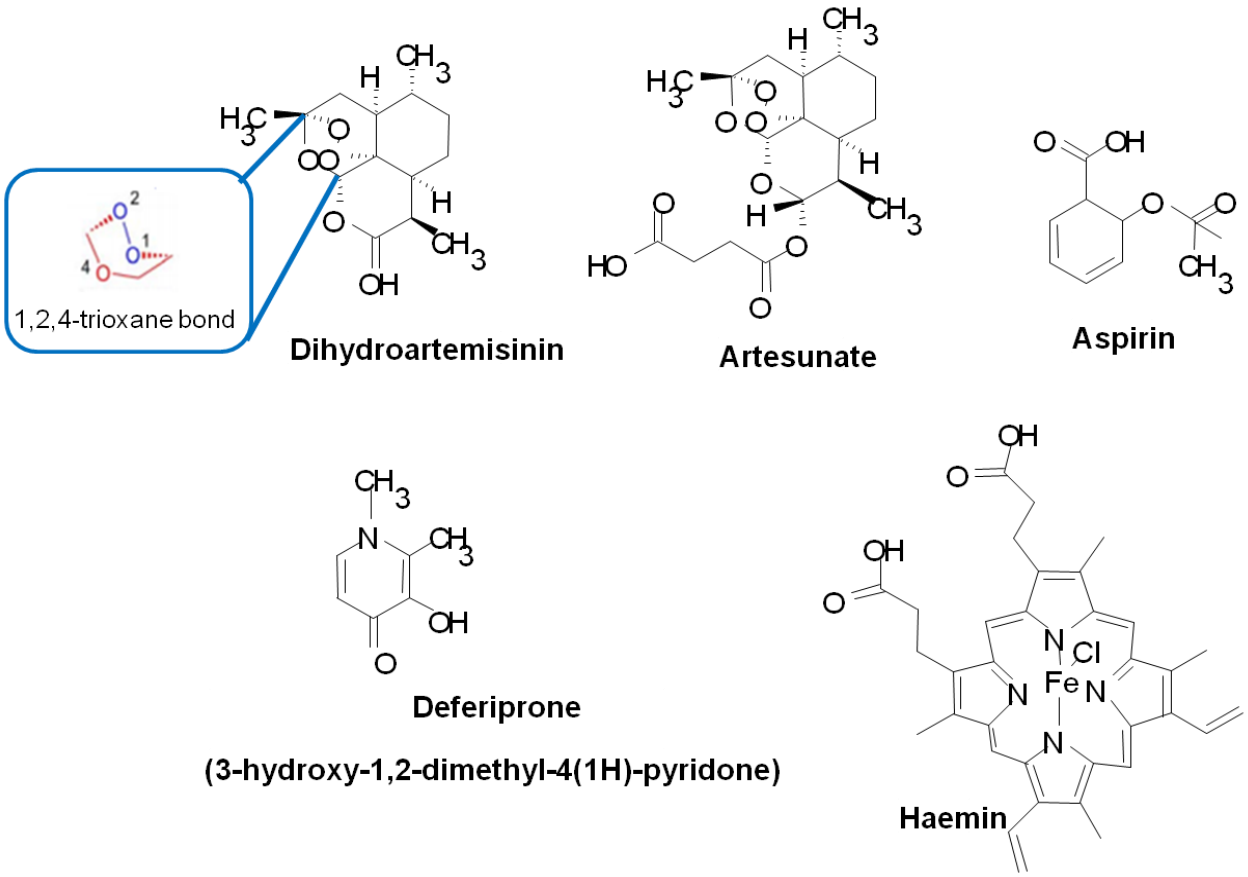

Figure 7: Chemical structures of the test compounds used in this study.

CHAPTER 2

MATERIALS & METHODS

2.1. REAGENTS AND CHEMICALS

ART and DHA were purchased from Dafra-Pharma (Turnhout, Belgium). All the ELISA kits which include human IL-6, human VEGF-α_{165}, human sTfR1 and human total survivin were purchased from R&D Systems (Abingdon, Oxfordshire, UK). The primers for qPCR include CLDN-1, E-cadherin, VEGF-α, survivin and HIF-1α were purchased from Invitrogen (Paisley, Renfrewshire, UK). Monoclonal antibodies against phospho-Akt (Ser473), total-Akt, HIF1-α (anti-human/mouse), MMP-9 (human/mouse) and polyclonal antibody against catalytically active cleaved caspase-3 were obtained from Cell Signaling Technology (Hitchin, Hertfordshire, UK). Primary antibody against CLND-1 (anti-human/mouse) was purchased from Invitrogen (Paisley, Renfrewshire, UK). Anti-hCA9 mouse monoclonal $IgG2_A$ and fluorescein conjugated mouse monoclonal IgG E-cadherin antibodies were purchased from R&D Systems (Abingdon, Oxfordshire, UK). Alexa-conjugated secondary antibody (Alexa Fluor 488 goat anti-mouse IgG H+L) was purchased from Molecular Probes (UK). Stabilised goat anti-rabbit and anti-biotin HRP-conjugated secondary antibodies were purchased from Thermo Scientific Pierce (Rockford, USA). APO-BrdU^{TM} TUNEL Assay Kit was supplied by Life Technologies (Paisley, Renfrewshire, UK). Deferiprone (3-hydroxy-1,2-dimethyl-4(1H)-pyridone, DFO), 3-(4,5-dimethylthiazol-2-yl)-2,5 diphenyltetrazolium bromide (MTT), saponin, sodium azide and all other chemicals and reagents, unless otherwise stated, were from Sigma-Aldrich (Poole, Dorset, UK). Culture plastics were purchased from Thermo Fisher Scientific (Loughborough, UK).

2.2. PROPAGATION OF CANCER CELLS

2.2.1. Cell lines and culture

The cell lines HL-60 (human promyelogenous leukaemic), HT-29-AK (human colorectal carcinoma) and Caco-2 (human epithelial colorectal adenocarcinoma) were obtained from the European Collection of Cell Cultures (ECACC). HL-60 cells were grown in suspension and cultured in RPMI 1640 medium obtained through PAA Cell Culture Company (Cambridge, UK). HT-29-AK and Caco-2 cell lines were maintained as monolayer cultures in MEM (Eagle's, with Earle's salts) medium supplied from PAA Cell Culture Company (Cambridge, UK). All media were supplemented with 10% fetal bovine serum (FBS) (Biosera, Ringmer, UK), 2mM L-glutamine (PAA Cell Culture Company, Cambridge, UK) and 1% antibiotic solution (100 U/ml penicillin, 0.1mg/ml streptomycin) purchased from PAA Cell Culture Company (Cambridge, UK). Caco-2 cells were additionally supplied with 1% MEM non Essential Amino Acids (Bosera, Ringmer, UK) and 1mM sodium pyruvate purchased from Sigma-Aldrich (Poole, Dorset, UK). All of the cells were maintained in the log phase of growth to avoid cell differentiation. For experiments performed under standard culture conditions, cells were grown at 37 °C in humidified atmosphere with the gas phase of 20% O_2, 5% CO_2, 75% N_2 (subsequently reffered to as normoxia). The normoxic conditions were obtained by a humidified incubator NuAire NU-5510/E (Polymouth, USA). For experiments in low oxygen tension (hypoxia), cells were incubated in a humidified Galaxy 48R incubator (New Brunswick Scientific, Cambridge, Cambridgeshire, UK) and flushed with 1% O_2, 5% CO_2, 94% N_2 at 37 °C. The hypoxic incubator was turned on one hour before the culture flasks with HL-60 and HT-29-AK cells were transferred from normoxic conditions (20% O_2) to the experimental conditions of hypoxia (1% O_2) and grown for 72h before any experiments were conducted.

2.2.2. Cell harvesting

The harvesting/collection of cells from tissue culture flasks was performed prior routine passaging, experiment setting up or freezing when cells were pre-confluent (middle-late log phase) observed as 70-80% confluency. Adherent HT-29-AK and Caco-2 cells were harvested by trypsynisation where flasks with cells were removed from incubator and depleted in nutrients medium was discarded by aspiration. Cells were washed twice with 5ml of PBS to remove remaining serum-containing medium and 1ml of proteinase trypsin-(EDTA) (0.1% trypsin/0.04% EDTA in DPBS) was added to the flasks to cover adhering cell layer. Flasks were incubated for 3mins at 37ºC to allow cells to detach. Once sufficiently un-attached, cells were dislodged by gently tapping the bottom of flask and 5ml of pre-warmed complete MEM medium was added to cells to neutralise trypsin. Re-suspended cells in 1:2 or 1:3 dilutions were sub-cultured into new 75cm^2 tissue culture flasks with added 10ml of fresh media and were returned to incubator. Optionally, re-suspended cells in complete MEM medium were transferred from flasks to universal bottles and used for the experimental set-up. Suspension HL-60 cells were harvested by transferring cells from flasks to universal bottles, centrifuged (1200 rpm, 2mins) and depleted in nutrients culture medium was discarded by aspiration. Cell pellets were re-suspended with 10ml of complete RPMI 1640 medium, transferred to fresh 75cm^2 flasks and placed to incubator or cell pellets were used in experiments.

2.2.3. Cell counting

Cell counting involved the use of an electronic counter (NucleoCounter®*,* Chemometec, Allerod, Denmark). Total number of cells in a cell suspension was determined by preparing 50µl medium-suspended cells, adding 50µl of lysis buffer to permeate the plasma membrane of cells, vortexing the mixture and adding 50µl of stabilising buffer to raise the

pH value of the mixture. Aliquot 50µl of the stabilised lysate was drawn into NucleoCassette® being impregnated with propidium iodine staining the nuclei of cells with impaired plasma membranes. The number of cells was automatically determined in the NucleoCounter® and multiplied by dilution factor of 3.

2.2.4. Cryopreservation of cells

The cell lines were stored in liquid nitrogen to keep stocks for long-term storage. Cells were transferred from culture flasks into universal bottles, pelleted by centrifugation *(*1200 rpm, 2mins) and the supernatant was discarded without disturbing the cells. Pellets at a density of at least 10^6cells/ml were re-suspended in 1ml of ice-cold freezing solution containing 10% dimethyl sulfoxide (DMSO) in FBS. Re-suspended cells were transferred into labelled 1,8ml polypropylene cryogenic vials (Fisher Scientific, Loughborough, UK), placed on wet ice during the procedure and transferred to a -80ºC freezer overnight before liquid nitrogen storage at -190ºC.

2.2.5. Recovery of cryopreserved cells

Frozen cells were taken out carefully of the liquid nitrogen and thawed rapidly (<1 min) to decrease the toxic effect on cells by DMSO. Cryovials were first placed in a 37ºC water bath and gently agitated until the cell suspension was thawed. The content of the cryovials was transferred to universal bottles, re-suspended with 5ml of pre-warmed RPMI 1640 or MEM complete growth medium and centrifuged (1200 rpm, 2mins). The supernatant containing freezing solution was discarded and cell pellets were re-suspended in 10ml of appropriate fresh medium prior seeding in 75cm^2 cell culture flasks. Flasks were incubated for 24h (at 37°C, 20% O_2, 5% CO_2, 75% N_2) before medium was exchanged or cells sub-cultured.

2.3. Drug solutions

Stock solutions of ART and DHA were prepared at the concentrations of 0.1, 1.0 10 and 100mM using sterile DMSO at >99% grade (Sigma-Aldrich, UK). ASA was dissolved in DMSO at stock concentrations of 1mM and 10mM. DFO was dissolved in DMSO as a 10mM stock solution, whereas stock solution of 3.5mM haemin was prepared using 0.1M NaOH. The final concentration of DMSO in culture media was less than 0.5%, which excluded the toxic effect by DMSO on cell viability.

2.4. MTT ASSAY

2.4.1. Measurement of cytotoxicity of ART, DHA and ASA

The anti-proliferative effects of ART, DHA against HL-60, Caco-2 and HT-29-AK cells were measured by the 3-(4,5-dimethyl-thizol-2-yl)-2,5-diphenyltetrazolium bromide (MTT) colorimetric assay. As depicted in figure 8, this assay is based on the ability of viable cells to metabolise yellow MTT tetrazolium to form the black formazan crystals by the mitochondrial succinate dehydrogenase. Because it was hypothesized that incubation length has an effect on the potency of test agents, the MTT cytotoxicity assays were performed for 24, 48 and 72h of incubation. All of the cell lines at a density of $1x10^4$cells/well were seeded in 96-well flat-bottomed microtitre plates (Thermo Fisher Scientific, UK). HL-60 cells were treated with varying concentrations of ART or DHA ranging from 0 µM to 100 µM, whereas HT-29-AK and Caco-2 cells were exposed to each compound at concentrations ranging from 0 µM to 750 µM. In similar MTT assay investigations, the cytotoxic effects of ASA (0-60mM) were evaluated against HL-60 and HT-29-AK cells and the results were used in subsequent combination studies. All of the plates were incubated for 24, 48, and 72h at 37°C either under normoxic (20% O_2, 5% CO_2, 75% N_2) or hypoxic (1% O_2, 5% CO_2, 94% N_2)

conditions. After incubation, the assays were terminated by adding 20µl of MTT solution at a working concentration of 5mg/ml to each well and the plates were incubated for additional 2h (at 37°C). At the end of the incubation, 100µl of lysis buffer (15% sodium dodecyl sulfate in 50% N,N-dimethyl formamide) was added to each well. The plates were incubated overnight to dissolve formazan crystals before the optical densities (OD) of the plates were read at 492nm using a plate reader (Anthos Labtech Instruments, Anthos 2001, Salzburg, Austria).

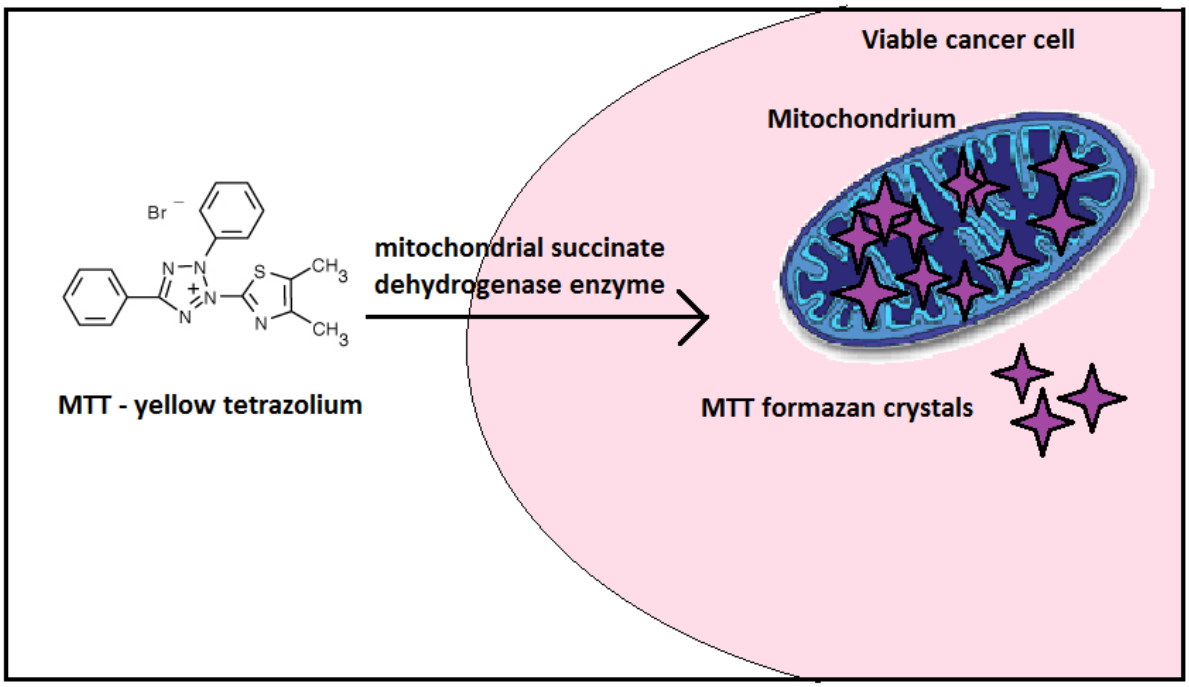

Figure 8: Simplified principle of MTT tetrazolium conversion into formazan crystals. MTT assay is a colorimetric technique where MTT tetrazolium is converted into black formazan crystals by the mitochondrial succinate dehydrogenase being present in highly respiring/living cells. The crystals are dissolved by adding lysis buffer to cells, which destroys their membranes. The absorbance read at 492nm using a plate reader is proportional with the numbers of living cells.

2.4.2. Data analysis

Data were expressed as percentage of control cell growth determined from following a formula:

Percentage of control cell growth = mean absorbance of drug treated wells/ average absorbance of control wells) x 100%.

The IC_{50} values (the 50% growth-inhibition concentrations) of ART, DHA and ASA at each of the incubation periods were estimated from sigmoidal-concentration-response curves of the results by the 4-parametric logistic analysis (Grafit Software, Erithacus, Staines, UK). Based on the results obtained, HL-60 and HT-29-AK cells as being most susceptible to cytotoxic effects of the test agents were used in subsequent investigations. In many of the subsequent experiments described herein, fixed concentrations of the test agents were used based on previously estimated ½IC_{50}, IC_{50} and 2xIC_{50} and etc.

2.4.3. Cytotoxicity of ART and DHA against confluent HT-29-AK cells

To investigate whether inoculums size has effect on the potency of test agents in normoxia (20% O_2), similar MTT assays were performed against confluent HT-29-AK cells. Cells ($1x10^4$cells/well) were seeded in 96-well flat-bottomed microtitre plates and incubated for 72h in normoxia as described above until ~80% confluency was reached. Thereafter, culture medium was discarded and replaced with fresh medium containing varying concentrations (0-750µM) of ART or DHA and incubated for 24h before the assays were terminated and analysed as described above.

2.4.4. Effect of iron on the activity of ART and DHA

The direct role of iron in the activity of ART and DHA against HL-60 and HT-29-AK cells was assessed by MTT assay in normoxia (20% O_2) and hypoxia (1% O_2). Cells were seeded at

$1x10^4$cells/well in 96-well flat bottomed microplates, and treated with varying concentrations (0-750μM) of ART or DHA in the absence or presence of 60μM (¼ the IC_{50} value of the iron chelator DFO measured) of DFO or iron haemin (at 1 μM or 3 μM) for 24h at 37°C. Following incubation, cells were terminated and analysed via Grafit Software as described above. The IC_{50} values for ART and DHA alone and agents in the presence of DFO or haemin were compared.

2.4.5. Cell rate of growth measurements

The proliferation rate of both cell lines under normoxic (20% O_2) and hypoxic (1% O_2) conditions were investigated using MTT assay. HL-60 and HT-29-AK cells ($1x10^4$/well) were seeded in 96-well flat-bottomed microtitre plates and incubated for 0, 24, 48, 72 and 96h at 37°C in normoxia or hypoxia. After incubation, plates were terminated as described previously and the OD was measured at 492nm using a plate reader (Anthos Labtech Instruments, Anthos 2001, Salzburg, Austria). The mean OD values and standard deviations were estimated from at least 3 independent experiments. The mean absorbance values derived from both oxygen tensions were analysed and plotted as ordinate, with incubation period as abscissa via Grafit Software using a linear model.

2.4.6. Irreversibility of cancer cell growth upon ART and DHA treatments

To investigate wheather ART and DHA have the ability to inhibit the re-growth of cancer cells, MTT assay with some modifications was performed. Adherent HT-29-AK cells ($1x10^4$cells/well) were plated in 96-well flat-bottomed microtitre plates, and incubated for 72h in normoxia (20% O_2) without or with ART (at 0μM, 7.22μM, 14.44μM, and 28.88μM) or DHA (at 0μM, 9.88μM, 19.75μM and 39.50μM). Following incubation, some of the plates were terminated as described above. The other plates had their incubation medium

removed and the cells were washed three times in 50µl of drug-free fresh MEM medium. Drug-free fresh MEM medium (100µl) was subsequently added to each well and the plates were incubated for additional 72h before the assays were terminated as above. In the case of HL-60 cells ($1x10^6$ cells/5ml/well), the cells were plated in duplicate into 6-well flat bottomed plates (Thermo Fisher Scientific, UK) and incubated for 72h without or with ART (at 0µM, 0.30µM, 0.60µM and 1.20µM) or DHA (at 0µM, 0.25µM, 0.49µM and 0.98 µM). After incubation, an aliquot of cell suspension from the control or drug-treated samples was transferred into 96-well flat-bottomed microtitre plates and immediately terminated as described previously. The cell suspension remaining in 6-well plates from the drug-treated and control samples was accordingly pelleted by centrifugation (1200rpm, 2mins). The supernatant from each sample was discarded and the pelleted cells were washed three times in drug-free RPMI 1640 medium. Cells were re-suspended in a drug-free fresh RPMI 1640 medium (100µl) and seeded in 6-well flat bottomed plates and left to grow for additional 72h. After incubation cells were plated in 96-well flat-bottomed microtitre plates, terminated and the absorbances read at 492nm as described above.

2.4.7. Combination studies

The microtitre MTT assay was performed to investigate whether ASA modulates the cytotoxicity of ART and DHA against cancer cells under different culture conditions. *C*ells ($5x10^6$ cells/75cm^2 tissue culture flask) were incubated with a fixed concentration of ASA (HL-60 cells under normoxic and hypoxic conditions 2.50mM and 2.21mM, respectively; HT-29-AK cells under normoxic and hypoxic conditions, 6.15mM and 8.47mM, respectively) and incubated for 72h under normoxic (20% O_2) or hypoxic (1% O_2) conditions, respectively. Cells were collected by centrifugation (1200 rpm, 2 mins) and re-suspended in 5ml of fresh culture medium. Cells ($1x10^4$ cells/well) were seeded in 96-well flat-bottomed microtitre

plates and treated without or with varying concentrations of ART or DHA (0-750µM) in the presence of fixed concentrations of ASA as stated above. The plates were incubated for 72h and the assay terminated by adding 20µl of MTT (5mg/ml) followed by a 2 h incubation step at 37ºC. The resultant formazan crystals were solubilised by adding 100µl of lysis buffer to each well and incubating the plates overnight. OD was measured of each plate and data were analysed via Grafit Software as previously.

2.5. ENZYME-LINKED IMMUNOSORBENT ASSAYS (ELISAs)

Enzyme-Linked Immunosorbent Assays (ELISAs) were used to determine the effects of the ART and DHA treatment on the cellular level of sTfR1, IL-6, VEGF-α_{165} and survivin according to the manufacturer's instructions (www.rndsystems.com). HT-29-AK and HL-60 cells ($5x10^6$cells/flask) were incubated for 72h without or with ART and DHA at concentrations determined for normoxic (20% O_2) and hypoxic (1% O_2) experiments. At the end of the incubation periods in both conditions, cells were harvested, washed twice in PBS (2ml) by centrifuged (1200 rpm, 2mins). Aliquot of the cell-free incubation media (1ml) was collected and stored at -20^oC for batch analyses for secreted sTfR1, IL-6 and VEGF α_{165} levels whereas pellets were used for survivin analysis.

2.5.1. The Quantikine® Human sTfR1 immunoassay

For sTfR1 measurements 100µl of sTfR1 assay diluent was loaded into each well of the 96-well plate, followed by the addition of 20µl of standard or thawed culture media. The plate was then incubated at 37ºC for 1h before being washed three times in 400µl wash buffer. Then 100µl/well of sTfR1 conjugate was immediately added to each well and the plate incubated (1h, at 37ºC). The wash step was repeated and 100µl/well of substrate solution was added. The plate was covered in foil to avoid light and further incubated (30 mins, at

37ºC). Stop solution (100µl/well) was added and absorbances at 492nm were measured immediately using a plate reader (Anthos Labtech Instruments, Anthos 2001, Salzburg, Austria).

2.5.2. The Quantikine® Human IL-6 immunoassay

The IL-6 assay was performed by pre-coating each well of the 96-well plate with 100µl of assay diluent followed by the addition of 100µl of standard or thawed sample culture medium. Following incubation (2h, at 37ºC), the plate was washed six times with 400µl wash buffer followed by the addition of 200µl/well of IL-6 conjugate After incubation (2h, at 37ºC), wash step was repeated before 50µl/well of substrate solution was added. The plate was incubated (1h, at 37ºC), followed by the addition of 50µl/well of amplifier solution and incubated (30mins, at 37ºC). Experiment was finished by addition of 50µl/well of stop solution and the plate was read at 492nm.

2.5.3. The Quantikine® Human VEGF-α_{165} immunoassay

Prior VEGF-α_{165} assay, frozen (at -20^{o}C) aliquot of the cell-free incubation medium was defrosted at RT and spun (at 1200rpm, 3mins) to remove cell debris. Assay diluents of 50µl was added to each well of the 96 well plate followed by the addition of 200µl/well of standard or thawed sample culture medium and the plate was incubated for 2h at 37ºC. Plate was washed three times with 400µl wash buffer and 200µl of VEGF-α_{165} conjugate was added to each well before incubation (2h, at 37ºC). After washing plate three times, 200µl of substrate solution (1:1 with colour reagents A and B) was added and plate was incubated in the dark for 25mins. Finally, 50µl of stop solution was added to each well and plate was read at 492nm.

2.5.4. The Quantikine® Human Survivin immunoassay

Pellets ($2x10^6$ cells) were solubilised in 200µl of lysis buffer before the cell lysates were stored at -20ºC and assayed for cellular survivin levels. Thawed samples were centrifuged (2500rpm, 5mins) and the supernatant diluted 2-fold in reagent diluent and assay diluents of 1:1. Standard or diluted sample (100µl/well) was loaded into a 96-well plate and incubated for 2h at 37ºC. After washing the plates three times, 100µl/well of diluted total survivin detection antibody (1:15 dilution with reagent diluent) was added and incubated at 37ºC for 2h. The wash step was repeated and 100µl/well of diluted streptavidin-HRP (1: 200 dilution with reagent diluent) was added and incubated (20mins, at 37ºC). After another wash step, 100µl/well of substrate solution (1:1 with colour reagents A and B) was added and the plate was incubated (20mins, at 37ºC,) in the dark before 50µl/well of stop solution was added and the absorbance read at 492nm.

2.5.5. Data analysis

The absorbances were read within 30mins and the concentrations of sTfR1, IL-6, VEGF-α_{165} and survivin were measured from the standard curve via Grafit Software (Erithacus, Staines, UK).

2.6. REAL-TIME QUANTITATIVE POLYMERASE CHAIN REACTION (RT-qPCR)

Real-time qPCR was used to determine the effects of the drug treatment on the cellular level of E-cadherin, CLDN-1, survivin, HIF-1α and VEGF-α. Cells, ($1x10^6$cells/well) were plated in 6-well sterile culture plates (Thermo Fisher Scientific, UK), treated without or with test agents alone or in combination with ASA at determined concentrations and incubated for 24h and 72h under normoxic conditions (20% O_2). At the end of the incubation periods, cells were harvested and washed twice in PBS.

2.6.1. RNA extraction

Total RNA from cell samples was extracted using Direct-zol RNA MiniPrep kit™ (Zymo Reseach, UK) directly from TRI Isolation Reagent® (Zymo Reseach, UK) according to the manufacturer's instructions (www.zymoresearch.com). Pelleted cells in 1,5 ml eppendorf tubes were homogenised by adding 800µl of the TRI Reagent® to each sample, mixing well by pipetting the mixture up and down and incubating for 5mins at RT. To remove particulates from cell lysates, samples were centrifuged (12000 rpm, 1 min, at 4ºC) and the supernatant (750µl) was carefully transferred into new eppendorf tubes for RNA purification. The same volume of ice-cold 100% ethanol (1:1 of sample homogenate and 100% ethanol) was added to each tube and vortexed. Cleared homogenate of 500µl was transferred into Zymo-Spin IIC Column™ in a Collection Tube, centrifuged (12000 rpm, 1 min, at 4ºC) and the flow-through was discarded. The loading of column with mixture (500µl) was repeated to process the volume of all samples. Samples were then washed with 400µl RNA Wash Buffer before centrifugation (12000 rpm, 1 min, at 4ºC) and the removal of the flow-through. Removal of any genomic DNA contamination was accomplished by adding 80µl of DNase I digestion mix (5µl DNase I (1U/µl), 8µl DNase I Reaction Buffer (10x), 3µl DNase/RNase-Free Water, 64µl RNA Wash Buffer in 80% ethanol) to each column, incubating for 15mins at RT and centrifuged (12000 rpm, 30sec, at 4ºC). Columns were transferred into new Collection Tubes, washed twice with 400µl Direct-zol™ RNA PreWash by centrifugation (12000 rpm, 1 min, at 4ºC) and the flow-through was discarded. Columns were washed with 700µl of RNA Wash Buffer, centrifuged (12000 rpm, 1 min, at 4ºC) and spun for an additional 2 mins in emptied Collection Tubes to ensure residual liquid removal. Columns were carefully transferred into fresh 1.5ml eppendorf tubes with lids cut off to allow tubes fit the centrifuge. Lids were kept sterile. DNase/RNase-Free Water of 50µl was added to

columns matrix and after centrifugation for 1min (12000 rpm, at 4ºC), RNA was eluted and kept on ice for immediate complement DNA (cDNA) preparation and the rest stored at -80ºC.

2.6.2. RNA concentration and quality

The concentration and quality of RNA samples were determined using an NanoDrop™ ND-1000 Spectrophotometer (NanoDrop Technology, Delaware, USA) and/or by Agilent 2100 Bioanalyser electrophoresis system using the Agilent RNA 6000 Pico Chips (Agilent Technologies, USA).

2.6.3. NanoDrop™ ND-1000 Sectrophotometer

The concentration and purity of extracted RNA was first measured using NanoDrop™ ND-1000 Spectrophotometer. After selecting NanoDrop program, machine pedestal was vigorously wiped and initialised using sterile MilliQ water (1µl). Aliquot of each sample (1µl) being kept on ice was sequentially analysed at 260 wavelength. The ratio of absorbances at 260nm and 280nm and at 260 and 230 was used to determine the purity of RNA (A260/A280>1.8; A260/A230>1.8).

2.6.4. Agilent 2100 Bioanalyser

Prior analysis of RNA quality and integrity, sample aliquots were diluted in sterile MilliQ water to final RNA concentration of 5ng/µl and kept on ice. Agilent RNA 6000 Pico reagents were left on bench to equilibrate to RT for 30mins before assay. The electrodes on the bioanalyser were decontaminated before starting and after an assay using electrode cleaner chips filled with RNaseZAP or RNAse-free distilled water, accordingly. Stock of gel matrix was prepared by filtering 550µl in filter column, centrifuged (4000rpm, 10mins), splitted into 65µl aliquots in RNAse-free tubes to be kept on ice for immediate use and the rest stored at

4 ºC. Stock of dye concentrate was vortexed for 10secs, centrifuged (1200rpm, 2mins), and 1µl was added to a 65µl gel-matrix aliquot which was then vortexed, centrifuged (12000rpm, 10mins) and kept on ice covered in foil. Samples and RNA 6000 Ladder (1.2µl) were denatured at 70ºC for 2mins in a heating block and placed on ice. RNA Chip was placed into Chip Priming Station being set at position C and the syringe clip at the top position. Aliquot of 9µl gel-dye mix was gently added into bottom G well, priming station was closed, syringe plunger (1ml location) was push down for 30secs and slowly released. Additional 9µl of gel-dye mix was added to other well marked G and 5µl of RNA 6000 Pico Marker was loaded into the 13 remaining wells of the chip. Denatured samples and ladder aliquots of 1µl were added to assigned wells, vortexed for 1min within vortex mixer, placed in Bioanalyser and run for 30mins using Eukaryote Total Nano Series II assay settings. The observation of the distinct 18s and 28s ribosomal peaks, their ratio (28s/18s) and the degradation in the peaks was used to assess RNA purity of samples. Representative picture of total RNA from cultured HT-29-AK cells upon drug treatment is shown in figure 9.

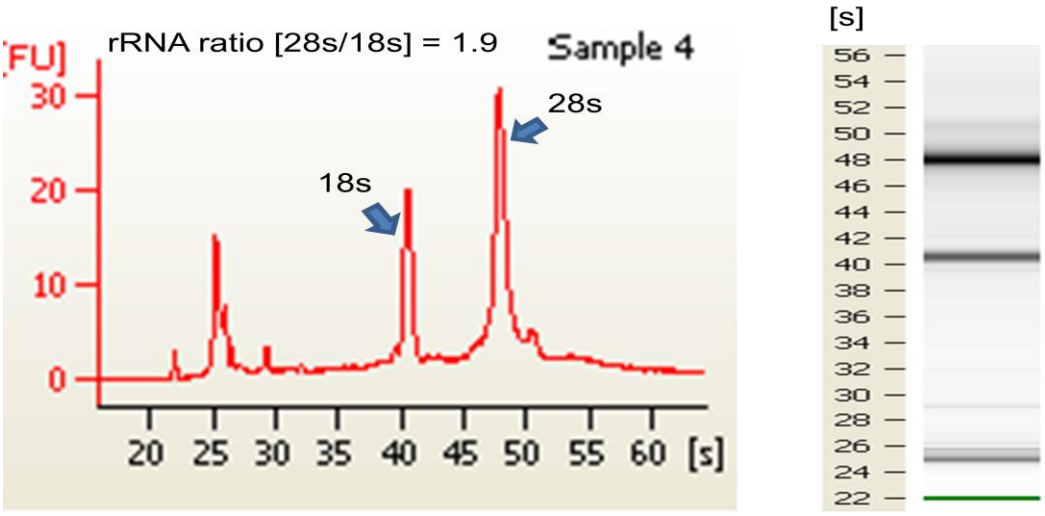

Figure 9: Electrophoretic separation of HT-29-AK cells total RNA upon drug treatment with the Agilent 2100 Bioanalyser using RNA 6000 Pico Chip.

2.6.5. cDNA synthesis

First-strand cDNA was synthesised using Tetro cDNA Synthesis Kit (Bioline, UK) according to the manufacturer's protocol (www.bioline.com). Total RNA for cells untreated and treated with the drug was prepared at 1µg in MilliQ sterile dH_20 to a final volume of 12µl in an RNase-free reaction tube and kept on ice. In a separate tube, the priming premix was prepared on ice containing 4µl Random Hexamer, 4µl dNTP mix (10mM), 4µl Ribosafe RNase Inhibitor, 4µl Tetro Reverse Transcriptase (200U/µl) and 16µl of 5x RT Buffer. Total volume of primer premix (32µl) was gently mixed by pipetting up and down. Primer premix (8µl) was added to each of 4 experimental tubes with 12µl of total RNA from each sample and gently mixed. The final reaction mixture of 20µl in each tube resulted in dilution of RNA to a final concentration of 50ng. The mixture was heated in a Gradient PCR machine (Eppendorf Mastercycler Gradient, UK) to 25ºC for 10mins, 45ºC for 30mins and to 85ºC for 5 mins to denature the reverse transcriptase. The resulting cDNA samples were chilled on ice, proceed to qPCR immediately or stored at -20ºC for long term storage.

2.6.6. qRT-PCR

The generated cDNA was then used as template for qPCR with the 2x SensiFAST™ SYBR Hi-ROX Mix (Bioline, UK) containing the SYBR® Green I dye, dNTPs, stabilizers, enhancers and hot-start Taq polymerase to avoid primer-dimer formation. Reaction primer pairs (forward and reverse) for genomic DNA targets are presented in table 2. ß-actin was used as an internal control for normalisation. Amplification condition for qPCR was performed using Hard-Shell® 96-Well Semi-Skirted PCR plate (Bio-Rad, UK) with a 10µl total reaction volume per each well composed of 5µl SYBR Mix, 0.4µl of each primer (10µM), 1µl cDNA template and 3.2µl MilliQ dH_2O. For each sample, the gene of interest 'target' and gene used for normalisation 'reference' which was β-actin, together with included no template

negative control (MilliQ sterile dH_20 instead of template cDNA) was measured in triplicate. PCR plate was sealed using Microseal® 'B' Adhesive film (Bio-Rad, UK), centrifuged (1200rpm, 30secs, 4ºC) and run on a BioRad CFX Connect Real Time System (Bio-Rad, UK). PCR thermocycling included an initial denaturation step at 95°C for 2mins, followed by 39 cycles of 95°C for 10s, annealing at 55°C for 30s and elongation for at 72°C for 60s. The melting curves of PCR amplicons were obtained with temparatures ranging from 65°C to 95°C with a 0.5°C increase in temperature for 0.05s.

Table 2: Primer sequences for qPCR and expected PCR products (bp).

Gene	Primer sequence (5'→3')	Product (bp)
β-actin	*Forward:* CTG GAA CGG TGA AGG TGA CA *Reverse:* AAG GGA CTT CCT GTA AAC AAT GCA	168
CLDN-1	*Forward:* CTG TCA TTG GGG GTG CGA TA *Reverse:* CTG GCA TTG ACT GGG GTC AT	118
E-cadherin	*Forward:* GGT GCT CTT CCA GGA ACC TC *Reverse:* GAA ACT CTC TCG GTC CAG CC	195
HIF-1α	*Forward:* AAG GTG TGG CCA TTG TAA AAA CTC *Reverse:* GCA TCA GTA GTT TCT TTA TGT ATG	167
Survivin	*Forward:* GTT CTT TGA AAG CAG TCG AG *Reverse:* GCC AGT TCT TGA ATG TAG AG	341
VEGF-α	*Forward:* GAG ATG AGC TTC CTA CAG CAC *Reverse:* TCA CCG CCT CGG CTT GTC ACA T	200

2.6.7. Quality determination of qRT-PCR products

The results of the qRT-PCR amplifications were analysed by a melt curve observation and/or by individual DNA band visualisation on a 2µl ethydium bromide (5mg/ml) stained 2% agarose gel in 50ml sterilised TBE buffer (0.1M Tris base, 0.1M Boric acid and 2.55mM EDTA Na_2 $2H_2O$, pH 8). Briefly, 0.7g of agarose powder (Sigma Aldrich, UK) in 35ml TBE buffer was heated carefully in microwave for 1mins and transferred to water bath (at 55ºC) for 10mins. Resulting 2% agarose gel was impregnated with 2µl ethidium bromide and poured into the gel tank to settle down for 20 mins. Combs forming 8 wells were removed and 50ml of TBE buffer was poured to a tank. The wells were loaded with 10µl of PCR product mixed with 2µl loading dye (6x) and with 3µl of molecular marker GeneRuler 1kb Plus DNA Ladder (Thermo Scientific, Hampshire, UK) in a separate well. DNA bands were separated on a Power-Pac (Bio-Rad, UK) at 50mA for 25 mins and visualised under a UV-light in GEL-DOC Imager (Bio-Rad Laboratories, USA).

2.6.8. mRNA concentration calculations

The mean threshold cycle values (C_t) determined for target genes and reference β-actin were used to calculate ΔC_t (ΔC_t = C_t of the target gene - C_t of the reference gene). The fold change in mRNA expression levels of target genes in drug treated cells as compared to untreated cells were determined using the $2^{-}\Delta\Delta C_t$ method in the following formula *2*-(ΔC_t of drug treated group – ΔC_t of control group). The normalised quantification values were ultimately expressed as relative fluorescence units (RFU) with a normalisation of the relative quantities of all target (gene) expression to the control quantity representing a value of 1.

2.7. IMMUNOCYTOCHEMISTRY STAINING

Immunocytochemistry was performed against adherent HT-29-AK cells to determine the effects of the drug treatment on the cellular localisation and intensity staining of CA-9, E-cadherin and CLDN-1. Cells ($4x10^4$cells/well) were seeded on 19mm glass coverslips in sterile 24-well tissue culture plates (Thermo Fisher Scientific, UK), and immediately treated without or with ART and DHA at specific concentrations before being incubated for 24 and 72h at 37°C in normoxia (20% O_2), respectively. At the end of the incubation periods, cells were fixed using paraformaldehyde method (for CA-9) or ice-cold methanol method (for E-cadherin and CLDN-1).

2.7.1. Paraformaldehyde fixation method and primary antibody staining

In CA-9 staining, cells were fixed by adding 100µl of 37% paraformaldehyde (Sigma Aldrich, UK) to cells with growth medium for 30mins. Thereafter, growth medium-paraformaldehyde mixture was removed and each cover slip was incubated in 500ul of blocking buffer (0.5% BSA and 0.1% saponin in PBS) for 1h at RT followed by incubation with 150µl of CA-9 primary antibody (5µg/1000µl) overnight at 4ºC, in the dark.

2.7.2. Methanol fixation method and primary antibody staining

In E-cadherin and CLDN-1 staining, the growth medium was removed from the wells and cells were washed three times with PBS, fixed in 500µl of 100% ice-cold methanol for 5mins, and incubated in 500µl blocking buffer (0.5% BSA and 0.1% saponin in PBS) for 1h at RT. Coverslips were bound in 250µl of primary antibody (E-cadherin and CLDN-1 antibodies; dilution 1:1000) overnight at 4ºC, in the dark.

2.7.3. Secondary antibody staining and confocal microscopic analysis

After incubation with primary antibodies in paraformaldehyde and methanol fixation methods, cells were washed three times in PBS and incubated with 250µl of the Alexa goat anti-mouse IgG conjugated secondary antibody (Invitrogen, UK) diluted 1:1000 with blocking buffer (0.5% BSA and 0.1% saponin in PBS) for 1h at RT, covered in foil. Coverslips were transferred into glass slides, mounted using DPX Mounting Medium (Fisher Scientific, Loughborough, Leicestershire, UK), and visualised on a confocal microscope (Zeiss LSM 510 META, Germany) at x 200 magnification using green argon laser at 488mn wavelength. Additionally, a He-Ne laser set to 543nm was used for phase contrast pictures acquisition. The objective used was EC Plan-Neofluar 20x/0.50 M27 and the pinhole channel set at 76µm.

2.7.4. Data analysis

The experiments were repeated at least two times and the representative images (from at least 10 images per coverslips) shows the localisation of specific protein in the majority of the cells being analysed by Zeiss laser scanning confocal microscope AIM Software (version 4,2,0,0). The scoring of target protein staining, localisation and intensity frequency was performed first by AIM Software settings optimisation for each fluorescent protein to obtain the highest signal-to-noise ratio followed by stack imaging (x- y- z- axis) and by using intensity frequency tools of AIM Software.

2.8. *IN VITRO* CELL SCRATCH WOUND ASSAY

2.8.1. Scratch wound assay of confluent HT-29-AK cells

For the *in vitro* wound healing assay, HT-29-AK cells ($2x10^6$/well) were seeded in 12-well flat bottomed plates (Thermo Fisher Scientific, UK) and grown for 3-4 days in normoxia

(20% O_2, 5% CO_2, at 37°C) until confluency was reached. At the appropriate time, a wound was created in some, but not all of the wells of the plates, by scrapping across the monolayer using the tip of a sterile 10µl Gilson pipette. The non-adherent cells were carefully removed by washing the wells three times with MEM medium supplemented with 10% FBS. Before cells were treated without or with ART and DHA, the diameter of the wounds of each well was monitored using a light microscope with a digital camera (3.0 Mega CMOS; Resolution 640x480; Premire® Texas, USA), photographed and analysed at four marked field of view per well using the TS view image analysis package (TS View Version 6.12.9). Cells were then incubated (at 37°C, 72h) with 2ml of fresh MEM medium and were treated with the drugs concentrations estimated on confluent cells (ART: 95.31µM, 190.62µM, 381.24 and 953.10µM; DHA 54.27µM, 108.53µM, 217.06 and 434.12µM). After incubation, the number of viable cells was assessed using the tryptan blue dye exclusion assay. Briefly, 50µl of the incubation medium was mixed with 50µl tryptan blue (Sigma Aldrich, UK) composed of 0.4% tryptan blue solution in 0.85% NaCl. An aliquot (~10µl) of this suspension was loaded onto a haemacytometer and counted using a light microscope at 10x magnification (Mazurek, Medilux-12, Southam, Warwickshire, UK). The average of viable cells were counted from four $1mm^2$ squares of a haemocytometer chamber, multiplied by the dilution factor of 2 and multiplied by 10^4 to estimate cell number in 1ml. The rest of the incubation medium containing the non-adherent/dead cells was removed and discarded before the wells were washed three times in fresh drug-free medium, with the wound diameter measured after the second wash. Assays were further incubated for 96h (20% O_2, 5% CO_2, 37°C) in fresh media without or with the test agents in the appropriate wells as before. The viable cell count was repeated using the tryptan blue exclusion assay and the diameter of the wound of each well also measured as described.

2.8.2. Data analysis

The mean number of dead cells and wound diameter were estimated from 2 independent experiments for each drug treatment and plotted against the concentrations of ART and DHA using Grafit Software.

2.9. FLOW CYTOMETRIC ANALYSIS OF PROTEIN LEVELS

2.9.1. Intracellular protein staining

2.9.1.1. Intracellular expression levels of COX-2, CLDN-1, catalytically active caspase-3, phospho-Akt, MMP-2 and MMP-9

To investigate the effects of drug treatment on the intracellular expression levels of proteins, the fluorescence activated cell sorter (FACS) analysis was performed. Cells ($5x10^6$cells/flask) were incubated without or with the drugs alone or in combination with ASA at concentrations described previously for 72h at 37°C in normoxia (20% O_2). After incubation, cells were collected and washed three times in PBS (5ml) by centrifugation (1200rpm for 5min). Cell pellets were fixed by being re-suspended in 250µl of PBS and 250µl of 6% formaldehyde, and incubated for 10mins at 37°C. Samples were then placed on ice for 1 min before being centrifuged (1200rpm, 5min). The cell pellets were blocked for 30 mins in 1ml of ice-cold 90% methanol and later stored at -20ºC for batch analyses. Thereafter, thawed cells were centrifuged at 1200rpm for 5min and the supernatant discarded. The pellets were washed twice in 200µl of incubation buffer (0.5% BSA and 0.1% saponin in PBS; stored at 4ºC) by centrifugation (at 1200rpm for 5min) and blocked for 10min in 100µl of incubation buffer. The cell pellets were collected by centrifugation and re-suspended in 100µl of following antibodies: CLDN-1 (dilution 1:1000), caspase-3 (dilution 1:100), phospho-Akt (dilution 1:100), COX-2 (dilution 1:80), MMP-2 (dilution 1:14) and

MMP-9 (dilution 1:14) and incubated in the dark for 1h. Thereafter, cells were washed in 100µl of incubation buffer and re-suspended in 0.5ml PBS. Finally the cells were transferred into Falcon™ round-bottom polystyrene tubes (Fisher Scientific, UK) and analysed on BD FACS Calibur ® flow cytometer (Becton Dickinson) using the FL-1 channel with an excitation wavelength of 488nm.

2.9.1.2. Intracellular levels of HIF-1α

In order to investigate intracellular levels of HIF-1α, the thawed cell pellets were washed twice in 300µl of Hanks' Balanced Salt Salution (HBSS) by centrifugation (1200rpm, 5min). The pelleted cells were then re-suspended in 0.8 ml of SAP buffer (0.1% saponin, 0.05% NaN_3 in HBSS), centrifuged (1200rpm, 5min) followed by discarding of 600µl of the supernatant from each eppendorf tube. To remaining 200µl of SAP buffer, 10µl of antibody conjugate was added and the samples were incubated in the dark for 45min at 37°C. Subsequently, the samples were washed twice in 0.8 ml of SAP buffer by centrifugation (1200rpm, 5min) before the samples were finally re-suspended in 800µl of PBS samples and analysed by flow cytometer as above.

2.9.2. Cell surface protein staining

2.9.2.1. Cell surface levels of E-cadherin and CA-9

The fluorescence levels of E-cadherin and CA-9 on cell surfaces were measured by terminating the flasks after incubation with/without ART and DHA (as described above) by transferring the content of flasks to labelled universal bottles, centrifugation (1200rpm, 5min) and discarding the supernatant. The cell pellets were then washed three times in 250µl of incubation buffer (PBS supplemented with 0.5% BSA; stored at 4ºC) by centrifugation (1200rpm, 5min) and Fc-blocked using 1µg of anti-human IgG-Fc antibody (abcam®, UK) in

100µl of incubation buffer for 15mins at RT. The pellets were collected by centrifugation (at 1200rpm for 5min), re-suspended in 30µl of E-cadherin and CA-9 antibodies (1:3 dilution) prior to incubation for 45mins at 4ºC. Following incubation, un-reacted antibodies were removed by washing the cells twice in 250 µl of incubation buffer by centrifugation (1200rpm, 5min) and finally the cells were re-suspended in 0.5ml PBS for flow cytometric analysis using 488nm wavelength laser excitation as described previously.

2.9.3. Data analysis

Data were analysed with the CellQuestTM software (Becton Dickinson, USA). The fluorescence of the cells was plotted against a total of 10 000 events and the results were expressed on a logarithmic scale from which relative fluorescence units were measured (RFU). RFU of analysed samples were ultimately normalised where ART, DHA and ASA treated cells were expressed relative to untreated cells (control) representing a value of 1.

2.10. WESTERN BLOTTING

Cells were seeded at a density of $5x10^6$cells into $75cm^2$ tissue culture flasks and treated with ART and DHA for 24h or 72h at 37ºC in normoxia (20% O_2). After incubation, cells were collected by centrifugation (1200rpm, 5mins), washed three times in PBS and proceed to protein extraction.

2.10.1. Extraction of protein from cultured cells

2.10.1.1. Extraction of protein using syringe with a 27-gauge hypodermic needle

The pelleted cells in plastic universal bottles were re-suspended in ice-cold 150µl of protein lysis buffer (100 mM NaCl, 10 mM (pH 7.6) Tris, 1 mM (pH 8) EDTA, 2 mM sodium pyrophosphate, 2 mM sodium fluoride, 2 mM β-glycerophosphate supplemented with

protease inhibitors of phenylmethylsulfonyl fluoride (0.1 mg/ml), 0.1 µg/ml aprotinin and 0.1 µg/ml leupeptin) and placed on ice to prevent denaturation of proteins. Samples were triturated on ice using syringe with a 27-gauge hypodermic needle (Becton Dickinson BD, UK) by pumping twenty times the mixture slowly into the syringe and ejecting with a single vigorous stroke. Samples were incubated on ice for 30 mins. The cell lysates were clarified of cell debris by centrifugation (14000rpm, 30mins, at 4ºC) and supernatant was transferred into new labelled eppendorf tubes. Protein concentration in lysates was measured at 280nm using a Nano-Drop Spectrophotometer (ND-1000 3.3 software, Labtech International, UK). In ratio 1:1, 100µl of cell lysates was mixed with 100µl of sample buffer (100mM Tris-Cl, (pH 6.8), 20% glycerol, DTT 200mM, 0.2% bromophenol blue in 2.5% SDS) and denatured at 95ºC for 10mins before being centrifuged at 4000rpm for 30 sec. Samples were chilled on ice prior electrophoretic separation or stored at -20ºC.

2.10.1.2. Extraction of protein using sonicator

To improve quality and quantity of extracted proteins, collected cells were sonicated with an ultrasonic probe. The procedure was normalised first by preparing the pellet of untreated HL-60 cells in a universal bottle, re-suspending with 900µl of ice-cold lysis buffer and dividing into 6 tubes with equal volume of 150µl cell-lysis buffer mixture and were kept on ice. Tubes were analysed either under earlier established homogenisation method with syringe or under different test conditions prepared for sonication procedure. The optimal procedure of sonication resulted in increased the concentration of proteins by about 3-fold without compromising its quality as compared to extraction using the syringe. Here, tube with cells was placed in a backer with ice and sonicated using an ultrasonic probe for 3 cycles lasting 5secs each with 30secs intervals. Homogenised cells were clarified by centrifugation (14000rpm, 30mins, at 4ºC) and lysates were transferred into new eppendorf

tubes to be quanified as described previously, used in SDS-PAGE electrophoresis or stored at -20ºC.

2.10.2. Sodium dodecyl sulphate-polyacrylamide gel electrophoresis (SDS-PAGE)

Equal amounts of sample protein lysates (60µg/well) prepared in total 20µl volume with sample buffer were separated by SDS-PAGE. 12-well Mini-Protean® TGX Stain-Free™ Any kD™ Precast Gels (Bio-Rad, UK) were placed into an Mini-PROTEAN® electrophoresis tank (Bio-Rad, UK). Approximately 150ml and 500ml of 1x running buffer composed of glycine 14.42g/l, SDS 1.0g/l and Tris 3.0 g/l was poured into the inner and outer chambers of tank, respectively and the gel combs were carefully removed. Samples were loaded to the wells alongside the protein molecular markers, 5µl (10-250kD) Precision Plus Protein™ Kaleidoscope™ (Bio-Rad, UK) and 5µl (9-200kDa) Biotylated Protein Ladder (Cell Signalling Technology, UK). The gel was run for 90min at 130V using Power-Pac 3000 (Bio-Rad, UK).

2.10.3. Transfer to PVDF membrane

Following electrophoresis, gels were removed from glass plates and placed into stain-free tray for Coomassie-like stain-free gel imaging on a Gel Doc™ EZ imaging system (Bio-Rad, UK) to visualise protein separation, ensure equal protein loading across samples and to verify protein transfer before immunoblotting (figure 10A). Transfer stack compromised of 7 layers of filter pads was placed on the bottom of transfer cassette electrode (anode) followed by polyvinylidene fluoride (PVDF) membrane (Trans-Blot® Turbo™ 0.2µm Midi PVDF Transfer Packs,Bio-Rad, UK), gel and second transfer stack on the top of cassette. During the procedure the air bubbles were removed using blot roller, cassette was closed using cassette lid (cathode) and placed into Trans-Blot® Turbo™ Transfer System

(Bio-Rad, UK). Protein bands transfer was conducted for mixed molecular weight settings of 7mins at 55V, 1.3A. Membranes were verified again for quality of protein transfer under Gel Doc™ EZ imaging system (Bio-Rad, UK) with stain-free tray for Ponceau-like stain-free membrane imaging (figure 10 B).

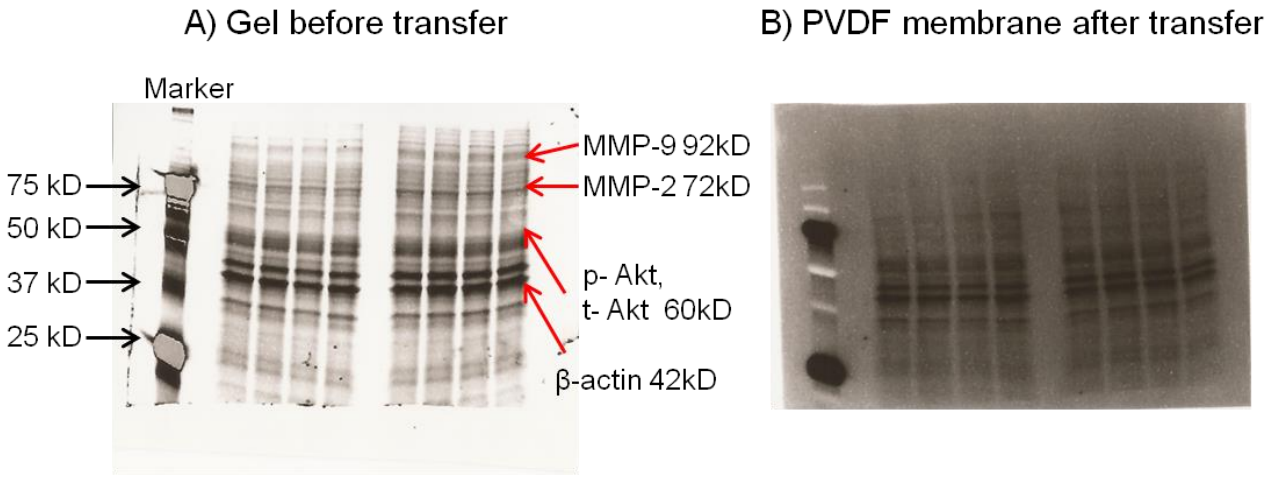

Figure 10: Representative Images of protein transfer and separation using a stain-free Gel Doc™ EZ imaging system (Bio-Rad, UK). Pictures showing A) total protein smears with estimated location of investigated proteins and B) PVDF membrane after protein transfer. MMP-2, matrix metalloproteinase-2; MMP-9, matrix metalloproteinase-9; p-Akt, phospho-Akt; t-Akt, total-Akt.

2.10.4. Immunolabelling and detection

To avoid non-specific binding, membranes were blocked with 25ml of 5% fat-free dry milk in Tris-buffered saline + 0.1% Tween®-20 (TBS/T) and placed on an orbital shaker for 1h at RT. Subsequently, membranes were probed 5ml of pre-titrated primary antibodies (1:1000 dilution) in antibody dilution buffer (0.25g BSA (5%), 0.25g dehydrated Marvel milk in TBS/T), placed on a roller mixer and incubated at 4ºC overnight. Unbound primary antibodies were removed by washing the membrane three times for 5 mins in 10ml TBS/T on an orbital shaker for 1h at RT. Membranes were then probed with 15ml of infra-red goat anti-rabbit IgG and infra-green anti-biotin HRP-conjugated secondary antibody dilutions

(1:7500 dilution), incubated on an orbital shaker for 1h at RT and excess of secondary antibodies was removed were through three washes (5mins/wash) in 10ml TBS/T. Immunodetection was performed using Super Signal® West Femto Maximum Sensitivity Substate chemiluminescent kit (Thermo Scientific Pierce, UK) according manufacturer's instructions and analysed under a UV-light in Chemi-Doc™ MP Imaging System (Bio-Rad, UK).

2.10.5. Membrane stripping and re-probing

Membrane stripping allowed detection of the next protein through removing initially bound antibody without losing the target protein. For total antibody detection, membrane previously probed with phospho antibody were always stripped by boiling the membrane for 5 mins in a glass backer with distilled water, re-blocking in 5% fat-free dry milk in Tris-buffered saline + 0.1% Tween®-20 (TBS/T) for 1h at RT and incubating with the different primary antibody.

2.10.6. Densitometry

The band intensity of samples from at least one experiment was quantified using densitometry software (Quantity One, Version 4.6.3, Bio-Rad Laboratories). β-actin was used as an internal control to ensure equal loading of proteins and additional normalisation between the samples. The procedure involved calculation of ratio between experimental protein intensity and β-actin intensity expressed in percentage, with the controls representing 100%.

2.11. APO-BrdU™ TUNEL ASSAY

APO-BrdU^{TM} terminal deoxynucleotidyl transferase-mediated nick end labelling (TUNEL) Assay (Life Technologies, UK) was used to determine whether ART- and DHA-induced cell death is incorporated with BrdU (5-bromo-2-deoxyuridine), a structural analog of thymidine being present at 3'-OH DNA break sites of apoptotic cells. Cells ($5x10^6$ cells/flask) were incubated in the absence or presence of ART and DHA for 24h or 72h in normoxia (20% O_2) at concentrations stated previously. Following the manufacturer's instructions, culture flasks were terminated and collected cells were re-suspended in 250µl of PBS, fixed in 250µl of 6% formaldehyde at 37°C for 10 minutes and placed immediately on ice for 2 mins. Samples were centrifuged at 1200 rpm for 2mins, before being permeabilised in 1ml of ice-cold methanol (90%) and left on ice for 30 mins. Samples were centrifuged (1200 rpm, 2mins), methanol was aspirated and cells washed twice in 1ml of wash buffer. DNA-labelling solution (50µl) was added and samples were incubated at 37°C for 1h. Samples were rinsed twice in 1ml of rinse buffer and centrifuged (1200 rpm, 2mins). The supernatant was discarded and cells were re-suspended in 100µl of antibody staining solution and incubated in the dark for 30 mins. Propidium iodine/RNase staining buffer (0.5ml) was added to samples and incubated in the dark for 30 mins before the samples were analysed on BD FACS Calibur ® flow cytometer (Becton Dickinson) at 488nm wavelength laser excitation. The principle of APO-BrdU™ TUNEL Assay is presented in figure 11.

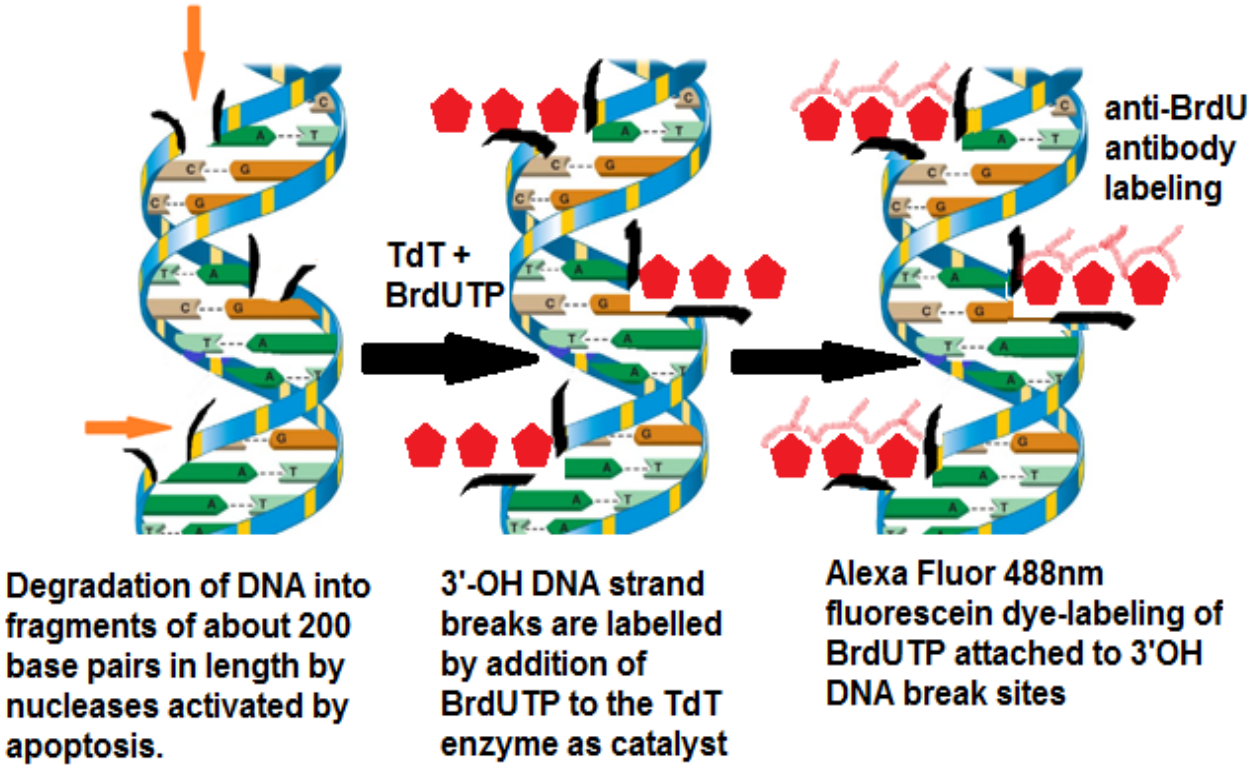

Figure 11: The principle of APO-BrdU™ TUNEL Assay. The determination whereby the drugs-induced cell death is linked with BrdU (5-bromo-2-deoxyuridine), a structural analog of thymidine being present at 3'-OH DNA break sites of apoptotic cells was investigated by flow cytometric analysis. To fixed samples the deoxythymidine analog 5-bromo-2'-deoxyurdine 5'-triphosphate (BrdUTP) and deoxynucleotidyl transferase (TdT) were added resulting in labelling DNA break sites which were detected by staining with anti-BrdU antibody (modified from www.phnxflow.com and www.lifetechnologies.com).

2.12. AGAROSE GEL ELECTROPHORESIS OF DNA

Agarose gel electrophoresis is a method used to separate DNA fragments based on their molecular size. It was performed to evaluate the effects of ART and DHA on DNA fragmentation. Cells (5x10^{6}cells/flask) were treated without or with the drugs and incubated for 72h in normoxia (20% O_2). Cells were collected and re-suspended in 200µl medium and DNA was isolated from samples using the Qiagen kit (Crawley, UK), according to

manufacturer's instructions. The DNA concentration in each sample was measured using Nano-Drop™ ND-1000 Spectrophotometer (ND-1000 3.3 software, Labtech International, UK). Equal amounts of purified DNA (50ng/µl or 70ng/µl) were prepared in total volume of 25µl mixed with 5µl of 6x DNA loading dye. Agarose gel buffer was composed of Tris Base 10.8g, Boric acid 5.5g, EDTA Na_2 H_2O 0.95g filled to 1l with dH_2O; pH 8.0 and sterilised. Agarose powder (Sigma Aldrich, UK) at 0.28g was added to agarose gel buffer aliquots of 35ml and the mixture was heated carefully in microwave oven for 1mins then transferred to water bath (at 55ºC) for 10mins. Agarose gel (0.8%) was impregnated with 2µl ethidium bromide (5mg/ml in dH_2O) and poured into the gel tank to settle down. Combs forming 8 wells were removed and 50ml of agarose gel buffer was additionally poured to a tank. The molecular marker used for DNA fragments size assessment being a α/ Eco 1301 16 or GeneRuler 1kb Plus DNA Ladder (Thermo Scientific, Hampshire, UK) alongside samples were loaded to wells. As a positive control, 50ng/µl or 70ng/µl DNA from a heat-treated control (at 95°C for 20 mins) was used. Samples were separated on a Power-Pac (Bio-Rad, UK) at 50mA for 25 mins and visualised under a UV-light in GEL-DOC apparatus at 366nm.

2.13. STATISTICAL ANALYSIS

Data were expressed as mean ± SD of at least three independent experiments and analysed for normality of distribution using the Shapiro-Wilk test. Statistically significant differences between control and appropriate drug treated samples were determined by the non-parametric Mann-Whitney-U-test and parametric Paired T- test or One Way Anova (Turkey test with multiple comparison or Dunnett test for comparison with control). $P \leq 0.05$ was considered as statistically significant.

CHAPTER 3

RESULTS

PART I: THE ANTI-CANCER ACTIVITY AND MOLECULAR MECHANISMS OF ACTION OF ART AND DHA AGAINST HT-29-AK AND HL-60 CELLS UNDER NORMOXIC CONDITIONS (20% O_2)

3.1. ART and DHA display growth inhibitory activities against HL-60, HT-29-AK and Caco-2 cells *in vitro* under standard normoxic conditions.

The aim of this study was to investigate the anti-cancer effects of ART and DHA, which are two main pharmacologically active metabolites of artemisinin derivatives, against human leukaemia HL-60 and CRC HT-29-AK and Caco-2 cells. Previous reports demonstrate that ART and DHA show anti-cancer effects against different cancer cell types both *in vitro* and *in vivo* (Efferth *et al.* 2002 and 2003; Lu *et al.* 2008). Therefore, the cytotoxicity of ART and DHA was first evaluated against all cell lines in normoxia (20% O_2, 5% CO_2, at 37°C) to identify agreement or to challenge previous experimental reports and to establish ART and DHA concentrations needed in subsequent mechanistic studies. As it was widely reported that 1,2,4-trioxanes exhibit their inhibitory activities in a time- and concentration dependent-manner (Lu *et al.* 2008; Zhou and Wang 2008; Lijuan *et al.* 2010), the cells were exposed to varying concentrations of ART and DHA (HL-60cells at 0-100μM; HT-29-AK and Caco-2 cells at 0-750μM) for 24, 48, 72h. The percentage of viable cells for each drug derived for specific cell line and time point was determined by thiazolyl blue MTT cytotoxicity assay as described in Materials & Methods (Sections 2.4.1. and 2.4.2) The results were then expressed as IC_{50} values (the 50% growth-inhibition concentrations) from sigmoidal-concentration-response curves by the 4-parametric logistic analysis via Grafit Software and

used in the subsequent experimental settings (Materials & Methods, Sections 2.4.1. and 2.4.2).

The results presented in table 3 show that ART and DHA inhibited the growth of all cell lines in a time-dependent manner, with cells being differentially susceptible to the drugs. From IC_{50} values in table 3, it is evident that HL-60, HT-29-AK and Caco-2 cells are most susceptible to the inhibitory effects of the drugs following 72h incubation and are least susceptible to the agents at 24h. Consistently with previous reports (Mercer *et al.* 2007; Hou *et al.* 2008; Lu *et al.* 2008; Zhou and Wang 2008; Lijuan *et al.* 2010), the study shows that ART and DHA are potent but show different inhibitory effects against the different tissue types (leukaemia vs. CRC) (table 3). Human leukaemia HL-60 cells were the most sensitive to ART and DHA while both HT-29-AK and Caco-2 colon cancer cell lines showed reduced susceptibility to drugs (table 3). Moreover, ART and DHA displayed distinct cytotoxic effects not only against different cancer types but also against different malignant differentiation state between cell lines derived from the same origin, gastrointestinal tract. Thus, ART and DHA were more cytotoxic at all incubation time points against well-differentiated CRC HT-29-AK cells in comparison to poorly-differentiated CRC Caco-2 cells (table 3). Prutki *et al.* (2006) reported previously that well-differentiated CRC cells had higher levels of TfR1 (responsible for iron endocytosis), as compared to poorly-differentiated cells. The findings indicate that the TfR1 diversity exhibited by well- and poorly-differentiated cancer cell lines might contribute to different cytotoxic effect of the drugs against HT-29-AK and Caco-2 cells.

Table 3: The effect of ART and DHA against HL-60, HT-29-AK and Caco-2 cells for 24h, 48h or 72h cultured in normoxia. Data points are means ± SD of at least three independent experiments with 18 replicates. ART, artesunate; DHA, dihydroartemisinin; **P<0.01; ***P<0.001

Incubation time (h)	Test agents	Cell lines		
		HL-60	HT-29-AK	Caco-2
		IC_{50} (μM, Mean±SD)		
24	ART	1.96 ± 0.28	165.06 ± 24.25	448.34 ± 59.49
	DHA	0.70 ± 0.12	58.02 ± 4.09	213.04 ± 24.47
48	ART	0.71 ± 0.15***	64.61 ± 6.61***	319.45 ± 62.10***
	DHA	0.65 ± 0.09	38.28 ± 2.44***	167.69± 17.72***
72	ART	0.60 ± 0.08***	14.44 ± 2.64***	42.13 ± 9.61***
	DHA	0.49 ± 0.03**	19.75 ± 1.07***	76.42 ± 8.14***

The inhibitory effects against cancer cells were further drug specific. DHA displayed the most potent activity against HL60 cells with IC_{50} values of 0.70 ± 0.12μM, 0.65 ± 0.09μM and 0.49 ± 0.03μM, as compared to ART values of 1.96 ± 0.28μM, 0.71 ± 0.15μM and 0.60 ± 0.08μM for 24, 48 and 72h incubations, respectively (table 3). After 72h where both drugs were most potent, DHA with an IC_{50} value of 0.49 ± 0.03μM was ~1.22 fold more potent (P<0.001), as compared to ART with an IC_{50} value of 0.70 ± 0.124μM (table 3). The concentration-response survival curves in figure 12 show that the cells are most susceptible to the inhibitory effects of the drugs at 72h, being least susceptible to the agents at 24h.

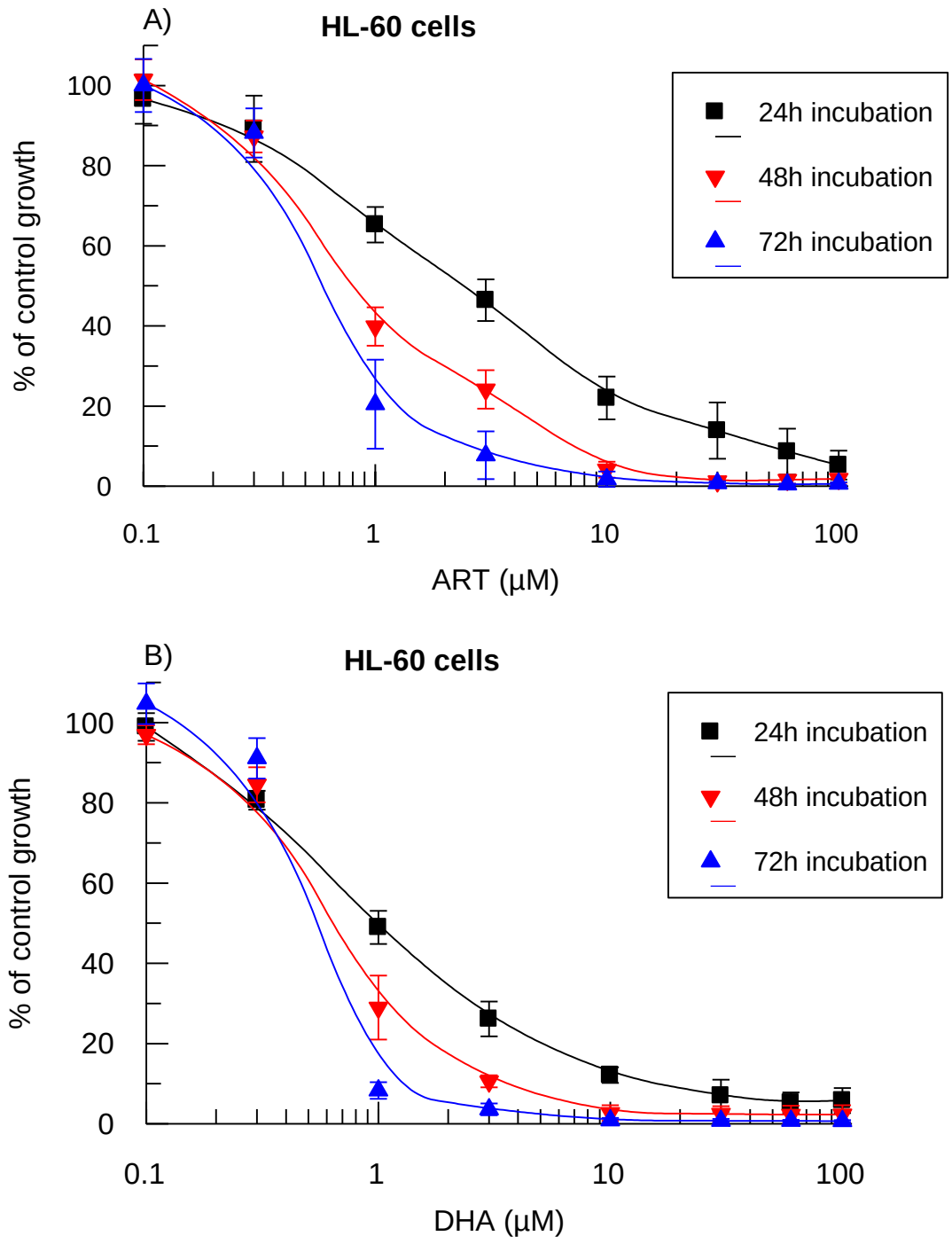

Figure 12: Concentration- and time-response effects of ART and DHA on the growth of HL-60 leukaemia cancer cells cultured in normoxia for 24-72h. The MTT assay was performed by treating HL-60 cells with varying concentrations (0-100µM) of A) ART and B) DHA for 24, 48, and 72h in normoxia (20% O_2) as described in Materials & Methods (Sections 2.4.1. and 2.4.2). Data points are means ± SD of at least three independent experiments with 18 replicates; ART, artesunate, DHA, dihydroartemisinin.

Similar observations were reported between ART and DHA against HT-29-AK and Caco-2 cells (table 3). The inhibitory profile of the agents against well-differentiated HT-29-AK cells over the incubation periods were as follows: ART, 165.06 ± 24.25µM, 64.61 ± 6.61µM and 14.44 ± 2.64µM at 24h, 48h and 72h, respectively (table 3). DHA significantly inhibited the growth of the cells resulting in IC_{50} values of 58.02 ± 4.09µM, 38.28 ± 2.44µM and 19.75 ± 1.07µM for 24, 48 and 72h incubation, respectively (table 3). DHA displayed a significant ($P< 0.001$) cytotoxic activity against HT-29-AK cells over ART for 24h (58.02 ± 4.09µM vs. 165.06 ± 24.25µM) and 48h (1.69~fold; 38.28 ± 2.44µM vs. 64.61 ± 6.61µM). In contrast, ART after 72h incubation was significantly ($P< 0.001$) more cytotoxic as compared to DHA (14.44 ± 2.64µM vs. 19.75 ± 1.07µM. The concentration-response curves for ART and DHA against HT-29-AK cells after 24, 48 and 72h incubation are shown in figures 13A and 13B.

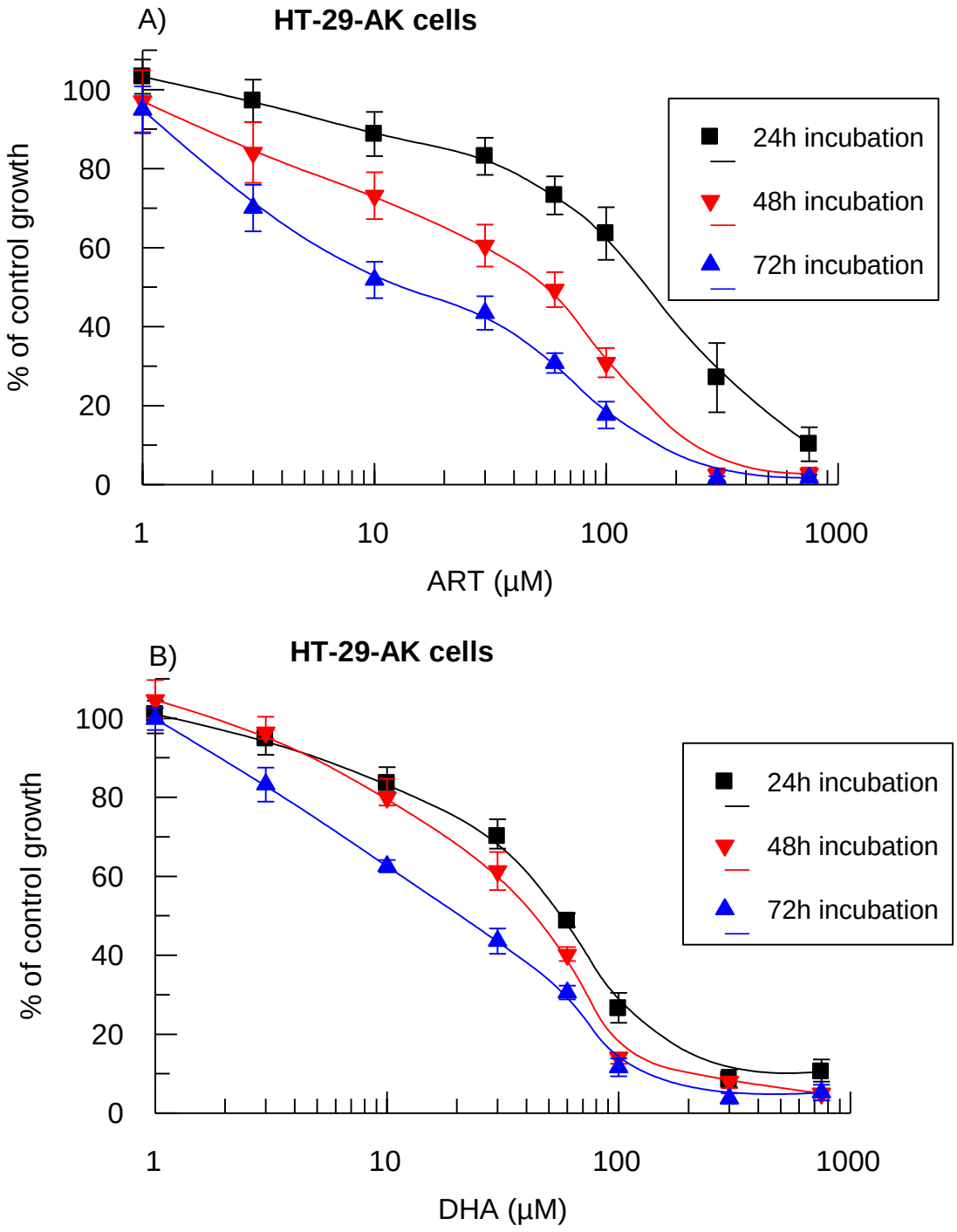

Figure 13: Concentration- and time-response effects of ART and DHA on the growth of HT-29-AK CRC cells cultured in normoxia for 24-72h. The MTT assay was performed by treating HT-29-AK cells with varying concentrations (0-750µM) of A) ART and B) DHA for 24, 48 or 72h in normoxia (20% O_2) as described in Materials & Methods (Sections 2.4.1. and 2.4.2). Data points are means ±SD of at least three independent experiments with 18 replicates; ART, artesunate, DHA, dihydroartemisinin.

In poorly-differentiated Caco-2 cells, ART inhibitory activities were as follows: 448.34 ± 59.49µM, 319.45 ± 62.10µM and 42.13 ± 9.61µM after 24h, 48h and 72h, respectively (table 3). DHA was more potent over ART after 24h and 48h resulting in IC_{50} values of 213.04 ± 24.47µM, 167.69 ± 17.72µM respectively (table 3). Following 72h, DHA was less potent than ART with cytotoxic activity against Caco-2 cells of 76.42 ± 8.14µM (table 3). The concentration-response curves for ART and DHA against Caco-2 cells after 24, 48 and 72h incubation are shown in figures 14A and 14B.

Due to relatively low activity of ART and DHA against Caco-2 cells, in the subsequent experiments HL60 cells and HT-29-AK cells were investigated. Having acquired the IC_{50} of the agents alone, the mechanistic basis of the effects of the drugs were evaluated at three selected concentrations based on their ½IC_{50}, IC_{50} and 2xIC_{50} obtained under that experimental condition.

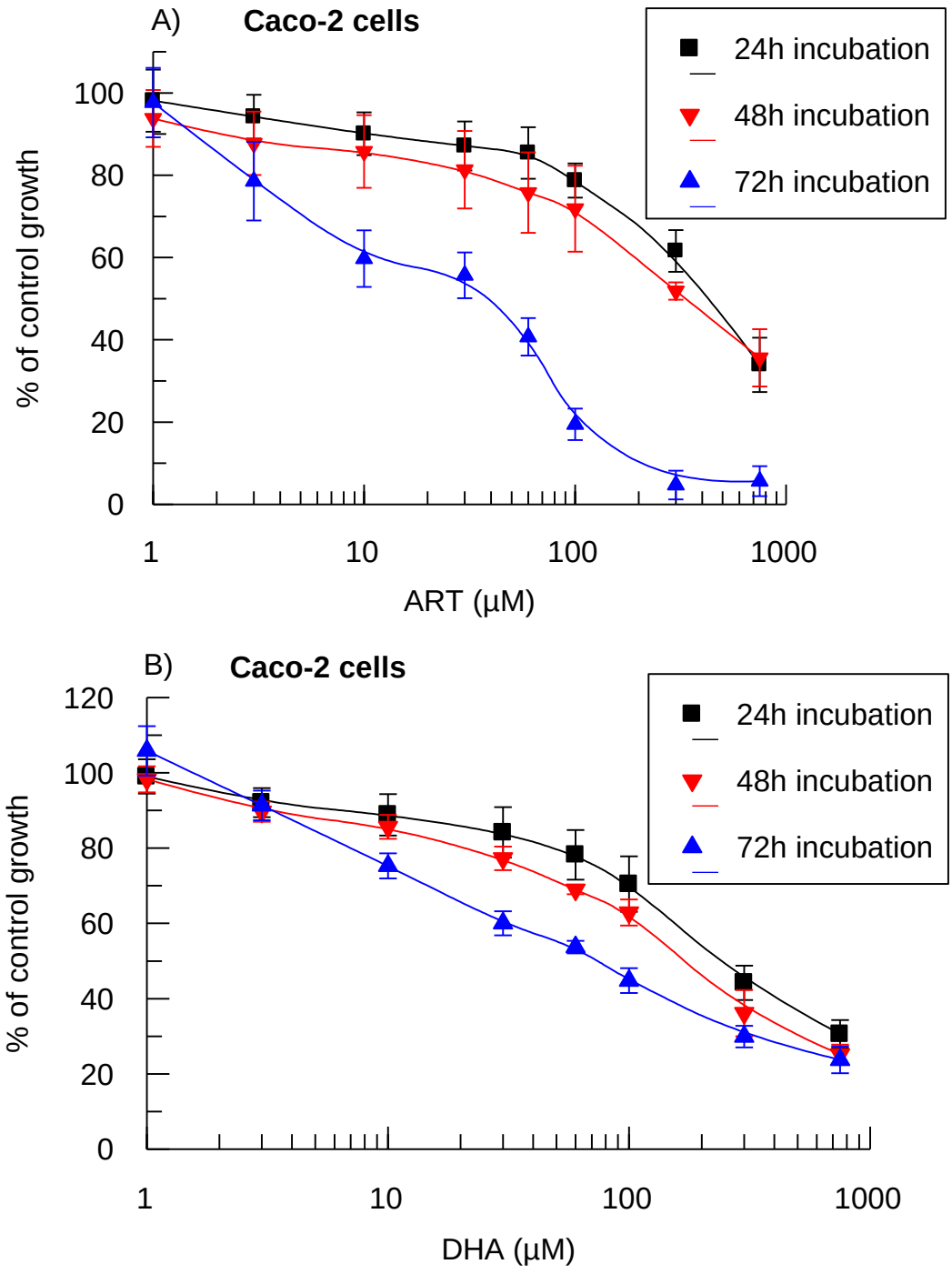

Figure 14: Concentration- and time-response effects of ART and DHA on the growth of Caco-2 CRC cells cultured in normoxia for 24-72h. The MTT assay was performed by treating the cells with varying concentrations (0-750µM) of A) ART and B) DHA for 24, 48 or 72h in normoxia (20% O_2) as described in Materials & Methods (Sections 2.4.1 and 2.4.2). Data points are means ±SD of at least three independent experiments with 18 replicates; ART, artesunate, DHA, dihydroartemisinin.

3.2. Cytotoxicity of ART and DHA against HT-29-AK is dependent on the proliferation state of the cells.

ART and DHA are reported to gain selectivity by targeting cancer cells, which have a high expression of TfR1 for iron absorption (Jiao *et al.* 2007; Zhao *et al.* 2013). Cellular iron is required to sustain unlimited and fast proliferation of cancer cells (Mercer *et al.* 2007; Oh *et al.* 2009; O'Neill *et al.* 2010). In addition, ART and DHA contain an endoperoxide bridge, which reductive cleavage by iron is a necessary prerequisite in their cytotoxicity (Mercer *et al.* 2007). It was reported previously that the effectiveness of some chemotherapeutic agents, which target highly proliferating cancer cells is decreased at highly hypoxic regions of tumour (Rustum *et al.* 2010). This is linked with the disproportional and incomplete vasculature in hypoxic tumours (Bhattacharya *et al.* 2004; Rustum *et al.* 2010; Goel *et al.* 2011). Disfunctional vasculature results in areas of lower rate of cancer cell proliferation, therefore, decreased effectiveness of some anti-cancer agents which target only highly proliferating cancer cells (Bhattacharya *et al.* 2004; Rustum *et al.* 2010; Goel *et al.* 2011). Remaining alive hypoxic cells enhance tumour aggressiveness through inhibition of cancer cell death which has been shown experimentally to be associated with development of therapeutic resistance and cancer recurrence (Milosevic *et al.* 2012; [b]Cho *et al.* 2013; Chen *et al.* 2014; Dekervel *et al.* 2014). Therefore, the potential of ART and DHA to preferentially kill rapidly proliferating cancer cells led to a question whether ART and DHA have the ability to target the relatively slow-proliferating cancer cells, which might cause treatment failure.

In this experiment, we explored the effects of ART and DHA against well-differentiated HT-29-AK cells ($1x10^4$cells/well) which were seeded first in 96-well flat-bottomed microtitre plates for 72h allowing the cells to reach ~80% confluency. Culture media was discarded and fresh media without/with ART and DHA (0-750µM) was added for 24h and the plates were

terminated and analysed as described in Materials & Methods (Section 2.4.3). As shown in table 4, the cytotoxicity of ART and DHA might be partly dependent on the proliferation state of cells at the time of the experiment. The confluent cells were less susceptible to the cytotoxic effects of ART and DHA compared to cells treated at t_0 (table 4). Treatment of confluent cells with DHA significantly ($P<0.001$) decreased the IC_{50} of DHA compared to their counterparts treated at t_0 (~1.87-folds; 108.53 ± 19.68 µM vs. 58.02 ± 4.09µM). In contrast to DHA, the cytotoxicity of ART was less affected by confluent HT-29-AK cells when compared to highly proliferating cells at t_0 (~1.15-folds;190.62µM vs. 165.06 ± 24.25µM; table 4). These results suggest that ART might more selectively and effectively target quiescent cancer cells within heterogeneic tumour interior as compared to DHA. The ability of ART to selectively kill the rapidly proliferating and the relatively slow dividing cells may be a promising therapeutic approach to improving survival of CRC patients. However, there were insufficient repeats done under confluent cell conditions to allow statistical analyses.

Table 4: The effect of ART and DHA against HT-29-AK cells, at time 0h and confluent cells, cultured in normoxia for 24h. Data points are means ± SD of at least three independent experiments with 18 replicates. ART, artesunate; DHA, dihydroartemisinin; ***P<0.001

	Test agents	State of cells used for experiments	HT-29-AK
			IC_{50} (µM, Mean±SD)
Incubation 24h	ART	highly proliferating cells at 0h	165.06 ± 24.25
	DHA		58.02 ± 4.09
	ART	confluent cells at 72h	190.62
	DHA		108.53 ± 19.68***

3.3. Cytotoxicity of ART and DHA against HL-60 and HT-29-AK cells is iron-dependent.

As iron is central to the activity of 1,2,4-trioxanes (Efferth 2005; O'Neill *et al.* 2010; Handrick *et al.* 2010; Rasheed *et al.* 2010; Ba *et al.* 2012), the role of iron (at 1 and 3µM haemin) and iron chelator DFO (at 60µM) in the anti-cancer activity of the drugs was evaluated. Data presented in table 5 show that DFO antagonised the activity of ART and DHA in both cell lines. ART in the presence of DFO was significantly ($P<0.001$) less cytotoxic against HL-60 cells compared to ART alone (IC_{50} of 29.5 ± 5.56 µM vs. 1.96 ± 0.28µM). Similarly, ART in the presence of DFO was significantly ($P<0.001$) less cytotoxic against HT-29-AK cells compared to ART alone (IC_{50} of 271.63 ± 10.49µM vs. 165.06 ± 24.25µM). DHA in the presence of DFO showed a significant ($P<0.001$) reduction in cytotoxicity against cells, respectively as compared to DHA alone (table 5). In contrast, haemin enhanced the cytotoxicity of the agents against both cell lines (table 5). HL-60 cells treated with ART and DHA in the presence of 1µM haemin showed a 60% ($P<0.001$) and 12.86% increase in cytotoxicity as compared to the drugs alone, respectively. Haemin (at 3µM) significantly ($P<0.001$) enhanced the activity of ART and DHA against HL-60 cells by 67% and 40%, respectively. A similar effect was observed against HT-29-AK cells where 1µM haemin increased the anti-cancer effects of ART by ~7.8% and DHA by ~24% ($P<0.001$). Haemin (at 3µM) increased cytotoxicity of ART by ~17.5% ($P<0.01$) and DHA by ~42% ($P<0.001$), as compared to the drug alone, respectively (table 5).

Table 5: The effect of ART and DHA alone and in the presence of deferiprone, DFO (60µM) and haemin (1µM or 3µM) against HL-60 and HT-29-AK cells for 24h cultured in normoxia. Data points are means ± SD of at least three independent experiments with 18 replicates. ART, artesunate; DHA, dihydroartemisinin; DFO, deferiprone. **P<0.01; ***P<0.001

	Test agents	HL-60	HT-29-AK
		IC_{50} (µM, Mean±SD)	
Incubation time 24h	ART	1.96 ± 0.28	165.06 ± 24.25
	DHA	0.70 ± 0.12	58.02 ± 4.09
	ART + DFO (60µM)	29.50 ± 5.56***	271.63 ± 10.49***
	DHA + DFO (60µM)	9.25 ± 1.20***	294.88 ± 31.97***
	ART + 1µM haemin	0.78 ± 0.08***	152.16 ± 12.75
	DHA + 1µM haemin	0.61 ± 0.04	43.90 ± 4.65 ***
	ART + 3µM haemin	0.65 ± 0.03***	133.49 ± 12.02**
	DHA + 3µM haemin	0.42 ± 0.03***	33.43 ± 1.61***

3.4. ART and DHA altered the secretion of sTfR1 in HL-60 and HT-29-AK cells in normoxia

Our previous experiments indicate that the availability of iron plays a pivotal role in the cytotoxicity of ART and DHA (table 5). Numerous reports demonstrate that ARTand DHA target selectively cancer cells, which have a high expression of the membrane TfR1 for enocytosis-mediated iron uptake (Jiao *et al.* 2007; Zhao *et al.* 2013). There are increasing reports showing that ART and DHA decrease expression of TfR1, thus resulting in diminished iron homeostasis through inhibiting iron endocytosis needed by cells to proliferate (Zhou *et al.* 2008; Ba *et al.* 2012 Zhao *et al.* 2013). TfR1 protein is proteolytically released from the surface of cells as a soluble protein through a highly regulated process known as ectodomain shedding (Hayashida *et al.* 2010). As a soluble form of TfR1 (sTfR1) in the incubation media is a quantitive marker of cell surface TfR1 *in vitro* (R'zik and Beguin

2001). Here, ELISA was performed to analyse the effect of ART and DHA treatment on sTfR1 concentrations in cell culture supernatants collected from HT-29-AK and HL-60 cells. For comparison purposes, culture supernatants from DHA-treated cells were collected at two different incubation time points (24h vs. 72h) and analysed as described in Materials & Methods (Section 2.5.1).

As can be seen in figure 15 A, there were measurable levels of sTfR1 equivalent to 3.40 nmol/L in ART-untreated HT-29-AK cells after 72h incubation. As compared to control (3.40nmol/L), sTfR1 levels in HT-29-AK cells treated at 7.22µM ART were increased by ~18.24% (4.02nmol/L). The levels of sTfR1 for ART-treated cells at 14.44µM and 28.88µM were lower than the lowest concentration of standard (< 3nmol/L).

DHA (at 29.01µM) upon 24h incubation resulted in a marked decrease in sTfR1 levels by ~75.66% (1.76nmol/L vs. control with 7.23 nmol/L) (figure 15A). High concentrations of DHA at 58.02µM and 116.04µM resulted in increased sTfR1 levels by ~2.15-fold (~114.52%, 15.51nmol/L) and ~2.87-fold (~186.86%, 20.74 nmol/L), respectively, as compared to control (7.23 nmol/L) (figure 15A). After 72h incubation, DHA-untreated cells showed a sTfR1 concentration of 1.84 nmol/L, which was increased by ~8.15% (1.99nmol/L) upon treating the cells with 9.88µM DHA. In contrast, the levels of sTfR1 for DHA-treated cells at 19.75µM were decreased by ~59.78% (0.74 nmol/L) and below limit of detection at 39.50µM DHA, respectively, as compared to control (figure 15A).

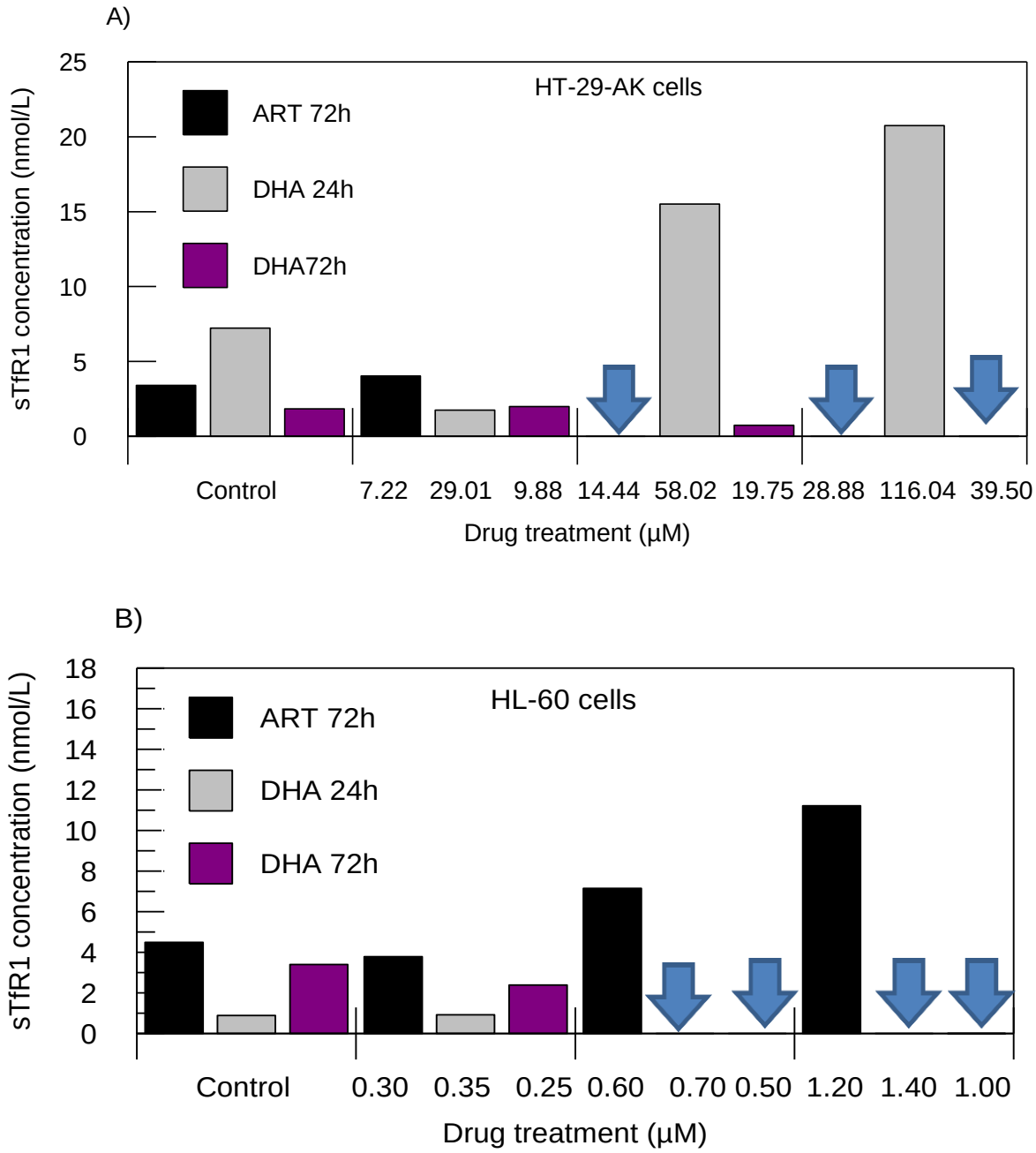

Figure 15: The secretion levels of sTfR1 in cancer cells upon ART and DHA treatments in normoxia. A) HT-29-AK and B) HL-60 cells were treated with the test compounds for 24h and 72h under normoxic conditions (20% O_2), before the cell-free incubation media were analysed for sTfR1 secretions by ELISA (Materials & Methods, Section 2.5.1). The histograms for ART-treated cells for 72h (black bars), DHA for 24h (grey bars) and DHA for 72h (purple bars) represent 2 independent experiments which are not powered to perform statistical analysis. Blue arrow indicates sTfR1 secretions below the limit of detection (< 3 nmol/L). ART, artesunate; DHA, dihydroartemisinin.

For comparison purposes similar investigations were performed for HL-60 cells treated with ART and DHA (figure 15B). Following 72h of incubation, ART-untreated HL-60 cells displayed sTfR1 concentration of 4.49 nmol/L which was decreased by ~15.37% (3.79 nmol/L) upon treating the cells at 0.30µM ART (figure 15B). HL-60 cells treated with 0.60µM and 1.20µM ART increased sTfR1 concentrations by 59.24% (7.15nmol/L) and ~2.50-folds (~149.67%; 11.21 nmol/L), as compared to control (4.49 nmol/L) (figure 15B).

As depicted in figure 15B, DHA-untreated cells following 24h incubation showed a sTfR1 concentration of 0.89nmol/L, which was increased slightly by ~3.37% (0.92nmol/L) at 0.35µM DHA. HL-60 cells treated with DHA at higher concentrations of 0.70µM and 1.40µM DHA resulted in sTfR1 concentrations being below the limit of detection. Inhibition of sTfR1 continued with prolonged incubation of HL-60 cells with DHA. This led to a 30% reduction (2.38 nmol/L) in sTfR1 with 0.25µM DHA and observed sTfR1 levels below the limit of detection with 0.50µM and 1.00µM DHA, respectively, as compared to control (3.40 nmol/L) (figure 15B).

Overall, ART and DHA have the ability to decrease sTfR1 secretions in HL-60 and HT-29-AK cells but this inhibition is strongly compound- and cell line- dependent (figure 15). When ART-treated HT-29-AK cells for 72h decreased sTfR1 secretions, ART against HL-60 cells for 72h increased sTfR1 concentration levels (figure 15). Similarly, DHA-treated HT-29-AK cells after 24h incubation markedly up-regulated the secretions of sTfR1 while DHA-treated HL-60 cells for 24h decreased sTfR1 levels (figure 15).

3.5. DHA altered the secretion of IL-6 in HL-60 and HT-29 cells in normoxia.

There is evidence that TfR1 expression is regulated by pro-inflammatory cytokines, including IL-6, which is strongly associated with CRC development and progression (Han *et al.* 1997; Chalaris *et al.* 2011; Harel *et al.* 2011). Experimental reports show that ART and DHA exert potent anti-inflammatory properties through the inhibition of pro-inflammatory cytokines, including IL-8 and IL-1β (Xu *et al.* 2007; Wu *et al.* 2010; Wang *et al.* 2011). Additionally, high IC_{50} values for ART and arteether correlated with high IL-6 signal transducer expression ($P<0.05$), thus showing potential impact of IL-6 on anti-cancer effects of 1,2,4-trioxanes (Anfosso *et al.* 2006).

Here, we wanted to evaluate if the effects of DHA on IL-6 secretion levels in HT-29-AK and HL-60 cells are time-dependent. Investigations were carried out at 24h and 72h using ELISA (Materials & Methods, Section 2.5.2).

As compared to control (0.16pg/mL), DHA at 29.01µM following 24h incubation in HT-29-AK cells did not alter IL-6 secretion levels (~0.30 fold; 0.18pg/mL) whereas the highest DHA concentration at 116.04µM had increased IL-6 secretions (~0.85 fold; 0.51pg/mL) (figure 16A). In contrast, middle DHA concentration (58.02µM) representing DHA IC_{50} value at this time point resulted in IL-6 secretions being below than the lowest concentration of standard (< 0.039pg/mL) (figure 16A). Similar pattern was observed with HT-29-AK cells after 72h (figure 16A). There was a ~1.6-fold (0.16pg/mL) and ~4.4-fold (0.44pg/mL) increase in IL-6 secretions upon treating the cells with 9.88µM, and 39.50µM of DHA, as compared to control (0.1pg/mL), respectively (figure 16A). However, IL-6 secretion with 19.75µM DHA (DHA IC_{50} value at this time point) was below the limit of detection (figure 16A).

In HL-60 cells after 24h, DHA (0.35µM) significantly (P<0.001) decreased IL-6 levels by ~2.75-fold (0.04pg/mL), as compared to control (0.11pg/mL; figure 16B). The levels of IL-6 concentrations were undetected with 0.70µM DHA (< 0.039pg/mL) and up-regulated with 1.40µM DHA (~7.55-fold, 0.83pg/mL), as compared to control (0.11pg/mL; figure 16B). Similar pattern was observed against HL-60 cells treated for 72h (figure 16B). DHA (at 0.25µM) markedly decreased IL-6 levels by ~2.38 fold (0.08pg/mL) whereas the levels of IL-6 were below the limit of assay detection (< 0.039pg/mL) with 0.50µM of DHA (figure 16B). An increased (~2.42-fold) secretion of IL-6 was observed with highest concentration of DHA (at 1.00 µM), as compared to control (0.19pg/mL) (figure 16B).

The results show that DHA exhibited a dual response on IL-6 secretion levels in HT-29-AK and HL-60 cancer cells, i.e. the levels of IL-6 were below limit of detection at the middle DHA concentrations and an increase of IL-6 was measured at the highest DHA concentrations. The undetected levels of IL-6 with DHA at IC_{50} (middle) concentrations might possibly relate to the specific unknown mechanisms of action of DHA in both cell lines.

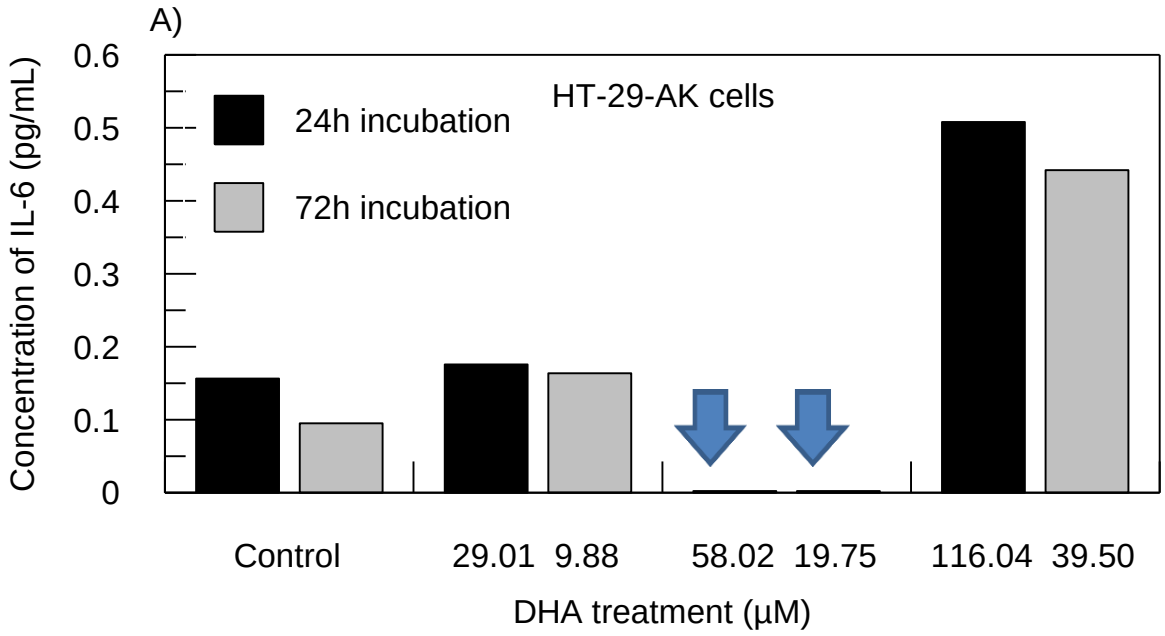

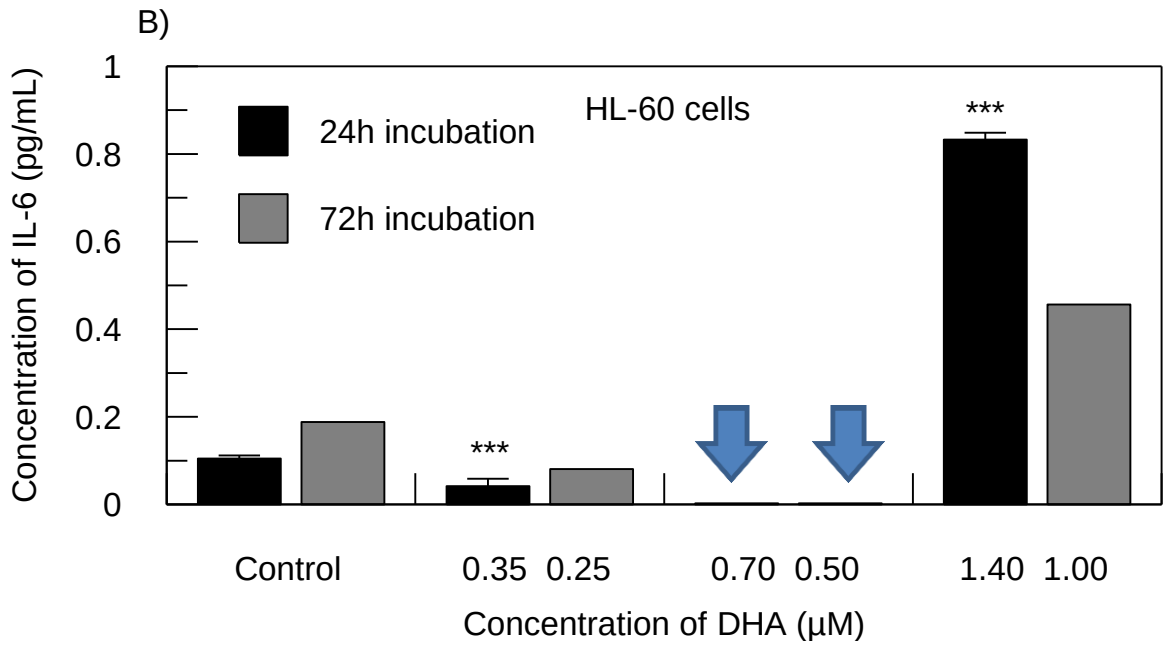

Figure 16: The secretion levels of pro-inflammatory cytokine IL-6 in cancer cells upon DHA treatment at 24h and 72h in normoxia. A) HT-29-AK and B) HL-60 cells were treated with DHA for 24h (black bars) and 72h (grey bars) under normoxic conditions (20% O_2), before IL-6 secreted into the culture media was measured by ELISA as described in Materials and Methods (Section 2.5.2). Blue arrow indicates IL-6 secretions below the limit of detection (< 0.039pg/mL). Data for DHA-treated HL-60 cells for 24h represent the mean ± S.D. of three independent experiments. ***P<0.001 as tested by Paired T test. Other results represent 2 independent experiments and are not powered to perform statistical analysis. DHA, dihydroartemisinin.

3.6. ART and DHA down-regulated intracellular protein levels of COX-2 in HT-29-AK cells in normoxia

Increasing reports show that the anti-cancer effects of ART and DHA in solid tumours are attributed to the inhibition of pro-inflammatory COX-2 protein, which is implicated clinically in enhanced mortality rates in patients and the development of chemo-resistance (Wang *et al.* 2011; Rahman *et al.* 2012; Roelofs *et al.* 2014; Zuo *et al.* 2014; Zhang *et al.* 2015). Due to limited reports of the effects of ART and DHA on COX-2 protein levels in haematological cancers, we initially aimed to evaluate and compare the effects of ART and DHA on COX-2

protein levels in HT-29-AK cells and HL-60 cells. However, due to COX-2 antibody limitations the experiments were only performed against HT-29-AK cells to challenge current reports on COX-2 expression in solid tumours. With prepared samples for flow cytometric analysis as described in Materials & Methods (Section 2.9.1.1), there was a concentration-dependent decrease in COX-2 protein levels by ~7% (0.93 ± 0.08 RFU), 15% (0.85 ± 0.07 RFU; P<0.001), 23% (0.77 ± 0.06 RFU; P<0.001) upon treating HT-29-AK cells with 7.22µM, 14.44µM and 28.88µM ART, respectively, as compared to control (1.00 ± 0.11 RFU) (figure 17A). Similarly, as shown in figure 17B, DHA-treated HT-29-AK cells for 72h significantly down-regulated COX-2 protein levels in a concentration-dependent manner by ~4.00% (0.96 ± 0.10 RFU; P<0.01), ~22% (0.78 ± 0.02 RFU; P<0.001) and ~33% (0.67 ± 0.002 RFU; P<0.001) with 9.88 µM, 19.75 µM and 39.50 µM DHA, respectively, as compared to untreated cells (1.00 ± 0.10 RFU) (figure 17B).

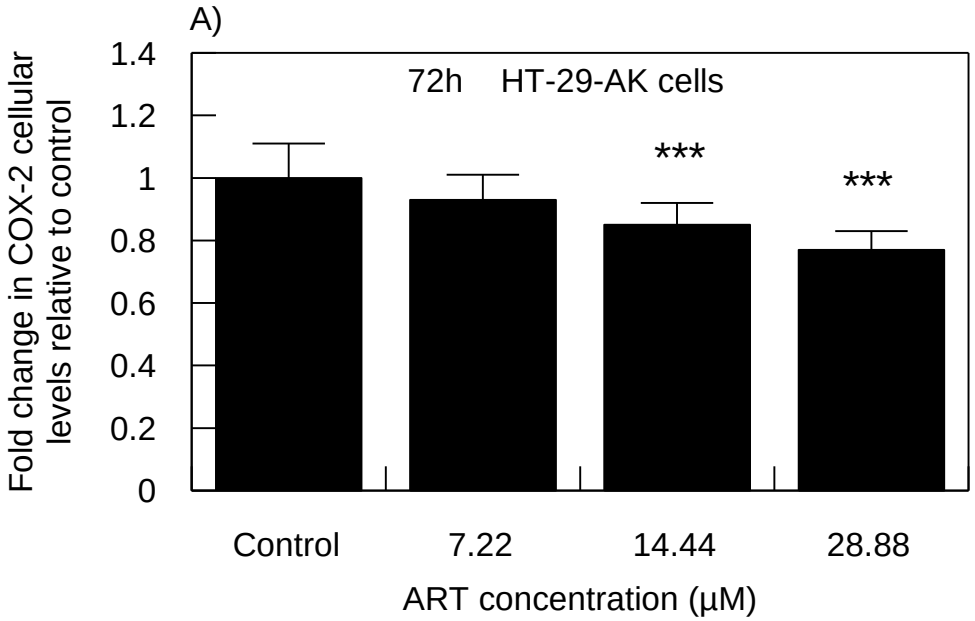

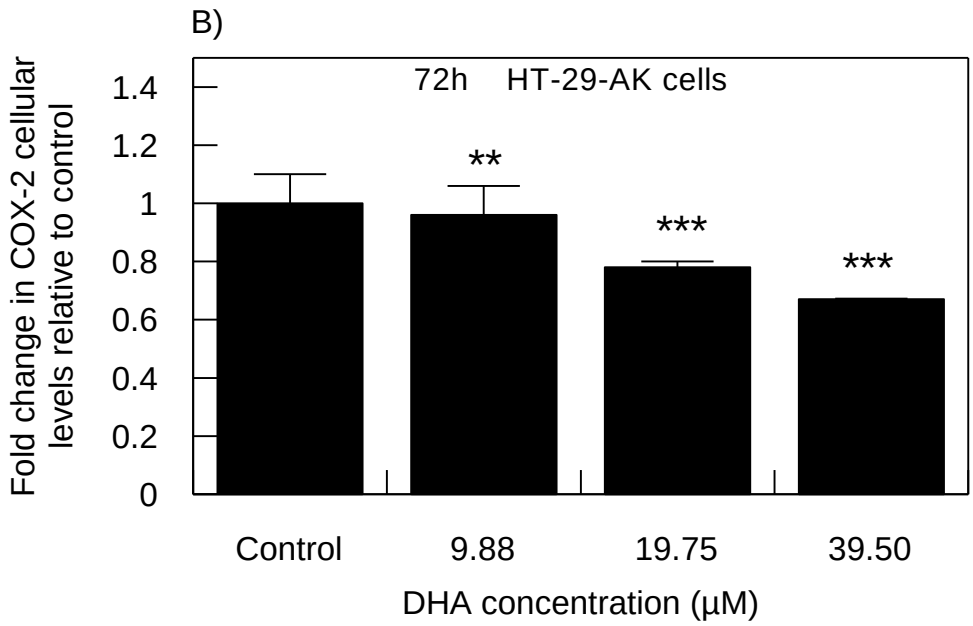

Figure 17: ART and DHA decreases the intracellular protein levels of COX-2 in HT-29-AK cells at 72h in normoxia. Cells were treated without or with A) ART (at 0µM, 7.22µM, 14.44µM and 28.88µM) and B) DHA (at 0µM, 9.88µM, 19.75µM and 39.50µM) for 72h in normoxia (20% O_2), stained with COX-2 antibody and analysed on flow cytometer (Materials and Methods, Section 2.9). Results are expressed as mean ± SD of three independent experiments. ***P<0.001 and **P<0.01 vs. control as tested by one-way Anova (Dunnett test for comparison with control). ART, artesunate; DHA, dihydroartemisinin.

3.7. Effect of ART and DHA on mRNA and protein expression levels of E-cadherin and its localisation.

Experimental reports show that ART and artemisinin inhibit invasion of cancer cells through restoring cell adhesion by increasing E-cadherin expression (Li *et al.* 2008; Lijuan *et al.* 2010; Weifeng *et al.* 2011). Therefore, in present study it was of interest to investigate the effect of ART and DHA on cell-cell adhesion molecule E-cadherin in both cell lines.

ART-mediated effect on E-cadherin was investigated in HT-29-AK cells using qPCR analysis as described in Materials and Methods (Section 2.6). For comparison purposes, HT-29-AK cells were exposed to ART for 24h and 72h. Treatment with 82.53 µM ART of

HT-29-AK cells for 24h had a minimal effect on mRNA E-cadherin levels with resulting a 10% decrease in E-cadherin levels as compared to control (ΔΔCt= 1.10 ± 0.13 vs. ΔΔCt= 1.00 ± 0.09, respectively; figure 18A). When HT-29-AK cells were incubated for 24h with high ART concentrations, E-cadherin mRNA levels increased by 94% at 165.06μM ART (ΔΔCt= 1.94 ± 0.37; P<0.001) and maximum increase by ~2.94-fold (ΔΔCt= 2.94 ± 0.61; P<0.001) was observed at 330.12μM ART, as compared to untreated cells (ΔΔCt= 1.00 ± 0.09), respectively (figure 18A). When compared to control group (ΔΔCt= 1.00 ± 0.03), E-cadherin mRNA levels were significantly (P<0.001) down-regulated in all ART-treated samples for 72h incubation by 2.27-fold (ΔΔCt= 0.44 ± 0.03 with 7.22μM ART and ΔΔCt= 0.44 ± 0.01 with 14.44μM ART P<0.001) and by 2.17-fold (ΔΔCt= 0.46 ± 0.10) with 28.88μM ART (figure 18B).

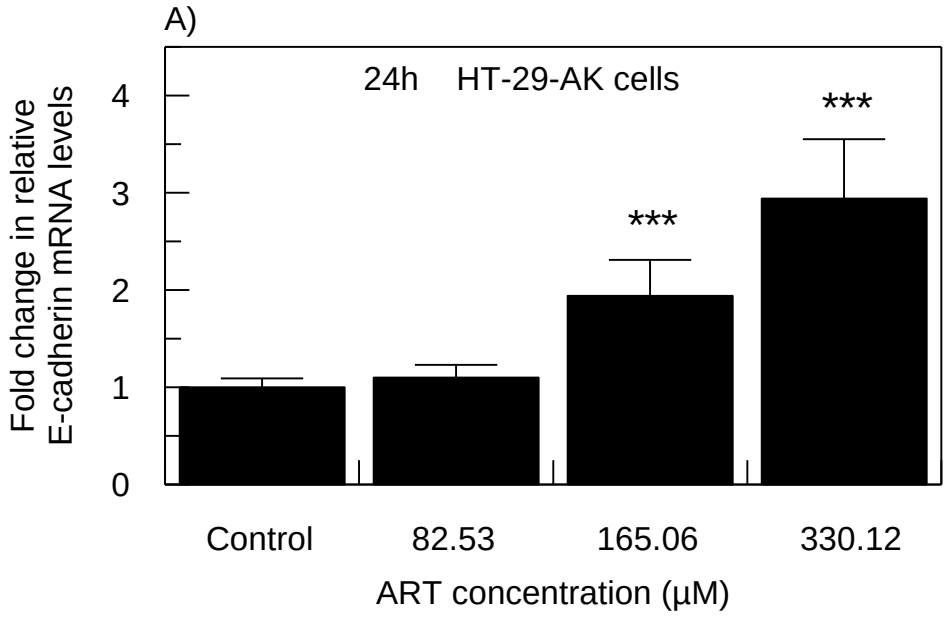

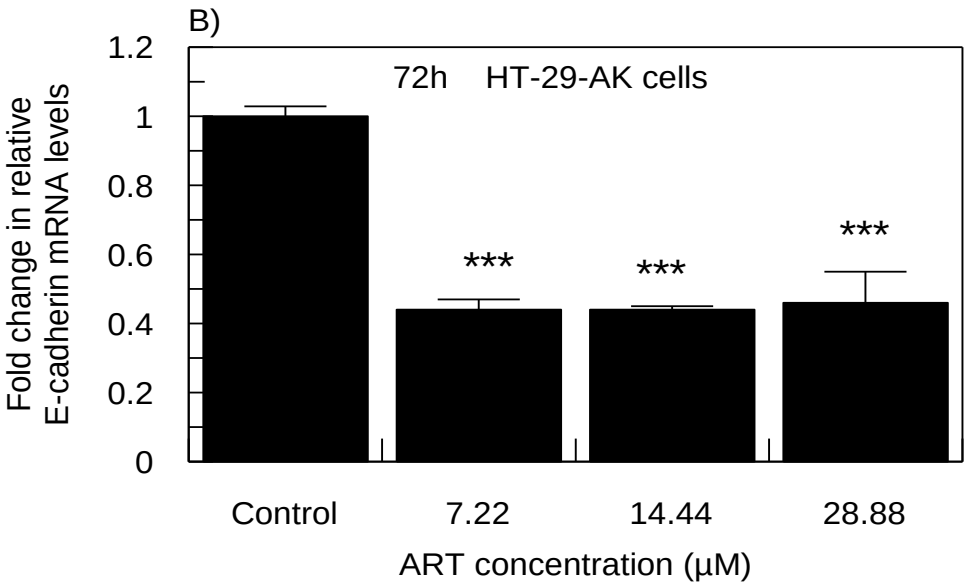

Figure 18: The effect of ART on E-cadherin mRNA expression in HT-29-AK cells at 24h and 72h in normoxia. qPCR analysis of E-cadherin gene expression was assessed in ART untreated and treated cells for (A) 24h (at 0µM, 82.53µM, 165.06µM, 330.12µM) and (B) 72h (at 0µM, 7.22µM, 14.44µM and 28.88µM) in normoxia (20% O_2) as described in Materials and Methods (Section 2.6). The results indicate means ± SD of three independent experiments. ***P<0.001 vs. control as tested by one-way Anova (Dunnett test for comparison with control). ART, artesunate.

The increase in E-cadherin mRNA levels upon ART treatment for 24h and subsequent down-regulation after 72h was considered provocative as E-cadherin plays a fundamental role in maintaining cell-cell contacts (Pećina-Šlaus 2003; Fujii *et al.* 2014). Therefore, it was hypothesized that triggered changes in E-cadherin mRNA levels upon ART treatments at both time points were associated with a disruption of cell epithelial integrity. To investigate this possibility, HT-29-AK cells were incubated with increasing concentrations of ART for 24h and 72h and immunocytochemical staining patterns for E-cadherin was analysed using Zeiss confocal microscope. As presented in a representative set of images in figure 19, for normalisation purposes some HT-29-AK cells were stained with secondary antibody only (figure 19i) to visualise any not specific signal. He-Ne laser set to 543nm was performed to

obtain cell surface phase contrast imaging of cells untreated and treated with compounds (figure 19ii). The background signal was removed (figure 19iii) using confocal microscope AIM software settings and all samples incubated with E-cadherin primary and secondary antibodies (complete staining) were further analysed. This step was repeated for every antibody used in next experiments and settings were constant for each sample set analysis.

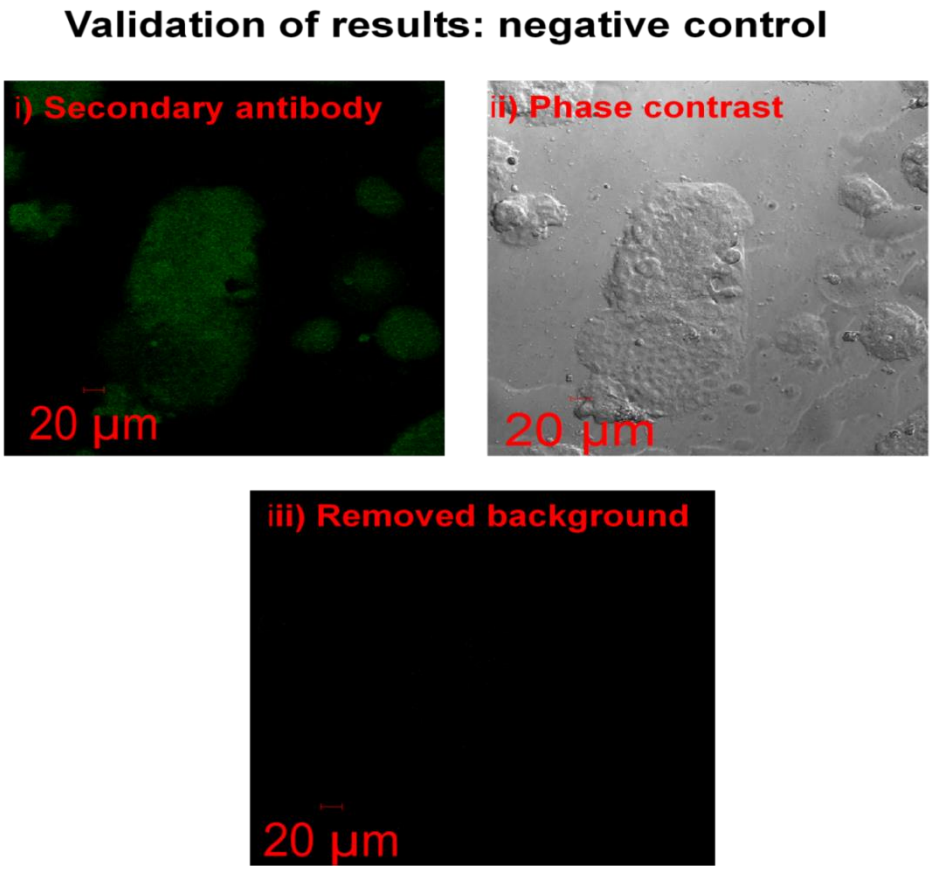

Figure 19: Normalisation of immunocytochemistry staining method for E-cadherin localisation in HT-29-AK cells. Cells were fixed, i) incubated with anti-mouse Alexa 488 secondary antibody (non-complete staining) prior analysis on confocal Zeiss LSM 510 META microscope with the objective used EC Plan-Neofluar 20x/0.50 M27 and the pinhole channel set at 76µm; ii) taking phase contrast image using He-Ne laser set to 543nm; and removing the background (iii) using confocal microscope Zeiss LSM 510 META settings tools (Materials & Methods, Section 2.7).

It was observed that an increase of mRNA E-cadherin levels upon ART for 24h resulted in mis-localisation of E-cadherin protein expressions (figure 20A). ART control cells had weak, diffusely distributed basal and lateral membranous staining of E-cadherin protein, while ART treatment resulted in concentration-dependent increase in E-cadherin lateral membrane staining and no changes in basal membranous staining, respectively (figure 20). Representative linear-profile histograms further confirm increase in intensity staining of E-cadherin at cell lateral area (blue marker) with 165.06µM ART as compared to weak and evenly distributed E-cadherin proteins over the membrane (red and blue markers) in ART control cells.

ART 24h HT-29-AK cells

A) Control

a) E-cadherin

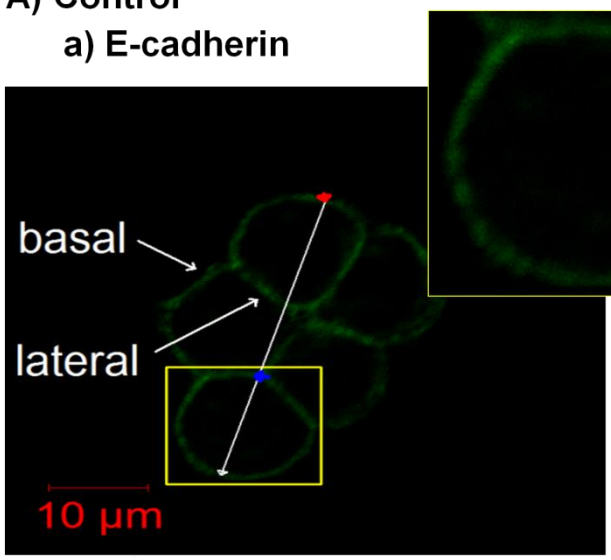

b) phase contrast

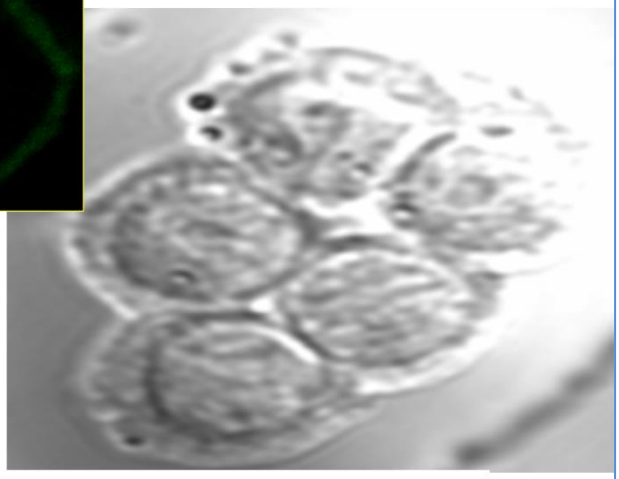

C) staining intensity of E-cadherin

	Red marker	Blue marker	Difference
Distance	0.30µm	23.07µm	22.78µm
Intensity	41	52	11

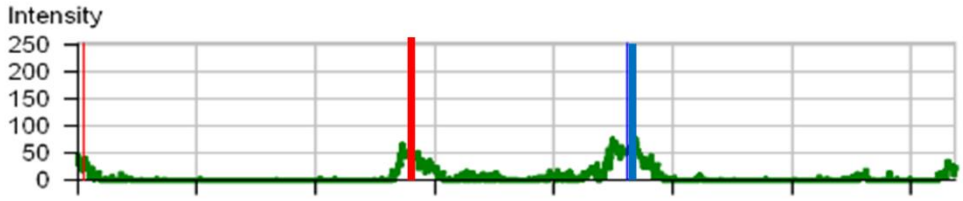

24h

B) 82.53µM ART

a) E-cadherin

b) phase contrast

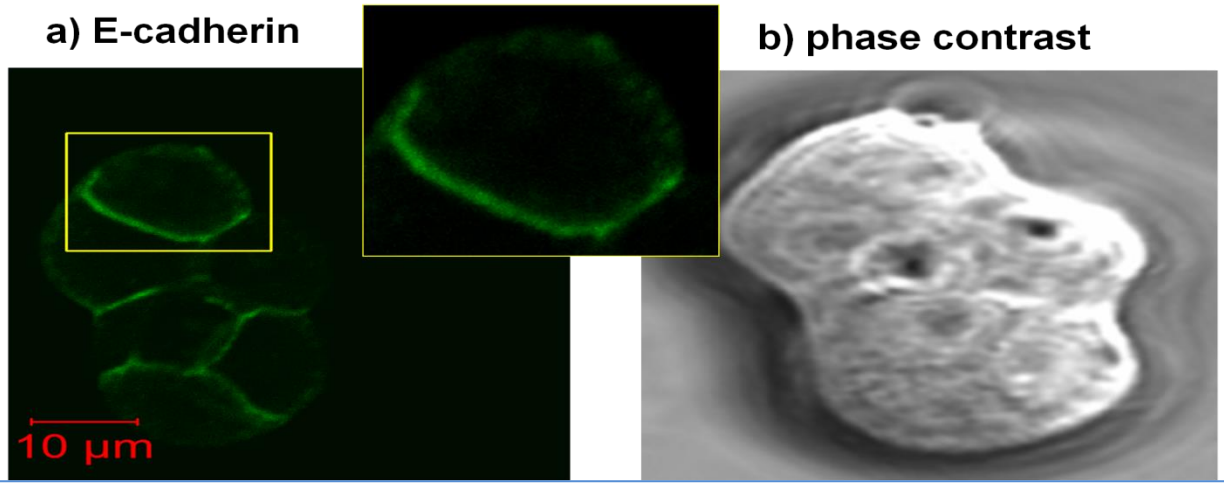

C) 165.06µM ART

a) E-cadherin

b) phase contrast

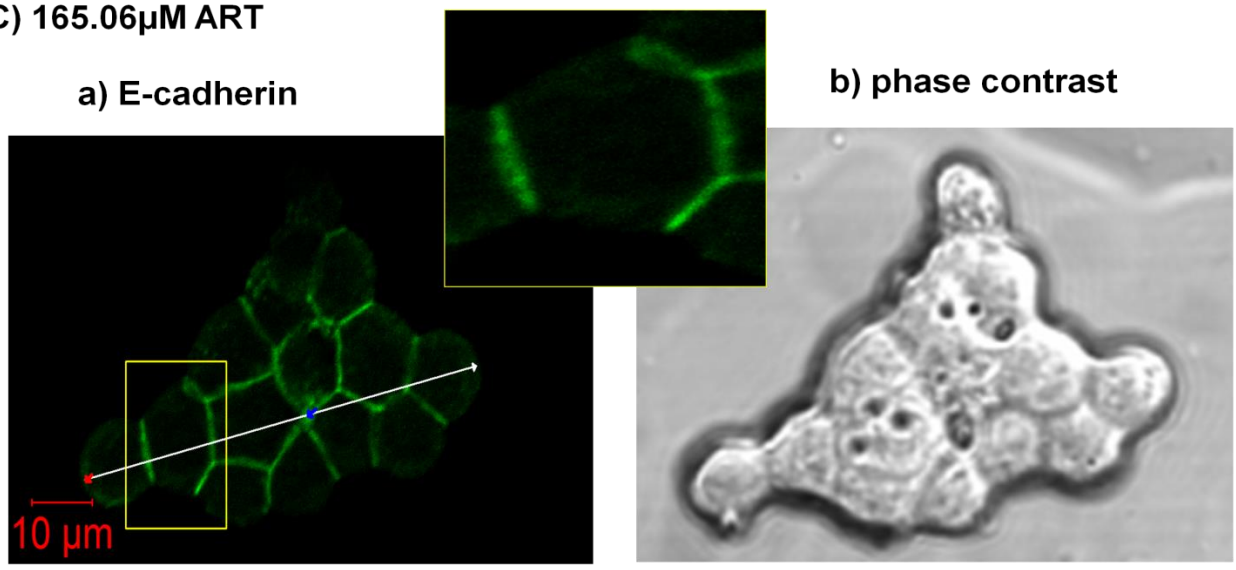

C) staining intensity of E-cadherin

	Red marker	Blue marker	Difference
Distance	0.47µm	38.02µm	37.55µm
Intensity	40	159	119

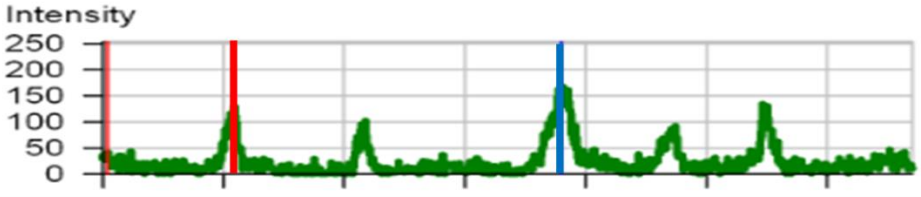

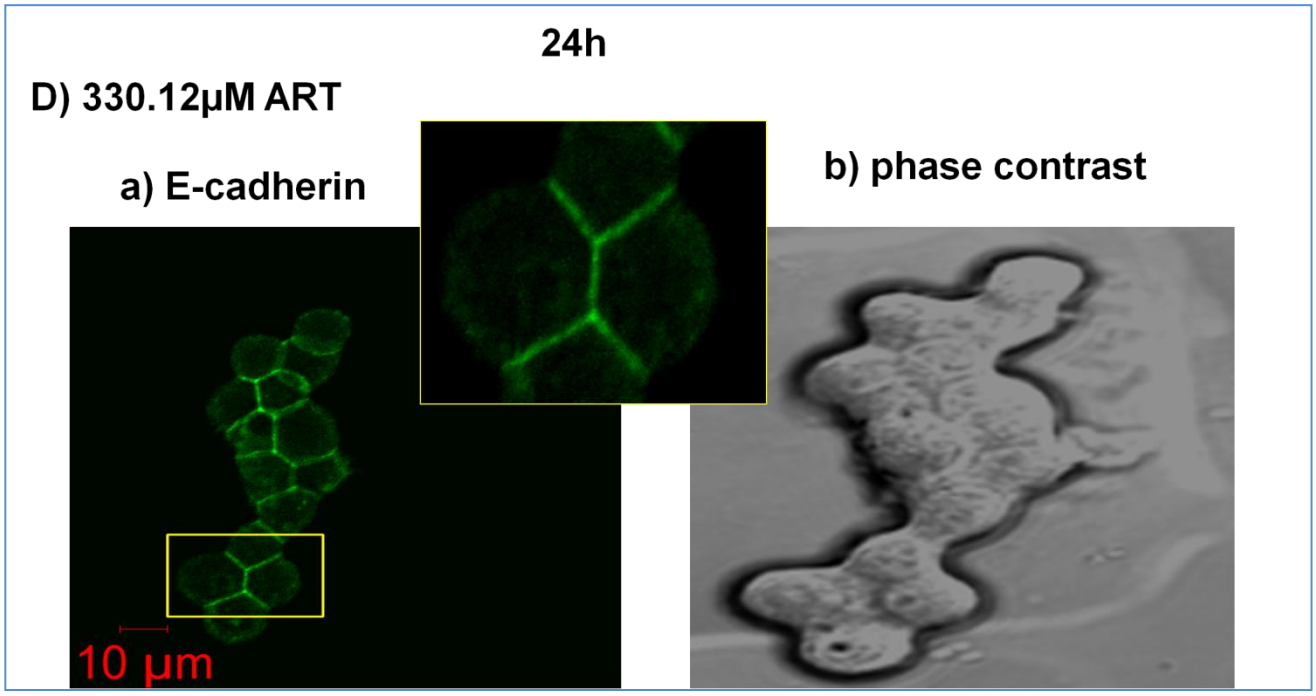

Figure 20: The effect of ART on E-cadherin cellular protein localisation in HT-29-AK cells at 24h in normoxia. Evaluation of E-cadherin localisation without/with ART treatment after 24h incubation: A) control, B) 82.53µM ART, C) 165.06µM ART, and D) 330.12µM ART. Cells were fixed, incubated with anti-E-cadherin and a) E-cadherin complete staining for each ART concentration was visualised using anti-mouse Alexa 488 secondary antibody prior analysis on confocal Zeiss microscope as described in Materials and Methods (Section 2.7). The objective used was EC Plan-Neofluar 20x/0.50 M27 and the pinhole channel set at 76µm. The representative images show the localisation and the staining intensity of E-cadherin in the majority of the cells analysed by AIM Software from 3 independent experiments. High-magnification images are located in upper right corner of representative picture whereas (b) phase contrast images are located on the left. Representative linear-profile histograms are indicated by white line upon ART treatment for 24h (control and 165.06µM) and presented in c) pictures. ART, artesunate.

In contrast, the membranous localisation of E-cadherin after 72h in all ART-untreated and treated cells was evenly distributed at baso-lateral level across all samples with representative images being shown for control and IC_{50} concentration at 14.44µM (figure 21 B and C). 3D side view of cells was obtained by Z-section scanning for control cells and ART-treated cells (at 14.44µM) in positions a, b and c (figure 21 B and C) and showed no changes in E-cadherin localisation at different cell sections.

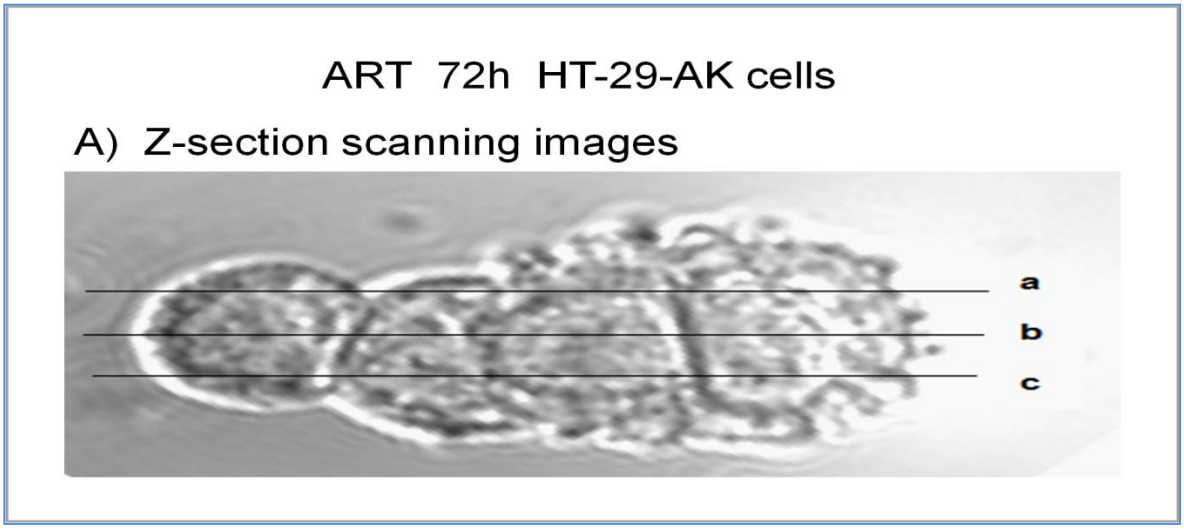

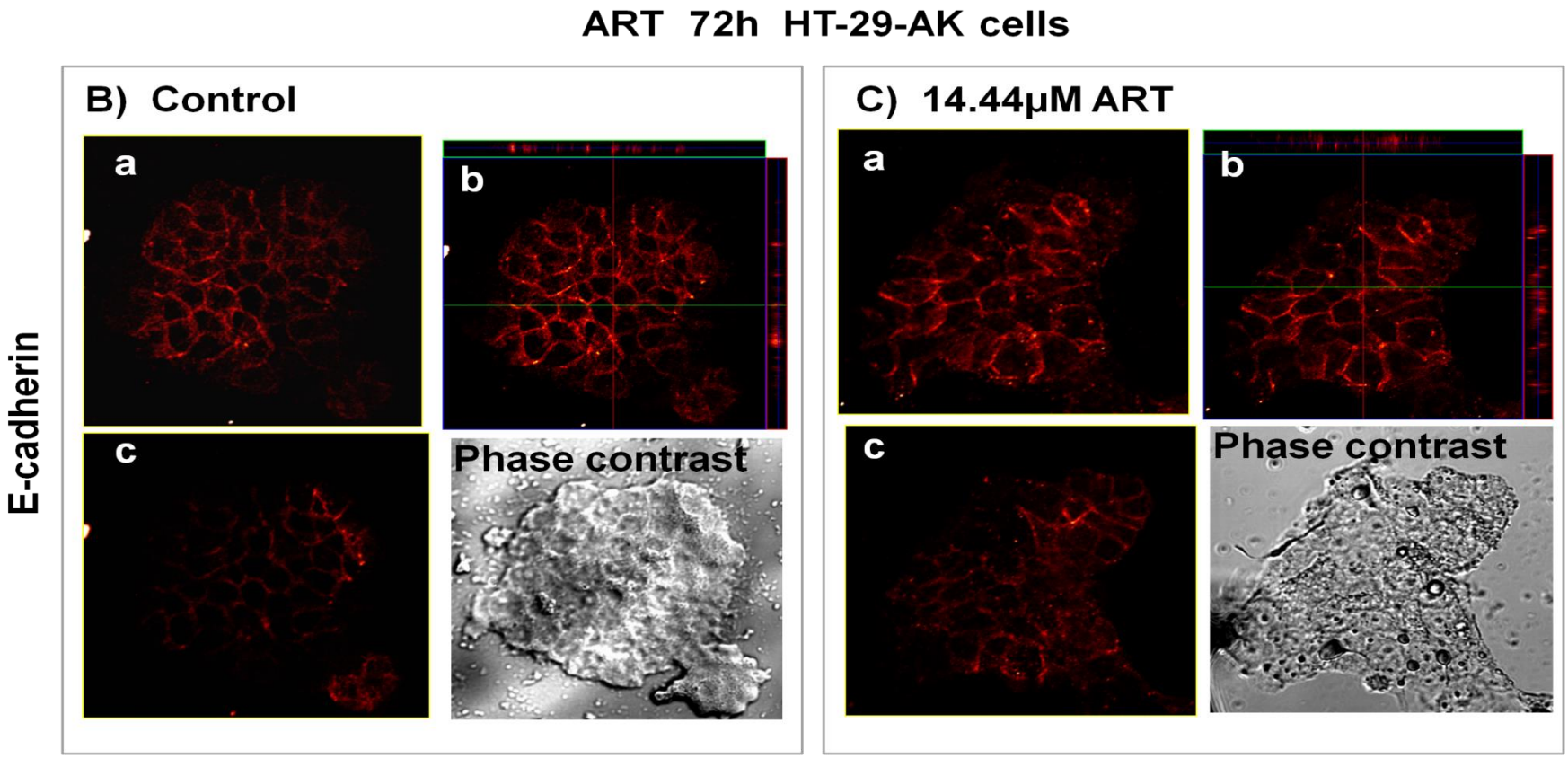

Figure 21: The effect of ART on E-cadherin cellular protein localisation in HT-29-AK cells at 72h in normoxia. Cells were fixed, incubated with anti-E-cadherin and visualised using anti-mouse Alexa 488 secondary antibody (complete staining) prior analysis on confocal Zeiss microscope. The objective used was EC Plan-Neofluar 20x/0.50 M27 and the pinhole channel set at 76µm. Representative 3D side view obtained by Z-section scanning of cells in positions a, b and c (as shown in A image).The representative images show the localisation of E-cadherin in the majority of the cells derived for B) ART-untreated cells (control) and C) at 14.44µM ART as analysed by AIM Software from 3 independent experiments. ART, artesunate.

In terms of DHA, E-cadherin expressions were only investigated using immunocytochemistry staining where HT-29-AK cells were treated with DHA for 24h and 72h incubations prior analysis (figures 22 and 23). Imaging of stained cells with E-cadherin antibody upon DHA treatment for 24h showed that untreated cells and cells treated with 29.01µM and 58.02 µM DHA had equally distributed basal and lateral membranous localisation of E-cadherin protein (figure 22). Interestingly, DHA treatment at 116.04µM in addition to baso-lateral membranous staining of cells also showed staining of cell nuclei (figure 22). Z-section imaging of all DHA untreated and treated cells in positions a, b, and c (figure 22a) was performed to evaluate potential changes in E-cadherin localisation at three different depths across the cells. Representative Z-section images are presented in figure 22 for DHA-untreated cells and treated with 116.04µM.

As illustrated in figure 23, treatment with DHA for 72h showed baso-lateral localisation of E-cadherin in all untreated and DHA-treated samples with not observed changes in E-cadherin localisation at different depths in cells while performing Z-section scanning (data not shown).

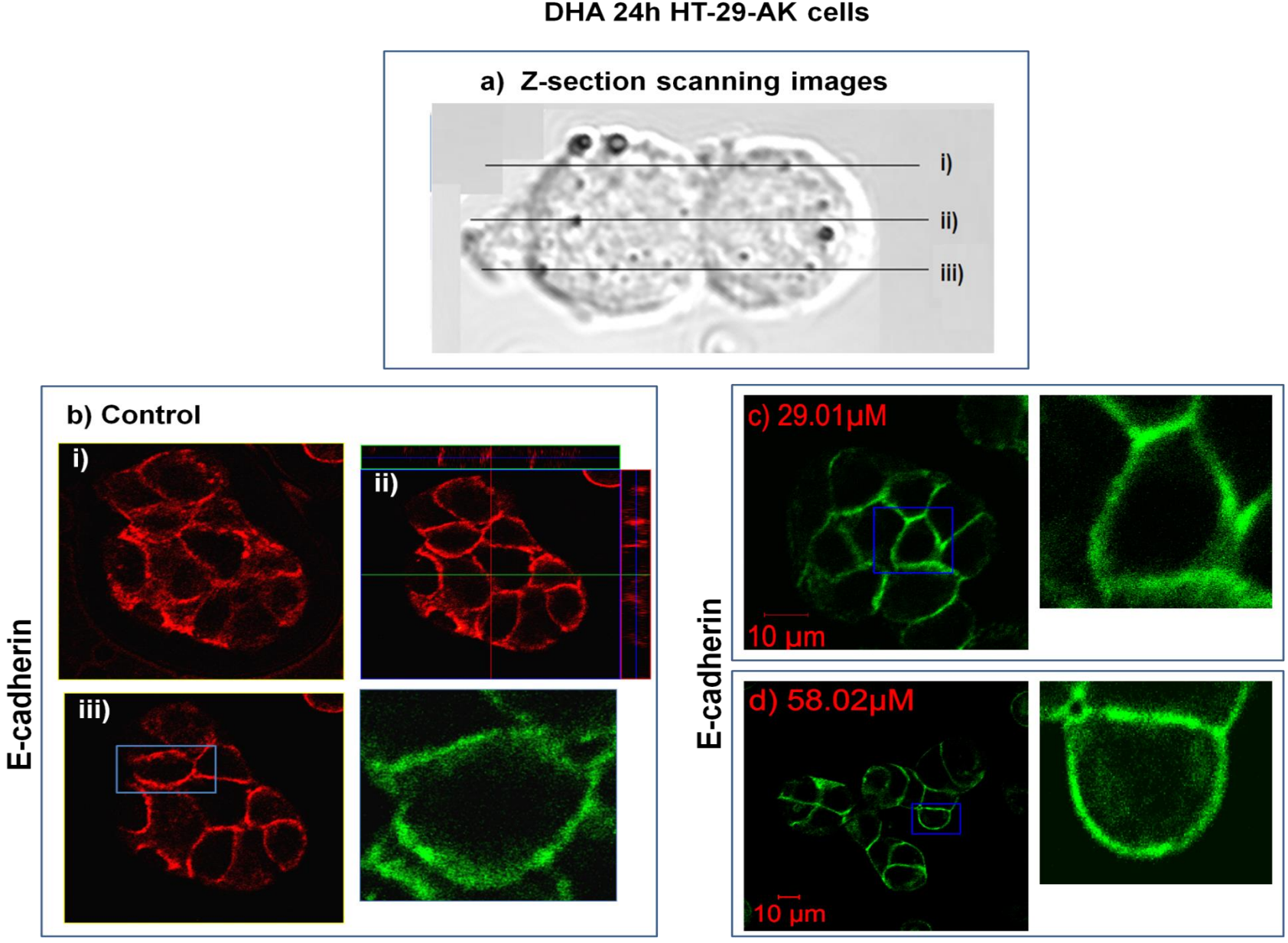
DHA 24h HT-29-AK cells
a) Z-section scanning images
i)
ii)
iii)
b) Control
E-cadherin
i)
ii)
iii)
c) 29.01μM
10 μm
d) 58.02μM
10 μm
E-cadherin

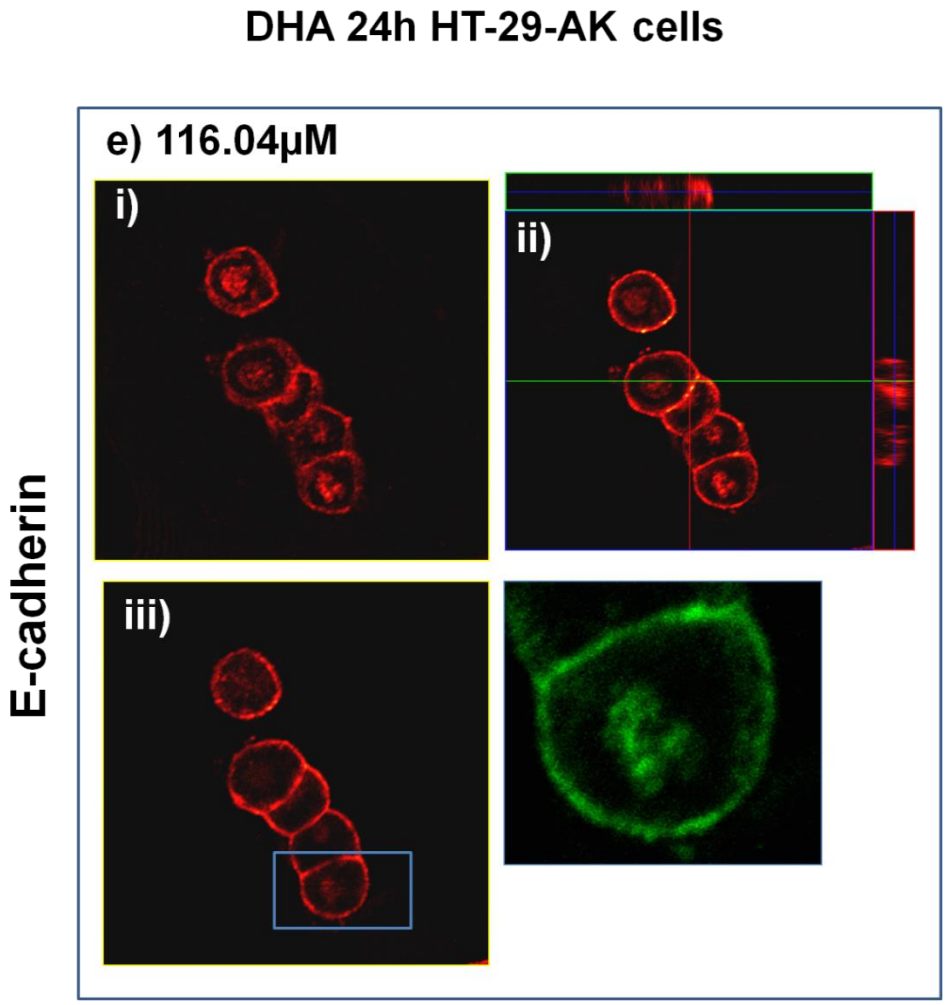

Figure 22: The effect of DHA on E-cadherin cellular protein localisation in HT-29-AK cells at 24h in normoxia. Evaluation of E-cadherin localisation using immunocytochemical staining was performed by seeding cells on glass coverslips with/without DHA at b) control, c) 29.01µM, d) 58.02µM, e) 116.04µM for 24h. Cells were then fixed, incubated with anti-E-cadherin and visualised using anti-mouse Alexa 488 secondary antibody on confocal microscope (Zeiss LSM 510 META) as described in Materials and Methods (Section 2.7). The objective used was EC Plan-Neofluar 20x/0.50 M27 and the pinhole channel set at 76µm. The representative images show the localisation and the staining intensity of E-cadherin in the majority of the cells analysed by AIM Software. Representative Z-section images of E-cadherin staining intensity were taken in i, ii and iii positions as shown in picture a) and represent DHA treatment for 24h with b) control and e) 116.04µM). The results represent 3 independent experiments. DHA, dihydroartemisin.

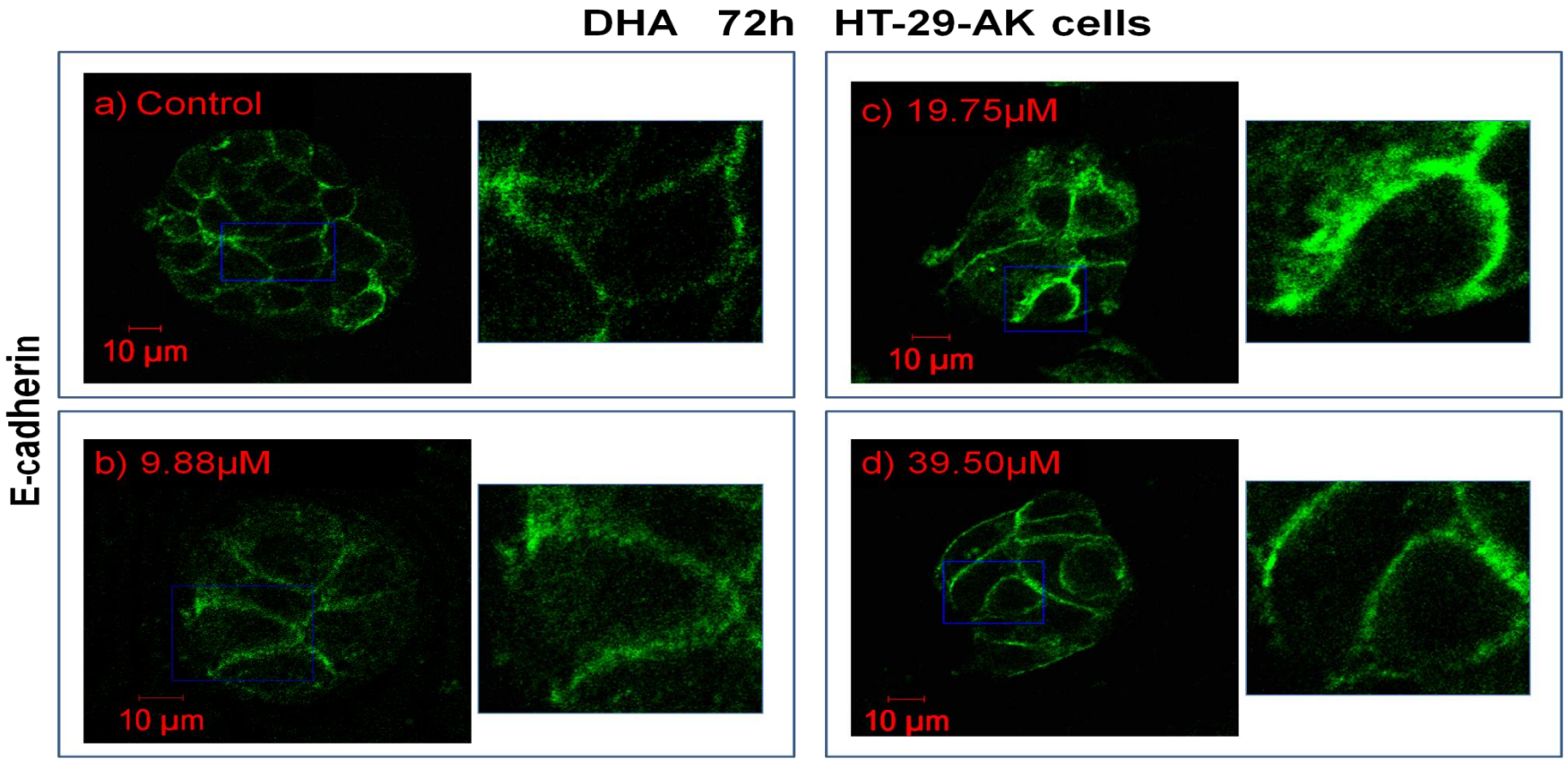

Figure 23: The effect of DHA on E-cadherin cellular protein localisation in HT-29-AK cells at 72h in normoxia. Evaluation of E-cadherin localisation using immunocytochemical staining was performed by seeding cells on glass coverslips with/without DHA at a) 0µM, b) 9.88µM, c) 19.75µM and d) 39.50µM for 72h in normoxia (20% O_2). Cells were then fixed, incubated with anti-E-cadherin and visualised using anti-mouse Alexa 488 secondary antibody on confocal microscope (Zeiss LSM 510 META as described in Materials and Methods (Section 2.7). The objective used was EC Plan-Neofluar 20x/0.50 M27 and the pinhole channel set at 76µm. The representative images show the localisation and the staining intensity of E-cadherin in the majority of the cells analysed by AIM Software. The results represent 3 independent experiments. DHA, dihydroartemisin.

To investigate whether ART and DHA modulate E-cadherin protein expression levels in HL-60 cells, cells were treated with drugs for 72h and stained with E-cadherin antibody prior flow cytometric analysis as described in Materials & Methods (Section 2.9.2.1). Figure 24A shows that ART treatment resulted in a significant ($P<0.001$) concentration-dependent increase in E-cadherin cell surface protein levels by ~52% (1.52 ± 0.10 RFU), ~65% (1.65 ± 0.13 RFU) and ~2.19-fold (2.19 ± 0.23 RFU) upon treating the cells with 0.30µM, 0.60µM and 1.20µM of ART for 72h, respectively, as compared to control (1.00 ± 0.05 RFU). In contrast, analysis of protein levels in DHA-treated cells for 72h resulted in E-cadherin protein expression levels to be decreasing with higher concentrations (figure 24B). Compared to control, treatment of cells with 0.25µM DHA caused no significant changes in E-cadherin protein expression (by 1%; 1.00 ± 0.09 RFU vs. 1.01 ± 0.09 RFU). Significantly down-regulated levels of E-cadherin protein secretions were observed with increasing concentrations of DHA by 11% (0.89 ± 0.05 RFU; $P<0.01$) and 12% (0.88 ± 3.88 RFU; $P<0.01$) with 0.49 µM and 0.98 µM DHA, respectively when compared to control (1.00 ± 0.09 RFU).

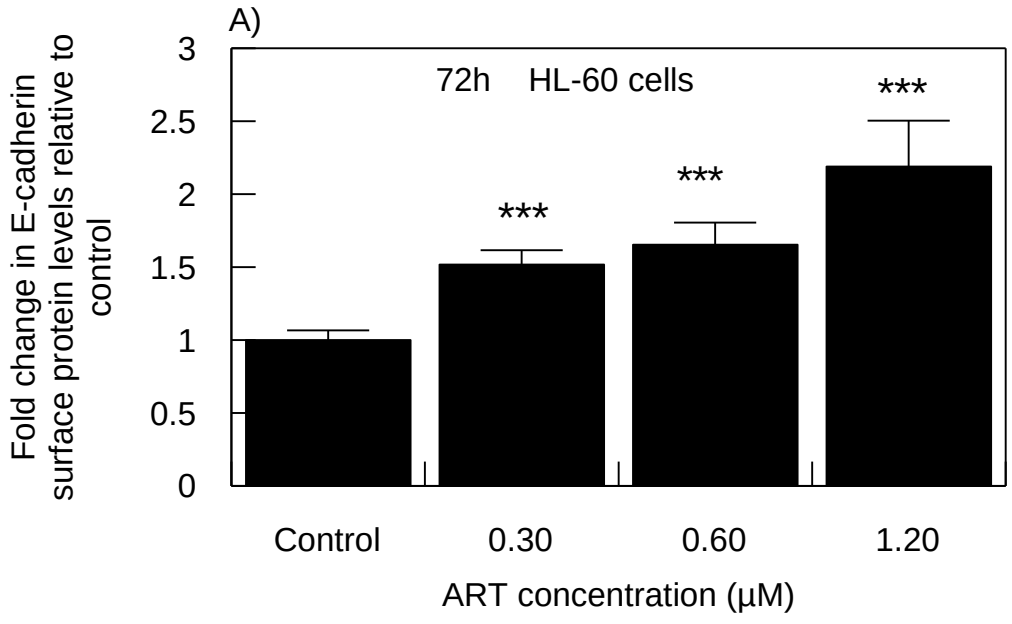

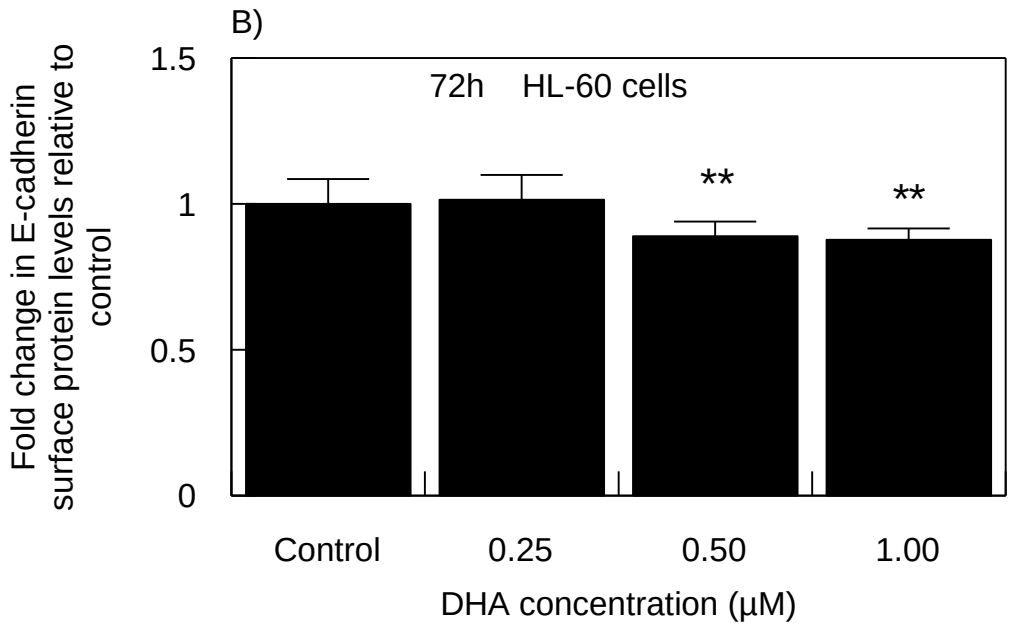

Figure 24: The effect of ART and DHA on surface E-cadherin protein expression levels in HL-60 cells at 72h in normoxia. Cells were treated without or with A) ART (at 0µM, 0.30µM, 0.60µM and 1.20µM) and B) DHA (at 0µM, 0.25µM, 0.50µM and 1.00µM) for 72h in normoxia (20% O_2), stained with E-cadherin antibody and analysed on flow cytometer as described in Materials & Methods (Section 2.9.2.1). Results are expressed as mean ± SD of three independent experiments. ***P<0.001 and **P<0.01 vs. control as tested by one-way Anova (Dunnett test for comparison with control). ART, artesunate; DHA, dihydroartemisinin.

3.8. Effect of ART and DHA on protein, mRNA and cellular localisation of CLDN-1

The up-regulation of CLDN-1 protein which maintains cell-cell integrity has been reported to enhance EMT and metastatic potential (Dhawan *et al.* 2005; Bezdekova *et al.* 2012). Besides, inverse relation between E-cadherin and CLDN-1 reported previously led us to evaluate the potential mechanisms of the cell death induced by ART and DHA by measuring CLDN-1 expressions at protein and mRNA levels together with its cell localisation using flow cytometric analyses, qPCR and immunocytochemisrty staining, respectively as described in Materials & Methods (Sections 2.6; 2.7 and 2.9.1.1).

To assess the role of ART-mediated expression change in CLDN-1mRNA levels and localisation, HT-29-AK cells were exposed to ART for 72h and for comparison purposes for 24h. Flow cytometric and immunocytochemistry analyses were only performed for 72h incubation with ART-treated HT-29-AK cells. qPCR analysis showed first that after 24h, measured CLDN-1 mRNA levels in samples treated with 82.53µM ART were highly up-regulated by ~6.97-fold, as compared to control (ΔΔCt= 6.97 ± 1.04 vs. ΔΔCt= 1.00 ± 0.03, P<0.001; figure 25A). These up-regulated mRNA CLDN-1 levels were decreasing with increasing concentrations of ART with resulting a fold change of ~ 2.66- (ΔΔCt= 2.66 ± 0.45, P<0.01) and ~2.65-fold (ΔΔCt= 6.95 ± 0.45, P<0.01) upon treating the cells with 165.06µM and 330.12µM ART for 24h respectively, as compared to control (ΔΔCt= 1.00 ± 0.03) (figure 25A). In contrast, mRNA CLDN-1 expression levels after 72h were significantly (P<0.001) decreased with increasing concentrations of ART and resulted in ~2.00- (ΔΔCt= 0.50 ± 0.06), ~2.13- (ΔΔCt= 0.47 ± 0.02) and ~1.92- (ΔΔCt= 0.52 ± 0.12) down-regulation with 7.22µM, 14.44µM and 28.88µM ART, respectively, as compared to untreated cells (ΔΔCt= 1.00 ± 0.04; figure 25B).

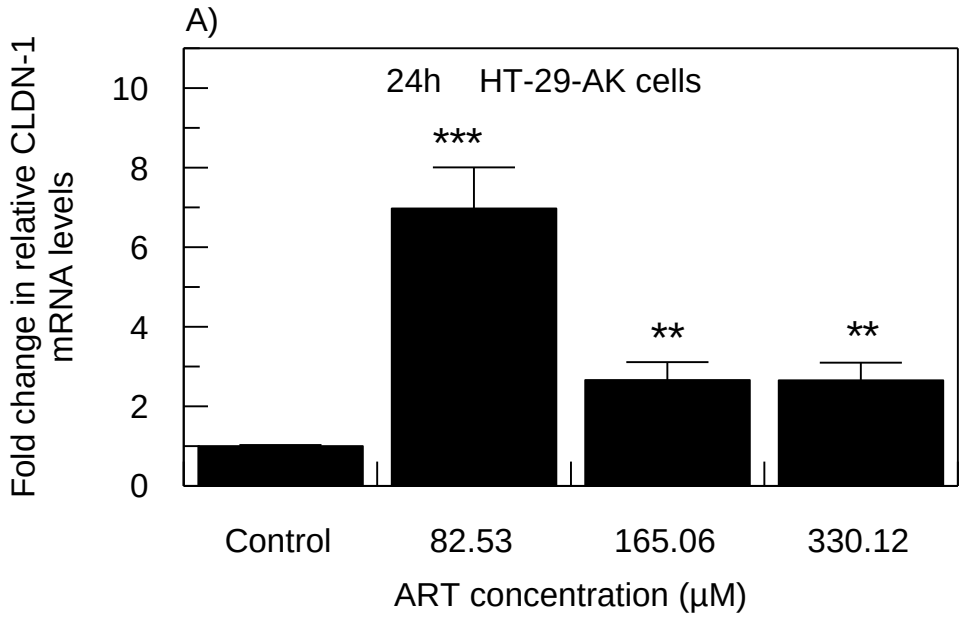

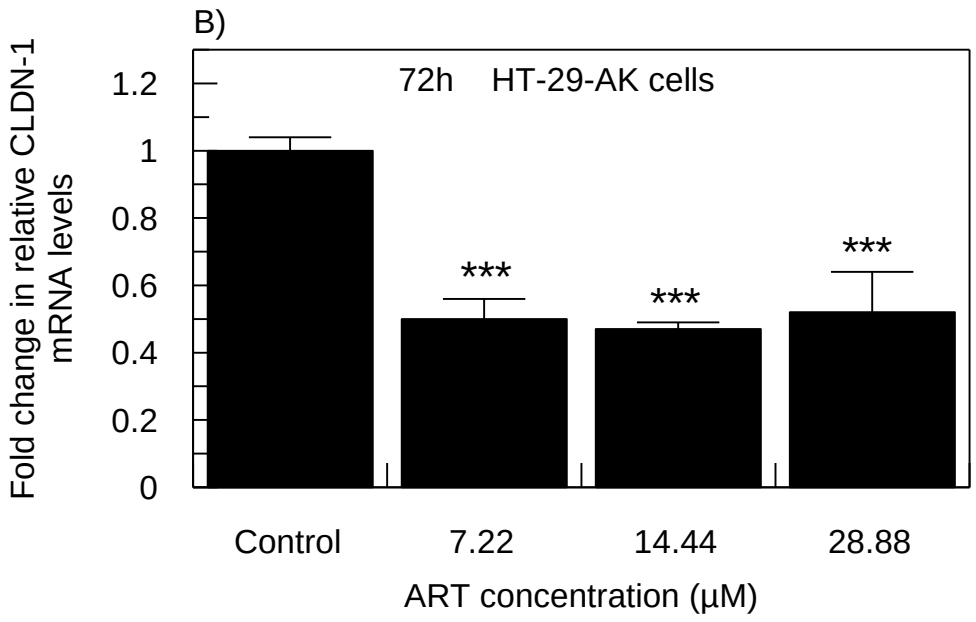

Figure 25: The effect of ART on CLDN-1 mRNA expression in HT-29-AK cells at 24h and 72h in normoxia. Cells were treated without or with A) ART (at 0µM, 82.53µM, 165.06µM and 330.12µM) for 24h and B) ART (at 0µM, 7.22µM, 14.44µM and 28.88µM) for 72h in normoxia (20% O_2) and mRNA CLDN-1 levels were measured by qPCR (Materials & Methods, Section 2.6). Results are expressed as mean ± SD of three independent experiments. **P<0.01 and ***P<0.001 vs. control as tested by one-way Anova (Dunnett test for comparison with control). ART, artesunate.

It was further investigated if CLDN1 suppression at the mRNA after 72hh treatment with ART was affected by any post-translational mechanisms. Therefore, the intracellular protein expression levels of CLDN-1 were measured by flow cytometry upon ART treatment for 72h as described in Materials & Methods (Section 2.9.1.1). Up-regulation of CLDN-1 protein levels were observed to be decreasing with increasing concentrations of ART (figure 26). As compared to control (1.00 ± 0.21 RFU), there was 80% (1.80 ± 0.18 RFU; P<0.001), 59% (1.59 ± 0.17 RFU; P<0.001) and 41% (1.41 ± 0.10 RFU; P<0.001) change in CLDN-1 protein levels upon treating the cells with 7.22µM, 14.44µM and 28.88µM ART, respectively (figure 26). Immunocytochemistry staining conducted as described in Materials & Methods (Section

2.7) showed membranous and cytoplasmic distribution of CLDN-1 in ART untreated cells (figure 27). In ART-treated cells at 7.22µM, 14.44µM and 28.88µM, re-location of CLDN-1 was observed from cytoplasm to the baso-lateral structures of the membrane (figure 27).

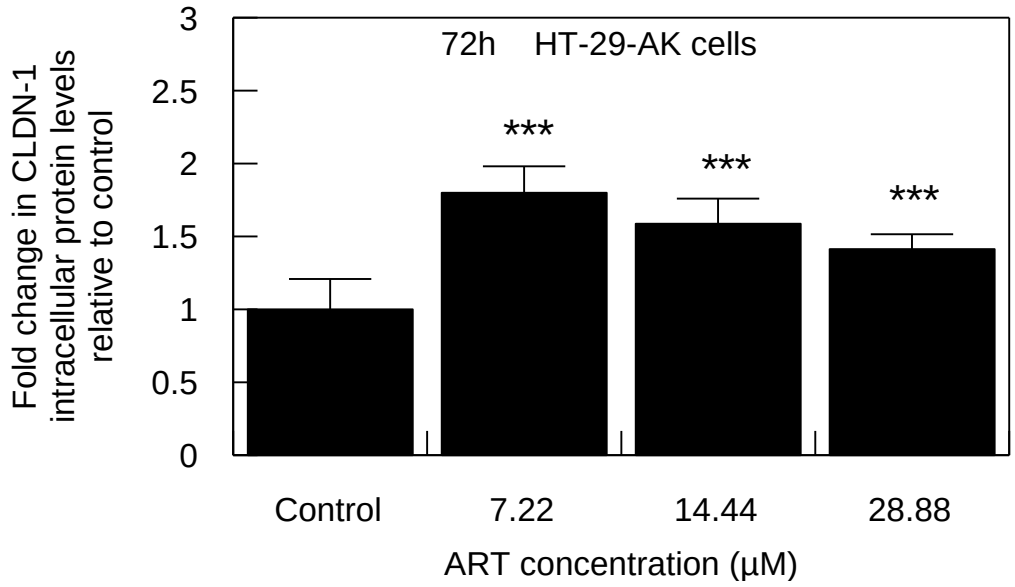

Figure 26: The effect of ART on intracellular CLDN-1 protein levels in HT-29-AK cells at 72h in normoxia. Cells were treated without or with ART (at 0 µM, 7.22µM, 14.44µM and 28.88µM) for 72h in normoxia (20% O_2) and CLDN-1 levels were measured on flow cytometer (Materials & Methods, Section 2.9.1.1). Results are expressed as mean ± SD of three independent experiments. ***P<0.001 vs. control as tested by one-way Anova (Dunnett test for comparison with control). ART, artesunate.

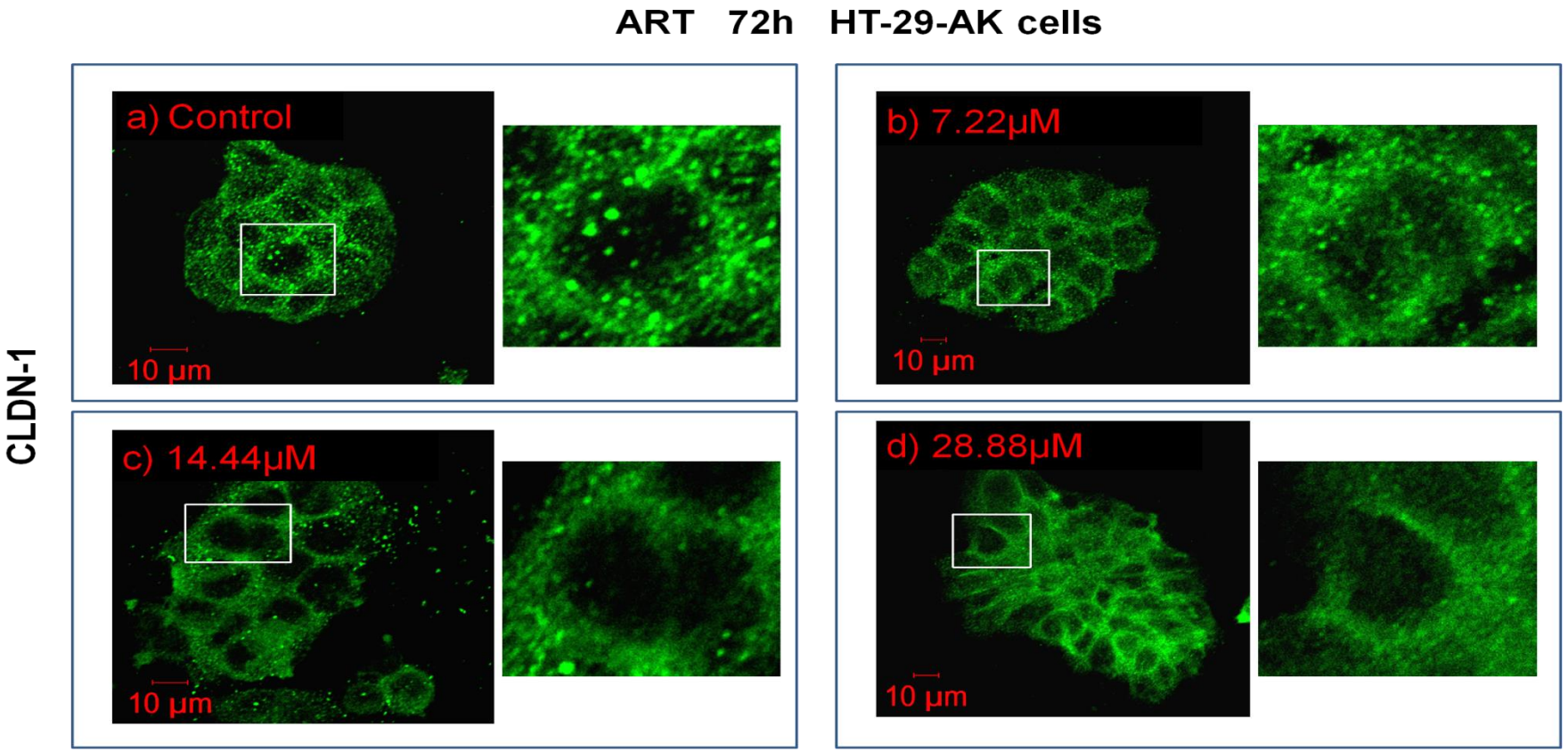

Figure 27: The effect of ART on CLDN-1 cellular protein localisatin in HT-29-AK cells at 72h in normoxia. Evaluation of CLDN-1 localisation using immunocytochemical staining was performed by seeding cells on glass coverslips with/without ART at a) 0µM, b) 7.22µM, c) 14.44µM and d) 28.88µM for 72h in normoxia (20% O_2). Cells were then fixed, incubated with anti-CLDN-1 and visualised using anti-mouse Alexa 488 secondary antibody on confocal microscope (Zeiss LSM 510 META). The objective used was EC Plan-Neofluar 20x/0.50 M27 and the pinhole channel set at 76µm. The representative images derived from 2 independent experiments show the localisation and the staining intensity of CLDN-1 in the majority of the cells analysed by AIM Software. High-magnification images are located next to respective sample. ART, artesunate.

As shown in figure 28, similar flow cytometric analysis was performed in HT-29-AK cells treated with DHA for 72h. The protein expression levels of CLDN-1 were up-regulated significantly (P<0.001) upon DHA treatment resulting in a 3.98-fold (3.98 ± 0.72 RFU) increase with a low DHA concentration (9.88µM), as compared to control (1.00 ± 0.31; figure 28). The higher concentrations of DHA at 19.75 µM and 39.50 µM lead to a steady decrease in CLDN-1 fold changes of ~3.79- (3.79 ± 0.56 RFU) and ~3.22-fold (3.22 ± 0.36 RFU), respectively, as compared to control (figure 28). DHA treated and untreated samples analysed by confocal microscope did not work properly and investigations should be repeated in the future (data not shown).

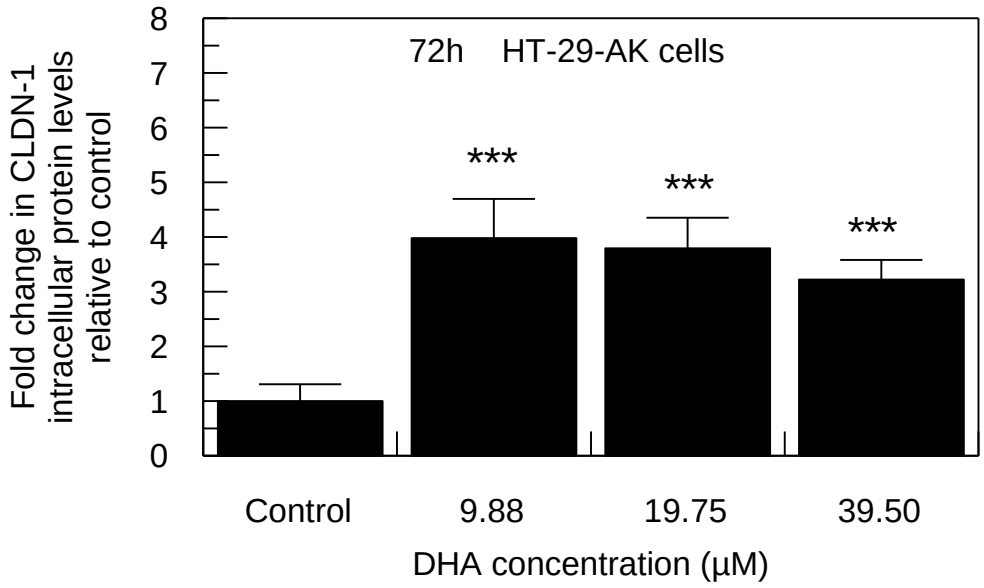

Figure 28: DHA decreases up-regulated levels of intracellular CLDN-1 in HT-29-AK cells at 72h in normoxia. Cells were treated without or with DHA (at 0 µM, 9.88µM, 19.75µM and 39.50µM) for 72h in normoxia (20% O_2), labelled with CLDN-1 antibody and analysed on flow cytometer as described in Materials & Methods (Section 2.9.2.1). Results are expressed as mean ± SD of three independent experiments. ***P<0.001 vs. control as tested by one-way Anova (Dunnett test for comparison with control). DHA, dihydroartemisinin.

With promising inhibitory activities of ART and DHA on CLDN-1 levels observed against HT-29-AK cells, flow cytometric analysis was performed to evaluate the effects of compounds on CLDN-1 protein levels in HL-60 cells (figure 29). ART treatment in HL-60 cells caused a significant ($P<0.001$) concentration-dependent increase in CLDN-1 protein expression levels by ~2.42-fold (2.42 ± 0.36 RFU), ~3.50-fold (3.50 ± 0.25 RFU) and ~4.40-fold (4.40 ± 0.50 RFU) upon treating the cells with 0.30µM, 0.60µM and 1.20µM of ART, respectively, as compared to control (1.00 ± 0.10 RFU) (figure 29A). Increase in CLDN-1 expression was also observed while treating HL-60 cells with DHA but CLDN-1 protein fold changes in all DHA-treated cells were not that high as compared to ART (figure 29A vs. 29B). As compared to control (1.00 ± 0.07 RFU), there was a marked but not significant increase in intracellular CLDN-1 levels by 13% (1.13 ± 0.08 RFU) upon treating HL-60 cells with 0.25µM DHA (figure 29B). Significantly ($P<0.001$), DHA-treated cells had up-regulated levels of CLDN-1 protein by 40% (1.40 ± 0.09 RFU) and 37% (1.37 ± 0.03 RFU) with 0.49 µM and 0.98 µM of DHA, respectively, as compared to control (1.00 ± 0.07 RFU) (figure 29B).

Overall, data show opposite activities of ART and DHA on CLDN-1 protein expression arising between HT-29-AK and HL-60 cells which could be due to cancer type differences (CRC vs. leukaemia) and morphology differences between investigated cells (adherent vs. non-adherent).

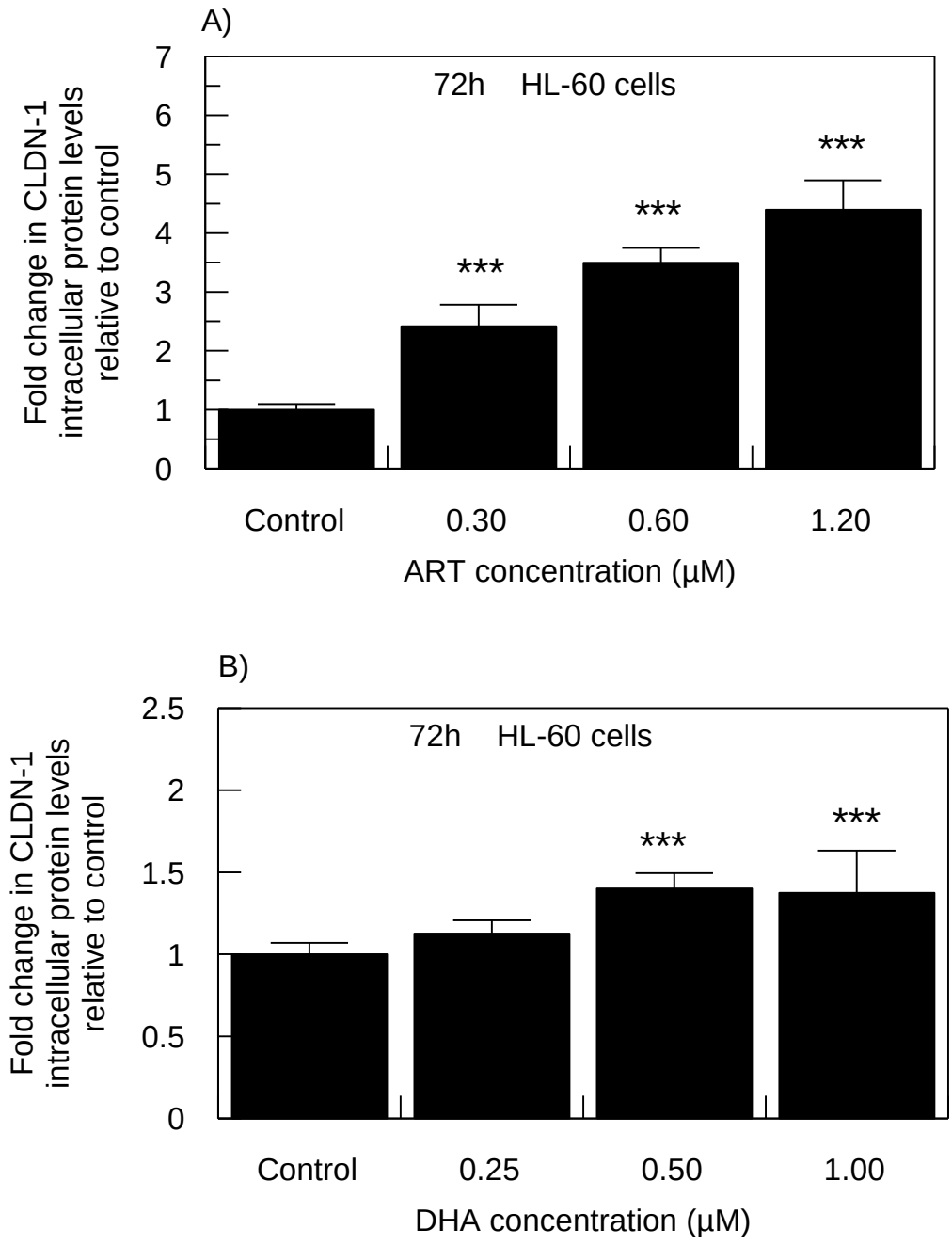

Figure 29: ART and DHA increase production of CLDN-1 intracellular protein in HL-60 cells at 72h in normoxia. Cells were treated for 72h without or with A) ART (at 0µM, 0.30µM, 0.60µM and 1.20µM) and B) DHA (at 0µM, 0.25µM, 0.50µM and 1.00µM) in normoxia (20% O_2), labelled with CLDN-1 antibody and analysed on flow cytometer as described in Materials and Methods (Section 2.9.2.1). Results are expressed as mean ± SD of three independent experiments. ***P<0.001 vs. control as tested by one-way Anova (Dunnett test for comparison with control). ART, artesunate; DHA, dihydroartemisinin.

3.9. ART and DHA reduced the wound healing capacity of HT-29-AK cells under normoxic conditions

The results have shown that ART and DHA display potent anti-cancer effects against highly proliferating HT-29-AK cells with reduced activity observed towards confluent cells (table 4). Reduced activity was more evident for DHA as compared to ART, hypothesizeng that ART is more likely to target slow proliferating cells within heterogeneic tumour mass. Therefore, using the concentrations of compounds derivered against confluent cells, *in vitro* wound healing assay was performed to assess the ability of ART and DHA to closure the wound gap made in HT-29-AK cells, as described in Matarials & Methods (Section 2.8).

The results displayed in figure 30 show representative photographs captured by light microscope at 10x (and x4) magnification. With an initial control wound diameter of 623.51µm (figure 30A ii), the wound diameter had reduced to 521.08µm after 3 days (figure 30 A iii) and the diameter further reduced to 45.06µm after 7 days of continuous culture (figure 30 A iiii). The monolayer of untreated ART cells throughout 7 days of the study was characterised by high cell-cell contact without changes in cell morphology (green arrows; figure 30 A). However, the capacity of the wound to close upon treating the cells with 95.31µM, 190.62µM, 381.24 µM and 953.10µM of ART for 72h was markedly reduced in a concentration-dependent manner as evidenced by the corresponding widening of the wound diameter to 833.68µm, 853.41µm, 966.05µm and ~1025.20µm, respectively (figure 30 B α, C α, D α, E α).

Further incubation for 96h with 95.31µM, 190.62µM, 381.24 µM and 953.10µM of ART resulted in an additional concentration-dependent widening of the wound to 1050µm, 1150µm, ~2000µm and ~4000µm, respectively (figure 30 B β, C β, D β, E β). The migration of the cells after this time was markedly reduced upon treating the cells with 95.31µM,

190.62μM of ART, with most of the cells killed by the higher concentrations of ART (381.24 μM and 953.10μM; figure 30 B β, C β, D β, E β). Single cancer cells observed at these high concentrations could mean that some cells had decreased ART susceptibility due to heterogeneic characteristics. Reduced sensitivity by some cells to ART could be also due to very high concentrations of ART being above concentrations used clinically which might contribute to the development of resistance. Furthermore, ART- treated exhibited a concentration-dependent manner inability to form cell-cell contact which might be linked with decreased E-cadherin mRNA levels observed previously (figure 18B). These characteristics might be linked with the induction of programmed cell death as there were changes in cancer cell morphology including cell shrinkage and formed balls of cell debris being typical features of apoptosis (figure 30, red *arrows*). These findings led to investigate in subsequent experiments the effect of ART on cleaved caspase-3 intracellular levels which is required for the execution of apoptosis.

A) Control HT-29-AK cells

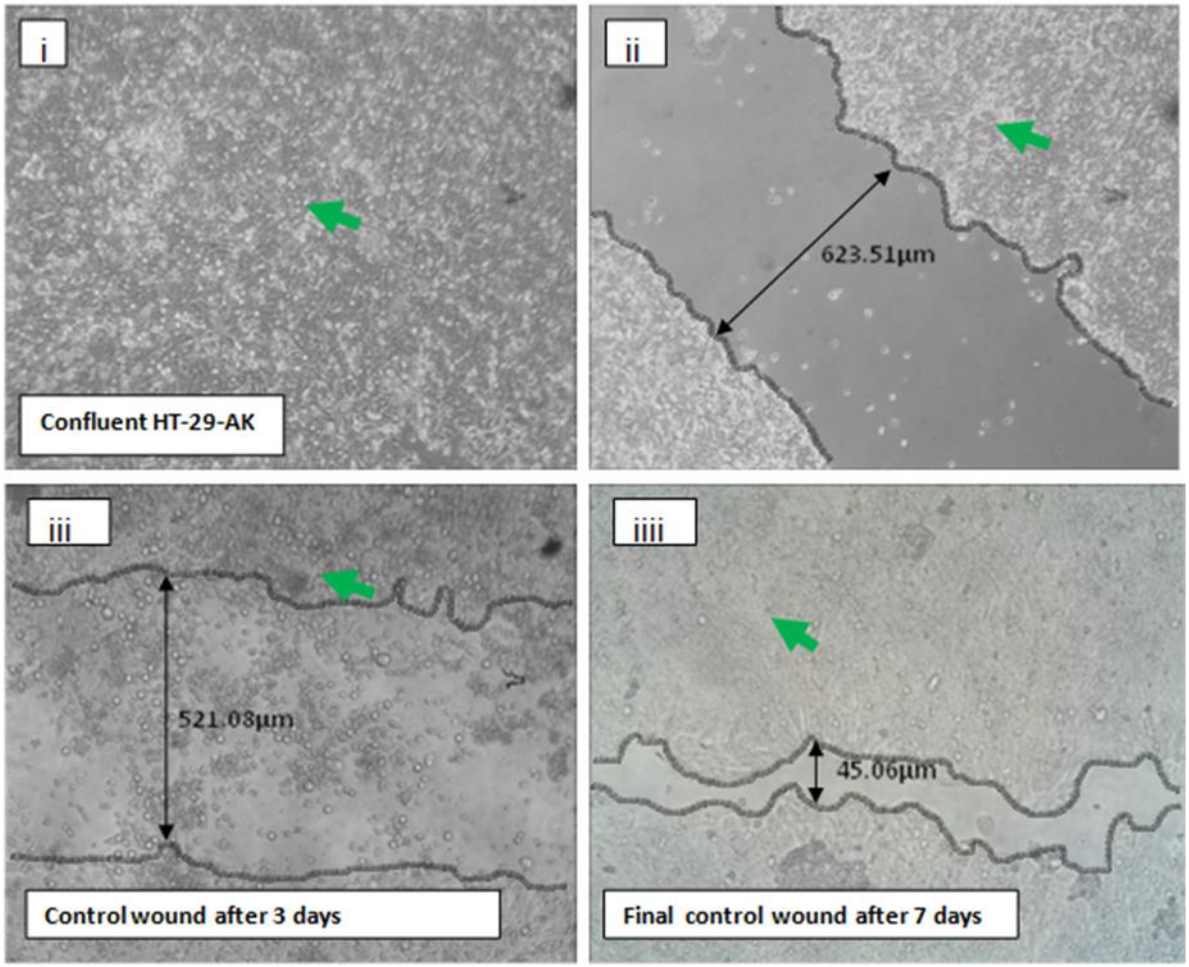

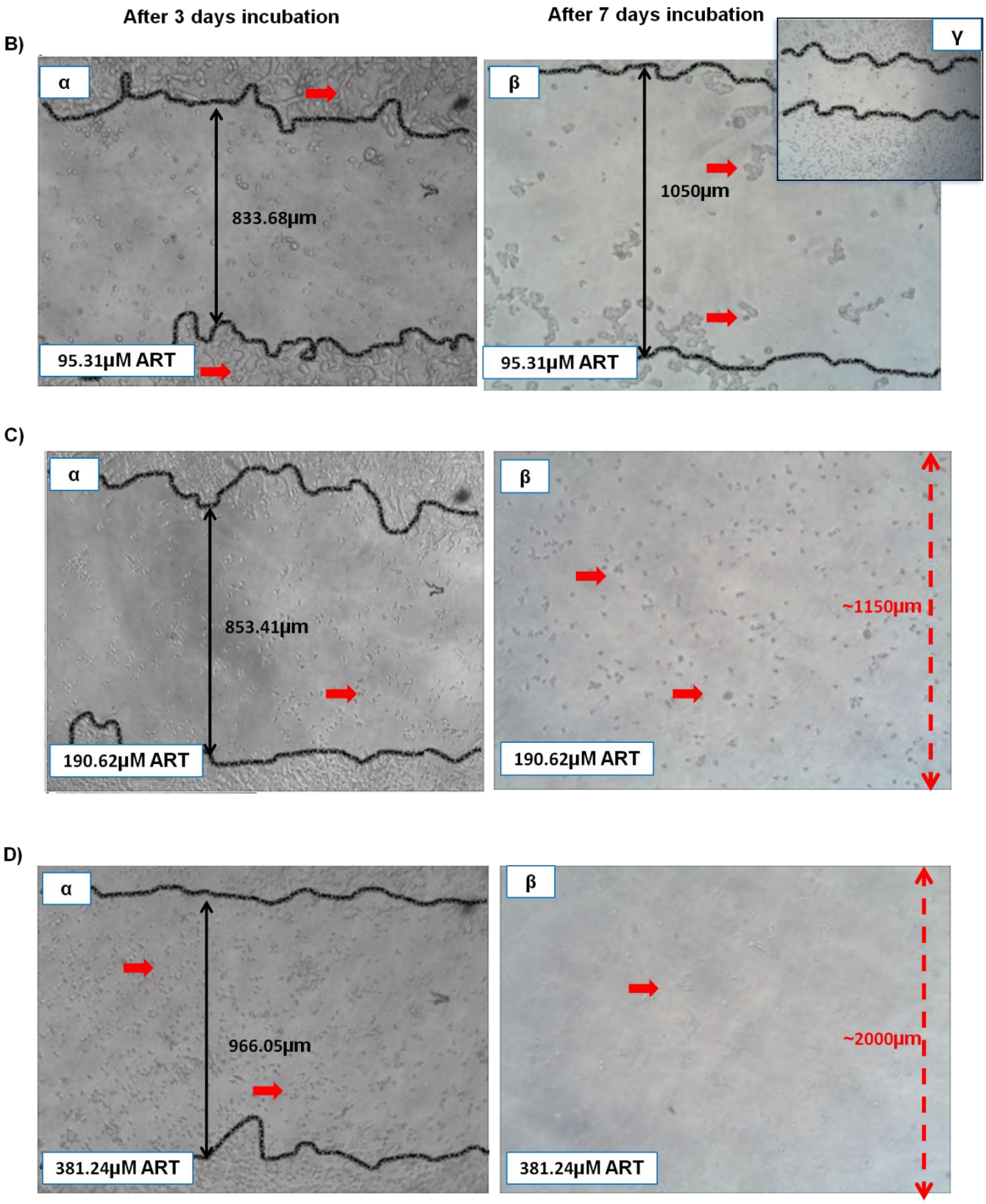
After 3 days incubation
After 7 days incubation
B)
α
833.68µm
95.31µM ART
β
1050µm
95.31µM ART
γ
C)
α
853.41µm
190.62µM ART
β
~1150µm
190.62µM ART
D)
α
966.05µm
381.24µM ART
β
~2000µm
381.24µM ART

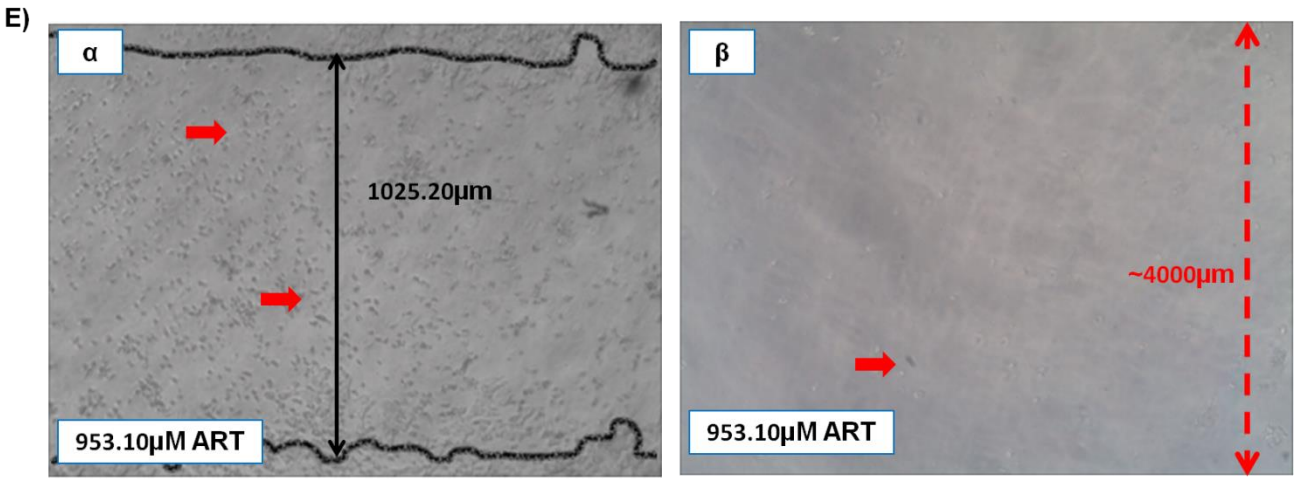

Figure 30: Wound healing capacity of HT-29-AK monolayers after treatment with ART in normoxia. Cells were seeded onto 24-well plate and grown in MEM growth media in normoxia (20% O_2) till confluency was reached (figure 30A i). An initial wound was created using a sterile 10µl Pasteur pipette (figure 30A ii) before the cells were treated without or with ART at A) 0µM, B) 95.31µM, C) 190.62µM and D) 381.24µM and E) 953.10 µM for 72h as described in Materials & Methods (Section 2.8). For each ART concentration (B-E), the wound diameter was measured after the first treatment with ART for 3 days which is represented as respective 'α' picture. After additional 96h (7 days in total) with ART, the wound diameter was measured again and is indicated as a respective 'β' picture for each ART concentration (B-E). Green arrows, normal cells; red arrows, damaged cells, dotted red arrows indicate wound healing diameter greater than 1100µm. ART, artesunate.

Due to the cytotoxic ability of ART (table 4) against HT-29-AK cells and its ability to increase the diameter of the wound (figure 30), it was of interest to determine whether the unattached cells in the vicinity of the wounds (which was visible under the microscope prior to the washing) were dead or alive. After 72h incubation with ART, the cells were collected from the wounds and counted using tryptan blue exclusion assay (Materials & Methods, Section, 2.8). The rest of the incubation media containing the non-adherent/dead cells was removed. The cells were washed three times in fresh ART-free media and the wound diameter was measured. The plates were incubated for additional 96h (7 days in total) in fresh media, in

the presence or absence of ART, as described in Materials & Methods (Section 2.8). The viable cell count was repeated using the tryptan blue exclusion assay and the diameter of the wound of each well was measures as before. The results after 72h and additional 96h were summarised (total 7 days) and the wound diameter and the mean number of dead cells was plotted against the concentrations of ART as shown in figure 31. As illustrated in figure 31, there was a concentration-dependent increase in the number of dead cells, which correlated with an increase in the wound diameter, as compared to initial control.

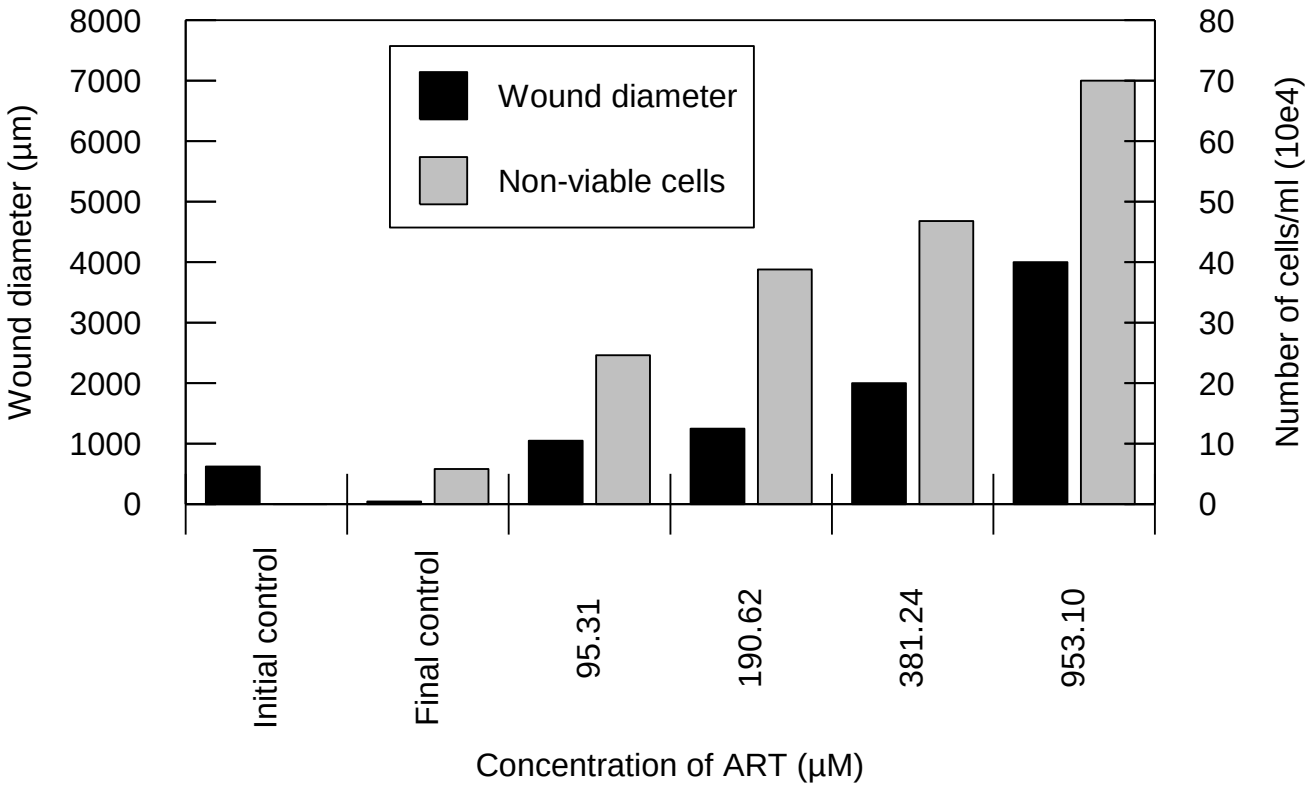

Figure 31: ART increases the diamater of the wound and the number of dead cells in HT-29-AK monolayers in normoxia. Following confluency, a wound was created and the cells were incubated in normoxia (20% O_2) without or with ART (at 0µM, 95.31µM, 190.62µM, 381.24 µM and 953.1µM) as described in Materials & Methods (Section 2.8). The results dead cells were estimated by tryptan blue exclusion assay. Data represent mean of 2 independent experiments and is not powered for statistical analysis. ART, artesunate.

Similar *in vitro* wound healing assay was performed for DHA-treated HT-29-AK cells. The results presented in figure 31 show the initial control wound (figure 32 Ai) with a diameter of 714.17µm which decreased in diameter to 374.76µm upon incubating the cells for 3 days without drug treatment (figure 32 A iii). There was complete closure of the wound after 7 days of incubation without drug treatment (figure 32 Aiiii). As with ART-untreated cells, it was observed that DHA-untreated cells had a high cell-cell contact and normal cell morphology (green arrows, figure 32 A) whereas DHA-treated cells were notably smaller, had shrunk and shown marked inhibition of cell-cell contact (red arrow head; figure 32 B, C, D, E). The results after 7 days of incubation show that upon treating the cells with 54.27µM, 108.53µM, 217.06 542.65µM of DHA, there was notable a concentration-dependent widening of the wound diameter to 984.74µm, 1278.24µm ~1600µm and ~3500µm, respectively (figure 32 B, C, D, E).

A) Control HT-29-AK cells

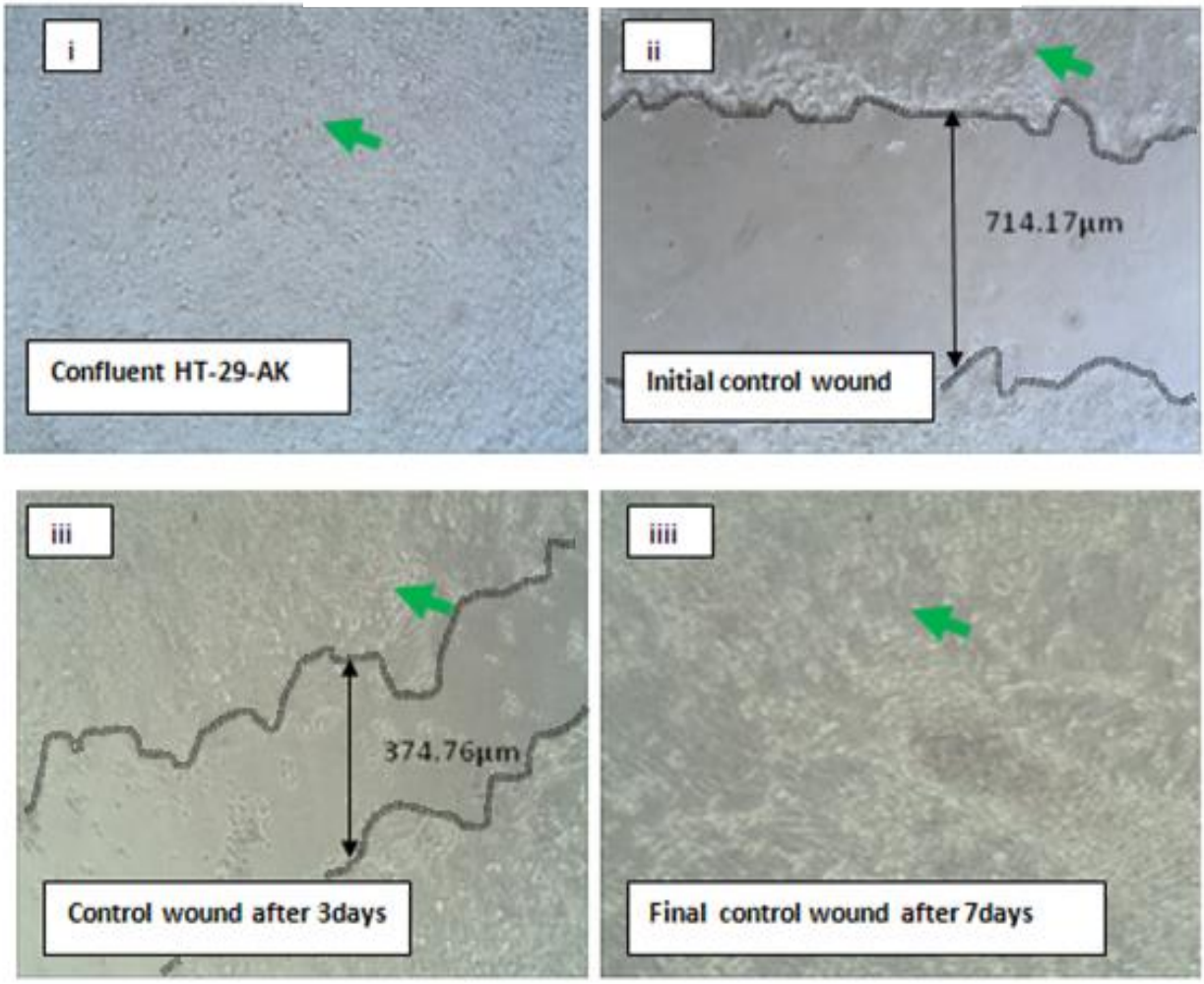

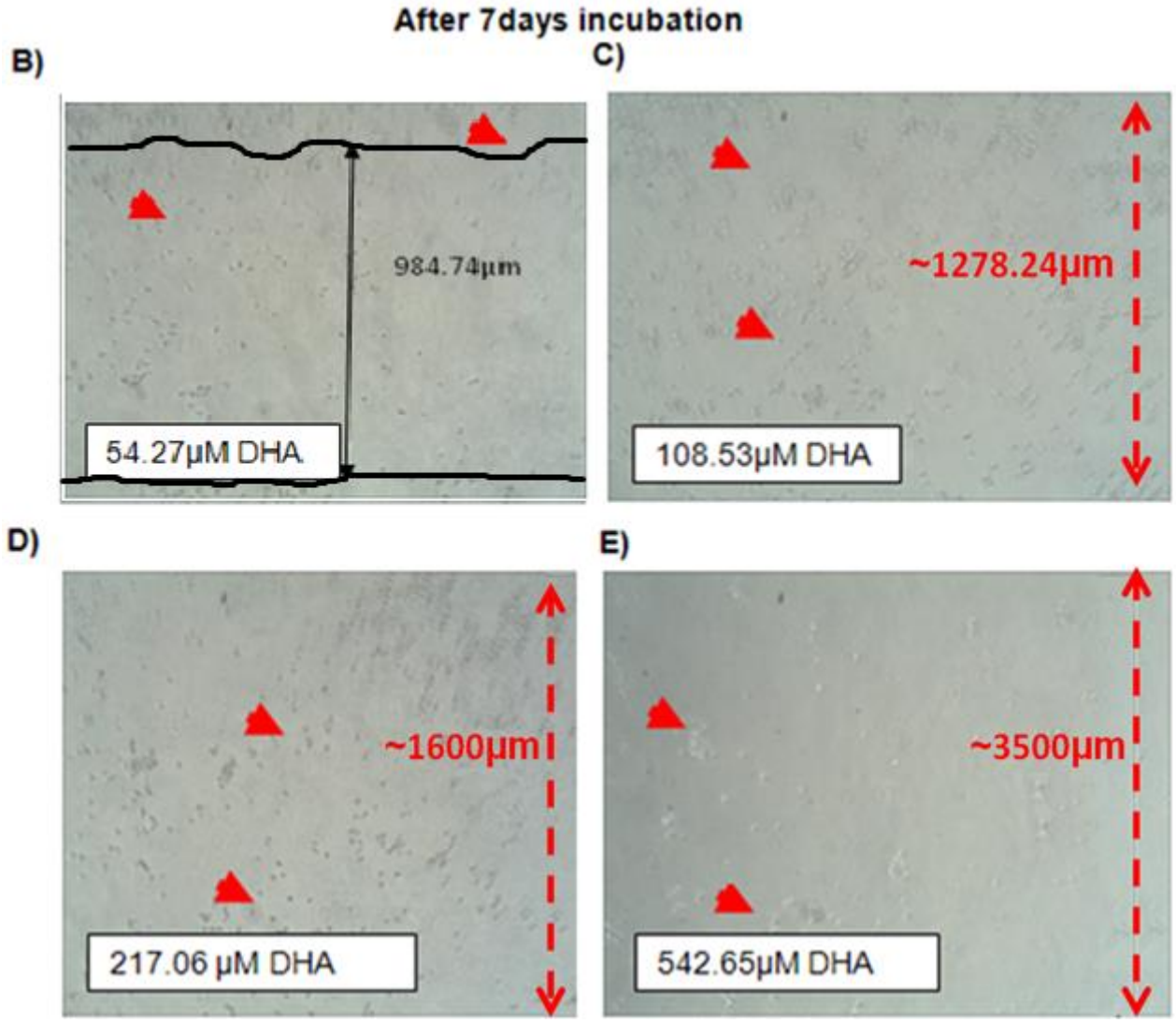

Figure 32: Wound healing capacity of HT-29-AK monolayers after treatment with DHA in normoxia. Cells were seeded onto 24-well plate and grown in MEM growth media in normoxia (20% O_2) till confluency was reached (figure 32A i). An initial wound was created using a sterile 10µl Pasteur pipette (figure 32A ii) before the cells were treated without or with DHA at A) 0µM, B) 54.27µM, C) 108.53µM and D) 217.06µM and E) 542.65µM as described in Materials & Methods (Section 2.8). For each DHA concentration (B-E), the wound diameter was measured after total 7 days of incubation with DHA. Green arrows, normal cells; red arrows, damaged cells, dotted red arrows indicate wound healing diameter greater than 1100µm. DHA, dihydroartemisinin.

Figure 33 shows that the number of dead cells in the incubation media correlated with an increase in the wound diameter, as compared to initial control.

Overall, ART and DHA exhibited comparable activity profiles in the inability of the wound to heal with observed increasing number of dead cells with ART and DHA increasing concentrations (figures 31 and 33).

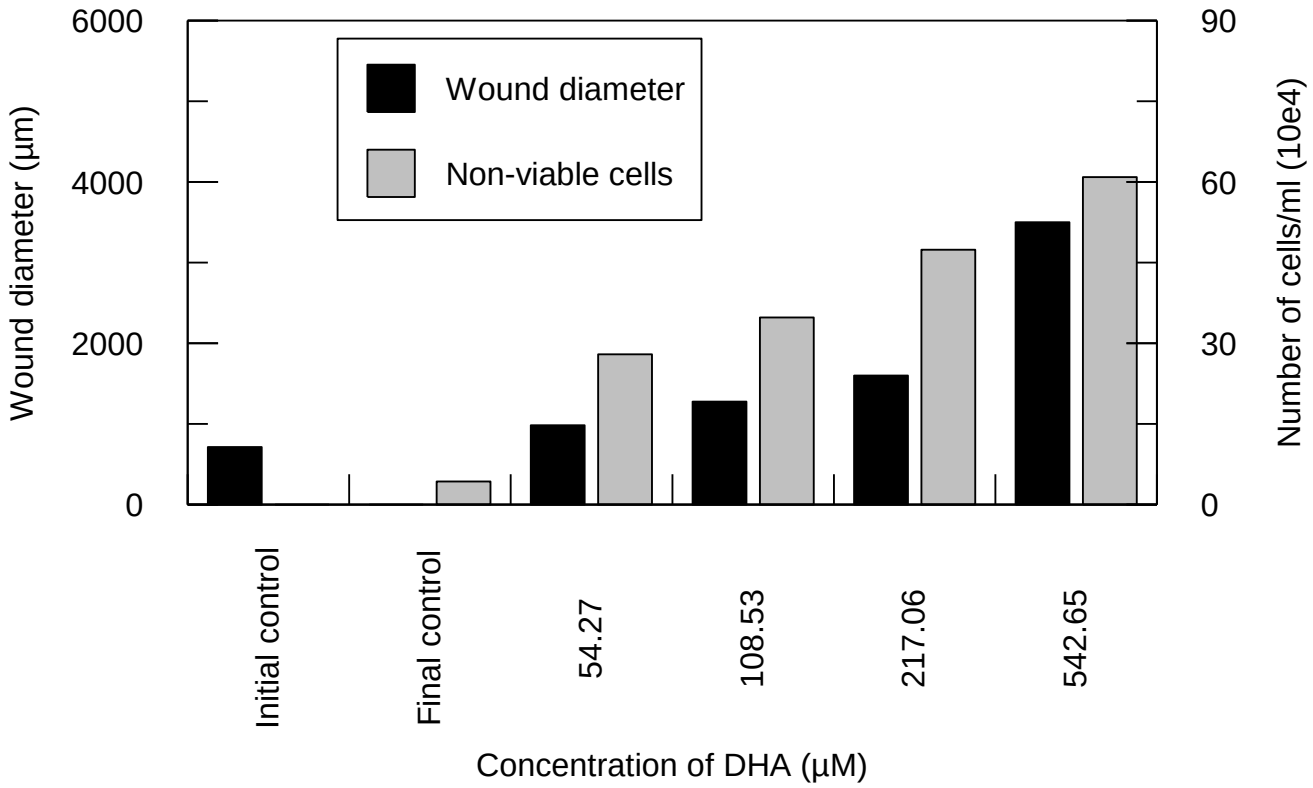

Figure 33: DHA increases the diamater of the wound and the number of dead cells in HT-29-AK monolayers in normoxia. Following confluency, a wound was created and the cells were incubated in normoxia (20% O_2) without or with DHA (at 0µM, 54.27µM, 108.53µM, 217.06 and 542.65µM) as described in Materials & Methods (Section 2.8). The results dead cells were estimated by tryptan blue exclusion assay. Data represent mean of 2 independent experiments and is not powered for statistical analysis. DHA, dihydroartemisinin.

3.10. Effect of ART and DHA on irreversibility of cell growth in normoxia

As the results of the wound healing assay indicate ART and DHA might inhibit migration/invasion of cancer cells through the inhibition of wound gap to heal, it was of interest to investigate if the agents inhibit the ability of cells to re-grow post drug treatment. For these experiments, MTT assay was performed as described in Materials & Methods (Section 2.4.6).

As illustrated in figure 34 A, cells treated with ART (at 7.22µM, 14.44µM, and 28.88µM) showed a significant ($P<0.001$) concentration-dependent inhibition of cell growth by ~38% (62.19 ± 0.34%), ~49% (51.19 ± 0.28%) and ~57% (43.09 ± 1.00%), respectively, as compared to control (100 ± 0.49%). There was a significant ($P<0.001$) concentration-dependent re-growth of the cells post-wash by ~44% (105.87 ± 4.04%) and ~43% (94.01 ± 6.79%) as compared to their matched pre-washed ART-treated samples. However, 28.88µM ART-treated cells showed a significant ($P<0.001$) inhibition of cells re-growth by ~19% (62.01 ± 11.49%). The initial treatment of cells with 9.88µM, 19.75µM, and 39.50µM of DHA resulted in a significant ($P<0.001$) concentration-dependent inhibition of cell proliferation by ~30% (69.69 ± 1.84%), ~51% (48.97 ± 1.11%) and ~ 66% (34.02 ± 1.38%), as compared to control (100 ± 0.67%). After wash, as compared to part 1, DHA (at 9.88µM) did not inhibit re-growth of cells whereas cells treated with 19.75µM of DHA demonstrated a ~43% ($P<0.001$; 48.97 ± 1.11% vs. 91.47 ± 5.64%) re-growth of the cells. The greatest inhibitory effect of DHA against HT-29-AK cells was observed when the cells were treated with 39.50µM of DHA. Here, the cells re-grew by 22.04% ($P<0.001$; 34.02 ± 1.38% vs. 56.06 ± 4.38%) post-wash (figure 34 B).

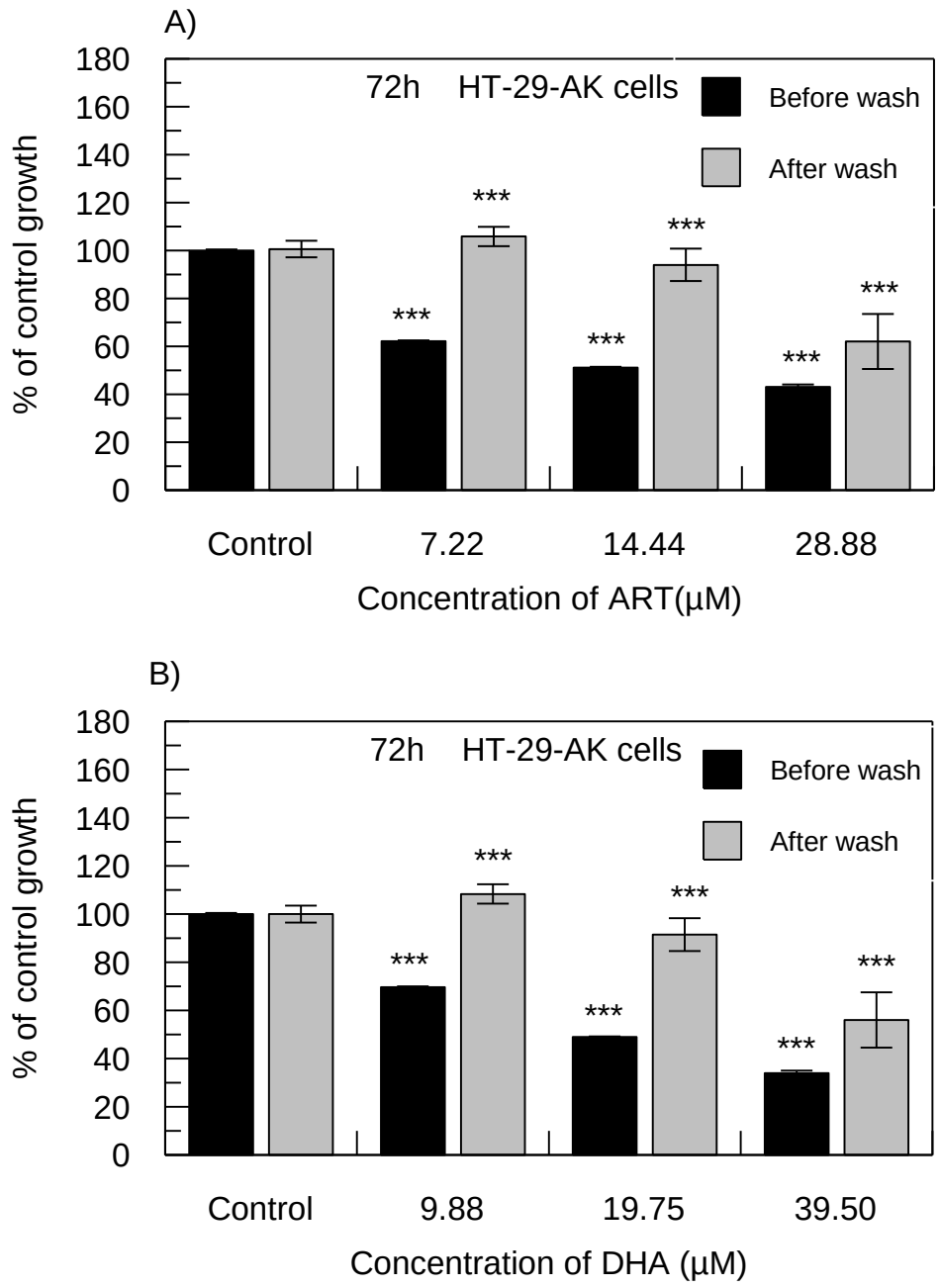

Figure 34: ART and DHA inhibit the re-growth of HT-29-AK cells cultured in normoxia. Initially (light grey bars), HT-29-AK cells were treated without or with (A) ART (at 0, 7.22, 14.44 and 28.88µM) and (B) DHA (at 0, 9.88, 19.75 and 39.50 µM) for 72h in normoxia (20% O_2) and terminated as described in Materials & Methods (Section 2.4.6). In the re-growth assay, the treated cells were washed and further incubated for 72h in drug-free media before the assay was terminated (Materials and Methods, Section 2.4.6). Data represent the mean ± S.D of 3 independent experiments. ***P<0.001 as tested by Paired T test. ART, artesunate; DHA, dihydroartemisinin.

For comparison purposes, similar investigations using MTT assay were performed with ART- and DHA-treated HL-60 cells (figure 35). As presented in figure 35 A, initial treatment without or with ART at 0.98µM, 1.96µM, and 3.92µM resulted in a significant ($P<0.001$) reduction in the growth of HL-60 cells by 37%, 70% and 91%, respectively as compared to control (100 ± 2.19%). Subsequent incubation of the cells, post wash for a further 72h in drug-free media revealed a significant ($P<0.001$) reduction in the ability of the cells to re-grow, i.e., none of the drug treated cells were able to re-grow to the levels observed in control samples (figure 35A). Nevertheless, there was significant ($P<0.001$) re-growth of the cells by 26% and 35%, as compared to the results of initial treatment with 0.98µM and 1.96µM ART, respectively (figure 35A). Interestingly, cells initially treated with ART (at 3.92µM) showed a re-growth of only 17% after the wash step ($P<0.001$; 9.5 ± 2.43% vs. 25.66 ± 3.28%) (figure 35A). Cells treated with DHA (at 0.70µM, 1.40 µM and 2.80µM) also showed significant inhibitory effect on cell growth by 2%, 76.1% ($P<0.001$) and 93.2% ($P<0.001$), respectively as compared to their corresponding control (figure 35 B). After the wash step, there was a significant ($P<0.001$) re-growth of the cells by 39% and 20% as compared with the pre-wash samples treated with DHA at 1.40µM and 2.80µM, respectively. Interestingly, data acquired from samples treated with 0.70µM of DHA post wash revealed a further reduction (~10%) in the ability of the cells to re-growth as compared to the corresponding pre-wash data ($P<0.001$; 3.55 ± 0.31% vs. 26.83 ± 5.45%) (figure 35 B).

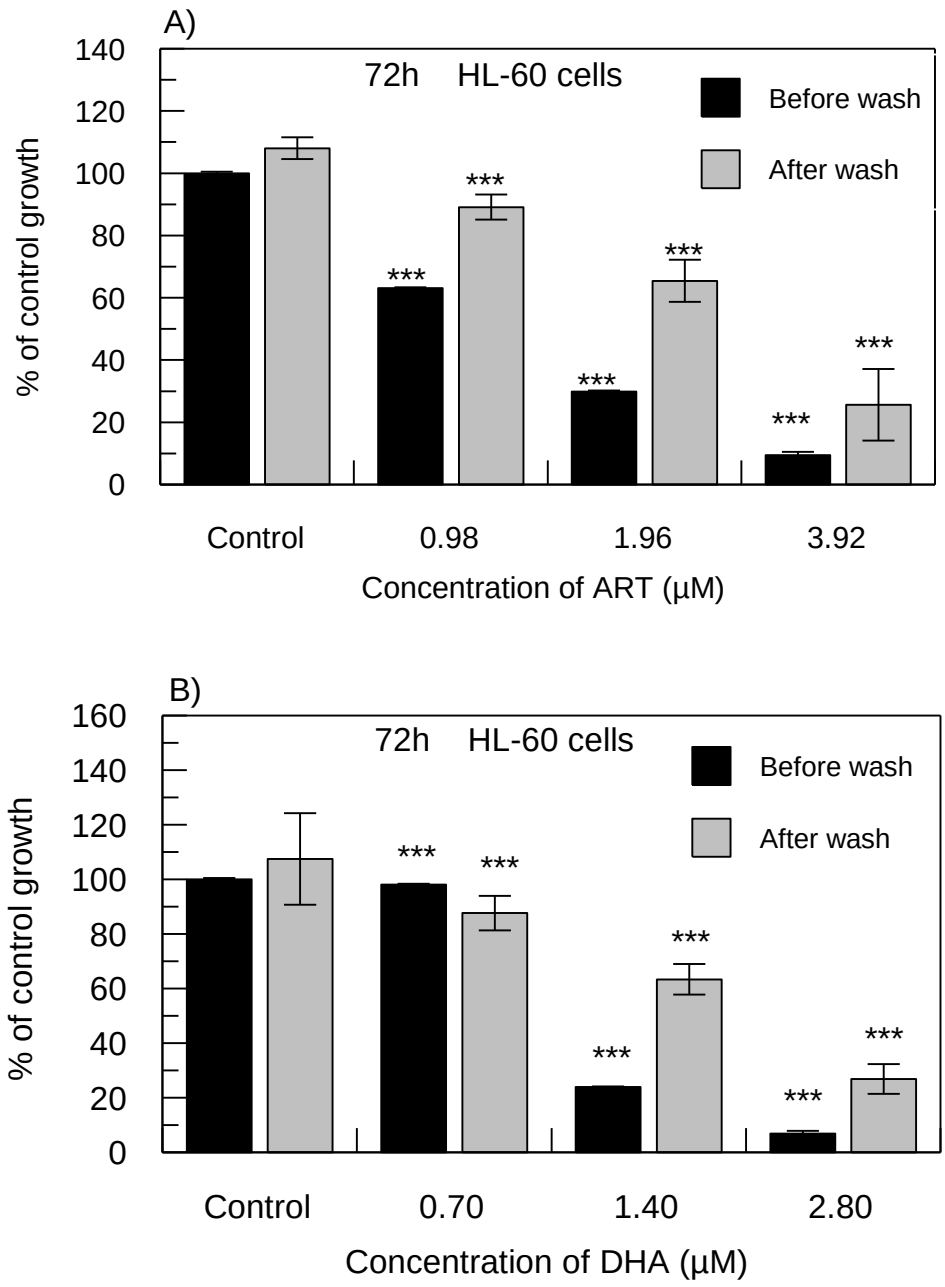

Figure 35: ART and DHA inhibit the re-growth of HL-60 cells cultured in normoxia. Initially (dark grey bars), HL-60 cells were treated without or with (A) ART (at 0, 0.98, 1.96, and 3.92µM) and (B) DHA (at 0, 0.70, 1.40 and 2.80µM) for 72h in normoxia (20% O_2) and the plates were terminated as described in Materials & Methods (Section 2.4.6). Some of the plates were washed and incubated in drug-free media for a further 72h (light grey bars) before the plates were terminated (Materials and Methods, Section 2.4.6). Data represent the mean ± S.D of 3 independent experiments. ***P<0.001 as tested by Paired T- test. ART, artesunate DHA, dihydroartemisinin.

3.11. Effect of ART and DHA on the expression of MMP-2 and MMP-9 proteins

The 2D wound healing assay showed that ART and DHA markedly reduced the capacity of the wound to heal/close (figures 30-33). In addition, MTT assay indicated the ability of ART and DHA to inhibit the re-growth of cancer cells after finishing drug therapy (figures 34 and 35). To investigate a possible molecular basis of these observations, the ability of ART and DHA to inhibit intracellular proteins MMP-2 and MMP-9 were investigated. Both proteins are associated with enhancing cancer cell migration, invasion, and metastatic abilities through decresing cell-EM interactions and were measured as described in Materials & Methods (Section 2.9.1.1) (Kim *et al.* 2012).

The protein levels of MMP-2 and MMP-9 were evaluated first upon ART and DHA treatment in HT-29-AK cells. Figure 36A shows that treatment with ART (at 7.22µM, 14.44µM and 28.88µM) caused an up-regulation in MMP-2 expressions with the highest observed at 14.44µM ART (~1.52-fold, 1.52 ± 0.17 RFU; $P<0.001$) and the lowest MMP-2 levels were observed with the highest concentration at 28.88µM ART (~1.09-fold, 1.09 ± 8.11 RFU), as compared to control (1.00 ± 0.13 RFU), respectively. The up-regulation of MMP-9 protein levels was decreasing with higher ART concentrations, resulting in a change in fold difference by ~3.35 (3.35 ± 0.31 RFU; $P<0.001$), ~3.12 (3.12 ± 0.27 RFU; $P<0.001$) and ~2.75 (2.75 ± 0.37 RFU; $P<0.001$) upon treating HT-29-AK cells with 7.22µM, 14.44µM and 28.88µM of ART, as compared with control (1.00 ± 0.03 RFU), respectively (figure 36B).

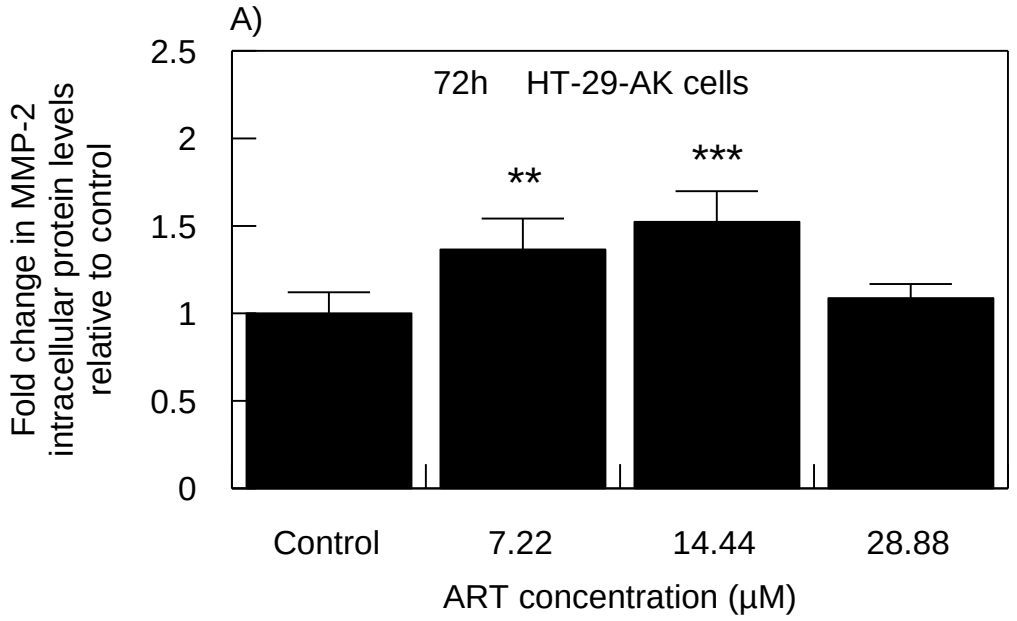
A)
72h HT-29-AK cells
Fold change in MMP-2 intracellular protein levels relative to control
2.5
2
1.5
1
0.5
0
**
***
Control
7.22
14.44
28.88
ART concentration (µM)

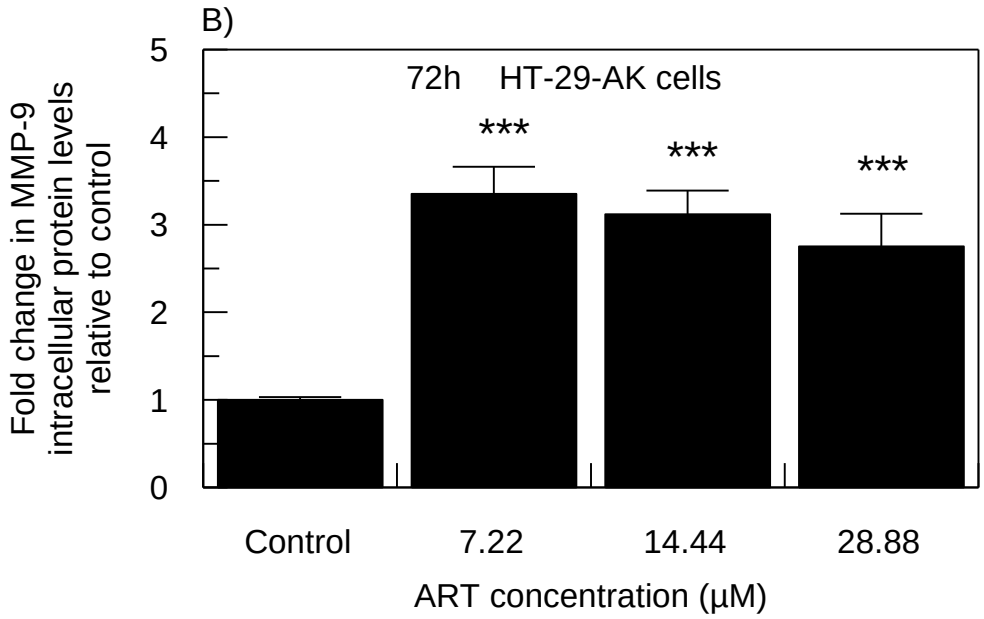
B)
72h HT-29-AK cells
Fold change in MMP-9 intracellular protein levels relative to control
5
4
3
2
1
0
***
***
***
Control
7.22
14.44
28.88
ART concentration (µM)

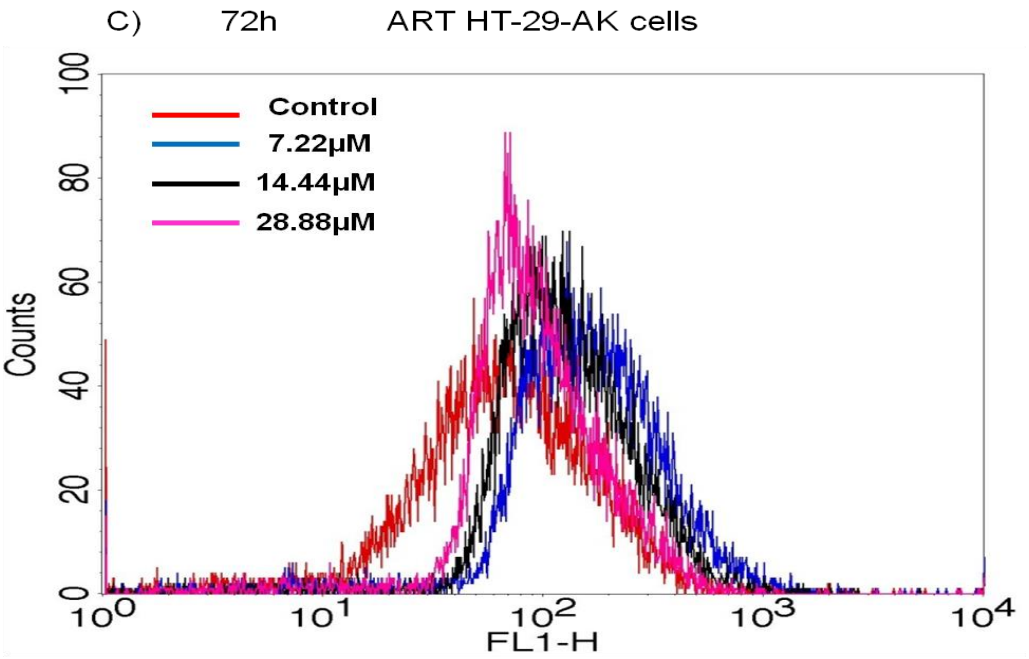

Figure 36: The effect of ART on intracellular MMP-2 and MMP-9 protein levels in HT-29-AK cells at 72h in normoxia. Cells were treated without or with ART (at 0µM, 7.22µM, 14.44µM and 28.88µM) for 72h in normoxia (20% O_2), labelled with either A) MMP-2 or B) MMP-9 antibodies and analysed on flow cytometer. C) Representative histograms showing changes in MMP-2 protein levels upon ART treatment as compared to untreated HT-29-AK cells as analysed by CellQueast Software on flow cytometer. Results are expressed as mean ± SD of three independent experiments. **P<0.01 and ***P<0.001 vs. control as tested by one-way Anova (Dunnett test for comparison with control). ART, artesunate.

MMP-2 intracellular protein expression levels were higher upon DHA treatment of HT-29-AK cells for 72h as compared to MMP-2 levels observed upon treating the cells with ART for 72h (figure 36A vs. figure 37A). Compared to control (0.99 ± 0.08 RFU), the up-regulated protein levels of MMP-2 in HT-29-AK cells were decreasing with increasing concentrations of DHA resulting in MMP-2 fold differerence of 2.45-fold (2.45 ± 0.30 RFU; P<0.001), 2.20-fold (2.20 ± 0.13 RFU; P<0.001) and 2.15-fold (2.15 ± 0.12 RFU; P<0.001) upon treating the cells with 9.88µM, 19.75µM and 39.50µM DHA, respectively (figure 37A).

The up-regulated levels of MMP-9 in HT-29-AK cells had steady lowering trend upon DHA treatment with increasing concentrations for 72h (figure 37B). Thus, compared to control (1.00 ± 0.21 RFU), there was 2.49-fold (2.49 ± 0.15 RFU; P<0.001), 2.39-fold (2.39 ± 0.17 RFU; P<0.001) and 2.03-fold (2.03 ± 0.08 RFU; P<0.001) increase in MMP-9 release upon treating HT-29-AK cells with DHA treatment at 9.88µM, 19.75µM and 39.50µM, respectively (figure 37B).

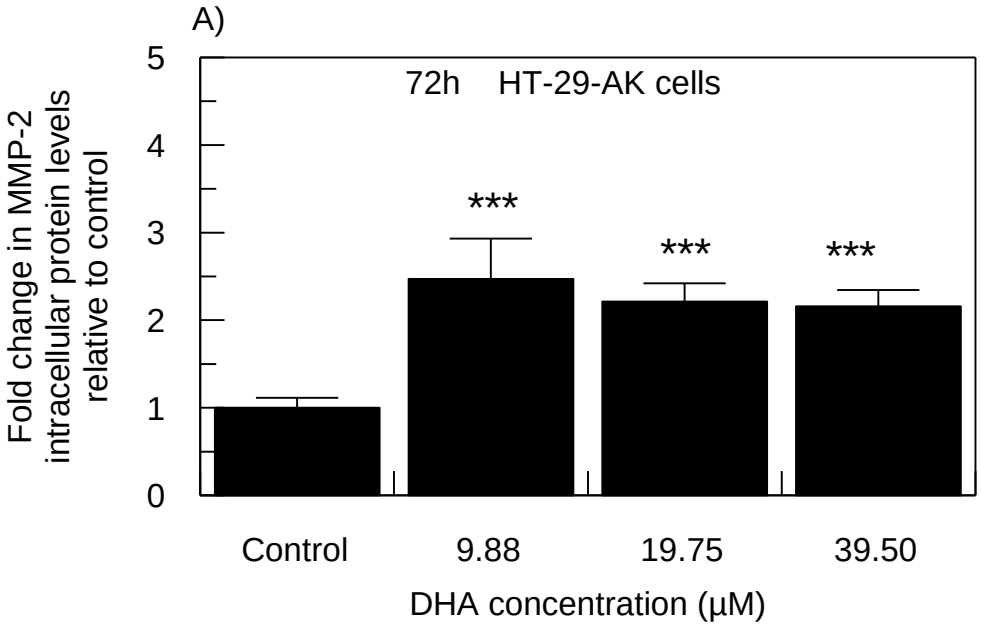

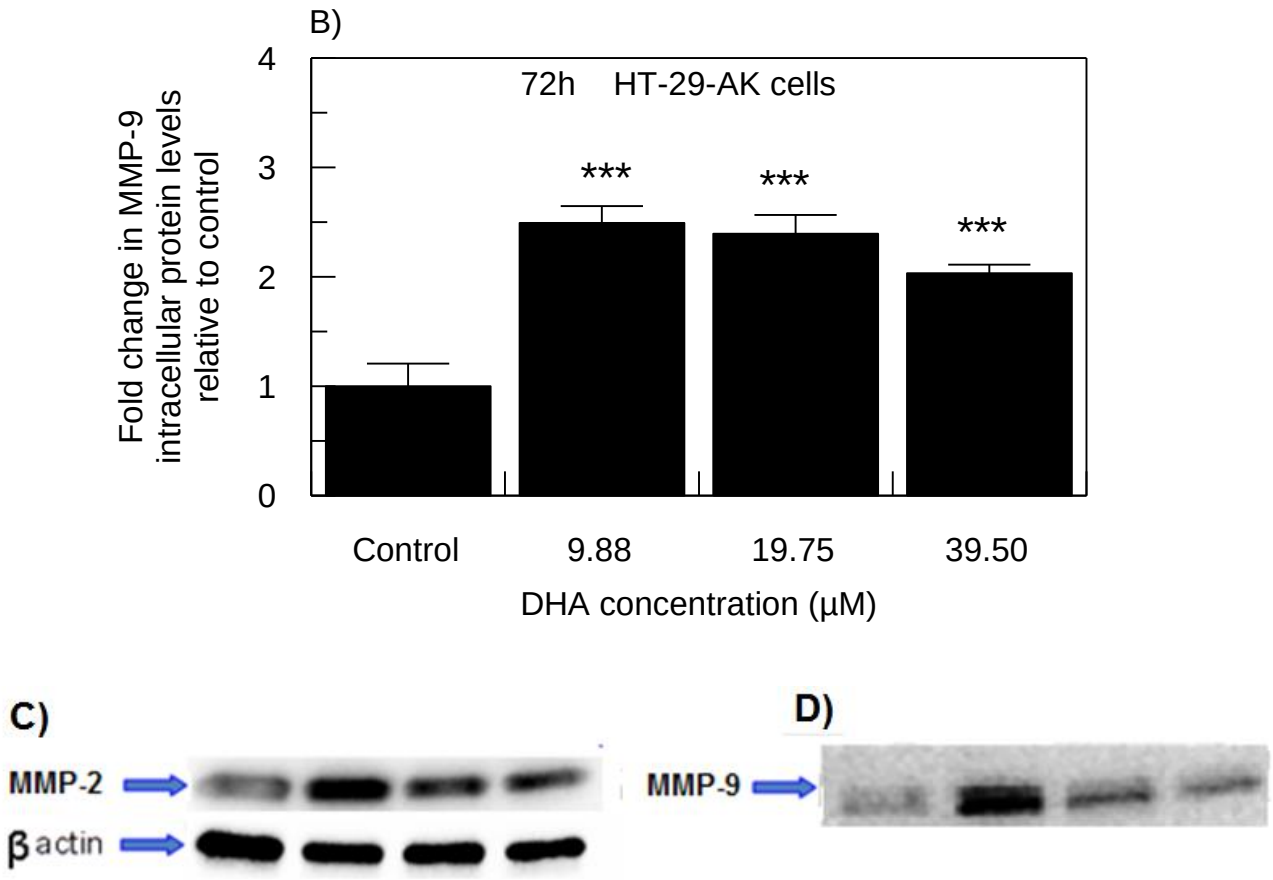

Figure 37: The effect of DHA on the protein expression of MMP-2 and MMP-9 in HT-29-AK cells at 72h in normoxia. Cells were treated without or with DHA (at 0µM, 9.88µM, 19.75µM and 39.50µM) for 72h under normoxic conditions, labelled with either A) MMP-2 or B) MMP-9 antibody and analysed on flow cytometer. In similar experiments, proteins were isolated from cells after DHA treatment, separated by SDS-PAGE and stained with C) MMP-2 and D) MMP-9 for Western blotting analysis as described in Materials and Methods (Section 2.10). Flow cytometry results represent the mean ± SD of three independent experiments where ***P<0.001 vs. control as tested by one-way ANOVA (Dunnett test for comparison with control). Western blotting data show results of 1 independent experiment. DHA, dihydroartemisinin.

The protein expression levels of MMP-2 and MMP-9 were additionally investigated for DHA-treated HT-29-AK cells for 72h using Western blotting performed as described in Materials & Methods (Section 2.10). Representative pictures show similar pattern in MMP-2 and MMP-9 protein expressions as compared with the results derived from flow cytometric analysis (figures 37 C and D). The dark bands at corresponding picture indicate high protein levels whereas light bands show low protein levels in those samples (figures 37 C and D).

MMP-2 and MMP-9 investigations in HL-60 cells treated with ART for 72h showed opposite results as compared to data on both proteins in HT-29-AK cells. As illustrated in figure 38A, HL-60 untreated cells showed MMP-2 intracellular protein levels of 1.00 ± 0.06 RFU which was increased in a concentration-dependent manner by 35% (1.35 ± 0.04 RFU; $P<0.05$), 45% (1.45 ± 0.18 RFU; $P<0.01$) and 63% (1.63 ± 0.15 RFU; $P<0.001$) upon treating HL-60 leukaemia cells with 0.30µM, 0.60µM and 1.20µM ART, respectively. It was further observed that expression of MMP-9 with ART after 72h was higher as compared to MMP-2 results (figures 38 A and B). ART-untreated cells demonstrated MMP-9 protein levels of 1.00 ± 0.02 RFU which was increased ~1.97- (1.97 ± 0.15 RFU; $P<0.001$), ~2.55- (2.55 ± 0.10 RFU; $P<0.001$) and ~3.06-fold (3.06 ± 0.25 RFU; $P<0.001$) upon ART treatment at 0.30µM, 0.60µM and 1.20µM, respectively (figure 38B).

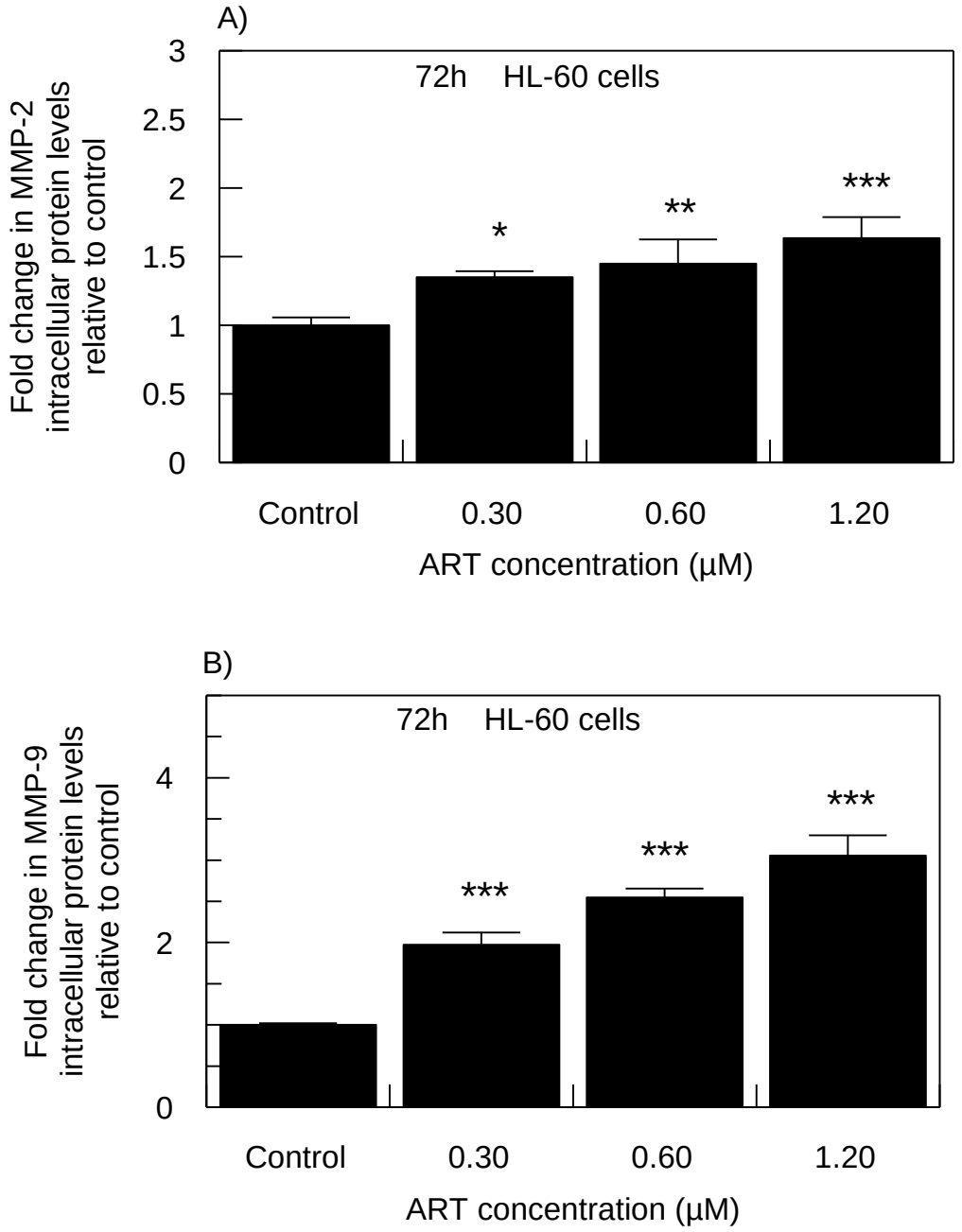

Figure 38: The effect of ART on the intracellular MMP-2 and MMP-9 protein expression in HL-60 cells at 72h in normoxia. Cells were treated without or with ART (at 0µM, 0.30µM, 0.60µM and 1.20µM) for 72h in normoxia (20% O_2), labelled with either A) MMP-2 or B) MMP-9 antibodies and analysed on flow cytometer as described in Materials and Methods (Section 2.9.1). Results are expressed as mean ± SD of three independent experiments. *P<0.05, **P<0.01 and ***P<0.001 vs. control as tested by one-way Anova (Dunnett test for comparison with control). ART, artesunate.

In comparison to the effects of ART in HL-60 cells, DHA-treated HL-60 cells at 0.25µM, 0.50µM and 1.00µM for 72h demonstrated not significant decreasing trend in MMP-2 protein levels by 1% (0.99 ± 0.03 RFU), 3% (0.97 ± 0.09 RFU) and 7% (0.93 ± 0.06 RFU), respectively, as compared to control (1.00 ± 0.02 RFU) (figure 39A). In addition, the expression levels of MMP-9 were increasing with increasing concentrations of DHA resulting in a percentage increase of 6% (1.06 ± 0.06 RFU), 13% (1.13 ± 0.03 RFU) and 22% (1.22 ± 0.04 RFU) upon treating the cells with 0.25µM, 0.50µM and 1.00µM of DHA, respectively, as compared with untreated cells (1.00 ± 0.07 RFU, figure 39B).

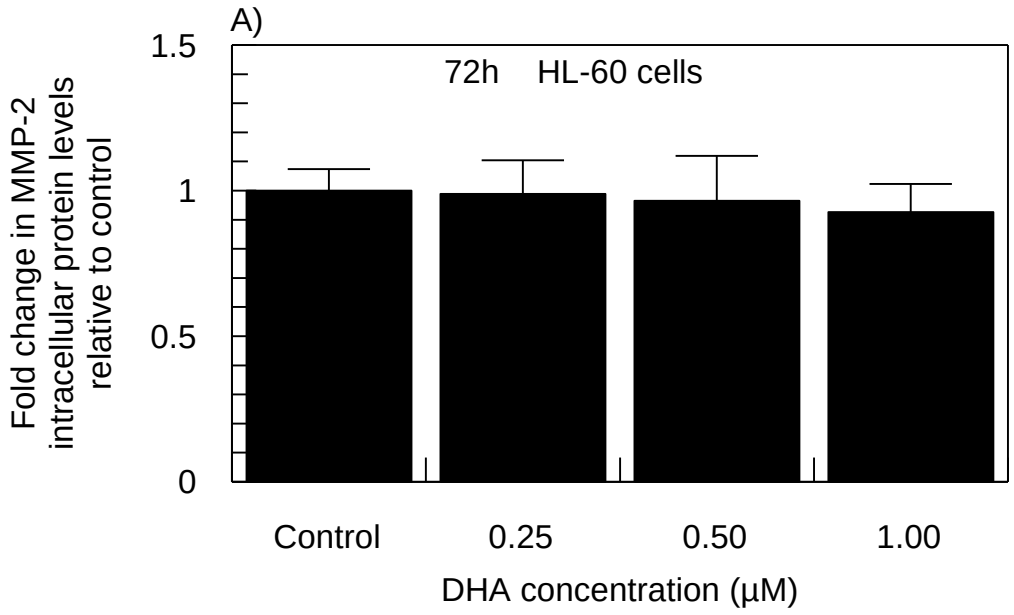

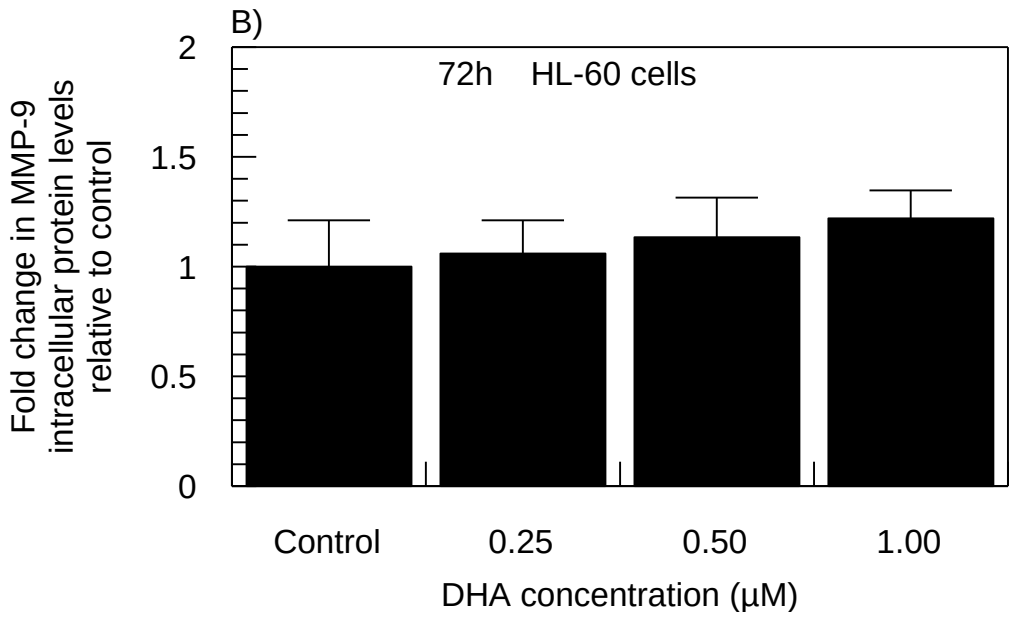

Figure 39: The effect of DHA on the intracellular MMP-2 and MMP-9 protein expression in HL-60 cells at 72h in normoxia. Cells were treated without or with DHA (at 0µM, 0.25µM, 0.50µM and 1.00µM) for 72h in normoxia (20% O_2), labelled with either A) MMP-2 or B) MMP-9 antibodies and analysed on flow cytometer as described in Materials and Methods (Section 2.9.1). Results are expressed as mean ± SD of three independent experiments. *P<0.05 vs. control as tested by one-way Anova (Dunnett test for comparison with control). DHA, dihydroartemisinin.

3.12. ART and DHA alter secretions and mRNA levels of pro-angiogenic VEGF-α in HT-29-AK and HL-60 cells

VEGF-α isoform is a key pro-angiogenic modulator, which has been demonstrated to have a central role in cancer metastasis through promoting angiogenesis (Niki *et al.* 2000). Increasing evidence indicates that ART and DHA inhibit two main pro-angiogenic factors, VEGF-α and HIF-1α in several cancer cell lines (Anfosso *et al.* 2006; Huang *et al.* 2007; Zhou *et al.* 2007; Aung *et al.* 2011; Wang *et al.* 2011). Therefore, to further study the cellular effects of action of ART and DHA against HT-29-AK and HL-60 cells, mRNA and protein levels of VEGF-α were investigated to identify agreement or to challenge previous reports (Materials & Methods, Sections 2.5.3 and 2.6).

In HT-29-AK cells, the mRNA expression levels of VEGF-α for 24h and 72h incubations with ART treatments were first measured by qPCR (figures 40A and B). HT-29-AK cells treated with ART for 24h showed increasing concentration levels of VEGF-α by 8.20-fold (ΔΔCt of 8.20 ± 1.10), 8.82-fold (ΔΔCt of 8.82 ± 0.69) and 9.13-fold (ΔΔCt of 9.13 ± 1.16) in a ART concentration-increasing manner with 82.53μM, 165.06μM and 330.12μM ART, respectively, as compared to control (ΔΔCt of 1.00 ± 00; $P<0.001$) (figure 40 A). In contrast, ART treatment for 72h significantly ($P<0.001$) inhibited VEGF-α mRNA expression in all samples by ~1.56 fold (ΔΔCt of 0.64 ± 0.04), ~1.45 fold (ΔΔCt of 0.69 ± 0.03) and ~1.64 fold (ΔΔCt of 0.61 ± 0.03) with 7.22μM, 14.44μM and 28.88μM ART, as compared to control (ΔΔCt of 1.00 ± 0.03, figure 40B), respectively.

ELISA investigating of the cellular VEGF-α_{165} secretions after 72h with ART in HT-29-AK cells was performed to evaluate if VEGF-α is modulated post-transcriptionaly by other mediators (figure 40C). VEGF-α_{165} protein levels in cell culture supernates from all ART-untreated and treated samples showed that ART treatment had variable effect on

VEGF-α_{165} secretion (figure 40C). Control cells showed VEGF-α_{165} secretion levels of 515.14pg/mL, which was decreased by ~1.20-fold (430.18pg/ml) upon treating the cells with 7.22µM of ART, followed by an increase by ~1.07-fold (551.27pg/mL) with 14.44µM ART. The VEGF-α_{165} secretion levels then dropped by ~1.29-fold (398.93pg/mL) at 28.88µM ART (figure 40C).

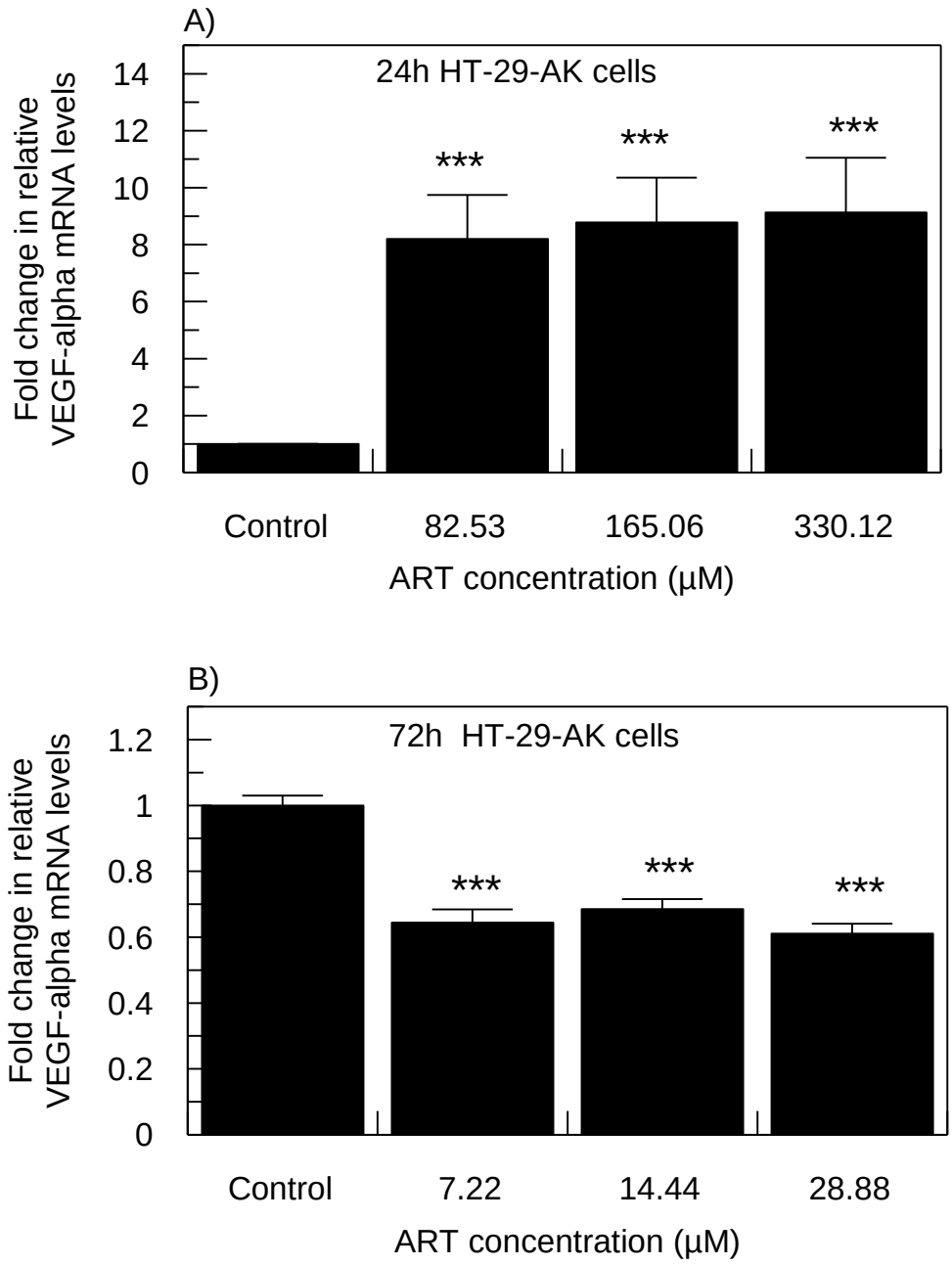

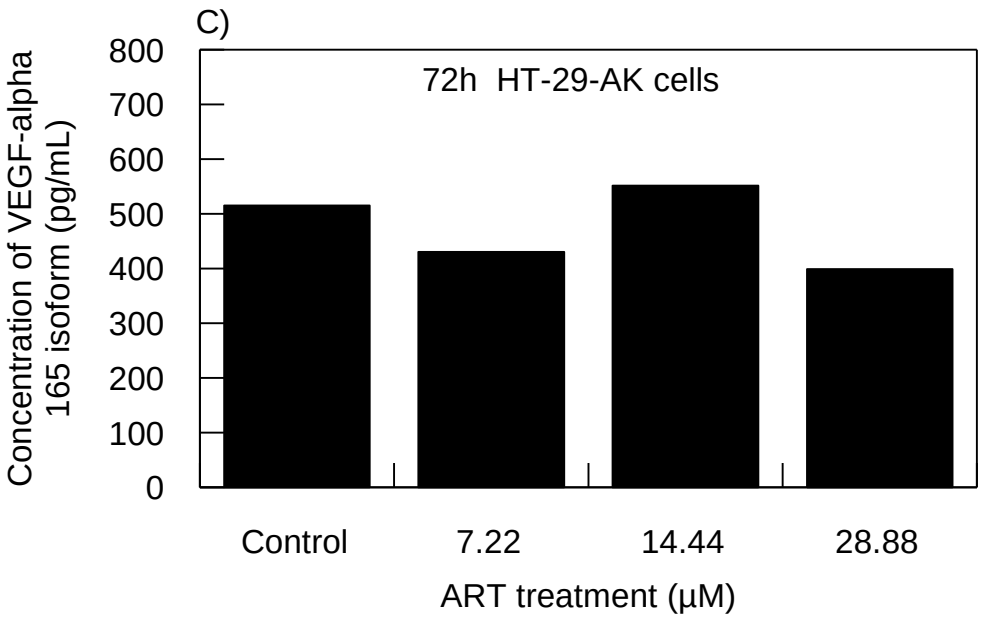

Figure 40: The effect of ART on VEGF-α mRNA expression levels and cellular VEGF-α165 secretion in HT-29-AK cells in normoxia. Cells were treated without or with ART (at 0µM, 82.53µM, 165.06µM and 330.12µM) for 24h and without or with ART (at 0µM, 7.22µM, 14.44µM and 28.88µM) for 72h in normoxia (20% O_2). After incubations cells were analysed for VEGF-α mRNA using qPCR analysis (A and B). In separate investigations culture media was collected and analysed for VEGF-$_{α165}$ levels by ELISA (C). Results are expressed as mean ± SD of three independent experiments. ***P<0.001 vs. control as tested by one-way Anova (Dunnett test for comparison with control). VEGF-$_{α165}$ protein levels represent 2 independent experiments which are not powered to perform statistical analysis. ART, artesunate.

Figure 41 shows that similar variable effects on VEGF-$α_{165}$ protein secretions were observed in HT-29-AK samples treated with DHA for 24h. There was an increase by ~1.06-fold (189.94pg/mL) in samples treated with 29.01µM of DHA, followed by a decrease by ~1.32- (136.23pg/mL) and ~1.29-fold (139.16pg/mL) when the cells were treated with DHA at 58.02µM and 116.04µM, as compared to control (139.16pg/mL), respectively. However, HT-29-AK cells treated for 72h at 9.88µM, 19.75µM and 39.50µM DHA showed a

reduction in VEGF-α_{165} secretion by ~1.27- (511.23pg/mL), ~1.26- (513.18pg/mL) and ~1.4-fold (464.36pg/mL), respectively, as compared to control (648.93 pg/mL) (figure 41).

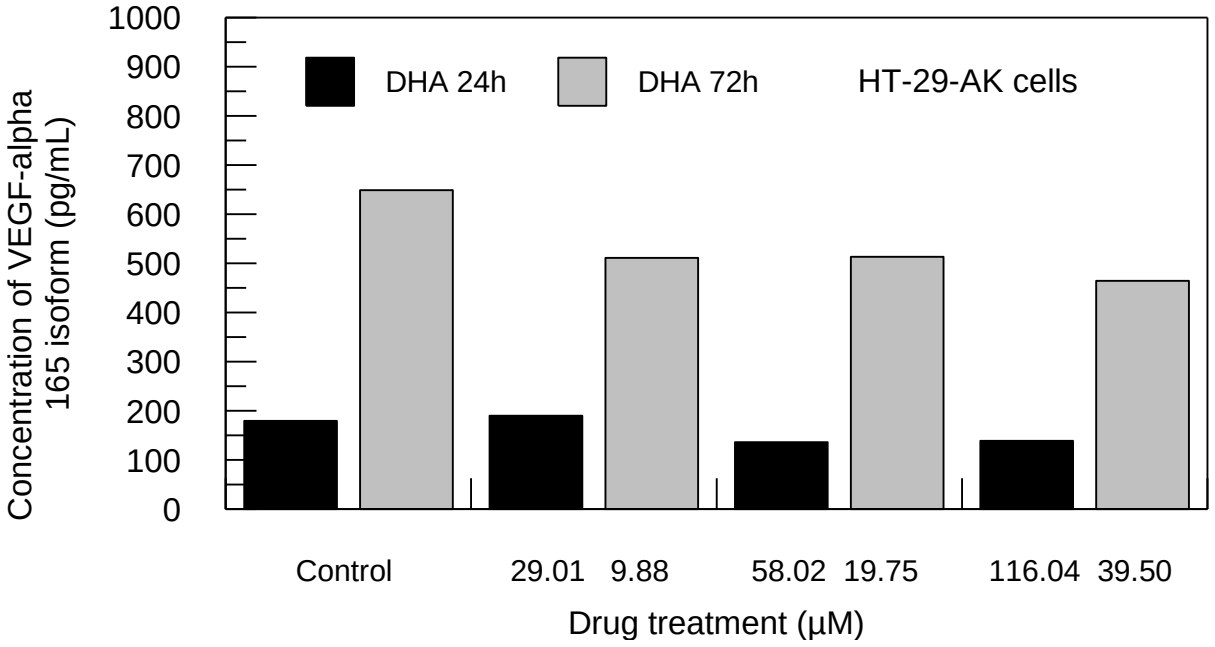

Figure 41: The effect of DHA on VEGF-α165 cellular secretion in HT-29-AK cells at 24h and 72h in normoxia. Cells were exposed to DHA for 24 h (striped bars) and 72h (dotted bars) with DHA concentrations shown under normoxic conditions (20% O_2). Following incubation cell-free culture media were analysed by ELISA as described in Materials & Methods (Section 2.5.3). The histograms represent the mean of 2 independent experiments which are not powered for statistical analysis. DHA, dihydroartemisinin.

Overall, data indicate that DHA treatment for 72h caused a decreased secretion of VEGF-α_{165} as compared to control at all concentrations tested. ART treatment for 72h and DHA for 24h produced some notable reductions in VEGF-α_{165} levels, but only at certain concentrations (ART at 7.22µM and 28.88µN; DHA at 58.02µM and 116.04µM; figures 40 and 41). In addition, we observed similar data patterns for mRNA and VEGF-α_{165} for ART-treated HT-29-AK cells for 72h, suggesting lack of other mediators affecting VEGF-α expression post-transcriptionaly (figure 41).

Similar investigations were performed to investigate the effects of ART and DHA on VEGF-α_{165} in HL-60 cells (figure 42). HL-60 cells showed measurable levels of VEGF-α_{165}, with more VEGF-α_{165} found in cells cultured for 72h with DHA, as compared to those cultured for 24h (figure 42). After 24h, DHA-untreated cells displayed the lowest VEGF-α_{165} secretions of 92.29 pg/ml, which was increased by ~22.21% (112.79) at 0.35µM and 0.70µM DHA, and by ~25.39% (115.72pg/mL) at 1.40µM DHA (figure 42). VEGF-α_{165} secretions in samples treated for 72h with 0.25µM. 0.49µM and 0.98µM DHA decreased with increasing DHA concentrations by ~1.25% (386.23pg/mL), ~9.24% (354.98pg/mL) and ~9.49% (354.00pg/mL), as compared to control (391.11pg/ml), respectively (figure 42). Similarly, as shown in figure 42, ART-untreated HL-60 cells for 72h showed a VEGF-α_{165} secretion of 490.72pg/mL which was decreased by ~15.52% (414.55pg/mL), ~5.37% (464.36pg/mL) and ~12.74% (428.22pg/mL) upon treating the cells with 0.30µM, 0.60µM, 1.20µM ART, respectively. Taken together, while DHA-treated HL-60 cells for 24h showed an increase in VEGF-α_{165} protein secretions, HL-60 cells treated with ART or DHA for 72h showed the ability to effectively decrease secretions of VEGF-α_{165} protein. The findings indicate anti-angiogenetic activity of both compounds against leukaemia HL-60 cells after 72h incubation. However, due to resources limitations presented results represent only 2 independent experiments which are not powered for statistical analysis.

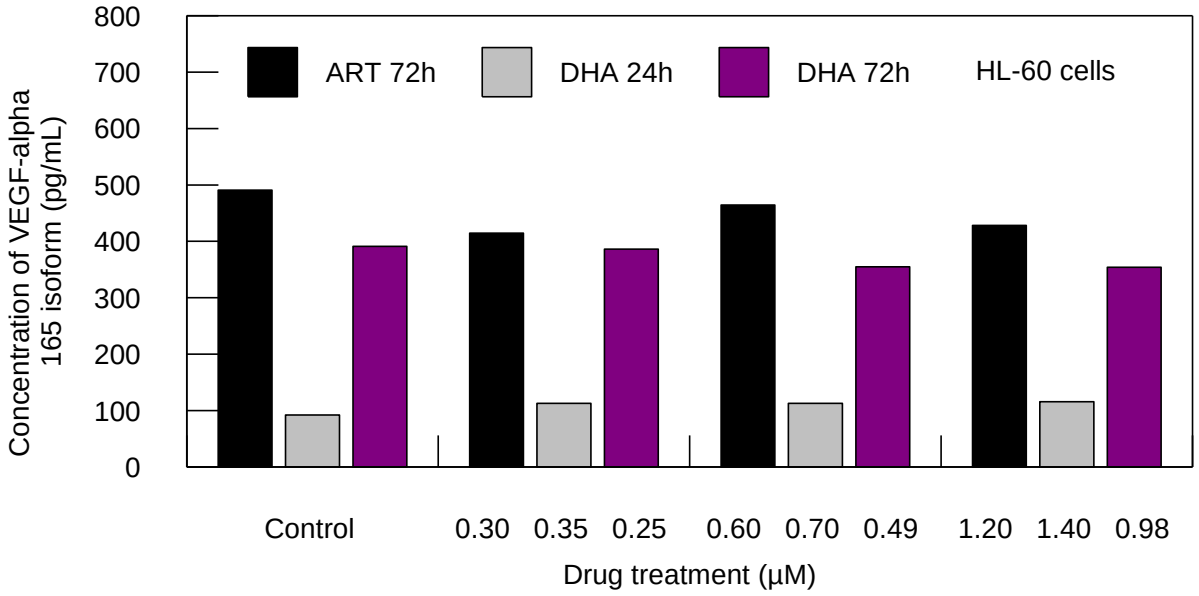

Figure 42: The effect of ART and DHA on VEGF-α165 cellular secretion in HL-60 cells in normoxia. Cells were exposed to ART for 72h (black bars), DHA for 24 h (grey bars) and 72h (purple bars) with the drug concentrations shown under normoxic conditions (20% O_2). Following incubation cell-free culture media were analysed by ELISA as described in Materials & Methods (Section 2.5.3). The histograms represent the mean of 2 independent experiments which are not powered for statistical analysis. ART, artesunate; DHA, dihydroartemisinin.

3.13. Effect of ART and DHA on HIF-1α protein and mRNA expression levels

The results indicate the ability of ART and DHA to produce variable effects on VEGF-α in cancer cells (figures 40-42). The expression of HIF-1α upon treatment with 1,2,4,-trioxanes in different experimental settings was variable and led to conflicting data regarding the effects of compounds on HIF-1α (Anfosso *et al.* 2006; Huang *et al.* 2007; Ba *et al.* 2012). Therefore, the effect of ART and DHA was evaluated in present study towards pro-angiogenic protein, HIF-1α. qPCR and flow cytometric analyses were performed to evaluate the effect of ART and DHA on expression change in HIF-1α mRNA and intracellular proteins levels, respectively, as described in Materials & Methods (Section 2.6 and 2.9.2).

Measured mRNA levels of HIF-1α upon treating HT-29-AK cells with ART for 24h were markedly up-regulated in a concentration-dependent manner by 10.12- (ΔΔCt= 10.12), 10.79- (ΔΔCt= 10.79) and 36.93-fold (ΔΔCt= 36.93) with 82.53μM, 165.06μM and 330.12μM ART, as compared to control (ΔΔCt=1.00), respectively (figure 43A). In contrast, HT-29-AK cells treated with ART for 72h showed HIF-1α mRNA levels to be significantly ($P<0.001$) decreased (figure 43B). There was a down-regulation of HIF-1α mRNA levels by 1.59-fold (ΔΔCt= 0.63 ± 0.05; $P<0.001$), 2.00-fold (ΔΔCt= 0.50 ± 0.03; $P<0.001$) and 6.25-fold (ΔΔCt= 0.16 ± 0.03; $P<0.001$) upon treating HT-29-AK cells with increasing concentrations of ART at 7.22μM, 14.44μM and 28.88μM, as compared to control (ΔΔCt= 1.00 ± 10), respectively (figure 43B). The protein expression of HIF-1α at intracellular level in HT-29-AK cells as measured by flow cytometric analysis was up-regulated upon ART treatment for 72h with levels to be decreasing with higher ART concentrations (figure 43C). This resulted in a significant ($P<0.001$) change in fold difference by ~2.81 (2.81 ± 0.17 RFU), ~2.52 (2.52 ± 0.12 RFU) and ~2.32 (2.32 ± 0.16 RFU) while treating HT-29-AK cells with 7.22μM, 14.44μM and 28.88μM ART for 72h, as compared to control (1.00 ± 0.11 RFU), respectively (figure 43C).

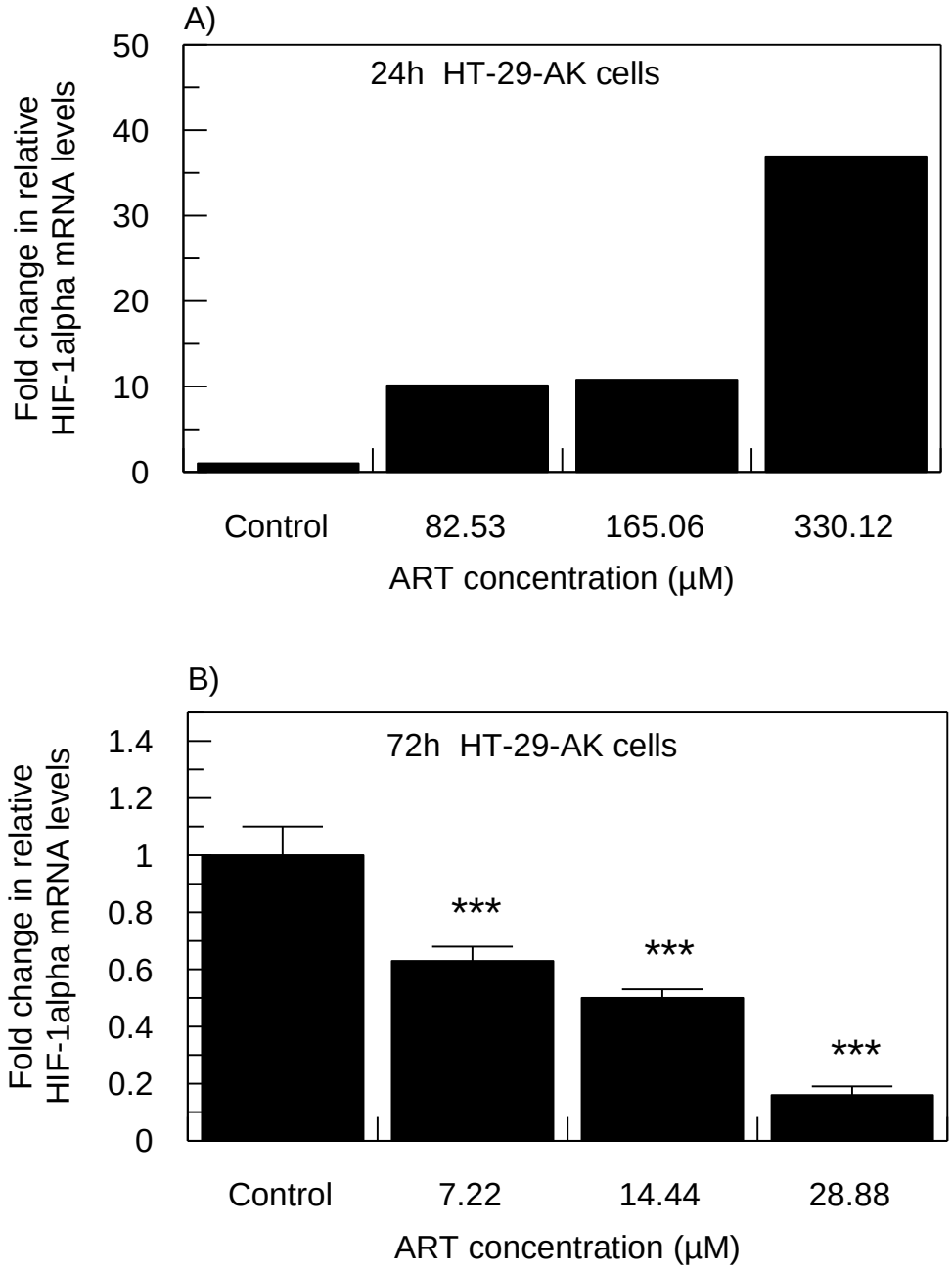
A)
24h HT-29-AK cells
Fold change in relative HIF-1alpha mRNA levels
50
40
30
20
10
0
Control
82.53
165.06
330.12
ART concentration (µM)
B)
72h HT-29-AK cells
Fold change in relative HIF-1alpha mRNA levels
1.4
1.2
1
0.8
0.6
0.4
0.2
0
***
***
***
Control
7.22
14.44
28.88
ART concentration (µM)

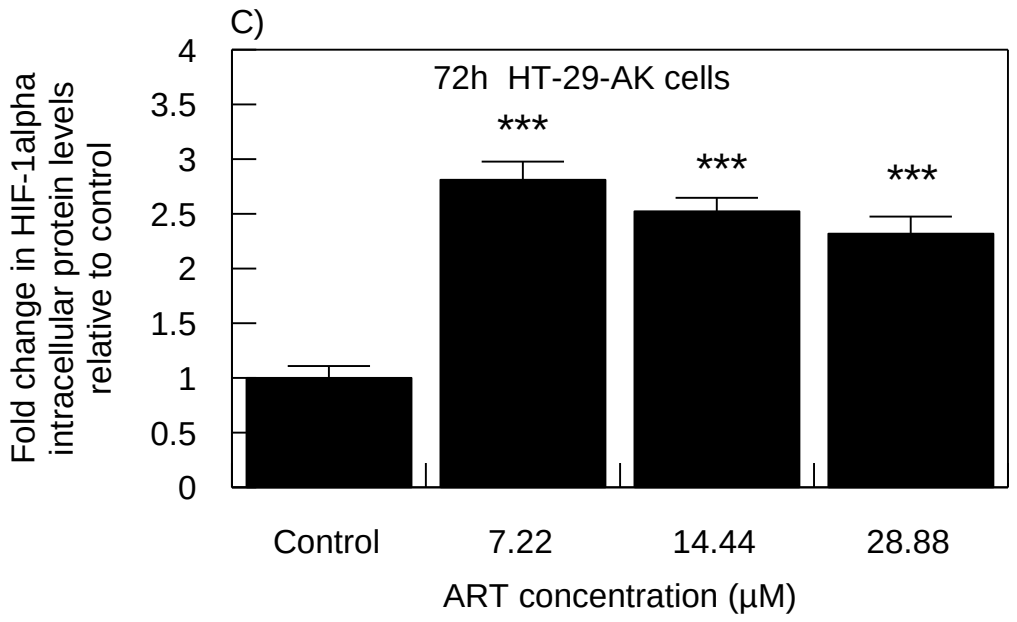

Figure 43: The effect of ART on HIF-1α mRNA expression and intracellular protein HIF-1α levels in HT-29-AK cells in normoxia. Cells were treated without or with ART for A) 24h (at 0µM, 82.53µM, 165.06µM and 330.12µM) and B) 72h (at 0µM, 7.22µM, 14.44µM and 28.88µM) in normoxia (20% O_2) and after incubations HIF-1α mRNA levels were analysed by qPCR as described in Materials & Methods (Section 2.6). C) In separate investigations after treating HT-29-AK cells for 72h with ART, cells were labelled with HIF-1α antibody and analysed for protein levels on flow cytometer (Materials & Methods 2.9.1.2). Results are expressed as mean ± SD of three independent experiments. ***P<0.001 vs. control as tested by one-way Anova. The mRNA HIF-1α expressions after 24h represent 2 independent experiments and are not powered for statistical analysis. ART, artesunate.

There was observed opposite effect in HIF-1α mRNA levels upon treating HT-29-AK cells for 24h and 72h with DHA as compared to results gathered for ART for the same time points, respectively (figures 43A and B vs. 44A and B). After 24h, variable effect on HIF-1α gene expression levels led to a significant down-regulation with 29.01μM DHA (by 42%, ΔΔCt=0.58 ± 0.08; P<0.001), up-regulation with 58.02μM DHA (by 33%, ΔΔCt=1.33 ± 0.10; P<0.001) and followed by down-regulation with 116.04μM DHA (by 15%, ΔΔCt=0.85 ± 0.11; P<0.05), as compared to untreated cells (ΔΔCt=1.00 ± 0.03; figure 44A), respectively. In contrast, qPCR analysis after 72h showed up-regulation in mRNA HIF-1α levels in all samples treated with DHA with the greatest increase observed at 39.50μM (~8.30-fold; ΔΔCt= 8.30 vs. ΔΔCt of 1.00) (figure 44B). Treating HT-29-AK cells for 72h with DHA at 9.88μM, 19.75μM and 39.50μM resulted in a decreasing trend of up-regulated levels of HIF-1α protein as investigated on flow cytometer by ~2.34-fold (2.34 ± 0.08 RFU), ~2.07-fold (2.07 ± 0.05 RFU) and ~1.77-fold (1.77 ± 0.19 RFU) as compared to control (1.00 ± 0.15 RFU; P<0.001), respectively (figure 44C).

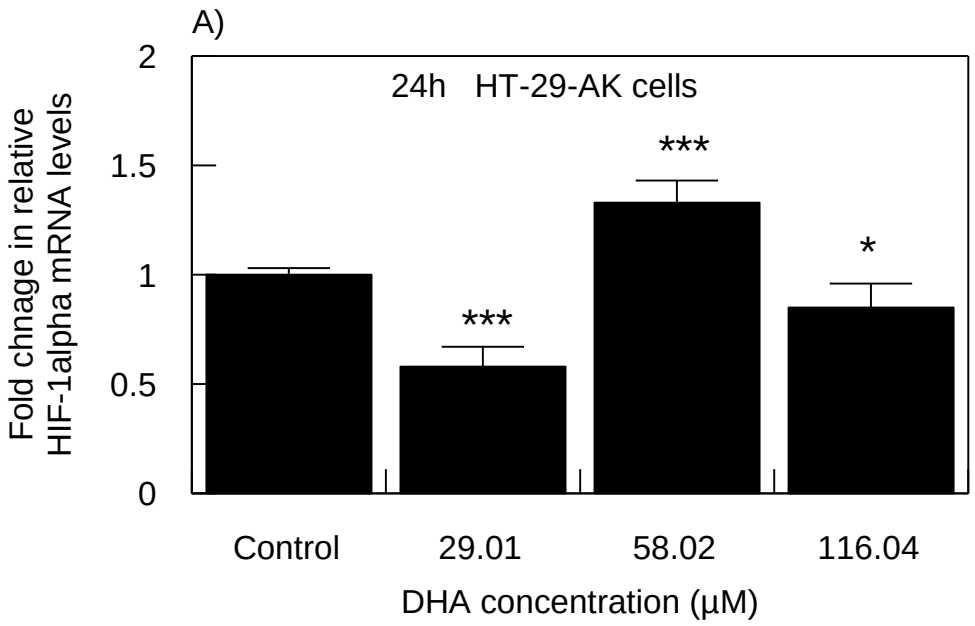
A)
24h HT-29-AK cells
Fold chnage in relative HIF-1alpha mRNA levels
2
1.5
1
0.5
0
***
***
*
Control
29.01
58.02
116.04
DHA concentration (µM)

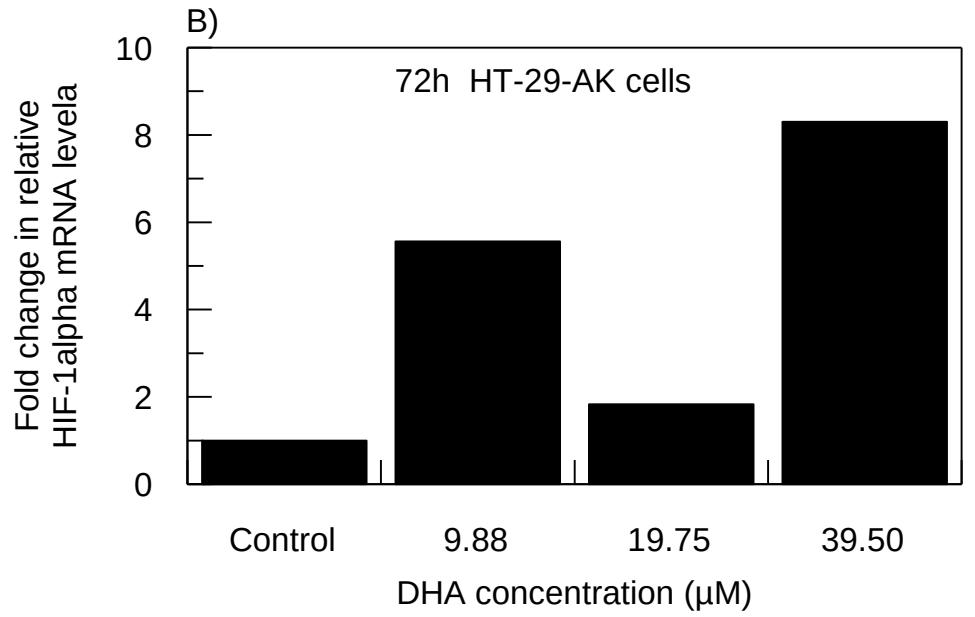
B)
72h HT-29-AK cells
Fold change in relative HIF-1alpha mRNA levela
10
8
6
4
2
0
Control
9.88
19.75
39.50
DHA concentration (µM)

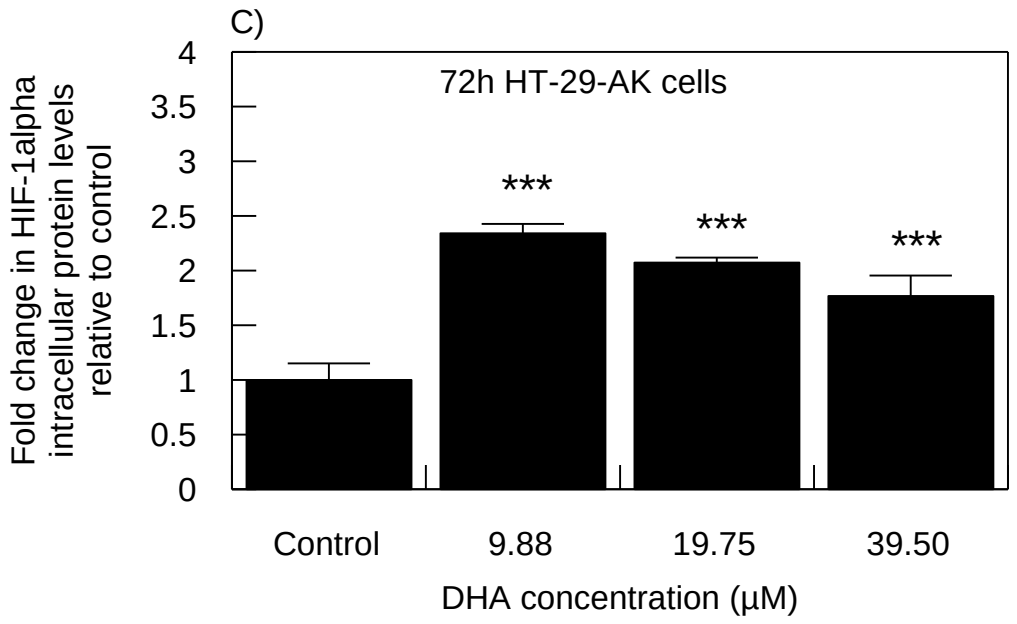

Figure 44: The effect of DHA on the mRNA expression and intracellular protein levels of HIF-1α in HT-29-AK cells in normoxia. Cells were treated without or with DHA for A) 24h (at 0µM, 29.01µM, 58.02µM and 116.04µM) and B) 72h (at 0µM, 9.88µM, 19.75µM and 39.50µM) in normoxia (20% O_2) and after incubations HIF-1α mRNA levels were analysed by qPCR as described in Materials & Methods (Section 2.6). C) In separate investigations after treating HT-29-AK cells for 72 with DHA, cells were labelled with HIF-1α antibody and analysed for protein secretions on flow cytometer (Materials & Methods, Section 2.9.1.2). Results are expressed as mean ± SD of three independent experiments. *P<0.05 and ***P<0.001 vs. control as tested by one-way Anova. The mRNA HIF-1α expressions after 72h represent 2 independent experiments and are not powered for statistical analysis. DHA, dihydroartemisinin.

The results show that mRNA HIF-1α levels in HL-60 cells treated with ART were markedly grater after 72h as compared to 24h (figure 45). The HIF-1α mRNA levels were viariable in ART-treated HL-60 cells for 24h resulting in a 2.33-fold (ΔΔCt= 0.43) decrease upon treating the cells with 0.98 μM ART, as compared to control (ΔΔCt= 1.00). In contrast, HIF-1α mRNA expressions increased by 7.23-fold (ΔΔCt= 7.23) and 3.24-fold (ΔΔCt= 3.24) upon treating the cells with 1.96 μM and 3.92 μM ART for 24h, as compared to control (ΔΔCt= 1.00), respectively (figure 45 A). After 72h, HIF-1α mRNA levels increased by 10.38-fold (ΔΔCt= 10.38) and 27.00-fold (ΔΔCt= 27.00) upon treating the cells with 0.30 μM and 0.60 μM ART as compared to control (ΔΔCt= 1.00), respectively (figure 45 B). The highest concentration at 1.20μM ART had the lowest HIF-1α mRNA expressions of ΔΔCt = 2.25 as compared to control (ΔΔCt= 1.00) (figure 45 B). At protein levels measured using flow cytometric analysis, HL-60 cells treated with ART at 0.30μM, 0.60μM and 1.20μM had a significant ($P<0.001$) concentration-dependent increase in HIF-1α protein activity by ~1.34- (1.34 ± 0.10 RFU), ~1.59- (1.59 ± 0.14 RFU) and ~1.71-fold (1.71 ± 0.27 RFU), respectively as compared to control (1.00 ± 0.17 RFU; figure 45C).

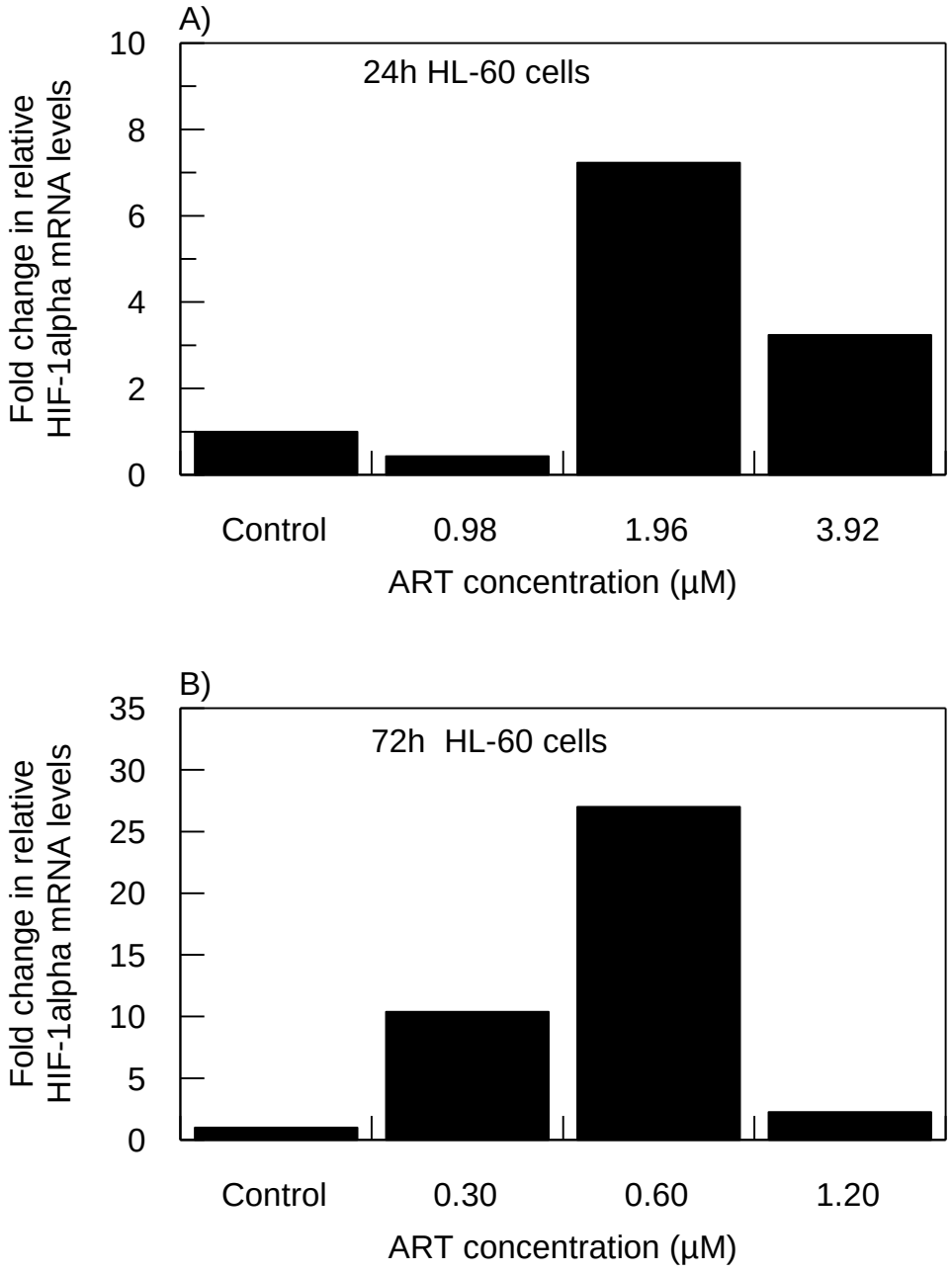
A)
24h HL-60 cells
Fold change in relative HIF-1alpha mRNA levels
10
8
6
4
2
0
Control
0.98
1.96
3.92
ART concentration (µM)
B)
72h HL-60 cells
Fold change in relative HIF-1alpha mRNA levels
35
30
25
20
15
10
5
0
Control
0.30
0.60
1.20
ART concentration (µM)

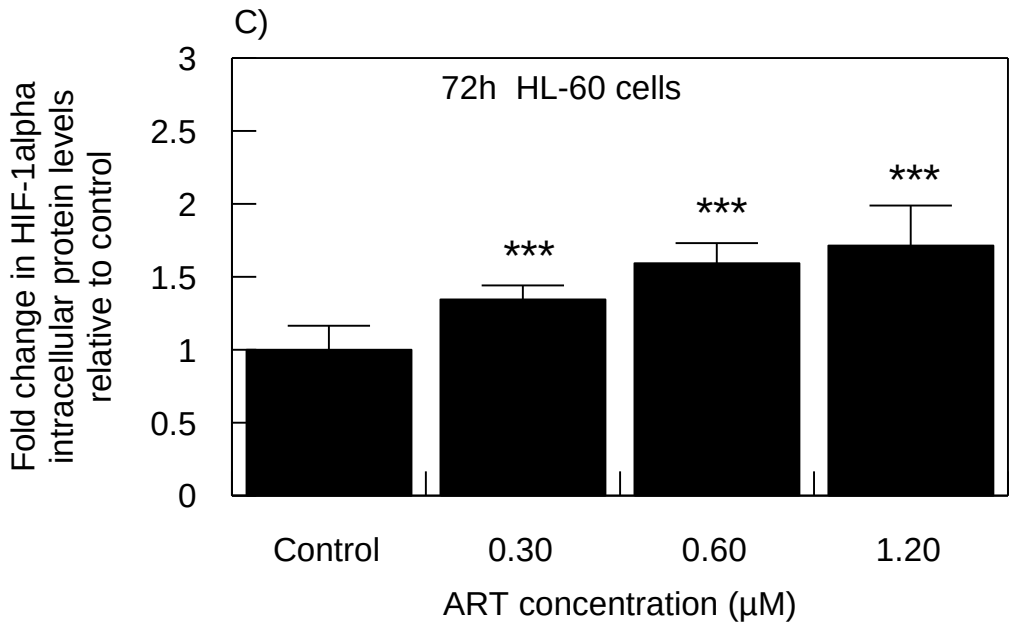

Figure 45: The effect of ART on the mRNA expression and intracellular protein levels of HIF-1α in HL-60 cells in normoxia. Cells were treated without or with ART for A) 24h (at 0µM, 0.98µM, 1.96µM and 3.92µM) and B) 72h (at 0µM, 0.30µM, 0.60µM and 1.20µM) in normoxia (20% O_2) and after incubations HIF-1α mRNA levels were analysed by qPCR as described in Materials & Methods (Section 2.6). In separate investigations after treating the cells for 72 with ART, cells were labelled with HIF-1α antibody and analysed for C) protein levels on flow cytometer (Materials & Methods 2.9.1.2). The results are expressed as mean ± SD of three independent experiments. ***P<0.001 vs. control as tested by one-way Anova (Dunnett test for comparison with control). The mRNA HIF-1α expressions represent 2 independent experiments and are not powered for statistical analysis. ART, artesunate.

There were variable effects of DHA treatment in HL-60 cells observed after 24h, with HIF-1α mRNA levels to be down-regulated markedly with 0.35μM and 1.40μM DHA by ~5-fold (ΔΔCt= 0.20) and ~1.12-fold (ΔΔCt= 0.89), as compared to control (ΔΔCt= 1.00), respectively (figure 46A). There was a 1.21-fold (ΔΔCt= 1.21) increase in HIF-1α mRNA levels in HL-60 cells when treated with DHA at 0.70μM, as compared to control (ΔΔCt= 1.00, figure 46B). In contrast, HIF-1α mRNA levels after 72h DHA treatment were increasing in a concentration-dependent manner with the peak observed at 1.00μM (ΔΔCt= 1.64 ± 0.17 vs. control of ΔΔCt= 1.00 ± 0.02; ~1.64-fold, $P<0.001$; figure 46B). There was a measured difference between mRNA and intracellular protein levels of HIF-1α upon treating HL-60 cells for 72h with DHA, which might indicate the involvement of post-transcriptional mediators or dalay in cellular response. Flow cytometric analysis showed noticeable but not significant increase in HIF-1α intracellular protein levels by 8.25% with 0.25μM DHA when compared to control (1.08 ± 0.11RFU vs. 1.00 ± 0.08 RFU; figure 46C). The significant ($P<0.01$) down-regulation was observed with increasing concentrations of DHA and led to 12.88% and 13.72% fall in HIF-1α levels upon treating the cells with 0.50μM and 1.00μM of DHA as compared to control, respectively (figure 46C).

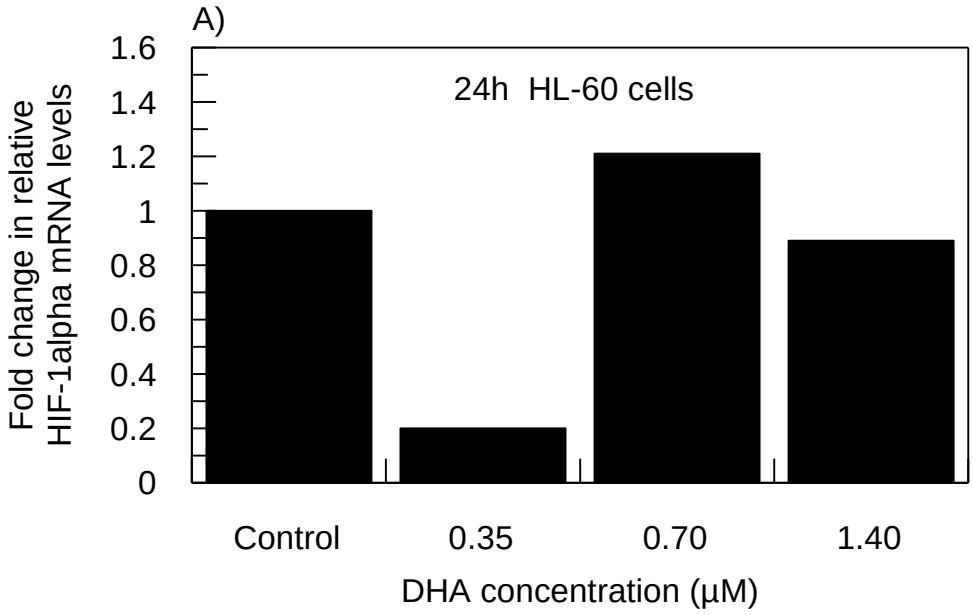
A)
24h HL-60 cells
Fold change in relative HIF-1alpha mRNA levels
1.6
1.4
1.2
1
0.8
0.6
0.4
0.2
0
Control
0.35
0.70
1.40
DHA concentration (µM)

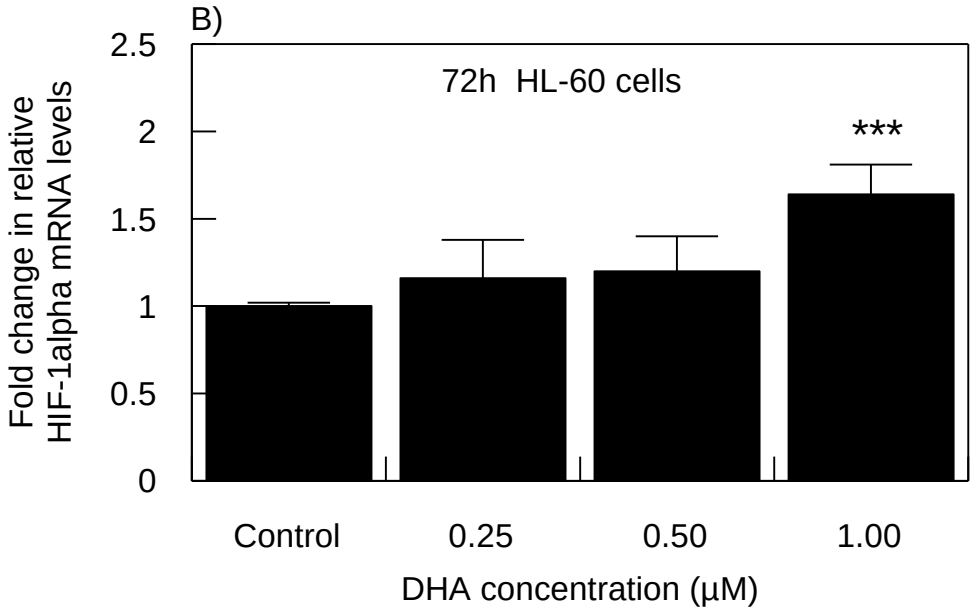
B)
72h HL-60 cells
***
Fold change in relative HIF-1alpha mRNA levels
2.5
2
1.5
1
0.5
0
Control
0.25
0.50
1.00
DHA concentration (µM)

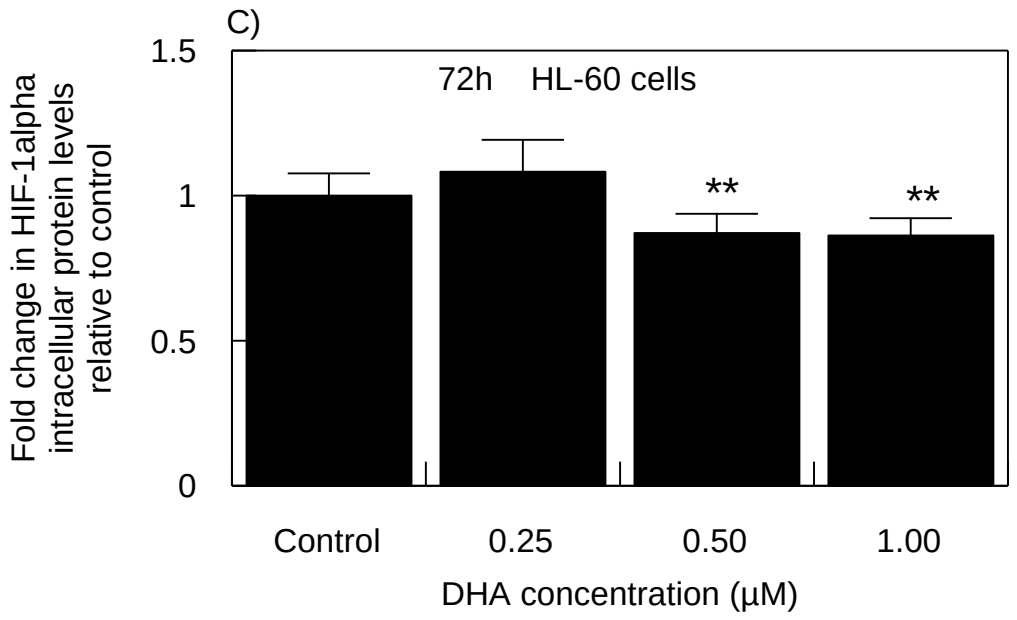

Figure 46: The effect of DHA on the mRNA expression and intracellular protein levels of HIF-1α in HL-60 cells in normoxia. Cells were treated without or with ART for A) 24h (0µM, 0.35µM, 0.70µM and 1.40µM) and B) 72h (0µM, 0.25µM, 0.50µM and 1.00µM) in normoxia (20% O_2) and after incubations HIF-1α mRNA levels were analysed by qPCR as described in Materials & Methods (Section 2.6). In separate investigations after treating the cells for 72 with DHA, cells were labelled with HIF-1α antibody and analysed for C) protein levels on flow cytometer (Materials & Methods 2.9.1.2). Results are expressed as mean ± SD of three independent experiments. ***P<0.001 and **P<0.01 vs. control as tested by one-way Anova. The mRNA HIF-1α expressions after 24h represent 2 independent experiments and are not powered for statistical analysis. DHA, dihydroartemisinin.

3.14. Effect of ART and DHA on CA-9 localisation in HT-29-AK cells

As the changes in HIF-1α mRNA and protein levels in HT-29-AK and HL-60 cells upon ART and DHA treatments were observed (figures 43-46), further attention was directed towards HIF-1α down-stream protein, CA-9. Epidemiological reports correlate CA-9 high protein expression and immunohistochemical staining with poor prognosis in solid tumours, including CRC (Saarnio *et al.* 1998; Rasheed *et al.* 2009; Ilie *et al.* 2010; Lock *et al.* 2013; Cheng *et al.* 2015; de Martino *et al.* 2015). Together with some reports of CA-9 involvement in enhancing EMT transformation and metastatic potential in cancers (Švastová *et al.* 2003), we focused on determining the localisation and possible changes of CA9 staining in HT-29-AK cells upon ART and DHA treatment for 24h and 72h incubations, respectively. Immunocytochemical staining of cell was performed as described in Materials & Methods (Section 2.7). As presented in figure 47, it was shown that CA-9 protein localisation in all samples untreated and treated with ART and DHA for both time points was membranous, equally distributed at basal and lateral levels. The findings indicate the lack of impact of ART and DHA on CA-9 protein localisation. However, additional studies are needed to verify the CA-9 expression at protein and mRNA levels.

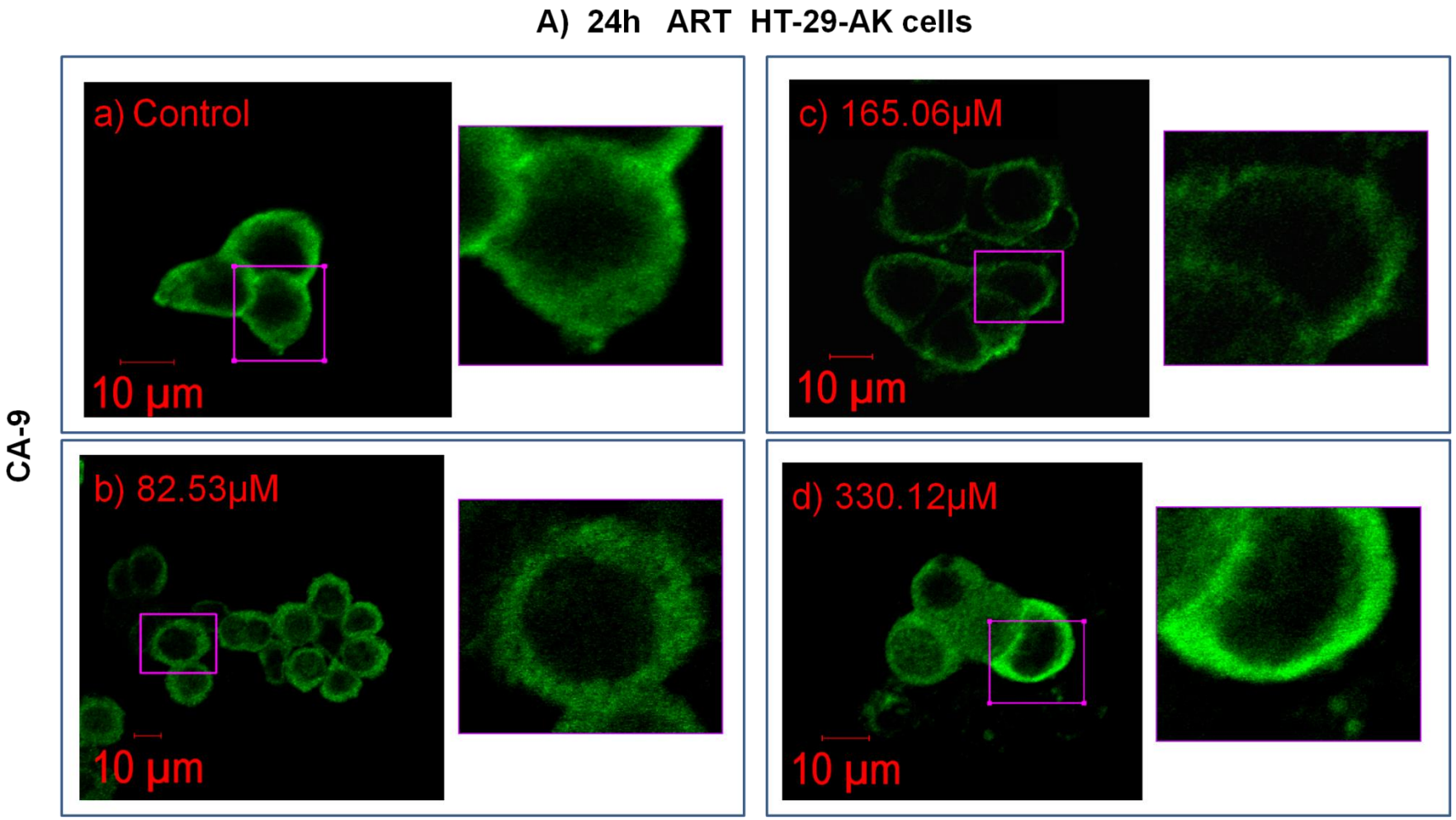
A) 24h ART HT-29-AK cells
CA-9
a) Control
10 µm
c) 165.06µM
10 µm
b) 82.53µM
10 µm
d) 330.12µM
10 µm

B) 72h ART HT-29-AK cells

CA-9

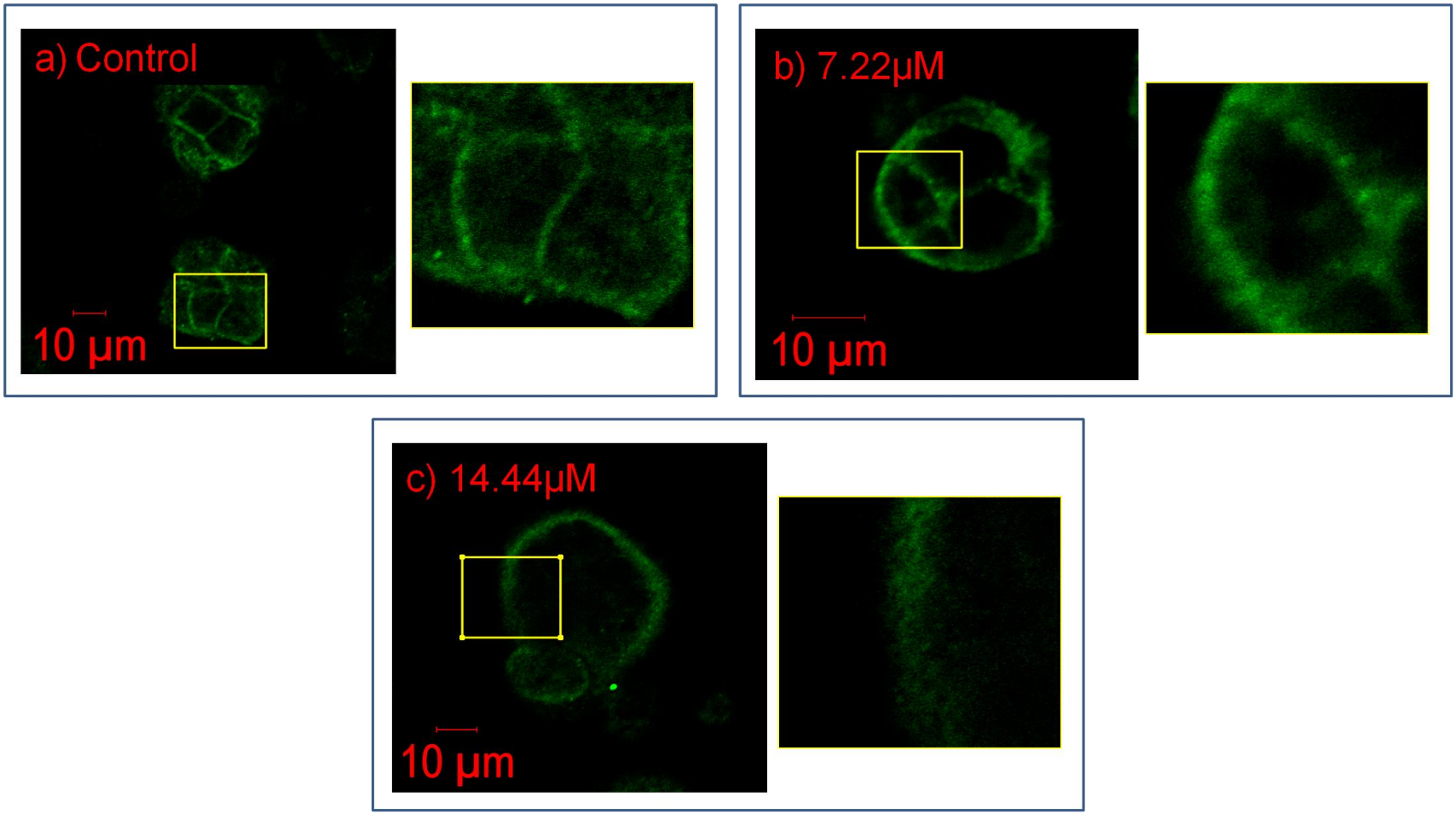

C) 24h DHA HT-29-AK cells

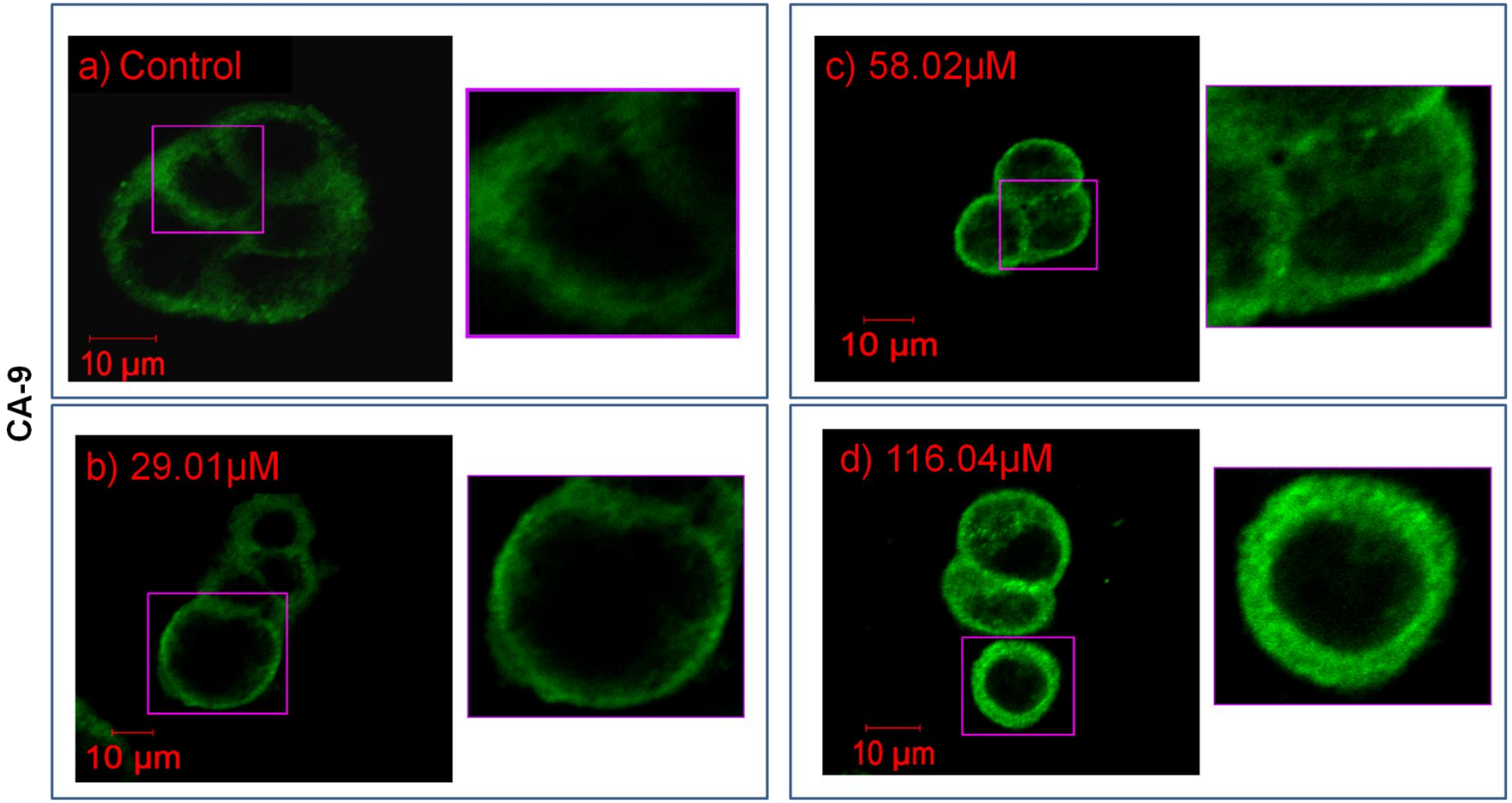

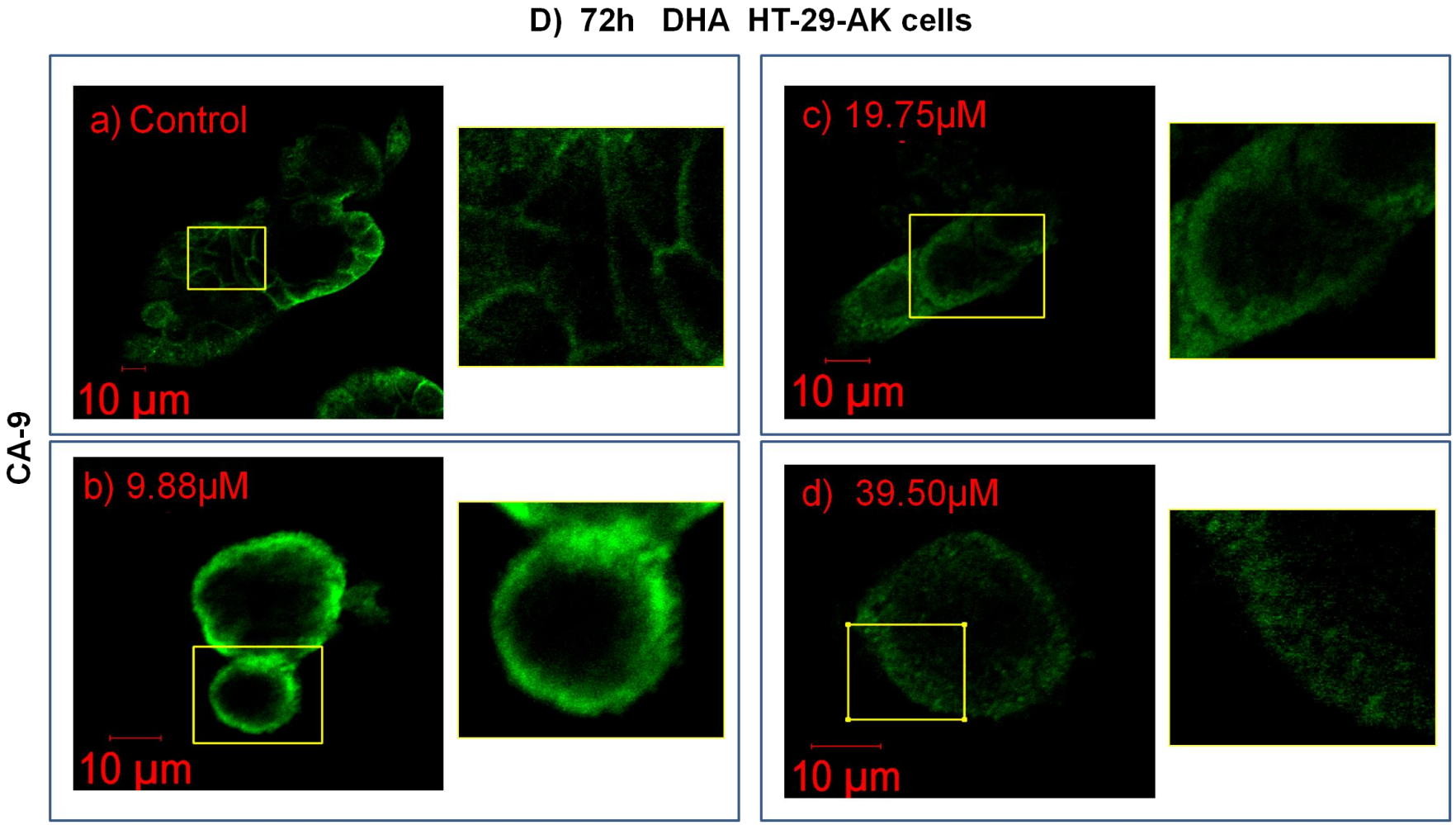
D) 72h DHA HT-29-AK cells
CA-9
a) Control
10 µm
c) 19.75µM
10 µm
b) 9.88µM
10 µm
d) 39.50µM
10 µm

Figure 47: The effect of ART and DHA treatment on CA-9 intracellular protein localisation in HT-29-AK cells at 24h and 72h in normoxia. Evaluation of CA-9 localisation using immunocytochemical staining was performed by seeding cells on glass coverslips with/without ART for A) 24h (at 0µM, 82.53µM, 165.06µM and 330.12µM) and B) 72h (at 0µM, 7.22µM, 14.44µM and 28.88µM); with/without DHA for C) 24h (at 0µM, 29.01µM, 58.02µM and 116.04µM) and D) 72h (0µM, 9.88µM, 19.75µM and 39.50µM) as described in Materials & Methods (Section 2.7). Cells were fixed, incubated with anti-CA-9 and visualised using anti-mouse Alexa 488 secondary antibody on confocal microscope (Zeiss LSM 510 META) at x 200 magnification. The objective used was EC Plan-Neofluar 20x/0.50 M27 and the pinhole channel set at 76µm. The representative images show the localisation and the staining intensity of CA-9 in the majority of the cells analysed by AIM Software. ART, artesunate; DHA, dihydroartemisinin.

3.15. ART and DHA treatment altered the cellular and mRNA survivin levels in HL-60 and HT-29-AK cells

The anti-cancer effects of ART and DHA in CRC SW480 cells and leukaemia KBM-5 cells *in vitro* and *in vivo* were reported previously to be linked with the inhibition of survivin (Shao *et al.* 2008; Kim *et al.* 2015). Survivin is a protein responsible for promoting motility and angiogenesis abilities of malignant cells, and the inhibition of cell apoptosis (Shin *et al.* 2001; Shao *et al.* 2008; Ye *et al.* 2014; Kim *et al.* 2015). Here, the effect of ART and DHA against HT-29-AK and HL-60 cells on mRNA and protein levels of survivin were measured by qPCR and ELISA as described in Materials & Methods (Sections 2.5.4 and 2.6). The aim of this investigation was to compare the results with previous reports and to provide additional knowledge of ART and DHA mode of action by evaluating 2 different time points (24h vs. 72h) at transcriptional level using qPCR and following 72h incubation to evaluate cellular protein survivin levels as analysed by ELISA.

The gene expression levels of survivin upon ART treatments in HT-29-AK cells were decreasing with increasing incubation time lengths (24h vs. 72h) (figure 48A and B). HT-29-AK cells treated with ART at 82.53µM, 165.06µM and 330.12µM for 24h had increased mRNA expressions of survivin by ~30.84-fold (ΔΔCt= 30.84 ± 10.53; P<0.001), ~8.33-fold (ΔΔCt= 8.33 ± 5.10), and a maximum fold change of ~39.64-fold (ΔΔCt= 39.64 ± 14.67; P<0.001), as compared to control (ΔΔCt= 1 ± 0.05), respectively (figure 48A). After 72, survivin mRNA levels increased by 1.90- (ΔΔCt= 1.90 ± 0.90), 6.83- (ΔΔCt= 6.83± 1.52) and 2.86-fold (ΔΔCt= 2.86 ± 1.20) upon treating the cells with 7.22µM, 14.44µM and 28.88µM ART, as compared to control (ΔΔCt= 1.00 ± 0.11), respectively (figure 48B).

Levels of survivin mRNA in ART-treated HL-60 cells were decreasing over a period of time between 24h and 72h (figure 48C vs. D). After 24h, there was up-regulation of survivin gene expression with ART at 0.98µM, 1.96µM, and 3.92µM by ~7.35-fold (ΔΔCt= 7.35 ± 1.62), ~15.64-fold (ΔΔCt= 15.64 ± 4.73; P<0.001), and the greatest up-regulation resulting in a fold change of ~36.02-fold (ΔΔCt= 36.02 ± 10.72; P<0.001), respectively, as compared to control (ΔΔCt= 1 ± 00; figure 48C). These survivin mRNA levels were still up-regulated after 72h but difference in survivin fold change decreased as compared to 24h. There was a ~5.51-fold (ΔΔCt= 5.51 ± 0.54; P<0.05), ~10.97-fold (ΔΔCt= 10.97 ± 2.70; P<0.001) and ~6.73-fold (ΔΔCt= 6.73 ± 1.04; P<0.01) increase upon treating HL-60 cells with ART at 0.30µM, 0.60µM, and 1.20µM, as compared to control (ΔΔCt= 1.00 ± 00), respectively (figure 48D).

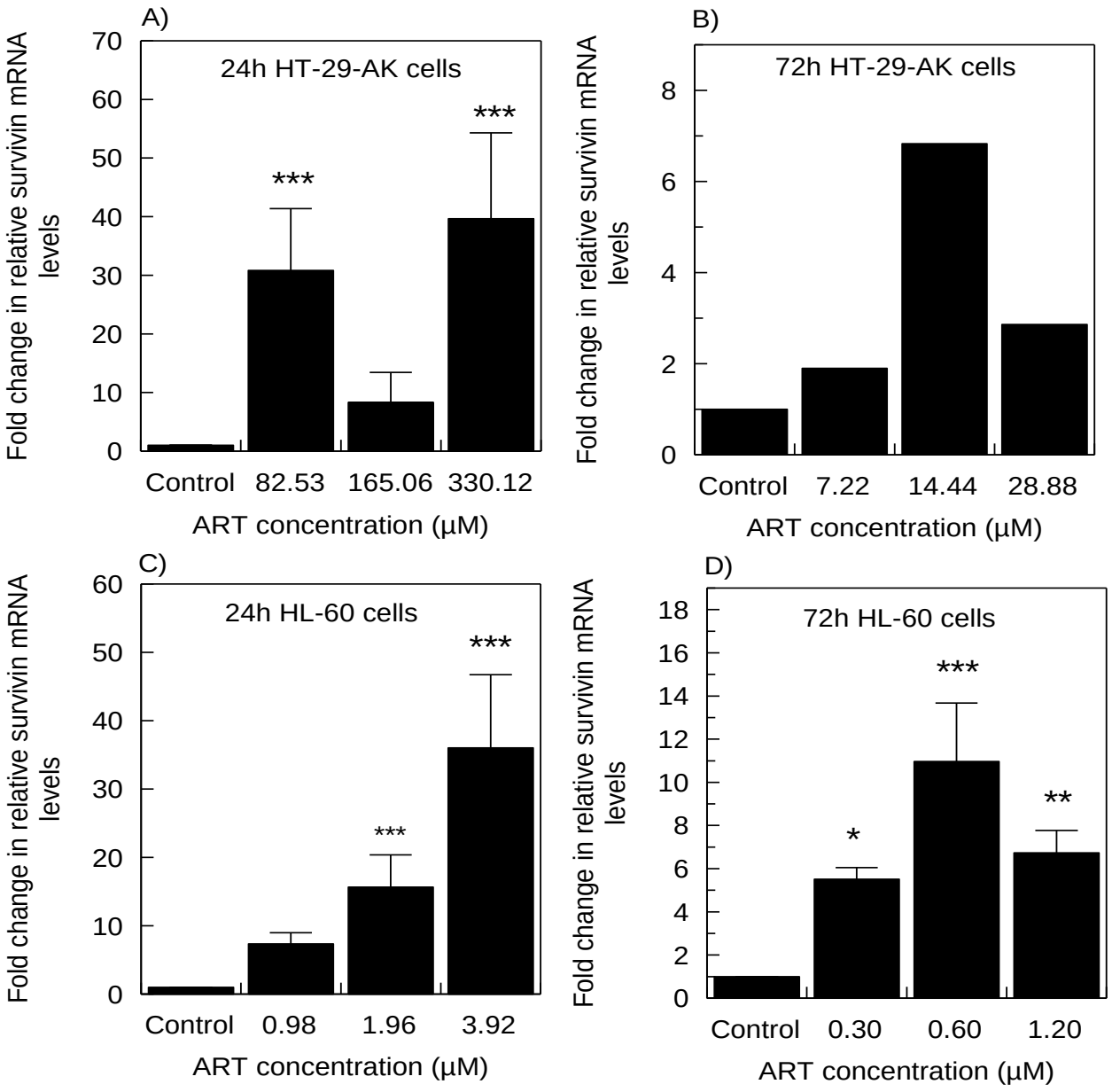

Figure 48: The effect of ART on the mRNA expression levels of survivin in HT-29-AK and HL-60 cells at 24h and 72h in normoxia. HT-29-AK cells were treated with ART for A) 24h (at 0 µM, 82.53µM, 165.06µM and 330.12µM) and B) 72h (at 0 µM, 7.22µM, 14.44µM and 28.88µM) whereas HL-60 cells were treated with ART for 24h C) (at 0 µM, 0.98µM, 1.96µM and 3.92µM) and 72h D) (at 0 µM, 0.30µM, 0.60µM and 1.20µM) and survivin mRNA levels were measured by qPCR as described in Materials and Methods (Section 2.6). Data for HT-29-AK cells treated with ART for 72h represent the mean of 2 independent experiments and is not powered for statistical analysis. *P<0.05, **P<0.01 and ***P<0.001 as tested by one-way ANOVA (Dunnett test). ART, artesunate.

Cell lysates analysed by ELISA showed that ART (at 7.22µM, 14.44µM and 28.88µM) after 72h treatment in HT-29-AK cells induced a slight decrease in survivin protein levels with the most noticeable of 16.39% (996.09pg/ml) at the highest concentration of ART (at 28.88µM), as compared to control (1191.41pg/ml; figure 49). ART-treated HL-60 cells for 72h at 0.30µM, 0.60µM, and 1.20µM had a slight decrease in survivin protein expressions with the highest decrease observed at 1.20µM ART (1824.22pg/ml), as compared to control (1957.03 pg/ml; figure 49).

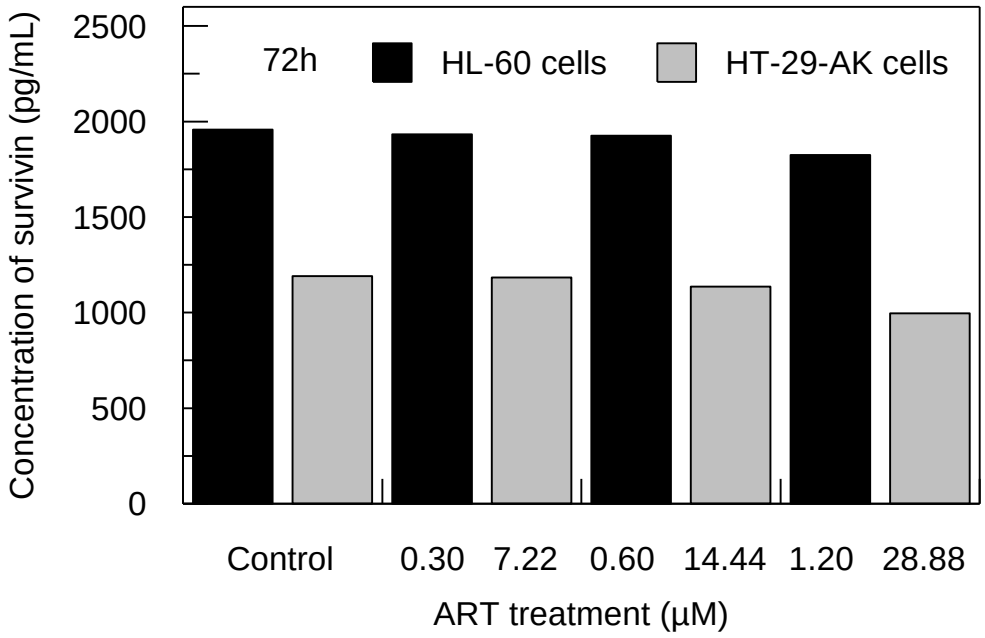

Figure 49: The effect of ART on cellular protein levels of survivin in HT-29-AK and HL-60 cells at 24h and 72h in normoxia. Survivin cellular protein levels from cell lysates were investigated by ELISA from ART-treated HT-29-AK cells for 72h (at 0µM, 7.22µM, 14.44µM and 28.88µM; grey bars) and ART-treated HL-60 cells for 72h (at 0µM, 0.30µM, 0.60µM and 1.20µM; black bars) as described in Materials and Methods (Section 2.5.4). Data for cells treated with ART for 72h represent the mean of 2 independent experiments and is not powered for statistical analysis. ART, artesunate.

The mRNA survivin levels upon DHA treatments at 29.01µM, 58.02µM and 116.04µM for 24h were significantly ($P<0.001$) decreased by 3.03- ($\Delta\Delta Ct= 0.33 \pm 0.23$), 2.17- ($\Delta\Delta Ct= 0.46 \pm 0.21$) and the same 2.17-fold ($\Delta\Delta Ct= 0.45 \pm 0.23$), as compared to control ($\Delta\Delta Ct= 1.00 \pm 0.04$), respectively (figure 50A). In contrast, survivin mRNA levels in HT-29-AK cells treated with DHA for 72h were all significantly ($P<0.001$) increased with the highest levels measured at 39.50µM (~35.33-fold; $\Delta\Delta Ct= 35.33 \pm 5.28$) (figure 50B). In accordance with decreased survivin mRNA levels observed after 24h with DHA, treatment of HT-29-AK cells with 29.01µM, 58.02µM and 116.04µM of DHA for 24h caused a 2.05% (1871.10pg/ml), 19.63% (1535.16pg/ml) and 31.08% (1316.41pg/ml) decrease in survivin levels as analysed by ELISA as compared to control (1910.16pg/ml), respectively (figure 50C). In opposite to increased survivin mRNA levels observed after 72h using qPCR, treatment of HT-29-AK cells for 72h at 9.88µM DHA decreased survivin levels by ~6.95% (1699.22 pg/ml), as compared to control (1826.17pg/ml) (figure 50C). DHA treatment at 19.75µM and 39.50µM decreased survivin protein levels by 14.22% (1566.41 pg/ml) and 15.94% (1535.16 pg/ml) as compared to control (1826.17pg/ml), respectively (figure 50C). The differences between survivin at mRNA and protein levels might indicate delay in response at transcriptional and post-transcriptional level or activity of other regulators modulating survivin protein expression (figure 50C).

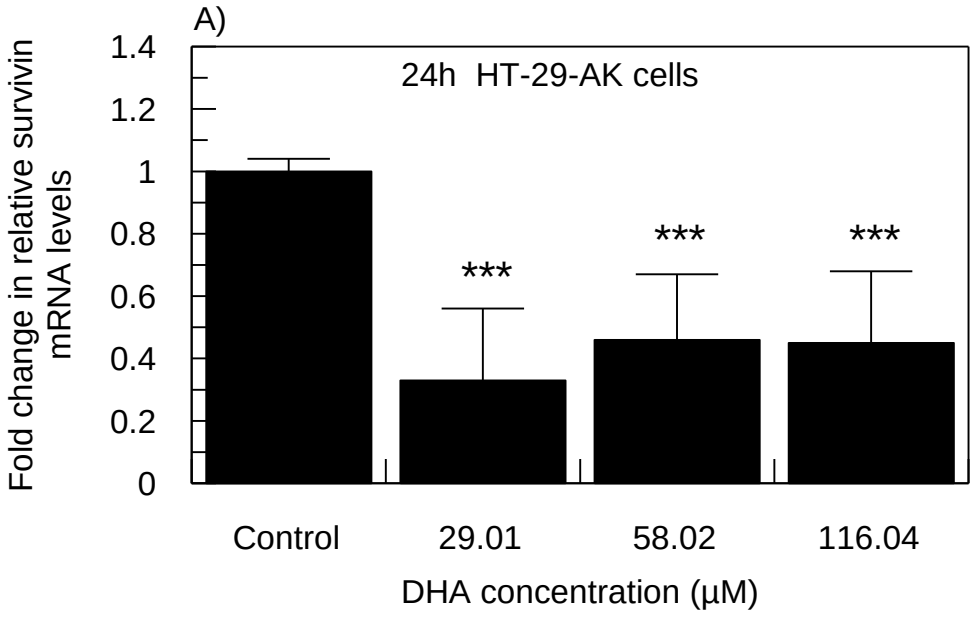
A)
24h HT-29-AK cells
Fold change in relative survivin mRNA levels
1.4
1.2
1
0.8
0.6
0.4
0.2
0
***
***
***
Control
29.01
58.02
116.04
DHA concentration (µM)

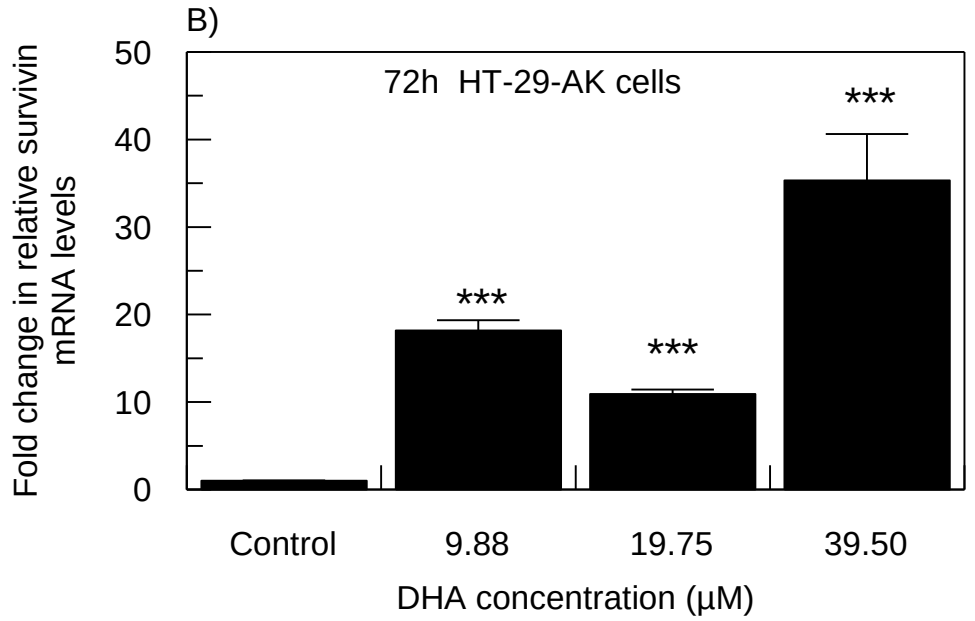
B)
72h HT-29-AK cells
Fold change in relative survivin mRNA levels
50
40
30
20
10
0
***
***
***
Control
9.88
19.75
39.50
DHA concentration (µM)

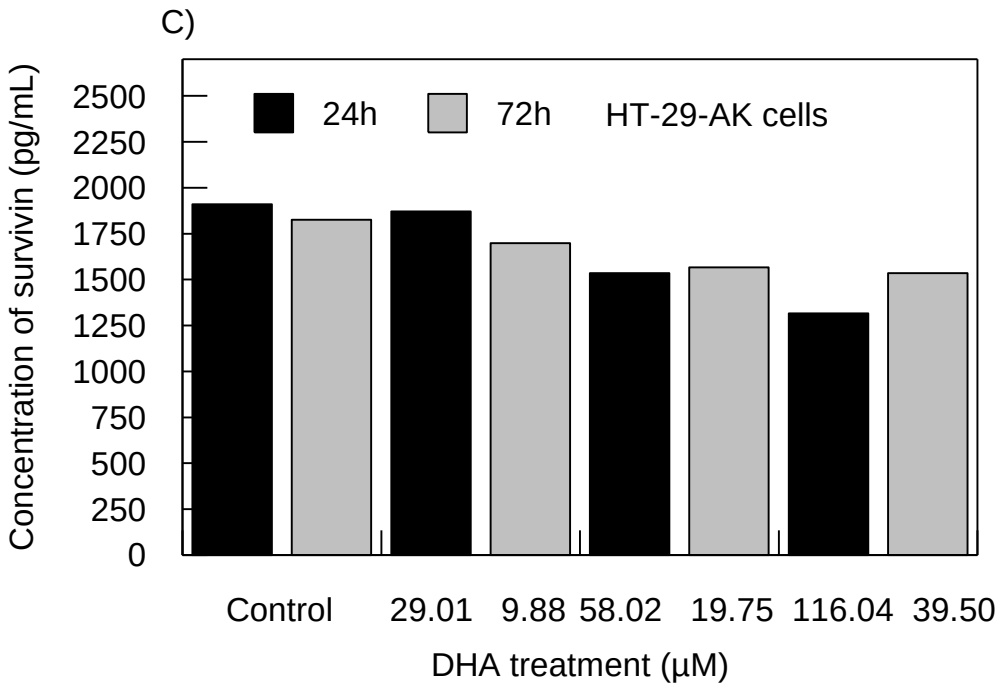

Figure 50: The effect of DHA on the mRNA expression and cellular protein levels of survivin in HT-29-AK cells at 24h and 72h in normoxia. Survivin mRNA levels measured for DHA-treated HT-29-AK cells for A) 24h (at 0 µM, 29.01µM, 58.02µM and 116.04µM) and B) for 72h (at 0 µM, 9.88µM, 19.75µM and 39.50µM) as analysed by qPCR as described in Materials & Methods (Section 2.6). C) A two-site sandwich ELISA was performed on the cell lysates upon treating HT-29-AK cells for 24h (black bars) and 72h (grey bars) (Materials & Methods, Section 2.5.4). The results derived from ELISA were not powered for statistical analysis. The results derived from qPCR represent 3 independent experiments where ***P<0.001 vs. control as tested by one-way ANOVA (Dunnett test). DHA, dihydroartemisinin.

The results from qPCR analysis showed that the survivin mRNA levels from DHA-treated HL-60 cells for 24h were down-regulated (figure 51A). These resulted in a ~1.27- (ΔΔCt= 0.79 ± 0.21), ~1.79- (ΔΔCt= 0.56 ± 0.28; P<0.05) and ~1.82-fold (ΔΔCt= 0.55 ± 0.19; P<0.01) decrease upon treated HL-60 cells for 24h with DHA at 0.30 µM, 0.70 µM and 1.40 µM, as compared to control of ΔΔCt equal to 1.00 ± 0.00, respectively (figure 51A). In contrast, as compared to control (ΔΔCt= 1.00), DHA treatment for 72h resulted in up-regulation of survivin mRNA levels at 0.25 µM (~19%; ΔΔCt= 1.19), 0.50µM (~85%; ΔΔCt= 1.85) and 1.00µM (~67%; ΔΔCt= 1.67), respectively (figure 51B).

Treatment of HL-60 cells for 24h with 0.35µM DHA did not alter the cellular protein level of survivin, as compared to control (1832.031pg/ml vs. 1832.31pg/ml; figure 51C). However, treatment of HL-60 cells with 0.70µM and 1.40µM caused a decrease in survivin concentrations by 9.38% (1660.16pg/ml) and 18.34% (1496.09 pg/ml), as compared to control (1832.031pg/ml), respectively (figure 51C). More noticeable decrease in protein survivin levels was observed at 72h incubation at 0.25µM DHA (by ~22.57%; 1527.34pg/ml) and 1.00µM (by ~32.48%; 1332.03pg/ml), as compared to untreated cells (1972.66pg/ml), respectively. The IC_{50} concentration of DHA representing 0.50µM resulted in un-changed survivin levels when compared to untreated cells (by 2%; 1933.60pg/ml vs. 1972.66pg/ml) (figure 51C).

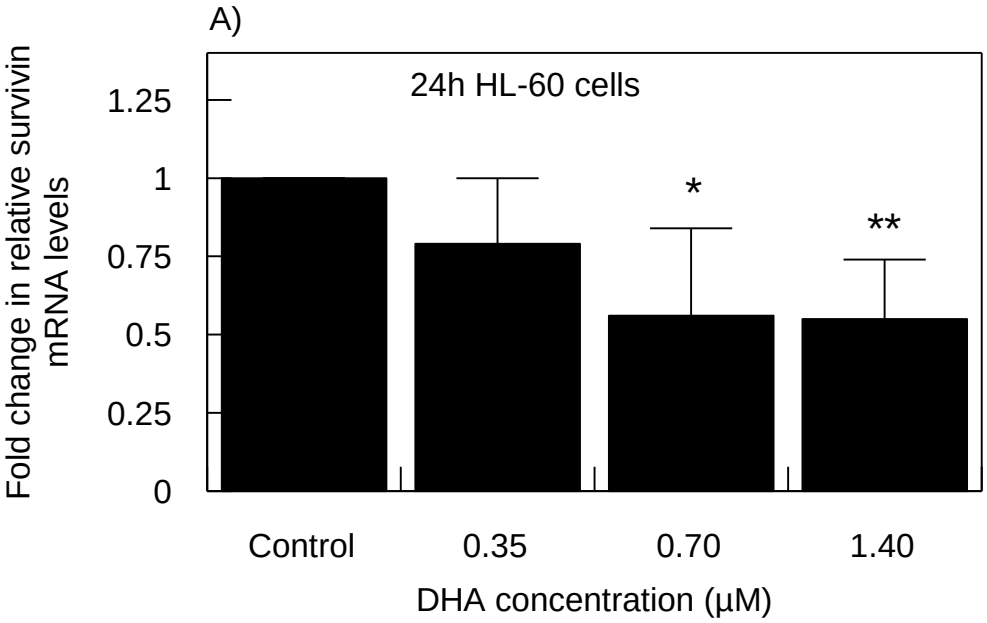
A)
24h HL-60 cells
Fold change in relative survivin mRNA levels
1.25
1
0.75
0.5
0.25
0
*
**
Control
0.35
0.70
1.40
DHA concentration (µM)

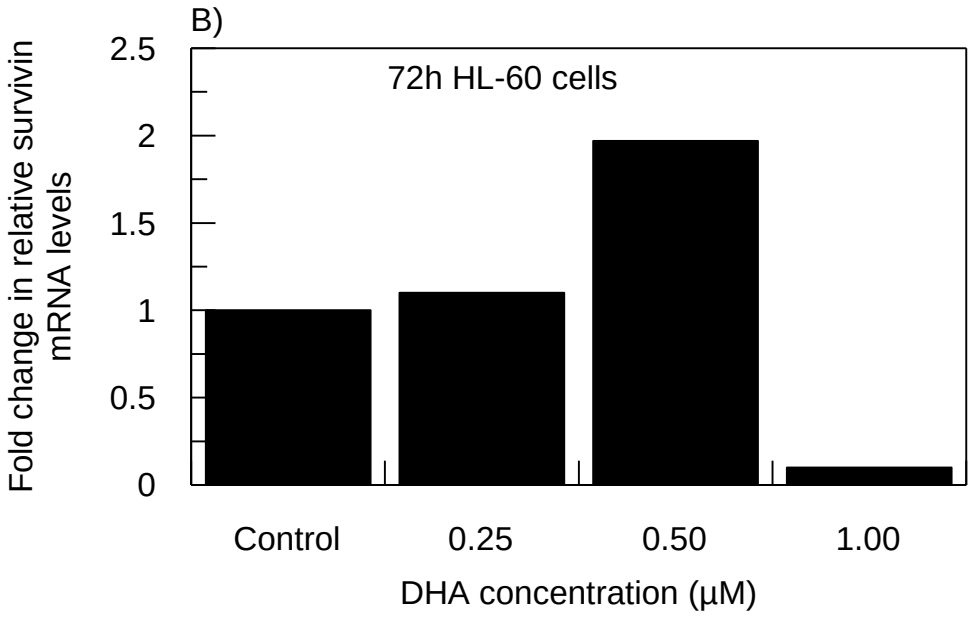
B)
72h HL-60 cells
Fold change in relative survivin mRNA levels
2.5
2
1.5
1
0.5
0
Control
0.25
0.50
1.00
DHA concentration (µM)

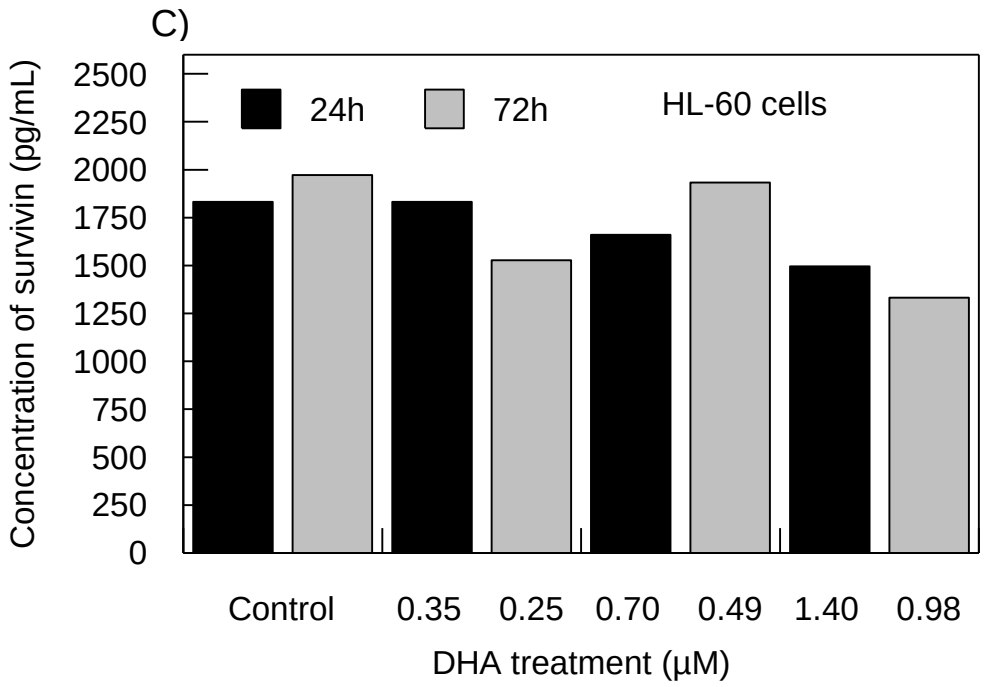

Figure 51: The effect of DHA on the mRNA expression and cellular protein levels of survivin in HL-60 cells at 24h and 72h in normoxia. Survivin mRNA levels measured for DHA-treated HL-60 cells for A) 24h (at 0 μM, 0.35μM, 0.70μM and 1.40μM) and B) for 72h (at 0 μM, 0.25μM, 0.50μM and 1.00μM) before being analysed by qPCR as describe in Materials & Methods (Section 2.6). C) A two-site sandwich ELISA was performed on the cell lysates upon treating HL-60 cells for 24h (black bars) and 72h (grey bars) (Materials & Methods, Section 2.5.4). The results derived from ELISA were not powered for statistical analysis. qPCR results for DHA-treated HL-60 cells for 24h represents 3 independent experiments where *P<0.05 and **P<0.01 as tested by one-way ANOVA (Dunnett test). DHA, dihydroartemisinin.

3.16. Effect of ART and DHA on phospho-Akt expression levels

Akt, is a serine/threonine-specific protein that plays a pivotal role in apoptosis inhibition by promoting malignant cell survival, proliferation and angiogenesis (Bortul *et al.* 2003; Altomare and Testa 2005; Stegeman *et al.* 2012). In colorectal HCT116 cells, TNF-α-activated Akt pathway contributed to inflammation-induced EMT, enhanced invasion and metastasis of cells (Wang *et al.* 2013). Previous reports demonstrated that ART in human cervical carcinoma cells and DHA in human prostate cancer cells promoted TRAIL-induced apoptosis through inhibition of the NF-κB and PI3K/Akt signaling pathways (He *et al.* 2010; Thanaketpaisarn *et al.* 2011). These observations show that ART and DHA have the ability to inhibit Akt, which could represent promising therapeutic approach for cancer therapy. Therefore, to further study the mode of action of ART and DHA in cancer cells, activated Akt (phosphorylated at Ser473) was investigated using flow cytometric and Western blotting analyses as described in Materials and Methods (Sections 2.9 and 2.10). It was hypothesized that ART and DHA in HT-29-AK and HL-60 cells would decrease expression of phoshorylated (phospho) Akt.

The findings derived from flow cytometic analysis showed that HT-29-AK cells treated with 7.22µM, 14.44µM and 28.88µM of ART had increased significantly ($P< 0.001$) phospho-Akt levels by ~3.31- (3.31 ± 0.53 RFU), ~3.47- (3.47± 0.32 RFU) and ~3.64-fold (3.64 ± 0.58 RFU), respectively, as compared to control (1.00 ± 0.04 RFU) (figure 52A).

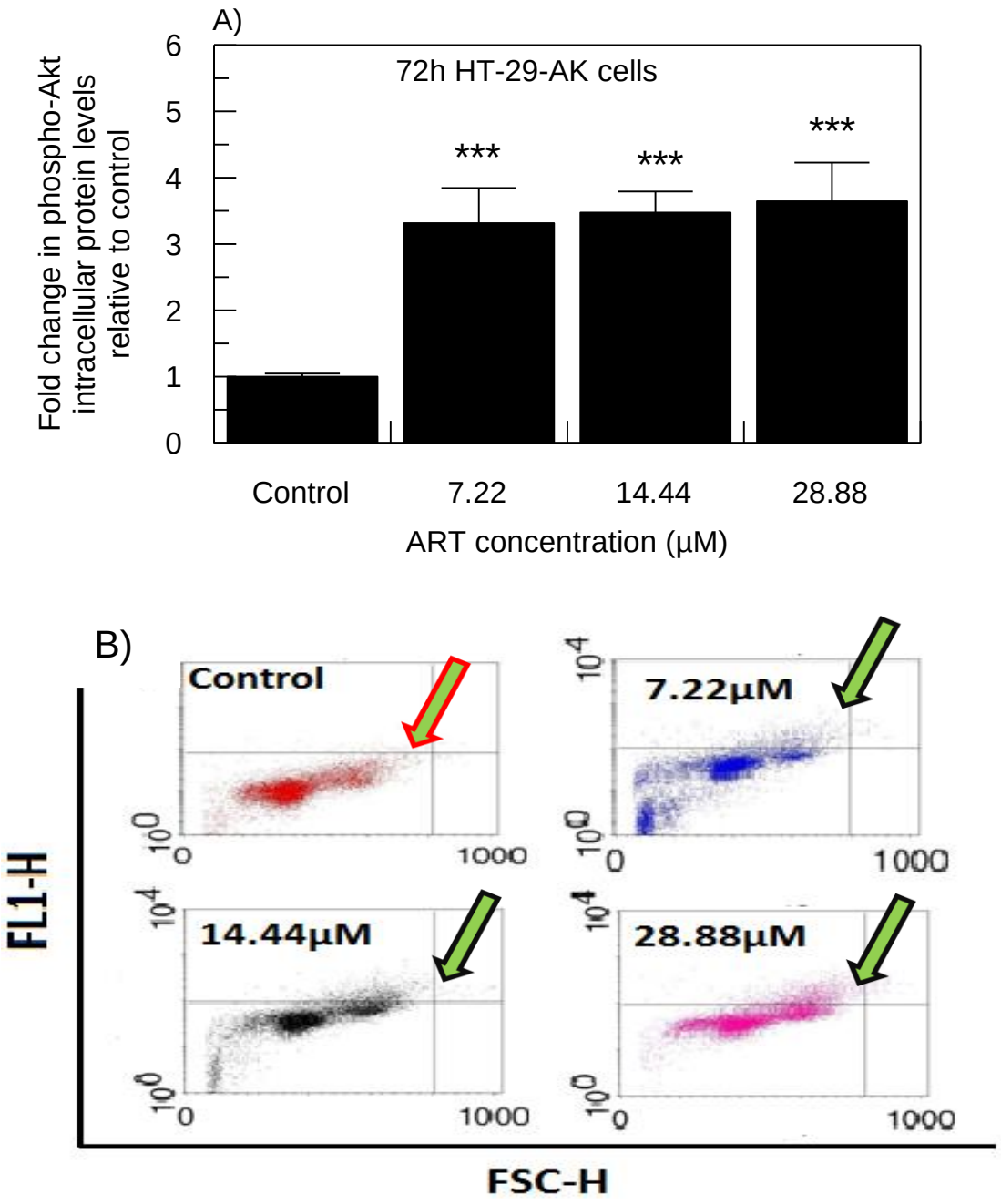

Figure 52: ART increases the protein levels of phospho-Akt in HT-29-AK cells at 72h in normoxia. Cells were exposed to ART (at 0µM, 7.22µM, 14.44µM and 28.88µM) for 72h in normoxia (20% O_2) and A) analysed for the presence of phospho-Akt on flow cytometer (Materials & Methods, Section 2.9). B) Representative dot plots derived from flow cytometer show (in arrow) an increase in phospho-Akt labelled cells between ART-treated and control cells. The results represent the mean ± SD of three independent experiments. ***P<0.001 vs. control as tested by one-way ANOVA (Dunnett test). ART, artesunate.

Interestingly, DHA treatment increased the levels of phospho-Akt protein in HT-29-AK cells in a time- and concentration-dependent manner (figures 53 A and B). HT-29-AK cells treated for 24h with DHA at 29.01µM, 58.02µM and 116.04µM showed a marked increase in phospho-Akt by ~1.26- (1.26 RFU), ~2.33- (2.33 RFU) and ~2.51-fold (2.51 RFU), as compared to control (1.00 RFU), respectively (figure 53 A). In contrast, DHA-treated HT-29-AK cells for 72h at 9.88µM and 19.75µM had increased the release of phosho-Akt by ~1.15-fold (1.15 RFU) and ~1.03-fold (1.03 RFU), as compared to control (1.00 RFU), respectively (figure 53 B). However, DHA at 39.50µM decreased the levels of phospho-Akt levels by ~1.11 fold (0.90 RFU), as compared to DHA untreated cells (1.00 RFU) (figure 53 B).

In order to validate flow cytometric results of DHA-mediated changes in phospho-Akt expression levels, Western blot analysis was performed for these two time points (figure 53 C and D). The results of Western blotting analysis are in accordance with flow cytometric observations and the dark bands correspond to the high protein levels of phospho-Akt whereas the lighter bands show the low protein phospho-Akt (figure 53).

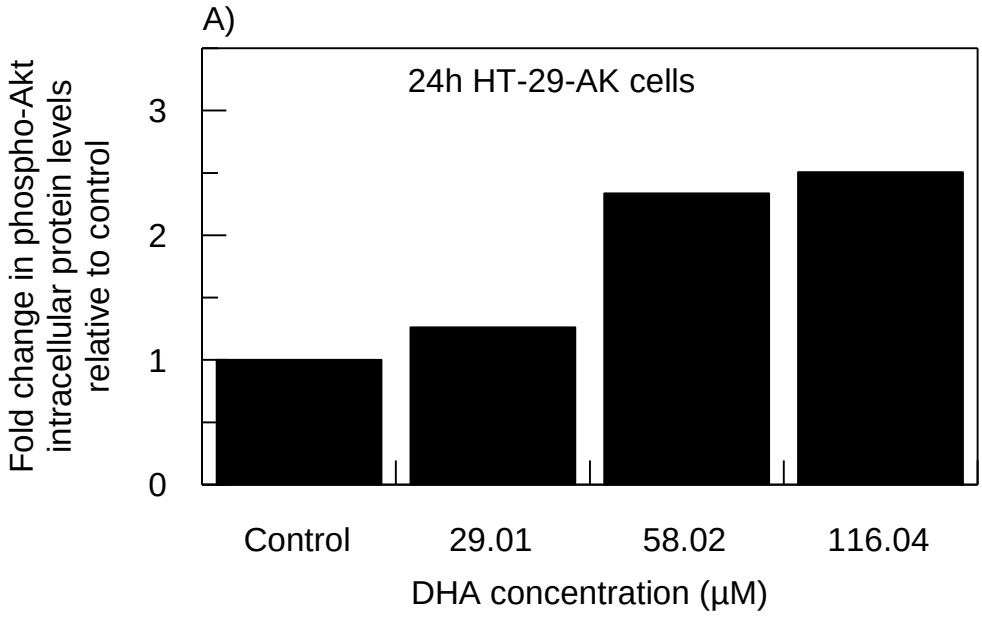

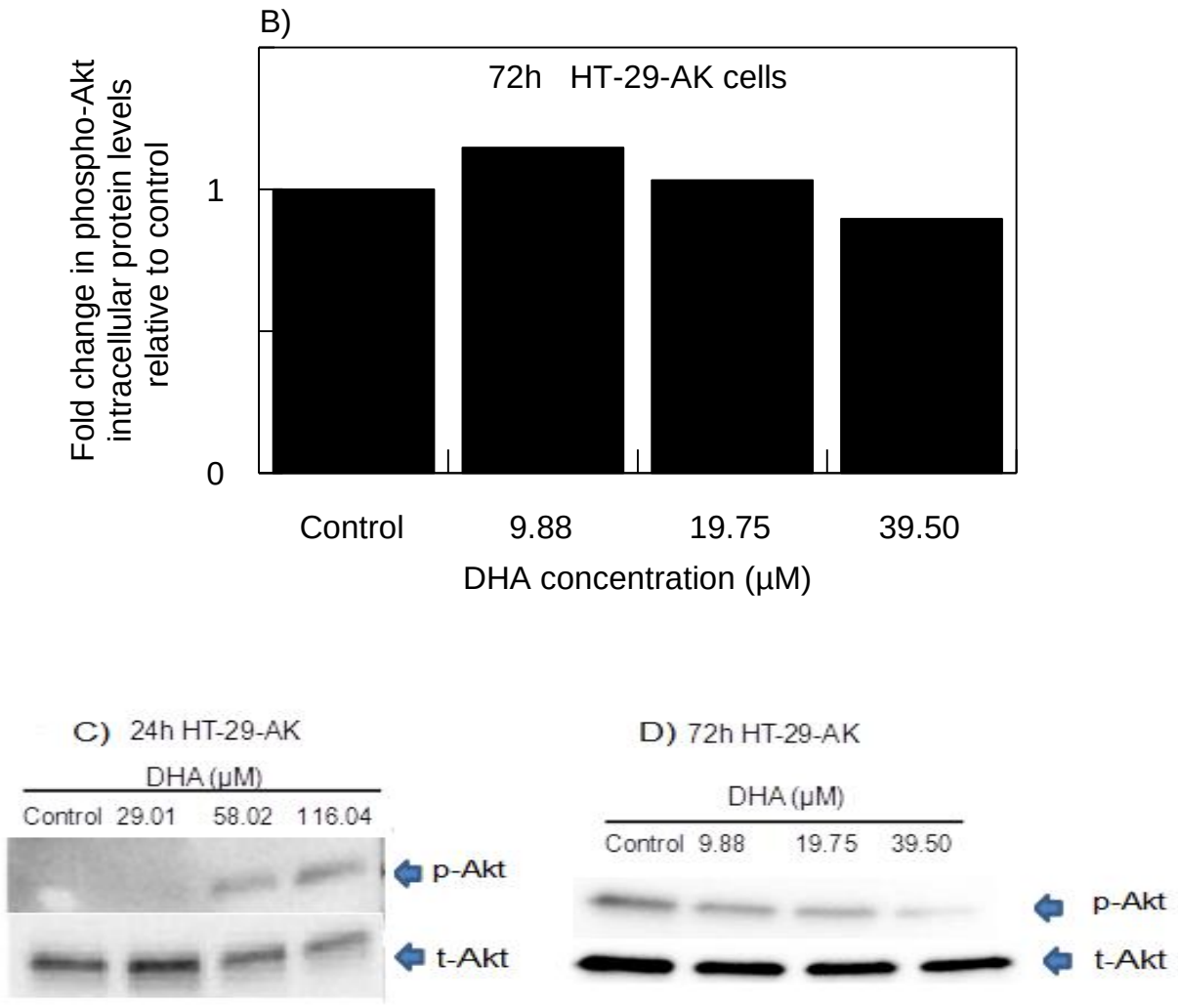

Figure 53: The effect of DHA on phospho-Akt intracellular protein levels in HT-29-AK cells at 24h and 72h in normoxia. Cells were exposed to A) DHA (at 0, 29.01µM. 58.02 µM and 116.04µM) for 24h and B) DHA (at 0, 9.88µM. 19.75µM and 39.50µM) for 72h in normoxia (20% O_2) and analysed for the presence of phospho(p)-Akt by flow cytometric analysis (Materials & Methods, Section 2.9). In similar experiments, proteins isolated from DHA-treated and control samples were separated by SDS-PAGE and Western blotting analysis was performed as described in Materials & Methods (Section 2.10). Re-probing of membrane for total (t)-Akt levels in cells treated for 24h with DHA confirmed equal loading of protein into all of the wells (lower panel of D). The results derived from flow cytometric and Western blotting analyses represent 2 independent experiments which are not powered for statistical analysis. DHA, dihydroartemisinin.

For comparison purposes similar flow cytometric investigations were performed in HL-60 cells treated with ART and DHA accordingly. As shown in figure 54 A, HL-60 cells treated with ART at 0.30µM, 0.60µM and 1.00µM had up-regulated phospho-Akt levels in a concentration-dependent manner by ~2.22-fold (2.22 ± 0.64 RFU; P<0.001), ~2.79-fold (2.79 ± 0.74 RFU; P<0.001) and ~3.16-fold (3.16 ± 0.51 RFU; P<0.001), as compared to control (1.01 ± 0.15 RFU), respectively. The phosphorylation of Akt protein increased in a concentration-dependent manner by ~5% (1.05 ± 0.17 RFU), ~10% (1.10 ± 0.18 RFU) and ~16% (1.16 ± 0.19 RFU) upon treating HL-60 cells for 72h with DHA at 0.25µM, 0.50µM and 1.00µM, as compared to control (1.00 ± 0.18 RFU), respectively but these changes were not significant (figure 54 B).

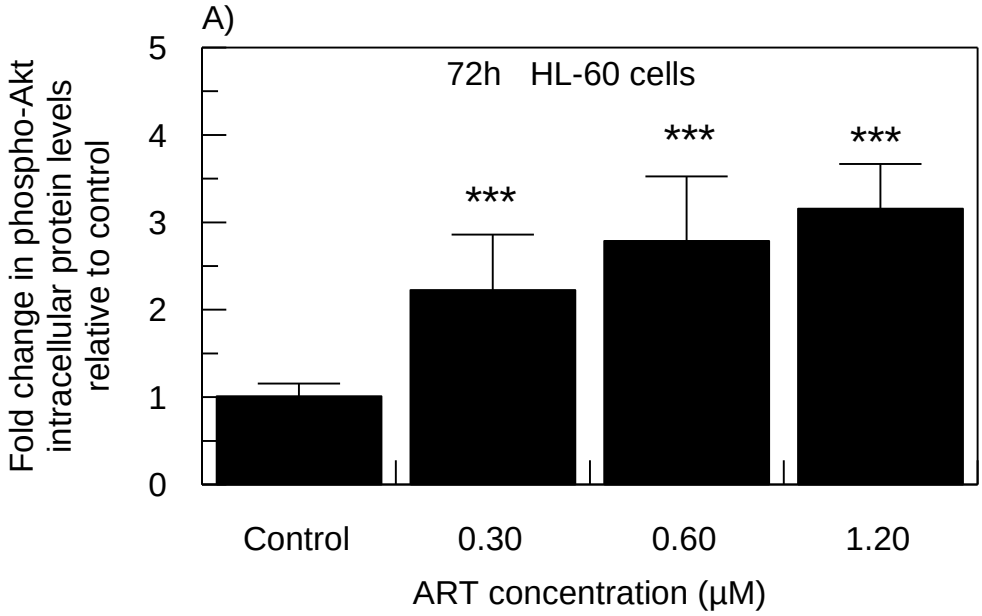

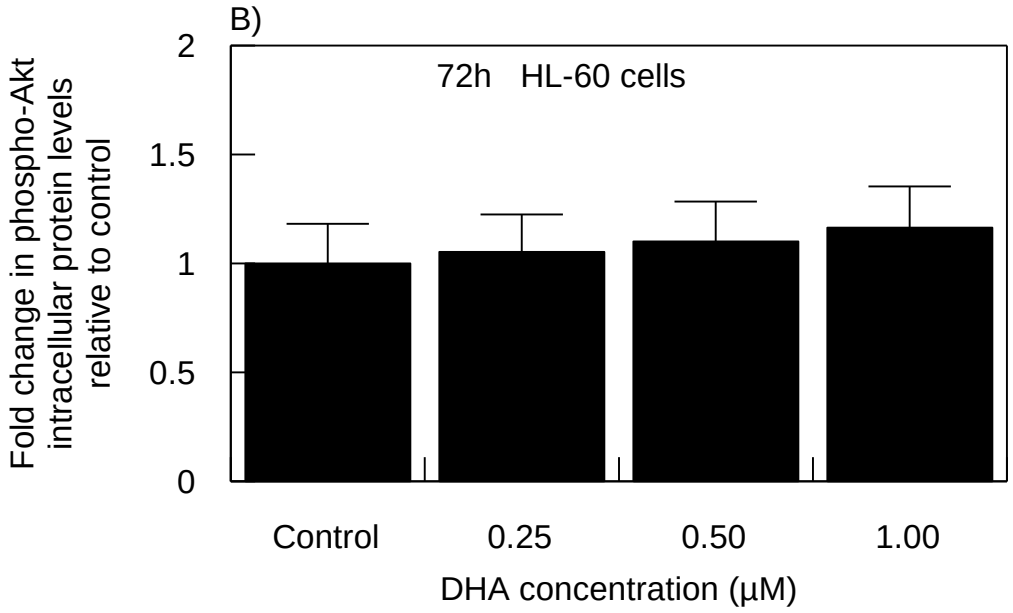

Figure 54: The effect of ART and DHA on phospho-Akt intracellular protein levels in HL-60 cells at 72h in normoxia. Cells were treated without or with A) ART (at 0.30µM, 0.60µM and 1.20µM) and B) DHA (at 0.25µM, 0.50µM and 1.00µM) for 72h under normoxic conditions (20% O_2), labelled with phospho-Akt antibody and analysed on flow cytometer (Materials & Methods, Section 2.9). The results represent the mean ± SD of three independent experiments where ***P<0.001 vs. control as tested by one-way ANOVA (Dunnett test). ART, artesunate; DHA, dihydroartemisinin.

3.17. ART and DHA increased caspase-3-dependent apoptosis of HT-29-AK and HL-60 cells

Since several studies have demonstrated that 1,2,4-trioxanes induce cell death via apoptosis (Mercer *et al.* 2007; Lu *et al.* 2008; Hamacher-Brady *et al*. 2010), the effects of ART and DHA was investigated on pro-apoptotic cleaved caspase-3 in HT-29-AK and HL-60 cells.

As presented in figure 55A, HT-29-AK cells treated with 7.22µM (3.09 ± 0.38), 14.44µM (3.24 ± 0.39 RFU) and 28.88µM (3.30 ± 0.27 RFU) of ART showed a significant (P<0.001) concentration-dependent increase in cellular level of caspase-3

as compared to control (1.00 ± 0.13), which was further presented as dots plots using flow cytometric analysis tools (figure 55B). Similarly, cells treated with DHA demonstrated a significant (P< 0.01) concentration-dependent increase of caspase-3 activity with the highest levels observed of 2.53 ± 0.73 RFU (at 39.5µM DHA) as compared to untreated samples (1.00 ± 0.10 RFU; figure 55C).

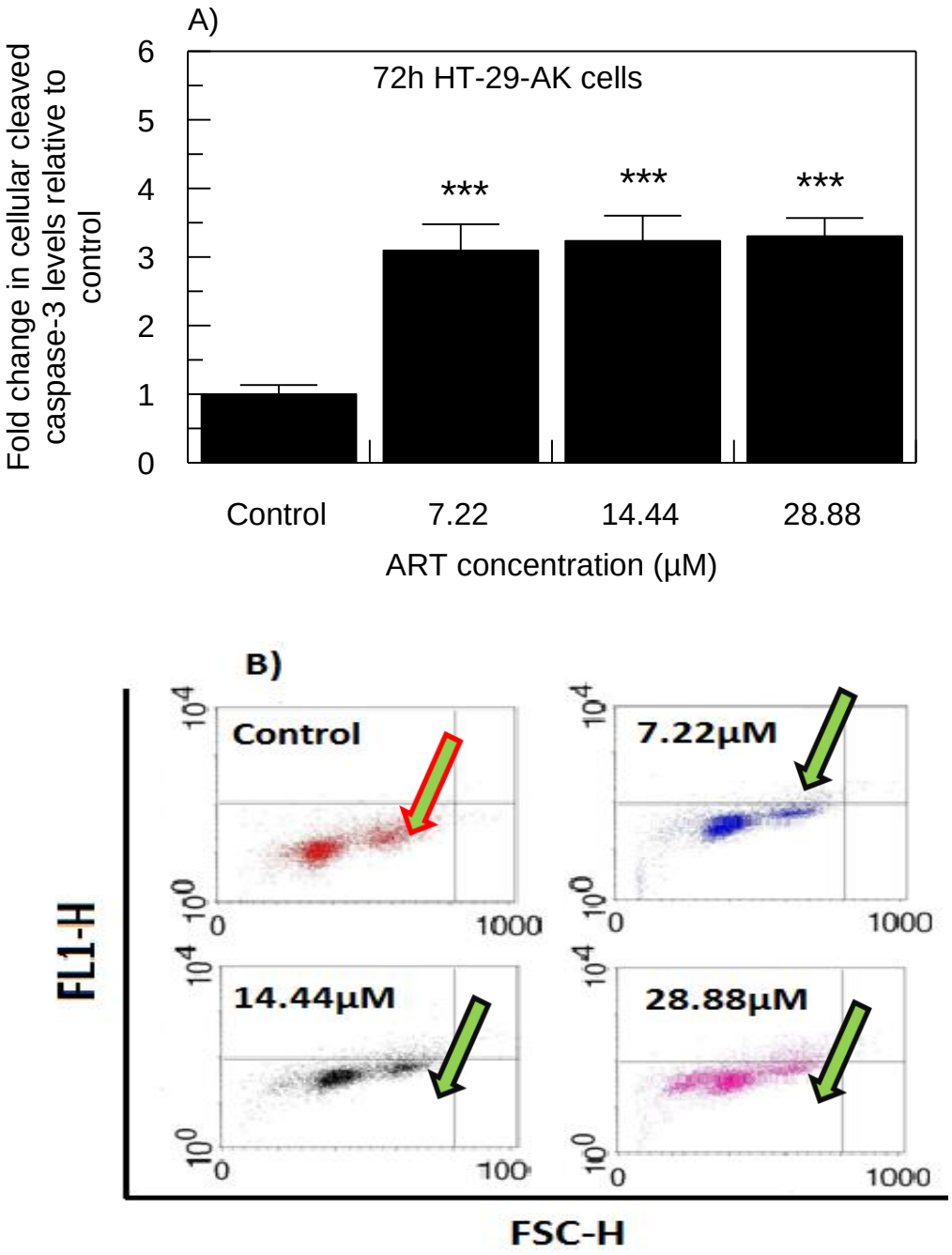

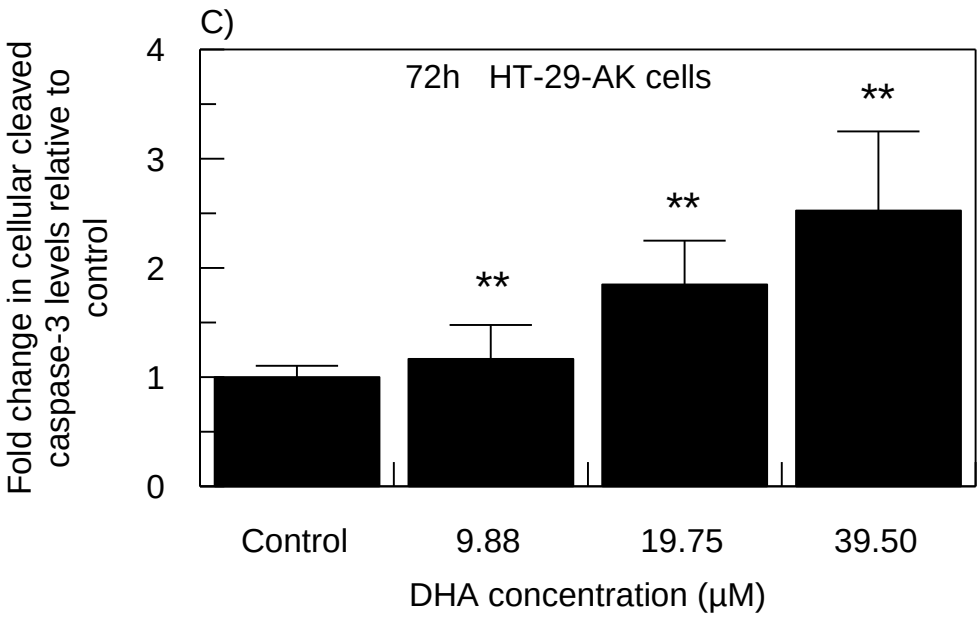

Figure 55: The effect of ART and DHA on the activity of cellular cleaved caspase-3 in HT-29-AK cells at 72h in normoxia. Cells were treated with A) ART (at 0µM, 7.22µM, 14.44µM and 28.88µM) and C) DHA (at 0µM, 9.88µM, 19.75µM and 39.50µM) for 72h in normoxia (20% O_2) and analysed for catalytically active caspase-3 by flow cytometry as described in Materials & Methods (Section 2.9). B) Representative dot plots derived from flow cytometer show (in arrow) an increase in cleaved caspase-3 labelled cells between ART-treated and control cells. The results represent the mean ± SD of three independent experiments. **P<0.01 and ***P<0.001 vs. control as tested by one-way Anova (Dunnett test). ART, artesunate; DHA, dihydroartemisinin.

As shown in figure 56 A, HL-60 cells treated with ART (at 0.30µM, 0.60µM and 1.00µM) had a significant (P<0.001) concentration-dependent increase in cleaved caspase-3 activity by ~1.48-fold (1.48 ± 0.13 RFU), ~2.04-fold (2.04 ± 0.18 RFU) and ~2.77-fold (2.77 ± 0.24 RFU), as compared to control (1.00 ± 0.14 RFU), respectively. Similarly, DHA-untreated cells showed a caspase-3 secretion of 1.00 ± 0.11 RFU which increased by ~1.06-fold (1.06 ± 0.11 RFU; P<0.05), ~1.07-fold (1.07 ± 0.13 RFU), ~1.12-fold (1.12 ± 0.13 RFU; P<0.05) upon treating the cells with 0.25µM, 0.50µM and 1.00µM DHA, respectively (figure 56 B).

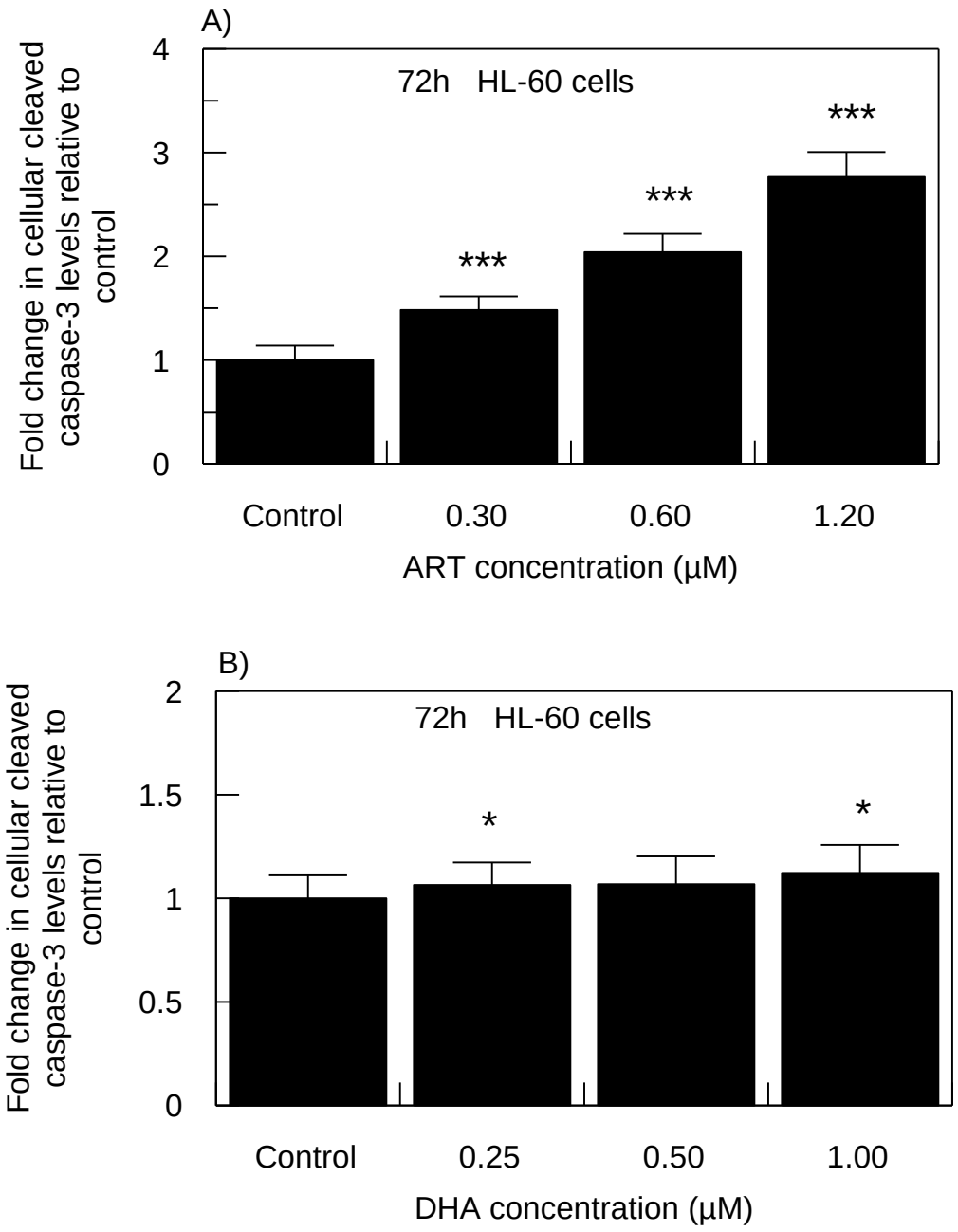

Figure 56: The effect of ART and DHA on the activity of cellular cleaved caspase-3 in HL-60 cells at 72h in normoxia. Cells were treated with A) ART (at 0, 0.30µM, 0.60µM and 1.00µM) and B) DHA (at 0, 0.25µM, 0.50µM and 1.00µM) for 72h in normoxia (20% O_2) and analysed for the presence of cleaved caspase-3 by flow cytometry as described in Materials & Methods (Section 2.9). The results represent the mean ± SD of three independent experiments. *P<0.05 and ***P<0.001 vs. control as tested by one-way ANOVA (Dunnett test). ART, artesunate; DHA, dihydroartemisinin.

3.18. DHA induces DNA strand breaks in treated HL-60 and HT-29-AK cells as measured by 5-bromo-2'-deoxyuridine (BrdU) assay under normoxic conditions

The results of previous study show that the anti-cancer effects of ART and DHA are linked with the induction of caspase-3 dependent apoptosis (figures 55 and 56). In order to further evaluate these observations, APO-BrdU^{TM} TUNEL Assay was used to determine whether DHA-induced cell death is incorporated with BrdU (5-bromo-2-deoxyuridine), a structural analog of thymidine being present at 3'-OH DNA break sites of apoptotic cells (Materials & Methods, Section 2.11).

As depicted in figure 57, there was a concentration-dependent increase in labelled BrdU levels upon treating HT-29-AK cells for 24h with the different concentrations of DHA. The BrdU levels increased by ~1.18-fold (1.18 RFU), ~1.36-fold (1.36 RFU), and ~1.65-fold (1.65 RFU) upon treating the cells with 9.88µM, 19.75µM and 39.50µM DHA for 72h as compared to control (1.00 RFU), respectively (figure 57).

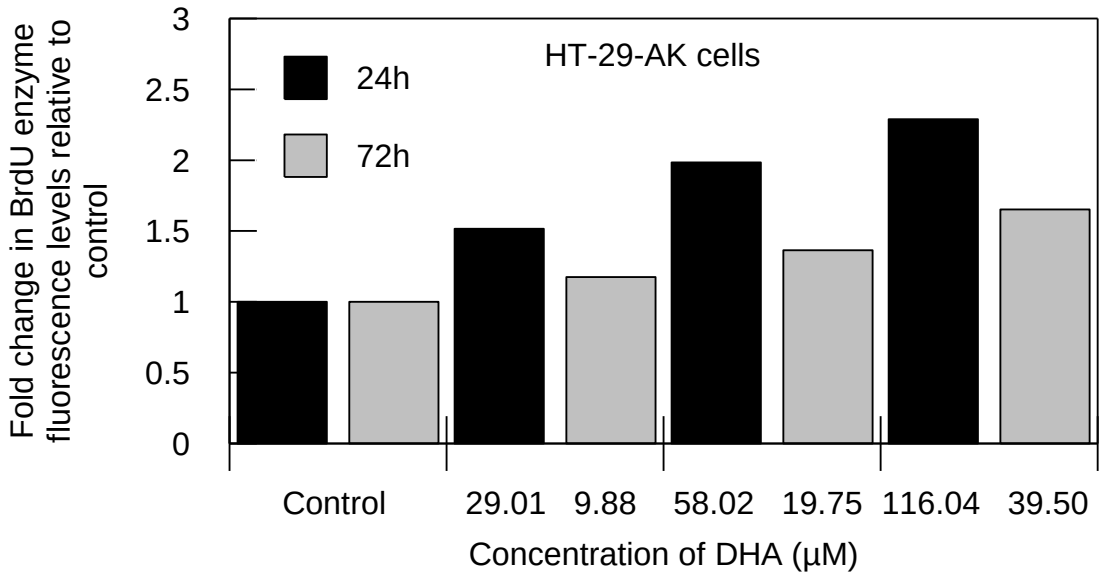

Figure 57: The effect of DHA on the presence of BrdU-labelled nicks in DNA in HT-29-AK cells at 24h and 72h in normoxia. Full bars represent cells treated for 24h with DHA (at 0µM, 29.01µM, 58.02µM and 116.04µM; black bars) and the grey bars represent cells treated with DHA for 72h (at 0µM, 9.88µM. 19.75µM and 39.50µM). The samples were analysed for the presence of BrdU-labelled DNA by flow cytometric analysis as described in Materials & Methods (Section 2.11). The results represent 1 independent experiment which is not powered for statistical analysis. DHA, dihydroartemisinin.

The results presented in figure 58 show that HL-60 cells treated for 24h with DHA at 0.35µM, 0.70µM and 1.40µM resulted in a marked concentration-dependent incorporation of BrdU into the nicked DNA strands by ~1.58-fold (1.58 RFU), ~1.97-fold (1.96 RFU) and ~2.47-fold (2.47 RFU), as compared to control (1.00 RFU), respectively. HL-60 cells treated for 72h with all of the concentrations tested of DHA (0.25µM, 0.49µM and 0.98µM) showed elevated BrdU levels, as compared to control (figure 58).

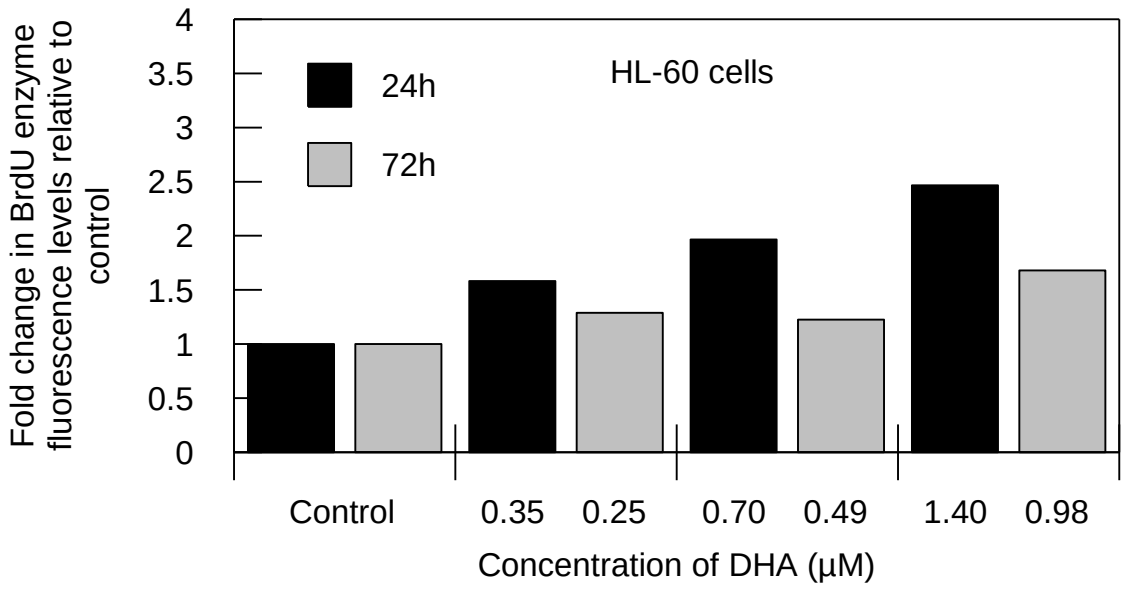

Figure 58: The effect of DHA on the presence of BrdU-labelled nicks in DNA in HL-60 cells at 24h and 72h in normoxia. Black bars represent cells treated for 24h with DHA (at 0, 0.35µM, 0.70µM and 1.40µM) and the grey bars represent cells treated with DHA for 72h with DHA (at 0, 0.25µM, 0.50µM and 1.00µM). The samples were analysed for the presence of incorporated BrdU by flow cytometric analysis as described in Materials & Methods (Section 2.11). The results represent 1 independent experiment which is not powered for statistical analysis. DHA, dihydroartemisinin.

3.19. ART and DHA induced DNA fragmentation in HT-29-AK and HL-60 cells in normoxia

In previous experiments, it was found that ART and DHA induced a concentration-dependent increase of pro-apoptotic caspase-3 in HT-29-AK and HL-60 cells (figures 55 and 56). DHA-treated HL-60 cells and HT-29-AK cells have also shown that DHA promote apoptosis by inducing DNA strand breaks, and observation which comes from an increase in BrdU-stained cells (figures 57 and 58). To investigate whether these results correlate with the presence of fragmented DNA in treated cells, HT-29-AK and HL-60 cells were treated with ART and DHA for varying incubation periods between 24h and 72h before the DNA was isolated and analysed using agarose gel

electrophoresis (Materials & Methods, Section 2.12). In order to validate the results, a positive control (heat-treated sample) was used. DNA damage was induced upon incubation of the isolated non-drug treated sample for 20min at 95°C (figure 59). This manipulation resulted in DNA smearing pattern which was compared to untreated and treated samples (figure 59).

As shown in figure 59, treatment of HT-29-AK cells for 72h with A) ART (at 7.22μM, 14.44μM, and 28.88μM) and B) DHA (at 9.88μM, 19.75μM and 39.50μM) led to the detection of ≥ 20 000 basepairs (bp) DNA fragments accumulated in all concentrations tested (red arrows). These DNA fragments represent the break-up of the large genomic DNA upon drug treatment into smaller, low molecular weight fragments being signs accompanying apoptosis.

The DNA damage upon ART treatment was not concentration-dependent, as compared to untreated cells [figure 59 A; lanes 3, 4, 5 (red arrows) vs. lane 2 (purple arrows)]. The heated samples (positive control) resulted in DNA smearing pattern ranging from ~20000-5000 bp (figure 59 A, lane 1, blue curly bracket). DNA isolated from DHA-treated cells (figure 59 B, lane 3, 4, 5) appeared to result in a greater DNA damage (more visible, lighter packed areas) at all concentrations tested as compared to negative control (barely visible; lane 2). DNA smearing pattern starting from 21226 bp and being lower than 4268 bp (figure 59 B, lane 1, blue curly bracket).

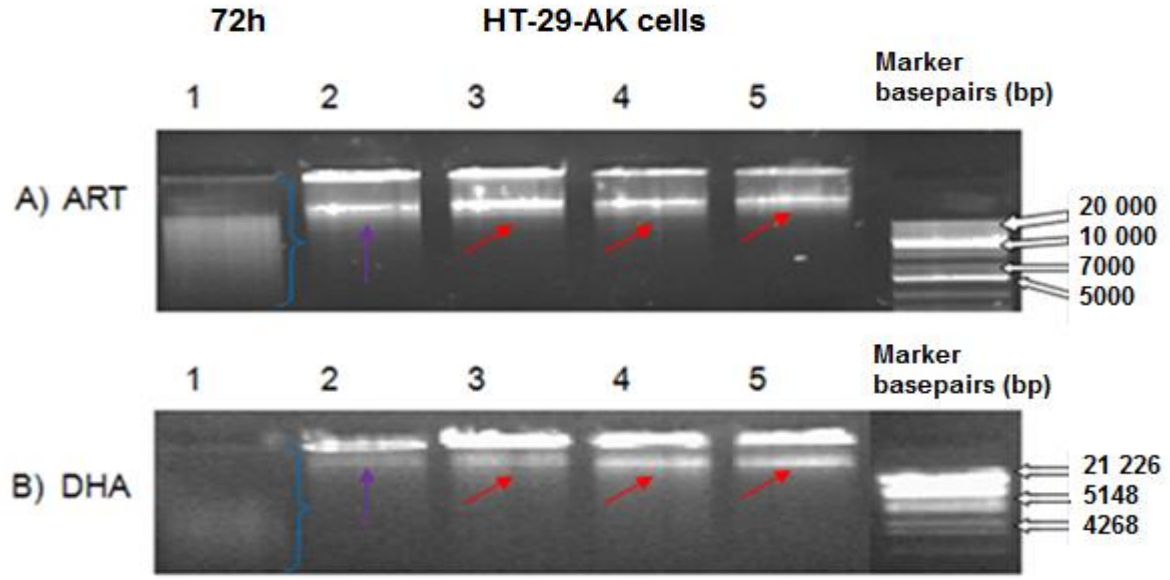

Figure 59: HT-29-AK cells DNA fragmentation analysis upon ART and DHA treatment for 72h in normoxia. Cells (5x10⁶cells/flask) were treated without/with ART and DHA for 72h in normoxia (20% O_2), before the DNA was isolated from cells and analysed using agarose gel electrophoresis (Materials & Methods, Section 2.12). Representative pictures: A) 72h, ART at 7.22 µM [*lane 3*], 14.44µM [*lane 4*], 28.88µM [lane 5]; B) 72h, DHA at 9.88µM [*lane 3*], 19.75 µM [*lane 4*], 39.50 µM [*lane 5*]. Positive controls (control DNA heated at 95°C for 20 mins) were used for both drugs for 72h (figure 58 A and B) [*lane 1*] and revealed DNA smearing (blue curly bracket). The drug untreated samples (negative control) are shown in *lane 2* (figure 58 A and B). Purified DNA from ART and DHA untreated and treated cells at 50ng/µL were separated on 0.8% agarose gel and visualised under UV light. Gene Ruler 1kb (A; 20000-5000 bp) or Lambda DNA/Eco 1301 16 (B; 21226- 4268 bp) molecular markers (Thermo Scientific, Hampshire, UK) were used to determine DNA bands. ART, artesunate; DHA, dihydroartemisinin.

As presented in figure 60, HL-60 cells treated with A) ART (at 0.98µM, 1.96µM, 3.92µM) for 24h; B) ART (at 0.36µM, 0.71µM, 1.42µM) for 48h; and 72h C) ART (at 0.30µM, 0.60µM and 1.20µM) for 72h resulted in the production of damaged DNA fragments (red arrows). Molecular weights of DNA fragments for all ART treated cells are ≥ 21226 bp (figure 60 A and B, lanes 3, 4, 5; and 60 C lanes 1-3). However, as

presented in figure 60 A and B (lane 2) and 60 C (lane 4) by purple arrows only a small appearance of DNA fragmentation is present in the DNA extracted from ART-untreated cells (negative control). As illustrated in lane 1 for 24h (A) and 48h (B), the heated controls also showed a small appearance of DNA fragmentation. Overall, cells treated with ART for 24h (lane 3, 4, 5) resulted in more visible DNA damage as compared to heated control (lane 1). For the 48h incubation, cells treated with 1.42µM ART appeared to result in greater DNA damage, as compared to the respective heated control (figure 60 B, lane 5 vs. lane 1). A heated control sample for was not evaluated for the 72h incubation (figure 60C).

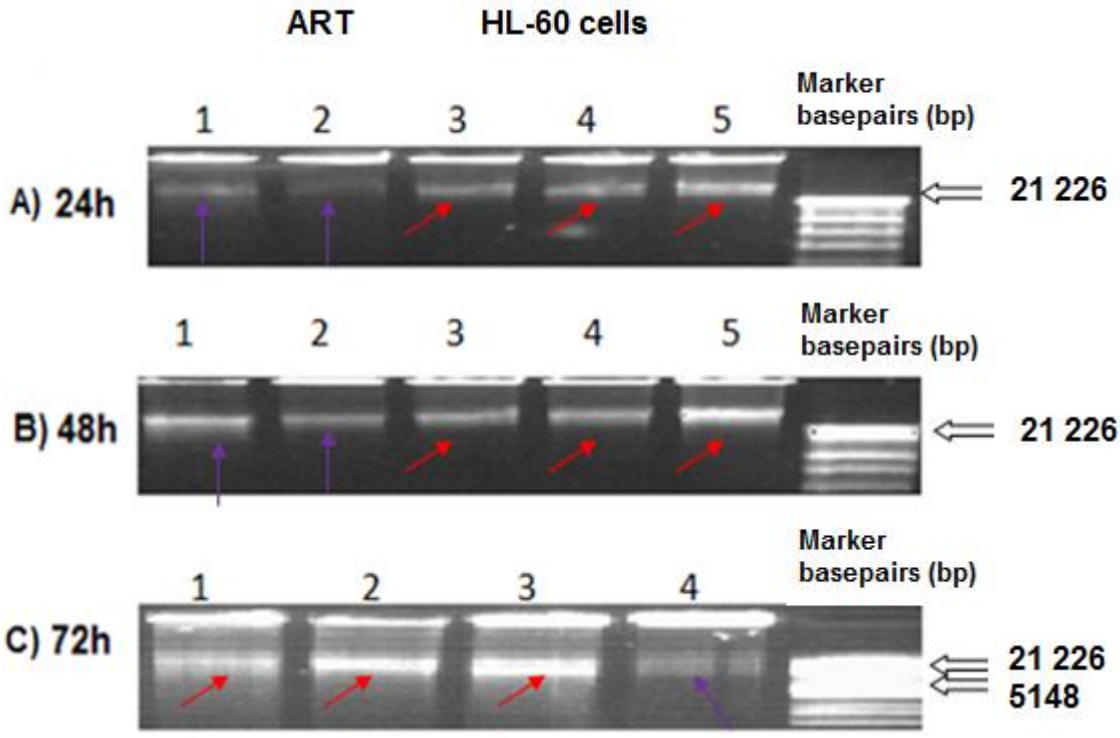

Figure 60: HL-60 cells DNA fragmentation analysis upon ART treatment for 24-72h in normoxia. Cells (5x10^{6}cells/flask) were treated without or with ART for 24, 48 or 72h in normoxia (20% O_2), before the DNA was isolated and assayed using agarose gel electrophoresis (Materials & Methods, Section 2.12). Representative pictures: A) 24h, ART at 0.98 µM [*lane 3*], 1.96 µM [*lane 4*], 3.92 µM [lane 5]; B) 48h, ART at 0.36 µM [*lane 3*], 0.71 µM [*lane 4*], 1.42 µM [*lane 5*]; C) 72h, ART at 0.30 µM [*lane 1*], 0.60 µM [*lane 2*], 1.20 µM [*lane 3*]. In this study, ART untreated samples (negative control) were used for all incubation periods (*lane 1* for 24h and 48h and *lane 4* for 72h). For data validation, positive control (DNA isolated from untreated samples which were heated at 95°C for 20 mins) was used for 24h (A) and 48h (B) incubations [*lane 1*]. Purified DNA from control and ART-treated cells at 70ng/µL were separated on 0.8% agarose gel and visualised under UV light. The Lambda DNA/Eco 1301 16 molecular marker (Thermo Scientific, Hampshire, UK) was used to determine DNA bands from 21226 bp to 5148 bp. ART, artesunate.

As presented in figure 61A and B, the results obtained for HL-60 cells treated with DHA for 24h (at 0.35μM, 0.70μM,1.40μM) and 72h (at 0.25μM, 0.50μM, 1.00μM) show a concentration-dependent increase in amount of smaller DNA fragmentation of ≥ 20 000 bp (more lighter, packed areas). DNA damage upon DHA treatment was indicated by red arrows (figure 61 A and B, lanes 3,4,5) whereas DHA untreated cells with almost undetectable DNA damage with purple arrows (figure 61 A and B, lanes 2). Positive controls for both incubations time points (figure 61 A and B, blue curly brackets) showed DNA damage with the appearance of smearing pattern reaching ~4268 bp for 24h and ~21226 bp for 72h.

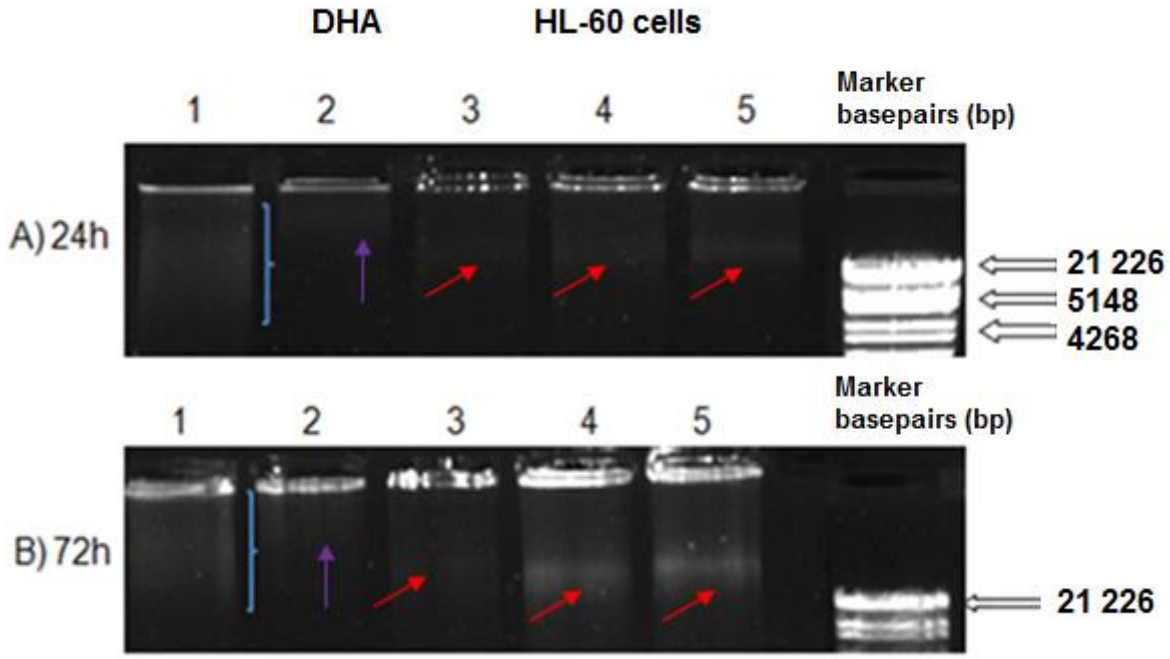

Figure 61: HL-60 cells DNA fragmentation analysis upon DHA treatment at 24h and 72h in normoxia. Cells (5x10⁶cells/flask) were treated without or with DHA for 24 or 72h under normoxic conditions (20% O_2), before the DNA was isolated and assayed using agarose gel electrophoresis (Materials & Methods, Section 2.12). Representative pictures: A) 24h, DHA at 0.35 µM [*lane 3*], 0.70 µM [*lane 4*], 1.4 µM [lane 5]; B) 72h, DHA at 0.25 µM [*lane 3*], 0.50 µM [*lane 4*], 1.00 µM [*lane 5*]. Here, positive control (non-drug treated isolated DNA which was heated at 95°C for 20 mins) used for the 24h (A) and 72h (B) [*lane 1*] incubations which show DNA smearing (blue curly bracket). DHA-untreated samples (negative control) were used for both incubation periods (*lane 2* for 24h and 72h). Purified DNA from control and DHA-treated cells at 70ng/µL were separatedon 0.8% agarose gel and visualised under UV light. The Lambda DNA/Eco 1301 16 molecular marker (Thermo Scientific, Hampshire, UK) was used to determine DNA bands from 21226 bp to 4268 bp. DHA, dihydroartemisinin.

CHAPTER 4

RESULTS

PART II: THE ANTI-CANCER ACTIVITY AND MOLECULAR MECHANISMS OF ART AND DHA AGAINST HT-29-AK AND HL-60 CELLS UNDER HYPOXIC CONDITIONS (1% O_2)

4.1. ART and DHA inhibit the growth of HL-60 and HT-29-AK cells in low oxygen tension

Since our previous study in normoxia (20% O_2, 5% CO_2, 75% N_2 at 37°C) has shown that ART and DHA exhibit profound cytotoxic activity (Section 3.1, table 3), the main focus of this study was to investigate whether low oxygen tension (1% O_2, 5% CO_2, 94% N_2 at 37°C) affected the sensitivity of HL-60 and HT-29-AK cells to ART and DHA. Similar to data acquired under normoxic conditions, it was revealed that treatment of HL-60 and HT-29-AK cells with ART and DHA under hypoxic conditions inhibited the growth of the cells in a time-dependent manner (tables 3 and 6). The 50% growth-inhibition concentration for ART-treated HL-60 cells for 24h was equal to IC_{50} value of 0.92 ± 0.23μM (table 6). There was a significant improvement in the activity of ART against leukaemic HL-60 cells with increase in incubation time, resulting in measured IC_{50} values of 0.73 ± 0.03μM (IC_{50} value of 0.92 ± 0.23μM vs. IC_{50} value of 0.73 ± 0.03μM ART; 1.26-fold enhancement; $P<0.05$), and 0.51 ± 0.06μM (IC_{50} value of 0.92 ± 0.23μM vs. IC_{50} value of 0.51 ± 0.06μM ART; 1.80-fold enhancement; $P<0.001$) after 48h and 72h, respectively (table 6).

There was a significant increase in the cytotoxicity of ART in hypoxia, as compared to normoxia after 24h incubation (hypoxia: IC_{50} value of 0.92 ± 0.23μM vs. normoxia: IC_{50} value of 1.96 ± 0.28μM, 2.13-fold enhancement; $P<0.001$) and after 72h incubation (hypoxia: IC_{50} value of 0.51 ± 0.06 μM vs.normoxia: IC_{50} value of 0.60 ± 0.08 μM, 1.18-fold enhancement; $P<0.05$) (tables 3 and 6). The cytotoxicity of ART in hypoxia for 48h, as compared normoxia was unchanged (hypoxia: IC_{50} value of 0.73 ± 0.03 μM vs. IC_{50} value of 0.71 ± 0.15 μM, $P>0.05$) (tables 3 and 6). These observations show the influence of low oxygen tumour microenvironment on ART response. ART was more potent against HL-60 cells after 24h and 72h in hypoxia, as compared to normoxia (tables 3 and 6).The cytotoxicity of ART after 48h incubation against HL-60 cells was unaffected by low oxygen microenvironment (tables 3 and 6). The findings show potential applications of ART for leukaemia therapy, especially towards leukaemic cells within hypoxic BM areas. In addition, the results show the importance of modeling the tumour microenvironment when developing novel therapeutic drug applications.

As compared to IC_{50} value of 1.10 ± 0.08μM for DHA-treated HL-60 cells for 24h in hypoxia, the cytotoxicity of DHA in low oxygen microenvironment significantly ($P<0.001$) increased with prolonged incubation (48h: IC_{50} value of 0.60 ± 0.09μM, 1.83-fold enhancement; 72h: IC_{50} value of 0.53 ± 0.07μM, 2.08-fold enhancement) (table 6). The inhibitory action of DHA for 24h in hypoxia was reduced by ~1.57-fold as compared to 24h in normoxia (hypoxia: IC_{50} value of 0.70 ± 0.12μM vs. normoxia: IC_{50} value of 1.10 ± 0.08μM) with a level of statistical significance of $P<0.001$ (tables 3 and 6). The changes in the cytotoxicity of DHA against HL-60 cells for 48h and 72h incubations under hypoxic conditions were too minimal to be considered significant (48h; hypoxia: IC_{50} value of 0.60 ± 0.09μM vs. normoxia: IC_{50} value of 0.65 ±

0.09µM, 72h; hypoxia: IC_{50} value of 0.53 ± 0.07µM vs. normoxia: IC_{50} value of 0.49 ± 0.03µM) (tables 3 and 6).

The findings show that DHA treatment of HL-60 cells in normoxia effectively inhibited the growth of both cell lines and this inhibition was decreased by hypoxia only for 24h treatment with DHA. The results show similar potency profiles of DHA in normoxia and hypoxia against leukaemic cells after 48h and 72h incubation, thus indicating potential applications of DHA to target leukaemia clinically. However, further studies are needed to support these observations.

After 72h incubation in low oxygen microenvironment (1% O_2) where ART and DHA were most potent against HL-60 cells, there was no significant difference in the cytotoxicity of compounds (ART with IC_{50} value of 0.51 ± 0.06µM vs. DHA with IC_{50} value of 0.53 ± 0.07µM; P>0.05, table 6). These results show similar potency profiles of ART and DHA against leukaemic cells after 72h incubation in hypoxia.

Table 6: The cytotoxic effect of ART and DHA alone at 24h, 48h or 72h incubation in hypoxia. The results for the drugs alone at each incubation point are expressed as the mean IC_{50} ± SD of at least three independent experiments with 18 replicates. *P<0.05; **P<0.01; ***P<0.001.

Incubation (hrs)	Compounds	HL-60 cells	HT-29-AK cells
		IC_{50} (µM, Mean±SD)	
24	ART	0.92 ± 0.23	269.86 ± 84.41
	DHA	1.10 ± 0.08	84.97 ± 2.72
48	ART	0.73 ± 0.03*	132.99 ± 31.83***
	DHA	0.60 ± 0.09***	50.36 ± 2.47***
72	ART	0.51 ± 0.06***	46.51 ± 4.74***
	DHA	0.53 ± 0.07***	27.10 ± 2.73***

As compared to the growth-inhibitory effect of ART with IC_{50} value of 269.86 ± 84.41µM against colorectal HT-29-AK cells after 24h incubation in hypoxia, the cytotoxic activity of ART against HT-29-AK cells in hypoxia significantly (P<0.001) increased with prolonged incubation, resulting in measured IC_{50} values of 132.99 ± 31.83µM (2.03-fold enhancement), and 46.51± 4.74µM (5.80-fold enhancement) after 48h and 72h, respectively (table 6).

When comparing the cytotoxic activity of ART against HT-29-AK cells under normoxic and hypoxic conditions, it was found that low oxygen microenvironment (1% O_2) reduced the cytotoxcity of ART at all time tested (tables 3 and 6). After 24h, HT-29-AK cells were 1.63-fold less susceptible to the cytotoxic effects of ART, as compared to normoxia (hypoxia: IC_{50} value of 269.86 ± 84.41µM vs. normoxia: IC_{50} value of 165.06 ± 24.25µM; P<0.01) (tables 3 and 6). After 48h, HT-29-AK cells were 2.06-fold less susceptible to the cytotoxic effects of ART, as compared to normoxia (hypoxia: IC_{50} value of 132.99 ± 31.83µM vs. normoxia: IC_{50} value of 64.61 ± 6.61µM; P<0.001) (tables 3 and 6). After 72h where ART was most potent against HT-29-AK cells under both tested conditions, the cytotoxicity of ART against the cells in hypoxia was reduced by 3.22-fold, as compared to normoxia (hypoxia: IC_{50} value of 46.51 ± 4.73µM vs. normoxia: IC_{50} value of 14.44 ± 2.64µM; P<0.001) (tables 3 and 6).

As compared to the growth-inhibitory effect of DHA with IC_{50} value of 84.97 ± 2.72µM against colorectal HT-29-AK cells after 24h incubation in hypoxia, the cytotoxic activity of DHA against HT-29-AK cells in hypoxia significantly (P<0.001) increased with prolonged incubation, resulting in measured IC_{50} values of 50.36 ± 2.47µM (1.69-fold enhancement), and 27.10 ± 2.73 µM (3.14-fold enhancement) after 48h and 72h, respectively (table 6).

When comparing the cytotoxicity of DHA against HT-29-AK cells under normoxic and hypoxic conditions, low oxygen microenvironment (1% O_2) was shown to antagonise growth-inhibitory effect of DHA at all time tested (tables 3 and 6). After 24h, HT-29-AK cells were 1.46-fold less susceptible to the cytotoxic effects of DHA, as compared to normoxia (hypoxia: IC_{50} value of 84.97 ± 2.72μM vs. normoxia: IC_{50} value of 58.02 ± 4.09μM; $P<0.001$) (tables 3 and 6). After 48h, HT-29-AK cells were 1.32-fold less susceptible to the cytotoxic effects of DHA, as compared to normoxia (hypoxia: IC_{50} value of 50.36 ± 2.47μM vs. normoxia: IC_{50} value of 38.28 ± 2.44μM; $P<0.001$) (tables 3 and 6). After 72h where DHA was most potent against HT-29-AK cells under both tested conditions, the cytotoxicity of DHA against the cells in hypoxia was reduced by 1.37-fold, as compared to normoxia (hypoxia: IC_{50} value of 27.10 ± 2.73μM vs. normoxia: IC_{50} value of 19.75 ± 1.07μM; $P<0.001$) (tables 3 and 6).

After 72h incubation in low oxygen microenvironment (1% O_2) where ART and DHA had the highest growth-inhibitory effects against HT-29-AK cells, DHA was more cytotoxic as compared to ART (DHA with IC_{50} value of 27.10 ± 2.73μM vs. ART with IC_{50} value of 45.70 ± 3.84μM; table 6) with a level of statistical significance of $P<0.001$.

The results show that the low oxygen microenvironment (1% O2) is a major factor that decreases the cytotoxicity of ART and DHA against human colorectal HT-29-AK cells. These data indicate the importance of developing novel therapeutic drug applications, including combination therapies to enhance the anti-cancer effects of ART and DHA for CRC treatment

4.2. Cytotoxicity of ART and DHA in hypoxia against HL-60 and HT-29-AK cells was affected by the presence of DFO and haemin.

As previous experiments in normoxia have shown that the cytotoxicity of ART and DHA in HL-60 and HT-29-AK cells is enhanced by the presence of 1μM and 3μM haemin and antagonised by the ferric iron chelator DFO at 60μM (table 5), it was of interest to evaluate whether hypoxia modulates these effects. Interestingly, the results obtained by MTT cytotoxicity assay under hypoxic conditions (table 7) showed that the presence of haemin antagonised the cytotoxic effects of ART and DHA. Lower haemin concentration (1μM) decreased the cytotoxicity of ART by ~5.03-fold (ART alone with IC_{50} value of 0.92 ± 0.23μM vs. ART+ 1μM haemin with IC_{50} value of 4.63μM; table 7). Haemin at 3μM further decreased the cytotoxicity of ART by ~18.42-fold (ART alone with IC_{50} value of 0.92 ± 0.23μM vs. ART+ 3μM haemin with IC_{50} value of 16.95μM). The cytotoxicity of DHA was antagonised by haemin (1μM) (IC_{50} value of 3.65μM) being a 3.32-fold increase in DHA IC_{50} value of 1.10 ± 0.08μM (table 7). Haemin at 3μM further decreased the cytotoxicity of DHA by ~4.98-fold (IC_{50} value of 5.48μM), as compared to DHA alone with IC_{50} value of 1.10 ± 0.08μM (table 7).

Similarly to normoxia (table 5), the presence of DFO (60μM) antagonised the cytotoxicity of ART and DHA against HL-60 cells under hypoxic conditions (table 7). The cytotoxicity of ART was antagonised the most in the presence of DFO (60μM) resulting in a ~58.90-fold increase in IC_{50} value of ART (0.92 ± 0.23 μM vs. 54.18μM; table 7). The cytotoxicity of DHA was also diminished by DFO (at 60μM) (IC_{50} value of 11.12μM) being a 10.11-fold increase in DHA IC_{50} value of 1.10 ± 0.08μM (table 7). As in normoxia (table 5), the results derived for HT-29-AK cells after 24h incubation showed that lower haemin concentration (1μM) increased the cytotoxicity of ART

by ~1.58-fold (ART alone with IC_{50} value of 269.86 ± 84.41µM vs. ART+ 1µM haemin with IC_{50} value of 170.5 ± 18.56µM). The anti-cancer properties of DHA against HT-29-AK cells were also enhanced by haemin (1µM) (IC_{50} value of 63.26µM) being a 1.34-fold increase in DHA IC_{50} value of 84.97 ± 2.72µM (table 7). Haemin at 3µM further increased the cytotoxicity of ART and DHA by ~1.72- (IC_{50} value of 156.52µM) and 1.64-fold (IC_{50} value of 51.91µM) when compared to ART IC_{50} value of 269.86 ± 84.41µM and DHA IC_{50} value of 84.97 ± 2.72µM alone, respectively (table 7). In addition, treatment of HT-29-AK cells with ART in combination with DFO (60µM) antagonised the activity of ART by at least ~2.78- fold (IC_{50} value of ≤ 750µM) when compared to ART alone (269.86 ± 84.41µM) (table 7). Similar effects were observed for DHA (IC_{50} value of 84.97 ± 2.72µM) where the presence of DFO (60µM) inhibited the cytotoxicity by ~7.78-fold (IC_{50} value of 660.68µM) (table 7).

Table 7: The cytotoxic effect of ART and DHA alone and in the presence of deferiprone (60µM) and haemin (1µM and 3µM) against HL-60 and HT-29-AK cells at 24h incubation in hypoxia. The results for the drugs alone at each incubation point are expressed as the mean IC_{50} ± SD of at least three independent experiments with 18 replicates. Data for the drugs in the presence of DFO and haemin (1µM and 3µM) represent 1 independent experiment with 18 replicates. ART, artesunate; DHA, dihydroartemisinin; DFO, deferiprone.

	Compounds	**HL-60 cells**	**HT-29-AK cells**
		IC_{50} (µM, Mean±SD)	
Incubation 24h	ART	0.92 ± 0.23	269.86 ± 84.41
	DHA	1.10 ± 0.08	84.97 ± 2.72
	ART + DFO (60µM)	54.18	≤ 750
	DHA + DFO (60µM)	11.12	660.68
	ART + 1µM haemin	4.63	170.50
	DHA + 1µM haemin	3.65	63.25
	ART + 3µM haemin	16.95	156.52
	DHA + 3µM haemin	5.48	51.91

Under normoxic conditions, it was shown that ART and DHA had increased cytotoxicity towards HL-60 and HT-29-AK cells in the presence of haemin (1µM and 3µM) (table 5). As presented in table 7, enhanced ART and DHA cytotoxicity in the presence of haemin (1µM and 3µM) was observed only towards CRC HT-29-AK cells which was in accordance with the results derived from normoxia (table 5 vs table 7). The lower anti-cancer activities of ART and DHA against HL-60 cells under hypoxic conditions in the presence of haemin (1µM and 3µM) might be resulted from different mechanisms by which iron is utilised by cancer cells in hypoxia, as compared to normoxia. The molecular regulation of iron up-take by malignant cells to sustain cell growth is mediated by the cell surface TfR1. Therefore, it was of interest to investigate wheather decreased activity of ART and DHA in the presence of haemin (1µM and 3µM) is associated with the changes of secreted levels of TfR1 upon the drugs treatment in hypoxia as compared to normoxia. Based on these considerations, ELISA to measure sTfR1 was performed in subsequent study.

4.3. Hypoxia modulates the effects of ART and DHA on the cellular secretion of sTfR1 in HL-60 and HT-29-AK cells

Data shown in table 7 demonstrate that the presence of haemin (1µM and 3µM) has variable effects on ART and DHA in both cell lines in hypoxia. Therefore, it was of interest to investigate the effects of ART and DHA on the levels of sTfR1 in cancer cells under hypoxia.

With prepared samples for ELISA as described in Materials & Methods (Section 2.5.1), we measured concentration-dependent increase in sTfR1 secretion levels by ~1.89-fold (4.34 nmol/L), ~3.28-fold (7.54 nmol/L), ~4.37-fold (10.04 nmol/L) upon treating HL-60 cells with 0.26µM, 0.52µM and 1.04µM ART, respectively, as

compared to control (2.30 nmol/L) (figure 62). In contrast, measured sTfR1 levels in samples treated with 0.27µM DHA were highly up-regulated by ~2.30-fold, as compared to control (2.07nmol/L vs. 0.90nmol/L, figure 62). These up-regulated sTfR1 secretions were decreasing with increasing concentrations of DHA. There was a fold change of ~ 1.51- (1.36 nmol/L) and ~1.36-fold (0.66 nmol/L) upon treating HL-60 cells with 0.54µM and 1.08µM DHA for 72h respectively, as compared to control (0.90nmol/L) (figure 62).

The findings show that ART and DHA exhibit distinct mechanisms towards TfR1 levels in HL-60 cells under hypoxic conditions. While ART increased TfR1 levels, DHA decreased TfR1 levels in HL-60 cells after 72h in hypoxia. The profile of activity of ART and DHA on TfR1 levels in HL-60 cells is similar to the observations in normoxia (figures 15 vs. 62), suggesting lack of influence of hypoxia on TfR1 levels in ART and DHA-treated HL-60 cells for 72h.

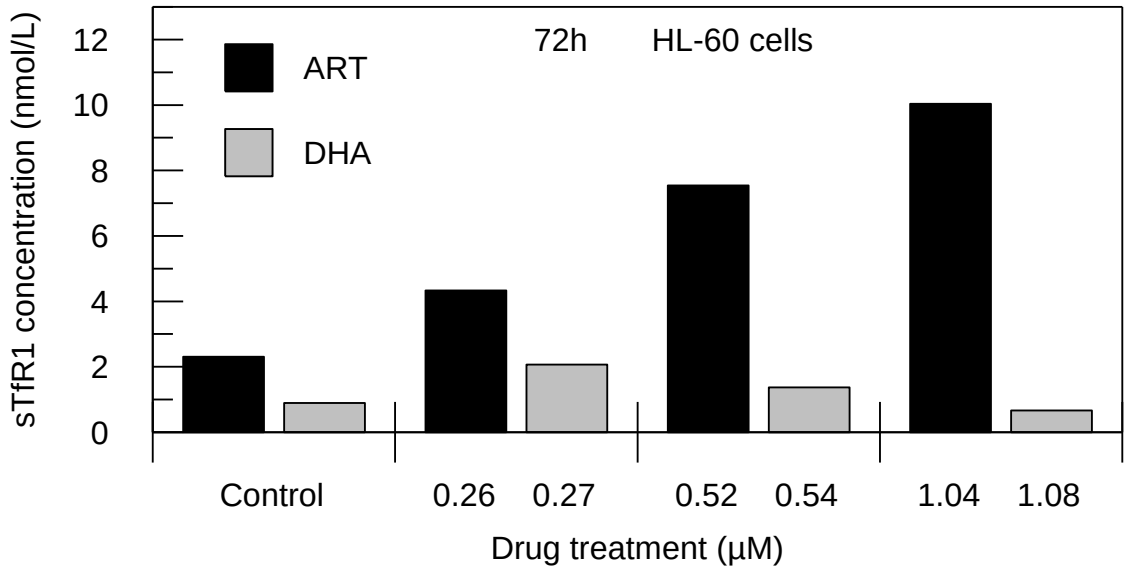

Figure 62: The secretion levels of sTfR1 in HL-60 cells upon ART and DHA treatments in hypoxia. Cells were exposed to ART (at 0µM, 0.26µM, 0.52µM and 1.04µM) and DHA (at 0µM, 0.27µM, 0.54µM and 1.08µM) for 72h under hypoxic conditions (1% O_2). After 72h incubation cell-free conditional media (from untreated and ART- and DHA-treated HL-60 cells) were analysed by ELISA for sTfR1 levels as described in Materials & Methods (Section 2.5.1). The histograms for ART treated cells (black bars) and DHA (grey bars) for 72h represent mean of 2 independent experiments which are not powered for statistical analysis. ART, artesunate; DHA, dihydroartemisinin.

The results displayed in figure 63 indicate that ART and DHA in hypoxia elicit opposite effects on sTfR1 secretions in HT-29-AK cells, as compared to the effects of compounds observed against HL-60 cells (figure 62 vs. figure 63).

Low concentration of ART (at 22.85µM) resulted in an increase of sTfR1 secretion levels by ~1.13-fold (5.43nmol/L), as compared to ART untreated cells (4.80nmol/L) (figure 63). These up-regulated sTfR1 secretions were decreasing with increasing concentrations of ART with resulting a fold change of ~ 2.15- (2.23nmol/L) and ~2.86-fold (1.68 nmol/L) upon treating HT-29-AK cells with 45.70µM and 91.40µM ART respectively, as compared to control (4.80 nmol/L) (figure 63). HT-29-AK cells treated

with 13.55µM, 27.10µM and 54.20µM DHA resulted in a concentration-dependent increase in sTfR1 concentrations by ~ 2.06- (3.79 nmol/L), ~ 2.48- (4.57 nmol/L) and ~9.66-folds (17.77 nmol/L), as compared to control (1.84nmol/L), respectively (figure 63).

Similarly to the observations in HL-60 cells, ART and DHA showed distinct mechanisms towards TfR1 levels in HT-29-AK cells under hypoxic conditions. While ART decreased TfR1 levels, DHA increased TfR1 levels in HT-29-AK cells after 72h in hypoxia. The profile of activity of ART on TfR1 levels in HT-29-AK cells is similar to the observations in normoxia (figures 15 and 63), suggesting lack of influence of hypoxia on TfR1 levels in ART and DHA-treated HL-60 cells for 72h. In contrast, DHA decreased TfR1 in HT-29-AK cells after 72h in normoxia but the TfR1 levels upon DHA treatment were increased in hypoxia, indicating the involvement of hypoxia in anti-cancer effects of DHA.

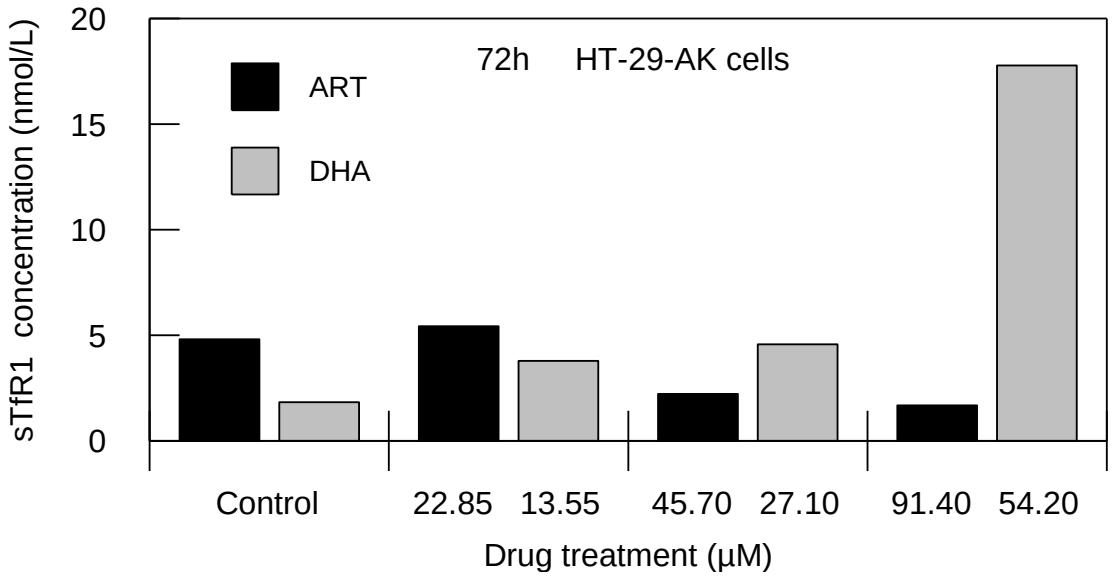

Figure 63: The secretion levels of sTfR1 in HT-29-AK cells upon ART and DHA treatments in hypoxia. Cells were exposed to ART (0, 22.85µM, 45.70µM and 91.40µM) and DHA (0µM, 13.55µM, 27.10µM and 54.20µM) for 72h under hypoxic conditions (1% O_2). After 72h incubation cell-free conditional media (from untreated and ART- and DHA-treated HL-60 cells) were analysed by ELISA for sTfR1 levels as described in Materials & Methods (Section 2.5.1). The histograms for ART treated cells (black bars) and DHA (grey bars) for 72h represent mean of 2 independent experiments which are not powered for statistical analysis. ART, artesunate; DHA, dihydroartemisinin.

4.4. The proliferation rate of HL-60 and HT-29-AK cells is affected by oxygen availabilty

In order to better understand the mode of action of ART and DHA, the proliferation rate of HL-60 and HT-29-AK cells at 0, 24, 48, 72 and 96h incubation was investigated under normoxic (20% O_2) and hypoxic (1% O_2) conditions as described in Materials & Methods (Section 2.4.5). As presented in figure 64, HL-60 and HT-29-AK cells in the first 24h were not proliferating rapidly (lag phase); there was no significant difference in the growth rate under both conditions. However, after 24h HL-60 and HT-29-AK cells under normoxia have turned into logarithmic growth

phase, followed by the plateau phase after 48h and again into logarithmic phase after 72h (figure 64). In contrast, the growth of HL-60 cells under hypoxia was slowly increasing from 0h to 72h, turning into death phase after 72h (figure 64A). The growth rate of HT-29- AK cells under hypoxia was linear up to 72h with a sharp decline (death phase) after 72h (figure 64B). Overall, the growth rate of HL-60 and HT-29-AK cells in normoxia after 48h was significantly (P<0.001) faster, as compared to the proliferation rate of the cells under hypoxia after 48h (figure 64).

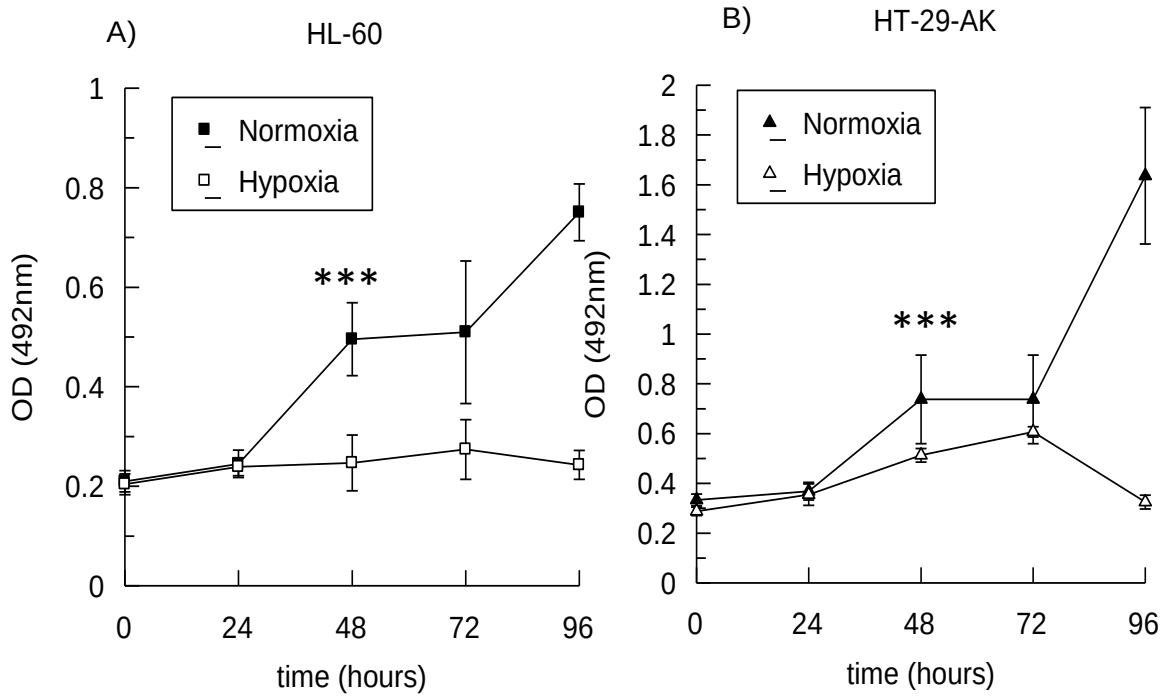

Figure 64: The growth kinetics of A) HL-60 and B) HT-29-AK cells cultured in normoxia and hypoxia. Cells ($1x10^4$cells/well) were plated in 96-well flat-bottomed microtitre plates and incubated for 0, 24, 48, 72 and 96h in normoxia (20% O_2) or hypoxia (1% O_2). Following incubation, the absorbance associated with viable cells following MTT assay was estimated as described in Materials & Methods (Section 2.4.5). The values are means± S.D. of at least 3 independent experiments, with 6 replicates per experiment and analysed by Mann Whitney U test. ***P<0.001 as per text above.

4.5. DHA treatment altered the secretion of cytokine IL-6 in HL-60 and HT-29-AK cells in hypoxia

In HL-60 cells after 24h, DHA at 0.27µM increased slightly IL-6 levels by ~1.11-fold (0.20pg/mL), as compared to control (0.18pg/mL; figure 65). The levels of IL-6 secretions were undetected with 0.53µM DHA (< 0.039pg/mL) and up-regulated with 1.06µM DHA (~2.94-fold, 0.53pg/mL), as compared to control (0.18pg/mL; figure 65). Similar pattern was observed against HT-29-AK cells treated with DHA for 72h (figure 65). As compared to control (0.17pg/mL), DHA (at 13.55µM) increased IL-6 levels by ~1.59- fold (0.27pg/mL) whereas the levels of IL-6 were below the limit of assay detection (< 0.039pg/mL) with 27.10µM of DHA (figure 65). Most detactable IL-6 secretion (~2.18-fold, 0.37pg/mL) was observed with the highest concentration of DHA (at 54.20 µM), as compared to control (0.17pg/mL) (figure 65).

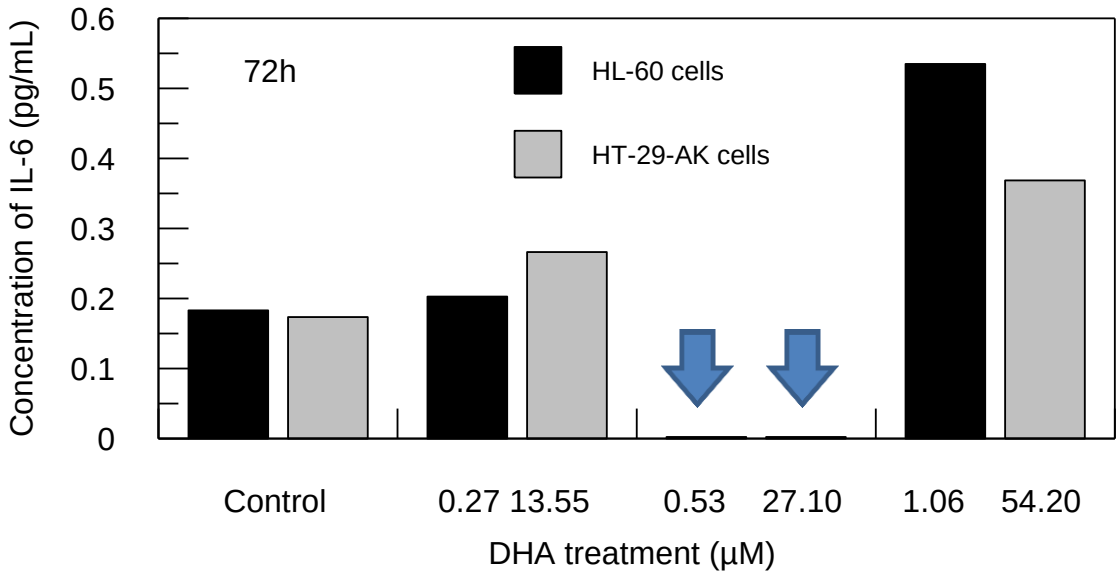

Figure 65: The secretion levels of pro-inflammatory cytokine IL-6 in HL-60 and HT-29-AK cells upon DHA treatment for 72h in hypoxia. HL-60 cells (black bars) were treated with 0µM, 0.27µM, 0.53µM and 1.06µM of DHA and HT-29-AK cells (grey bars) were treated with 0µM, 13.55µM, 27.10µM and 54.20µM of DHA for 72h before the incubation media was measured for secreted IL-6 levels by ELISA following manufacturer's instructions (www.rndsystems.com) (Materials & Methods, Section 2.5.2). As shown in arrow, the level of IL-6 secretions with DHA at 0.53µM and 27.10µM was below the limit of detection (< 0.039pg/mL). Data represent mean of 2 independent experiments and is not powered for statistical analysis. DHA, dihydroartemisinin.

4.6. ART and DHA reduced the levels of VEGFα$_{165}$ in HL-60 and HT-29-AK cells in hypoxia

As in normoxia, the effect of ART and DHA on the level of VEGF-α$_{165}$ secretion in HL-60 and HT-29-AK cells in hypoxia was investigated (figure 66). With measurable levels of VEGF-α$_{165}$ in all samples, ART at 0.26µM, 0.51µM, and 1.02µM produced identical levels of reduction in VEGF-α$_{165}$ secretions of 82.52 pg/mL, 81.54 pg/mL and 82.52 pg/mL, as compared to control (93.26pg/mL), respectively (figure 66). In contrast, measured VEGF-α$_{165}$ secretions in cells treated with 0.27µM and 0.54µM

DHA were slightly up-regulated by ~1.07-fold (89.36 pg/mL) and 1.01-fold (84.47 pg/mL), respectively, as compared to control (83.50 pg/mL) (figure 66). The levels of VEGF-α_{165} secretions were decreased with 1.06µM DHA (~1.08-fold, 77.64 pg/mL), as compared to control (83.50 pg/mL; figure 66).

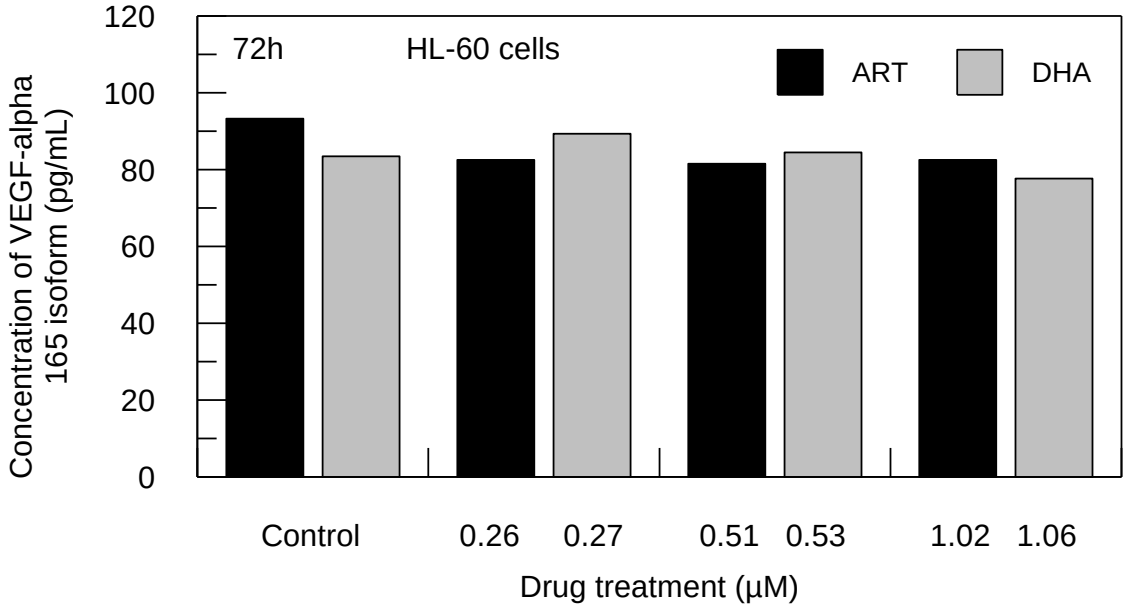

Figure 66: The effect of ART and DHA on VEGF-α165 cellular secretion in HL-60 cells at 72h in hypoxia. Cells were exposed to ART (at 0µM, 0.26µM, 0.51µM and 1.02µM) or DHA (at 0µM, 0.27µM, 0.53µM and 1.06µM) for 72 h under hypoxic conditions (1% O_2) before the cell-free culture media were analysed by ELISA as described in Materials & Methods (Section 2.5.2). The histograms for ART treated cells (black bars), DHA for 72h (grey bars) represent 2 independent experiments which are not powered for statistical analysis. ART, artesunate; DHA, dihydroartemisinin.

The results displayed in figure 67, show that HT-29-AK cells treated with 22.85 µM and 91.40µM ART resulted in a minimal reduction of VEGF-α_{165} secretion by ~1.03-fold (433.11 pg/mL) and ~1.06-fold (424.32pg/mL), as compared to control (447.75 pg/mL), respectively. The levels of VEGF-α_{165} were minimally increased with 45.70µM ART (461.43 pg/mL) as compared to control (447.75 pg/mL; figure 67).

DHA-treated HT-29-AK cells for 72h down-regulated VEGF-α_{165} secretions in a concentration-dependent manner by ~1.19-fold (453.61 pg/mL), ~1.23-fold (438.96 pg/mL) and ~1.30-fold (415.53 pg/mL) with 13.55 µM, 27.10 µM and 54.20 µM DHA, respectively when compared to untreated cells (541.50 pg/mL) (figure 67).

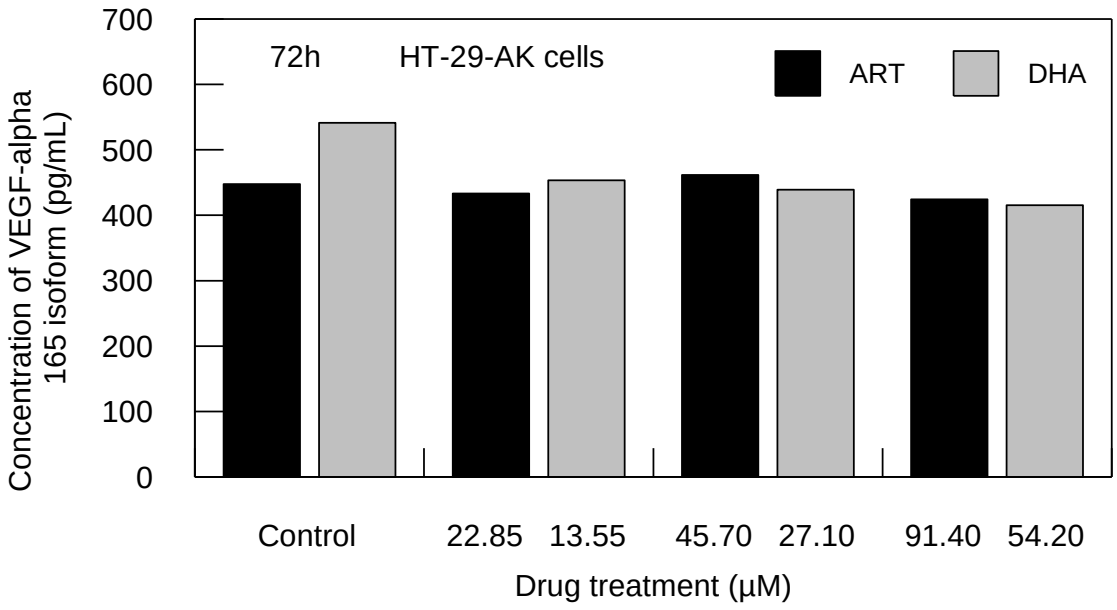

Figure 67: The effect of ART and DHA on VEGF-α165 cellular secretion in HT-29-AK cells under hypoxia. Cells were exposed to ART (at 0µM, 22.85µM, 45.70µM and 91.40µM) or DHA (at 0µM, 13.55µM, 27.10µM and 54.20µM) for 72 h under hypoxic conditions (1% O_2). Thereafter, cell-free incubation media were analysed by sandwich ELISA as described in Materials & Methods (Section 2.5.2). The histograms for ART treated cells (black bars) and DHA (grey bars) represent mean of 2 independent experiments which are not powered for statistical analysis. ART, artesunate; DHA, dihydroartemisinin.

4.7. ART and DHA treatment altered cellular survivin levels in HL-60 and HT-29-AK cells in hypoxia

To investigate whether hypoxia modulates the expression of survivin, HL-60 and HT-29-AK cells were incubated without or with the test agents for 72h in low oxygen tension (1% O_2). As shown in figure 68, cellular survivin concentration was up-regulated in a concentration-dependent manner with 0.26µM and 0.51µM ART against HL-60 cells by ~1.04- (910.16 pg/mL) and ~1.13-fold, (988.28 pg/mL), as compared to control (871.09 pg/mL), respectively. However, as compared with control (871.09pg/mL), ART at 1.02µM resulted in a reduction in survivin concentration by ~1.11-fold (785.16 pg/mL) (figure 68). Moreover, as compared to control (339.84pg/mL), there was a marked increase in survivin concentrations by ~2.98- (1011.72pg/mL), ~2.77- (941.41pg/mL) and ~4.08-fold (1386.72pg/mL) upon treating the cells with 0.27µM, 0.53µM and 1.06µM of DHA, respectively (figure 68).

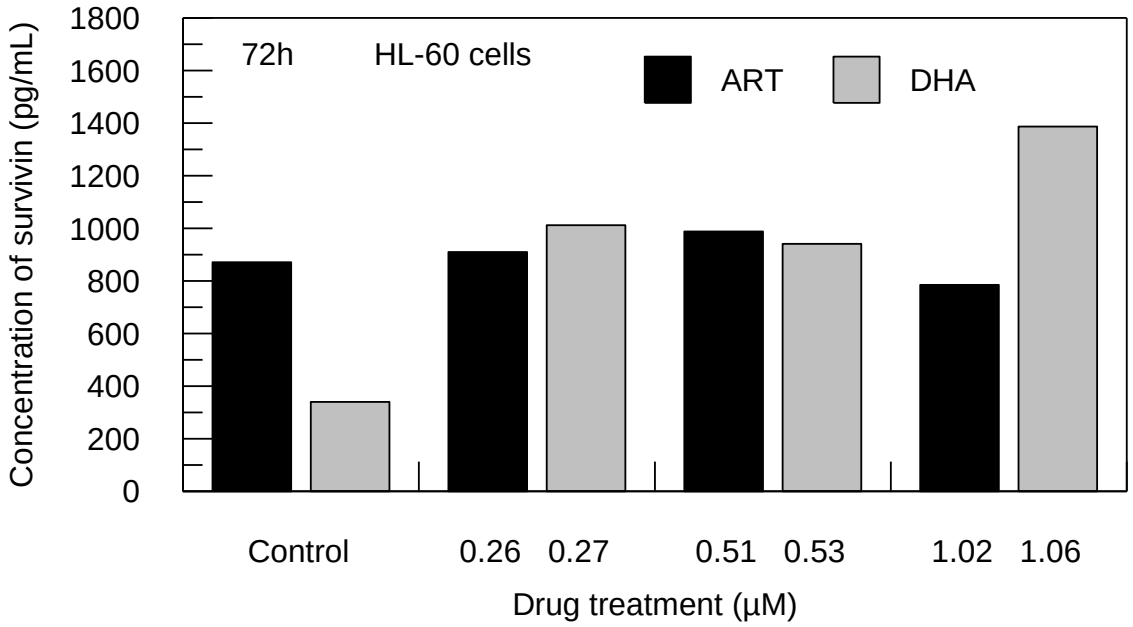

Figure 68: The effect of ART and DHA on cellular survivin levels in HL-60 cells at 72h in hypoxia. Cells were exposed to ART (at 0µM, 0.26µM, 0.51µM and 1.02µM) or DHA (at 0µM, 0.27µM, 0.53µM and 1.06µM) for 72 h under hypoxic conditions (1% O_2) before the cell-free culture media were analysed by ELISA as described in Materials & Methods (Section 2.5.4). The histograms for ART treated cells (black bars), DHA for 72h (grey bars) represent 2 independent experiments which are not powered for statistical analysis.. ART, artesunate; DHA, dihydroartemisinin.

In addition, HT-29-AK cells treated with 22.85µM of ART showed decreased survivin levels by ~1.34-fold (746.09 pg/mL), as compared to control (996.09 pg/mL) (figure 69). Compared to control (996.09 pg/mL), there was a marked increase by ~1.79– (1785.16 pg/mL) and ~1.59-fold (1582.03 pg/mL) when the cells were treated with 45.70µM and 91.40µM of ART, respectively (figure 69). DHA at 13.55µM (1433.59 pg/mL) and 54.20µM (1441.41 pg/mL) had no effect on survivin levels in HT-29-AK cells, as compared to control (1433.59pg/mL) (figure 69). However, DHA at 27.10µM markedly decreased the concentration of survivin by ~1.42-fold (1011.719pg/mL) as compared to control (1433.59pg/mL) (figure 69).

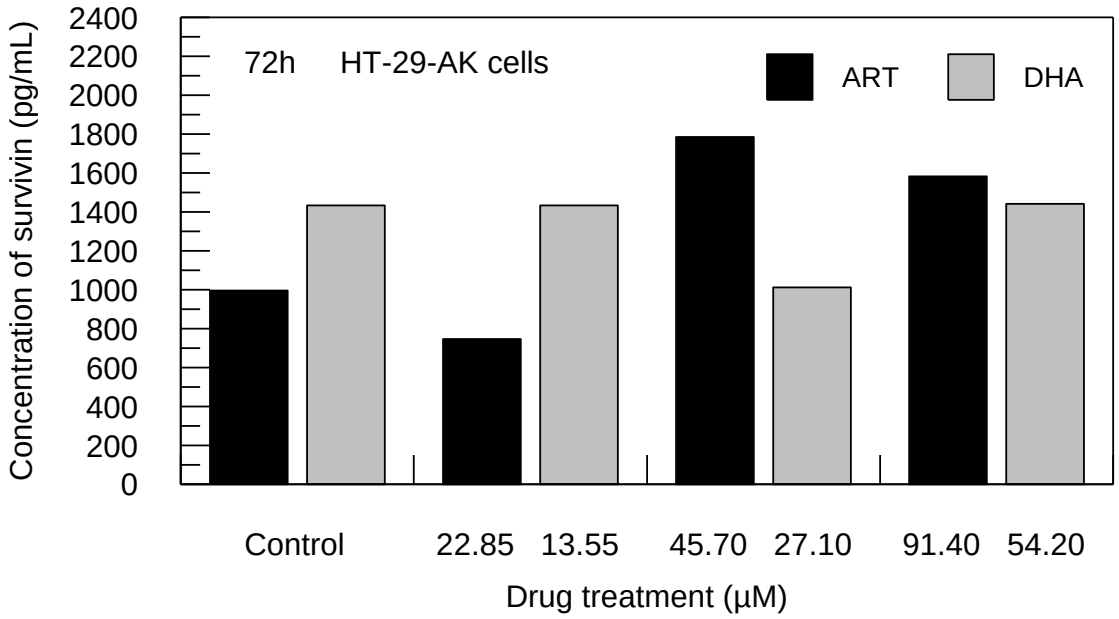

Figure 69: The effect of ART and DHA on cellular survivin levels in HT-29-AK cells in hypoxia. Cells were incubated without or with ART at 0µM, 22.85µM, 45.70µM and 91.40µM (black bars) or DHA at 0µM, 13.55µM, 27.10µM, 54.20µM (grey bars) for 72h under hypoxic conditions (1% O_2). A two-site sandwich ELISA was used to measure survivin in cell lysates as described in Materials and Methods (Section 2.5.4). The results represent 2 independent experiments which are not powered for statistical analysis. ART, artesunate, DHA, dihydroartemisinin.

4.8. ART and DHA induced the release of phospho-Akt in HT-29-AK cells in hypoxia

To determine the effect of ART and DHA on phospho-Akt secretion against HT-29-AK cells in hypoxia, a flow cytometric analysis was performed as described in Materials & Methods (Section 2.9.1). The treatment of HT-29-AK cells for 72h with 22.85µM, 45.70µM and 91.40µM of ART induced a significant ($p < 0.001$) increase in phospho-Akt levels by ~2.9- (2.90 ± 0.04 RFU), ~2.74- (2.74 ± 0.13 RFU) and ~3.01-fold (3.01 ± 0.03 RFU), as compared to control (1.00 ± 0.01 RFU), respectively (figure 70). ART-mediated increase in phosho-Akt in HT-29-AK cells under hypoxia after 72h was not in a concentration-dependent manner, as compared to the results

obtained in normoxia (figure 52 A vs. figure 70). As in normoxia, HT-29-AK cells treated with DHA under hypoxia induced a concentration-dependent increase in phospho-Akt protein levels by ~1.42- (1.42 ± 0.37 RFU), ~2.01- (2.01 ± 0.48 RFU) and ~2.39-fold (2.39 ± 0.35 RFU; P<0.01), as compared to control (1.00 ± 0.26 RFU), respectively (figure 70).

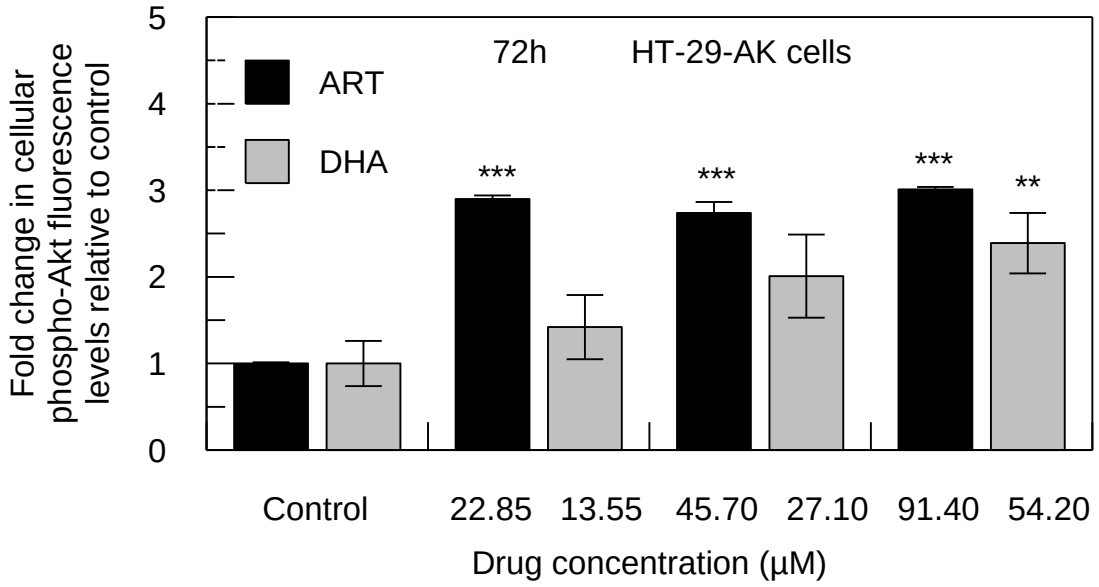

Figure 70: ART and DHA increase the protein levels of phospho-Akt in HT-29-AK cells at 72h in hypoxia. Cells were exposed to ART (0µM, 22.85µM, 45.70µM and 91.40µM) and DHA (0µM, 13.55µM. 27.10µM and 54.20µM) for 72h in hypoxia (1% O_2) and analysed for the presence of phosho-Akt by flow cytometric analysis as described in Materials & Methods (Section 2.9.1). The results for ART and DHA treated cells represent the mean ± SD of three independent experiments. **P<0.01 ***P<0.001 vs. control as tested by the Mann-Whitney test.

4.9. ART and DHA induced the release of cleaved caspase-3 in HL-60 and HT-29-AK cells under hypoxic conditions

It was observed that ART and DHA induced a concentration-dependent increase of caspase-3 in HL-60 and HT-29-AK cells under normoxic conditions (figures 55 and 56). To further investigate whether apoptosis of cancer cells upon ART and DHA

treatment is affected by oxygen availability, caspase-3 activity was measured in cells treated without or with the test agents under hypoxic conditions. As shown in figure 71, treatment of HL-60 cells with ART and DHA for 72h increased not-significantly cellular levels of caspase-3.

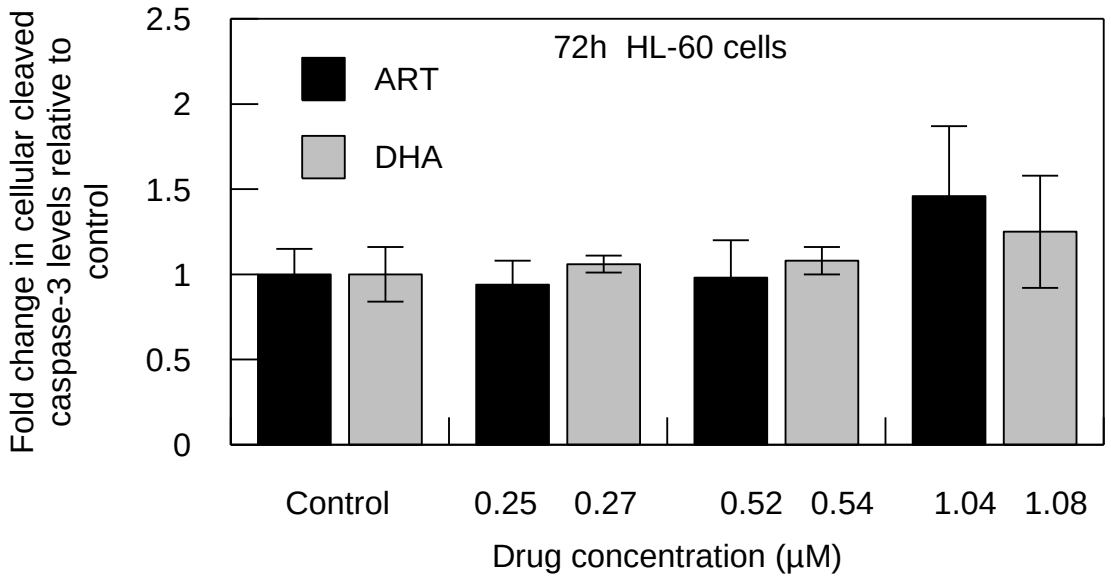

Figure 71: The effect of ART and DHA on the activity of cellular cleaved caspase-3 in HL-60 cells at 72h in hypoxia. Cells were treated with ART (at 0µM, 0.25µM, 0.52µM and 1.04µM; black bars) and DHA (at 0µM, 0.27µM, 0.54µM and 1.08µM; grey bars) for 72h under hypoxic conditions (1% O_2) and analysed for the presence of caspase-3 by flow cytometry as described in Materials & Methods (Section 2.9.1). The histograms represent the mean ± SD of three independent experiments. ART, artesunate; DHA, dihydroartemisinin.

As shown in figure 72, treatment of the HT-29-AK cells at 22.85µM, 45.70µM, and 91.40µM ART showed a marked ~2.86- (2.86 ± 0.09 RFU), ~2.68- (2.69 ± 0.09 RFU) and ~2.96-fold (2.96 ± 0.16 RFU) increase in the cellular levels of caspase-3, as compared to control (1.00 ± 0.03 RFU), respectively. HT-29-AK cells treated at 13.55µM, 27.10µM, and 54.20µM DHA had a noticeable increase in caspase-3 levels by ~1.36- (1.36 ± 0.17 RFU), ~1.38- (1.38 ± 0.29 RFU) and ~1.63-

fold (1.63 ± 0.24 RFU), as compared to control (1.00 ± 0.07 RFU), respectively (figure 72).

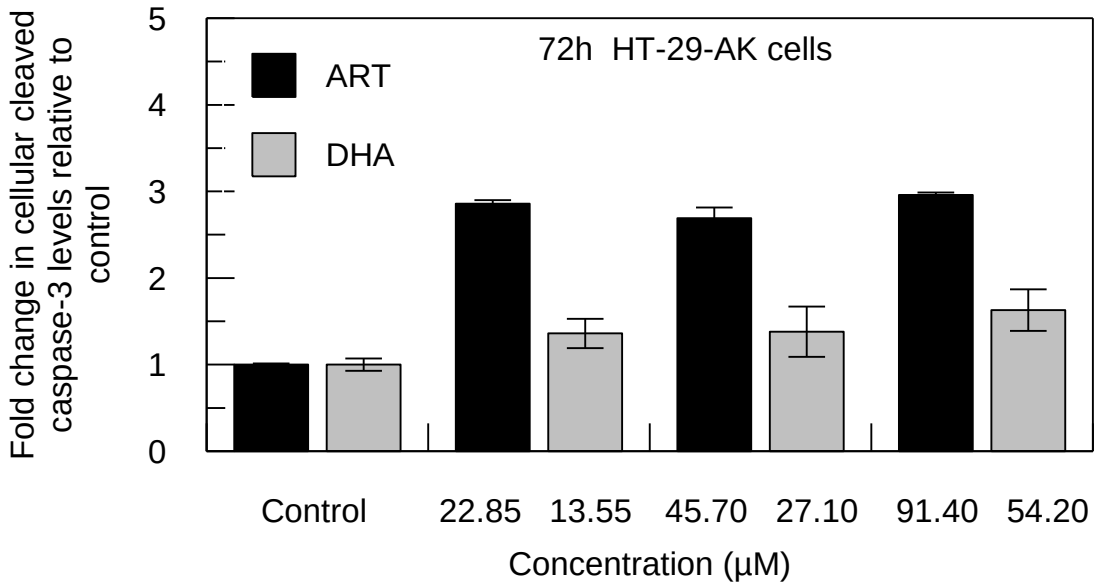

Figure 72: The effect of ART and DHA on the activity of cellular cleaved caspase-3 in HT-29-AK cells in hypoxia. Cells were treated with ART (at 0µM, 22.85µM, 45.7µM, and 91.4µM) and DHA (at 0µM, 13.55µM, 27.10µM, and 54.20µM) for 72h under hypoxic conditions (1% O_2) and analysed for the presence of caspase-3 activity by flow cytometry as described in Materials & Methods (Section 2.9.1). The results represent the mean ± SD of three independent experiments. ART, artesunate, DHA, dihydroartemisinin.

4.10. DHA induced DNA damage as measured by BrdU staining in HL-60 and HT-29-AK cells under hypoxia

To further investigate the effect of DHA under hypoxic conditions, the levels of BrdU-labelled cells were determined by flow cytometry (Materials & Methods, Section 2.11). HT-29-AK cells treated for 72h with DHA resulted in an increase in BrdU staining as compared to control (figure 73). As depicted in figure 73A, HL-60 cells treated with 1.06µM DHA unchanged the level of BrdU stained cells, as compared to untreated cells (1.00 RFU vs. 1.01 RFU). DHA-treated HT-29-AK cells increased

BrdU levels by ~1.16- (1.16 RFU), ~1.13- (1.13 RFU) and ~1.28-fold (1.28 RFU) upon treating the cells with 13.55µM, 27.10µM and 54.20µM, as compared to untreated cells (1.00 RFU), respectively (figure 73B).

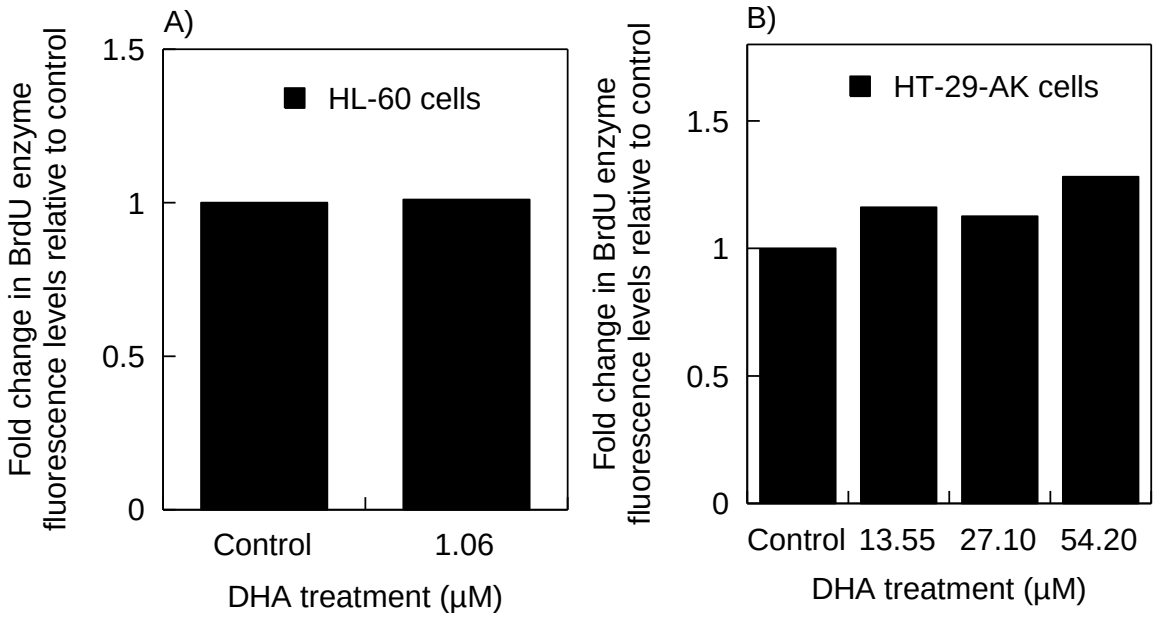

Figure 73: The effect of DHA on the presence of BrdU-stained cells as a marker of DNA damage in HL-60 and HT-29-AK cells in hypoxia. Representative histograms: A) DHA treated HL-60 cells at 0µM and 1.06µM and B) DHA treated HT-29-AK cells at 0µM, 13.55µM, 27.10µM and 54.20µM for 72h under hypoxic conditions (1% O_2). The samples were analysed for the presence of BrdU-labelled cells by flow cytometric analysis as described in Materials & Methods (Section 2.11). The results represent 1 independent experiment. DHA, dihydroartemisinin.

4.11. DHA induced DNA fragmentation in HL-60 cells in hypoxia

To determine whether DHA treatment induced DNA damage in HL-60 cells, a DNA isolated from untreated and treated samples were separated on an agarose gel. As depicted in figure 74, HL-60 cells treated without (negative control) or with 0.27µM, 0.54µM and 1.08µM of DHA for 72h under hypoxia resulted in a DNA damage with DNA fragments of ≥ 20 000 bp in all concentrations tested (red arrows). DHA-treated cells (lanes 3, 4 and 5) resulted in a greater DNA damage characterised by

lighter smeared areas as compared to negative control (lane 2, purple arrow). Heating of control sample led to a DNA smear pattern ranging from 20000 to 1500 bp (lane 1, blue curly bracket).

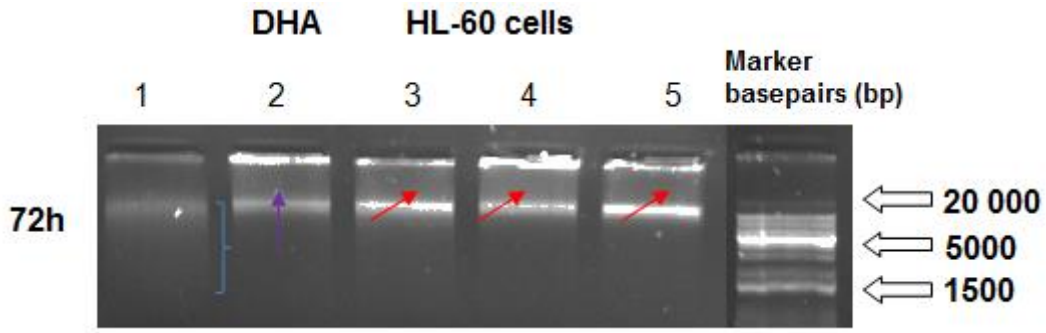

Figure 74: A representative DNA fragmentation analysis of DHA-treated HL-60 cells for 72h in hypoxia using agarose gel electrophoresis. HL-60 cells ($5x10^6$ cells/flask) were treated with 0.27µM [*lane 3*], 0.54µM [*lane 4*] and 1.08µM [*lane 5*] DHA for 72h under hypoxic conditions (1% O_2). In this study, two controls were used: DHA untreated sample (negative control) [*lane 2*] and DHA untreated sample which were heated at 95°C for 20 mins (positive control). DNA damage observed in heated control led to a DNA smearing pattern ranging from 20000 to 1500kDa (blue curly bracket). Purified DNA from control and DHA-treated cells at 70ng/µL were loaded separated on 0.8% agarose gel and visualised under UV light. The GeneRuler 1kb Plus DNA molecular marker (Thermo Scientific, Hampshire, UK) was used to determine DNA bands from 20000 bp to 1500 bp as shown on right. DHA, dihydroartemisinin.

CHAPTER 5

RESULTS

PART III: THE ANTI-CANCER EFFECTS OF ART AND DHA (ALONE AND IN COMBINATION WITH ASA) AGAINST HT-29-AK AND HL-60 CELLS UNDER NORMOXIC AND HYPOXIC CONDITIONS

5.1. Cytotoxicity of ASA against HT-29-AK and HL-60 cells is dependent on oxygen availability

It was established that ART and DHA inhibit the growth of HL-60 and HT-29-AK cells in time and concentration manners, both under normoxic (standard 20% O_2) and hypoxic (1% O_2) conditions (tables 3 and 6). Here, to explore whether ART and DHA exhibit synergy with ASA, both cell lines were initially treated with ASA to screen its cytotoxic activities through MTT assay as described in Materials & Methods (Section 2.4.7). Similar experiments were performed in normoxia and hypoxia to evaluate whether different oxygen levels influenced the sensitivity of HL-60 and HT-29-AK cells to ASA (Materials & Methods, Section 2.4.7). The cells were exposed to ASA (0- 60mM) for 24, 48 and 72h under either normoxic (20% O_2) or hypoxic (1% O_2) conditions.

As compared to the growth-inhibitory effect of ASA against HL-60 cells in normoxia after 24h incubation with an IC_{50} value of 16.89 ± 2.5mM, the cytotoxicity of ASA against HL-60 cells in normoxia significantly ($P<0.001$) increased with prolonged incubation, resulting in IC_{50} values of 3.12 ± 0.46mM (~5.41-fold enhancement) and 2.50 ± 0.18mM (~6.76-fold enhancement) after 48h and 72h, respectively (table 8). When HL-60 cells were treated with ASA under hypoxic conditions at 24, 48 and 72h, IC_{50} values increased, as compared to normoxia by at least ~3.55-fold (>60mM

vs. 16.89 ± .5mM), ~19.23fold (>60mM vs. 3.12 ± 0.46mM), and ~8.82-fold (22.05 ± 2.7mM vs. 2.5 ± 0.18mM; P<0.001), respectively. Treatment of HT-29-AK cells with ASA for 24h in normoxia resulted in ASA IC_{50} value of 21.35 ± 2.12mM with a significant (P < 0.001) drop of cell viability in a time-dependent manner, thus enhanced ASA cytotoxic activities with IC_{50} values as follow: 13.25 ± 0.79mM (~1.61-fold enhancement) and 6.15 ± 0.83mM (~3.47-fold enhancement) after 48h and 72h, respectively (table 8). When comparing the cytotoxicity of ASA against HT-29-AK cells under normoxic and hypoxic conditions, low oxygen microenvironment (1% O_2) was shown to antagonise growth-inhibitory effect of ASA at all time tested (table 8). After 24h, HT-29-AK cells were 1.50-fold less susceptible to the cytotoxic effects of ASA, as compared to normoxia (hypoxia: IC_{50} value of 31.95 ± 2.59mM vs. normoxia: IC_{50} value of 21.35 ± 2.12mM; P<0.001) (table 8). After 48h, HT-29-AK cells were 1.34-fold less susceptible to the cytotoxic effects of ASA, as compared to normoxia (hypoxia: IC_{50} value of 17.73 ± 1.64mM vs. normoxia: IC_{50} value of 13.25 ± 0.79mM; P<0.001) (table 8). After 72h where ASA was most potent against HT-29-AK cells under both tested conditions, the cytotoxicity of ASA against the cells in hypoxia was reduced by 1.38-fold, as compared to normoxia (hypoxia: IC_{50} value of 8.47 ± 2.18mM vs. normoxia: IC_{50} value of 6.15 ± 0.83mM; P<0.01) (table 8). Overall, low oxygen tension (1% O_2) reduced the sensitivity of HL-60 cells and HT-29-AK cells to ASA, as compared to normoxic conditions (table 8).

ASA was dissolved in DMSO at stock concentrations of 1mM and 10mM. In order to exclude any cytotoxic effects of DMSO on cancer cells, the cells were treated with equivalent concentrations of DMSO (positive control) as present in drug treated samples (under both test conditions of hypoxia and normoxia). The final

concentration of DMSO in culture media was less than 0.5% and the results showed that DMSO did not produce any cytotoxic effects against the cells (data not shown).

Table 8: The effect of ASA on the growth of HL-60 and HT-29-AK cells cultured for 24h, 48h or 72h under normoxic or hypoxic conditions. The cells were seeded in 96-well flat-bottomed microtitre plates and treated with graded concentrations of ASA (0-60mM) against HL-60 and HT-29-AK cells for 24, 48 or 72h in a) *top* table: normoxia (20% O_2, 5% CO_2, 75% N_2; 37°C,) or b) *bottom* table: hypoxia (1% O_2, 5% CO_2, 94% N_2; 37°C) as described in Materials & Methods (Section 2.4.7). Cell growth upon ASA treatment at each time point was measured by the MTT colorimetric assay and IC_{50} values were derived via Grafit Software. All results are expressed as the mean IC_{50} ± SD of at least three independent experiments. ***P<0.001 vs. 24h as tested by Paired-T test.

	Incubation condition	**Incubation (hrs)**	**HL-60 cells**	**HT-29-AK cells**
			ASA IC_{50} (mM, Mean ± SD)	
a)	Normoxia	24	16.89 ± 2.5	21.35 ± 2.12
		48	3.12 ± 0.46***	13.25 ± 0.79 ***
		72	2.50 ± 0.18***	6.15 ± 0.83 ***
b)	Hypoxia	24	> 60	31.95 ± 2.59
		48	> 60	17.73 ± 1.64 ***
		72	22.05 ± 2.70***	8.47 ± 2.18 ***

5.2. ASA modulates the cytotoxicity of ART and DHA against cancer cells

To investigate whether a fixed concentration of ASA, equivalent to their IC_{50} concentrations as estimated under specific test condition (HL-60 cells: normoxia: 2.50mM ASA; HT-29-AK cells: normoxia: 6.15mM ASA; hypoxia: 8.47mM ASA), has any effects on ART and DHA cytotoxicity against HL-60 and HT-29-AK cells, the combination studies were performed using MTT assay as described in Materials & Methods (Section 2.4.7). During investigations under hypoxic conditions with HL-60

cells, ASA IC_{50} value used for combination studies resulted in cancer cells to be all dead. Therefore, 1/10 of ASA IC_{50} value (2.21mM) estimated in hypoxia was used in further combination studies. For HL-60 cells in normoxia, combination of 2.50mM ASA significantly (P<0.001) increased the cytotoxicity of ART (IC_{50} value of 0.48 ± 0.02 µM) as compared to ART alone (IC_{50} value of 0.59 ± 0.08 µM) whereas the cytotoxicity of DHA was not affected (DHA IC_{50} value of 0.49 ± 0.03 µM vs. DHA combined with ASA with IC_{50} value of 0.49 ± 0.04 µM; table 9). For HT-29-AK cells treated under normoxic conditions, the presence of 6.15mM ASA significantly (P< 0.001) improved the cytotoxicity of DHA (IC_{50} value of 5.93 ± 0.58 µM) and ART (IC_{50} value of 6.67± 0.73 µM) resulting in a 3.33-fold and 2.16-fold greater activity as compared to DHA (IC_{50} value of 19.75 ± 1.07µM) and ART (IC_{50} value of 14.44 ± 2.64 µM) alone, respectively (table 9).

Table 9: The effect of ART and DHA alone and in the presence of fixed concentrations of ASA against HT-29-AK and HL-60 cells in normoxic conditions. The results are expressed as the mean IC_{50} ± SD of three independent experiments. ART, artesunate; ASA; aspirin; DHA, dihydroartemisinin. ***P<0.001 as tested by Paired-T test.

Normoxia		
	HL-60 cells	**HT-29-AK cells**
Test agents	**IC_{50} (µM ± SD)**	
ART	0.59 ± 0.08	14.44 ± 2.64
DHA	0.49 ± 0.03	19.75 ± 1.07
	Test agents + 2.50mM ASA	*Test agents +6.15mM ASA*
ART	0.48 ± 0.02***	6.67 ± 1.73***
DHA	0.49 ± 0.04	5.93 ± 0.58***

Table 10: The effect of ART and DHA alone and in the presence of fixed concentrations of ASA against HT-29-AK and HL-60 cells in hypoxic conditions. The results are expressed as the mean IC_{50} ± SD of three independent experiments. The results ([z]) are derived from 1 independent experiment. ART, artesunate; ASA; aspirin; DHA, dihydroartemisinin. ***P<0.001 as tested by Paired-T test.

Hypoxia		
	HL-60 cells	**HT-29-AK cells**
Test agents	**IC_{50} (µM ± SD)**	
ART	0.51 ± 0.06	46.51 ± 4.74
DHA	0.53 ± 0.07	27.10 ± 2.73
	Test agents + 2.21mM ASA	*Test agents +8.47mM ASA*
ART	0.46[z]	1.63 ± 0.50***
DHA	0.23[z]	7.90 ± 0.99***

For HL-60 cells in hypoxia, the presence of 2.21mM of ASA led to a marked improvement in the activity of ART (IC_{50} value of 0.46µM) and DHA (IC_{50} value of 0.23µM), increasing their cytotoxicity by ~11% and ~43% as compared to ART (IC_{50} value of 0.51 ± 0.06 µM) and DHA (IC_{50} value of 0.53 ± 0.07µM) alone, respectively (table 10). The results obtained from HT-29-AK cells show that the presence of 8.47mM ASA significantly increased the cytotoxicity of ART (IC_{50} of value 1.63 ± 0.50 µM; P<0.001) and DHA (IC_{50} value of 7.90 ± 0.99µM; P< 0.001) resulting in a 28.53- and 3.43-folds greater activity, as compared to the measured IC_{50} values for ART (IC_{50} value of 46.51 ± 4.74 µM) and DHA (IC_{50} value of 27.10 ± 2.73 µM) alone, respectively (table 10).

Overall, the results show that a fixed concentrations of ASA in combination with DHA and ART (except ASA combined with DHA against HL-60 cells in normoxia) in both

conditions tested pharmaco-enhanced DHA and ART. The enhancement effect was more marked for HT-29-AK cells than for HL-60 cells.

5.3. Effect of ART and DHA (alone and in combination with ASA) on COX-2 protein

The expression levels of pro-inflammatory COX-2 protein in HT-29-AK cells of either, ASA, ART and DHA alone or ASA in combination with drugs is presented in figure 75. As compared to control group (1.00 ± 0.08 RFU), treatment of cells with ART (at 14.44 µM) and DHA (at 19.75 µM) for 72h significantly ($P<0.001$) enhanced the protein levels of COX-2 by 3.36-fold (3.36 ± 0.45 RFU) and 3.05-fold (3.05 ± 0.29 RFU), respectively (figure 75). There was an average increase in the percentage of COX-2 protein levels by ~40% (1.40 ± 0.15 RFU) upon ASA treatment (at 6.15mM) compared to control, however these changes were not found to be significant. COX-2 expressions levels in the ASA combined groups with ART (3.61 ± 0.40 RFU) or DHA (3.72 ± 0.50 RFU) were significantly ($P<0.001$) up-regulated when compared to control but not statistically increased when compared to ART (by ~6.93%, 3.36 ± 0.45 RFU) and DHA (by ~18.01%, 3.05 ± 0.29 RFU) alone (figure 75).

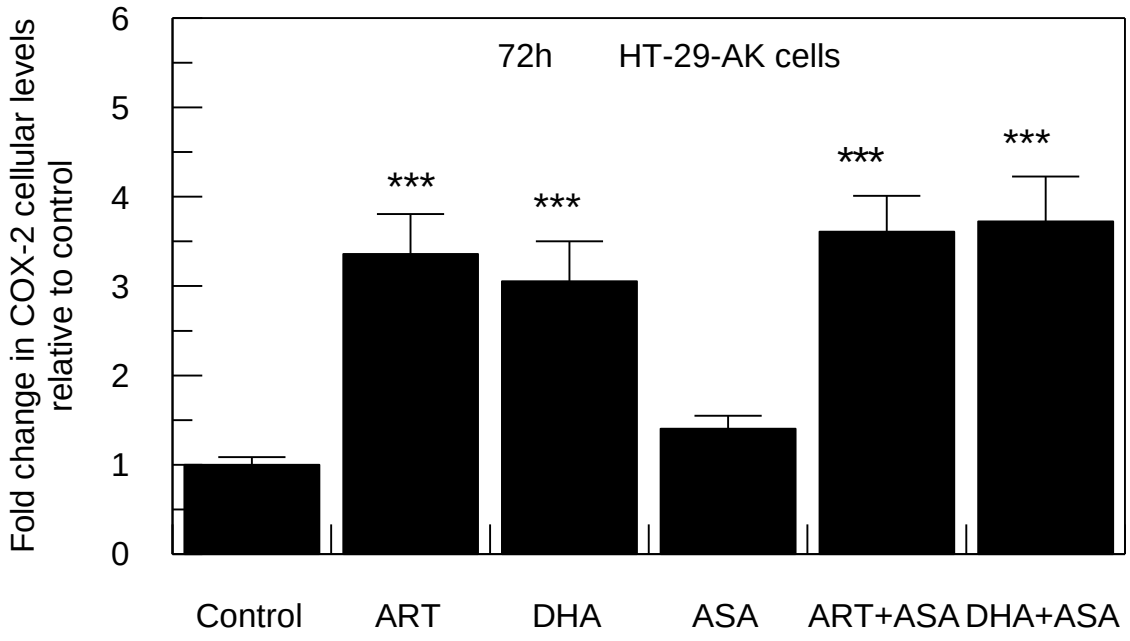

Figure 75: The effect of ART, DHA and ASA (alone and in combination) on cellular COX-2 protein levels in HT-29-AK cells. Cells were treated without or with the test agents for 72h in normoxia (20% O_2), harvested, incubated with COX-2 antibody and analysed on flow cytometer as described in Materials & Methods (Section 2.9). The results represent 3 independent experiments were ***P<0.001 vs. control as tested by one-way ANOVA (Turkey test with multiple comparison). ART, artesunate; ASA, aspirin; DHA, dihydroartemisinin.

5.4. Effect of ART and DHA (alone and in combination with ASA) on survivin cellular and mRNA levels

Survivin is a pro-survival protein associated with the development of drug resistance, thus favouring the progression and metastasis of cancer (Shin *et al.* 2001; Shao *et al.* 2008; Ye *et al.* 2014; Kim *et al.* 2015). This led to investigate whether ASA co-treatment modulates survivin mRNA expression in HT-29-AK cells (figure 76). Compared to control (ΔΔCt= 1.00± 0.02), qPCR analysis showed significant increase of survivin mRNA levels in samples treated with ART, DHA and ASA by ~1.58-fold (ΔΔCt= 1.58 ± 0.37; P<0.01), ~1.78-fold (ΔΔCt= 1.78 ± 0.43; P<0.001) and ~1.62-fold (ΔΔCt= 1.62 ± 0.29; P<0.01), respectively (figure 76). When HT-29-AK cells

were incubated with ART and ASA combination, survivin mRNA levels increased by 22% (ΔΔCt= 1.92 ± 0.49), as compared to ART alone but these protein changes were not significant (figure 76). Interestingly, combination of DHA with ASA reduced the increase in survivin mRNA by 18% caused by DHA alone (ΔΔCt= 1.46 ± 0.15 vs. ΔΔCt= 1.78 ± 0.43, respectively; P>0.05; figure 76).

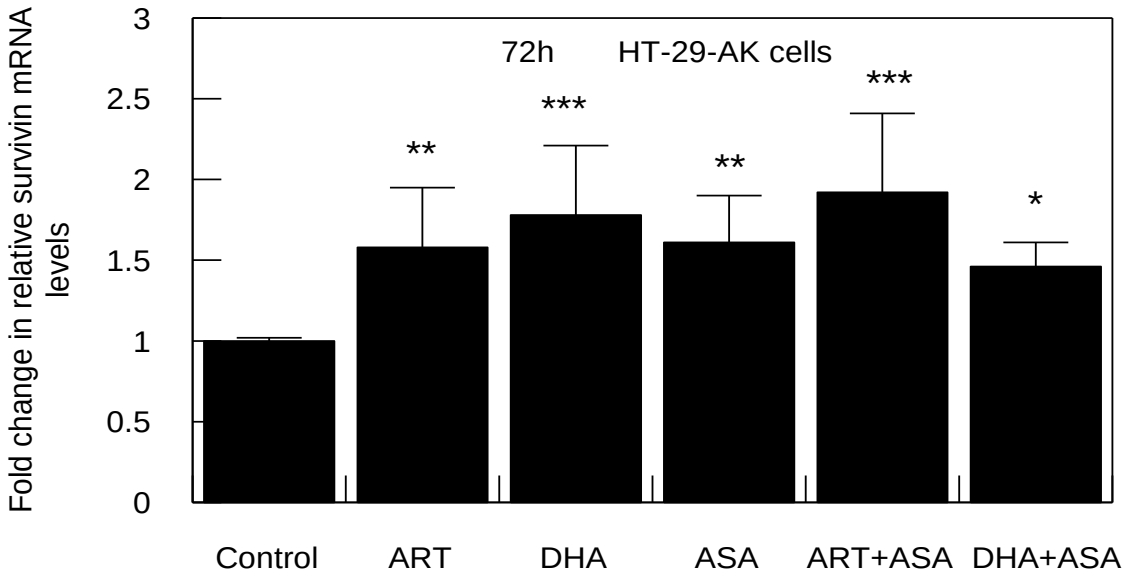

Figure 76: The effect of ART, DHA and ASA (alone and in combination) on survivin mRNA levels in HT-29-AK cells. Cells were exposed to the test agents in normoxia (20% O_2) as shown and as described in Materials and Methods (Section 2.6). The results represent the mean ± SD of three independent experiments. ***P<0.001, **P<0.01 and *P<0.01 vs. control as tested by one-way ANOVA (Turkey test with multiple comparison). ART, artesunate; ASA, aspirin; DHA, dihydroartemisinin.

5.5. Effect of ART and DHA (alone and in combination with ASA) on HIF-1α mRNA levels

qPCR analysis of HIF-1α mRNA levels showed that HT-29-AK-treated cells for 72h with ASA not significantly reduced levels of HIF-1α (by 8.08%), as compared to control cells (ΔΔCt= 0.91 ± 0.14 vs. ΔΔCt= 0.99 ± 0.04, respectively) (figure 77). Treatment with ART led to a significant decrease of HIF-1α gene expression levels

by ~16.16%, as compared to control (ΔΔCt= 0.83 ± 0.08 vs. ΔΔCt= 0.99 ± 0.04, respectively; P<0.01) whereas treatment with DHA alone did not have any effect on HIF-1α levels (ΔΔCt= 1.00 ± 0.11) (figure 77). Combining ASA with ART further enhanced the reduction effect of ART alone in the expressions of HIF-1α mRNA in cancer cells by 14.46% (ΔΔCt= 0.71 ± 0.05 vs. ΔΔCt= 0.83 ± 0.08, respectively) and by 28.28%, compared to control group alone (ΔΔCt= 0.71 ± 0.05 vs. ΔΔCt= 0.99 ± 0.04; P<0.001, respectively) (figure 77). Co-treatment of DHA with ASA reduced the mRNA levels of HIF-1α by 9%, as compared to DHA alone (ΔΔCt= 0.91 ± 0.07 vs. ΔΔCt= 1.00 ± 0.11, respectively) but the difference was not statistically significant (figure 77).

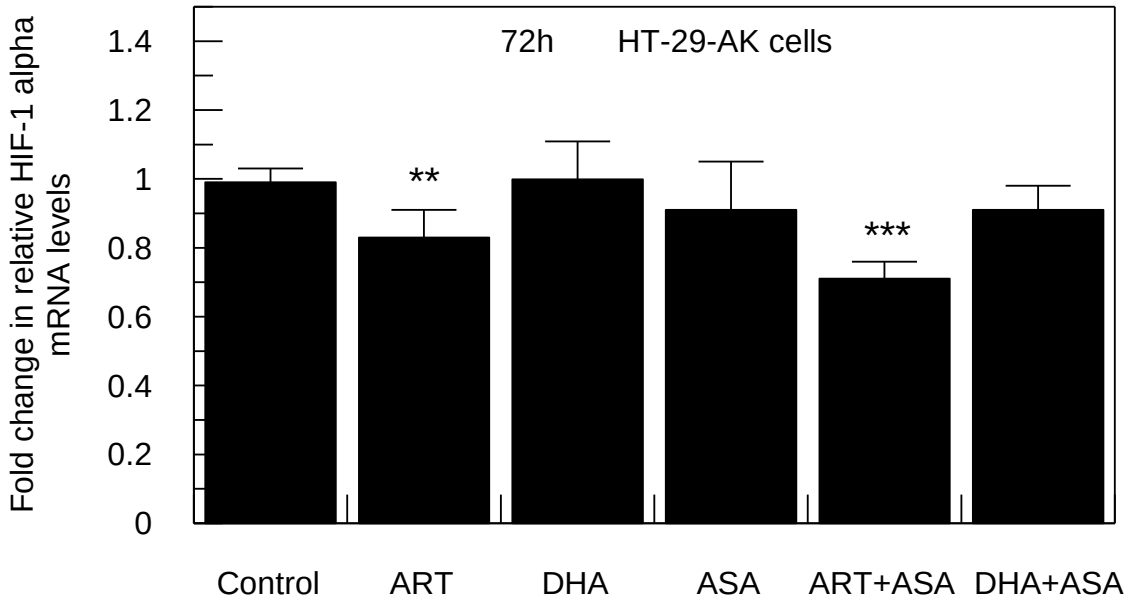

Figure 77: The effect of ART, DHA and ASA (alone and in combination) on HIF-1α mRNA levels in HT-29-AK cells. Cells were exposed to the test agents in normoxia (20% O_2) as shown and as described in Materials and Methods (Section 2.6). The result histograms represent the mean ± SD of three independent experiments. ***P<0.001 and **P<0.01 vs. control as tested by one-way ANOVA (Turkey test with multiple comparison). ART, artesunate; ASA, aspirin; DHA, dihydroartemisinin.

5.6. Effect of ART and DHA (alone and in combination with ASA) on VEGF-α mRNA levels

VEGF-α is a key mediator contributing to cancer angiogenesis and metastasis (Schneider *et al.* 2011; Yoshioka *et al.* 2012; Panoilia *et al*. 2015). Therefore, the effects of ART and DHA in combination with ASA against HT-29-AK cells under 72h incubations were examined on possible changes in VEGF-α transcriptional stability (figure 78). As compare to control cells, the expression pattern of VEGF-α mRNA was slightly decreased by ART (by 4%, ΔΔCt= 0.96 ± 0.15 vs. ΔΔCt= 1.00 ± 0.09, respectively) and ASA (by 7%, ΔΔCt= 0.93 ± 0.13 vs. ΔΔCt= 1.00 ± 0.09, respectively) as single agents but increased by DHA (by 6%, ΔΔCt= 1.06 ± 0.21 vs. ΔΔCt= 1.00 ± 0.09, respectively) (figure 78). However, these VEGF-α mRNA expression changes were not statistically significant. Cells treatment with DHA and ASA combination did not alter markedly VEGF-α transcriptional levels, as compared to DHA alone (ΔΔCt= 1.04 ± 0.10 vs. ΔΔCt= 1.06 ± 0.21 vs. respectively). Interestingly, combination of ART with ASA attenuated the decrease in VEGF-α mRNA levels measured with ART alone by additional 17.71% (ΔΔCt= 0.79 ± 0.06 vs. ΔΔCt= 0.96 ± 0.15 vs. respectively) and by 21%, as compared to control (ΔΔCt= 0.79 ± 0.06 vs. ΔΔCt= 1.00 ± 0.09, $P<0.05$, respectively) (figure 78).

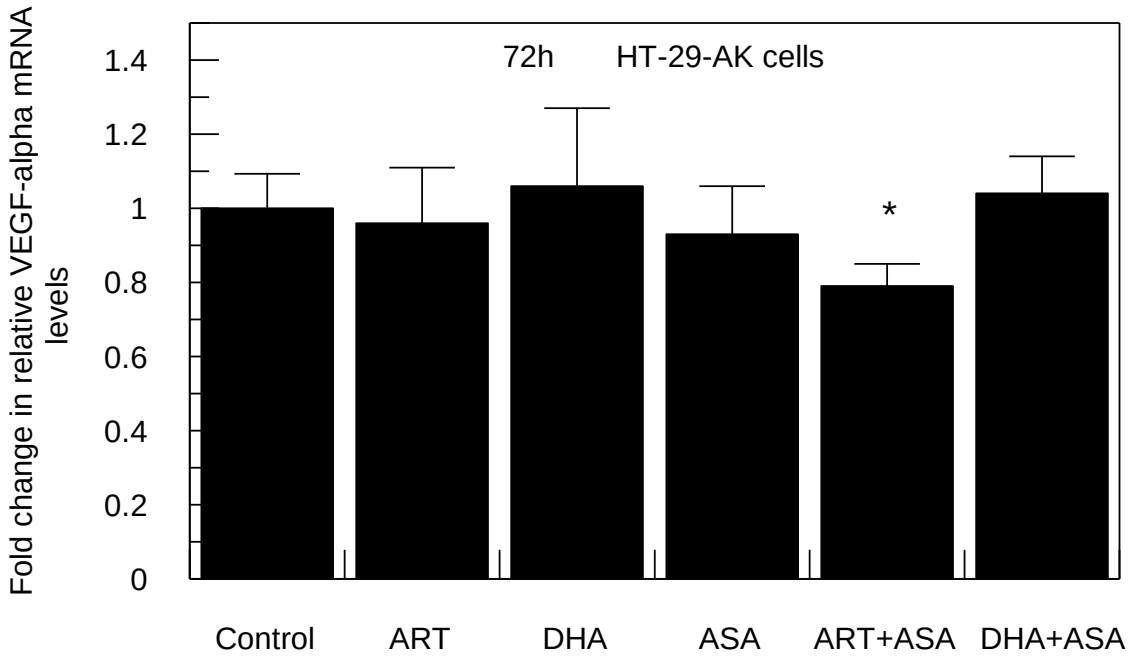

Figure 78: The effect of ART, DHA and ASA (alone and in combination) on VEGF-α mRNA levels in HT-29-AK cells. Cells were exposed to the test agents in normoxia (20% O_2) as shown and as described in Materials and Methods (Section 2.6). The result histograms represent the mean ± SD of three independent experiments. *P<0.05 vs. control as tested by one-way ANOVA (Turkey test with multiple comparison). ART, artesunate; ASA, aspirin; DHA, dihydroartemisinin.

5.7. ASA combination with ART and DHA increased cellular phospho-Akt levels

The cellular expression levels of anti-apoptotic phosho-Akt upon treatment of HT-29-AK cells with ART, DHA and ASA (alone and in combination) were measured by flow cytometric analyses and are presented in figure 79. Data acquired show significant (P<0.001) increase in phosho-Akt levels by ~2.62-fold (2.62 ± 0.24 RFU) and ~2.28-fold (2.28 ± 0.78 RFU) upon treating the cells with ART and DHA alone, respectively, as compared to control (1.00 ± 0.31 RFU). Cellular levels of phosho-Akt increased by 11% when treated with ASA alone, as compared to control (1.11 ± 0.07 RFU vs. 1.00 ± 0.31 RFU, respectively) but these changes were not significant. The

combination of ART with ASA up-regulated levels of phospho-Akt to 3.06 ± 0.73 RFU, which led to a fold difference of ~1.17, as compared to ART alone (2.62 ± 0.24 RFU) and by 3.06-fold increase as compared to control (3.06 ± 0.73 RFU vs. 1.00 ± 0.31 RFU; P<0.001, respectively). Similarly, co-treatment of DHA with ASA caused an increase in phospho-Akt levels by 1.43-fold as compared to DHA alone (3.27 ± 0.87 RFU vs. 2.28 ± 0.78 RFU, respectively) and significant up-regulation by 3.27-fold as compared to untreated cells (P<0.001; 3.27 ± 0.87 RFU vs. 1.00 ± 0.31 RFU, respectively).

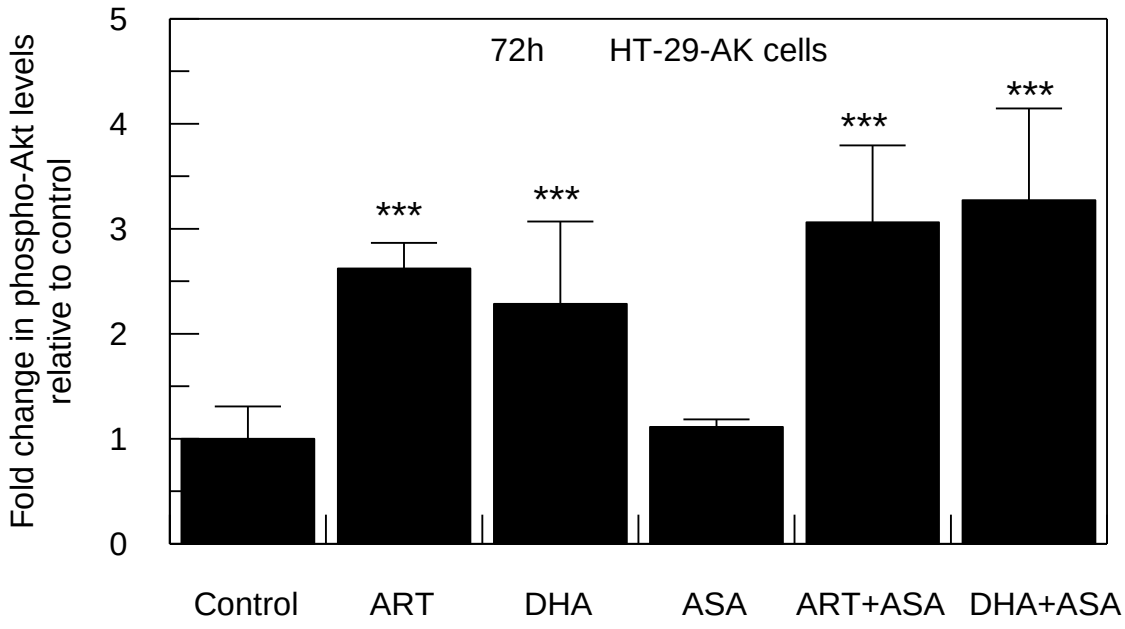

Figure 79: The effect of ART, DHA and ASA (alone and in combination) on cellular phospho-Akt levels in HT-29-AK cells in normoxia. HT-29-AK cells were exposed to the test agents in normoxia (20% O_2) as shown and as described in Materials and Methods (Section 2.9). The results for ART and DHA treated cells represent the mean ± SD of three independent experiments. ***P<0.001, vs. control as tested by one-way ANOVA (Turkey test with multiple comparison). ART, artesunate; ASA, aspirin; DHA, dihydroartemisinin.

5.8. ASA enhanced ART- and DHA- caspase-3-dependent apoptosis

As ART and DHA were shown in vast number of reports, including in our previous studies to induce cancer cells apoptosis (Kim *et al.* 2015; Zhang *et al.* 2015; Zhao *et al.* 2015; figures 55 and 56), we examined whether ASA can enhance ART- and DHA-mediated cell death. Expression of cleaved caspase-3 protein levels measured by flow cytometric analysis following treatment of cells with ART, DHA or ASA (alone and in combination) for 72h is shown in figures 80 and 81. Significantly ($P<0.001$), HL-60 cells treated with ART, DHA and ASA increased levels of cleaved caspase-3 to 3.10 ± 0.16 RFU, 1.79 ± 0.06 RFU and 2.02 ± 0.04 RFU, as compared to control cells (1.00 ± 0.01 RFU), respectively (figure 80). Used in combination, ART and ASA significantly ($P<0.001$) up-regulated levels of caspase-3 to 9.88 ± 0.51 RFU, which resulted in a fold difference of ~3.19, as compared to ART alone (3.10 ± 0.16 RFU) (figure 80). Alongside this, co-treatment of DHA with ASA caused a significant increase (~7.59-fold; 13.59 ± 0.42 RFU; $P<0.001$) in the levels of cleaved caspase-3, as compared to DHA alone (1.79 ± 0.06 RFU) (figure 80).

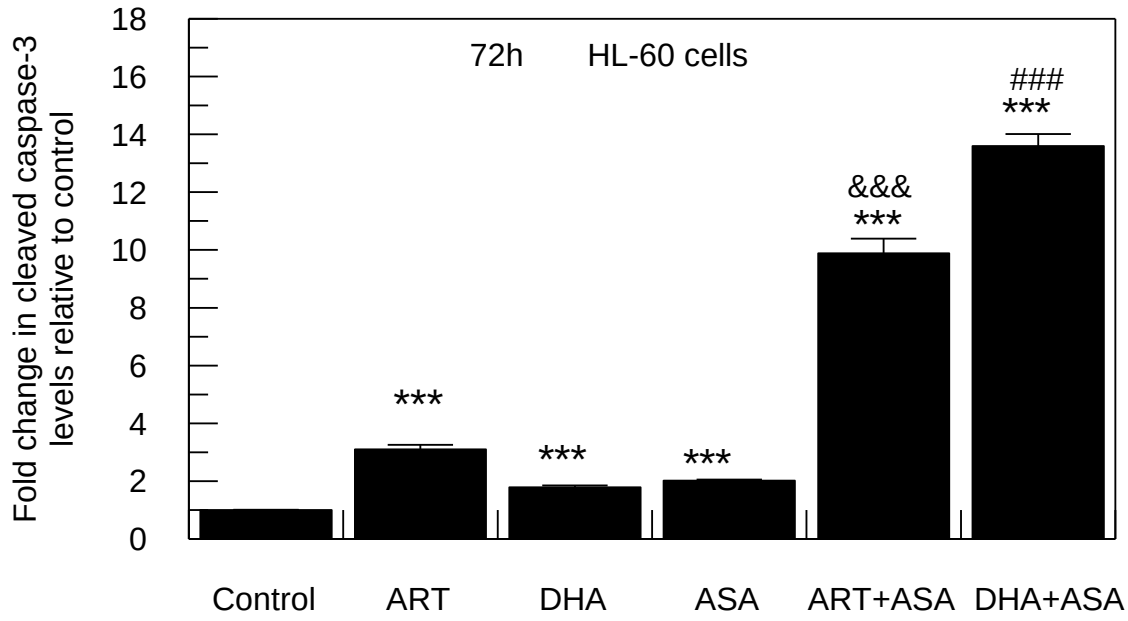

Figure 80: The effect of ART, DHA and ASA (alone and in combination) on cellular cleaved caspase-3 levels in HL-60 cells. HL-60 cells were exposed to the test agents in normoxia (20% O_2) as shown and as described in Materials and Methods (Section 2.9). The result histograms represent the mean ± SD of three independent experiments. ***P<0.001, vs. control; ###P<0.001 vs. DHA; &&&P<0.001 vs. ART as tested by one-way ANOVA (Turkey test with multiple comparison). ART, artesunate; ASA, aspirin; DHA, dihydroartemisinin.

As shown in figure 81 cleaved caspase-3 release in HT-29-AK cells was activated by a single agent of ART (3.28 ± 0.20 RFU; ~3.28-fold; P<0.001), DHA (3.05 ± 0.09 RFU; ~3.04-fold; P<0.001) and ASA (1.66 ± 0.11 RFU; ~1.66-fold; P<0.01), as compared to control (1.00 ± 0.05 RFU). Combination treatment of ASA with either, ART and DHA significantly increased caspase-3 protein levels in cells, as compared to ART alone (by 81.65%; 4.10 ± 0.49 RFU; vs. 3.28 ± 0.20 RFU; P<0.01) and DHA alone (by ~125%; 4.30 ± 0.74 RFU vs. 3.05 ± 0.09 RFU; P<0.001), respectively (figure 81).

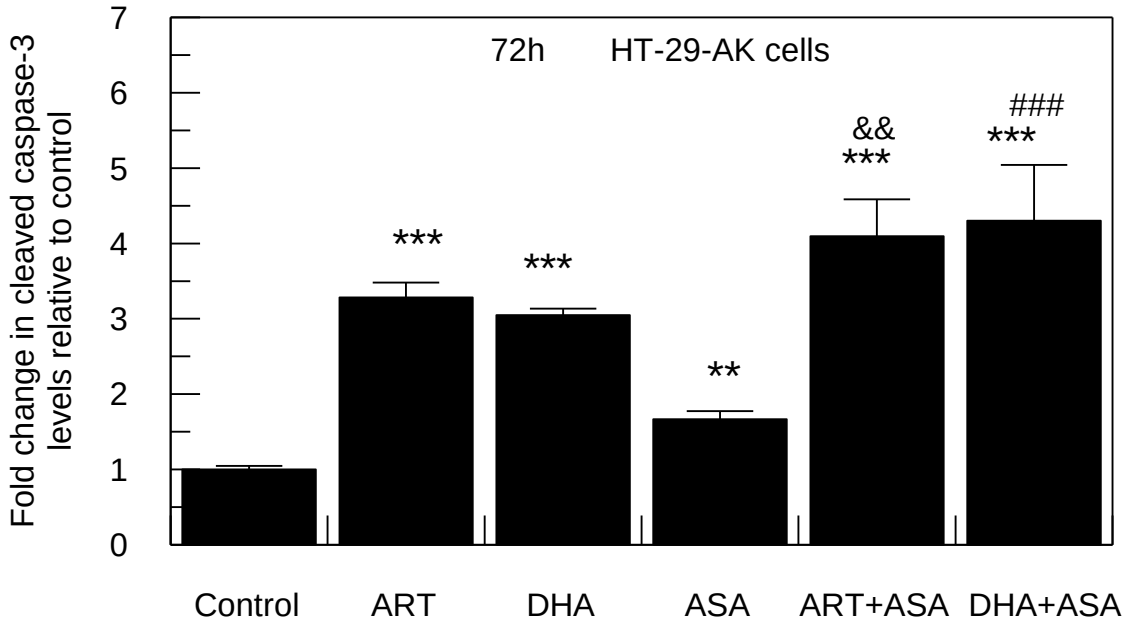

Figure 81: The effect of ART, DHA and ASA (alone and in combination) on cellular cleaved caspase-3 levels in HT-29-AK cells. HT-29-AK cells were exposed to the test agents in normoxia (20% O_2) as shown and as described in Materials and Methods (Section 2.9). The result histograms represent the mean ± SD of three independent experiments. ***P<0.001, vs. control; **P<0.01, vs. control; $^{\#\#\#}$P<0.001 vs. DHA; $^{\&\&}$P<0.01 vs. ART as tested by one-way ANOVA (Turkey test with multiple comparison). ART, artesunate; ASA, aspirin; DHA, dihydroartemisinin.

CHAPTER 6

DISCUSSION

Part 1: THE MOLECULAR BASIS OF THE ANTI-CANCER EFFECTS OF ART AND DHA AGAINST HT-29-AK AND HL-60 CELLS IN NORMOXIA AND HYPOXIA

6.1. Cytotoxicity of ART and DHA under normoxic and hypoxic conditions

Extensive anti-cancer effects of ART and DHA have been reported in multiple cancer types of human tumour including leukaemia and CRC (Lu *et al.* 2008; Zhou *et al.* 2008; Jones *et al.* 2009; Lu *et al.* 2011; Zhao *et al.* 2015). However, the molecular activity of ART and DHA against cancer cells remains still incompletely understood. As increasing reports are describing the potential clinical utility of ART and DHA (Singh and Verma 2002; Singh and Panwar 2006; Jansen *et al.* 2011; Krishna *et al.* 2015), further studies are needed to provide additional molecular basis of their action to enhance greater understanding of the fundamental cellular processes targeted by the agents.

Non-adherent human leukaemia HL-60 cells and adherent human CRC HT-29-AK cells are highly-proliferating cells, extensively reported to be very sensitive to ART and DHA and for these properties were selected for *in vitro* experimental settings in the present study (Anfosso *et al.* 2006; Mercer *et al.* 2007; Li *et al.* 2008; Lu *et al.* 2008; Zhou *et al.*2008; Zhao *et al.* 2015). Second gastrointestinal cell Caco-2 line was used to compare the effects of ART and DHA between cells of the same tissue origin but characterised by different differentiation state of cells (well-differentiated HT-29-AK cells vs. non-differentiated Caco-2 cells) (Li *et al*. 2008; Bourseau-Guilmain *et al.* 2011).

Under standard normoxic experimental conditions (20% O_2), ART and DHA inhibited the growth of leukaemia HL-60 cells and CRC HT-29-AK and Caco-2 cells in a time-dependent manner (table 3; figures 12, 13 and 14). These results were in accordance with several previous studies, such as Lu *et al.* (2008), Zhou and Wang (2008), Buommino *et al.* (2009), Li *et al.* (2009) and Lijuan *et al.* (2010). Our results also showed that leukaemia HL-60 cells were the most sensitive to ART and DHA followed by CRC HT-29-AK and Caco-2 cells (table 3). The distinct anti-cancer effect of ART and DHA against different cancer cell lines and malignant phenotypes was found in several previous studies (Efferth *et al.* 2001; Mercer *et al.* 2007; Hou *et al.* 2008; Lu *et al.* 2008). Prolonged incubation of the cells with the drugs enhanced their activity, with the following rank order, 72h>48h>24h. After 72h, DHA was more potent than ART against HL-60 cells (0.60 ± 0.08μM vs. 0.49 ± 0.03μM) whereas ART was more potent than DHA against HT-29-AK cells (14.44 ± 2.64μM vs. 19.75 ± 1.07μM) and against Caco-2 cells (42.13 ± 9.61μM vs. 76.42 ± 8.14μM) (table 3). Distinct profiles of anti-cancer effect of ART and DHA between cells of the same origin such as gastric and bladder cancers but different sub-types (gastric BGC-823, HGC-27 and MGC-803 cell lines; bladder T24 and RT4 cell lines) were determined previously (Hou *et al.* 2008; Zuo *et al.* 2014; Zhang *et al.* 2015). The differences arising between HT-29-AK and Caco-2 colorectal cell lines could be linked with different status of TfR1 receptors which are needed for endocytosis-mediated iron and drug intake (Dautry-Varsat *et al.* 1983; Eckenroth *et al.* 2011). Further support for the latter comes from numerous reports which demonstrate the ability of 1,2,4-trioxanes to conjugate with TfR1-transferrin complex at the cell membrane (Zhou *et al.* 2008; Ba *et al.* 2012 Zhao *et al.* 2013). The complex is then internalised into the cell through endocytosis and released iron within an endosome result in the

cleavage of 1,2,4-trioxanes' endoperoxide bridge leading to the formation of free radicals which kill cancer cells (Mercer *et al.* 2007; Lai *et al.* 2005; Oh *et al.* 2009).

In previous studies, well-differentiated carcinoma tissues were characterised by high distribution of TfR1 (15; $P<0.05$) whereas poor-differentiated samples had low distribution of TfR1 (1; $P<0.05$) (Prutki *et al.* 2006). It could be postulated that ART and DHA in well-differentiated HT-29-AK cells are more rapidly internalised by the highly distributed TfR1 on cell surface whereas in poorly-differentiated Caco-2 cells the transport of the drugs was limited due to lower numbers of TfR1. In addition, Caco-2 cells over-express a pentaspan stem cell marker CD133, which was shown to inhibit endocytosis of iron carrying transferrin molecule, which could further result in decreased activation of ART and DHA through iron-mediated cleavage of endoperoxide bond within the cell (Bourseau-Guilmain *et al.* 2011). However, in cancer cell line xenografts it has been reported that well-differentiated cells have features of poorly distributed microvessels within the tumour biomass, which limit transport and distribution of chemotherapeutic agents (Rustum *et al.* 2010). In contrast, poorly-differentiated human tumour xenografts were characterised by a well-vascularised tumour biomass featuring more developed blood vessels (Rustum *et al.* 2010). This allows a better drug transport and penetration within the tumour, thus a better therapeutic response (Rustum *et al.* 2010). Therefore, it is important to develop xenografts model of ART and DHA activity against both gastrointestinal cell lines as current *in vitro* study may not reflect completely their response *in vivo*.

The changes in cytotoxicity of ART and DHA against HT-29-AK cells were further linked with different proliferation status of the cells (table 4). Highly proliferative HT-29-AK cells treated with ART and DHA for 24h immediately after seeding (t_0) were more susceptible to drugs as compared to confluent cells (80% confluency)

treated with drugs for 24h (t_0 : ART IC_{50} of 165.06 ± 24.25µM, DHA IC_{50} of 58.02 ± 4.09µM vs. 80% confluent cells: ART IC_{50} of 190.62µM, DHA IC_{50} of 108.53 ± 19.69µM). It could be explained by the fact that confluent cells have lower requirements for iron, thus reduced cytotoxicity of ART and DHA as compared to highly proliferative HT-29-AK cells at t_0 with greater requirement for iron. ART and DHA might have decreased access to TfR1 in confluent cells due to tight cell-cell interactions as compared to 'loosely' growing cells at t_0.

As in normoxia (20% O_2), ART and DHA in hypoxia (1%O_2) inhibited the growth of HL-60 and HT-29-AK cells in a time-dependent manner (table 6). In HL-60 cells, after 72h when the drugs were most potent, ART was more potent in hypoxia than normoxia (normoxia: IC_{50} of 0.60± 0.08µM vs. hypoxia: IC_{50} of 0.51 ± 0.06µM; 1.18-fold enhancement; $P<0.05$); while cytotoxicity of DHA was not affected by different oxygen tensions (normoxia: IC_{50} of 0.49± 0.03µM vs. hypoxia: IC_{50} of 0.53 ± 0.07µM; $P>0.05$). These results suggest that ART and DHA in HL-60 cells effectively overcome unfavourable hypoxic environment to exert their cytotoxic activities and from the clinical point of view may decrease risk of cancer therapy failure and the development of chemo-resistance.

In contrast, the cytotoxicity of ART and DHA against HT-29-AK cells was significantly ($P<0.01$) inhibited in hypoxia (1% O_2) compared to normoxia (20% O_2) at all time point tested. The findings suggest reduced sensitivity of the cells towards ART and DHA and the impact of hypoxic condition on the drugs-mediated cytotoxicity (table 3 vs. table 6). Encouragingly, the reduced sensitivity to ART and DHA against HT-29-AK cells was decreasing with longer incubations, showing enhanced killing mechanisms of ART and DHA over a period of time (table 6). The hypoxia-dependent anti-cancer effect of DHA against cancer cells was investigated in

previous experimental studies (Aung *et al.* 2011; Ontikatze *et al.* 2014). In human CRC cells (HCT15, HCT116, and Coco 205), hypoxic microenvironment (0.2% O_2) was induced 2h before DHA (0-80µM) was added for 48h and showed the effective inhibition of all cell lines in both normoxic and hypoxic conditions (Ontikatze *et al.* 2014). It could be possible that incubation of cells for 2h in hypoxic chamber was not enough to effectively induce hypoxic environment in cancer cells, thereby to observe decreased sensitivity of cells towards ART and DHA as it was observed in our study (table 3 vs. table 6). Before each treatment in the investigations, cells were grown in hypoxia (1% O_2) for 72h to effectively induce hypoxia. In addition, into account should be taken different CRC types used in the studies. Here, HT-29-AK cells were selected to study the anti-cancer effects of ART and DHA. In contrast, Ontikatze *et al.* (2014) investigated the anti-cancer effect of DHA against a panel of human CRC lines, including HCT15, HCT116, and Coco 205 cancer cells but not HT-29-AK cells. According to the literature, Ontikatze *et al.* (2014) studied DHA against a panel of CRC cell lines at low oxygen tension of 0.2%. In the present study, the oxygen tension of 1% was investigated, which might further result in different effects of DHA between the studies. Other parameters which could affect the results between different laboratory settings include length of cell incubations with DHA (24-48-72h vs. 48h) and composition of culture media.

6.2. Cytotoxicity of ART and DHA in cancer cells is iron-dependent

It is reported that the endoperoxide bridge of 1,2,4-trioxanes requires activation by an iron (II) species to produce ROS and CCR to exert their cytotoxicity (Efferth *et al.* 2004; Mercer *et al.* 2007). In normoxia (20% O_2), it was found that haemin, an iron carrying molecule (at 1µM and 3µM) enhanced the activity of ART and DHA in HL-60

and HT-29-AK cells following 24h incubation. The findings support the importance of iron in ART- and DHA-mediated activity and are consistent with previous reports (Smith *et al.* 1997; Efferth *et al.* 2004; Singh and Lai 2004; Lai *et al.* 2005; Kelter *et al.* 2007; Zhang and Gerhard 2008; Zhang and Gerhard 2009). As shown in table 5, iron chelating molecule, DFO (60μM) antagonised ART and DHA cytotoxicity in both cell lines after 24h by mopping out available iron needed to activate their endoperoxide bridge. These observations were consistent with previous studies where iron chelators or compounds without the endoperoxide bridge were used and this resulted in decreased or loss of cytotoxic effects of the agents (Mercer *et al.* 2007; Zhao *et al.* 2015).

In hypoxia (1% O_2), surprisingly, the cytotoxicity of ART and DHA against HL-60 cells was antagonised by the presence of haemin at 1μM, and further at 3μM haemin (compounds+1μM haemin: DHA IC_{50} of 3.65μM, ART IC_{50} of 4.63μM; compounds+3μM haemin: DHA IC_{50} of 5.48μM, ART IC_{50} of 16.95μM vs. DHA IC_{50} of 1.10 ± 0.08μM and ART IC_{50} of 0.92 ± 0.23μM alone; table 7). The results indicate that adaptive responses of HL-60 cells to hypoxia are mediated by haemin where increasing haemin concentrations at 1μM and 3μM decreased ART and DHA cytotoxicity. The molecular mechanisms responsible for antagonised effects of ART and DHA to cancer cells upon haemin co-adminstration are unknown and require further investigations. In addition, decreased cytotoxicity of ART was reported when co-adminstrated with Ferrosanol® (10μg/ml) in normoxia (20% O_2) against breast cancer MCF7 cells, suggesting that TfR1 on cell surfaces of some cell lines under specific experimental conditions do not react with drug-iron complex which could inhibit endocytosis-mediated drug-iron complex internalisation within the cells and activation of drug (Kelter *et al.* 2007).

In contrast, the cytotoxicity of ART and DHA in HT-29-AK cells was increased in the presence of haemin (at 1µM and 3µM) and was antagonised in the presence of DFO, thus showing similar molecular mechanisms of action of the drugs as in normoxia (20% O_2) (table 7 vs. table 5).

However, the inhibition of cytotoxicity of ART and DHA with DFO was much greater in hypoxia (1% O_2) than in normoxia (20% O_2), suggesting additional inhibitory mechanisms involved (table 5 vs. table 7). It was reported that HIF-1α in normoxia is rapidly degraded in an O_2 and Fe^{2+}- dependent manner, resulting in a no detectable HIF-1α secretion (Ke and Costa 2006; Romney *et al.* 2011). Other studies showed that at low oxygen levels, HIF-1α is more stable and detectable which result in the up-regulation of genes involved in angiogenesis and drug resistance (Ke and Costa 2006; Romney *et al.* 2011). It can be hypothesized that DFO by diminishing the availability of Fe^{2+} in culture media lead to further stabilization of HIF-1α, thus resulting in decreased inhibitory effects of the drug.

A high expression of TfR1 has been implicated with tumour stage and poor prognostic subsets in breast cancer (Habashy *et al.* 2010). In addition, the over-expression of TfR1 in a panel of *in vitro* cell models of acquired resistance to tamoxifen indicated TfR1 as a candidate marker of tamoxifen resistance (Habashy *et al.* 2010). The concentration of sTfR1 in the incubation media is a quantitative marker of cellular TfR1 levels (R'zik and Beguin, 2001). In the present study, DHA-treated HT-29-AK cells under normoxic conditions for 24h resulted in overall up-regulated levels of sTfR1 whereas after 72h there was observed down-regulation of sTfR1 upon DHA treatment (figure 15). When comparing results from hypoxia, sTfR1 in DHA-treated HT-29-AK cells for 72h increased in a concentration-dependent manner, showing the involvement of low oxygen microenvironment as compared to

normoxia (figure 15 vs. figure 63). In contrast, under both conditions, ART-treated HT-29-AK cells for 72h decreased levels of sTfR1 as compared to control, thus indicating that hypoxic environment did not have impact on ART-mediated sTfR1 levels (figures 15 and 61). ART-mediated sTfR1 decrease is in agreement with data reported by others (Zhou *et al.* 2008; Ba *et al*. 2012). Therefore, ART-mediated decrease in sTfR secretion may be a consequence of the deleterious effects of ART on the cells. This might be linked with inhibited recycling of TfR1 to the cell surface and decreased cell iron uptake capacity as triggered by ART. The cells depleted in iron, which is required for continous cell proliferation and DNA synthesis have reduced stability of intracellular proteins, thus resulting ultimately in cell death. For HL-60 cells, DHA-treated cells for 24h and 72h in normoxia resulted in a decrease of sTfR1 and this was consistent with down-regulation of sTfR1 in hypoxia with DHA-treated cells for 72h (figures 15 and 62). The different mode of action was reported with ART against HL-60 cells. Here, sTfR1 levels in normoxia and hypoxia increased after ART treatment for 72h (figures 15 and 62). The results of these studies indicate that ART and DHA may exhibit different mechanisms of action against different cell lines and different time point tested (figures 15 and 62). ART- and DHA-mediated effect on sTfR1 might be also dependent on the availability of oxygen (figures 15 and 62). Unfortunately, due to resources limitations presented data represent only 2 independent experiments and further studies are needed to confirm these findings and allow statistical analysis.

The results of growth kinetics of HL-60 and HT-20-AK cells further suggest that the cytotoxicity of ART and DHA is not related with proliferation rates observed in both conditions (figure 64).

6.3. Effect of ART and DHA on IL-6 and COX-2 levels

IL-6 is a pro-tumourigenic cytokine, involved in tumour cell proliferation, survival and invasiveness (Grivennkov *et al.* 2009; Nagasaki *et al.* 2014; Rokavec *et al.* 2014). The higher levels of TfR1 in gut mucosal and leukaemic cells were reported to be stimulated and regulated by a number of pro-inflammatory cytokines, including TNF-α, lL-6 and IL-1β (Nezu *et al.* 1994; Han *et al.* 1997; Chalaris *et al.* 2011; Harel *et al.* 2011). Previous studies showed that 1,2,4-trioxanes exert anti-inflammatory activities through inhibition of interleukins, including IL-8 and IL-1β (He *et al.* 2011; Wang *et al.* 2011). The cytotoxicity of ART and arteether also correlated with high IL-6 signal transducer expression ($P<0.05$), thus potentially affecting their anti-cancer effects (Anfosso *et al.* 2006). Therefore, the next step of this study was focused on investigating IL-6 secretion levels in media collected following the treatment of HT-29-AK and HL-60 cells with DHA.

HT-29-AK and HL-60 cells treated with DHA for 24h and 72h showed a dual response on IL-6 expression (figure 16). In both cell lines, there were undetectable levels of IL-6 expression (below the lowest concentration of standard 0.039pg/mL) with concentrations representing IC_{50} value of DHA followed by increased levels of IL-6 with concentrations representing $2xIC_{50}$ value of DHA at 24h and 72h, respectively (figure 16).

Hypoxia is reported to stimulate IL-6 over-expression which further may enhance expression of HIF-1α via STAT-3 signaling pathway (Anglesio *et al.* 2011). In the present study, as in normoxia, HT-29-AK and HL-60 cells treated with DHA for 72h incubation showed a dual response on IL-6 expression (figures 16 and 65) with secretions levels of IL-6 being unchanged by hypoxic microenvironment when compared to normoxia. Overall, despite limited number of repeats, the results may

indicate that DHA-mediated IL-6 changes are independent from oxygen tension levels but strictly dependent on the concentrations tested of DHA.

Increasing invasive and the migratory potential of cells in cancer progression require the up-regulation of many pro-inflammatory mediators including COX-2 (Jang *et al.* 2009). COX-2, an inducible isoform of COX enzyme, induces the release of prostaglandins (PGs) involved in inflammatory, wound healing, and malignancy processes (Jang *et al.* 2009). 1,2,4-trioxanes were reported to exert potent anti-inflammatory activities through COX-2 inhibition in cancer cells (Wang *et al.* 2011; Zhang *et al.* 2014; Zuo *et al.* 2014) and non-cancer studies (Okorji and Olajide 2014). These previous reports are similar to our observations were DHA- and ART-treated HT-29-AK cells for 72h down-regulated the COX-2 protein levels in a concentration-dependent manner, thus confirming their anti-inflammatory effects in both cell lines (figure 17).

6.4. Effect of ART and DHA on expression and localisation of E-cadherin and CLDN-1 in cancer cells

Enhanced inflammation within tumour microenvironment contributes to EMT, a differentiation cascade which promotes the breakdown of the epithelial integrity and facilitates cell motility and invasiveness (Jang *et al.* 2009; Imbert *et al.* 2012; Rokavec *et al.* 2014; Gu *et al.* 2015). One of the major steps enabling EMT through invasion of cancer cells is dysregulation of the epithelial marker E-cadherin (Ca^{2+}-binding transmembrane molecule), which is pivotal in cell-cell adhesion (Li *et al.* 2008). Previous reports showed that E-cadherin levels increased upon treatment with ART and artemisinin in some cancer cell types, including colorectal poorly-differentiated CLY and moderately-differentiated Lovo cells, endometrial HEC-1B

cells and hepatocarcinoma HepG2 cells (Li *et al.* 2008; Lijuan *et al.* 2010; Weifeng *et al.* 2011). In the same study of Li *et al.* 2008, ART treatment (0-200µM for 72h) in well-differentiated HT-29 cells demonstrated a decreasing E-cadherin protein expression as analysed by a Western blotting technique and with membranous localisation of E-cadherin detected by immunofluorescence. The significant observation of our study was that ART treatment for 24h incubation resulted in up-regulation in E-cadherin mRNA levels in HT-29-AK cells while treatment with ART for 72h resulted in E-cadherin mRNA down-regulation, suggesting that ART modulates E-cadherin mRNA levels in a time-dependent manner (figure 18). The localisation of E-cadherin within the cells upon ART treatment was further explored by immunocytochemical staining (figures 20 and 21). After 24h treatment with ART, control cells had equally distributed membranous E-cadherin localisation whereas ART-treated cells had minimal basal localisation and ART-mediated increase in lateral membranous staining (figure 20). It was reported previously that a biological response modifier and anti-cancer agent, ubenimex enhanced cell-cell adhesion through aggregation of E-cadherin at cell-cell contact sites in a human breast YMB-S cancer cell line (Fujioka *et al.* 1995). The results of a present study might indicate that ART through increasing the localisation of E-cadherin at cell-cell contact sites enhanced cell-cell adhesion in HT-29-AK cells after 24h treatment with ART. Nevertheless, Doki *et al.* (1993) demonstrated that cell clones from human esophageal cancer TE-2 cells with negative E-cadherin expression were relatively more invasive than cell clones with positive E-cadherin expression. This absent or down-regulated expression of E-cadherin was frequently reported in diverse metastatic and invasive cancers, including CRC, breast, pancreatic, hepatocellular carcinoma, ovarian and endometrial cancers (Deep *et al.* 2014; He *et al.* 2013; Zhou

et al. 2013; Kashiwagi *et al*. 2010; Jang *et al.* 2009; Sawada *et al.* 2008; Mell *et al.* 2003). It has also been shown clinically that decreased expression of E-cadherin correlated with worse survival rate in patients with CRC (Elzagheid *et al.* 2012; He *et al.* 2013). Therefore, the results of this study might indicate that ART by enhancing the aggregation of E-cadherin at cell-cell contacts is contributing to the inhibition of migration and invasiveness in HT-29-AK cells.

Despite it was not investigated in the present study, we further postulate E-cadherin localisation to be associated with enhanced activity of ankyrin-G. Ankyrin-G (gene ank3) is a scaffolding protein being required for protein trafficking of various membrane domains, including epithelial lateral membranes (Durak *et al.* 2014). The results from the study of Kizhatil and colleagues (2007) on human bronchial epithelial cells may suggest that ankyrin-G binds to the cytoplasmic domain of E-cadherin and simultaneously recruits β-2-spectrin, resulting in accumulation of E-cadherin at lateral membranes, thus increasing cell-cell interactions and inhibiting the process of EMT. However, further studies are needed to confirm this hypothesis. The down-regulation of E-cadherin mRNA levels in all samples with ART-treated HT-29-AK cells for 72h treatment was linked with equally distributed E-cadherin at basal and lateral membranous sites as analysed with immunocytochemical staining (figure 18 vs. 21), and this was in agreement with previous observations of Li *et al.* (2008). The treatment of HT-29-AK cells with ART for 24h resulted in an inverse relationship between increased levels of E-cadherin and decreased levels of CLDN-1 (figure 18A and 25A). CLDN-1 is a tight junction protein which regulates normal epithelial physiology and its dysfunction is implicated with tumorigenesis and EMT (Dhawan *et al.* 2005; Bezdekova *et al.* 2012; Blanchard *et al.* 2013; Huang *et al*. 2015). Singh *et al.* (2011) showed that increased levels of CLDN-1 mediated down-

regulation of E-cadherin by up-regulating the expression of Zeb-1. This resulted in progression from normal colonic epithelium to colon adenocarcinoma (Singh *et al.* 2011). It could be possible that augmented mRNA levels of E-cadherin had negative impact on CLDN-1 mRNA levels but further studies are needed to exactly analyse this association. Quantitative PCR results of our study showed that HT-29-AK cells treated for 72hrs with ART showed decreased CLDN-1mRNA expression (figure 25). At protein level, flow cytometric analysis showed increased CLDN-1 protein levels upon treating HT-29-AK cells with ART for 72 (figure 26). However, these increased CLDN-1 levels were decreasing with higher ART, suggesting delay in transcription response mediated by ART (figure 26). Conflicting results have been published with respect to CLDN-1 expression in colon cancer and its clinical outcome (Dhawan *et al.* 2005; Shibutani *et al.* 2013). Analysis of CLDN-1 expression in tissue samples from healthy and CRC patients showed loss of CLDN-1 expression in normal colon tissues, increased CLDN-1 levels in 3 patients with primary colon cancer and marked over-expression in CLDN-1 protein levels in 2 patients with metastatic CRC (Dhawan *et al.* 2005). Under investigation is also localisation of CLDN-1 within CRC cells and their potential importance in CRC progression (Dhawan *et al.* 2005; Bezdekova *et al.* 2012). CLDN-1 in normal colonic epithelium typically is localised at cell membrane, altered mislocalisation stained as membranous/cytoplasmic is observed in adenomacarcinoma (p=0.0001) and adenomas (p=0.0002) where cytoplasmic localisation was linked with a higher degree of dysplastic lesions (Bezdekova *et al.* 2012). In CRC tissue samples membranous/cytoplasmic is more frequent when compared to adenomas (87% vs. 51%, respectively; p=0.001), thus suggesting the importance of CLDN-1 localisation in CRC progression (Bezdekova *et al.* 2012). Our data of the effects of ART-untreated and -treated HT-29-AK cells for 72h indicate

that CLDN-1 in untreated cells has membranous and cytoplasmic localisation, whereas ART-treated cells shows re-localisation of CLDN-1 from cytosolic structures to the membrane, thus possibly reversing EMT and inhibiting CRC progression (figure 27).

For comparison purposes, we performed some studies investigating the effect of DHA treatment on the localisation of E-cadherin in HT-29-AK cells. DHA-treatment for 24h resulted in basolateral-E-cadherin localisation at 29.01µM and 58.02µM, whereas the highest DHA concentration (at 116.04µM) resulted in a partly membranous and nuclear accumulation (figure 22). It can be hypothesized that DHA at a highest concentration of 116.04µM reached a threshold of E-cadherin up-regulation, possibly resulting in its gene-regulatory activities. Treatment of HT-29-AK cells for 72h was consistent with previous results with ART and showed baso/lateral membranous localisation in all DHA-untreated and –treated cells and with concomitant decreasing pattern of CLDN-1 protein levels analysed using flow cytometric analyses (figures 23 and 28).

Similar investigations of ART and DHA were performed against HL-60 cells. Flow cytometric analysis showed that ART-treated cells for 72h had a concentration-dependent increase in E-cadherin protein surface levels and augmented CLDN-1 levels (figures 24 and 28). In contrast, DHA treated HL-60 cells for 72h had down-regulated E-cadherin levels and concentration-dependent increase in CLDN-1 levels (figures 24 and 29). These results show that the effects of ART and DHA could differ between each drug and cell line used. However, the associated clinical meaning and the basis molecular mechanisms of these changes require further studies.

6.5. Inhibition of cell migration and invasion by ART and DHA

The ability of cancer cells to invade and metastasise is related with high mortality and morbidity in patients (Steeg *et al.* 2006; Shapiro *et al.* 2007). The anti-invasive and anti-metastatic activities of ART and DHA were evaluated previously by various techniques, including 2D wound healing assay, 3D transwell chamber invasion assays and *in vivo* metastasis settings (Hwang *et al.* 2010; Rasheed *et al.* 2010; Weifeng *et al.* 2011; [a]Chen *et al.* 2013). In 2D wound-healing assay, artemisinin treatment (0-75µM) for 24-48-72h resulted in a concentration- and time- dependent inhibition of hepatoma cells (HepG2 and SMMC-7721) migration and invasion which was linked with blocking the ability of cells to close the wound gap (Weifeng *et al.* 2011). Consistent with these findings, it was observed here using a crude invasion assay that ART and DHA inhibited the capacity of HT-29-AK cells to heal the wound (figures 30-32). Together with concentration-dependent wound diameter inhibition, there were increasing numbers of floating dead cells (non-viable cells) (figures 31-33). ART- and DHA- treated HT-29-AK cells which remained attached to the well looked small and had noticeable damaged membranes under microscope, as compared to healthy control cells. It was hypothesized that ART and DHA-induced genotoxicity marked these cells to undergo a programmed cell death, apoptosis, were some of these typical cell features to apoptosis were observed (figures 30 and 32).

To determine the potential molecular basis of these findings, the ability of DHA and ART to suppress MMPs, which are responsible for enhancing invasion and metastasis of tumour cells, was investigated. In the present study, ART-treated HT-29-AK cells for 72h decreased up-regulated protein levels of MMP-2 with the highest concentration used (at 28.88µM) resulting in MMP-2 levels being comparable

with untreated cells (1.09 ± 0.08RFU vs. 1.00 ± 0.13RFU, figure 36A). The expression levels of MMP-9 upon ART treatment for 72h resulted in a concentration-dependent decrease of up-regulated MMP-9 levels, as compared to control (figure 36B). The results from flow cytometric and Western blotting analyses further showed that DHA treatment for 72h decreased the up-regulated MMP-2 and MMP-9 levels in a concentration-dependent manner (figure 37 A-D). For comparison purposes, we performed flow cytometric studies for the effects of ART and DHA on MMP-2 and MMP-9 levels against HL-60 cells (figure 38). It was observed that ART treatment following 72h incubation resulted in a concentration-dependent increase in MMP-2 and MMP-9 levels as compared to control (figure 38). Whereas treatment with DHA for 72h unchanged MMP-2 levels in all DHA untreated and treated cells but resulted in a slight increase of MMP-9, as compared to control cells (figure 39). There are various previous studies describing the potent inhibitory effects of ART and DHA towards several MMPs, including MMP-2 and MMP-9 (Buommino *et al.* 2009; Rasheed *et al.* 2010; Wang *et al.* 2011; Weifeng *et al.* 2011). Here, ART and DHA showed their inhibitory properties against MMP-2 and MMP-9 in adherent HT-29-AK cells whereas unfavorable effects of the compounds against both MMPs were observed against suspension HL-60 cells. These observations warrant further investigations to better understand the biological meaning of these results and possible clinical outcomes.

A major clinical problem is associated with the ability of tumour cells to re-grow, causing local re-currence of cancer even after surgery and the threat of the development of resistance to anti-cancer agents (Abulafi and Williams 1994). The results of ART and DHA in a wound healing/migration assay and their ability to alter MMP-2 and MMP-9 expression levels indicate that ART and DHA might inhibit

migration and invasion of HT-29-AK cells in our study. Therefore, it was of interest to further determine the effect of the drugs on HT-29-AK cells capacity to re-grow. The initial treatment of HT-29-AK cells with either ART (at 7.22, 14.44, 28.88µM) or DHA (at 9.88, 19.75 and 39.50µM) for 72h showed a concentration-dependent growth-inhibition by the agents (figure 34). After washing the cells following 72h incubation, the ability of ART and DHA to inhibit the re-growth of cells was noticed, with the most prominent inhibition observed with the highest concentrations of ART (28.88µM) and DHA (39.50µM) (figure 34). For comparison purposes, similar experiments with ART and DHA were performed for HL-60 cells (figure 35). We observed that none of ART and DHA treated HL-60 cells were able to re-grow to the levels observed in control samples (figure 35). The re-growth inhibition abilities of ART and DHA were more marked in HL-60 cells as compared to HT-29-AK cells (figure 34 vs. figure 35), with the exact molecular mechanisms of these observations required to be further determined. The results indicate a promising potential of ART and DHA to inhibit cancer cell re-growth, thus contributing to better therapeutic effects in patients through decreasing the risk of cancer re-currence and the development of resistance.

6.6. ART and DHA to modulate VEGF-α and HIF-1α levels

Angiogenesis, a process of new blood vessel formation is associated with uncontrolled tumour growth, metastasis and cancer cell resistance to anti-cancer agents (Zhou *et al.* 2007; Mohammadi-Motlagh *et al.* 2010; Schneider *et al.* 2011). The secretion of the main cancer pro-angiogenic factor VEGF-α and cytokines is enhanced during angiogenesis and occurs via multiple processes, including hypoxia-mediated activation of HIF-1α (Duffy *et al.* 2003). There is evidence that ART and

DHA inhibit two main pro-angiogenic factors VEGF-α and HIF-1α in several cancer cell lines (Anfosso *et al.* 2006; Huang *et al.* 2007; Zhou *et al.* 2007; Aung *et al.* 2011; Wang *et al.* 2011). In normoxic conditions of the present study, ART-treated HT-29-AK cells for 24h resulted in a significant ($P<0.001$) increase of VEGF-α mRNA levels with concomitant decrease of VEGF-α mRNA levels observed after 72h (figure 40 A and B). The measurement of VEGF-α165 secretion levels from collected media after ART treatment for 72h showed decrease in its expression with the lowest ART concentration of 7.22µM and the highest 28.88µM while unchanged levels with 14.44µM ART (figure 40 C). The VEGF-α165 secretion levels were decreasing with increasing concentrations of DHA (at 58.02µM and 116.04µM) following treatment for 24h and decreased with DHA treatment (at 9.88µM, 19.75µM and 39.50µM) for 72h when compared to their respective controls (figure 41). The secretion levels of VEGF-α165 were also measured in HL-60 cells, where DHA treatment for 24h showed no change in VEGF-α165 levels in all sample treated and un-treated cells whereas decreased secretion levels of VEGF-α165 were measured for DHA and ART treated HL-60 cells for 72h (figure 41). Despite of some limitations of these studies, including not enough repeats to allow statistical analysis we can conclude that ART and DHA show the ability to decrease VEGF-α levels. Thus, the results might indicate a crucial role of ART and DHA in angiogenesis inhibition but further experiments are needed to clarify the exact mechanisms of their effects.

Hypoxia has been reported to be a major stimulus for the up-regulation of VEGF-α and HIF-1α (Ankoma-Sey *et al.* 2000; Hendriksen *et al.* 2009). In addition, knockdown of HIF-1α or survivin in the ovarian cancer cell lines suppressed VEGF-α expression, thus showing the correlation between VEGF-α expression and other proteins (Huang *et al.* 2008). Under hypoxic conditions in the present study, ART-

and DHA-treated HL-60 and HT-29-AK cells for 72h had variable effects on VEGF-α which were specific for the drug used and cell line tested (figures 66 and 67). The secretion levels of VEGF-$_{α165}$ were similar to those obtained in normoxia, suggesting that the anti-cancer effects of ART and DHA towards VEGF-$_{α165}$ are not affected by hypoxic microenvironment (figures 40-42 vs. figures 64 and 65).

Previous studies have shown that DHA (5-25μM) inhibited the expression of HIF-1α in rat C6 glioma cells (Huang *et al.* 2007). Similar observations with the ability of artesunate and artemisinin to inhibit HIF-1α were reported in human rheumatoid arthritis fibroblast-like syniviocytes and in mouse embryonic stem cell-derived embryoid bodies, respectively (Wartenberg *et al.* 2003; He *et al.* 2011). More recently Ba *et al.* (2012) demonstrated that the treatment with DHA (0-25μM) for 24h or with 25μM DHA for different times from 0h to 24h increased HIF-1α levels in a human hepatoma HepG2 cancer cell line.The aim of our further investigations was to investigate the effect of ART and DHA on HIF-α mRNA and intracellular protein levels in both cell lines. Due to time and resources limitations, the studies were performed under normoxic conditions only. ART-treated HT-29-AK cells for 24h showed increased HIF-α mRNA at all concentrations tested (at 82.53μM, 165.06μM and 330.12μM) while 72h incubation resulted in a concentration-dependent significant ($p<0.001$) decrease of HIF-α mRNA (figure 43 A and B). At protein level, investigated using flow cytometric analysis, ART-treated cells for 72h resulted in decreasing levels of HIF-α with increasing concentrations of ART (at 7.22μM, 14.44μM and 28.88μM) (figure 43 C). These results indicate that ART effect on mRNA HIF-α expression levels is time-dependent and can be modulated post-transcriptionally. Variable results for HIF-α mRNA levels between 24h and 72h incubation together with variations in HIF-α protein expression were observed for

ART against HL-60 cells and for DHA against HT-29-AK and HL-60 cells (figures 44, 44 and 46). The molecular mechanisms responsible for the different expression of HIF-α in cancer cells are unknown and need to be better clarify.

The observed changes in HIF-1α expressions upon ART and DHA treatments resulted in further investigations of CA-9, another hypoxia marker directly regulated by HIF-1α (Li *et al.* 2014). In squamous cell head and neck SSCHNC cancer cells, CA-9 had strong membrane and cytoplasmic expression (26.6%) seen mainly in areas of focal necrosis and was related with resistance to radiotherapy (Koukourakis *et al.* 2001). Here, it was observed that CA-9 protein localisation in all ART and DHA untreated and treated cells for both time points was membranous, without signs of mislocalisation to cytoplasm and without changes in CA-9 intensity (figure 47). The findings indicate the lack of impact of ART and DHA on CA-9 protein localisation in HT-29-AK cells (figure 47). It would be beneficial to investigate CA-9 at mRNA and protein levels stimulatenously to determine any potential variations in their levels and to compare these effects to CA-9 main regulator, HIF-1α.

6.7. ART and DHA modulate the expression of proteins which are responsible for caspase-dependent cell death

Protection against apoptosis is a key mechanism implicated in malignant transformation by enhanced cell survival, avoidance of immune surveillance and development of resistance to chemotherapeutic agents (Yang *et al.* 2001; Hector and Prehn 2009). Akt plays a pivotal role in apoptosis inhibition by promoting malignant cell survival, proliferation and angiogenesis through a number of downstream effectors (Bortul *et al.* 2003; Altomare and Testa 2005; Stegeman *et al.* 2012). ART in human cervical carcinoma cells and DHA in human prostate cancer cells have been shown to enhance TRAIL- mediated apoptosis through inhibition of

the NF-κB and PI3K/Akt signaling pathways (He *et al.* 2010; Thanaketpaisarn *et al.* 2011). These events were accompanied by inhibition of pro-survival proteins, such as survivin, XIAP, and Bcl-XL (Thanaketpaisarn *et al.* 2011). In human rheumatoid arthritis fibroblast–like synoviocytes, ART inhibited the PI3K/Akt activation and secretion of VEGF and IL-8 which were stimulated in synoviocytes by TNF-α or hypoxia (He *et al.* 2011). The observations of He and collegues (2011) demonstrated that ART has the ability to inhibit the expression of angiogenic factors in synoviocytes which could represent promising therapeutic approach for Rheumatoid arthritis.

In this study, incubation of HT-29-AK cells with DHA for the first 24h resulted in a transient, concentration-dependent increase in protein levels of anti-apoptotic phospho-Akt concentrations followed by a concentration-dependent decrease in phospho-Akt after 72h (figure 53). In contrast, HT-29-AK cells treated with ART for 72h resulted in a concentration-dependent increase in phospho-Akt levels (figure 52). We also noted increasing proteins levels of phosho-Akt upon ART and DHA treatment for 72h of HL-60 cells which stand in contrast with majority of previous reports (figure 54) (Ma *et al.* 2011; Thanaketpaisarn *et al.* 2011; Kim *et al.* 2015). It suggests that the compounds may activate other pathways implicated in inhibition of apoptosis. These observations are important from clinical point of view, as even short activation of phospho-Akt may be associated with enhanced inflammatory responses and induction of resistance to chemotherapy (Bortul *et al.* 2003; Wang *et al.* 2013). Further studies of ART and DHA alone and in the presence of allosteric Akt inhibitors may clarify the effects of the drugs on phospho-Akt levels. Up-regulated levels of Akt were reported in ART and DHA-treated HT-29-AK cells in

hypoxia, thus indicating similar profiles of activities of compounds in both conditions (figure 70).

To investigate the mechanistic basis of anti-cancer effects of ART and DHA, a suppressor of apoptosis, survivin protein was evaluated (Shin *et al.* 2001; Ye *et al.* 2014). Previous studies have shown that 1,2,4-trioxanes induce apoptosis by causing significant decreases in cellular survivin levels (Mu *et al.* 2007; Shao *et al.* 2008). Here, the cellular levels of survivin measured upon drug treatment were dependent on the incubation length and cell line-specific (figures 48-50). Survivin expression can be regulated by several stimuli, such as Akt, HIF-α, IL-6 and IL-4 (through activation of the STAT-6 signaling pathway). For HT-29-AK cells treated with ART, we noted decreasing levels of survivin at the level of mRNA with the length of incubation (24h vs. 72h) while protein levels also showed decreasing trend after 72h, suggesting that post-transcriptionally survivin is not affected significantly by other mediators (figure 48). In contrast, DHA-treated HT-29-AK cells showed increasing expressions of survivin mRNA with prolonged incubations (24h vs. 72h) whereas protein levels measured by ELISA showed concentration-dependent decrease in survivin, indicating that survivin is modulated post-transcriptionally (figure 50). For comparison purposes, studies of ART against HL-60 cells demonstrated decreasing mRNA levels of survivin with longer incubation (24h vs. 72h) while at protein survivin levels were unchanged at all ART treatments (figure 49). DHA-treated HL-60 cells for 24h had decreased survivin mRNA expressions as investigated by qPCR, whereas after 72h the levels of survivin mRNA were only low with the highest concentration of DHA at1.00μM (figure 49). ELISA analysis showed decreasing protein levels of survivin after treating HL-60 cells for 24 and 72h with DHA (figure 49). Further studies are needed to clarify the role of survivin and other

mediators of survivin in the cytotoxicity of ART and DHA against HL-60 and HT-29-AK cells.

Survivn levels in hypoxia upon treating the both cell lines with ART and DHA were variable and distinctive from those effects observed in normoxia (figures 67 and 68). The results might indicate the influence of low oxygen tension and presumable other mediators on the effects of ART and DHA in HL-60 and HT-29-AK cells (figures 67 and 68). Data for the effects of ART and DHA in both cell lines under hypoxic conditions represent 2 independent experiments and requires additional repeats for statistical analysis (figures 68 and 69).

There is ample data which suggest that 1,2,4-trioxanes exert their anti-tumour activities via apoptosis by its primary effecter molecule, caspase-3 (Lu *et al.* 2008; Kong *et al.* 2012; Dong and Wang 2014; Zuo *et al.* 2014; Kim *et al.* 2015). These observations are consistent with our own data in which ART and DHA treatment for 72h increased catalytically cleaved caspase-3 in HL-60 and HT-29-AK cells, suggesting that these agents promote cancer cell apoptosis (figures 55 and 56). These observations were accompanied by morphological changes observed in ART- and DHA-treated HT-29-AK cells under light microscope showing characteristic cell shrinkage, blebbing and “a mass of cell debris”, being typical hallmarks of apoptosis (Coelho *et al.* 2000; Bestwick *et al.* 2006; Sanmartin *et al.* 2012). The DHA-induced caspase-3 production was consistent with elevated or concentration-dependent increased levels of BrdU-labelled nicks in DNA strands which are present in apoptotic cells only (figure 57 and 58). Together with the drug-induced increase in caspase-3 and BrdU-labelled DNA levels, there were accumulated DNA fragments in samples treated with the test agents upon separating the DNA on agarose gel electrophoresis as compared to respective controls (figures 59-61). The results have

not showed small DNA fragments or features of smear ladder as compared to previous studies (Li *et al*. 2009; Yang *et al.* 2009). This could be due to technical problem related with a too high the percentage of agarose gel resulting in inhibited separation of damaged DNA and this should be checked in the future.

As in normoxia, cells treated for 72h with ART and DHA under low oxygen (1%) showed up-regulated secretions of caspase-3 (figures 71 and 72), suggesting that these agents promote cancer cell apoptosis even in hypoxia. DHA mediated caspase-3 secretion was consistent with elevated levels of BrdU-labelled nicks in DNA strands, which are present in apoptotic cells only (figure 73). Together with DHA-induced increased caspase-3 and BrdU-labelled DNA levels in HL-60 cells, there were observable presence of fragmented DNA in samples treated with DHA upon separating on agarose gel electrophoresis (figure 74), which is consistent with previous reports in normoxia but was not investigated previously in hypoxia (Li *et al.* 2009; Yang *et al.* 2009).

6.8. Conclusions and future studies

Overall, despite of some limitations (e.g. small sample size, selection of DHA only for some experiments) the results of this study indicate that ART and DHA in standard normoxic experimental settings (20% O_2) effectively induced a time-dependent growth inhibition in HL-60, HT-29-AK and Caco-2 cells. The importance of modelling tumour microenvironment in drug discovery and development is becoming more popular due to the potential benefits for cancer therapy through reducing the risk of chemo-resistance. Therefore, the cytotoxicity of ART and DHA was additionally investigated under low oxygen tension (1% O_2) to mimic tumour hypoxia. Hypoxic environment reduced the susceptibility of the cells to ART and DHA, as compared to

normoxia. The anti-cancer activity of ART and DHA was iron-dependent in normoxia while low oxygen tension (1%) showed that ART and DHA against HL-60 cells was not exclusively dependent on their interaction with iron. Given the broad spectrum of mediators involved in ART and DHA anti-cancer effects showed from data collected, further studies are required to validate our observations and translate them into significance for cancer therapy.

CHAPTER 7

DISCUSSION 2

Part 2: THE MOLECULAR BASIS OF THE ANTI-CANCER EFFECTS OF ART AND DHA COMBINED WITH ASA AGAINST HT-29-AK AND HL-60 CELLS IN NORMOXIA AND HYPOXIA

7.1. Anti-cancer effects of ART and DHA (alone and in combination with ASA) against HL-60 and HT-29-AK cells under normoxic and hypoxic conditions

This study investigated ART and DHA in combination with ASA, as a chemo-sensitizing agent on the growth of human HT-29-AK colorectal and human HL-60 leukaemic cancer cells. Specifically, we have shown that ART and DHA in combination with ASA had improved inhibitory effects on the growth in cultured cancer cells under normoxic (in ART and ASA combination) and hypoxic conditions. The combination regimen with ASA in HT-29-AK cells under normoxic conditions enhanced the caspase-3-dependent apoptotic effects of ART and DHA at least in part through down-regulation of tumour angiogenesis-stimulating growth factors, including survivin, HIF-1α and VEGF-α.

Due to the anti-inflammatory properties of ASA, its ability to inhibit cancer cell growth and induce apoptosis, ASA has become an attractive agent to investigate in

combination with currently used chemo-therapeutic compounds (Bellosillo *et al.* 1998; Gao *et al.* 2004; Pathi *et al.* 2012; Li *et al.* 2013). It was reported previously that ASA successfully potentiated the inhibitory effects of troglitazone ([a]Yan *et al.* 2010), doxorubicin (Hossain *et al.* 2012), cisplatin (Kumar and Singh 2012), valproic acid (Li *et al.* 2013) and reversine (Qin *et al.* 2013) in cancer cells. ART and DHA have shown to enhance anti-cancer effect of several anti-cancer compounds in cultured cells (including cisplatin-resistant ovarian cancer cells and doxorubicin-resistant T leukaemia cells) and carcinoma xenografts (Efferth *et al.* 2007; Wang *et al.* 2010; Liu and Cui 2013; Zhang *et al.* 2013; Feng *et al.* 2014). Because the primary mechanisms of action of 1,2,4-trioxanes (ART, DHA, artemisinin) and ASA are linked with the inhibition of crucial cell signaling factors, including survivin, COX-2, HIF-1α and VEGF-α involved in angiogenesis and the induction of apoptosis through similar intermediates (caspase-3), it was hypothesized that ASA would enhance the cytotoxic effects of ART and DHA.

Before investigating ASA in combination with ART and DHA our first studies aimed to evaluate the effects of ASA under normoxic and hypoxic conditions in HL-60 and HT-29-AK cells to allow determination of ASA fixed concentrations which were used in further experimental settings. In initial normoxic (20% O_2) studies, it was found that ASA inhibited the growth of HL-60 and HT-29-AK cells in a time-dependent manner (table 8). These results are consistent with the observations previously reported in several other cancers *in vitro,* including B-cell chronic lymphocytic human leukaemic cells (Bellosillo *et al.* 1998), human colon cancer SW480, RKO, HT-29, and HCT116 cell lines (Zhou *et al.* 2011; Pathi *et al.* 2012), YD8 human oral squamous cancer cells (Park *et al.* 2010), human HeLa and mouse U14 cervical carcinoma (Qin *et al.* 2013). The mean ASA IC_{50} values determined by Bellosillo *et*

al. (1998) in leukaemic cells under 48h were in the range between 4.4 and 7.3mM/L and were comparable to ASA IC_{50} value of 3.12 ± 0.46mM calculated in our study when treating HL-60 cells for 48h (table 8). The ASA IC_{50} value after 72h in present study was 2.50 ± 0.18mM and was within the range of effective concentrations of ASA against leukaemic cancer cells reported previously (Bellosillo *et al.* 1998). In cultured HT-29-AK cells, the inhibitory effect of ASA observed in present investigation was also time-dependent, resulting in IC_{50} values as follow: 21.35 ± 2.12mM, 13.25 ± 0.79mM and 6.15 ± 0.83mM after 24, 48 and 72h incubations, respectively (table 8). ASA IC_{50} value of 6.15 ± 0.83mM was similar with IC_{50} values observed upon ASA treatment of 4 colon cancer cell lines (SW480, RKO, HT-29, and HCT116) for 72h with resulted IC_{50} values ranging from 2.5mM to 5mM in all cell lines (Pathi *et al.* 2012).

In previous chapters we have shown the importance of the oxygen concentration in ART- and DHA-mediated cytotoxicity (table 3 vs. table 6). Therefore, we further investigated the effect of low oxygen levels (1%) on ASA-mediated anti-cancer effects in both cell lines. HL-60 and HT-29-AK cells were less susceptible to ASA under each time point tested (24, 48h and 72h) in hypoxia as compared to respective time points in normoxia (table 8). Interestingly, HL-60 cells were far less sensitive to ASA in hypoxia as compared to HT-29-AK cells (ASA HL-60 cells IC_{50} values of >60mM at 24 and 48h; and 22.05 ± 2.7mM at 72h; ASA HT-29-AK cells IC_{50} values of 31.95 ± 2.59mM, 17.73 ± 1.63mM and 8.47 ± 2.18mM after 24, 48 and 72h, respectively; figure 8). The findings are unexpected in view of the fact that in previous our studies, ART and DHA were more cytotoxic towards HL-60 cells in both normoxic and hypoxic conditions as compared to HT-29-AK cells (reduced sensitivity of cells in hypoxia). These discrepancies might arise from different contribution of

hypoxic signaling mediators on ASA-mediated cytotoxicity in cancer cells of different line and cell state (suspension vs. attached cells).

We further wished to determine whether ASA fixed concentrations derived for HL-60 cells (normoxia: 2.50mM) and HT-29-AK cells (normoxia: 6.25mM; hypoxia: 8.47mM) after 72h can synergistically enhance anti-cancer effects of ART and DHA. We have chosen these fixed ASA concentrations after 72h for two reasons. First, they are most potent against each cell line and secondly, there are in the range of ASA serum concentrations achievable in humans, thus being most practical for therapeutic use (Juárez *et al.* 2004). Because ASA IC_{50} concentration of 22.05mM derived from hypoxia in HL-60 cells at 72h was resulting in dead of all cells during MTT experiments (data not shown), we decided to use 1/10 of this concentration equal to 2.21mM. MTT combination studies demonstrated a synergistic interaction between fixed concentration of ASA (2.50mM) when co-treated with ART but not with DHA in HL-60 cells under normoxic conditions (ASA+ART IC_{50} value of 0.48 ± 0.02µM vs. ART alone with IC_{50} of 0.59 ± 0.08µM, $P<0.001$; ASA+DHA IC_{50} value of 0.49 ± 0.03µM vs. DHA alone with IC_{50} of 0.49 ± 0.04µM; table 9). Hypoxia enhanced the cytotoxicity of ART and DHA in HL-60 cells when combined with ASA (2.21mM) but there was not enough repeats to perform statistical analyses (ASA+ART IC_{50} value of 0.46mM vs. ART alone with IC_{50} of 0.51 ± 0.06mM; ASA+DHA IC_{50} value of 0.23mM vs. DHA alone with IC_{50} of 0.53 ± 0.07mM; table 10). ASA (6.15mM) in normoxia significantly ($P<0.001$) enhanced the cytotoxic effects of ART and DHA on the inhibition of CRC growth and proliferation (ASA+ART IC_{50} value of 6.67 ± 1.73µM vs. ART alone with IC_{50} of 14.44 ± 2.64µM; ASA+DHA IC_{50} value of 5.93 ± 0.58µM vs. DHA alone with IC_{50} of 19.75 ± 1.07µM; table 9). However, even greater enhancement of ART and DHA-mediated anti-cancer effects when combined with

ASA was seen in hypoxic microenvironment, suggesting high selectivity of combination regimen towards hypoxic cells (ASA+ART IC_{50} value of 1.63 ± 0.50µM vs. ART alone with IC_{50} of 46.51 ± 4.74µM; ASA+DHA IC_{50} value of 7.90 ± 0.99µM vs. DHA alone with IC_{50} of 27.10 ± 12.73µM; $P<0.001$; table 10). This data indicate that ART and DHA combination with ASA could reverse decreased susceptibility of cells under hypoxic conditions to ART and DHA alone. Thus, ART and DHA in combination with ASA might be an effective combination regimen to enhance efficacy of chemotherapy in cancer cells. Due to time and resources limitations further studies were concentrated on possible mechanisms of action of ART and DHA combined with ASA under normoxic conditions.

A pleiotropic enzyme COX-2 belongs to the COX membrane-bound haemo- and glycol-proteins family (COX-1, COX-2 and COX-3 isoforms) (Thun *et al.* 2002; Grrenhough *et al.* 2009). COX-2 is implicated in carcinogenesis by promoting the proliferation, survival, angiogenesis, migration and the invasiveness of malignant cells (Thun *et al.* 2002; Grrenhough *et al.* 2009). The mechanisms of action responsible for the inhibitory effects of ASA on cancer cells, including colorectal carcinoma is reported to stem in part from its ability to directly suppress the expression of COX-1 and COX-2 enzymes (Thun *et al.* 2002; Vane and Botting 2003; Weiss *et al.* 2006; Yoo and Lee 2007; Rahman *et al.* 2012; [a]Cho *et al.* 2013). In addition, it has been reported by others (Wang *et al.* 2011; Zuo *et al.* 2014; Zhang *et al.* 2015) and us (figure 17) that ART and DHA decrease COX-2 expression in cancers. Therefore, we hypothesized that ART and DHA combination with ASA would synergistically decrease COX-2 protein expression in HT-29-AK cells. In contrast, it was observed using flow cytometric analyses that COX-2 levels in all single drug treatments were increased, with the highest changes observed when

cells were treated with ART and DHA combined to ASA (figure 75). This suggests that the anti-cancer mechanisms of ART and DHA combinations with ASA are independent of COX-2 inhibition. Our observations are consistent with some other ASA studies, including in B-cell chronic lymphocytic leukaemic cells, colon cancer cells and COX-null mouse embryo fibroblasts where ASA-dependent inhibitory and apoptotic effects were postulated to be COX-independent (Hanif *et al.* 1996; Bellosillo *et al.* 1998; Zhang *et al.* 1999). [a]Cho *et al.* 2013 indicated important function of COX-1 in carcinogenesis, therefore we cannot rule out possibility that enhanced cytotoxicity effects of ART and DHA when combined with ASA are mediated through down-regulation of COX-1 isoform which require further investigations. Considering the mechanisms of the drugs combinations inhibitory effects cannot be explained by COX-2 protein expression, we decided to investigate survivin mRNA levels.

Previous studies showed that 1,2,4-trioxanes-induced apoptosis in single drug treatments was accompanied by a significant decrease or loss in a key apoptosis inhibitor survivin protein or mRNA levels (Shao *et al.* 2008; Odaka *et al.* 2014; Kim *et al.* 2015). In human myeloid leukaemic KBM-5 cells investigated by Kim *et al.* 2015, combination of ART (10µM) with doxorubicin (30µM), paclitaxel (1.50nM) and docetaxel (1.50nM) for 24h potentiated the inhibitory effect in survivin down-regulation in these cells more effectively as compared to single agents. The anti-cancer effects of ASA (alone or in combination) were also reported to be associated with survivin mRNA and protein levels down-regulation (Yang *et al.* 2011; Li *et al.* 2013; Dong *et al.* 2014). Combination of ASA (3mM/l) with cisplatin (10µg/ml) was reported in gastric SGC7901/cisplatin cell cultures to significantly reduce mRNA and protein levels of survivin when compared to ASA (3mM/l) or cisplatin (10µg/ml) alone

(Dong *et al.* 2014). In the current study, ASA combination with ART resulted in a marked increase of survivin mRNA levels as compared to single drugs (figure 76). However, ASA was shown to markedly decrease survivin mRNA levels in HT-29-AK cells when combined with DHA (figure 76). Survivin down-regulation of ASA and DHA combination was further confirmed in preliminary ELISA cellular survivin levels (data not shown) but repetition of experiments is necessary to allow statistical analysis. Our observations indicate that synergistic effect of ART and DHA with ASA on colon cancer inhibition might be drug specific were different mechanistic mechanisms are involved. It can be postulated that survivin over-expression in ART and ASA combination might contribute to the development of drug resistance and/or the inhibition of cell sensitivity towards drug treatment. In contrast, combined treatment with DHA and ASA resulting in survivin down-regulation might inhibit the process of angiogenesis more effectively and enhance cell sensitivity towards drug combination, thus reducing the risk of chemo-resistance. It is possible that combination of ART and ASA which resulted in increased of survivin mRNA is linked with lower fold difference in inhibitory effects against HT-29-AK cells, as compared to inhibitory effects of DHA co-treatment with ASA and their respective single agents (ART IC_{50} value of 14.44 ± 2.64µM vs. ART combined with ASA IC_{50} value of 6.67 ± 1.73µM, 2.16-fold enhancement; DHA IC_{50} value of 19.75 ± 1.07µM vs. DHA combined with ASA IC_{50} value of 5.93 ± 0.58µM, 3.33-fold enhancement; table 9). Survivin down-regulation as a strategy to increase the cytotoxic effects of chemotharapy agents was evidenced by Ghanbari *et al.* (2014). Ghanbari *et al.* (2014) showed that combination of docetaxel with vinblasite lowered the expression of survivin and decreased the IC_{50} value of docetaxel (from 70 to 5nM; $P<0.05$). However, similar studies of docetaxel with vinblasite combination in the presence of

survivin inhibitor deguelin resulted in significant ($P<0.05$) enhancement in synergistic efficacy of docetaxel and vinblastine (Ghanbari *et al.* 2014). We can hypothesize that the enhancement of sensitivity of HT-29-AK cells by ASA and DHA combination therapy and down-regulation of the same cellular pathway mediator survivin simultaneously is resulting in drugs synergistic cytotoxic effects, therefore better anti-cancer efficacy and higher target selectivity. The enhanced therapeutic effects and selectivity of the artemisinins would lead to lower concentrations of drugs used clinically and decrease potential side effects in humans. Furthermore, highly effective and selective drug combinations could be used against already resistant cancer cells lines for superior clinical outcome and prolonging survival times for patients with colorectal cancer. Further studies using survivin inhibitors could help to confirm this hypothesis.

HIF-1 is a heterodimeric transcription factor which has been demonstrated to play an important role in promoting the expression of pro-angiogenesis and pro-resistance proteins in carcinogenesis (Tacchini *et al.* 1999; Švastová *et al.* 2003; Jeong *et al.* 2005; [a]Cho *et al.* 2013; Chen *et al.* 2014; Li *et al.* 2014). Therefore, the inhibition of this protein by chemotherapeutic agents alone or in combinations is an attractive therapeutic approach. A number of preclinical reports in cancer cells, such as rat C6 glioma cells treated with DHA (5-25μM) (Huang *et al.* 2007) and non-cancer settings (Wartenberg *et al.* 2003; He *et al.* 2011) have shown that the 1,2,4-trioxanes inhibit HIF-1α expression. There are also some reports showing induction of HIF-1α in cancers, including human hepatoma cell line HepG2 treated with DHA (0-25μM) for 24h or with 25μM DHA for different times from 0h to 24h (Ba *et al.* 2012). Our previous experiments showed that the effects of ART and DHA on HIF-1α were linked with used compound and cancer type (human leukaemic HL-60 cells vs.

human colorectal HT-29-AK cells) (figures 43-46). Other factors were associated with investigated target (mRNA or protein levels) and incubation time (24h vs. 72h) (figures 43-46). In current study, it has been reported that mRNA HIF-1α levels in ASA and ART-treated samples were decreased whereas in DHA-treated samples were unchanged as compared to control (figure 77). The pronounced down-regulation of mRNA HIF-1α levels was observed in ART and DHA combination with ASA, suggesting synergistic effect of drugs to be due to inhibition of HIF-1α levels (figure 77). This data further suggest that by combining ASA with ART or DHA we can enhance the inhibition of drug resistance and angiogenesis of HT-29-AK cells more effectively as compared with single agents and achieve better efficacy of chemotherapy in these cells.

According to numerous studies, the VEGF family members and their receptors have shown to play various biological functions, including in vasculogenesis (Krusche *et al.* 2013), angiogenesis (Niki *et al.* 2000), metastasis and tumour survival (Jayasinghe *et al.* 2013). The expression and concentration of soluble VEGFR-1 as investigated by a Western blot analysis and ELISA in samples of patients with CRC were significantly ($P<0.001$) increased as compared to those in controls (Abbasi *et al.* 2015). The observations of Abbasi *et al.* (2015) indicated soluble VEGFR-1 as a useful indicator of the malignant potential and tumour progression (Abbasi *et al.* 2015). Especially, VEGF-α isoform has been demonstrated to have a crucial role in cancer metastasis through promoting angiogenesis (Niki *et al.* 2000). Mechanistic studies on ASA (5 and 10mM) inhibitory effects against colon cancer cells (RKO, SW480, HT-29 and HCT-116) were reported to be associated with the down-regulation of pro-angiogenic mediators VEGF-α and its receptor VEGFR1 (Pathi *et al.* 2012). Furthermore, ASA (100mg/kg, twice a day orally) administrated to male

mice injected with a solution containing Lewis lung carcinoma cells led to reduction in lung cancer metastasis to regional lymph nodes and significantly ($P<0.0001$) reduced mice mortality (Ogawa *et al.* 2014). There is much evidence that 1,2,4-trioxanes inhibit angiogenesis through VEGF-α suppression or decrease in cultured cancer cells and non-cancer studies *in vitro*; and *in vivo* using xenograft tumours (Wartenberg *et al.* 2003; Aung *et al.* 2011; Wang *et al.* 2011; Zhang *et al.* 2013). Zhang *et al.* (2013) demonstrated that a synergistic anti-proliferative effect in human lung carcinoma (A549 and A549/DDP cells) of DHA combined with cisplatin was attributed to reduced tumour microvessel density and suppression of angiogenesis-related proteins HIF-1α and VEGF-α both *in vitro* and *in vivo.* Krusche *et al.* (2013) also demonstrated synergistic inhibition of angiogenesis by ART and captopril (angiotensin-I-converting enzyme inhibitor) of human umbilical vein endothelial cells (HUVEC) *in vitro* using wound healing assay and vascularisation processes *in vivo* using a chorioallantoic membrane (CAM) assay of quail embryos. In our study, examination of mRNA levels of VEGF-α in HT-29-AK cells showed down-regulation of their transcriptional stability upon combination of ART with ASA, as compared to ART alone, and significantly ($P<0.05$) as compared to control (figure 78). These results are further showing that ART and DHA-mediated synergistic effects in HT-29-AK cells might be due to the inhibition of angiogenesis through down-regulation of VEGF-α mRNA levels.

Previous studies showed that ART and DHA decreased the levels of phosho-Akt in cultured cancer cells and xenograft tumor model (He *et al.* 2010; Ma *et al.* 2011; Thanaketpaisarn *et al.* 2011; Lee *et al.* 2013; Odaka *et al.* 2014). [a]Cho *et al.* 2013 demonstrated that the inhibitory effect of ASA (1mM) on EGFR-activated cell viability in ovarian OVCAR-3 cancer cells was associated with blocking phospho-Akt and

phospho-Erk protein expressions. The phosphorylation of Akt in present study was showed to be up-regulated upon combination of ASA with ART and DHA in HT-29-AK cells (figure 79). Uddin *et al.* 2010 showed that clinically activated phospho-Akt was associated with over-expressed COX-2 levels and not linked with COX-1 in epithelial ovarian cancer (EOC). *In vitro* studies using EOC cells of Uddin and colleagues *(*2010), further showed that the inhibition of COX-2 using ASA selective inhibitor NS398 and gene silencing impaired phospho-Akt levels and resulted in cell growth inhibition and induction of apoptosis. These results might indicate link between COX-2 and phospho-Akt up-regulation observed in our study when combining ASA with ART and DHA. Future experiments with using COX-2 selective inhibitor NS398 or gene silencing would clarify the signaling mechanisms involved in the up-regulation of phospho-Akt expression in our study.

Key proteins involved in the process of apoptosis include caspases, where caspase-3 is an executor protein activated by extrinsic and intrinsic signaling cascades (Hector *et al.* 2009). Anti-cancer effects of ASA (alone or in combination) treatment regimen has been reported to be attributed with the activation of caspase-dependent apoptosis, especially caspases-3,7,8 and 9 (Gao *et al.* 2004; Hossain *et al.* 2012; Pathi *et al.* 2012; Li *et al.* 2013; Qin *et al.* 2013; Thakkar *et al.* 2013). Similarly, ART and DHA-induced apoptosis (alone and in combination with other chemotherapeutic agents) against cell lines, including colorectal and leukaemia cells is reported with intrinsic and extrinsic dependent activation of caspases (Jiang *et al.* 2013; Liu and Cui 2013; Feng *et al.* 2014; Wang *et al.* 2014; Zhang *et al.* 2015). Here, studies using flow cytometic analyses (figure 80 and 81) showed that ASA co-treatment significantly enhanced caspase-3-dependent apoptotic effect of ART and DHA in cultured leukaemic HL-60 and colorectal HT-29-AK cells *in vitro* as compared

to monotherapy drugs effect. The findings further support our previous results of the drugs combinatorial synergistic effects in cancer cells.

7.2. Conclusions and future directions

In conclusion, we presented evidence showing better anti-cancer activity of ART and DHA when combined with ASA against HT-29-AK cells under normoxic and hypoxic conditions *in vitro*. The inhibitory effect of combination treatments against HL-60 cells was improved in normoxia (in ART and ASA combination) but hypoxic microenvironment was showed to enhance the efficacy of ART and DHA when combined with ASA. However, more repeats are needed to perform statistical analyses for ART and DHA combined with ASA against HL-60 cells in hypoxia. As presented in simplified diagram of drugs combinations mechanisms of action (figure 82), we found that synergistic activity of combinations in colorectal cancer HT-29-AK cells was COX-2 independent and potentially correlated with up-regulation of survivin mRNA (in ART and ASA combination) and phospho-Akt protein expressions, which might unfavourably decrease combinational cytotoxicity effects. Most importantly, we observed combination treatments efficacy in HT-29-AK cells to be associated with enhanced anti-angiogenic effects in HT-29-AK cells via survivin (in DHA and ASA combination), HIF-1α, and VEGF-α (in ART and ASA combination) inhibition as well as the induction of caspase-3-dependent apoptosis (figure 82). Therefore, by inhibiting cancer cell growth, restricting angiogenesis and promoting apoptosis of HT-29-AK cells, ART and DHA combination with ASA may potentially be of great value in the treatment of CRC. MTT cytotoxicity assay showed that the cytotoxicity of DHA in combination with ASA against HL-60 cells was not enhanced under normoxic conditions (table 9). However, there was a significant enhancement

in the production of caspase-3 in HL-60 cells when DHA was combined with ASA in normoxia (figure 81). The mechanisms involved are not clear and further investigations are needed. Other future studies might include investigation of the effect of combinations on mediators implicated in angiogenesis, migration and invasion in both cell lines. Additional cancer cell lines to study the effects of ART and DHA in combination with ASA under normoxic and hypoxic conditions would increase further the understanding of their effects. These studies should be performed to clearly answer the question whether the effects of these combinations are at pre- or post-transcriptional level. Determination of mechanistic basis of the combined treatments on the tumour inhibition, metastasis and vasculogenesis *in vivo* experiments in rodents is also needed.

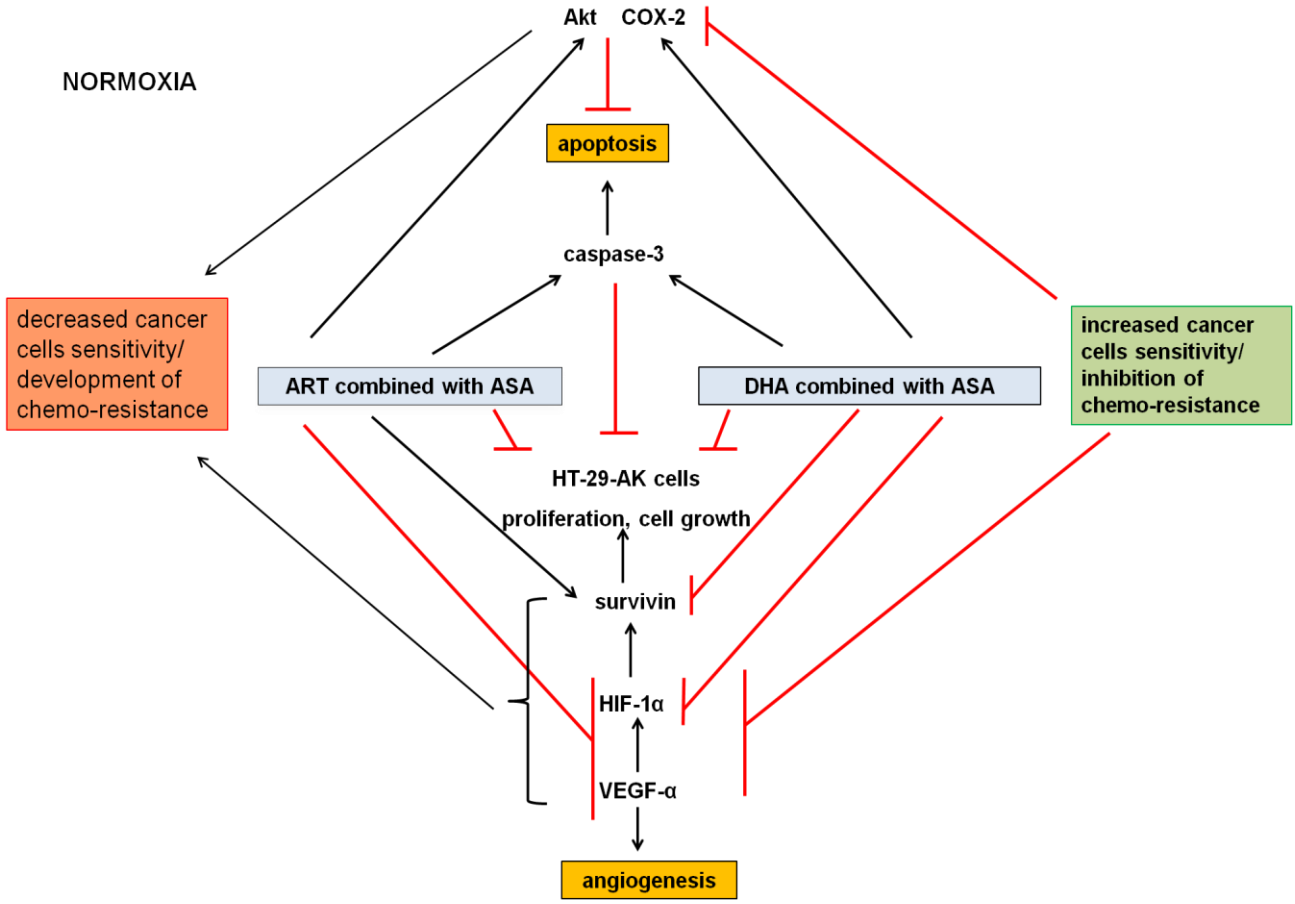

Figure 82: The proposed shema of the mechanisms of action of ART and DHA combined with ASA in induced apostosis in human colorectal HT-29-AK cancer cells under normoxic conditions. Symbol ⊥ means decrease and the arrow ↑means increase.

References

Abbasi, O., Mashayekhi, F., Mirzajani, E., Asl, S.F., Mahmoudi, T., and Saedi, H.S. (2015) 'The soluble VEGFR1 concentration in the serum of patients with colorectal cancer'. *Surgery Today*, 45 (2) 215-20

Abulafi, A.M. and Williams, N.S. (1994) 'Local recurrence of colorectal cancer: The problem, mechanisms, management and adjuvant therapy'. *British Journal of Surgery*, 81 (1) 7-19

Aguayo, A., Kantarjian, H., Manshouri, T., Gidel, C., Estey, E., Thomas, D., Koller, C., Estrov, Z., O'Brien, S., Keating, M., Freireich, E., and Albitar, M. (2000) 'Angiogenesis in acute and chronic leukemias and myelodysplastic syndromes'. *Blood,* 96(6) 2240-5

Altomare, D.A. and Testa, J.R. (2005) 'Perturbations of the Akt signaling pathway in human cancer'. *Oncogene*, (24) 7455-64

Anfosso, L., Efferth, T., Albini, A., and Pfeffer, U. (2006) 'Microarray expression profiles of angiogenesis-related genes predict tumor cell response to artemisinins'. *Pharmacogenomics Journal*, 6(4) 269-78

Anglesio, M.S., George, J., Kulbe, H., Friedlander, M., Rischin, D., Lemech, C., Power, J., Coward, J., Cowin, P.A., House, C.M., Chakravarty, P., Gorringe, K.L., Campbell, I.G., Australian Ovarian Cancer Study Group, Okamoto, A., Birrer, M.J., Huntsman, D.G., de Fazio, A., Kalloger, S.E., Balkwill, F., Gilks, C.B., and Bowtell, D.D. (2011) 'IL6-STAT3-HIF signaling and therapeutic response to the angiogenesis inhibitor sunitinib in ovarian clear cell cancer'. *Clinical Cancer Research,* 17 (8) 2538-48

Ankoma-Sey, V., Wang, Y., and Dai, Z. (2000) 'Hypoxic stimulation of vascular endothelial growth factor expression in activated rat hepatic stellate cells'. *Hepatology*, 31(1) 141-8

Antoine, T., Fisher, N., Amewu, R., O'Neill, P.M., Ward, S.A., and Biagini, G.A. (2014) 'Rapid kill of malaria parasites by artemisinin and semi-synthetic endoperoxides involves ROS-dependent depolarization of the membrane potential'. *The Journal of Antimicrobial Chemotherapy*, 69(4) 1005-16

Ashley, E. A., Dhorda, M., Fairhurst, R. M., Amaratunga, C., Lim, P., Suon, S., Sreng, S., Anderson, J. M., and Mao, S. (2014) 'Spread of artemisinin resistance in *Plasmodium falciparum* malaria'. *The New England Journal of Medicine*, 371(5) 411-423

Ashton, M., Nguyen, D.S., Nguyen, V.H., Gordi, T., Trinh, N.H., Dinh, X.H., Nguyen, T.N., and Le, D.C. (1998) 'Artemisinin kinetics and dynamics during oral and rectal treatment of uncomplicated malaria'. *Clinical Pharmacology and Therapeutics*, 63(4) 482-93

Aung, W., Sogawa, C., Furukawa, T., and Saga, T. (2011) 'Anticancer effect of dihydroartemisinin (DHA) in a pancreatic tumor model evaluated by conventional methods and optical imaging'. *Anticancer Research*, 31(5) 1549-58

Ba, Q., Zhou, N., Duan, J., Chen, T., Hao, M., Yang, X., Li, J., Yin, J., Chu, R., Wang, H., (2012) 'Dihydroartemisinin exerts its anticancer activity through depleting cellular iron via transferring receptor-1'. *PLoS ONE* 7(8): e42703

Bachmeier, B., Fichtner, I., Killian, P.H., Kronski, E., Pfeffer, U., and Efferth, T. (2011) 'Development of resistance towards artesunate in MDA-MB-231 human breast cancer cells'. *PLoS ONE* 6 (5), art. no. e20550

Banović, M., Veliki, I., Stanec, M., and Lesar, M. (2005) 'Acetysalicylic acid (ASA) and non-steroidal anti-inflammatory drugs (NSAID) for prevention of thrombosis and cancer (Review)'. *Libri Oncologici*, 33 (1-3) 61-72

Bastiaannet, E., Sampieri, K., Dekkers, O.M., De Craen, A.J.M., Van Herk-Sukel, M.P.P., Lemmens, V., Van Den Broek, C.B.M., Coebergh, J.W., Herings, R.M., Van De Velde, C.J., Fodde, R., and Liefers, G.J. (2012) 'Use of Aspirin postdiagnosis improves survival for colon cancer patients'. *British Journal of Cance*r, 106 (9) 1564-70

Bellosillo, B., Piqué, M. Barragán, M., Castaño, E., Villamor, N., Colomer, D., Montserrat, E., Pons, G., and Gil, J. (1998) 'Aspirin and salicylate induce apoptosis and activation of caspases in B-cell chronic lymphocytic leukemia cells'. *Blood* 92 (4) 1406–14

Bennett, A., Tacca, M. D., Stamford, I. F., and Zebro, T. (1977). 'Prostaglandins from tumours of human large bowel'. *British Journal of Cancer*, 35 (6) 881–4

Berger, T.G., Dieckmann, D., Efferth, T., Schultz, E.S., Funk, J.-O., Baur, A., and Schuler, G. (2005) 'Artesunate in the treatment of metastatic uveal melanoma - first experiences'. *Oncology Reports*, 14 (6) 1599-1603(5)

Bestwick, C.S., and Milne, L. (2006) 'Influence of galangin on HL-60 cell proliferation and survival'. *Cancer Letters*, 243(1) 80-9

Bezdekova, M., Brychtova, S., Sedlakova, E., Langova, K., Brychta, T., and Belej, K. (2012) 'Analysis of Snail-1, E-cadherin and Claudin-1 expression in colorectal adenomas and carcinomas'. *International Journal of Molecular Sciences*, 13(2)1632–43

Bhattacharya, A., Tóth, K., Mazurchuk, R., Spernyak, J.A., Slocum, H.K., Pendyala, L., Azrak, R., Cao, S., Durrani, F.A., and Rustum, Y.M. (2004) 'Lack of microvessels in well-differentiated regions of human head and neck squamous cell carcinoma A253 associated with functional magnetic resonance imaging detectable hypoxia, limited drug delivery, and resistance to irinotecan therapy'. *Clinical Cancer Research*, 10 (23) 8005-17

Blanchard, A.A., Ma, X., Dueck, K.J., Penner, C, Cooper, S.C., Mulhall, D., Murphy, L.C., Leygue, E., and Myal, Y. (2013) 'Claudin 1 expression in basal-like breast cancer is related to patient age'. *BMC Cancer*, 13: 268, doi: 10.1186/1471-2407-13-268

Boland, C. R., Luciani, M. G., Gasche, C., and Goel, A. (2005) 'Infection, Inflammation, and gastrointestinal cancer'. *Gut,* 54 (9) 1321-31

Bonnet, M., Buc, E., Sauvanet, P., Darcha, C., Dubois, D., Pereira, B., Déchelotte, P., Bonnet, R., Pezet, D., and Darfeuille-Michaud, A. (2013) 'Colonization of the human gut by *E. coli* and colorectal cancer risk'. *Clinical Cancer Research*, 20(4) 859-67

Borka, K., Kaliszky, P., Szabó, E., Lotz, G., Kupcsulik, P., Schaff, Z., Kiss, A. (2007) 'Claudin expression in pancreatic endocrine tumors as compared with ductal adenocarcinomas'. *Virchows Archiv: an international journal of pathology*, 450(5) 549-57

Bortul, R., Tazzari, P.L., Cappellini, A., Tabellini, G., Billi, A.M., Bareggi, R., Manzoli, L., Cocco, L., and Martelli, A.M. (2003) 'Constitutively active Akt1 protects HL60 leukemia cells from TRAIL-induced apoptosis through a mechanism involving NF-kappaB activation and cFLIP(L) up-regulation'. *Leukemia, 17* (2) 379-389

Bourseau-Guilmain, E., Griveau, A., Benoit, J.P., and Garcion, E. (2011) 'The importance of the stem cell marker prominin-1/CD133 in the uptake of transferrin and in iron metabolism in human colon cancer Caco-2 cells'. *PLoS One.* 6(9):e25515

Brahimi-Horn, M.C., Chiche, J., and Pouysségur, J. (2007) 'Hypoxia and cancer'. *Journal of Molecular Medicine*, 85 (12) 1301-7

Buommino, E., Baroni, A., Canozo, N., Petrazzuolo, M., Nicoletti, R., Vozza, A., and Tufano, M.A. (2009) *'*Artemisinin reduces human melanoma cell migration by down-regulating αvβ3 integrin and reducing metalloproteinase 2 production'. *Investigational New Drugs*, 27(5) 412-18

Chalaris, A., Garbers, C., Rabe, B., Rose-John, S., and Scheller, J. (2011) 'The soluble Interleukin 6 receptor: generation and role in inflammation and cancer'. *European Journal of Cell Biology*, 90(6-7) 484-94

Chang, S. E., Huh, J., Choi, J. H., Sung, K. J. Moon, K. C., and Koh, J. K. (1999) 'Cutaneous relapse in acute promyelocytic leukaemia following treatment with all-trans retinoic acid'. *The British Journal of Dermatology*, 141(3) 586-7

Chen, J., Ding, Z., Peng, Y., Pan, F., Li, J., Zou, L., Zhang, Y., and Liang, H. (2014) 'HIF-1[alpha] inhibition reverses multidrug resistance in colon cancer cells via downregulation of MDR1/P-glycoprotein'. *PLoS ONE*, 9(6)

[a]Chen, X., Han, K., Chen, F., Wu, C., and Huang, W. (2013). 'Effects of Artesunate on the invasion of lung adenocarcinoma A549 cells and expression of ICAM-1 and MMP-9'. *Chinese Journal of Lung Cancer, 16*(11) 567-571

Chen, J., Imanaka, N., Chen, J., and Griffin, J. D. (2010) 'Hypoxia potentiates Notch signaling in breast cancer leading to decreased E-cadherin expression and increased cell migration and invasion'. *British Journal of Cancer*, 102(2) 351-60

Chen, J., Kobayashi, M., Darmanin, S., Qiao, Y., Gully, C., Zhao, R., Yeung, S. C., and Lee, M. H. (2009) 'Pim-1 plays a pivotal role in hypoxia-induced chemoresistance'. *Oncogene*, 28 (28) 2581-92

[b]Chen, Y., Sun, Y., Chen, L., Xu, X., Zhang, X., Wang, B., Min, L., and Liu, W. (2013) 'miRNA-200c increases the sensitivity of breast cancer cells to doxorubicin through the suppression of E-cadherin-mediated PTEN/Akt signaling'. *Molecular Medicine Reports*, 7(5) 1579-84

Cheng, C., Ho, W. E., Goh, F. Y., Guan, S. P., Kong, L. R., Lai, W.-Q., Leung, B. P., Wong, W. S. F., and Idzko, M. (2011) 'Anti-malarial drug artesunate attenuates experimental allergic asthma via inhibition of the phosphoinositide 3-kinase/Akt pathway'. *PLoS ONE,* 6(6),e20932

Cheng, F., Wang, X.'E ; Zhong, D., Sun, L., Wang, Q., and Liu, C. (2015) 'Significance of detection of serum carbonic anhydrase IX in the diagnosis of lung cancer'. *Chinese Journal of Lung Cancer*, 18(1) 29-33

Chim, C.S., Wong, A.S.Y., and Kwong, Y. L*. (2004) '*Epigenetic dysregulation of the Jak/STAT pathway by frequent aberrant methylation of SHP1 but not SOCS1 in acute leukaemias'. *Annals of Hematology,* 83 (8) 527-32

[a]Cho, M., Kabir, S.M., Dong, Y., Lee, E., Rice, V.M., Khabele, D., and Son, D.S. (2013) 'Aspirin blocks EGF-stimulated cell viability in a COX-1 dependent manner in ovarian cancer cells'. *Journal of Cancer,* 4(8) 671-78

[b]Cho, K., Shin, H.W., Kim, Y.I., Cho, C.H., Chun, Y.S., Kim, T.Y., Park, J.W. (2013) 'Mad1 mediates hypoxia-induced doxorubicin resistance in colon cancer cells by inhibiting mitochondrial function'. Free Radical Biology & Medicine, 60:201-10

Choi, J.Y., Jang, Y.S., Min, S.Y., and Song, J.Y. (2011) 'Overexpression of MMP-9 and hif-1α in breast cancer cells under hypoxic conditions'. *Journal of Breast Cancer*, 14 (2) 88-95

Coelho, D., Holl, V., Weltin, D., Lacornerie, T., Magnenet, P., Dufour, P., Bischoff, P. (2000) 'Caspase-3-like activity determines the type of cell death following ionizing radiation in MOLT-4 human leukaemia cells'. *British Journal of Cancer*, 83(5) 642-9

Cohen, T., Nahari, D., Cerem, L.W., Neufeld, G., and Levi, B.Z. (1996) 'Interleukin 6 induces the expression of vascular endothelial growth factor'. *The Journal of Biological Activity,* 271(2) 736-41

Cooks, T., Pateras, I.S., Tarcic, O., Solomon, H., Schetter, A.J., Wilder, S., Lozano, G., Pikarsky, E., Forshew, T., Rozenfeld, N., Harpaz, N., Itzkowitz, S., Harris, C.C. Rotter, V., Vassilis G. Gorgoulis, V.G., and Oren, M., (2013) 'Mutant p53 prolongs NF-κB activation and promotes chronic inflammation and inflammation-associated colorectal cancer'. *Cancer Cell,* 23 (5) 634-46

Cui, L. and Su, X.Z. (2009) 'Discovery, mechanisms of action and combination therapy of artemisinin'. *Expert Review of Anti-infective Therapy*, 7(8) 999-1013

Dambacher, J., Beigel, F., Seiderer, J., Haller, D., Göke, B., Auernhammer, C.J., and Brand, S. (2007) 'Interleukin 31 mediates MAP kinase and STAT1/3 activation in intestinal epithelial cells and its expression is upregulated in inflammatory bowel disease'. *Gut*, 56(9) 1257-65

Dautry-Varsat, A., Ciechanover, A. and Lodish, H. F. (1983) 'pH and the recycling of transferrin during receptor-mediated endocytosis'. *Proceedings of the National Academy of Sciences of the United States of America*, 80(8) 2258-62

De Bont, E. S. J. M., Rosati, S., Jacobs, S., Kamps, W., and Vellenga, E., (2001) 'Increased bone marrow vascularization in patients with acute myeloid leukaemia: a possible role for vascular endothelial growth factor'. *British Journal of Haematology*, 113 (2) 296-304

De Botton, S., Sanz, M.A., Chevret, S., Dombret, H., Martin, G., Thomas, X., Mediavilla, J.D., Recher, C., Ades, L., Quesnel, B., Brault, P., Fey, M., Wandt, H., Machover, D., Guerci, A., Maloisel, F., Stoppa, A.M., Rayon, C., Ribera, J.M., Chomienne, C., Degos, L., Fenaux, P., European APL Group, PETHEMA Group (2006) 'Extramedullary relapse in acute promyelocytic leukemia treated with all-trans retinoic acid and chemotherapy'. *Leukemia*, 20(1) 35-41

De Martino, M., Lucca, I., Mbeutcha, A., Wiener, H.G., Haitel, A., Susani, M., Shariat, S.F., and Klatte, T. (2015) 'Carbonic anhydrase IX as a diagnostic urinary marker for urothelial bladder cancer'. *European Urology*, 68 (4) 552-4

De Vries, P.J. and Dien, T.K. (1996) 'Clinical pharmacology and therapeutic potential of artemisinin and its derivatives in the treatment of malaria'. *Drugs*, 52 (6) 818-36

Deep, G., Jain, A. K., Ramteke, A., Ting, H., Vijendra, K. C., Gangar, S. C., Subhash, C., and Agarwal, R. (2014) 'SNAI1 is critical for the aggressiveness of prostate cancer cells with low E-cadherin'. *Molecular Cancer*, 13, 37

Dekervel, J., Hompes, D., Van Malenstein, H., Popovic, D., Sagaert, X., De Moor, B., Van Cutsem, E., D'Hoore, A., Verslype, C., and Van Pelt, J. (2014) 'Hypoxia-driven gene expression is an independent prognostic factor in stage II and III colon cancer patients'. *Clinical Cancer Research*, 20(8) 2159-68

Dell'Eva, R., Pfeffer, U., Vené, R., Anfosso, L., Forlani, A., Albini, A., and Efferth, T. (2004) 'Inhibition of angiogenesis in vivo and growth of Kaposi's sarcoma xenograft tumors by the anti-malarial artesunate'. *Biochemical Pharmacology*, 68(12) 2359-66

Des Guetz, G., Uzzan, B., Nicolas, P., Cucherat, M., Morere, J.-F., Benamouzig, R., Breau, J.L., and Perret, G.-Y. (2006) 'Microvessel density and VEGF expression are prognostic factors in colorectal cancer. Meta-analysis of the literature'. *British Journal of Cancer*, 94 (12) 1823–32

Devarajan, E., Sahin, A.A., Chen, J.S., Krishnamurthy, R.R., Aggarwal, N., Brun, A.M., Sapino, A., Zhang, F., Sharma, D., Yang, X.H., Tora, A.D., and Mehta, K. (2002) 'Down-regulation of caspase 3 in breast cancer: a possible mechanism for chemoresistance'. *Oncogene*, 21(57) 8843-51

Dhawan, D., Craig, B. A., Cheng, L., Snyder, P. W., Mohammed, S. I., Stewart, J. C., Zheng, R., Loman, R.A., Foster, R.S., and Knapp, D. W. (2010).' Effects of short-term Celecoxib treatment in patients with invasive transitional cell carcinoma of the urinary bladder'. *Molecular Cancer Therapeutics*, 9(5) 1371–77

Dhawan, P., Singh, A.B., Deane, N.G., No, Y., Shiou, S.R., Schmidt, C., Neff, J., Washington, M.K., and Beauchamp, R.D. (2005) 'Claudin-1 regulates cellular transformation and metastatic behavior in colon cancer'. *The Journal of Clinical Investigation*, 115(7) 1765-76

Din, F .V. N., Dunlop, M. G., Stark, L. A. (2004) 'Evidence for colorectal cancer cell specificity of aspirin effects on NF kappa B signaling and apoptosis'. *British Journal of Cancer*, 91 (2) 381-8

Din, F.V.N., Theodoratou, E., Farrington, S.M., Tenesa, A., Barnetson, R.A., Cetnarskyj, R., Stark, L., Porteous, M.S., Campbell, H., and Dunlop, M.G. (2010) 'Effect of aspirin and NSAIDs on risk and survival from colorectal cancer'. *Gut*, 59 (12) 1670- 79

Doki, Y., Shiozaki, H., Tahara, H., Inoue, M., Oka, H., Iihara, K., Kadowaki, T., Takeichi, M., and Mori, T. (1993)'Correlation between E-cadherin expression and invasiveness *in vitro* in a human esophageal cancer cell line.' *Cancer Research*, 53(14) 3421-6

Dong, H., Liu, G., Jiang, B., Guo, J., Tao, G., Yiu, W., Zhou, J., and Li, G. (2014) 'The effects of aspirin plus cisplatin on SGC7901/CDDP cells *in vitro*'. *Biomedical Reports*, 2(3) 344(5)

Dovizio, M., Tacconelli, S., Ricciotti, E., Bruno, A., Maier, T. J., Anzellotti, P., Di Francesco, L., Sala, P., Signoroni, S., Bertario, L., Dixon, D. A., Lawson, J. A., Steinhilber, D., Fitzgerald, G. A., Patrignani, P. (2012) 'Effects of celecoxib on prostanoid biosynthesis and circulating angiogenesis proteins in familialadenomatous polyposis'. *The Journal of Pharmacology and Experimental Therapeutics,* 341 (1) 242-50

Drew, M.G.B., Metcalfe, J., Dascombe, M.J., and Ismail, F.M.D. (2007) 'De novo identification and stability of the artemisinin pharmacophore: Studies of the reductive decomposition of deoxyartemisinins and deoxyarteethers and the implications for the mode of antimalarial action'. *Journal of Molecular Structure: THEOCHEM*, 823 (1-3) 34-46

Du, X.X., Li, Y.J., Wu, C.L., Zhou, J.H., Han, Y., Sui, H., Wei, X.L., Liu, L., Huang, P., Yuan, H.H., Zhang, T.T., Zhang, W.J., Xie, R., Lang, X.H., Jia, D.X., Bai, Y.X., (2013) 'Initiation of apoptosis, cell cycle arrest and autophagy of esophageal cancer cells by dihydroartemisinin'. *Biomedicine & Pharmacotherapy*, 67 (5) 417-24

Duc, D.D., de Vries, P.J., Nguyen, X.K., Le Nguyen, B., Kager, P.A., and van Boxtel, C.J. (1994) 'The pharmacokinetics of a single dose of artemisinin in healthy Vietnamese subjects'. *The American Journal of Tropical Medicine and Hygiene*, 51(6) 785-90

Duffy, J. P., Eibl, G., Reber, H. A., and Hines, O. J. (2003) 'Influence of hypoxia and neoangiogenesis on the growth of pancreatic cancer'. *Molecular Cancer*, 2, (12) http://doi.org/10.1186/1476-4598-2-12

Durak, O., de Anda, F.C., Singh, K.K., Leussis, M.P., Petryshen, T.L., Sklar, P., and Tsai, L.H. (2014) 'Ankyrin-G regulates neurogenesis and Wnt signaling by altering the subcellular localisation of β-catenin'. *Molecular Psychiatry*, 20 (3) 388-97

Eckenroth, B. E., Steere, A. N., Chasteen, N. D., Everse, S. J., and Mason, A. B. (2011). 'How the binding of human transferrin primes the transferrin receptor potentiating iron release at endosomal pH'. *Proceedings of the National Academy of Sciences of the United States of America,* 108 (32) 13089–94

Eckstein-Ludwig, U., Webb, R. J., Van Goethem, I. D. A., East, J. M., Lee, A. G., Kimura, M., O'Neill, P. M., Bray, P. G., Ward, S. A., and Krishna, S. (2003) 'Artemisinins target the SERCA of *Plasmodium falciparum*'. *Nature*, 424(6951) 957-61

Efferth, T. (2005) 'Mechanistic perspectives for 1,2,4-trioxanes in anti-cancer therapy'. *Drug Resistance Updates*, 8 (1-2) 85-97

Efferth, T., Benakis, A., Romero, M.R., Tomicic, M., Rauh, R., Steinbach, D., Häfer, R., Stamminger, T., Oesch, F., Kaina, B., and Marschall, M. (2004) 'Enhancement of cytotoxicity of artemisinins towards cancer cells by ferrous iron'. *Free Radical Biology and Medicine* 37, (7) 998-1009

Efferth, T., Dunstan, H., Sauerbrey, A., Miyachi, H., and Chitambar, C.R. (2001) 'The anti-malarial artesunate is also active against cancer'. *International Journal of Oncology,* 18(4) 767-73

Efferth, T., Giaisi, M., Merling, A., Krammer, P.H., and Li-Weber M. (2007) 'Artesunate induces ROS-mediated apoptosis in doxorubicin-resistant T leukemia cells'. *PLoS One* 2 (8): e693

Elzagheid, A., Buhmeida, A., Laato, M., El-Faitori, O., Syrjanen, K., Collan, Y. and Pyrhönen, S. (2012) 'Loss of E-cadherin expression predicts disease recurrence and shorter survival in colorectal carcinoma'. *APMIS,* 120, 539–48

Faderl, S., Do, K.-A., Johnson, M.M., Keating, M., O'Brien, S., Jilani, I., Ferrajoli, A., Ravandi-Kashani, F., Aguilar, C., Dey, A., Thomas, D.A., Giles, F.J., Kantarjian, H.M., and Albitar, M. (2005) 'Angiogenic factors may have a different prognostic role in adult acute lymphoblastic leukemia'. *Blood*, 106 (13) 4303-07

Farrow, D.C., Vaughan, T.L., Hansten, P.D., Stanford, J.L., Risch, H.A., Gammon, M.D., Chow, W.H., Dubrow, R., Ahsan, H., Mayne, S.T., Schoenberg, J.B., West, A.B., Rotterdam, H., Fraumeni, J.F. Jr, and Blot, W.J. (1998) 'Use of aspirin and other nonsteroidal anti-inflammatory drugs and risk of esophageal and gastric cancer'. *Cancer Epidemiology*, *Biomarkers* & Prevention,7 (2) 97-102

Feng, X., Li, L., Jiang, H., Jiang, K., Jin, Y., and Zheng, J., (2014) 'Dihydroartemisinin potentiates the anticancer effect of cisplatin via mTOR inhibiti'on in cisplatin-resistant ovarian cancer cells: involvement of apoptosis and autophagy'. *Biochemical and Biophysical Research Communications*, 444(3) 376-81

Ferlay, J., Shin, H.R., Bray, F., Forman, D., Mathers, C. and Parkin, D.M. (2016) 'GLOBOCAN 2008, Cancer Incidence and Mortality Worldwide'. IARC Cancer Base No. 10, Lyon: IARC Press

Fisher, R., Pusztai, L., and Swanton, C. (2013) 'Cancer heterogeneity: implications for targeted therapeutics'. *British Journal of Cancer*, 108(3) 479-85

Fleming, M., Ravula, S., Tatishchev, S.F. and Wang, H.L. (2012) 'Colorectal carcinoma: Pathologic aspects'. *Journal of Gastrointestinal Oncology*, 3 (3) 153-73

Fujii, R., Imanishi, Y., Shibata, K., Sakai, N., Sakamoto, K., Shigetomi, S., Habu, N., Otsuka, K., Sato, Y., Watanabe, Y., Ozawa, H., Tomita, T., Kameyama, K., Fujii, M., and Ogawa, K. (2014) 'Restoration of E-cadherin expression by selective Cox-2 inhibition and the clinical relevance of the epithelial-to-mesenchymal transition in head and neck squamous cell carcinoma'. *Journal of Experimantal & Clinical Cancer Research: CR*, 10: 33-40

Fujioka, S., Kohno, N., and Hiwada, K. (1995) 'Ubenimex activates the E-cadherin-mediated adhesion of a breast cancer cell line YMB-S'. *Japanese Journal of Cancer Research: Gann*, 86(4) 368-73

Gallagher, R.E., Moser, B.K., Racevskis, J., Poiré, X., Bloomfield, C.D., Carroll, A.J., Ketterling, R.P., Roulston, D., Schachter-Tokarz, E., Zhou, D.C., Chen, I.M., Harvey, R., Koval, G., Sher, D.A., Feusner, J.H., Tallman, M.S., Larson, R.A., Powell, B.L., Appelbaum, F.R., Paietta, E., Willman, C.L., and Stock, W. (2012) 'Treatment-influenced associations of PML-RARα mutations, FLT3 mutations, and additional chromosome abnormalities in relapsed acute promyelocytic leukemia'. *Blood*, 120(10) 2098-108

García Rodríguez, L.A., Lin, K.J., Hernández-Díaz, S., and Johansson, S. (2011) 'Risk of upper gastrointestinal bleeding with low-dose acetylsalicylic acid alone and in combination with clopidogrel and other medications'. *Circulation*, 123 (10)1108-15

Ghanbari, P., Mohseni, M., Tabasinezhad, M., Yousefi, B., Saei, A.A., Sharifi, S., Rashidi, M. R., and Samadi, N. (2014) 'Inhibition of survivin restores the sensitivity of breast cancer cells to docetaxel and vinblastine'. *Applied Biochemistry and Biotechnology*, 174 (2) 667-81

Goel, S., Duda, D.G., Xu, L., Munn, L.L., Boucher, Y., Fukumura, D., and Jain, R.K. (2011) 'Normalization of the vasculature for treatment of cancer and other diseases'. *Physiological Reviews*, 91(3) 1071-121

Gopalakrishnan, A. M., and Kumar, N., (2015) 'Antimalarial action of artesunate involves DNA damage mediated by reactive oxygen species'. *Antimicrobial Agents and Chemotherapy*, 59 (1) 317-25

Greenhough, A., Smartt, H.J.M., Moore, A.E., Roberts, H.R., Williams, A.C., Paraskeva, C., and Kaidi, A. (2009) 'The COX-2/PGE2 pathway: Key roles in the hallmarks of cancer and adaptation to the tumour microenvironment'. *Carcinogenesis,* 30 (3) 377-86

GRIN Taxonomy Databases (2015). USDA, ARS, National Genetic Resources Program. Germplasm Resources Information Network - (GRIN), National Germplasm Resources Laboratory, Beltsville, Maryland. [online] available from <http://www.ars-grin.gov/cgi-bin/npgs/ html/splist.pl?997> [02 November 2015]

Grivennikov, S., Greten, F.R., Karin, M. (2010) 'Immunity, inflammation, and cancer'. *Cell*, 140(6) 883-99

Grivennikov, S., Karin, E., Terzic, J., Mucida, D., Yu, G.Y., Vallabhapurapu, S., Scheller, J., Rose-John, S., Cheroutre, H., Eckmann, L., and Karin, M. (2009) 'IL-6 and Stat3 are required for survival of intestinal epithelial cells and development of colitis-associated cancer'. *Cancer Cell*, 15(2)103-13

Groblewska, M., Mroczko, B., Wereszczynska-Siemiatkowska, Kedra, B., Lukaszewicz, M., Baniukiewicz, A., Szmitkowski, M. (2008) 'Serum interleukin (IL-6) and C-reactive protein (CRP) levels in colorectal adenoma and cancer patients'. *Clinical Chemistry and Laboratory Medicine,* 46 (10) 1423-8

Gu, K., Li, M.M., Shen, J., Liu, F., Cao, J.Y., Jin, S., and Yu, Y. (2015) 'Interleukin-17-induced EMT promotes lung cancer cell migration and invasion via NF-κB/ZEB1 signal pathway'. *American Journal of Cancer Research*, 5(3) 1169-79

Gunter, M.J., and Leitzmann, M.F., (2006) 'Obesity and colorectal cancer: epidemiology, mechanisms and candidate genes'. *The Journal of Nutritional Biochemistry*, 17 (3) 145-56

Győrffy, H., Holczbauer, A., Nagy, P., Szabó, Z., Kupcsulik, P., Páska, C., Papp, J., Schaff, Z., and Kiss, A. (2005) 'Claudin expression in Barrett's esophagus and adenocarcinoma'. *Virchows Archiv: an international journal of pathology,* 447(6) 961-8

Habashy, H.O, Powe, .DG., Staka, C.M., Rakha, E.A., Ball, G., Green, A.R., Aleskandarany, M., Paish, E.C., Douglas, M.R., Nicholson, R.I., Ellis, I.O., and Gee, J.M. (2010) 'Transferrin receptor (CD71) is a marker of poor prognosis in breast cancer and can predict response to tamoxifen'. *Breast Cancer Research and Treatment,* 119 (2) 283-93

Hakacova, N., Klingel, K., Kandolf, R., Engdahl, E., Fogdell-Hahn, A., and Higgins T.(2013) 'First therapeutic use of Artesunate in treatment of human herpesvirus 6B myocarditis in a child'. *Journal of Clinical Virology*, 57(2) 157-60

Hamacher-Brady, A., Stein, H.A., Turschner, S., Toegel, I., Mora, R., Jennewein, N., Efferth, T., Eils, R., and Brady, N.R. (2010) 'Artesunate activates mitochondrial apoptosis in breast cancer cells via iron-catalyzed lysosomal reactive oxygen species production'. *Journal of Biological Chemistry*, 286 (8) 6587-6601

Han, O., Failla, M.L., and Smith, J.C. (1997) 'Transferrin-iron and proinflammatory cytokines influence iron status and apical iron transport efficiency of Caco-2 intestinal cell line'. *Journal of Nutritional Biochemistry*, 8 (10) 585–91

Handrick, R., Ontikatze, T., Bauer, K.D., Freier, F., Rübel, A., Dürig, J., Belka, C., and Jendrossek, V. (2010) 'Dihydroartemisinin induces apoptosis by a Bak-dependent intrinsic pathway'. *Molecular Cancer Therapeutics*, 9 (9) 2497-510

Hanif, R., Pittas, A., Feng, Y., Koutsos, M.I., Qiao, L. Staiano-Coico,L., Shiff, S.I., and Rigas, B. (1996) 'Effects of nonsteroidal anti-inflammatory drugs on proliferation and on induction of apoptosis in colon cancer cells by a prostaglandin-independent pathway'. *Biochemical Pharmacology*, 52(2) 237–45

Harada, H., Kizaka-Kondoh, S. and Hiraoka, M. (2005) 'Optical imaging of tumor hypoxia and evaluation of efficacy of a hypoxia-targeting drug in living animals'. *Molecular Imaging*, 4 (3) 182-193

Harel, E., Rubinstein, A., Nissan, A., Khazanov, E., Nadler Milbauer, M., Barenholz, Y., and Tirosh, B. (2011) 'Enhanced transferrin receptor expression by proinflammatory cytokines in enterocytes as a means for local delivery of drugs to inflamed gut mucosa'. *PLoS ONE*, 6(9)

Harpaz, N., and Polydorides, A.D. (2010) 'Colorectal dysplasia in chronic inflammatory bowel disease: pathology, clinical implications, and pathogenesis'. *Arhives of pathology & laboratory medicine,* 134 (6) 876-95

Hassan, M., Watari, H., AbuAlmaaty, A., Ohba, Y., and Sakuragi, N. (2014) 'Apoptosis and molecular targeting therapy in cancer'. *BioMed Research International*, *2014*, 150845

Hayashida, K., Bartlett, A.H., Chen, Y., and Park, P.W. (2010) 'Molecular and cellular mechanisms of ectodomain shedding'. *The Anatomical Record*, 293(6) 925-37

Haynes, R.K., and Vonwiller, S.C. (1996) 'The behaviour of qinghaosu (artemisinin) in the presence of non-heme iron(II) and (III)'. *Tetrahedron Letters*, 37(2) 257-260

He, X., Chen, Z., Jia, M., and Zhao, X. (2013) 'Downregulated E-cadherin expression indicates worse prognosis in Asian patients with colorectal cancer: evidence from meta-analysis'. *PloS One,* 8(7): e70858

He, Y., Fan, J., Lin, H., Yang, X., Ye, Y., Liang, L., Zhan, Z., Dong, X., Sun, L.,and Xu, H. (2011) 'The anti-malaria agent artesunate inhibits expression of vascular endothelial growth factor and hypoxia-inducible factor-1α in human rheumatoid arthritis fibroblast-like synoviocyte'. *Rheumatology International,* 31(1) 53-60

He, Q., Shi, J., Shen, X.-L., An, J., Sun, H., Wang, L., Hu, Y.-J., Sun, Q., Fu, C., Sheikh, M.S., and Huang, Y. (2010) 'Dihydroartemisinin upregulates death receptor 5 expression and cooperates with TRAIL to induce apoptosis in human prostate cancer cells'. *Cancer Biology and Therapy*, 9 (10) 817-23

Hector, S., Conlon, S., Schmid, J., Dicker, P., Cummins, R. J., Concannon, C. G., Johnston, P. G., Kay, E. W., and Prehn, J. H. M. (2012) 'Apoptosome-dependent caspase activation proteins as prognostic markers in Stage II and IIIcolorectal cancer'. *British Journal of Cancer*, 106(9) 1499-1505

Hector, S. and Prehn, J.H. (2009) 'Apoptosis signaling proteins as prognostic biomarkers in colorectal cancer: A review'. *Biochimica et Biophysica Acta,* 1795 (2) 117-29

Heidland, A., Klassen, A., Rutkowski, P., and Bahner, U. (2006) 'The contribution of Rudolf Virchow to the concept of inflammation: what is still of importance?' *Journal of Nephrology*, 19 Suppl 10:S102-9

Hendriksen, E.M., Span, P.N., Schuuring, J., Peters, J.P., Sweep, F.C., van der Kogel, A.J., and Bussink, J. (2009) 'Angiogenesis, hypoxia and VEGF expression during tumour growth in a human xenograft tumour model'. *Microvascular Research*, 77(2) 96-103

Herr, I. and Debatin, K.M. (2001) 'Cellular stress response and apoptosis in cancer therapy'. *Blood*, 98(9) 2603-14

Ho, W.E., Peh, H.Y., Chan, T.K., and Wong, W.S. (2014) 'Artemisinins: pharmacological actions beyond anti-malarial'. *Pharmacology & Therapeutics*, 142(1)126-39

Holla, V. R., Mann, J.R., Shi, Q., and Dubois, R. N. (2006) 'Prostaglandin E2 regulates the nuclear receptor NR4A2 in colorectal cancer'. *The Journal of Biological Chemistry*, 281(5) 2676-82

Holla, V.R., Wang, D., Brown, J.R., Mann, J.R., Katkuri, S., and DuBois, R.N. (2005) 'Prostaglandin E2 regulates the complement inhibitor CD55/decay-accelerating factor in colorectal cancer'. *The Journal of Biological Chemistry*, 280(1) 476-83

Hossain, M.A., Kim, D.H., Jang, J.Y., Kang, Y.J., Yoon, J.-H., Moon, J.-O., Chung, H.Y., Kim, G.-Y., Choi, Y.H., Copple, B.L., and Kim, N.D. (2012) 'Aspirin enhances doxorubicin-induced apoptosis and reduces tumor growth in human hepatocellular carcinoma cells *in vitro* and *in vivo'. International Journal of Oncology*, 40(5) 1636-42

Hou, J., Wang, D., Zhang, R., and Wang, H. (2008) 'Experimental therapy of hepatoma with artemisinin and its derivatives: *in vitro* and *in vivo* activity, chemosensitization, and mechanisms of action'. *Clinical Cancer Research* 17, (14) 5519-30

Hu, C.J., Zhou, L., and Cai, Y. (2014) 'Dihydroartemisinin induces apoptosis of cervical cancer cells via upregulation of RKIP and downregulation of bcl-2'. *Cancer Biology &Therapy, 15(3) 279-88*

Huang, Y., Hua, K., Zhou, X., Jin, H., Chen, X., Lu, X., Yu, Y., Zha, X., and Feng, Y. (2008) 'Activation of the PI3K/AKT pathway mediates FSH-stimulated VEGF expression in ovarian serous cystadenocarcinoma'. *Cell Research,* 18(7) 780-91

Huang, X.J., Ma, Z.Q., Zhang, W.P., Lu, Y.B., and Wei, E.Q. (2007) 'Dihydroartemisinin exerts cytotoxic effects and inhibits hypoxia inducible factor-1alpha activation in C6 glioma cells'. *The Journal of Pharmacy and Pharmacology,* 59 (6) 849-56

Huang, J., Zhang, L., He, C., Qu, Y., Li,J., Zhang,J., Du,T., Chen, X., Yu, Y., Liu, B., and Zhu, Z. (2015) 'Claudin-1 enhances tumor proliferation and metastasis by regulating cell anoikis in gastric cancer'. *Oncotarget*, 6 (3) 1652-65

Hung, W.-C., Tseng, W.-L., Shiea, J., Chang, H.-C. (2010) 'Skp2 overexpression increases the expression of MMP-2 and MMP-9 and invasion of lung cancer cells'. *Cancer Letters*, 288 (2) 156-161

Hwang, Y.P., Yun, H.J., Kim, H.G., Han, E.H., Lee, G.W., and Jeong, H.G.(2010) 'Suppression of PMA-induced tumor cell invasion by dihydroartemisinin via inhibition of PKCα/Raf/MAPKs and NF-κB/AP-1-dependent mechanisms'. *Biochemical Pharmacology*, 79(12) 1714-26

Iglesias-Serret, D., Piqué, M., Barragán, M., Cosialls, A.M., Santidrián, A.F., González-Gironès, D.M., Coll-Mulet, L., de Frias, M., Pons, G., and Gil, J. (2010) 'Aspirin induces apoptosis in human leukemia cells independently of NF-κB and MAPKs through alteration of the Mcl-1/Noxa balance'. *Apoptosis*, 15 (2) 219-29

Ilie, M., Mazure, N. M., Hofman, V., Ammadi, R. E., Ortholan, C., Bonnetaud, C., Havet, K., Venissac, N., Mograbi, B., Mouroux, J., Pouysségur, J., and Hofman, P. (2010) 'High levels of carbonic anhydrase IX in tumour tissue and plasma are biomarkers of poor prognostic in patients with non-small cell lung cancer'. *British Journal of Cancer,* 102(11) 1627-35

Im, S.R. and Jang, Y.J. (2012) 'Aspirin enhances TRAIL-induced apoptosis via regulation of ERK1/2 activation in human cervical cancer cells'. *Biochemical and Biophysical Research Communications,* 424 (1) 65-70

Imbert, A.-M., Garulli, C., Choquet, E., Koubi, M., Aurrand-Lions, M., and Chabannon, C. (2012) 'CD146 expression in human breast cancer cell lines induces phenotypic and functional changes observed in epithelial to mesenchymal transition'. *PLoS ONE*, *7*(8) e43752

Jaffe, B.M. (1974) 'Prostaglandins and cancer: an update'. *Prostaglandins*, 6: 453–61

Jang, T.J., Jeon, K.H., and Jung, K.H. (2009) 'Cyclooxygenase-2 expression is related to the epithelial-to-mesenchymal transition in human colon cancers'. *Yonsei Medical Journal*, 50 (6) 818–24

Jansen, F.H., Adoubi, I., J C KC, DE Cnodder T, Jansen, N., Tschulakow, A., and Efferth, T. (2011) 'First study of oral Artenimol-R in advanced cervical cancer: clinical benefit, tolerability and tumor markers'. *Anticancer Research*, 31(12) 4417-22

Jayasinghe, C., Simiantonaki, N., and Kirkpatrick, C. J. (2013) 'VEGF-B expression in colorectal carcinomas and its relevance for tumor progression'. *Histology and Histopathology : cellular and molecular biology,* pages: 647-653

Jeong, H.J., Hong, S.-H., Park, R.-K., Shin, T., An, N.-H., and Kim, H.-M. (2005) 'Hypoxia-induced IL-6 production is associated with activation of MAP kinase, HIF-1 and NF-κB on HEI-OC1 cells'. *Hearing Research*, 207(1) 59-67

Ji, Y., Yang, X., Li, J., Lu, Z., Li, X., Yu, J., and Li, N. (2014) 'IL-22 promotes the migration and invasion of gastric cancer cells via IL-22R1/AKT/MMP-9 signaling'. *International Journal of Clinical and Experimental Pathology*, 7(7) 3694-703

Jiang, W., Huang, Y., Wang, J.P, Yu, X.Y., and Zhang, L.Y. (2013) 'The synergistic anticancer effect of artesunate combined with allicin in osteosarcoma cell line *in vitro* and *in vivo'*. *Asian Pacific Journal of Cancer Prevention*, 14(8) 4615–19

Jiang, W., Li, B, Zheng, X., Liu, X., Cen, Y., Li, J., Pan, X., Cao, H., Zheng, J., and Zhou, H. (2011) 'Artesunate in combination with oxacillin protect sepsis model mice challenged with lethal live methicillin-resistant *Staphylococcus aureus* (MRSA) via its inhibition on proinflammatory cytokines release and enhancement on antibacterial activity of oxacillin'. *International Immunopharmacology*, 11(8) 1065-73

Jiao, Y., Ge, C.M., Meng, Q.H., Cao, J.P., Tong, J., and Fan, S.J. (2007) 'Dihydroartemisinin is an inhibitor of ovarian cancer cell growth'. *Acta Pharmacologica Sinica*, 28 (7) 1045-56

Jodele, S., Chantrain, C.F., Blavier, L., Lutzko, C., Crooks, G.M., Shimada, H., Coussens, L.M., and Declerck, Y.A. (2005) 'The contribution of bone marrow-derived cells to the tumor vasculature in neuroblastoma is matrix metalloproteinase-9 dependent'. *Cancer Research*, 65(8) 3200-8

John, B.J., Abulafi, A.M., Poullis, A., and Mendall, M.A. (2007) 'Chronic subclinical bowel inflammation may explain increased risk of colorectal cancer in obese people'. *Gut*, 56(7) 1034-5

Johnson, T.W., Anderson, K.E., Lazovich D, and Folsom, A.R. (2002) 'Association of aspirin and nonsteroidal anti-inflammatory drug use with breast cancer'. *Cancer Epidemiology*, *Biomarkers & Prevention,* 11(12) 1586-91

Jones, M., Mercer, A.E., Stocks, P.A., La Pensée, L.J., Cosstick, R., Park, B.K., Kennedy, M.E., Piantanida, I., Ward ,S.A., Davies, J., Bray, P.G., Rawe, S.L., Baird, J., Charidza, T., Janneh, O., and O'Neill, P.M. (2009) 'Antitumour and antimalarial activity of artemisinin-acridine hybrids'. *Bioorganic & Medicinal Chemistry Letters* 19, (7) 2033-7

Joseph, B., Ekedahl, J., Lewensohn, R., Marchetti, P., Formstecher, P., and Zhivotovsky, B. (2001) 'Defective caspase-3 relocalization in non-small cell lung carcinoma'. *Oncogene,* 20 (23) 2877-88

Juárez Olguín, H., Flores Pérez, J., Lares Asseff, I., Loredo Abdalá, A. and Carbajal Rodríguez, L. (2004) 'Comparative pharmacokinetics of acetyl salicylic acid and its metabolites in children suffering from autoimmune diseases'. *Biopharmaceutics & Drug Disposition*, 25: 1–7. doi: 10.1002/bdd.379

Kaiser, M., Wittlin, S., Nehrbass-Stuedli, A., Dong, Y., Wang, X., Hemphill, A., Matile, H., Brun, R., and Vennerstrom, J.L. (2007) 'Peroxide bond-dependent antiplasmodial specificity of artemisinin and OZ277 (RBx11160)'. *Antimicrobial Agents and Chemotherapy*, 51(8) 2991-3

Kashiwagi, S., Yashiro, M., Takashima, T., Nomura, S., Noda, S., Kawajiri, H., Ishikawa, T., Wakasa, K., and Hirakawa, K. (2010) 'Significance of E-cadherin expression in triple-negative breast cancer'. *British Journal of Cancer,* 103 (2) 249-55

Kasum, C.M., Blair, C.K, Folsom, A.R., and Ross, J.A. (2003) 'Non-steroidal anti-inflammatory drug use and risk of adult leukaemia'. *Cancer Epidemiology*, *Biomarkers & Prevention*, 12(6) 534-7

Katanyoo, K., Rongsriyam, K., and Chongtanakon, M. (2013) 'Association between pretreatment levels of serum vascular endothelial growth factor (VEGF) and survival outcomes in locally advanced cervical cancer patients'. *Journal of Cancer Therapy*, 04 (10) 1478-84

Ke, Q., and Costa, M. (2006) 'Hypoxia-inducible factor-1 (HIF-1)'. *Molecular Pharmacology,* 70 (5) 1469-80

Kehrer, J.P. (2000) 'The Haber-Weiss reaction and mechanisms of toxicity'. *Toxicology*, 149 (1) 43-50

Kelly, J.D., Williamson, K.E., Irvine, A.E., Hamilton, P.W., Weir, H.P., Anderson, N.H., Keane, P.F. and Johnston, S.R. (1999) 'Apoptosis and its clinical significance for bladder cancer therapy'. *BJU International*, 83 (1) 1–10

Kelter, G., Steinbach, D., Konkimalla, V.B., Tahara, T., Taketani, S., H.-H. Fiebig, and Efferth, T. (2007) 'Role of transferrin receptor and the ABC transporters ABCB6 and ABCB7 for resistance and differentiation of tumor cells towards artesunate'. *PLoS ONE* 2(8): e798. doi:10.1371/journal.pone.0000798

[a]Kim, W.D., Kim, Y.W., Cho, I.J., Lee, C.H., and Kim, S.G. (2012) 'E-cadherin inhibits nuclear accumulation of Nrf2: implications for chemoresistance of cancer cells'. *Journal of Cell Science*, 125(5) 1284-95

[b]Kim, Y. H., Kwon, H.-J., and Kim, D.-S. (2012) 'Matrix metalloproteinase 9 (MMP-9)-dependent processing of βig-h3 protein regulates cell migration, invasion, and adhesion'. *The Journal of Biological Chemistry*, 287(46) 38957-69

Kim, C., Lee, J.H., Kim, S.-H., Sethi, G., and Ahn, K. S. (2015) 'Artesunate suppresses tumor growth and induces apoptosis through the modulation of multiple oncogenic cascades in a chronic myeloid leukemia xenograft mouse model'. *Oncotarget*, 6(6) 4020-35

Kim, S.-H., Park, Y.-Y., Kim, S.-W., Lee, J.-S., Wang, D., Dubois, R.N. (2011) 'ANGPTL4 induction by prostaglandin E2 under hypoxic conditions promotes colorectal cancer progression'. *Cancer Research*, 71(22) 7010-20

Kizhatil, K., Davis, J.Q., Davis, L., Hoffman, J., Hogan, B.L., and Bennett, V. (2007) 'Ankyrin-G is a molecular partner of E-cadherin in epithelial cells and early embryos'. *Journal of Biological Chemistry*, 282(36) 26552-61

Ko**,** Y.H., Roh**,** S.-Y**.,** Won**,** H.S., Jeon**,** E.K., Hong**,** S.H., Lee**,** M.A., Kang**,** J.H., Hong**,** Y.S., Kim, M.S., and Jung, C.-K. (2010) 'Prognostic significance of nuclear survivin expression in resected adenoid cystic carcinoma of the head and neck'. *Head & Neck Oncology,* 2:30 doi:10.1186/1758-3284-2-30

Kolonics, A., Apáti, A., Nahajevszky, S., Gáti, R., Brózik, A., and Magócsi, M. (2001)'Unregulated activation of STAT-5, ERK1/2 and c-Fos may contribute to the phenotypic transformation from myelodysplastic syndrome to acute leukaemia'. *Haematologia,* 31(2) 125-38

Kong, R., Jia, G., Cheng, Z.-x., Wang, Y.-w., Mu, M., Wang, S.-j., Pan, S.-h., Gao, Y., Jiang, H.-c., Dong, D.-l., and Sun, B. (2012) 'Dihydroartemisinin enhances Apo2l/TRAIL-mediated apoptosis in pancreatic cancer cells via ROS-mediated up-regulation of death receptor 5'. *PLoS ONE* 7 (5) art. no. e37222

Koomagi, R*.,* Zintl, F*.,* Sauerbrey, A*., and* Volm, M. (2001) 'Vascular endothelial growth factor in newly diagnosed and recurrent childhood acute lymphoblastic leukemia as measured by real-time quantitative polymerase chain reaction'. *Clinical Cancer Research*, 7(11) 3381-4

Koukourakis, M.I., Giatromanolaki, A., Sivridis, E., Simopoulos, K., Pastorek, J., Wykoff, C.C., Gatter, K.C., and Harris, A.L. (2001) 'Hypoxia-regulated carbonic anhydrase-9 (CA9) relates to poor vascularization and resistance of squamous cell head and neck cancer to chemoradiotherapy'. *Clinical Cancer Research*, 7(11) 3399-403

Krishna, S., Ganapathi, S., Ster, I.C., Saeed, M.E.M., Cowan, M., Finlayson, C., Kovacsevics, H., Jansen, H., Kremsner, P.G., Efferth, T., and Kumar, D. (2015) 'A randomised, double blind, placebo-controlled pilot study of oral artesunate therapy for colorectal cancer'. *EBioMedicine*, 2 (1) 82-90

Krishna, S., Uhlemann, A.C., and Haynes, R.K. (2004) 'Artemisinins: mechanisms of action and potential for resistance'. *Drug Resistance Updates*, 7(4-5) 233-44

Krungkrai, J., Imprasittichai, W., Otjungreed, S., Pongsabut, S., and Krungkrai, S.R. (2010) 'Artemisinin resistance or tolerance in human malaria patients'. *Asian Pacific Journal of Tropical Medicine*, 3(9) 748-53

Krusche, B., Arend, J., and Efferth, T. (2013) 'Synergistic inhibition of angiogenesis by artesunate and captopril *in vitro* and *in vivo*'. *Evidence-Based Complementary and Alternative Medicine*, 2013, 10 pages, Article ID 454783, doi:10.1155/2013/454783

Kumar, B., Koul, S., Petersen, J., Khandrika, L., Hwa, J.S., Meacham, R. B., Wilson, S., and Koul, H.K. (2010) 'p38 mitogen-activated protein kinase-driven MAPKAPK2 regulates invasion of bladder cancer by modulation of MMP-2 and MMP-9 activity'. *Cancer Research,* 70(2) 832-41

Kumar, A., and Singh, S.M. (2012) 'Priming effect of aspirin for tumor cells to augment cytotoxic action of cisplatin against tumor cells: implication of altered constitution of tumor microenvironment, expression of cell cycle, apoptosis, and survival regulatory molecules'. *Molecular* and Cellular *Biochemistry*, 371(1-2) 43-54

Lai, H., Sasaki, T., Singh, N.P. and Messay, A. (2005) 'Effects of artemisinin-tagged holotransferrin on cancer cells'. *Life Sciences* 76, 1267-79

Lee, J., Shen, P., Guobing Zhang, G., Wu, X., and Zhang, X. (2013) 'Dihydroartemisinin inhibits the Bcr/Abl oncogene at the mRNA level in chronic myeloid leukemia sensitive or resistant to imatinib'. *Biomedicine & Pharmacotherapy,* 67 (2) 157-63

Li, W., Albrecht, A.M., and Li, M. (2012) 'Inflammation and pancreatic. cancer: A tale of two cytokines'. *Cell Biology: Research & Tharapy,* 1 (1) art. No. 1000e 104

Li, M., Song, J., and Pytel, P. (2014) 'Expression of HIF-1 regulated proteins vascular endothelial growth factor, carbonic anhydraseIX and hypoxia inducible gene 2 in hemangioblastomas'. *Folia neuropathologica / Association of Polish Neuropathologists and Medical Research Centre, Polish Academy of Sciences,* 52(3) 234-42

Li, S., Xue, F., Cheng, Z., Yang, X., Wang, S., Geng, F., and Pan, L. (2009) 'Effect of artesunate on inhibiting proliferation and inducing apoptosis of SP2/0 myeloma cells through affecting NFκB p65'. *International Journal of Hematology,* 90(4) 513-521

Li, Y., Zhang, L., Simayi, D., Zhang, N., Tao, L., Yang, L., Zhao, J., Chen, Y., Li, F., and Zhang, W. (2015) 'Human Papillomavirus Infection Correlates with Inflammatory Stat3 Signaling Activity and IL-17 Level in Patients with Colorectal Cancer'. *PLoS One*, 10 (2)

Li, L.-N., Zhang, H.-D., Yuan, S.-J., Yang, D.-X., Wang, L., and Sun, Z.-X. (2008) 'Differential sensitivity of colorectal cancer cell lines to artesunate is associated with expression of beta-catenin and E-cadherin'. *European Journal of Pharmacology*, 588 (1) 1-8

Li, Y.J., Zhou, J.H., Du, X.X., Jia de X., Wu, C.L., Huang, P., Han, Y., Sui, H., Wei, X.L., Liu, L., Yuan, H.H., Zhang, T.T., Zhang, W.J., Xie, R., Lang, X.H., Liu,T., Jiang, C.L., Wang, L.Y., and Bai, Y.X. (2014) 'Dihydroartemisinin accentuates the anti-tumor effects of photodynamic therapy via inactivation of NF-κB in Eca109 and Ec9706 esophageal cancer cells'. *Cellular Physiology and Biochemistry*, 33(5) 1527-36

Li, X., Zhu, Y., He, H., Lou, L., Ye, W., Chen, Y., and Wang, J. (2013) 'Synergistically killing activity of aspirin and histone deacetylase inhibitor valproic acid (VPA) on hepatocellular cancer cells'. *Biochemical and Biophysical Research Communications,* 436 (2) 259-64

Lijuan, W., Yucong, Y., and Wenli, G., (2010) 'Effect of artesunate on human endometrial carcinoma HEC-1B cells'. *Journal of Medical Colleges of PLA* 3, 25 (3) 143-51

Liu, Y. and Cui, Y.F. (2013) 'Synergism of Cytotoxicity Effects of Triptolide and Artesunate combination treatment in pancreatic cancer cell lines'. *Asian Pacific Journal of Cancer Prevention,* 14(9) 5243-48

Lock, F.E., McDonald,P.C., Lou,Y., Serrano,I., Chafe, S.C., Ostlund,C., Aparicio, S., Winum, J.-Y., Supuran, C.T., and Dedhar, S., (2013) 'Targeting carbonic anhydrase IX depletes breast cancer stem cells within the hypoxic niche'. *Oncogene* 32, 5210-5219

Lok, Cn., and Ponka, P. (1999) 'Identification of a hypoxia response element in the transferrin receptor gene'. *Journal of Biological Chemistry*, 274 (34) 24147-52

Lu, C.C., Kuo, H.C., Wang, F.S., Jou, M.H., Lee, K.C., and Chuang, J.H.(2015) 'Upregulation of TLRs and IL-6 as a marker in human colorectal cancer'. *International Journal of Molecular Sciences*, 16 (1) 159-77

Lu, J.J., Meng L.H., Cai, Y.J., Chen, Q., Tong, L.J., Lin, L.P., and Ding, J. (2008) 'Dihydroartemisinin induces apoptosis in HL-60 leukemia cells dependent of iron and p38 mitogen-activated protein kinase activation but independent of reactive oxygen species'. *Cancer Biology and Therapy* 7, (7) 1017-23

Lu, J.J., Chen, S.M., Zhang, X.W., Ding, J., and Meng, L.H. (2011) 'The anti-cancer activity of dihydroartemisinin is associated with induction of iron-dependent endoplasmic reticulum stress in colorectal carcinoma HCT116 cells'. *Investigational New Drugs,* 29(6) 1276-83

Lu, J.J., Chen, S.M., Zhang, X.W., Ding, J., and Meng, L.H. (2010) 'The anti-cancer activity of dihydroartemisinin is associated with induction of iron-dependent endoplasmic reticulum stress in colorectal carcinoma HCT116 cells'. *Investigational new drugs,* 1-8

Luger, T.A., Krutmann, J., Kirnbauer, R., Urbanski, A., Schwarz, T., Klappacher, G., Köck, A., Micksche, M., Malejczyk, J., and Schauer, E. (1989) 'IFN-beta 2/IL-6 augments the activity of human natural killer cells'. *The Journal of Immunology*, 143 (4) 1206–9

Lyu, C.J., Rha, S.Y., and Won, S.C. (2007) 'Clinical role of bone marrow angiogenesis in childhood acute lymphocytic leukemia'. *Yonsei Medical Journal,* 48 (2) 171-5

Ma, H., Wu, L., Wang X.X., Lin, S., Zhang, A.M., Yao, Q., Sun, J.G. and Chen, Z.T., (2011) 'The effects of artesunate on the expression of EGFR and ABCG2 in A549 human lung cancer cells and a xenograft model'. *Molecules,* 16 (12) 10556-69

Martínez, M.E., McPherson, R.S., Levin, B., and Annegers, J.F. (1995) 'Aspirin and other nonsteroidal anti-inflammatory drugs and risk of colorectal adenomatous polyps among endoscoped individuals'. *Cancer Epidemiology*, *Biomarkers &* Prevention, 4 (7) 703-7

Meenaghan, T., Dowling, M., and Kelly, M. (2012) 'Acute leukaemia: making sense of a complex blood cancer'. *British Journal of Nursing*. 21(2):76, 78-83

Mell, L.K., Meyer, J.J., Tretiakova, M., Khramtsov, A., Gong, C., Yamada, D., Montag, A.G., and Mundt, A.J. (2003) 'Prognostic significance of decreased E-cadherin protein expression in pathologic stage I - III endometrial cancer: an immunohistochemical analysis'. *Radiation Oncology*, 57(2) S402-S403

Mercer, A.E., Maggs, J.L., Xiao-Ming sun, Cohen, G.M., Chadwick, J., O'Neil, P.M., and Park, B.K. (2007) 'Evidence for the involvement of carbon –centerd radicals in the induction of apoptotic cell death by artemisinin compounds'. *The Journal of Biological Chemistry,* 282 (13) 9372-82

Meshnick, S. R., Taylor, T. E., and Kamchonwongpaisan, S. (1996) 'Artemisinin and the antimalarial endoperoxides: from herbal remedy to targeted chemotherapy'. *Microbiological Reviews*, 60 (2) 301(15)

Milosevic, M., Warde, P., Ménard, C., Chung, P., Toi, A., Ishkanian, A., McLean, M., Pintilie, M., Sykes, J., Gospodarowicz, M., Catton, C., Hill, R.P., and Bristow, R. (2012) 'Tumor hypoxia predicts biochemical failure following radiotherapy for clinically localized prostate cancer'. *Clinical Cancer Research*, 18(7) 2108-14

Miyamoto, T., Tanaka, N., Eishi, Y., and Amagasa, T. (1994) 'Transferrin receptor in oral tumors'. *Journal of Oral* and *Maxillofacial Surgery,* 23 (6 Pt 2) 430-33

Mohamed, M., Dun, K., and Grabek, J. (2013) 'Atypical features in a patient with acute promyelocytic leukaemia: a potential diagnostic pitfall'. *BMJ Case Reports*, doi: 10.1136/bcr-2013-200152

Mohammadi-Motlagh, H.-R., Mansouri, K., and Mostafaie, A. (2010) 'Plants as useful agents for angiogenesis and tumor growth prevention'. *Physiology and Pharmacology*, 14, (3) 302-17

Moysich, K.B., Menezes, R.J., Ronsani, A., Swede, H., Reid, M.E., Cummings, K.M., Falkner, K.L., Loewen, G.M., and Bepler, G. (2002) 'Regular aspirin use and lung cancer risk'. *BMC Cancer*, 2, art. no. 31

Moysich, K.B., Mettlin, C., Piver, M.S., Natarajan, N., Menezes, R.J., Swede, H. (2001) 'Regular use of analgesic drugs and ovarian cancer risk'. *Cancer Epidemiology*, *Biomarkers & Prevention*, 10(8) 903-6

Mu, D., Chen, W., Yu, B., Zhang, C., Zhang, Y., and Qi, H. (2007) 'Calcium and survivin are involved in the induction of apoptosis by dihydroartemisinin in human lung cancer SPC-A-1 cells'. *Methods and Findings in Experimental and Clinical Pharmacology,* 1 (29) 33-8

Nagamune, K., Beatty, W.L., and Sibley, L. D. (2007) 'Artemisinin induces calcium-dependent protein secretion in the protozoan parasite *Toxoplasma gondii*'. *Eukaryotic cell,* 6(11) 2147-56

Nagasaki, T., Hara, M., Nakanishi, H., Takahashi, H., Sato, M., Takeyama, H. (2014) 'Interleukin-6 released by colon cancer-associated fibroblasts is critical for tumour angiogenesis: anti-interleukin-6 receptor antibody suppressed angiogenesis and inhibited tumour-stroma interaction'. *British Journal of Cancer*, 110(2) 469-78

Nesaretnam, K., and Meganathan, P. (2011) 'Tocotrienols: inflammation and cancer'. *Annals of the New York Academy of Science*, 1229:18-22

Neufeld, G., Cohen, T., Gengrinovitch, S., Poltorak, Z. (1999) 'Vascular endothelial growth factor (VEGF) and its receptors'. *FASEB Journal,* 13(1) 9-22

Nezu, M., Iwagaki, H., Aoki, H., Tanaka, N., and Orita, K. (1994) 'Tumour necrosis factor-alpha upregulates transferrin receptors in K 562 cells'. *The Journal of International medical Research*, 22(3) 145-52

Ng, D.S., Liao, W., Tan, W.S., Chan, T.K., Loh, X.Y., and Wong, W.S. (2014) 'Anti-malarial drug artesunate protects against cigarette smoke-induced lung injury in mice'. *Phytomedicine,* 21(12) 1638–44

Niki, T., Iba, S., Tokunou, M., Yamada, T., Matsuno, Y., and Hirohashi, S. (2000) 'Expression of vascular endothelial growth factors A, B, C, and D and their relationships to lymph node status in lung adenocarcinoma'. *Journal of the American Association for Cancer Research,* 6(6) 2431-9

Nishikawa, M., Oshitani, N., Matsumoto, T., Nishigami, T., Arakawa, T., and Inoue, M. (2005) 'Accumulation of mitochondrial DNA mutation with colorectal carcinogenesis in ulcerative colitis'. *British Journal of Cancer*, 93(3) 331-7

Noedl, H., Se, Y., Sriwichai, S., Schaecher, K., Teja - Isavadharm, P., Smith, B., Rutvisuttinunt, W., Bethell, D., Surasri, S., Fukuda, M.M., Socheat, D., and Chan Thap, L. (2010) 'Artemisinin resistance in Cambodia: a clinical trial designed to address an emerging problem in Southeast Asia. (Clinical report)'. *Clinical Infectious Diseases,* 51(11) e82-9

Nosten, F., and White, N.J. (2007) 'Artemisinin-based combination treatment of falciparum malaria'. *The American Journal of Tropical Medicine and Hygiene*, 77(6) 181-92

Nsobya, S.L., Kiggundu, M., Nanyunja, S., Joloba, M., Greenhouse, B., and Rosenthal, P.J. (2010) '*In vitro* sensitivities of *Plasmodium falciparum* to different antimalarial drugs in Uganda'. *Antimicrobial Agents and Chemotherapy*, 54(3) 1200-6

O'Donnell, K.A., Yu, D., Zeller, K.I., Kim, J.W., Racke, F., Thomas-Tikhonenko, A., Dang, C.V. (2006) 'Activation of transferrin receptor 1 by c-Myc enhances cellular proliferation and tumorigenesis'. *Molecular and Cellular Biology*, 26(6) 2373-86

Odaka,Y., Xu, B., Luo, Y., Shen, T., Shang, C., Wu, Y., Zhou, H., and Huang, S. (2014) 'Dihydroartemisinin inhibits the mammalian target of rapamycin-mediated signaling pathways in tumor cells'. *Carcinogenesis,* 35(1) 192-200

Ogawa, F., Amano, H., Ito, Y.,Matsui, Y., Hosono, K., Kitasato, H., Satoh, Y., and Majima, M. (2014) 'Aspirin reduces lung cancer metastasis to regional lymph nodes'. *Biomedicine & Pharmacotherapy,* 68 (1) 79-86

Oh, S., Kim, B.J., Singh, N.P., Lai, H., and Sasaki, T. (2009) 'Synthesis and anti-cancer activity of covalent conjugates of artemisinin and a transferrin-receptor targeting peptide'. *Cancer Letters* 274, (1) 33-9

Okorji, U.P., and Olajide, O.A. (2014) 'A semi-synthetic derivative of artemisinin, artesunate inhibits prostaglandin E2 production in LPS/IFNγ-activated BV2 microglia'. *Bioorganic and Medicinal Chemistry,* 22 (17) 4726-34

O' Neill, P.M., Barton, V.E., and Ward, S.A. (2010) **'**The molecular mechanism of action of artemisinin—The debate continues'. *Molecules* 15, (3) 1705-21

Ontikatze, T., Rudner, J., Handrick, R., Belka, C. and Jendrossek, V. (2014) 'Dihydroartemisinin is a hypoxia-active anti-cancer drug in colorectal carcinoma cells'. *Frontiers in Oncology,* 4:116

Pai, R., Nakamura, T., Moon, W.S., and Tarnawski, A.S. (2003) 'Prostaglandins promote colon cancer cell invasion; signaling by cross-talk between two distinct growth factor receptors'. *FASEB Journal*, 17(12) 1640-7

Panoilia, E., Schindler, E., Samantas, E., Aravantinos, G., Kalofonos, H.P., Christodoulou, C., Patrinos, G.P., Friberg. L.E., and Sivolapenko, G. (2015) 'A pharmacokinetic binding model for bevacizumab and VEGF165 in colorectal cancer patients'. *Cancer Chemotherapy and Pharmacology*, 75(4) 791-803

Park, I.-S., Jo, J.-R., Hong, H., Nam, K.-Y., Kim, J.-B., Hwang, S.-H., Choi, M.-S., Ryu, N.-H., Jang, H.-J., Lee, S.-H., Kim, C.-S., Kwon, T.-G., Park, G.-Y., Park, J.-W., and Jang, B.-C. (2010) 'Aspirin induces apoptosis in YD-8 human oral squamous carcinoma cells through activation of caspases, down-regulation of Mcl-1, and inactivation of ERK-1/2 and AKT'. *Toxicology in Vitro*, 24 (3) 713-20

Paschoud, S., Bongiovanni, M., Pache, J.C., and Citi, S. (2007) 'Claudin-1 and claudin-5 expression patterns differentiate lung squamous cell carcinomas from adenocarcinomas'. *Modern Pathology,* 20(9) 947-54

Pathi, S., Jutooru, I., Chadalapaka, G., Nair, V., Lee, S.-O., Safe, S. (2012) 'Aspirin inhibits colon cancer cell and tumor growth and downregulates Specificity Protein (Sp) transcription factors'. *PLoS ONE* 7 (10). art. no. e48208

Patrono, C. (2015) 'The multifaceted clinical readouts of platelet inhibition by low-dose aspirin'. *Journal of the American College of Cardiology*, 66(1) 74-85

Pećina-Šlaus, N. (2003) 'Tumor suppressor gene E-cadherin and its role in normal and malignant cells'. *Cancer Cell International*, 3:17

Prutki, M., Poljak-Blazi, M., Jakopovic, M., Tomas, D., Stipancic, I., and Zarkovic, N. (2006) 'Altered iron metabolism, transferrin receptor 1 and ferritin in patients with colon cancer'. *Cancer Letters*, 238 (2) 188-96

Qiao, L., and Li, X. (2014) 'Role of chronic inflammation in cancers of the gastrointestinal system and the liver: where we are now'. *Cancer Letters*, 345 (2)150-2

Qin, H.-x., Yang, J., Cui, H.-k., Li, S.-p., Zhang, W., Ding, X.-l., and Xia, Y.h. (2013) 'Synergistic antitumor activity of reversine combined with aspirin in cervical carcinoma in vitro and in vivo'. *Cytotechnology*, 65 (4) 643-53

Rahman, M., Selvarajan, K., Hasan, M.R., Chan, A. P., Jin, C., Kim, J., Chan, S., K., Le, N. D., Kim, Y.-B., and Tai, I. T. (2012) 'Inhibition of COX-2 in colon cancer modulates tumor growth and MDR-1 expression to enhance tumor regression in therapy-refractory cancers in vivo'. *Neoplasia*, 14(7) 624–33

Rasheed, S. A, Efferth T, Asangani I.A., Allgayer H. (2010) 'First evidence that the antimalarial drug artesunate inhibits invasion and in vivo metastasis in lung cancer by targeting essential extracellular proteases'. *International Journal of Cancer*, 127 (6) 1475-1485

Rasheed, S., Harris, A.L., Tekkis, P.P., Turley, H., Silver, A., McDonald, P.J., Talbot, I.C., Glynne-Jones, R., Northover, J.M., and Guenther, T. (2009) 'Assessment of microvessel density and carbonic anhydrase-9 (CA-9) expression in rectal cancer'. *Pathology, Research and Practice*, 205(1) 1-9

Ress, S. R., Morris, C. D., and Jacobs, P. (1990) 'Enhanced natural killer cell activity and long survival in acute non-lymphoblastic leukaemia. A case report'. *South African Medical Journal,* 77 (12) 648-50

Ringshausen, I., Dechow, T., Schneller, F., Weick, K., Oelsner, M., Peschel, C., and Decker, T. (2004) 'Constitutive activation of the MAPkinase p38 is critical for MMP-9 production and survival of B-CLL cells on bone marrow stromal cells. (Original Manuscript) (MTT)'. *Leukemia,* 18(12) 1964

Roelofs, H.M., Te Morsche, R.H., van Heumen, B.W., Nagengast, F.M., and Peters, W.H. (2014) 'Over-expression of COX-2 mRNA in colorectal cancer'. *BMC Gastroenterology*, 14 (1), doi: 10.1186/1471-230X-14-1

Rokavec, M., Öner, M. G., Li, H., Jackstadt, R., Jiang, L., Lodygin, D., Kaller, M., Horst, D., Ziegler, P.K., Schwitalla, S., Slotta-Huspenina, J., Bader, F.G., Greten, F.R., and Hermeking, H. (2014) 'IL-6R/STAT3/miR-34a feedback loop promotes EMT-mediated colorectal cancer invasion and metastasis'. *The Journal of Clinical Investigation*, 124(4) 1853–67

Romney, S.J., Newman, B.S., Thacker, C., and Leibold, E.A. (2011) 'HIF-1 regulates iron homeostasis in Caenorhabditis elegans by activation and inhibition of genes involved in iron uptake and storage'. *PLoS Genetics*, 7(12):e1002394

Ross, J.A, Blair, C.K., Cerhan, J.R, Soler, J.T., Hirsch, B.A., Roesler, M.A., Higgins, R.R., and Nguyen, P.L. (2011) 'Nonsteroidal anti-inflammatory drug and acetaminophen use and risk of adult myeloid leukemia'. *Cancer Epidemiology, Biomarkers & Prevention,* 20(8) 1741-50

Rossiello, L., Ruocco, E., Signoriello, G., Micheli, P., Rienzo, M., Napoli, C., and Rossiello, R. (2007) 'Evidence of COX-1 and COX-2 expression in Kaposi's sarcoma tissues'. *European Journal of Cancer,* 43(8) 1232-41

Ruffin, M. T., Krishnan, K., Rock, C. L., Normolle, D., Vaerten, M. A., Peters-Golden, M., Crowell, J., Kelloff, G., Boland, C. R., and Brenner, D. E. (1997) 'Suppression of human colorectal mucosal prostaglandins: determining the lowest effective aspirin dose'. *Journal of the National Cancer Institute*, 89(15) 1152-60

Rustum, Y. M., Tóth, K., Seshadri, M., Sen, A., Durrani, F. A., Stott, E., Morrison, C.D., and Bhattacharya, A. (2010) 'Architectural heterogeneity in tumors caused by differentiation alters intratumoral drug distribution and affects therapeutic synergy of antiangiogenic organoselenium compound'. *Journal of Oncology*, http://doi.org/10.1155/2010/396286

Ryschich, E., Huszty, G., Knaebel, H.P., Hartel, M., Büchler, M.W., and Schmidt, J. (2004) 'Transferrin receptor is a marker of malignant phenotype in human pancreatic cancer and in neuroendocrine carcinoma of the pancreas'. *European Journal of Cancer*, 40(9) 1418-22

R'zik, S., and Beguin, Y. (2001) 'Serum soluble transferrin receptor concentration is an accurate estimate of the mass of tissue receptors'. *Experimental Hematology,* 29(6) 677-85

Saarnio, J., Parkkila, S., Parkkila, A.K., Haukipuro, K., Pastoreková, S., Pastorek, J., Kairaluoma, M.I., Karttunen, T.J. (1998) 'Immunohistochemical study of colorectal tumors for expression of a novel transmembrane carbonic anhydrase, MN/CA IX, with potential value as a marker of cell proliferation'. *The American Journal of Pathology*, 153(1) 279-85

Saito, T., Yoshida, K., Matsumoto, K., Saeki, K., Tanaka, Y., Ong, S.M., Sasaki, N., Nishimura, R., and Nakagawa, T. (2014) 'Inflammatory cytokines induce a reduction in E-cadherin expression and morphological changes in MDCK cells'. *Research in Veterinary Science*, 96(2) 288-91

Sanmartín, C., Plano, D., Sharma, A.K., and Palop, J.A. (2012) 'Selenium compounds, apoptosis and other types of cell death: an overview for cancer therapy'. *International Journal of Molecular Sciences*, 13(8) 9649-72

Sasaki, Y., Takeda, H., Sato, T., Orii, T., Nishise, S., Nagino, K., Iwano, D., Yaoita, T., Yoshizawa, K., Saito, H., Tanaka, Y., Kawata, S. (2012) 'Serum Interleukin-6, insulin, and HOMA-IR in male individuals with colorectal adenoma'. *Clinical Cancer Research*, 18 (2) 392-9

Satimai, W., Sudathip, P., Vijaykadga, S., Khamsiriwatchara, A., Sawang, S., Potithavoranan, T., Sangvichean, A., Delacollette, C., Singhasivanon, P., Kaewkungwal, J., and Lawpoolsri, S. (2012) 'Artemisinin resistance containment project in Thailand. II: responses to mefloquine-artesunate combination therapy among falciparum malaria patients in provinces bordering Cambodia'. *Malaria Journal,* 11(1) 300

Sawada, K., Mitra, A. K., Radjabi, A. R., Bhaskar, V., Kistner, E. O., Tretiakova, M., Jagadeeswaran, S., Montag, A., Becker, A., Kenny, H.A., Peter, M.E., Ramakrishnan, V., Yamada, S.D., and Lengyel, E. (2008) 'Loss of E-cadherin promotes ovarian cancer metastasis via α5-Integrin, which is a therapeutic target'. *Cancer Research*, 68(7) 2329–39

Schneider, P., Dubus, I., Gouel, F., Legrand, E., Vannier, J.P. and Vasse, M. (2011) 'What role for angiogenesis in childhood acute lymphoblastic leukaemia?' *Advances in Hematology*, 2011, 274628

Sertel, S., Eichhorn, T., Simon, C.H., Plinkert, P.K., Johnson, S.W., and Efferth, T. (2010) 'Pharmacogenomic identification of c-Myc/Max-regulated genes associated with cytotoxicity of artesunate towards human colon, ovarian and lung cancer cell lines'. *Molecules*, 15 (4) 2886-910

Shahrokni, A., Rajebi, M.R., and Saif, M.W. (2009) 'Toxicity and efficacy of 5-fluorouracil and capecitabine in a patient with TYMS gene polymorphism: A challenge or a dilemma?'. *Clinical Colorectal Cancer*, 8 (4) 231-4

Shao, Y., Zhu, Y., and Liu, M. (2008) 'Effects of dihydroartemisinin on the proliferation and apoptosis of colon carcinoma cell line SW480'. *Medical Journal of Wuhan University*, 3 (29) 319-23

Shapiro, S., Hughes, G., Al-Obaidi, M.J., O'Reilly, E., Ramesh, S., Smith, J., Ahmad, R., Dawson, C., Riddle, P, and Sekhar, M. (2007) 'Acute myeloid leukaemia secondary to treatment with capecitabine for metastatic colorectal cancer'. *European Journal of* Haematology, 78(6) 543-4

Shi, C., Li, H., Yang, Y., and Hou, L. (2015) 'Anti-inflammatory and immunoregulatory functions of artemisinin and its derivatives'. *Mediators of Inflammation*, Vol.2015, Article ID 435713

Shibutani, M., Noda, E., Maeda, K., Nagahara, H., Ohtani, H., and Hirakawa, K. (2013) 'Low expression of claudin-1 and presence of poorly-differentiated tumor clusters correlate with poor prognosis in colorectal cancer'. *Anticancer Research,* 33 (8) 3301-6

Shin, S., Sung, B.J., Cho, Y.S., Kim, H.J., Ha, N.C., Hwang, J.I., Chung, C.W., Jung, Y.K., and Oh, B.H. (2001) 'An antiapoptotic protein human survivin is a direct inhibitor of caspase-3 and -7'. *Biochemistry,* 40, 1117-23

Singh, N.P., and Lai, H.C. (2004) 'Artemisinin induces apoptosis in human cancer cells'. *Anticancer Research,* 24 (4) 2277-80

Singh, A.B., Sharma, A., Smith, J.J., Krishnan, M., Chen, X., Eschrich, S., Washington, M.K., Yeatman, T.J., Beauchamp, R.D., and Dhawan, P. (2011) 'Claudin-1 up-regulates the repressor ZEB-1 to inhibit E-cadherin expression in colon cancer cells'. *Gastroenterology,* 141 (6) 2140-53

Singh, N.P., and Panwar, V.K. (2006) 'Case report of a pituitary macroadenoma treated with artemether'. *Integrative Cancer Therapies*, 5 (4) 391–4

Singh, N., and Verma, K. (2002) 'Case report of a laryngeal squamous cell carcinoma treated with artesunate'. *Archive of Oncology, 10(4)* 279–80

Smith, S.L., Fishwick, J., McLean, W.G., Edwards, G., and Ward, S.A. (1997) 'Enhanced *in vitro* neurotoxicity of artemisinin derivatives in the presence of haemin'. *Biochemical Pharmacology*, 53 (1) 5-10

Steeg, P.S. (2006) ‘Tumor metastasis: mechanistic insights and clinical challenges’. *Nature Medicine,* 12, 895 - 904

Stegeman, H., Kaanders, J.H., Wheeler, D.L., van der Kogel, A.J., Verheijen, M.M., Waaijer, S.J., Iida, M., Grénman, R., Span, P.N., and Bussink, J. (2012) ‘Activation of AKT by hypoxia: a potential target for hypoxic tumors of the head and neck’. *BMC Cancer*, 12 art. no. 463

Suzuki, H., Tomida, A., and Tsuruo, T. (1998) ‘A novel mutant from apoptosis-resistant colon cancer HT-29 cells showing hyper-apoptotic response to hypoxia, low glucose and cisplatin’. *Japanese Journal of Cancer Research,* 89(11) 1169-78

Szkaradkiewicz, A., Marciniak, R., Chudzicka-Strugała, I., Wasilewska, A., Drews, M., Majewski, P., Karpiński, T., and Zwoździak, B. (2009) ‘Proinflammatory cytokines and IL-10 in inflammatory bowel disease and colorectal cancer patients’. *Archivum Immunologiae et Therapiae Experimentalis (Warsz),* 57(4) 291-4

Švastová, E., Žilka, N., Zat'ovičová, M., Gibadulinová, A., Čiampor, F., Pastorek, J., and Pastoreková, S. (2003) ‘Carbonic anhydrase IX reduces E-cadherin-mediated adhesion of MDCK cells via interaction with β-catenin’. *Experimental Cell Research*, 290(2) 332-45

Tacchini, L., Bianchi, L., Bernelli-Zazzera, A., and Cairo, G. (1999) ‘Transferrin receptor induction by hypoxia. HIF-1-mediated transcriptional activation and cell-specific post-transcriptional regulation’. *The Journal of Biological Chemistry*, 274(34) 24142-6

Takami, T., and Sakaida, I. (2011) ‘Iron regulation by hepatocytes and free radicals’. *Journal of Clinical Biochemistry and Nutrition*, *48* (2) 103–06

Takeuchi, K., Araki, H., Umeda, M., Komoike, Y., and Suzuki, K. (2001) ‘Adaptive gastric cytoprotection is mediated by prostaglandin EP1 receptors: a study using rats and knockout mice’. *The Journal of Pharmacology and Experimental Therapeutics,* 297(3) 1160-5

Tanaka, T. (2012) 'Development of an inflammation-associated colorectal cancer model and its application for research on carcinogenesis and chemoprevention'. *International Journal of Inflammation,* 2012, 658786

Thakkar, A., Sutaria, D., Grandhi, B.K. Wang, J., and Sunil Prabhu, S. (2013) 'The molecular mechanism of action of aspirin, curcumin and sulforaphane combinations in the chemoprevention of pancreatic cancer'. *Oncology Reports*, 29(4)1671-77

Thanaketpaisarn, O., Waiwut, P., Sakurai, H., and Saiki, I. (2011) 'Artesunate enhances TRAIL-induced apoptosis in human cervical carcinoma cells through inhibition of the NF-κB and PI3K/Akt signaling pathways'. *International Journal of Oncology,* 39(1) 279-85

Thun, M.J., Jane Henley, S., and Patrono, C. (2002) 'Nonsteroidal anti-inflammatory drugs as anticancer agents: Mechanistic, pharmacologic, and clinical issues'. *Journal of the National Cancer Institute,* 94 (4) 252-66

Tran, T.H., Dolecek, C., Pham, P.M., Nguyen, T.D., Nguyen, T.T., Le, H.T., Dong, T.H., Tran, T.T., Stepniewska, K., White, N.J., Farrar, J. (2004) 'Dihydroartemisinin-piperaquine against multidrug-resistant *Plasmodium falciparum* malaria in Vietnam: randomised clinical trial'. *Lancet,* 363(9402)18-22

Tsimberidou, A.M., Estey, E., Whitman, G.J., Dryden, M.J., Ratnam, S., Pierce, S., Faderl, S., Giles, F., Kantarjian, H.M., and Garcia-Manero, G. (2004) 'Extramedullary relapse in a patient with acute promyelocytic leukemia: successful treatment with arsenic trioxide, all-trans retinoic acid and gemtuzumab ozogamicin therapies'. *Leukemia Research*, 28(9) 991-4

Uchiyama T.,Takahashi, H., Endo, H., Sakai, E., Hosono, K., Nagashima, Y., and Nakajima, A. (2012) 'IL-6 plays crucial roles in sporadic colorectal cancer through the cytokine networks including CXCL7'. *Journal of Cancer Therapy* 3 (No. 6A) 874-79

Uddin, S., Ahmed, M., Hussain, A., Assad, L., Al-Dayel, F., Bavi, P., Al-Kuraya, K.S., and Munkarah, A. (2010) 'Cyclooxygenase-2 inhibition inhibits PI3K/AKT kinase activity in epithelial ovarian cancer'. *International Journal of Cancer,* 126(2) 382-94

Ueda, M., Imada, K., Imura, A., Koga, H., Hishizawa, M. and Uchiyama, T. (2005) 'Expression of functional interleukin-21 receptor on adult T-cell leukaemia cells'. *British Journal of Haematology*, 128: 169–76

Valentini, C.G., Fianchi, L., Voso, M.T., Caira, M., Leone, G., and Pagano, L. (2011) 'Incidence of acute myeloid leukemia after breast cancer'. *Mediterranean Journal of Hematology and Infectious Diseases*, 3(1) e2011069

Vane, J.R. and Botting R.M. (2003) 'The mechanism of action of aspirin'. *Thrombosis Research*, 110(5-6) 255-8

Vordermark D. (2010) 'Hypoxia-specific targets in cancer therapy: role of splice variants'. *BMC Medicine* 8 (1) 43-5

Waldner, M. J., Wirtz, S., Jefremow, A., Warntjen, M., Neufert, C., Atreya, R., Becker, C., Weigmann, B., Vieth, M., Rose-John, S., and Neurath, M. F. (2010) 'VEGF receptor signaling links inflammation and tumorigenesis in colitis-associated cancer'. *The Journal of Experimental Medicine*, *207*(13) 2855–68

Wang, S.J., Gao, Y., Chen, H., Kong, R., Jiang, H.C., Pan, S.H., Xue, D.B., Bai, X.W., and Sun, B. (2010) 'Dihydroartemisinin inactivates NF-kappaB and potentiates the anti-tumor effect of gemcitabine on pancreatic cancer both *in vitro* and *in vivo'*. *Cancer Letters,* 293 (1) 99-108

Wang, S.J., Sun, B., Cheng, Z.X., Zhou, H.X., Gao, Y., Kong, R., Chen, H., Jiang, H.C., Pan,S.H., Xue, D.B., and Bai, X.W. (2011) 'Dihydroartemisinin inhibits angiogenesis in pancreatic cancer by targeting the NF-κB pathway'. *Cancer Chemotherapy and Pharmacology*, 68 (6) 1421-30

Wang, H., Wang, H.S., Zhou, B.H., Li, C.L., Zhang, F., Wang, X.F., Zhang, G., Bu, X.Z., Cai, S.H., and Du, J. (2013) 'Epithelial-mesenchymal transition (EMT) induced by TNF-α requires AKT/GSK-3β-mediated stabilization of snail in colorectal cancer'. *PLoS One*, 8(2):e56664

Wang, Y., Yang, J., Chen, L., Wang, J., Wang, Y., Luo, J., Pan, L., and Zhang, X. (2014) 'Artesunate induces apoptosis through caspase-dependent and -independent mitochondrial pathways in human myelodysplastic syndrome SKM-1 cells'. *Chemico-biological interactions*, 219, 28-36

Wang, J., Zhang, B., Guo, Y., Li, G., Xie, Q., Zhu, B., Gao, J., and Chen, Z.(2008) 'Artemisinin inhibits tumor lymphangiogenesis by suppression of vascular endothelial growth factor C'. *Pharmacology*, 82(2) 148-55

Wartenberg, M., Wolf, S., Budde, P., Grünheck, F., Acker, H., Hescheler, J., Wartenberg, G., and Sauer, H. (2003) 'The antimalaria agent artemisinin exerts antiangiogenic effects in mouse embryonic stem cell-derived embryoid bodies'. *Laboratory Investigations,* 83 1647-55

Wei, Y., Chen, R., Dimicoli, S., Bueso - Ramos, C., Neuberg, D., Pierce, S., Wang, H., Yang, H., Jia, Y., Zheng, H., Fang, Z., Nguyen, M., Ganan - Gomez, I., Ebert, B., Levine, R., Kantarjian, H., and Garcia - Manero, G.(2013) 'Global H3K4me3 genome mapping reveals alterations of innate immunity signaling and overexpression of JMJD3 inhuman myelodysplastic syndrome CD34+ cells'. *Leukemia,* 27(11) 2177(10)

Weifeng, T., Feng, S., Xiangji, L., Changqing, S., Zhiquan, Q., Huazhong, Z., Peining, Y., Yong, Y., Mengchao, W., Xiaoqing, J., and Wan-Yee, L. (2011) 'Artemisinin inhibits *in vitro* and *in vivo* invasion and metastasis of human hepatocellular carcinoma cells'. *Phytomedicine*, 18(2-3) 158-62

Weil, J., Colin-Jones, D., Langman, M., Lawson, D., Logan, R., Murphy, M., Rawlins, M., Vessey, M., and Wainwright, P. (1995) 'Prophylactic aspirin and risk of peptic ulcer bleeding'. *British Medical Journal*, 310 (6983) 827-30

Weiss, J.R., Baker, J.A., Baer, M.R., Menezes, R.J., Nowell, S., and Moysich, K.B. (2006) 'Opposing effects of aspirin and acetaminophen use on risk of adult acute leukemia'. *Leukemia Research,* 30(2) 164-9

Wu, X., Zhang, W., Shi, X., An, P., Sun, W., and Wang, Z. (2010) 'Therapeutic effect of artemisinin on lupus nephritis mice and its mechanisms'. *Acta Biochim Biophys Sin (Shanghai),* 42(12) 916-23

Xiang, S., Sun, Z., He, Q., Yan, F., Wang, Y., and Zhang, J. (2010) 'Aspirin inhibits ErbB2 to induce apoptosis in cervical cancer cells'. *Medical Oncology*, 27 (2) 379-87

Xie, J., and Itzkowitz, S. H. (2008) 'Cancer in inflammatory bowel disease'. *World Journal of Gastroenterology, 14*(3) 378–89

Xiong, H., Hong, J., Du, W., Lin, Y.W., Ren, L.L., Wang, Y.C, Su, W.Y., Wang, J.L., Cui, Y., Wang, Z.H., and Fang, J.Y. (2012) 'Roles of STAT3 and ZEB1 proteins in E-cadherin down-regulation and human colorectal cancer epithelial-mesenchymal transition'. *The Journal of Biological Chemistry*, *287*(8) 5819–32

Xu, H., He, Y., Yang, X., Liang, L., Zhan, Z., Ye, Y., Yang, X., Lian, F., and Sun, L. (2007) 'Anti-malarial agent artesunate inhibits TNF-α-induced production of proinflammatory cytokines via inhibition of NF-κB and PI3 kinase/Akt signal pathway in human rheumatoid arthritis fibroblast-like synoviocytes'. *Rheumatology,* 6 (46) 920-6

Xu, Q., Li, Z.X., Peng, H.Q., Sun, Z.W., Cheng, R.L., Ye, Z.M., and Li, W.X. (2011) 'Artesunate inhibits growth and induces apoptosis in human osteosarcoma HOS cell line *in vitro* and *in vivo*'. *Journal of Zhejiang University. Science B,* 12(4) 247-55

Yadav, A., Kumar, B., Datta, J., Teknos, T. N., and Kumar, P. (2011) 'IL-6 promotes head and neck tumor metastasis by inducing epithelial-mesenchymal transition via the JAK-STAT3-SNAIL signaling pathway'. *Molecular Cancer Research : MCR*, *9*(12) 1658–67

[a]Yan, K.H., Yao, C.J., Chang, H.Y., Lai, G.M., Cheng, A.L., Chuang, S.E. (2010) 'The synergistic anticancer effect of troglitazone combined with aspirin causes cell cycle arrest and apoptosis in human lung cancer cells'. *Molecular Carcinogenesis*, 49(3) 235-46

[b]Yan, L., Lin, B., Gao, L., Gao, S., Liu, C., Wang, C., Wang, Y., Zhang, S., and Iwamori, M. (2010) 'Lewis (y) antigen overexpression increases the expression of

MMP-2 and MMP-9 and invasion of human ovarian cancer cells'. *International Journal of Molecular Sciences*, 11(11) 4441-52

Yang, Q., Shi, M., Shen, Y., Cao, Y., Zuo, S., Zuo, C., Zhang, H., Gabrilovich, D.I., Yu, Y., and Zhou, J. (2014) 'COX-1-derived thromboxane A2 plays an essential role in early B-cell development via regulation of JAK/STAT5 signaling in mouse'. *Blood, 124(10) 1610-21*

Yang, X. H., Sladek, T. L ., Liu, X., Butler, B. R., Froelich, C. J., and Thor, A. D. (2001) 'Reconstitution of caspase 3 sensitizes MCF-7 breast cancer cells to doxorubicin- and etoposide-induced apoptosis'. *Cancer Research*, 61(1) 348-54

Yang, X., Wang, W., Tan, J., Song, D., Li, M., Liu, D., Jing, Y. and Zhao, L. (2009) 'Synthesis of a series of novel dihydroartemisinin derivatives containing a substituted chalcone with greater cytotoxic effects in leukemia cells'. *Bioorganic and Medicinal Chemistry Letters,* 19(15) 4385-88

Yang, L., Zhu, H., Liu, D., Liang, S., Xu, H., Chen, J., Wang, X., and Xu, Z. (2011) 'Aspirin suppresses growth of human gastric carcinoma cell by inhibiting survivin expression'. *Journal of Biomedical Research*, *25* (4) 246–53

Yao, X., Ireland, S.K., Pham, T., Temple, B., Chen, R., Raj, M.H.G., and Biliran, H. (2014) 'TLE1 promotes EMT in A549 lung cancer cells through suppression of E-cadherin'. *Biochemical and Biophysical Research Commun*ications, 455 (3) 277–84

Ye, Q., Cai, W., Zheng, Y., Evers, B. M., and She, Q.-B. (2014) 'ERK and AKT signaling cooperate to translationally regulate survivin expression for metastatic progression of colorectal cancer'. *Oncogene*, 33(14) 1828-39

Yoo, J. and Lee, Y.J. (2007) 'Aspirin enhances tumor necrosis factor-related apoptosis-inducing ligand-mediated apoptosis in hormone-refractory prostate cancer cells through survivin down-regulation'. *Molecular Pharmacology*, 72 (6) 1586-92

Yoshioka, Y., Shimizu, S., Ito, T., Taniguchi, M., Nomura, M., Nishida, T., and Sawa, Y. (2012) 'p53 inhibits vascular endothelial growth factor expression in solid tumor'. *Journal of Surgical Research,* 174(2) 291-7

Zaki, M.H., Vogel, P., Body-Malapel, M., Lamkanfi, M., and Kanneganti, T.D. (2010) 'IL-18 production downstream of the Nlrp3 inflammasome confers protection against colorectal tumor formation'. *Journal of Immunology,* 185(8) 4912-20

Zhang, S., and Gerhard, G.S. (2008) 'Heme activates artemisinin more efficiently than hemin, inorganic iron, or hemoglobin'. *Bioorganic & Medicinal Chemistry,* 16 (16) 7853-61

Zhang, S., and Gerhard, G.S. (2009) 'Heme mediates cytotoxicity from artemisinin and serves as a general anti-proliferation target'. *PLoS ONE* 4(10), 1-10

Zhang, P., Luo, H.S., Li, M., and Tan, S.Y. (2015) 'Artesunate inhibits the growth and induces apoptosis of human gastric cancer cells by downregulating COX-2'. *OncoTargets and Therapy*, 16(8) 845-54

Zhang, X., Morham, S. G., Langenbach, R., and Young, D. A. (1999) 'Malignant transformation and antineoplastic actions of nonsteroidal antiinflammatory drugs (Nsaids) on cycloxygenase-null embryo fibroblasts'. *The Journal of Experimental Medicine, 190*(4) 451–60

Zhang, H. M., Rao, J.N., Guo, X., Liu, L., Zou, T., Turner, D.J., and Wang, J.-Y. (2004) 'Akt kinase activation blocks apoptosis in intestinal epithelial cells by inhibiting caspase-3 after polyamine depletion'. *The Journal of Biological Chemistry*, 279(21) 22539-47

Zhang, J.L., Wang, Z., Hu, W., Chen, S. S., Lou, X. E., and Zhou, H.J. (2013) 'DHA regulates angiogenesis and improves the efficiency of CDDP for the treatment of lung carcinoma'. *Microvascular Research*, 87, 14(11)

Zhang, Z.Y., Yu, S.Q., Miao, L.Y., Huang, X.Y, Zhang, X.P., Zhu, Y.P., Xia, X.H., and Li, D.Q.(2008) 'Artesunate combined with vinorelbine plus cisplatin in treatment of advanced non-small cell lung cancer: a randomized controlled trial'. *Zhong Xi Yi Jie He Xue Bao,* 6(2)134-8

Zhang, B., Zhang, B., Chen, X., Bae, S., Singh, K., Washington, M. K., and Datta, P. K. (2014) 'Loss of Smad4 in colorectal cancer induces resistance to 5-fluorouracil through activating Akt pathway'. *British Journal of Cancer*, 110(4) 946-57

Zhao, F., Wang, H., Kunda, P., Chen, X., Liu, Q., and Liu, T. (2013) 'Artesunate exerts specific cytotoxicity in retinoblastoma cells via CD71'. *Oncology Reports*, (30) 3 1473-1482

Zhao, X., Zhong, H., Wang, R., Liu, D., Waxman, S., Zhao, L., and Jing, Y. (2015) 'Dihydroartemisinin and its derivative induce apoptosis in acute myeloid leukemia through Noxa-mediated pathway requiring iron and endoperoxide moiety'. *Oncotarget*, 6(8) 5582-96

Zhou, H.-J., Wang, Z., and Li, A. (2008) 'Dihydroartemisinin induces apoptosis in human leukemia cells HL60 via downregulation of transferrin receptor expression'. *Anti-Cancer Drugs* 3, (19) 247-55

Zhou, L., Wang, D.S., Li, Q.J., Sun, W., Zhang, Y., and Dou, K.F. (2013) 'The down-regulation of Notch1 inhibits the invasion and migration of hepatocellular carcinoma cells by inactivating the cyclooxygenase-2/Snail/E-cadherin pathway *in vitro'*. *Digestive Diseases and Sciences*, 58(4) 1016-25

Zhou, H.-J., Wang, W.-Q., Wu, G.-D., Lee, J., Li, A. (2007) 'Artesunate inhibits angiogenesis and downregulates vascular endothelial growth factor expression in chronic myeloid leukemia K562 cells'. *Vascular Pharmacology,* 47 (2-3) 131-138

Zhou, Q., Zhu, Y., Deng, Z., Long, H., Zhang, S., and Chen, X. (2011) 'VEGF and EMMPRIN expression correlates with survival of patients with osteosarcoma'. *Surgical Oncology*, 20 (1) 13-9

Zhu, H.H., Qin, Y.Z, and Huang, X.J. (2014) 'Resistance to arsenic therapy in acute promyelocytic leukemia'. *The New England Journal of Medicine*, 370(19) 1864-6

Zuo, W., Wang, Z.-Z., and Xue, J. (2014) 'Artesunate induces apoptosis of bladder cancer cells by miR-16 regulation of COX-2 expression'. *International Journal of Molecular Sciences*, *15 (8)* 14298-312